НАУЧНО-ПРАКТИЧЕСКИЙ ЖУРНАЛ

ISSN 1682-0363 (print)
ISSN 1819-3684 (online)

БЮЛЛЕТЕНЬ СИБИРСКОЙ МЕДИЦИНЫ

BULLETIN OF SIBERIAN MEDICINE

Том 21
№ 4. 2022

20 ЛЕТ ЖУРНАЛУ «БЮЛЛЕТЕНЬ СИБИРСКОЙ МЕДИЦИНЫ»

BULLETIN OF SIBERIAN MEDICINE

Peer-reviewed scientific-practical journal
Issued quarterly

Volume 21, No. 4, 2022

ISSN 1682-0363 (print)
ISSN 1819-3684 (online)

FOUNDER AND PUBLISHER:
Siberian State Medical University, Ministry of Healthcare of the Russian Federation

Registered by the Ministry of Mass Media and Communications of the Russian Federation
Certificate of registration
No. 77-7366 of 26.03.2001

The journal "Bulletin of Siberian Medicine" is included in the list of peer-reviewed scientific journals and publications issued in the Russian Federation, which should publish main scientific results of doctoral and Candidate of Sciences theses

Bulletin of Siberian Medicine is indexed in:
Scopus
Web of Science (WoS (ESCI))
Science Index
RSCI
Ulrich's International Periodicals Directory
Cyberleninka
DOAS

Editorial Board Office:
107, Lenina Av., Tomsk, 634050, Russian Federation
Telephone: +7-(382-2)-51-41-53.
http://bulletin.tomsk.ru
E-mail: bulletin.tomsk@mail.ru

Publisher: Siberian State Medical University.
2, Moscow Trakt, Tomsk, 634050,
Russian Federation.
Editors: E.E. Stepanova, Yu.P. Gotfrid
Translators: M.E. Orlova, K.Yu.Skvortsova
Electronic makeup, cover design
L.D. Krivtsova

Printed in Litburo LLC,
4, Koroleva Str., Tomsk, 634055, Russian Federation

Signed to print on 30.12.2022
Format 60 × 84/8. Offset print.
Coated paper. Times font.
P.s. 26,75. C.p.s. 26,0.
500 copies. Order No. 921.

The price – free.
Date of publication 30.12.2022.

Pass-through copyright.
Advertising providers are liable for the truthfulness of information in advertising materials.

© Siberian State Medical University, 2022

EDITOR-IN-CHIEF
O.I. Urazova, *Corresponding Member of RAS (Tomsk)*

DEPUTY EDITORS-IN-CHIEF:
L.M. Ogorodova, *Corresponding Member of RAS (Tomsk)*
SCIENCE EDITOR
V.V. Kalyuzhin, *Professor (Tomsk)*

EDITORIAL BOARD:
V.M. Alifirova, *Professor (Tomsk)*
L.I. Aftanas, *Academician of RAS (Novosibirsk)*
A.A. Baranov, *Academician of RAS (Moscow)*
A.I. Vengerovsky, *Professor (Tomsk)*
Ye.G. Grigoriyev, *Corresponding Member of RAS (Irkutsk)*
A.M. Dygai, *Academician of RAS (Tomsk)*
M.V. Zav'yalova, *Professor (Tomsk*)
L.V. Kapilevich, *Professor (Tomsk)*
S.I. Karas, *Professor (Tomsk)*
R.S. Karpov, *Academician of RAS (Tomsk)*
V.I. Kiselyov, *Corresponding Member of RAS (Barnaul)*
S.V. Logvinov, *Professor (Tomsk)*
À.D. Makatsaria, *Corresponding Member of RAS (Moscow)*
L.S. Namazova-Baranova, *Academician of RAS (Moscow)*
S.A. Nekrylov, *Professor (Tomsk)*
V.P. Puzyryov, *Academician of RAS (Tomsk)*
V.I. Starodubov, *Academician of RAS (Moscow)*
Ye.A. Stepovaya, *Professor (Tomsk)*
A.T. Teplyakov, *Professor (Tomsk)*
V.A. Tkachuk, *Academician of RAS (Moscow)*
V.A. Trufakin, *Academician of RAS (Novosibirsk)*
O.S. Fedorova, *Professor (Tomsk)*
I.A. Khlusov, *Professor (Tomsk)*
Ye.L. Choinzonov, *Academician of RAS (Tomsk)*
A.G. Chuchalin, *Academician of RAS (Moscow)*
A.V. Shabrov, *Academician of RAS (St.-Petersburg)*
V.A. Shkurupiy, *Academician of RAS (Novosibirsk)*
M.S. Yusubov, *Professor (Tomsk)*
A. Antsaklis, *Professor (Greece)*
F. Chervenak, *Professor (USA)*
C. Dadak, *Professor (Austria)*
Y. Dekhtyar, *Professor (Latvia)*
M. Epple, *Professor (Germany)*
D. Gailani, *Professor (USA)*
P. Odermatt *(Switzerland)*
J. Odland *(Norway)*
M. Poyurovsky, *Professor (Israel)*
V. Zhdankin, *Professor (USA)*

БЮЛЛЕТЕНЬ СИБИРСКОЙ МЕДИЦИНЫ

Научно-практический журнал
Выходит 4 раза в год

Том 21, № 4, 2022

ISSN 1682-0363 (print)
ISSN 1819-3684 (online)

УЧРЕДИТЕЛЬ И ИЗДАТЕЛЬ:
ФГБОУ ВО «Сибирский государственный медицинский университет» Минздрава России

Журнал основан в 2001 году
Зарегистрирован в Министерстве РФ по делам печати, телерадиовещания и средств массовых коммуникаций
Свидетельство регистрации ПИ № 77-7366 от 26.03.2001 г.

Журнал входит в Перечень ведущих рецензируемых научных журналов и изданий, выпускаемых в РФ, в которых должны быть опубликованы основные научные результаты диссертаций на соискание ученой степени доктора и кандидата наук

Индексация:
Scopus
Web of Science (WoS (ESCI))
РИНЦ (Science Index)
RSCI
Ulrich's International Periodicals Directory
Cyberleninka
DOAS

Редакция:
634050, г. Томск, пр. Ленина, 107.
Тел.: (382-2)-51-41-53.
http://bulletin.tomsk.ru
E-mail: bulletin.tomsk@mail.ru

Оригинал-макет:
Издательство СибГМУ.
634050, г. Томск, Московский тракт, 2.
Редакторы: Е.Е. Степанова, Ю.П. Готфрид
Перевод: М.Е. Орлова, Дж. Палацца
Электронная верстка, дизайн обложки Л.Д. Кривцова

Отпечатано в ООО «Литбюро»,
634055, г. Томск, ул. Королёва, 4.

Подписано в печать 30.12.2022 г.
Формат 60 × 84/8. Печать офсетная.
Бумага мелованная. Гарнитура «Times».
Печ. л. 26,75. Усл. печ. л. 26,0.
Тираж 500 экз. Заказ 921.

Цена – свободная.
Дата выхода в свет 30.12.2022.

При перепечатке ссылка на «Бюллетень сибирской медицины» обязательна.

Ответственность за достоверность информации, содержащейся в рекламных материалах, несут рекламодатели.

© Сибирский государственный медицинский университет, 2022

ГЛАВНЫЙ РЕДАКТОР
О.И. Уразова, *член-корреспондент РАН (Томск)*

ЗАМЕСТИТЕЛЬ ГЛАВНОГО РЕДАКТОРА:
Л.М. Огородова, *член-корреспондент РАН (Томск)*

НАУЧНЫЙ РЕДАКТОР
В.В. Калюжин, *профессор, д-р мед. наук (Томск)*

РЕДКОЛЛЕГИЯ:
В.М. Алифирова, *профессор, д-р мед. наук (Томск)*
Л.И. Афтанас, *академик РАН (Новосибирск)*
А.А. Баранов, *академик РАН (Москва)*
А.И. Венгеровский, *профессор, д-р мед. наук (Томск)*
Е.Г. Григорьев, *член-корреспондент РАН (Иркутск)*
А.М. Дыгай, *академик РАН (Томск)*
М.В. Завьялова, *профессор, д-р мед. наук (Томск)*
Л.В. Капилевич, *профессор, д-р мед. наук (Томск)*
С.И. Карась, *профессор, д-р мед. наук (Томск)*
Р.С. Карпов, *академик РАН (Томск)*
В.И. Киселев, *член-корреспондент РАН (Барнаул)*
С.В. Логвинов, *профессор, д-р мед. наук (Томск)*
А.Д. Макацария, *член-корреспондент РАН (Москва)*
Л.С. Намазова-Баранова, *академик РАН (Москва)*
С.А. Некрылов, профессор, *д-р ист. наук (Томск)*
В.П. Пузырев, *академик РАН (Томск)*
В.И. Стародубов, *академик РАН (Москва)*
Е.А. Степовая, *профессор, д-р мед. наук (Томск)*
А.Т. Тепляков, *профессор, д-р мед. наук (Томск)*
В.А. Ткачук, *академик РАН (Москва)*
В.А. Труфакин, *академик РАН (Новосибирск)*
О.С. Федорова, *профессор, д-р мед. наук (Томск)*
И.А. Хлусов, *профессор, д-р мед. наук (Томск)*
Е.Л. Чойнзонов, *академик РАН (Томск)*
А.Г. Чучалин, *академик РАН (Москва)*
А.В. Шабров, *академик РАН (Санкт-Петербург)*
В.А. Шкурупий, *академик РАН (Новосибирск)*
М.С. Юсубов, *профессор, д-р хим. наук (Томск)*
A. Antsaklis, *профессор (Греция)*
F. Chervenak, *профессор* (США)
C. Dadak, *профессор* (Австрия)
Y. Dekhtyar, *профессор* (Латвия)
M. Epple, *профессор* (Германия)
D. Gailani, *профессор* (США)
P. Odermatt *(Швейцария)*
J. Odland *(Норвегия)*
M. Poyurovsky, *профессор* (Израиль)
V. Zhdankin, *профессор* (США)

СОДЕРЖАНИЕ

CONTENTS

УДК 618.19-006.6-021.3:577.171.6]-037:615.849
https://doi.org/10.20538/1682-0363-2022-4-6-12

Possibilities of predicting the HER2 / neu status in a primary tumor in breast cancer patients using ^{99m}Tc-DARPinG3

Bragina O.D.[1, 2], Tashireva L.A.[1], Chernov V.I.[1, 2], Deyev S.M.[2, 3], Tolmachev V.M.[2, 4]

[1] *Cancer Research Institute, Tomsk National Research Medical Center (NRMC), Russian Academy of Sciences*
5, Kooperativny Str., Tomsk, 634009, Russian Federation

[2] *National Research Tomsk Polytechnic University*
30, Lenina Av., 634050, Tomsk, Russian Federation

[3] *Shemyakin – Ovchinnikov Institute of Bioorganic Chemistry, Russian Academy of Sciences*
16/10, Miklukho-Maklaya Str., 117997, Moscow, Russian Federation

[4] *Uppsala University*
7, Dag Hammarskjölds väg, Segerstedthuset, 75236, Uppsala, Sweden

ABSTRACT

Aim. To determine informative prognostic criteria for assessing the HER2 / neu status in primary breast cancer using ^{99m}Tc-DARPinG3.

Materials and methods. The study included 10 patients with breast cancer ($T_{1-4}N_{0-2}M_0$) before systemic therapy, who underwent a radionuclide study using ^{99m}Tc-DARPinG3 at a dose of 3,000 μg. Five patients were characterized by HER2 / neu overexpression in primary breast cancer, whereas 5 patients were HER2-negative. For all patients, morphological and immunohistochemical studies and fluorescence in situ hybridization (FISH) of the primary tumor nodule were carried out. Single-photon emission computed tomography (SPECT) of the chest was performed for all patients 4 hours after the injection of ^{99m}Tc-DARPinG3.

Results. The total activity of ^{99m}Tc-DARPinG3 was 522.4 ± 341.8 MBq. The comparative analysis showed that higher uptake of the labeled protein in HER2-positive breast cancer was significant ($p = 0.0159$, Mann – Whitney U test). The analysis of the ratios showed significant differences in the tumor-to-background ratios in patients with HER2-positive breast cancer ($p < 0.0159$, Mann – Whitney U test). Based on the logistic regression analysis, a mathematical model was developed to predict the status of HER2 / neu in primary breast cancer patients (specificity and sensitivity 100%; $p = 0.0004$) using ^{99m}Tc-DARPinG3 at a dose of 3,000 mcg 4 hours after the injection of the radiopharmaceutical.

Conclusion. The results of the study allow to consider the tumor-to-background ratio 4 hours after the injection of ^{99m}Tc-DARPinG3 as an additional prognostic parameter for determining the HER2 / neu status in primary breast cancer.

Keywords: breast cancer, radionuclide diagnosis, alternative scaffolds, DARPinG3, HER2 / neu

Conflict of interest. The authors declare the absence of obvious or potential conflict of interest related to the publication of this article.

Source of financing. The study was supported by the grant of the Ministry of Science and Higher Education, Agreement No. 075-15-2022-1103, on the topic “Development of targeted molecules based on scaffold proteins for the diagnosis and therapy of malignant neoplasms: a theranostic approach”.

Conformity with the principles of ethics. All patients signed an informed consent to participate in the study. The study was approved by the Bioethics Committee at Cancer Research Institute, Tomsk NRMC.

✉ *Bragina Olga D.,* bragina_od@mail.ru

For citation: Bragina O.D., Tashireva L.A., Chernov V.I., Deyev S.M., Tolmachev V.M. Possibilities of predicting the status of the HER2 / neu receptor in a primary tumor in breast cancer patients using a targeted radiopharmaceutical «99mTc-DARPinG3». *Bulletin of Siberian Medicine.* 2022;21(4):6–12. https://doi.org/10.20538/1682-0363-2022-4-6-12.

Возможности прогнозирования статуса рецептора HER2/neu в первичной опухоли у больных раком молочной железы с применением таргетного радионуклидного препарата «^{99m}Tc-DARPinG3»

Брагина О.Д.[1, 2], Таширева Л.А.[1], Чернов В.И.[1, 2], Деев С.М.[2, 3], Толмачев В.М.[2, 4]

[1] Научно-исследовательский институт (НИИ) онкологии, Томский национальный исследовательский медицинский центр (НИМЦ) Российской академии наук
634009, Россия, г. Томск, пер. Кооперативный, 5

[2] Национальный исследовательский Томский политехнический университет (НИ ТПУ)
634050, Россия, г. Томск, пр. Ленина, 30

[3] Институт биоорганической химии (ИБХ) им. акад. М.М. Шемякина и Ю.А. Овчинникова Российской академии наук (РАН)
117997, Россия, г. Москва, ул. Миклухо-Маклая, 16/10

[4] Уппсальский университет
75236, Швеция, г. Уппсала, Segerstedthuset, Dag Hammarskjölds väg 7

РЕЗЮМЕ

Цель. Определить информативные прогностические критерии для оценки статуса HER2/neu в первичной опухоли у больных раком молочной железы (РМЖ) с применением радиофармпрепарата «^{99m}Tc-DARPinG3».

Материалы и методы. В работу включены 10 больных РМЖ ($T_{1–4}N_{0–2}M_0$), которым до начала системного лечения выполнялось радионуклидное исследование с применением препарата «^{99m}Tc-DARPinG3» в дозировке основного вещества 3 000 мкг: у пяти пациентов была выявлена гиперэкспрессия HER2/neu в первичной опухоли молочной железы, у пяти – нет. Во всех случаях проводились морфологическое и иммуногистохимическое исследования и FISH-анализ ткани основного опухолевого узла. Через 4 ч после введения препарата всем больным выполнялась однофотонная компьютерная томография органов грудной клетки.

Результаты. Суммарная активность препарата «^{99m}Tc-DARPinG3» составила 522,4 ± 341,8 МБк. При сравнительном анализе статистически значимым являлось более высокое накопление меченного протеина в HER2-позитивных опухолях молочной железы (p = 0,0159, U-критерий Манна – Уитни). Анализ соотношений продемонстрировал значимые различия показателя опухоль/фон у больных в подгруппе с HER2-позитивными опухолями молочной железы ($p < 0,0159$, U-критерий Манна – Уитни). На основании проведенного исследования с применением метода логистической регрессии разработана математическая модель для прогнозирования статуса HER2/neu в первичной опухоли у больных РМЖ (специфичность и чувствительность 100%; $p = 0,0004$) при использовании препарата «^{99m}Tc-DARPinG3» в дозировке 3 000 мкг через 4 ч после введения.

Заключение. Результаты данного исследования позволяют рассматривать показатель опухоль/фон через 4 ч после введения препарата «^{99m}Tc-DARPinG3» в качестве дополнительного перспективного параметра для определения статуса HER2/neu в первичной опухоли у больных РМЖ.

Ключевые слова: рак молочной железы, радионуклидная диагностика, альтернативные каркасные белки, DARPinG3, HER2/neu

Конфликт интересов. Авторы декларируют отсутствие явных и потенциальных конфликтов интересов, связанных с публикацией настоящей статьи.

Источник финансирования. Работа выполнена в рамках гранта Министерства науки и высшего образования по теме «Разработка таргетных молекул на основе каркасных белков для диагностики и терапии злокачественных новообразований: тераностический подход» (соглашение № 075-15-2022-1103).

Соответствие принципам этики. Все пациенты подписали информированное согласие на участие в исследовании. Исследование одобрено биоэтическим комитетом НИИ онкологии Томского НИМЦ.

Для цитирования: Брагина О.Д., Таширева Л.А., Чернов В.И., Деев С.М., Толмачев В.М. Возможности прогнозирования статуса рецептора HER2/neu в первичной опухоли у больных раком молочной железы с применением таргетного радионуклидного препарата «^{99m}Tc-DARPinG3». *Бюллетень сибирской медицины.* 2022;21(4):6–12. https://doi.org/10.20538/1682-0363-2022-4-6-12.

INTRODUCTION

HER2-positive breast cancer (BC) is diagnosed in more than 20% of BC cases. This cancer subtype is characterized by an unfavourable prognosis and a high risk of distant metastasis. High expression of HER2 / neu is a predictor of tumor sensitivity to specific (targeted) therapy, which requires strict selection of BC patients [1, 2].

Immunohistochemistry (IHC) and fluorescence in situ hybridization (FISH), currently used in clinical practice, do not have optimal characteristics for determining the HER2 / neu status. In particular, they do not allow for a simultaneous study of the state of a primary tumor and regional and distant metastasis, as well as for determination of molecular characteristics of detected tumor growth areas. This fact is of particular importance in terms of heterogeneity of HER2 / neu expression in primary tumors and metastatic sites, which can occur in 6–48% of cases. Harvesting material for a morphological examination in this case is not always technically possible or may result in serious complications [3, 4].

One of the modern directions in determining the HER2 / neu status is targeted radionuclide diagnosis using alternative scaffolds [5–7]. DARPinG3 molecules, which are ankyrin repeat proteins, belong to scaffolds [8, 9]. Results of phase I clinical trials of ^{99m}Tc-DARPinG3 in BC patients revealed the absence of complaints and toxic effects on the patient's body throughout the entire follow-up and higher uptake of the compound in HER2-positive BC. Besides, the optimal dose of the protein (3,000 μg) and the optimal time interval for the study after administration of the radiopharmaceutical (4 hours) were determined [10].

To continue the study in the subgroup of patients who received DARPinG3 at a dose of 3,000 μg, we conducted an additional analysis to identify prognostic criteria and the cut-off value for the tumor-to-background ratio for ^{99m}Tc-DARPinG3 to assess the HER2 / neu status in primary BC.

The aim of the study was to determine informative prognostic criteria for assessing the HER2 / neu status in primary BC patients using 99mTc-DARPinG3.

MATERIALS AND METHODS

The clinical trial was registered on ClinicalTrials.gov (Identifier: NCT04277338) and approved by the Bioethics Committee at Cancer Research Institute of Tomsk NRMC (Protocol No. of). The study included 10 BC patients (T1-3N0-1M0) who underwent a radionuclide study using ^{99m}Tc-DARPinG3 at a dose of 3,000 μg 4 hours after the injection of the radiopharmaceutical: 5 patients had HER2 overexpression, while 5 patients were HER2-negative.

All patients underwent a standard morphological examination and IHC of breast tumors; verification of axillary lymph node metastasis was carried out by cytology. IHC was performed according to a standard procedure; Dako oncoprotein c-erbB-2 antibodies were used. The expression of HER2 / neu was assessed according to the American Society of Clinical Oncology (ASCO) guidelines adopted in 2018 [1].

^{99m}Tc-DARPinG3 was prepared in sterile conditions at the Department of Radionuclide Diagnosis of Cancer Research Institute, Tomsk NRMC using the "CRS Isolink" kit (Center for Radiopharmaceutical Science, Paul Scherrer Institute, Villigen, Switzerland). Purification of the radiopharmaceutical was performed using NAP-5 columns (GE Healthcare, Sweden). After the purification, ^{99m}Tc-DARPinG3 was diluted to 10 ml with a sterile 0.9% sodium chloride solution, filtered, and slowly injected to the patient [9].

Single-photon emission computed tomography (SPECT) of the chest was conducted in the supine position 4 hours after the injection. SPECT acquisition included 32 projections. The data were evaluated using the E. Soft software package (Siemens, Germany) with determination of the radiopharmaceutical uptake in the primary breast tumor, the same area in the opposite breast, and the area projected at the latissimus dorsi and liver by outlining the region of interest (ROI) on axial slices with the best visualization (v = 3.53 cm^3). Tumor-to-background ratio (TBR), tumor-to-latissimus dorsi ratio, and tumor-to-liver ratio were calculated.

Statistical processing of the results was carried out using the STATISTICA 10.0 software package and Prism 9 (GraphPad, USA). The normality of distribution of variables was checked using the Shapiro – Wilk test. Taking into account non-normal distribution of the studied quantitative variables, the nonparametric Mann – Whitney test was used to assess the significance of differences for independent samples. The results were presented as the median and the interquartile range *Me* [Q_1–Q_3]. The prognostic value of the studied parameters was assessed using the ROC analysis. The logistic regression analysis was used to assess the risk. The differences were considered statistically significant at $p < 0.05$.

RESULTS

The activity of ^{99m}Tc-DARPinG3 before administration to the patient was 522.4 ± 341.8 MBq. The comparative analysis of ^{99m}Tc-DARPinG3 uptake revealed that higher uptake of the radiopharmaceutical in primary breast tumors with HER2 / neu overexpression ($p = 0.0159$, Mann – Whitney *U* test) was significant (Table 1, Fig. 1).

Table 1

Comparative analysis of ^{99m}Tc-DARPinG3 uptake in breast cancer patients 4 hours after the injection, *Me* [Q_1–Q_3]

^{99m}Tc-DARPinG3 uptake	HER2-negative breast tumors (total number of impulses)	HER2- positive breast tumors (total number of impulses)
Tumor	835.0 (654.5–2,534.0)	8,184.0 (5,174.0–13,453.0)
	$p = 0.0159$	
Background	450.0 (81.0–1,206.0)	413.5 (391.5–566.0)
	$p = 0.9048$	
Latissimus dorsi muscle	183.0 (58.0–790.5)	390.5 (298.8–588.0)
	$p = 0.7302$	
Liver	1,060.0 (690.5–6,421.0)	4,481.0 (2,300.0–5,126.0)
	$p = 0.2857$	

Analysis of the ^{99m}Tc-DARPinG3 uptake ratio demonstrated significant differences in the tumor-to-background ratio in patients with HER2-positive BC ($p < 0.0159$, Mann – Whitney *U* test) (Table 2, Fig. 2).

Table 2

Tumor-to-background ratio, tumor-to-latissimus dorsi ratio, and tumor-to-liver ratio in breast cancer patients 4 hours after the ^{99m}Tc-DARPinG3 injection, *Me* [Q_1–Q_3]

Parameter	HER2-negative breast tumors	HER2- positive breast tumors
Tumor-to-background ratio	2.4 (1.8–8.0)	15.3 (12.6–32.0)
	$p = 0.0159$	
Tumor-to latissimus dorsi ratio	4.5 (3.2–12.8)	22.5 (9.4–45.1)
	$p = 0.0635$	
Tumor-to-liver ratio	0.8 (0.4–1.1)	2.3 (1.0–5.6)
	$p = 0.0635$	

Additionally, to determine the prognostic value of the tumor-to-background ratio in assessing the HER2 / neu status in the primary tumor, we constructed ROC curves following the ROC analysis. The area under the curve (AUC) was 1.000 (95% confidence interval (CI) 1.000–1.000), $p < 0.0143$. The cut-off value was 10.39, sensitivity was 100.0%, and specificity was 100.0% (Fig. 3).

The logistic regression analysis revealed that the tumor-to-background ratio of more than 10.39 4 hours after the injection of ^{99m}Tc-DARPinG3 at a dose of 3,000 μg was a prognostic factor for the positive HER2 / neu status in primary BC patients (Chi-square = 12.36, $p = 0.0004$). The sensitivity and specificity of the model were 100%.

CONCLUSION

Determining the HER2 / neu status is an essential component for the prescription of optimal systemic therapy for BC patients. Unfortunately, despite a big number of currently used diagnostic techniques, they cannot simultaneously analyze the spread of the tumor in the patient's body and assess the molecular characteristics of the detected metastatic sites. Rapid development of targeted radionuclide imaging methods and addressing the potential of this research method at international scientific and clinical sites have significantly expanded the understanding of the role of this technique in the diagnosis of patients with BC and confirmed its potential.

In particular, the first clinically tested scaffold (a novel group of synthetic proteins with optimal properties for delivering a radionuclide to a tumor cell) was the affibody molecule. Radiolabeled ^{111}In-ABY-025 and ^{68}Ga-ABY-025 demonstrated its

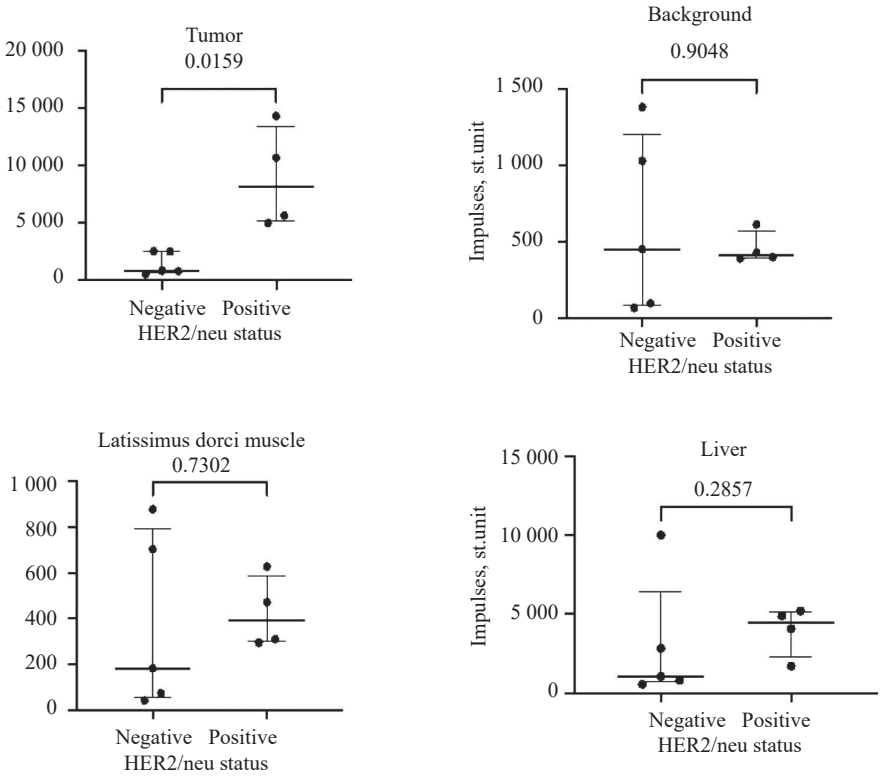

Fig. 1. Uptake of ^{99m}Tc-DARPinG3 in breast cancer patients 4 hours after the injection of the radiopharmaceutical

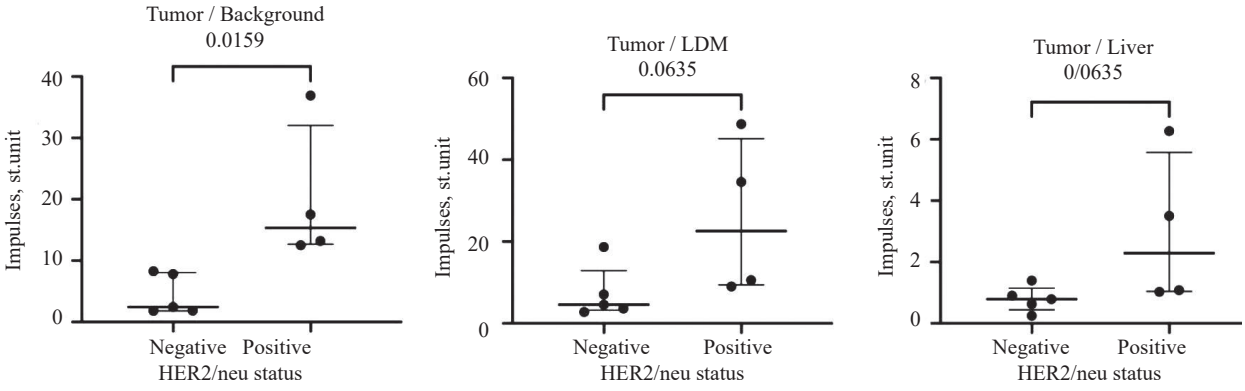

Fig. 2. Tumor-to-background ratio, tumor-to-latissimus dorsi ratio, and tumor-to-liver ratio in breast cancer patients 4 hours after the ^{99m}Tc-DARPinG3 injection

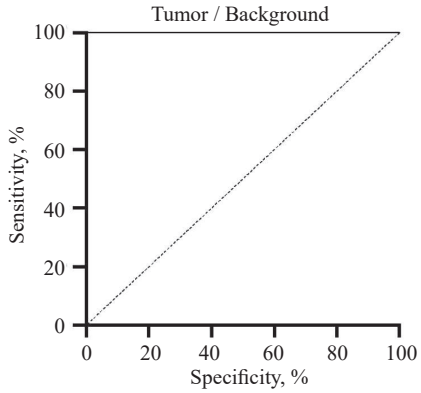

Fig. 3. ROC curve for the tumor-to-background ratio for assessing the HER2 / neu status in the primary tumor in breast cancer patients 4 hours after the ^{99m}Tc-DARPinG3 injection

effectiveness in SPECT / CT and PET for diagnosing metastatic BC with HER2/neu overexpression [11, 12]. A phase I clinical radionuclide study on alternative scaffolds in the diagnosis of HER2-positive BC was performed at Tomsk Polytechnic University and Tomsk NRMC using the synthetic ADAPT6 molecule labeled with technetium-99m (^{99m}Tc-ADAPT6) [13, 14]. The results demonstrated good tolerability of ^{99m}Tc-ADAPT6 and its high diagnostic efficiency in determining the HER2 / neu status in BC [15].

The present work is a continuation of the study using another alternative scaffold – the DARPinG3 molecule labeled with technetium-99m (^{99m}Tc-DARPinG3) with tropism to HER2 / neu. The results obtained during the recently completed phase I clinical trials also demonstrated good tolerability of ^{99m}Tc-DARPinG and its potential use for visualization of tumor sites in the breast, axillary lymph nodes, and visceral organs. This fragment of the study allowed to identify the most informative parameters for determining the HER2 / neu status in BC.

In particular, the tumor-to-background ratio in the mathematical model allows to predict the status of HER2 / neu in primary BC patients with high sensitivity and specificity (100 and 100%, respectively, $p = 0.0004$). Besides, it allows to consider the tumor-to-background ratio 4 hours after the injection of the radiopharmaceutical as an additional prognostic criterion for determining the HER2 / neu status in this group of patients.

REFERENCES

1. Wolff A.C., Hammond M.E.H., Hicks D.G., Dowsett M., McShane L.M., Allison K.H. et al. Recommendations for human epidermal growth factor receptor 2 testing in breast cancer: American Society of Clinical Oncology/College of American Pathologists clinical practice guideline update. *J. Clin. Oncol*. 2013;31(31):3997–4013. DOI: 10.1200/JCO.2013.50.9984.
2. Zavyalova M., Vtorushin S., Krakhmal N., Savelieva O., Tashireva L., Kaigorodova E. et al. Clinicopathological features of non-specific invasive breast cancer according to its molecular subtypes. *Experimental Oncology.* 2016;38(2):122–127.
3. Bartley A.N., Washington M.K., Ventura C.B., Ismaila N., Colasacco C. Benson 3rd A.B. et al. HER2 testing and clinical decision making in gastroesophageal adenocarcinoma: guideline grom the College of American Pathologists, American Society for Clinical Pathology, and the American Society of Clinical Oncology. *J. Clin. Oncol.* 2017;35(4):446–464. DOI: 10.1200/JCO.2016.69.4836.
4. Furrer D., Sanschagrin F., Jabod S., Diorio C. Advantages and disadvantages of technologies for HER2 testing in breast cancer specimens. *Am. J. Clin. Pathol.* 2015;144(5):686–703. DOI: 10.1309/AJCPT41TCBUEVDQC.
5. Bragina O.D., Chernov V.I., Zelchan R.V., Sinilkin I.G., Medvedeva A.A., Larkina M.S. Alternative scaffolds in radionuclide diagnosis of malignancies. *Bulletin of Siberian Medicine*. 2019;18(3):125–133 (in Russ.). DOI: 10.20538/1682-0363-2019-3-125-133.
6. Bragina O.D., Deyev S.M., Chernov V.I., Tolmachev V.M. Evolution of targeted radionuclide diagnosis of HER2-positive breast cancer. *Acta Naturae.* 2022 (in press) (in Russ).
7. Krasniqi A., D'Huyvetter M., Devoogdt N., Frejd F.Y., Sorensen J., Orlova A. et al. Same-day imaging using small proteins: clinical experience and translational prospects in oncology. *Journal of Nuclear Medicine*. 2018;59(6):885–891. DOI: 10.2967/jnumed.117.199901.
8. Shilova O.N., Deyev S.M. DARPins: Promising scaffolds for theranostics. *Acta Nature.* 2019;11(4):42–53. DOI: 10.32607/20758251-2019-11-4-42-53.
9. Vorobyeva A., Schulga A., Konovalova E., Güler R., Löfblom J., Sandström M. et al. Optimal composition and position of histidine-containing tags improves biodistribution of 99mTc-labeled DARPin G3. *Scientific Reports.* 2019;9(1):9405. DOI: 10.1038/s41598-019-45795-8.
10. Bragina O., Chernov V., Schulga A., Konovalova E., Garbukov E., Vorobyeva A.et. al. Phase I trial of 99mTc-(HE)3-G3, a DARPin-based probe for imaging of HER2 expression in breast cancer. *Journal of Nuclear Medicine.* 2022;Apr.;63(4):528–535. DOI: 10.2967/jnumed.121.262542.
11. Sandström M., Lindskog K., Velikyan I., Wennborg A., Feldwisch J., Sandberg D. et al. Biodistribution and radiation dosimetry of the anti-HER2 Affibody molecule 68Ga-ABY-025 in breast cancer patients. *J. Nucl. Med*. 2016;57(6):867–871. DOI: 10.2967/jnumed.115.169342.
12. Sörensen J., Velikyan I., Sandberg D., Wennborg A., Feldwisch J., Tolmachev V. et al. Measuring HER2-receptor expression in metastatic breast cancer using [^{68}Ga]ABY-025 affibody PET/CT. *Theranostics*. 2016;6(2):262–271. DOI: 10.7150/thno.13502.
13. Bragina O., Witting E., Garousi J., Zelchan R., Sandström M., Medvedeva A. et al. Phase I study of 99mTc-ADAPT6, a scaffold protein-based probe for visualization of HER2 expression in breast cancer. *J. Nucl. Med*. 2021;62(4):493–499. DOI: 10.2967/jnumed.120.248799.
14. Bragina O.D., Chernov V.I., Garbukov E.Yu., Doroshenko A.V., Vorobyeva A.G., Orlova A.M., Tolmachev V.M. Possibilities of radionuclide diagnostics of Her2-positive breast cancer using technetium-99m-labeled target molecules: the first experience of clinical use. *Bulletin of Siberian Medicine*. 2021;20(1):23–30 (in Russ.). DOI: 10.20538/1682-0363-2021-1-23-30.
15. Bragina O.D., Chernov V.I., Tashireva L.A., Zelchan R.V., Medvedeva A.A., Lukina N.M., Goldberg V.E., Tolmachev V.M. Determination of the most informative prognostic parameters for assessing the status of the epidermal growth factor receptor Her2/neu in the primary tumor in breast cancer patients using the targeted radiopharmaceutical ^{99m}Tc-ADAPT6. *Problems in Oncology.* 2021;67(3):368–373 (in Russ.). DOI: 10.37469/0507-3758-2021-67-3-368-373.

Authors contribution

Bragina O.D., Chernov V.I., Deyev S.M., Tolmachev V.M. – conception and design or analysis and interpretation of the data; justification of the manuscript, critical revision of the manuscript for important intellectual content, final approval of the manuscript for publication. Tashireva L.A. – statistical processing of the material.

Authors information

Bragina Olga D. – Dr. Sci. (Med.), Oncologist, Senior Researcher, Radionuclide Diagnosis Department, Cancer Research Institute, Tomsk NRMC; Senior Researcher, Oncotheranostics Research Center, National Research Tomsk Polytechnic University, Tomsk, bragina_od@mail.ru, https://orcid.org/0000-0001-5281-7758

Tashireva Lyubov A. – Cand. Sci. (Med.), Senior Researcher, General and Molecular Pathology Department, Cancer Research Institute, Tomsk NRMC, Tomsk, tashireva@oncology.tomsk.ru, https://orcid.org/0000-0003-2061-8417

Chernov Vladimir I. – Dr. Sci. (Med.), Professor, Head of the Radionuclide Diagnosis Department, Cancer Research Institute, Tomsk, chernov@tnimc.ru, https://orcid.org/0000-0002-5524-9546

Deyev Sergei M. – Dr. Sci. (Biology), Professor, RAS Academician, Head of the Molecular Immunology Department, Shemyakin – Ovchinnikov Institute of Bioorganic Chemistry, Russian Academy of Sciences, Moscow, deev_sm@tpu.ru, https://orcid.org/0000-0002-3952-0631

Tolmachev Vladimir M. – Professor, Head of the Laboratory for Immunology, Genetics, and Pathology, Uppsala University, Uppsala, Sweden; Head of the Oncotheranostics Research Center, National Research Tomsk Polytechnic University, Tomsk, Vladimir.tolmachev@igp.uu.se, https://orcid.org/0000-0002-6122-1734

(✉) **Bragina Olga D.,** bragina_od@mail.ru

Received 22.12.2021;
approved after peer review 08.02.2022;
accepted 09.06.2022

УДК 615.273.2:547.992
https://doi.org/10.20538/1682-0363-2022-4-13-19

Assessment of the effect of iron-rich humic substances on hematological parameters in the model of acute posthemorrhagic and iron deficiency anemia

Bratishko K.A.[1], Logvinova L.A.[1], Ivanov V.V.[1], Zhirkova A.M.[2], Ufandeew A.A.[1], Buyko E.E.[1], Zima A.P.[1], Rabcevich E.S.[1, 3], Kuznecova M.V.[1], Belousov M.V.[1], Perminova I.V.[2], Zykova M.V.[1]

[1] *Siberian State Medical University*
2, Moscow Trakt, Tomsk, 634050, Russian Federation

[2] *Lomonosov Moscow State University*
1, Leninskie Gory, Moscow, 119991, Russian Federation

[3] *National Research Tomsk State University*
36, Lenina Av., Tomsk, 634050, Russian Federation

ABSTRACT

Aim. To assess the effect of iron-rich humic substances on hematological parameters in acute post-hemorrhagic and iron deficiency anemia.

Materials and methods. Materials for the study were samples of iron-rich active pharmaceutical ingredients based on humic substances (Fe(III) hydroxide complexes with humic substances and polymaltose): HA-Fe^{3+}, HA-PM-Fe^{3+}, FA-Fe^{3+}, and FA-PM-Fe^{3+}. The anti-anemic activity of the substances was studied on 53 female Wistar rats of the conventional rat line in the model of acute posthemorrhagic and iron deficiency anemia. Anti-anemic activity was assessed by the hemoglobin level, erythrocyte count, hematocrit, and serum iron level.

Results. The studied substances HA-Fe^{3+} and FA-Fe^{3+} are the most effective in correcting the consequences of both experimental acute posthemorrhagic anemia and iron deficiency anemia. Their effect is comparable to that of the positive control drug Ferrum Lek.

Conclusion. Fe(III) hydroxide complexes stabilized by humic and fulvic acids exhibit anti-anemic activity.

Keywords: acute posthemorrhagic anemia, iron deficiency anemia, humic substances, ligands, Fe(III) hydroxide complexes

Conflict of interest. The authors declare the absence of obvious and potential conflicts of interest related to the publication of this article.

Source of financing. The study was carried out within the state assignment of the Ministry of Health of the Russian Federation (No. 056-00071-22-02).

Conformity with the principles of ethics. The protocol of animal experiments complies with the ethical standards and principles of biomedical research and was approved by the Ethics Committee at Siberian State Medical University (Protocol No. 8461/1 of 05.11.2020).

For citation: Bratishko K.A., Logvinova L.A., Ivanov V.V., Zhirkova A.M., Ufandeew A.A., Buyko E.E., Zima A.P., Rabcevich E.S., Kuznecova M.V., Belousov M.V., Perminova I.V., Zykova M.V. Assessment of the effect of iron-rich humic substances on hematological parameters in the model of acute posthemorrhagic and iron deficiency anemia. *Bulletin of Siberian Medicine.* 2022;21(4):13–19. https://doi.org/10.20538/1682-0363-2022-4-13-19.

✉ *Logvinova Lyudmila A.,* ludmila_logvinova@mail.ru

Оценка влияния железосодержащих субстанций на основе гуминовых веществ на гематологические показатели на модели острой постгеморрагической и алиментарной анемии

Братишко К.А.[1], Логвинова Л.А.[1], Иванов В.В.[1], Жиркова А.М.[2], Уфандеев А.А.[1], Буйко Е.Е.[1], Зима А.П.[1], Рабцевич Е.С.[1, 3], Кузнецова М.В.[1], Белоусов М.В.[1], Перминова И.В.[2], Зыкова М.В.[1]

[1] Сибирский государственный медицинский университет (СибГМУ)
Россия, 634050, г. Томск, Московский тракт, 2

[2] Московский государственный университет (МГУ) им. М.В. Ломоносова
Россия, 119991, г. Москва, Ленинские горы, 1

[3] Национальный исследовательский Томский государственный университет (НИ ТГУ)
Россия, 634050, г. Томск, пр. Ленина, 36

РЕЗЮМЕ

Цель. Оценить степень влияния железосодержащих субстанций на основе гуминовых веществ на гематологические показатели при острой постгеморрагической и алиментарной анемии.

Материалы и методы. Образцы железосодержащих активных фармацевтических субстанций на основе гуминовых веществ (комплексы гидроксида Fe(III) с гуминовыми веществами и полимальтозатом): ГК-Fe^{3+}, ГК-ПМ-Fe^{3+}, ФК-Fe^{3+} и ФК-ПМ-Fe^{3+}. Противоанемическая активность субстанций исследована на 53 самках крыс линии Вистар конвенциональной категории на модели острой постгеморрагической и алиментарной анемии. Противоанемическая активность оценена по показателям: уровень гемоглобина, содержание эритроцитов, гематокрит и уровень сывороточного железа.

Результаты. Исследуемые вещества ГК-Fe^{3+} и ФК-Fe^{3+} являются наиболее эффективными в коррекции последствий как экспериментальной острой постгеморрагической анемии, так и алиментарной анемии. Их эффект сопоставим с препаратом положительного контроля «Феррум Лек».

Заключение. Комплексы гидроксида Fe(III), стабилизированные гуминовыми кислотами и фульвокислотами, проявляют антианемическую активность.

Ключевые слова: острая постгеморрагическая анемия, железодефицитная анемия, гуминовые вещества, лиганды, комплексы гидроксида Fe(III)

Конфликт интересов. Авторы декларируют отсутствие явных и потенциальных конфликтов интересов, связанных с публикацией настоящей статьи.

Источник финансирования. Работа выполнена при финансовой поддержке государственного задания Министерства здравоохранения РФ (№ 056-00071-22-02).

Соответствие принципам этики. Эксперименты на животных соответствуют этическим нормам и принципам биомедицинских исследований и одобрены этическим комитетом СибГМУ (протокол № 8461/1 от 05.11.2020).

Для цитирования: Братишко К.А., Логвинова Л.А., Иванов В.В., Жиркова А.М., Уфандеев А.А., Буйко Е.Е., Зима А.П., Рабцевич Е.С., Кузнецова М.В., Белоусов М.В., Перминова И.В., Зыкова М.В. Оценка влияния железосодержащих субстанций на основе гуминовых веществ на гематологические показатели на модели острой постгеморрагической и алиментарной анемии. *Бюллетень сибирской медицины.* 2022;21(4):13–19. https://doi.org/10.20538/1682-0363-2022-4-13-19.

INTRODUCTION

High biological value of iron and significance of this transition metal and its compounds are proven by high abundance of iron in nature in general and in living beings in particular (as it is a cofactor of more than 70 metalloenzymes and porphyrins), electron-donating and electron-withdrawing properties of its ions, and its participation in complex metabolic pathways (hematopoiesis, glycolysis, cellular respiration, detoxification, etc.) [1–3]. Functional iron deficiency (mainly, in the composition of hemoglobin) and decreased iron in macrophages and hepatocytes contribute to the emergence of iron deficiency anemia (IDA), which is diagnosed in almost every tenth person in the world, according to WHO [4–7].

The clinical significance of IDA is associated not only with the pandemic prevalence, but also with the adverse effect of IDA on the most vulnerable to this disease age groups, including children, women of reproductive age, pregnant women, and the elderly [3–15]. They have a history of growth retardation, hydrops, premature and complicated births, inflammatory processes, decreased physical activity and disability, cognitive impairment, mental impairment, etc. [6, 7, 10].

Long-term oral iron therapy is one of the fundamental principles of sideropenia therapy, set forth by L.I. Idelson back in the 1980s [3] and described in the Russian "Clinical guidelines for Iron Deficiency Anemia Management 2020" [3]. Moreover, patients should not discontinue to take drugs when the hemoglobin level and the erythrocyte count are restored. Instead, they should continue taking medications in the adjusted dose until the iron level is restored, which should last for at least 6 months.

Currently, the pharmaceutical market has more than 30 monocomponent and combined drugs of ferrous (mainly sulfate) and trivalent iron (hydroxide polymaltose complex) and about 70 multivitamin drugs [3]. Due to various chemical structure, iron preparations can differ significantly in terms of bioavailability. Absorption of iron(II) (in the form of sulfate and fumarate) occurs along a concentration gradient in the intestinal region (passive diffusion) and exceeds the rate of adsorption of iron(III), which ultimately can increase the level of serum Fe^{2+} and cause intensification of oxidative processes (oxidative stress in the gastrointestinal tract is observed in more than 20 % of patients) [3, 6, 8, 10].

Moreover, adverse drug reactions take place, such as erythema, a metallic taste in the mouth (as severe as ulceration of the mucous membrane), darkening of tooth enamel and gums, dyspepsia (nausea, vomiting, diarrhea, constipation, etc.), and epigastric pain [3, 10]. Low digestibility of trivalent iron ions is associated with their ability to hydrolyze in the gastrointestinal tract with the formation of a precipitate. The iron(III)-hydroxide polymaltose complex (the active ingredient of such drugs as Ferrumlek, Maltofer, Ferinject) is a promising molecule among the compounds of iron(III), as it overcomes the enterocyte membrane barrier by means of active transport, therefore, the risk of siderosis development is reduced [6]. Moreover, it is redox – inert and does not interact with food components and other drugs [4]. Its only drawback is that patients may develop allergic reactions, which can be as severe as anaphylactic shock [3, 8]. Therefore, there is an urgent need to search for new promising ligands for iron(III) ions used for prevention and therapy in manifest iron deficiency, which include humic substances (HS) [16–23].

HS are refractory polydisperse copolymers, which are carriers of a large number of functional groups, including carboxyl, phenolic, quinoid, amide, ester, ether, etc. [16]. Polyfunctionality, developed inner surface, and, consequently, high reactivity (the ability to participate in ionic, redox reactions, van der Waals interactions, etc.) determined the affinity of HS to cells of various organs and systems, and their natural origin ensured safety, the absence of toxic effects in large concentrations, and a mild effect on metabolic processes at the cellular, organ, and organ system levels. Due to all this, HS are used as hepatoprotectors, anti-inflammatory and immunomodulatory agents [17], antihypoxants, antioxidants [18, 19], and detoxification and anti-allergic agents [20].

This class of natural biomolecules is now actively studied in a wide range of research areas because of the ability of HS to act as polydentate ligands due to electron-donating groups and slow down the migration of toxic metals in natural biological media. At the same time, a number of studies established a strong correlation between metal toxicity and the capacity of HS to bind metal ions [21, 22]. HS can act not only as effective chelate sorbents [23], but also as carriers of biogenic metals (namely, iron) in an easily accessible complex form, which, along with the absence of enzymatic systems in the body that metabolize them, contributes to a longer therapeutic effect.

In this regard, the aim of this study was to assess the effect of iron-containing active pharmaceutical ingredients (API) based on complexes of iron(III) hydroxide with HS on hematological parameters in the model of acute posthemorrhagic and iron deficiency anemia.

MATERIALS AND METHODS

In the experiment, samples of iron-containing API based on HS (complexes of iron(III) hydroxide with HS and polymaltose) were synthesized in the Laboratory of Natural Humic Systems of the Department of Medical Chemistry and Fine Organic Synthesis, Faculty of Chemistry, Lomonosov Moscow State University: HA-Fe^{3+} (with potassium humate), HA-PM-Fe^{3+} (with potassium humate and polymaltose (1 : 1)), FA-Fe^{3+} (with fulvic acid), and FA-PM-Fe^{3+} (with fulvic acid and polymaltose (1 : 1)). The first stage of the study involved screening of the anti-anemic properties of the substances in order to find the most effective candidate drugs to treat acute posthemorrhagic anemia (APHA) and was performed on 30 female Wistar rats of the conventional rat line (weighing 270–310 g). The animals were kept, cared for, and treated in accordance with the recommendations of international ethics committees. The protocol of experiments carried out in this study complied with the ethical standards and principles of biomedical research and was approved by the Ethics Committee at Siberian State Medical University (Protocol No. 8461/1 of 05.11.2020).

At the first stage, the animals were randomly divided into 6 experimental groups; in each group, APHA was caused by blood loss (the sample volume of the collected biofluid was 1.5 % of body weight) [24]. Interspecies dose conversion was performed to calculate the dose of iron to be administered [25]. The animals of group 1 (control, $n = 5$) were intragastrically injected with 1 ± 0.1 ml of purified water for 5 days after acute blood loss. The animals of group 2 were intragastrically injected with the reference listed drug Ferrum Lek® syrup (Slovenia) at a dose of 17 mg / kg of elemental iron ($n = 5$ positive control, control-3). The animals of groups 3, 4, 5, and 6 ($n = 5$) were intragastrically injected with iron-containing APIs based on HS (HA-Fe^{3+}, HA-PM-Fe^{3+}, FA-Fe^{3+}, FA-PM-Fe^{3+}, respectively) at a dose of 17 mg / kg of elemental iron for 5 days. Blood from the caudal vein of the animals of all groups was taken on day 6; euthanasia by CO_2 asphyxiation then followed. Next, hematological tests of the collected biological material were performed to assess hemoglobin level (HGB), g / l; erythrocyte count (RBC), $*10^3$ / μl, and hematocrit (HCT), %. Spectrophotometry was used to determine the content of serum iron (reagents "Vector-Best" (Novosibirsk), spectrophotometer SF-2000 (Russia)).

At the second stage, we studied the effect of the most effective preparations based on HS, identified during the first stage of the experiment, on the course of IDA. A total of 23 female Wistar rats of the conventional rat line weighing 216–256 g were used in the experiment. During 4.5 months, part of the animals (5 animals) had unlimited access to complete feed with a normal iron content (76.8 μg / g), and 18 female rats received *ad libitum* diet with a low iron content (28.2 μg / g). After 4.5 months, the main hematological parameters were measured in all animals (see above). After that, five animals were intragastrically injected with 1 ± 0.1 ml of purified water for 14 days. The other 18 animals with developed anemia were divided into three groups ($n = 6$), and in the next 2 weeks of the experiment, they continued to receive a low-iron diet while getting daily intragastric injections of the reference listed drug Ferrum Lek® syrup (Slovenia), HA-Fe^{3+}, and FA-Fe^{3+}, respectively. The iron content in Ferrum Lek®, HA-Fe^{3+}, and FA-Fe^{3+} was 17 mg / kg of elemental iron. After that, blood was taken from the caudal vein (followed by CO_2 asphyxiation), and morphological and biochemical parameters were measured (see above).

Statistica 8.0 (StatSoft Inc.) was used for the statistical data analysis. Methods of non-parametric statistics were used in the study: namely, the Friedman and Kruskal – Wallis tests. For each sample, we calculated the mean value X and the error of the mean SE. Differences between observations / groups were considered statistically significant at $p < 0.05$.

RESULTS AND DISCUSSION

Following the data analysis, it was found that acute blood loss in rats of the control group led to a drop in the studied hematological parameters. At the same time, these parameters did not reach the corresponding baseline values when purified water was used further on in the experiment. In the group of the positive control (after APHA, the reference listed drug Ferrum Lek® was used), a significant increase in hemoglobin, hematocrit, and RBC levels was observed compared with animals in the control group, but the parameters also did not reach the baseline level ($p < 0.05$) (Table 1).

Table 1

Hematological parameters after 5 days of the experiment, $X \pm SE$

Group	Before a course of medication (control-1)				After a course of medication			
	HGB, g / l	HCT, %	RBC, $\times 10^3$ / mcl	Fe, µmol / l	HGB, g / l	HCT, %	RBC, $\times 10^3$ / mcl	Fe, µmol / l
Water, $n = 5$ (control-2)	176.9 ± 2.0	45.1 ± 0.8	8.1 ± 0.1	61.7 ± 2.2	149.4 ± 2.1*	43.2 ± 0.5*	7.4 ± 0.1*	47.3 ± 1.7*
Ferrum Lek®, $n = 5$ (control-3)	189.4 ± 5.3	46.6 ± 1.8	8.5 ± 0.4	64.0 ± 8.9	158.4 ± 6.9*	45.8 ± 2.1	7.6 ± 0.3	44.4 ± 2.9
HA-Fe^{3+}, $n = 5$	178.8 ± 3.9	47.0 ± 2.3	8.4 ± 0.4	74.4 ± 6.4	158.4 ± 7.1*	45.8 ± 2.1	7.6 ± 0.4	51.6 ± 5.8*
HA-PM-Fe^{3+}, $n = 5$	191.1 ± 13.3	43.6 ± 1.6	7.8 ± 0.3	56.3 ± 7.0	146.0 ± 2.9*	42.6 ± 0.8	7.1 ± 0.3	38.8 ± 7.3
FA-Fe^{3+}, $n = 5$	182.1 ± 6.1	43.9 ± 3.5	7.9 ± 0.6	60.6 ± 2.2	145.3 ± 8.4*	42.6 ± 2.3	7.2 ± 0.6	48.0 ± 7.1
FA-PM-Fe^{3+}, $n = 5$	172.1 ± 3.0	43.5 ± 2.8	7.9 ± 0.4	58.7 ± 3.9	143.6 ± 6.8*	41.4 ± 1.9	7.1 ± 0.4	51.1 ± 4.4

The differences were statistically significant, $p < 0.05$: * with control-1 (the Friedman test); # with control-2 (the Kruskal – Wallis test); ^ with control-3 (the Kruskal – Wallis test).

Some hematological parameters in the rats were normalized after intragastric administration of the studied API at a dose of 17 mg / kg / day for 5 days after modeling APHA. It should be noted that during intragastric course administration, the studied substances HA-Fe^{3+} and FA-Fe^{3+} demonstrated greater efficiency in correcting the consequences of experimental APHA in comparison with samples of iron-containing APIs HA-PM-Fe^{3+} and FA-PM-Fe^{3+}, as the former resulted in a more significant increase in the levels of hematological parameters under study than the latter. At the same time, all the studied samples of iron-containing APIs based on HS had the same effect as the positive control drug Ferrum Lek®, which led to effective normalization of hematological parameters in the laboratory animals. No significant differences were found between the efficiency of the studied substances and the reference listed drug.

Following daily intragastric administration of HA-Fe^{3+} and FA-Fe^{3+}, as well as the reference listed drug Ferrum Lek® for 14 days at a dose of 17 mg / kg of elemental iron, serum iron concentrations returned to the baseline values ($p < 0.05$) (Table 2). It should be noted that the course administration of HA-Fe^{3+}increased the serum iron concentration in comparison with Ferrum Lek®, which was observed as a consistent trend ($p > 0.05$) (Table 2). However, administration of the studied substances and the reference listed drug for 14 days did not allow to bring hemoglobin and hematocrit levels to the control values ($p < 0.05$) (Table 2). It should also be noted that course administration of Ferrum Lek®, HA-Fe^{3+}, and FA-Fe^{3+} at a dose of 17 mg / kg / day for 14 days did not affect the body weight of rats and the absolute and relative weights of the liver and spleen in the model of IDA ($p > 0.05$).

Table 2

Hematological parameters after 14 days of the experiment, $X \pm SE$

Group	After modeling anemia				After a course of medication			
	HGB, g / l	HCT, %	RBC,$\times 10^6$/ mcl	Fe, µmol	HGB, g / l	HCT, %	RBC,$\times 10^6$ / mcl	Fe, µmol
Water, $n = 5$	198.8 ± 3.2	59.6 ± 0.9	10.3 ± 0.2	64.5 ± 1.6	197.8 ± 4.5^	59.5 ± 1.7^	9.7 ± 0.3	67.3 ± 1.1
Ferrum Lek®, $n = 6$	170.6 ± 6.7	51.1 ± 2.2	10.0 ± 0.4	25.4 ± 5.8	169.6 ± 3.2#	50.3 ± 0.9#	9.5 ± 0.3	60.6 ± 8.0*
HA-Fe^{3+}, $n = 6$	180.8 ± 5.7	53.6 ± 1.7	10.0 ± 0.4	34.1 ± 3.7	172.0 ± 1.9#	51.3 ± 0.6#	9.4 ± 0.1	75.0 ± 6.7*
FA-Fe^{3+}, $n = 6$	164.8 ± 11.7	50.1 ± 3.3	10.2 ± 0.5	20.4 ± 5.5	166.0 ± 1.7#	49.7 ± 0.7#	9.3 ± 0.2	62.3 ± 7.9*

The differences are statistically significant, $p < 0.05$: * with the group "After modeling anemia" (the Friedman test); # with the group "Water" (the Kruskal –Wallis test); ^ with the group "Ferrum Lek" (the Kruskal – Wallis test).

CONCLUSION

It was found that daily intragastric administration of the studied APIs after modeling APHA contributed to partial normalization of hematological parameters. Among the four samples studied, the most pronounced increase in hemoglobin concentration, erythrocytosis, and serum iron was observed in two iron-containing samples of APIs, namely, HA-Fe^{3+} and FA-Fe^{3+}. At the same time, the effect of all samples of iron-containing APIs based on HS was similar to the positive control drug Ferrum Lek®. No significant differences were found between the efficiency of the studied substances, as well as the reference listed drug.

The anti-anemic activity of iron(III) hydroxide complexes stabilized by humic and fulvic acids was

shown on the model of chronic IDA. At the same time, both APIs (HA-Fe^{3+}, whose matrix is 100% potassium humate, and FA-Fe^{3+}, whose matrix is 100 % fulvic acids) exhibit comparable activity. The results obtained confirmed the prospects of using HS as ligands in order to obtain APIs to normalize IDA.

REFERENCES

1. Levina A.A., Tsybulskaya M.M., Minina L.T., Tsvetaeva N.V. The ratio between the basic microelements (Fe, Cu, Zn) under anemia of different etiology. *Russian Clinical Laboratory Diagnostics.* 2013;7:45–48 (in Russ.).
2. Powers J.M., Buchanan G.R., Adix L., Zhang S., Gao A., McCavit T.L. Effect of low-dose ferrous sulfate vs iron polysaccharide complex on hemoglobin concentration in young children with nutritional iron-deficiency anemia. *JAMA.* 2017;137(22):2297–2304. DOI: 10.1001/jama.2017.6846.
3. Chilova R.A., Murashko A.V., Vechorko V.I., Chushkov Yu.V., Korolev V.S. Prevention and treatment of iron deficiency in pregnant and lactating women. *RMJ. Mother and Child.* 2017;15:1092–1095 (in Russ.).
4. Atadzhanyan A.S., Zainulina M.S., Malakhovskaya E.A. Comparative efficiency of intravenous and oral iron preparations in anemic pregnant women. *Journal of Obstetrics and Women's Diseases.* 2019;68(2):23–32 (in Russ.).
5. Jose A., Mahey R., Sharma J.B., Bhatla N., Saxena R., Kalaivani M. et al. Comparison of ferric carboxymaltose and iron sucrose complex for treatment of iron deficiency anemia in pregnancy- randomised controlled trial. *BMC Pregnancy Childbirth.* 2019;19(1):54. DOI: 10.1186/s12884-019-2200-3.
6. Lepanto M.S., Luigi R., Cutone A., Conte M.P., Paesano R., Valenti P. Efficacy of lactoferrin oral administration in the treatment of anemia and anemia of inflammation in pregnant and non-pregnant women: an interventional study. *Front Immunol.* 2018;9:2121. DOI: 10.3389/fimmu.2018.02123.
7. Lasocki S., Asfar P, Jaber S., Ferrandiere M., Kerforne T., Asehnoune K. et al. Impact of treating iron deficiency, diagnosed according to hepcidin quantification, on outcomes after a prolonged ICU stay compared to standard care: a multicenter, randomized, single-blinded trial. *Crit. Care.* 2021;25(1):62. DOI: 10.1186/s13054-020-03430-3.
8. Cappellini M.D., Musallam K.M., Taher A.T. Iron deficiency anaemia revisited. *J. Intern. Med.* 2020;287(2):153–170. DOI: 10.1111/j.1365-2141.2011.09012.x10.1111/joim.13004.
9. Kononova S.V., Kuzin V.B., Lovtsova L.V., Zueva I.A., Ganenkov A.A. Pharmacological and clinical-economic aspects of the use of iron preparations (review). *Medical Almanac.* 2010;3(12):197–201 (in Russ.).
10. Gorokhovskaya G.N., Yun V.L. Iron deficiency in the practice of a therapist. Character of iron deficiency and prevention of iron deficiency anemia. *Medical Council.* 2014;2:85–92 (in Russ.).
11. Andreichev N.A., Andreicheva E.N. The differential diagnostic of anemias associated with iron metabolism. *Russian Medical Journal.* 2016;22(4):213–221 (in Russ.).
12. Lukina E.A., Ledina A.V., Rogovskaya S.I. Iron deficiency anemia: a view of hematologist and gynecologist. Optimizing diagnostic and treatment approach. *RMJ. Mother and Child.* 2020;3(4):248–253 (in Russ.).
13. Savchenko T.N., Agaeva M.I. Anemia and pregnancy. *RMJ. Mother and Child.* 2016;15:971–975 (in Russ.).
14. Strutynsky A.V. Iron deficiency anemia. Diagnostics and treatment. *Difficult Patient.* 2013;11(12):38–43 (in Russ.).
15. Egorova N.A., Kanatnikova N.V. Iron metabolism in the human body and its hygienic limits for drinking water. Review. Part 1. *Hygiene and Sanitation.* 2020;99(4):412–417 (in Russ.).
16. Perminova I.V. From green chemistry and nature-like technologies towards ecoadaptive chemistry and technology. *Pure Appl. Chem.* 2019;91(5):851–864. DOI: 10.1515/pac-2018-1110.
17. Trofimova E.S., Danilets M.G., Ligacheva A.A., Sherstoboev E.Y., Zykova M.V., Tsupko A.V. et al. Immunomodulating properties of humic acids extracted from oligotrophic sphagnum magellanicum peat. *Bulletin of Experimental Biology and Medicine.* 2021;170(4):461–465. DOI: 10.1007/s10517-021-05088-5.
18. Bratishko K.A., Zykova M.V., Ivanov V.V., Buiko E.E., Drygunova L.A., Perminova I.V., et al. Peat humic acids – prospective biologically active substances with antioxidant activity for the development of protective agents. *Chemistry of Plant Raw Material.* 2021;1:287–298 (in Russ.).
19. Zykova M.V., Logvinova L.A., Bratishko K.A., Yusubov M.S., Romanenko S.V., Schepetkin I.A. et al. Physicochemical characterization and antioxidant activity of humic acids isolated from peat of various origins. *Molecules.* 2018;23(4):753. DOI: 10.3390/molecules23040753.
20. Trofimova E.S., Ligacheva A.A., Danilets M.G., Sherstoboev E.Y., Zykova M.V., Logvinova L.A. et al. Anti-allergic properties of humic acids isolated from pine-sphagnum-cotton sedge peat. *Bulletin of Experimental Biology and Medicine.* 2022;172(3):324–327. DOI: 10.1007/s10517-022-05385-7.
21. Avvakumova N.P. Humin substances – the factor of biosystems protection from ecotoxicogenic substances. *Izvestia of Samara Scientific Center of the Russian Academy of Sciences.* 2009;11(1-2):197–201 (in Russ.).
22. Buiko E.E., Zykova M.V., Ivanov V.V., Bratishko K.A., Ufandeev A.A., Grigorieva I.O., et al. Antioxidant activity of silver-containing bionanocompositions based on humic substances in cell culture. *Drug Development & Registration.* 2021;10(4):46–53 (in Russ.).
23. Pankratov D.A., Anuchina M.M., Konstantinov A.I., Perminova I.V. Analyzing the dynamics of interaction between humic coal substances and metallic iron. *Russian Journal of Physical Chemistry.* 2019;93(7):992–1001 (in Russ.).
24. Ostroushko A.A., Tonkushina M.O., Gagarin I.D., Grzhegorzhevsky K.V., Danilova I.G., Gette I.F. A method for correcting posthemorrhagic anemia. RF Patent. 2018: 2671077 C1 (in Russ.).
25. Shekunova E.V., Kovaleva M.A., Makarova M.N., Makarov V.G. Dose selection in preclinical studies: cross-species dose conversion. *The Bulletin of the Scientific Center for Expert Evaluation of Medicinal Products.* 2020;10(1):19–28 (in Russ.).

Authors contribution

Bratishko K.A., Ufandeew A.A., Buyko E.E., Rabcevich E.S., Kuznecova M.V. – carrying out of the experiment, analysis and interpretation of the data. Logvinova L.A. – analysis and interpretation of the data, drafting of the manuscript. Ivanov V.V. – formulation of the aim and objectives, carrying out of the experiment, analysis and interpretation of the data. Zhirkova A.M. – synthesis and modification of the studied compounds. Zima A.P., Belousov M.V. – formulation of the aim and objectives, analysis and interpretation of the data. Perminova I.V. – conception and design, synthesis and modification of the studied compounds. Zykova M.V. – conception and design, formulation of the aim and objectives, critical revision of the manuscript for important intellectual content, editing of the manuscript, presentation of the published work.

Authors information

Bratishko Kristina A. – Senior Lecturer, Chemistry Division, Siberian State Medical University, Tomsk, kr-1295@mail.ru, http://orcid.org/0000-0001-6571-4061https://orcid.org/0000-0001-6571-4061

Logvinova Lyudmila A. – Cand. Sci. (Chemistry), Senior Lecturer, Chemistry Division, Siberian State Medical University, Tomsk, ludmila_logvinova@mail.ru, http://orcid.org/0000-0002-0167-7043

Ivanov Vladimir V. – Cand. Sci. (Biology), Head of the Center for Preclinical Research, Siberian State Medical University, Tomsk, ivanovvv1953@gmail.com, http://orcid.org/0000-0001-9348-4945

Zhirkova Anastasia M. – Junior Researcher, Laboratory of Natural Humic Systems, Department of Medical Chemistry and Fine Organic Synthesis, Lomonosov Moscow State University, Moscow, nastya12349@mail.ru, http://orcid.org/0000-0001-6571-4061https://orcid.org/0000-0001-6571-4061

Ufandeew Alexander A. – Junior Researcher, Center for Preclinical Research, Siberian State Medical University, Tomsk, ufandeev@gmail.com, http://orcid.org/0000-0002-3837-1179

Buyko Evgeny E. – Laboratory Assistant, Center for Preclinical Research, Siberian State Medical University, Tomsk, buykoevgen@yandex.ru, http://orcid.org/0000-0002-6714-1938https://orcid.org/0000-0002-6714-1938

Zima Anastasia P. – Dr. Sci. (Med.), Professor, Pathological Physiology Division, Siberian State Medical University, Tomsk, zima2302@gmail.com, http://orcid.org/0000-0002-9034-7264https://orcid.org/0000-0002-9034-7264

Rabcevich Evgeniya S. – Cand. Sci. (Chemistry), Assistant, Chemistry Division, Siberian State Medical University; Research Engineer, Testing Laboratory "Analytical Center of Natural Systems Geochemistry", National Research Tomsk State University, Tomsk, evgenia882-a@mail.ru, http://orcid.org/0000-0002-9275-4453

Kuznecova Maria V. – 6th-year Student, Department of Biomedicine, Siberian State Medical University, Tomsk, mary35889@gmail.com, http://orcid.org/0000-0002-2446-9108

Belousov Mikhail V. – Dr. Sci. (Pharm.), Head of the Pharmaceutical Analysis Division, Siberian State Medical University, Tomsk, mvb63@mail.ru, http://orcid.org/0000-0002-2153-7945

Perminova Irina V. – Dr. Sci. (Chemistry), Professor, Head of the Laboratory of Natural Humic Systems, Department of Medical Chemistry and Fine Organic Synthesis, Lomonosov Moscow State University, Moscow, iperminova@gmail.com, http://orcid.org/0000-0001-9084-7851

Zykova Maria V. – Dr. Sci. (Pharm.), Associate Professor, Head of the Chemistry Division, Siberian State Medical University, Tomsk, gmv2@rambler.ru, http://orcid.org/0000-0002-1973-8983

(✉) **Logvinova Lyudmila A.,** ludmila_logvinova@mail.ru

Received 22.12.2021;
approved after peer review 08.02.2022;
accepted 09.06.2022

УДК 616.151.511: 615.273.5:616.153.962.4]-092.4
https://doi.org/10.20538/1682-0363-2022-4-20-28

Comparative study of predisposition to thrombosis with administration of known systemic hemostatic agents and fibrin monomer in the experiment

Vdovin V.M.[1], Shakhmatov I.I.[1], Momot A.P.[1, 2]

[1] *Altai State Medical University (ASMU)*
40, Lenina Av., Barnaul, 656038, Russian Federation

[2] *Altai Branch of the National Research Center for Hematology*
1/2, Lyapidevskogo Str., Barnaul, 656045, Russian Federation

ABSTRACT

Aim. To compare predisposition to thrombosis caused by administration of known systemic hemostatic agents and fibrin monomer under the conditions of normal coagulation versus drug-induced hypocoagulation in the experiment.

Materials and methods. The prothrombotic effect of intravenous (IV) administration of various systemic hemostatic agents was compared in a series of *in vivo* experiments. These agents included fibrin monomer (FM) (0.25 mg / kg), prothrombin complex concentrate (PCC) (40 IU / kg) or recombinant factor VIIa (rFVIIa) (270 mcg / kg). The studies were conducted under the conditions of hypocoagulation induced by the administration of warfarin (*per os* at a dose of 0.4–0.5 mg / kg / day for 14 days) or dabigatran etexilate (*per os* at a single dose of 15–20 mg / kg). Hemostatic system parameters were evaluated using thromboelastometry and calibrated automated thrombography.

Results. It was found that PCC reversed anticoagulant effects and led to an overcompensated increase in the density characteristics of the blood clot along with an excessive increase in thrombin generation in the groups of animals with warfarin-induced coagulopathy. The use of PCC and rFVIIa in the groups of animals with dabigatran-induced hypocoagulation also resulted in an increase in blood thrombogenic properties. In the administration of PCC, it was manifested though an increased D-dimer level and in administration of rFVIIa – through an increase in the clot density characteristics. At the same time, replacement of these hemostatic agents with FM did not affect the hemostatic system parameters.

Conclusion. FM at a dose of 0.25 mg / kg, as opposed to PCC and rFVIIa, is safer in terms of the risk of thrombosis.

Keywords: thrombosis, hypocoagulation, prothrombin complex concentrate, Eptacog alfa (activated), fibrin monomer, warfarin, dabigatran etexilate

Conflict of interest. The authors declare the absence of obvious and potential conflicts of interest related to the publication of this article.

Source of financing. The study was supported by the grant of the Russian Foundation for Basic Research (No. 18-415-220001), Technology Standard LLC, and ASMU.

Conformity with the principles of ethics. The study was approved by the local Ethics Committee at Altai State Medical University (Protocol No. 12 of 12.11.2015).

For citation: Vdovin V.M., Shakhmatov I.I., Momot A.P. Comparative study of predisposition to thrombosis with administration of known systemic hemostatic agents and fibrin monomer in the experiment. *Bulletin of Siberian Medicine.* 2022;21(4):20–28. https://doi.org/10.20538/1682-0363-2022-4-20-28.

✉ *Vdovin Vyacheslav M.,* erytrab@gmail.com

Сравнительный анализ предрасположенности к тромбообразованию при применении известных системных гемостатических средств и фибрин-мономера в эксперименте

Вдовин В.М.[1], Шахматов И.И.[1], Момот А.П.[1, 2]

[1] Алтайский государственный медицинский университет (АГМУ)
Россия, 656038, г. Барнаул, пр. Ленина, 40

[2] Национальный медицинский исследовательский центр (НМИЦ) гематологии (Алтайский филиал)
Россия, 656045, г. Барнаул, ул. Ляпидевского, 1/2

РЕЗЮМЕ

Цель. Провести сравнительную оценку предрасположенности к тромбообразованию, обусловленную применением известных системных гемостатических средств и фибрин-мономера в условиях нормокоагуляции и на фоне фармакологически индуцированной гипокоагуляции в эксперименте.

Материалы и методы. В сериях экспериментов *in vivo* сопоставляли протромботический эффект внутривенного введения различных системных гемостатических препаратов. В их числе использовались фибрин-мономер (ФМ) (0,25 мг/кг), концентрат факторов протромбинового комплекса (КФПК) (40 МЕ/кг) или рекомбинантный фактор VIIa (rFVIIa) (270 мкг/кг). Исследования проводились на фоне гипокоагуляции, обусловленной приемом варфарина (*per os* в дозе 0,4–0,5 мг/кг/сут на протяжении 14 сут) или дабигатрана этексилата (*per os* в разовой дозе 15–20 мг/кг). Оценивали показатели системы гемостаза, включая проведение тромбоэластометрии и калиброванной тромбографии.

Результаты. Установлено, что в группах животных с индуцированной варфарином коагулопатией КФПК реверсировал эффекты антикоагулянта, но приводил к сверхкомпенсированному усилению плотностных характеристик сгустка крови наряду с избыточным усилением генерации тромбина. Использование КФПК и rFVIIa в группах животных с гипокоагуляцией, вызванной приемом дабигатрана, также приводило к нарастанию тромбогенных свойств крови. Это иллюстрировалось в случаях использования КФПК увеличением уровня D-димера, а применения rFVIIa – усилением плотностных характеристик сгустка. В то же время замена данных гемостатиков на ФМ не отражалась на показателях системы гемостаза.

Заключение. ФМ в дозе 0,25 мг/кг в сравнении с КФПК и rFVIIa более безопасен с позиции риска возникновения внутрисосудистого тромбообразования.

Ключевые слова: тромбообразование, гипокоагуляция, концентрат факторов протромбинового комплекса, эптаког альфа (активированный), фибрин-мономер, варфарин, дабигатрана этексилат

Конфликт интересов. Авторы декларируют отсутствие явных и потенциальных конфликтов интересов, связанных с публикацией настоящей статьи.

Источник финансирования. Исследование выполнено за счет средств гранта РФФИ (№ 18-415-220001), при финансовой поддержке ООО «Технология-Стандарт» и Алтайского государственного медицинского университета.

Соответствие принципам этики. Исследование одобрено локальным этическим комитетом Алтайского государственного медицинского университета (протокол № 12 от 12.11.2015).

Для цитирования: Вдовин В.М., Шахматов И.И., Момот А.П. Сравнительный анализ предрасположенности к тромбообразованию при применении известных системных гемостатических средств и фибрин-мономера в эксперименте. *Бюллетень сибирской медицины.* 2022;21(4):20–28. https://doi.org/10.20538/1682-0363-2022-4-20-28.

INTRODUCTION

Currently, a whole range of systemic hemostatic agents with a known mechanism of action is available in clinical practice [1]. These include antiplatelet agents, fibrinogen, as well as cryoprecipitate enriched with fibrinogen, prothrombin complex concentrate (PCC), factors VIII and IX, eptacog alfa (activated) also known as recombinant factor VIIa (rFVIIa), anti-inhibitor coagulant complex (FEIBA), tranexamic acid, etc. The mentioned hemostatic agents are in demand in practical medicine for prevention of bleeding disorder or management of bleeding in injuries and major surgeries, including thromboprophylaxis. It is noted that their use in general leads to a shift in the hemostatic balance toward increased blood coagulation, which provides a hemostatic effect [2].

Safety of drugs and their effectiveness are priority conditions for the selection of certain drugs that affect the hemostatic system. It is known that the use of some systemic hemostatic agents at recommended doses is associated with the risk of developing venous or arterial thrombosis, as they may lead to an excessive hemostatic potential.

Previously, we conducted original studies that showed the presence of independent hemostatic activity of exogenous fibrin monomer (FM) in the experimental model of liver injury [3]. Similar results were obtained using the same model with drug-induced hypocoagulation [4, 5]. According to the results of the above studies, FM was as efficient as both rFVIIa and PCC. These publications emphasized the comparison of the listed drugs with FM in terms of their effectiveness, while safety issues (in terms of the risk of thrombosis) were not analyzed and discussed. Obviously, this serious aspect should be considered in an additional analysis, which involves assessing the odds for the so-called thrombotic preparedness, characterized by corresponding changes in the hemostatic system [6].

In this regard, the aim of this study was to conduct a comparative assessment of predisposition to thrombosis due to the use of known systemic hemostatic agents and FM under the conditions of normal coagulation and drug-induced hypocoagulation in the experiment.

MATERIALS AND METHODS

The data were collected from 94 healthy male Chinchilla rabbits weighing 3.0-4.5 kg, kept in standard vivarium conditions. The animals were divided into 7 groups by block randomization. Animal experiments were carried out in accordance with the European Convention and Directives for the Protection of Vertebrate Animals Used in the Experiment 86/609/EEC, as well as the Declaration of Helsinki and the "Rules for Conducting Work with the Use of Experimental Animals". The study was approved by the local Ethics Committee at Altai State Medical University (Protocol No. 12 of 12.11.2015).

At the beginning of the experiment, animals in groups 1 (n = 13), 2 (n = 14), and 3 (n = 16) received warfarin dissolved in water (Nycomed, Denmark) *per os* at a dose of 0.4–0.5 mg / kg / day for 14 days until international normalized ratio (INR) values of 2.0 and above were reached. After this period, blood was collected from the marginal ear vein of the animals (by the free flow technique) to study the hemostatic system. Then, these animals received a placebo administered intravenously at a dose of 0.5 ml (3.75 M urea solution corresponding to its concentration in the FM solution), PCC (Prothromplex 600, Baxter, Italy) at a dose of 40 IU / kg, or FM at a dose of 0.25 mg / kg, respectively. The FM-based agent was obtained using the original technology [7]. One hour after the intravenous administration of a placebo or a systemic hemostatic agent, blood was sampled again.

At the beginning of the experiment, the animals in groups 4 (n = 10), 5 (n = 14), 6 (n = 14), and 7 (n = 13) received dabigatran etexilate dissolved in water (Pradaxa®, Boehringer Ingelheim, Germany) *per os* at a dose of 15–20 mg / kg. To achieve a sufficient anticoagulant effect, the dose of the drug for the animals was determined taking into account the correction factor for dose conversion between animals and humans [8] and the recommendations specified in the medication guide (Pradaxa®, registration certificate No. LSR-007065/09). After two hours, blood was taken from these animals to study hemostasis, and then a placebo was injected intravenously at a dose of 0.5 ml, PCC (Protromplex 600, Baxter, Italy) was administered at a dose of 40 IU / kg, rFVIIa (NovoSeven, Novo Nordisk A/C, Denmark) was administered at a dose of 270 mcg / kg or FM was administered at a dose of 0.25 mg / kg, respectively. The doses for PCC and rFVIIa were determined according to the current guidelines [9–11]. One hour after the intravenous administration

of a placebo or a hemostatic agent, blood was taken again.

Blood from all animals in the study was placed in plastic tubes with EDTA potassium salt to determine platelet count and with 0.11 M (3.8%) sodium citrate solution (the ratio of blood and stabilizer was 9:1) to identify other parameters. Platelet-poor plasma in all samples was obtained according to the generally accepted method. In venous blood samples, the platelet count was assessed on the automatic hematology analyzer Drew-3 (Drew Scientific Inc., UK – USA). In the blood plasma, the international normalized ratio (INR), the echitoxic time (ET) of coagulation, and fibrinogen concentration according to the Clauss assay were determined on the Thrombostat 2 coagulometer (Behnk Electronik, Germany) using reagents from Technology-Standard Ltd. (Russia). D-dimer level was determined using the NycoCard Reader II (Axis-Shield PoC AS, Norway) and NycoCard® D-Dimer test systems (Axis-Shield PoC AS, Norway).

Thromboelastometry of the blood stabilized with citrate was performed on the ROTEM® Gamma thromboelastometer (Pentapharm GmbH, Germany) with the star-TEM reagent in the NATEM assay. The following parameters were determined: CT – coagulation time; CFT – clot formation time; α angle – clot amplitude; MCF – the maximum clot firmness; A10 – clot amplitude after 10 minutes. To assess thrombin generation, the calibrated automated thrombography according to N.S. Hemker (2003) was used on the Fluoroskan Ascent FL microplate fluorometer (ThermoFisher SCIENTIFIC, Finland) with Thrombinoscope™ 3.0.0.26 software and reagent kits from Thrombinoscope® (Netherlands) (PPP-Reagent, Thrombin Calibrator, FluCa-Kit) with tissue factor at a concentration of 5.0 pM. The following parameters were taken into account: lag time – initiation of thrombin generation; ETP – endogenous thrombin potential; peak thrombin – peak thrombin concentration; ttPeak – time to reach peak thrombin concentration; V – the rate of thrombin generation [12].

The distribution of characteristics in the samples was evaluated using the Shapiro – Wilk test. Depending on the distribution of the characteristics, Student's *t*-test, Mann – Whitney *U*-test, or Wilcoxon *W*-test were used. The differences were considered statistically significant at $p \leq 0.05$. The results were processed using the MedCalc software version 17.9.7 (license BU556-P12YT-BBS55-YAH5M-UBE51). The data were presented as the median and the interquartile range (Me [Q_{25}÷Q_{75}]).

RESULTS

When systemic hemostatic drugs including PCC (group 2) and FM (group 3) were used in the groups of animals with warfarin-induced coagulopathy (verified in group 1 – placebo), the achieved effects in the hemostatic system differed (Table 1). In particular, the administration of PCC led to the normalization of INR and a statistically significant decrease in the platelet count in the peripheral blood. It was accompanied by an overcompensated increase in the density characteristics of the blood clot (according to the thromboelastometry data, for MCF (+21%, $p < 0.005$) and A10 (+49%, $p < 0.006$)) in comparison with placebo [13] and excessive thrombin generation (according to the calibrated automated thrombography data, for ETP, peak thrombin and thrombin generation V) (Table 1). It should be noted that in the group of warfarinized animals who received FM (group 3), despite a sharp decrease in blood loss (by 9.1 times compared with placebo – in group 1) [5], high INR and a hypocoagulation shift according to calibrated automated thrombography were not corrected toward normal physiological values.

In the following groups of animals, in which dabigatran was used for direct thrombin inhibition, the hemostatic system parameters also differed after the administration of PCC, rFVIIa, and FM: in groups 5, 6, and 7, respectively (Table 2). The administration of PCC or rFVIIa to animals receiving dabigatran etexilate led to an increase in D-dimer by 2.8 and 8.0 times, respectively, which was not specific for the experimental group that received FM. In addition, the use of PCC in groups 5 and 2 was accompanied by a statistically significant decrease in the platelet count in peripheral blood (by 17.0 and 6.1%, respectively), which was not characteristic of the FM effects. According to the data obtained in group 6, where rFVIIa was used as a systemic hemostatic agent, a shift to hypercoagulability was seen in such thromboelastometry parameters as CT, MCF, CFT and A10, which was not noted in animals receiving FM (group 7). According to several parameters, the density characteristics of the clot (α angle (+28.2%, $p < 0.001$), CFT (–44.7%, $p < 0.001$) and A10 (+30.2%, $p < 0.019$)) exceeded those in the placebo

group [13]. As it was shown earlier, the use of FM reduced blood loss by 2.9 times compared with group 4, while the administration of PCC and rFVIIa did not affect blood loss [14].

DISCUSSION

Researchers around the world published findings indicating the risk of thrombotic complications in patients receiving rFVIIa or PCC for prevention or relief of overt bleeding. A number of foreign researchers expressed their concern regarding this issue. So, in the study by A. Girolami et al., cases of arterial and venous thrombosis with unspecified localization were observed in patients with several bleeding disorders (deficiency of FVII and FXI, dysfibrinogenemia, von Willebrand disease, Glanzmann thrombasthenia) when they received rFVIIa [15]. Cases of thrombosis after the use of rFVIIa in cardiac surgical patients were also described in the literature [16, 17]. The review by M. Levi et al. is of particular interest, as it presented the results of safety analysis of rFVIIa in 35 randomized trials involving 4,468 patients. It was shown that thromboembolic events were documented in 9.0% of patients included in the study; these events took place mainly in the arterial bed [18].

Many authors also associated the use of PCC with various types of intravascular coagulation. S.G. Yates and R. Sarode noted that the risk of thromboembolic complications (TEC) after the PCC administration in the treatment of bleeding associated with coumarin intake remained an important clinical problem [19]. A number of authors described various thrombotic events associated with PCC, namely, superficial thrombophlebitis, deep vein thrombosis, pulmonary embolism, arterial and cavitary thrombosis, and disseminated intravascular coagulation (DIC) [20–24]. At the same time, the risk of thrombosis increases in patients with cardiovascular diseases and the elderly, as well as in the combined use of rFVIIa and PCC [25].

Previously published studies showed that the administration of exogenous FM was accompanied by an increase in D-dimer, a marker of coagulation and fibrinolysis, by 7.0 and 8.0 times in groups of animals receiving this agent at doses of 2.5 and 5.0 mg / kg [3]. This was accompanied by an increase in the density characteristics of the blood clot (based on thromboelastometry findings) [13] and consumption of platelets with a 1.5-fold decrease in their number in the peripheral blood (with FM at a dose of 5.0 mg / kg) [3]. At the same time, the use of FM at a dose of 0.25 mg / kg did not lead to changes characteristic of a shift to hypercoagulability [3, 13]. It should be noted that, according to the calibrated automated thrombography data, the intensity of thrombin generation did not increase, regardless of the used FM dose [13].

In these studies, both rFVIIa and PCC recipients showed a trend toward intravascular thrombosis. When using rFVIIa, thromboelastometry detected an increase in the density of the blood clot (for α angle, CT, CFT, MCF, and A10) and an 8-fold increase in D-dimer compared with the baseline value before the administration of this agent ($p < 0.005$). The use of PCC was also accompanied by a rise in D-dimer by 2.8 times compared with the baseline value ($p < 0.003$), an overcompensated increase in the density of the blood clot (based on MCF and A10 parameters of thromboelastometry), as well as excessive thrombin generation (in terms of ETP, peak thrombin, and V). At the same time, the replacement of the above systemic hemostatic agents with FM did not lead to intravascular coagulation, according to the methods used to assess the hemostastic system.

Table 1

The results of the hemostatic system evaluation in the experimental animals with administration of warfarin, *Me* (Q_{25}÷Q_{75})

Parameters	Group 1 (placebo)		Group 2 (PCC)		Group 3 (FM 0.25 mg / kg)	
	before placebo administration (1a)	after placebo administration (1b)	before FM administration (2a)	after PCC administration (2b)	before FM administration (3a)	after PCC administration (3b)
Platelet count, $\times 10^9$ / l	555.0 [471.0÷591.0]	512.0 [474÷700.0] $p_{1a–1b} = 0.382$	425.0 [392.8÷531.3]	399.0 [334.0÷454.5] $p_{2a–2b} = 0.049$ Δ –6.1%	509.0 [417.8÷578.0]	479.5 [408.3÷551.5] $p_{3a–3b} = 0.328$
INR, ratio	2.4 [2.0÷4.0]	2.5 [2.2÷4.6] $p_{1a–1b} = 0.650$	2.1 [1.7÷6.2]	1.1 [1.0÷1.2] $p_{2a–2b} = 0.002$ Δ –47.6%	2.0 [1.6÷3.6]	2.0 [1.5÷2.9] $p_{3a–3b} = 0.063$

Table 1 (continued)

Parameters	Group 1 (placebo)		Group 2 (PCC)		Group 3 (FM 0.25 mg / kg)	
	before placebo administration (1a)	after placebo administration (1b)	before FM administration (2a)	after PCC administration (2b)	before FM administration (3a)	after PCC administration (3b)
Fibrinogen, g / l	2.8 [2.6÷4.3]	3.0 [2.6÷4.4] $p_{1a–1b}$ = 0.814	3.3 [2.8÷4.1]	2.9 [2.5÷3.6] $p_{2a–2b}$ = 0.260	3.1 [2.7÷3.5]	3.0 [2.5÷3.3] $p_{3a–3b}$ = 0.065
D-dimer, ng / ml	150.0 [100.0÷200.0]	150.0 [100.0÷200.0] $p_{1a–1b}$ = 0.351	100.0 [100.0÷100.0]	100.0 [100.0÷200.0] $p_{2a–2b}$ = 0.180	200.0 [100.0÷250.0]	200.0 [150.0÷400.0] $p_{3a–3b}$ = 0.075
Thromboelastometry						
CT, sec	2,122.5 [1,328.3÷2,464.8]	2,095.0 [1,052.0÷2,398.0] $p_{1a–1b}$ = 0.530	1,573.5 [948.3÷2,394.0]	494.0 [355.0÷626.0] $p_{2a–2b}$=0.002 Δ –3.2 times	1,459.0 [783.5÷2,198.8]	1,559.5 [734.0÷1,918.8] $_{3a–3b}$ = 0.221
α angle, degrees	n.r. in 9 cases	n.r. in 7 cases	48.0 [39.5÷52.0] n.r. in 8 cases	68.0 [59.0÷71.0]	39.5 [30.3÷60.8] n.r. in 6 cases	37.0 [32.8÷55.3] n.r. in 4 cases $p_{3a–3b}$ = 0.767
CFT, sec	n.r. in 10 cases	n.r. in 8 cases	356.0 [307.5÷794.5] n.r. in 8 cases	166.0 [110.0÷181.0]	452.5 [218.5÷522.5] n.r. in 8 cases	367.0 [187.0÷404.8] n.r. in 6 cases p_{3a-3b}=0.735
MCF, mm	n.r. in 8 cases	n.r. in 7 cases	22.5 [9.0÷49.5] n.r. in 4 cases	70.0 [67.0÷76.0] $p_{2a–2b}$=0.008 Δ –3.1 times	32.5 [15.8÷50.5] n.r. in 6 cases	44.0 [32.0÷49.5] n.r. in 4 cases $p_{3a–3b}$ = 0.139
A10, mm	n.r. in 9 cases	n.r. in 8 cases	8.5 [4.0÷34.5] n.r. in 4 cases	64.0 [55.0÷68.0] $p_{2a–2b}$=0.007 Δ –7.5 times	24.5 [18.8÷38.0] n.r. in 6 cases	32.0 [27.0÷41.0] n.r. in 5 cases $p_{3a–3b}$ = 0.260
Calibrated automated thrombography						
Lagtime, min	3.5 [2.7÷4.5] n.r. in 2 cases	4.4 [3.4÷5.6] n.r. in 3 cases $p_{1a–1b}$ = 0.592	5.0 [4.3÷5.3] n.r. in 6 cases	1.7 [1.5÷2.0] $p_{2a–2b}$ Δ –2.9 times	4.5 [4.5÷5.3]	6.0 [5.9÷6.3] n.r. in 2 cases $p_{3a–3b}$ = 0.593
ETP, nmol × min	150.2 [92.3÷183.9] n.r. in 2 cases	103.0 [60.9÷158.8] n.r. in 3 cases $p_{1a–1b}$ = 0.109	97.8 [68.2÷104.9] n.r. in 6 cases	582.0 [444.9÷806.4] $p_{2a–2b}$ Δ +6.0 times	131.7 [81.3÷145.2]	149.3 [111.3÷189.6] n.r. in 2 cases $p_{3a–3b}$ = 0.514
Peak thrombin, nmol	28.2 [18.9÷56.2] n.r. in 2 cases	12.5 [7.5÷21.8] n.r. in 3 cases $p_{1a–1b}$ = 0.041 Δ –2.3 times	10.9 [7.3÷14.8] n.r. in 6 cases	65.4 [41.3÷74.5] $p_{2a–2b}$ Δ +6.0 times	10.5 [10.3÷13.6]	13.3 [10.9÷21.9] n.r. in 2 cases $p_{3a–3b}$ = 0.285
ttPeak, min	6.5 [4.7÷7.2] n.r. in 2 cases	9.2 [8.3÷10.5] n.r. in 3 cases $p_{1a–1b}$ = 0.108	9.5 [7.9÷9.9] n.r. in 6 cases	9.5 [8.8÷9.6]	10.5 [10.2÷11.0]	10.8 [10.3÷11.1] n.r. in 2 cases $p_{3a–3b}$ = 0.922
V, nmol / min	9.4 [7.1÷25.9] n.r. in 2 cases	3.4 [2.0÷6.5] n.r. in 3 cases $p_{1a–1b}$ = 0.085	2.4 [1.6÷4.7] n.r. in 6 cases	7.8 [6.4÷11.8] $p_{2a–2b}$ Δ +3.3 times	2.3 [1.6÷3.0]	2.8 [2.3÷5.2] n.r. in 2 cases $p_{3a–3b}$ = 0.592

Note: in tables 1 and 2: PCC – prothrombin complex concentrate, FM – fibrin monomer, p – statistical significance of the differences in the compared parameters, Δ is the difference between the values, n.r. – not registered.

Table 2

The results of the hemostatic system evaluation in the experimental animals with direct thrombin inhibition, *Me* (Q_{25}÷Q_{75})

Parameters	Group 4 (Placebo)		Group 5 (PCC)		Group 6 (rFVII)		Group 7 (FM 0.25 mg / kg)	
	before placebo administration (4a)	after placebo administration (4b)	before FM administration (5a)	after PCC administration (5b)	before FM administration rFVII (6a)	after PCC administration rFVII (6b)	before FM administration (7a)	after PCC administration (7b)
Platelet count, ×10 ^{9} / l	541.5 [481.3÷553.0]	501.0 [421.5÷517.5] $p_{4a–4b}$ = 0.116	521.0 [458.0÷601.8]	432.5 [379.8÷501.5] $p_{5a–5b}$ = 0.050 Δ –17.0%	638.5 [535.3÷709.5]	638.0 [523.8÷717.5] $p_{6a–6b}$ = 0.972	559.0 [528.3÷566.5]	550.5 [499.8÷565.3] $p_{7a–7b}$ = 0.600
Echitoxic time, ratio	3.4 [3.1÷3.8]	3.5 [3.1÷4.1] $p_{4a–4b}$ = 0.333	2.1 [1.8÷2.5]	2.5 [2.0÷3.3] $p_{5a–5b}$ = 0.016 Δ +19.1%	2.5 [2.1÷3.7]	3.0 [2.2÷3.6] $p_{6a–6b}$ = 0.156	2.6 [2.2÷2.9]	2.5 [2.2÷2.7] $p_{7a–7b}$ = 0.600
Fibrinogen, g / l	2.9 [2.3÷4.2]	2.9 [2.4÷3.1] $p_{4a–4b}$ = 0.139	4.1 [3.4÷5.0]	3.6 [3.0÷4.7] $p_{5a–5b}$ = 0.033 Δ –12.2%	2.9 [2.4÷3.2]	2.8 [2.4÷3.4] $p_{6a–6b}$ = 0.969	3.2 [2.9÷3.5]	3.1 [2.9÷3.5] $p_{7a–7b}$ = 0.433
D-dimer, ng / ml	100.0 [100.0÷200.0]	100.0 [100.0÷200.0] $p_{4a–4b}$ = 0.480	200.0 [200.0÷300.0]	550.0 [400.0÷800.0] $p_{5a–5b}$ = 0.003 Δ 2.8 times	100.0 [100.0÷150.0]	800.0 [300.0÷1,100.0] $p_{6a–6b}$ = 0.005 Δ 8.0 times	100.0 [100.0÷200.0]	200.0 [100.0÷300.0] $p_{7a–7b}$ = 0.075
Thromboelastometry								
CT, sec	925.0 [619.0÷995.0]	713.0 [673.0÷853.0] $p_{4a–4b}$ = 0.515	1023.0 [776.0÷1404.8]	964.5 [768.5÷1087.8] $p_{5a–5b}$ = 0.037 Δ –5.7 %	675.5 [573.5÷996.8]	484.0 [274.0÷948.3] $p_{6a–6b}$ = 0.048 Δ –28.3%	660.0 [477.5÷907.0]	480.0 [348.3÷637.0] $p_{7a–7b}$ = 0.139
α angle, degree	59.0 [48.0÷66.0]	62.0 [60.0÷66.0] $p_{4a–4b}$ = 0.953	61.5 [54.3÷67.3] n.r. in 3 cases	57.0 [50.5÷62.0] n.r. in 2 cases $p_{5a–5b}$ =0.327	61.5 [56.3÷68.8]	70.5 [63.3÷75.0] $p_{6a–6b}$ = 0.059	64.5 [59.3÷75.3]	65.5 [59.8÷76.3] $p_{7a–7b}$ = 0.767
CFT, sec	169.0 [140.0–210.0]	151.0 [134.0–167.0] $p_{8a–8b}$ = 0.767	175.0 [143.0÷231.5] n.r. in 3 cases	231.5 [182.3÷425.8] n.r. in 1 case $p_{5a–5b}$ = 0.137	166.5 [112.0–196.0]	114.0 [84.0–147.8] $p_{6a–6b}$ = 0.035 Δ –31.5%	132.0 [82.5÷165.5]	150.0 [123.0÷165.0] $p_{7a–7b}$ = 0.859
MCF, mm	56.0 [54.0÷66.0]	62.0 [48.0÷66.0] p_{4a-4b} = 0.953	65.5 [58.3÷74.0] n.r. in 3 cases	69.5 [62.0÷70.8] n.r. in 3 cases $p_{5a–5b}$ = 0.889	59.5 [45.0÷64.8]	65.5 [56.0÷73.0] $p_{6a–6b}$ = 0.021 Δ +10.1%	63.0 [55.8÷67.8]	62.5 [58.0÷68.8] $p_{7a–7b}$ = 0.779
A10, mm	48.0 [47.0÷59.0]	52.0 [45.0÷60.0] $p_{4a–4b}$ = 0.374	57.5 [47.3÷65.8] n.r. in 2 cases	54.0 [48.0÷59.0] n.r. in 2 cases $p_{5a–5b}$ = 0.441	48.0 [39.8÷55.0]	56.0 [49.5÷65.8] $p_{6a–6b}$ = 0.034 Δ +16.6%	55.0 [48.0÷65.8]	54.0 [49.0÷67.0] $p_{7a–7b}$ = 0.889

Note: rFVII – recombinant factor VIIa.

CONCLUSION

The presented data revealed prothrombotic effects of the above hemostatic agents, namely, PCC and rFVIIa. The latter were tested in two experimental models with drug-induced hypocoagulation associated with warfarin or dabigatran. The effects were manifested through overcompensated changes in hemostatic system parameters (compared with intact animals), including an increase in D-dimer and a shift toward hypercoagulability according to thromboelastometry.

It should be noted that FM at a dose of 0.25 mg / kg resulted in significant reduction of blood loss without the above-described thrombogenic effects in the blood, which distinguished it from the known hemostatic agents. Therefore, we suppose that FM is safer in terms of adverse events, such as spontaneous thrombosis in the bloodstream.

REFERENCES

1. Melnik A.A. The mechanism of action of hemostatic drugs. *News of Medicine and Pharmacy*. 2017;10(622) (in Russ.).
2. Rossaint R., Bouillon B., Cerny V., Coats T.J., Duranteau J., Fernández-Mondéjar E. et al. The European guideline on management of major bleeding and coagulopathy following trauma: fourth edition. *Crit. Care*. 2016;20:100. DOI: 10.1186/s13054-016-1265-x.
3. Momot A.P., Vdovin V.M., Shakhmatov I.I., Tolstokorov I.G., Orekhov D.A., Shevchenko V.O., et al. Systemic hemostatic and prothrombotic effects of fibrin-monomer in experiment with dosed liver therapy. *Siberian Scientific Medical Journal*. 2019;39(1):6–12 (in Russ.). DOI: 10.15372/SSMJ20190101.
4. Vdovin V.M., Momot A.P., Krasyukova V.O., Tolstokorov I.G., Orekhov D.A., Shevchenko V.O., et al. Systemic hemostatic and hemostasiological effects of fibrin monomer in direct thrombin inhibition in experiment. *Russian Journal of Physiology*. 2019;105(2):207–215 (in Russ.). DOI: 10.1134/S0869813919020109.
5. Vdovin V.M., Momot A.P., Orekhov D.A., Tolstokorov I.G., Shevchenko V.O., Shakhmatov I.I., et al. Systemic hemostatic and hemostasiological effects of fibrin monomer in low dose under warfarin action in experiment. *Thrombosis, Hemostasis and Rheology*. 2019;79(3):16–23 (in Russ.). DOI: 10.25555/THR.2019.3.0885.
6. Momot A.P., Tsyvkina L.P., Taranenko I.A., Mamaev A.N., Serdyuk G.V., Shakhmatov I.I., et al. Modern methods of recognizing the state of thrombotic readiness. Barnaul: Altai State University, 2011:138 (in Russ.).
7. Momot A.P., Shakhmatov I.I., Lomaev I.S., Terekhov S.S. Method of industrial production of fibrin monomer from blood plasma. RF Patent No. 2522237. 10.07.2014. Bul. No. 19 (in Russ.).
8. Guskova T.A. Preclinical toxicological study of drug as a guarantee of their safe clinical investigation. *Toxicological Review*. 2010;104(5):2–5 (in Russ.).
9. Ryn J., Stangier J., Haertter S., Liesenfeld K.-H., Wienen W., Feuring M. et al. Dabigatran etexilate – a novel, reversible, oral direct thrombin inhibitor: interpretation of coagulation assays and reversal of anticoagulant activity. *Thromb. Haemost*. 2010;103(6):1116–1127. DOI: 10.1160/TH09-11-0758.
10. Bavalia R., Abdoellakhan R., Brinkman H.J.M., Brekelmans M.P.A., Hamulyák E.N., Zuurveld M. et al. Emergencies on direct oral anticoagulants: Management, outcomes, and laboratory effects of prothrombin complex concentrate. *Res. Pract. Thromb. Haemost*. 2020;4(4):569–581. DOI: 10.1002/rth2.12336.
11. Zozulya N.I., Kumskova M.A., Polyanskaya T.Yu., Svirin P.V. Clinical guidelines for the diagnosis and treatment of hemophilia. RHS, 2018:34 (in Russ.).
12. Papayan L.P., Golovina O.G., Chechetkin A.V., Bessmeltsev S.S., Kapustin S.I., Kargin V.D., et al. Algorithm of hemostasis diagnostics and monitoring of antithrombotic therapy. Guidelines. St. Petersburg: Russian Research Institute of Hematology and Transfusion Medicine, 2016:18 (in Russ.).
13. Vdovin V.M., Momot A.P., Orekhov D.A., Bobrov I.P., Momot D.A., Shakhmatov I.I., et al. Influence of exogenous fibrin monomer on hemostatic potential and formation of fibrin in the area of dosed liver injury in experiment. *Russian Journal of Physiology*. 2020;106(9):1132–1143 (in Russ.). DOI: 10.31857/S0869813920070092.
14. Vdovin V.M., Momot A.P., Krasyukova V.O., Tolstokorov I.G., Orekhov D.A., Shevchenko V.O., et al. Systemic hemostatic and hemostasiological effects of fibrin monomer in direct thrombin inhibition in experiment. *Russian Journal of Physiology*. 2019;105(2):207–215 (in Russ.). DOI: 10.1134/S0869813919020109.
15. Girolami A., Marinis G.B., Bonamigo E., Lombardi A.M. Recombinant FVIIa concentrate-associated thrombotic events in congenital bleeding disorders other than hemophilias. *Hematology*. 2012;17(6):346–349. DOI: 10.1179/1607845412Y.0000000027.
16. Pichon N., Bellec F., Sekkal S., Marsaud J.P., Laskar M., François B. et al. Fatal thrombotic event after infusion of recombinant activated factor VII after cardiac surgery. *J. Thorac. Cardiovasc. Surg*. 2008;136(1):220–221. DOI: 10.1016/j.jtcvs.2007.10.084.
17. Hajj-Chahine J., Jayle C., Tomasi J., Houmaida H., Corbi P. Acute aortic valve thrombosis secondary to recombinant factor VIIa. *Ann. Thorac. Surg*. 2012;93:999. DOI: 10.1016/j.athoracsur.2011.08.050.
18. Levi M., Levy J.H., Andersen H.F., Truloff D. Safety of recombinant activated factor VII in randomized clinical trials. *N. Engl. J. Med*. 2010;363(19):1791–1800. DOI: 10.1056/NEJMoa1006221.
19. Yates S.G., Sarode R. New strategies for effective treatment of vitamin K antagonist-associated bleeding. *J. Thromb. Haemost*. 2015;13(Suppl.1):S180–S186. DOI: 10.1111/jth.12970.
20. Köhler M. Thrombogenicity of prothrombin complex concentrates. *Thromb. Res*. 1999;95(4Suppl.1):S13–S17. DOI: 10.1016/s0049-3848(99)00079-1.
21. Ehrlich H.J., Henzl M.J., Gomperts E.D. Safety of factor VIII inhibitor bypass activity (FEIBA): 10-year compilation of

thrombotic adverse events. *Haemophilia.* 2002;8(2):83–90. DOI: 10.1046/j.1365-2516.2002.00532.x.
22. Goldhammer J.E., Bakowitz M.J., Milas B.L., Patel P.A. Intracardiac thrombosis after emergent prothrombin complex concentrate administration for warfarin reversal. *Anesthesiology*. 2015;123(2):458. DOI: 10.1097/ALN.0000000000000464.
23. Brinkman H.J.M. Prothrombin complex concentrate, a general antidote for oral anticoagulation. In the book: Basaran O. Anticoagulation Therapy, 2016. Chapter 5:79–109. DOI: 10.5772/64304.
24. Gavva C., Reddy M., Sarode R. Four-factor prothrombin complex concentrates effectiveness in the reversal of anticoagulation. *International Journal of Clinical Transfusion Medicine*. 2017;2017(5):39–47. DOI: 10.2147/IJCTM.S114736.
25. Rajpurkar M., Croteau S.E., Boggio L., Cooper D.L. Thrombotic events with recombinant activated factor VII (rFVIIa) in approved indications are rare and associated with older age, cardiovascular disease, and concomitant use of activated prothrombin complex concentrates (aPCC). *J. Blood Med*. 2019;10:335–340. DOI: 10.2147/JBM.S219573.

Authors contribution

Vdovin V.M. – conception and design, experimental model formulation, analysis and interpretation of the data, critical revision of the manuscript for important intellectual content, final approval of the manuscript for publication. Momot A.P. – conception and design, analysis and interpretation of the data, critical revision of the manuscript for important intellectual content, final approval of the manuscript for publication. Shakhmatov I.I. – conception and design, analysis and interpretation of the data.

Authors information

Vdovin Vyacheslav M. – Cand. Sci. (Med.), Associate Professor, Head of the Department of Pathological Physiology, ASMU, Barnaul, erytrab@gmail.com, https://orcid.org/0000-0002-4606-3627

Shakhmatov Igor I. – Dr. Sci. (Med.), Associate Professor, Head of the Department of Normal Physiology, ASMU, Barnaul, iish59@yandex.ru, https://orcid.org/0000-0002-0979-8560

Momot Andrey P. – Dr. Sci. (Med.), Professor, Director, Altai Branch of the National Research Center for Hematology; Head of the Laboratory for Hemostasis, Institute of Clinical Medicine, ASMU, Barnaul; xyzan@yandex.ru, http://orcid.org/0000-0002-8413-5484

(✉) **Vdovin Vyacheslav M.,** erytrab@gmail.com

Received 18.02.2022;
approved after peer review 31.03.2022;
accepted 09.06.2022

УДК 616-008.9-021.6:616.233-008.8-076.5
https://doi.org/10.20538/1682-0363-2022-4-29-36

Features of the cytogram and cytokine profile of bronchoalveolar lavage fluid in experimental metabolic syndrome

Voronkova O.V., Birulina J.G., Ivanov V.V., Buyko E.E., Esimova I.E., Grigorieva A.V., Osikhov I.A., Chernyshov N.A., Motlokhova E.A.

Siberian State Medical University (SSMU)
2, Moscow Trakt, Tomsk, 634050, Russian Federation

ABSTRACT

The aim of the study was to identify the features of the cellular composition and cytokine profile of bronchoalveolar lavage fluid in rats in a model of diet-induced metabolic syndrome.

Materials and methods. In an experiment on animals (rats), a model of metabolic syndrome (MS) induced by a high-fat and high-carbohydrate diet was reproduced. To assess the viability of the reproduced model, biochemical and morphometric methods were used, such as measurement of body weight, specific gravity of liver and visceral fat, and blood pressure, determination of glucose concentration in the blood (including a glucose tolerance test), as well as determination of blood lipid parameters. To assess the intensity of the inflammatory response in the blood, the concentration of total protein, the total number of leukocytes, and the levels of immunocytokines (interleukin (IL)-6, IL-10, tumor necrosis factor (TNF)α, monocyte chemoattractant protein (MCP)-1) were determined. Open bronchoalveolar lavage was performed on the isolated heart – lung complex. The concentration of protein, immunocytokines (IL-6, IL-10, TNFα, MCP-1), the total number of leukocytes, and the ratio of their morphological types were determined in the bronchoalveolar lavage fluid (BALF).

Results. In animals with MS, an increase in the total number of leukocytes in the blood due to granulocytes and a rise in the concentration of protein, TNFα, and IL-10 were revealed compared with the parameters in the controls. BALF analysis revealed an increase in the concentration of protein, the total number of leukocytes, and the absolute number of alveolar macrophages, neutrophil granulocytes, and lymphocytes. The levels of IL-6 and MCP-1 were more than 1.5 times higher.

Conclusion. Changes in the qualitative and quantitative parameters of BALF are inflammatory in nature and are formed during a systemic inflammatory response accompanying metabolic disorders in modeling MS in rats in the experiment.

Keywords: metabolic syndrome, bronchoalveolar lavage fluid, inflammation

Conflict of interest. The authors declare the absence of obvious or potential conflict of interest related to the publication of this article.

Source of financing. The study was supported by the grant of the Russian Science Foundation No. 22-25-20039, https://rscf.ru/project/22-25-20039, and funded by the Administration of the Tomsk Region.

Conformity with the principles of ethics. The study was approved by the local Ethics Committee at Siberian State Medical University (Protocol No. 8201 of 27.03.2020).

For citation: Voronkova O.V., Birulina J.G., Ivanov V.V., Buyko E.E., Esimova I.E., Grigorieva A.V., Osikhov I.A., Chernyshov N.A., Motlokhova E.A. Features of the cytogram and cytokine profile of bronchoalveolar lavage fluid in experimental metabolic syndrome. *Bulletin of Siberian Medicine.* 2022;21(4):29–36. https://doi.org/10.20538/1682-0363-2022-4-29-36.

✉ *Voronkova Olga V.,* voronkova-ov@yandex.ru

Особенности цитограммы и цитокинового профиля жидкости бронхоальвеолярного лаважа при экспериментальном метаболическом синдроме

Воронкова О.В., Бирулина Ю.Г., Иванов В.В., Буйко Е.Е., Есимова И.Е., Григорьева А.В., Осихов И.А., Чернышов Н.А., Мотлохова Е.А.

Сибирский государственный медицинский (СибГМУ)
Россия, 634050, г. Томск, Московский тракт, 2

РЕЗЮМЕ

Цель. Выявить особенности клеточного состава и цитокинового профиля жидкости бронхоальвеолярного лаважа у крыс в модели диет-индуцированного метаболического синдрома.

Материалы и методы. В эксперименте на животных (крысах) воспроизведена модель метаболического синдрома (МС), индуцированного высокожировой и высокоуглеводной диетой. Для оценки состоятельности воспроизведенной модели использованы биохимические и морфометрические методы: измерение массы тела, удельной массы печени и висцерального жира, измерение артериального давления, определение содержания в крови глюкозы (в том числе в глюкозотолерантном тесте (ГТТ)), определение параметров липидного спектра крови. Для оценки интенсивности воспалительного ответа в крови определяли концентрацию общего белка, общее количество лейкоцитов и концентрацию иммуноцитокинов (интерлейкина (IL) -6, IL-10, фактора некроза опухоли альфа (TNFα), моноцитарного хемотоксического фактора-1 (MCP-1)). Открытым способом на изолированном комплексе «сердце–легкие» выполняли бронхоальвеолярный лаваж. В бронхоальвеоларной жидкости (БАЛЖ) определяли концентрацию белка, иммуноцитокинов (IL-6, IL-10, TNFα, MCP-1), общее количество лейкоцитов и соотношение их отдельных морфологических форм.

Результаты. У животных с МС выявлено повышение в крови общего количества лейкоцитов за счет гранулоцитарного компонента, увеличение концентрации белка и цитокинов TNFα и IL-10 по сравнению с соответствующими параметрами у крыс контрольной группы. В результате анализа БАЛЖ выявлено повышение концентрации белка, общего количества лейкоцитов, абсолютного числа альвеолярных макрофагов, нейтрофильных гранулоцитов и лимфоцитов; более чем в 1,5 раза превышена концентрация IL-6 и MCP-1.

Заключение. Изменения качественных и количественных параметров БАЛЖ носят воспалительный характер и формируются на фоне системного воспалительного ответа, сопровождающего нарушение обмена веществ при моделировании МС у крыс в эксперименте.

Ключевые слова: метаболический синдром, бронхоальвеолярная жидкость, воспаление

Конфликт интересов. Авторы гарантируют отсутствие потенциальных и явных конфликтов интересов, связанных с публикацией данной статьи.

Источник финансирования. Исследование выполнено за счет гранта Российского научного фонда № 22-25-20039, https://rscf.ru/project/22-25-20039, и средств Администрации Томской области.

Соответствие принципам этики. Исследование одобрено локальным этическим комитетом СибГМУ (протокол № 8201 от 27.03.2020).

Для цитирования: Воронкова О.В., Бирулина Ю.Г., Иванов В.В., Буйко Е.Е., Есимова И.Е., Григорьева А.В., Осихов И.А., Чернышов Н.А., Мотлохова Е.А. Особенности цитограммы и цитокинового профиля жидкости бронхоальвеолярного лаважа при экспериментальном метаболическом синдроме. *Бюллетень сибирской медицины.* 2022;21(4):29–36. https://doi.org/10.20538/1682-0363-2022-4-29-36.

INTRODUCTION

A cluster of metabolic conditions united under the term metabolic syndrome (MS) accelerate the development and progression of a number of diseases, including cardiovascular and cerebrovascular diseases, type 2 diabetes mellitus, kidney and biliary tract diseases, and some types of cancer [1–3]. In the clinical medicine with wide-spread comorbidity, one of the discussed issues is the effect of the MS components on the state of the respiratory system. In some clinical studies, MS has been identified as an independent risk factor for impaired lung function and aggravation of respiratory symptoms in multifactorial

diseases, such as bronchial asthma and chronic obstructive pulmonary disease.

It has been established that the most significant MS components contributing to respiratory pathology are abdominal obesity, hyperglycemia, and hyperinsulinemia [4–6]. Early mechanisms of the damaging effect of the MS components on the bronchopulmonary system remain the least studied. To some extent, this is due to the fact that most studies are clinical in nature. Since the cardiorespiratory system has broad adaptive capabilities, patients with pronounced manifestations of respiratory failure against the background of MS are in the focus of attention of doctors. In this regard, it is advisable to study the complex mechanisms of the effect of metabolic disorders on the morphological and functional state of the bronchopulmonary system in an experiment using animal models.

Collecting and studying bronchoalveolar lavage fluid (BALF) are reliable methods for studying the cytological, immunological, biochemical, and microbiological characteristics of the bronchoalveolar parts of the respiratory system. The study of BALF not only provides significant assistance in diagnosing and determining the activity of the pathological process, but also allows for a deeper understanding of the pathogenetic patterns of lung damage in the underlying or concomitant pathology [7, 8].

The aim of the study was to reveal the features of the cellular composition and cytokine profile of BALF in rats in a model of diet-induced MS.

MATERIALS AND METHODS

The experiment was performed on 33 outbred male Wistar rats (average weight 280.5 ± 36.1 g) aged 6 weeks at the beginning of the study, which were divided into control (15 animals) and experimental (18 animals) groups. The animals were kept in the conditions of a vivarium. The studies were carried out in compliance with the principles of humanity set out in the directives of the European Community (86/609/EEC) and the Declaration of Helsinki.

A model of diet-induced MS was reproduced in the animals of the experimental group. The rats were fed with a high-fat and high-carbohydrate diet containing standard feed (66%) with the addition of animal fat (17%), fructose (17%), and cholesterol (0.25%); drinking water was replaced with a 20% fructose solution (total calorie content of the daily diet was 440 kcal / 100 g). The rats of the control group received a standard diet (Delta Feeds, BioPro, Russian Federation, total calorie content 300 kcal / 100 g, proteins 24%, fats 6%, carbohydrates 44%) with free access to food and water.

To assess the viability of the reproduced MS model, body weight and blood pressure were measured in the animals at the beginning and at the end of the experiment (Systola, Neurobotics, Russian Federation). In the last week of the experiment, a glucose tolerance test (GTT) was performed: fasted rats (fasting for 12 hours) were intragastrically injected with a glucose solution at a dose of 2 g / kg (D-glucose, Sigma-Aldrich, USA). After 0, 15, 30, 60, 90, and 120 min, the blood glucose concentration was determined by the enzymatic colorimetric method using a reagent kit (Chronolab, Spain). 12 weeks after the start of the experiment, the animals were euthanized by CO2 asphyxia. Blood was taken from the heart of the animals to assess hematological parameters (vacutainer K2EDTA tubes) and obtain blood serum (vacutainer serum clot activator tubes). Hematological parameters were assessed on the automatic hematology analyzer (BC-2800 Vet, Mindray, China). Biochemical parameters were determined in the blood serum, including lipid indices (on the Architect c4000 Automatic Biochemistry Analyzer, Abbot, USA). The levels of immunocytokines (interleukin (IL)-6, IL-10, tumor necrosis factor (TNF)α, monocyte chemoattractant protein (MCP)-1) were measured by the enzyme-linked immunosorbent assay (ELISA) (Bender MedSystems kits, GmbH, Austria). The liver and visceral adipose tissues (mesenteric, epididymal, and retroperitoneal adipose tissue) were isolated by dissection and weighed on the analytical balance, and their specific gravity was calculated.

Open bronchoalveolar lavage was performed on the isolated heart – lung complex. Cold saline was used as a lung lavage fluid [9]. Both lungs were washed 2–3 times with a truncated syringe inserted via the trachea. The initial volume of the lavage fluid for a single injection was 3 ml, the return volume was at least 2 ml. In the BALF, the protein concentration was determined spectrophotometrically by the BCA assay (BCA Protein Assay Kit, Sigma-Aldrich), and cytokines IL-6, IL-10, TNFα, and MCP-1 were measured by ELISA (Bender MedSystems GmbH kits, Austria).

BALF cytology was performed to identify the total number of leukocytes and the ratio of their morphological types. For this purpose, BALF was centrifuged, and cell pellet sections were placed on a glass slide, fixed in formaldehyde vapor, and stained

using the Romanowsky – Giemsa stain. Cellular elements were counted per 200 cells using microscopy with immersion oil objective.

Statistical analysis was performed using the SPSS Statistics 23 software. Normally distributed data (Shapiro – Wilk test) were presented as the mean and the standard deviation ($M \pm SD$). Non-normally distributed data were presented as the median and the interquartile range Me (Q_{25};Q_{75}). Differences between the samples were analyzed using the Student's *t*-test or the Mann – Whitney *U* test. The differences were considered statistically significant at $p < 0.05$.

RESULTS

The impact of a high-fat and high-carbohydrate diet on the animals of the experimental group led to statistically significant changes in the physiological and biochemical parameters compared with the controls: an increase in the body weight, an increase in the specific gravity of the liver and visceral adipose tissue, a rise in the blood pressure, an increase in the concentration of total protein and glucose in the blood (Table 1). Changes in the blood lipid indices were characterized by an increase in the concentration of triacylglycerols, total cholesterol, low-density lipoprotein cholesterol (LDL-C), and very-low-density lipoprotein cholesterol (VLDL-C). The concentration of high-density lipoprotein cholesterol (HDL-C) was lower than that in the controls, which was manifested through the atherogenic coefficient, which was more than 1.5 times ($p = 0.02$) higher than in the control group (Table 1).

Table 1

The effect of a high-fat and high-carbohydrate diet on the physiological and biochemical parameters of rats, $M \pm SD$

Parameter	Control group ($n = 15$)	Model of MS ($n = 18$)
Body weight, g	433.3 ± 39.4	489.1 ± 47.9; $p = 0.01$
Systolic blood pressure, mm Hg	130.4 ± 9.5	145.1 ± 8.7; $p = 0.01$
Diastolic blood pressure, mm Hg	86.5 ± 9.3	101.4 ± 12.2; $p = 0.028$
Fasting blood glucose, mmol / l	4.7 ± 0.5	6.6 ± 0.4; $p < 0.001$
Total protein, g / l	52.7 ± 3.4	66.7 ± 3.8; $p = 0.004$
Total cholesterol, mmol / l	1.7 ± 0.2	2.3 ± 0.3; $p = 0.001$
HDL-C, mmol / l	0.6 ± 0.1	0.4 ± 0.1; $p = 0.003$
LDL-C, mmol / l	0.9 ± 0.2	1.4 ± 0.4; $p = 0.02$
VLDL-C, mmol / l	0.3 ± 0.1	0.5 ± 0.1; $p = 0.03$
Triacylglycerols, mmol / l	0.7 ± 0.2	1.7 ± 0.5; $p = 0.001$
Atherogenic coefficient	2.5 ± 0.3	3.8 ± 0.7; $p = 0.02$
Specific gravity of the adipose tissue, g	2.2 ± 0.2	4.3 ± 0.6; $p < 0.001$
Specific gravity of the liver, g	3.1 ± 0.4	4.2 ± 0.5; $p < 0.001$

Table 1 (continued)

Note: here and in Tables 2–4: *p* is the level of statistical significance of the differences compared with the parameters in the control group.

In the animals with MS, GTT revealed a decrease in glucose tolerance. An increase in the area under the "glucose concentration – time" curve by 1.3 times was recorded on the graph showing changes in the blood glucose levels compared with values in intact animals ($AUC_{0\text{-}120}$). In the control group, the area under the curve (AUC) was 752.2 ± 50.4 mmol / l × 120 min, in the experimental group – 940.9 ± 55.8 mmol / l × 120 min ($p = 0.001$) (Figure).

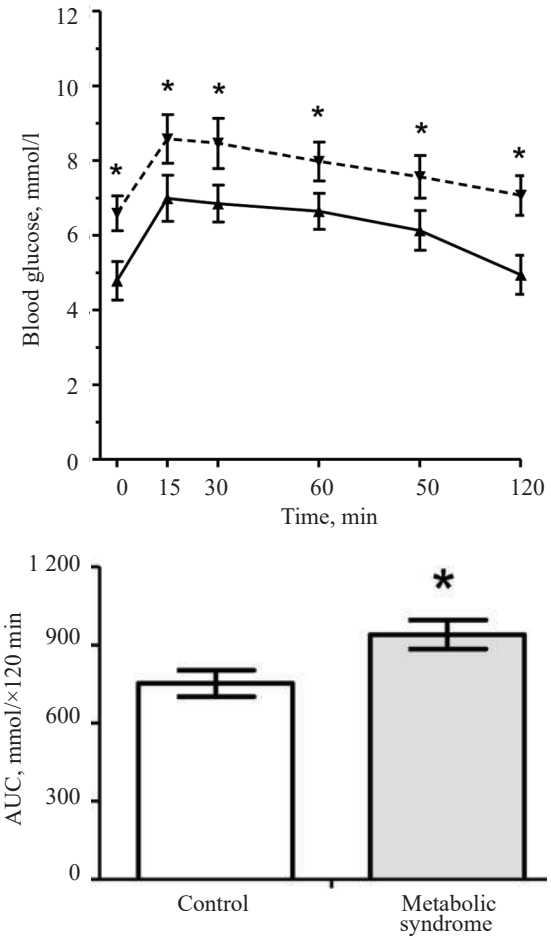

Figure. Changes in the concentration of glucose in the blood of rats (*a*) and the area under the "glucose concentration – time" curve ($AUC_{0\text{-}120}$) (*b*) in the glucose tolerance test: solid line – control group, dotted line – experimental group.

*$p < 0.05$ compared with the control group

The analysis of hematological parameters revealed an increase in the total number of leukocytes in the blood of the experimental group animals by 1.4 times compared with the values in the control group. The quantitative analysis of the leukocyte differential revealed a statistically significant increase in the absolute and relative number of granulocytes per unit volume of blood (Table 2).

According to the results of the biochemical analysis, the protein concentration in the BALF in the animals of the experimental group was 1.08 (±0.30) g / l, which, on average, was 1.5 times higher ($p = 0.037$) than the corresponding value in the intact animals (Table 3). The qualitative and quantitative analysis of the BALF cytogram revealed an increase in the total number of leukocytes per unit volume of fluid, compared with the control values, due to an increase in the absolute number of all types of leukocytes in the BALF – alveolar macrophages, neutrophil granulocytes, and lymphocytes (Table 3).

The study of the concentration of cytokines in the blood serum of the experimental animals revealed higher levels of IL-10 and TNFα compared with the control values. The concentration of IL-6 and MCP-1 in the BALF significantly exceeded the control values (Table 4).

Table 2

Total number of leukocytes and hemogram parameters in the experimental animals, *Me* (Q_{25}; Q_{75})

Parameter		Control group ($n = 15$)	Model of MS ($n = 18$)
Total number of leukocytes, $\times 10^9$ / l		9.9 (9.4; 10.9)	13.7 (11.4; 15.0); $p = 0.001$
The quantitative composition of cells (in the numerator – in %, in the denominator – in absolute numbers, $\times 10^9$/l)	Granulocytes	28.2 (25.9; 31.3) 2.5 (1.7; 3.6)	33.2 (31.5; 34.2); $p = 0.001$ 3.9 (3.2; 4.4); $p = 0.003$
	Lymphocytes	65.3 (64.2; 67.6) 7.6 (5.9; 8.3)	64.2 (62.7; 66.2); $p = 0.343$ 7.1 (6.4; 8.5); $p = 0.84$
	Monocytes	3.4 (3.0; 3.6) 0.4 (0.2; 0.4)	3.5 (3.1; 4.0); $p = 0.1$ 0.5 (0.3; 0.4) $p = 0.166$

Table 3

Protein concentration, *M* ± *SD*, the total number of leukocytes, and the parameters of the BALF cytogram in the experimental animals, *Me* (Q_{25}; Q_{75})

Parameter		Control group ($n = 15$)	Model of MS ($n = 18$)
Total protein, g / l		0.74 (±0.20)	1.08 (±0.30) $p = 0.037$
Total number of leukocytes, $\times 10^9$ / l		0.55 (0.30; 0.84)	0.80 (0.65; 1.55) $p = 0.047$
Quantitative composition of cells (in the numerator – in %, in the denominator – in absolute numbers, $\times 10^9$ / l)	Alveolar macrophages	42.60 (38.50; 53.00) 0.23 (0.13; 0.39)	51.50 (33.88; 55.25) $p = 0.677$ 0.66 (0.51; 0.87) $p = 0.0007$
	Neutrophil granulocytes	47.00 (41.60; 55.50) 0.27 (0.14; 0.36)	45.25 (36.50; 55.50) $p = 0.589$ 0.58 (0.02; 0.09) $p = 0.035$
	Lymphocytes	5.50 (1.75; 7.75) 0.02 (0.01; 0.04)	7.00 (2.38; 9.88) $p = 0.146$ 0.05 (0.02; 0.09) $p = 0.039$

Table 4

Concentration of cytokines, pg / ml, in the blood serum and BALF of the experimental animals, *Me* (Q_{25}; Q_{75})

Parameter	Blood serum		BALF	
	Control group ($n = 15$)	Model of MS ($n = 18$)	Control group ($n = 15$)	Model of MS ($n = 18$)
IL-6	5.5 (2.3; 6.3)	7.8 (4.7; 14.1); $p = 0.152$	5.3 (4.7; 9.2)	9.7 (9.4; 15.7); $p = 0.007$
IL-10	11.8 (6.0; 23.8)	43.3 (21.9; 54.7); $p = 0.029$	59.9 (37.4; 74.5)	66.1 (38.4; 85.9); $p = 0.351$
TNFα	2.6 (2.6; 5.2)	10.8 (6.4; 11.7); $p = 0.035$	40.1 (20.6; 46.2)	39.6 (31;5; 42.5); $p = 0.863$
MCP-1	158.6 (91.7; 454.6)	155.7 (111.7; 407.3); $p = 0.423$	166.7 (131.5; 352.5)	284.3 (184.0; 498.1); $p = 0.045$

DISCUSSION

Reproduction of genetic or diet- and drug-induced models of MS in experiments on animals makes it possible to study changes in homeostatic parameters and analyze the effect of emerging metabolic disorders on various organs and systems. Diet-induced combined *in vivo* models of MS with a high content of fat and carbohydrates in the diet are more similar to the unbalanced human diet, are most consistent with alimentary obesity, and are adequate in terms of the mechanisms of development of MS and associated comorbidity [10–12].

The model reproduced in our experiment reflected the main biometric and biochemical changes typical of MS. The rats receiving a 12-week high-fat and high-carbohydrate diet had an increase in the body weight due to the accumulation of visceral adipose tissue and hepatomegaly. Besides, arterial hypertension with an increase in both systolic and diastolic blood pressure was noted in the animals with MS (Table 1). Blood biochemistry revealed changes indicating carbohydrate and lipid metabolism disorders, such as fasting hyperglycemia, low glucose tolerance, as well as dyslipoproteinemia with an increase in the blood level of triacylglycerols and atherogenic fractions of lipoproteins (LDL-C, VLDL-C) and a decrease in the concentration of high-density lipoproteins.

A number of studies have confirmed that factors of the immune system are actively involved in the pathogenesis of digestive diseases [13, 14]. An important role in the pathogenesis of MS is attributed to sterile inflammation in the adipose tissue, which is induced by macro- and micronutrients, as well as metabolic products formed in the visceral adipose tissue with its excessive accumulation [15]. Such metabolic inflammation often does not have pronounced clinical manifestations, but is accompanied by local stromal vascular and functional changes in the adipose tissue – adipocyte hypertrophy, infiltration by immune cells, fibrosis of the extracellular matrix, impaired microcirculation, and changes in the secretory phenotype of cellular elements [14]. However, in some cases, laboratory tests reveal an increase in the level of nonspecific inflammatory markers in the blood, such as C-reactive protein, fibrinogen, procalcitonin, etc., which correlates with the severity of inflammation in the adipose tissue [16].

As a result of our experiment, we revealed an increase in the total number of leukocytes due to granulocytes, as well as an increase in the protein concentration in the blood serum of the animals with induced MS compared with the intact animals (Tables 1, 2). At the same time, we registered an increase in the levels of TNFα and IL-10 in the blood serum (Table 4). The identified changes are common signs of an inflammatory response that develops against the background of diet-induced metabolic disorders [17–19].

Factors of systemic inflammation associated with MS and obesity contribute to the development of pathology in various organs and systems, which is confirmed by a large number of experimental and clinical studies [2, 20]. One of the informative methods for detecting biological markers of most lung diseases is the study of BALF (cytological, biochemical, immunological), which gives accurate information about the direction and severity of protective, adaptive, and pathological reactions in the lungs and allows to study the systemic mechanisms for maintaining structural and functional homeostasis in the bronchopulmonary system [7, 8].

Following the analysis of the BALF cytogram, we found an increase in the total number of leukocytes, as well as their individual morphological types (the absolute number of alveolar macrophages, neutrophil granulocytes, and lymphocytes) in the animal models of MS compared with the control values (Table 3). In normal conditions, macrophages represent the majority of phagocytes in the lower respiratory tract [21]. During inflammation, the proportion of alveolar macrophages increases both due to proliferation of tissue-resident cells (to a larger extent) and due to recruitment of macrophages of monocytic origin from peripheral blood (to a lesser extent) [22]. Monocytes infiltrating tissues find themselves in a specific microenvironment and develop into macrophages with altered functions, often exacerbating inflammatory responses [23]. It is assumed that it is monocytes recruited from the blood, and not proliferating tissue-resident alveolar macrophages, that are the precursors of M1-polarized macrophages in the lungs. The latter are distinguished by pronounced cytotoxic and antimicrobial activity, secrete a large number of reactive oxygen species, nitrogen, and proinflammatory cytokines, and contribute to alteration and progression of inflammation in the bronchial mucosa [24].

The analysis of the BALF cytokine profile revealed a more than 1.5-fold increase in the concentration of IL-6 and MCP-1 in the animals with MS compared with the controls (Table 4). It is known that the monocyte chemotactic factor is predominantly secreted by macrophages and

monocytes, dendritic cells, and lung fibroblasts and increases the chemotactic activity of monocytes, but not neutrophils [25]. IL-6 is a pleiotropic cytokine with both pro- and anti-inflammatory properties due to implementation of different types of signaling [26]. In chronic obstructive pulmonary disease, IL-6 is crucial for attracting neutrophils to the site of inflammation, as it leads to synthesis of the necessary chemokines by endothelial cells as a result of trans-signaling. At the same time, neutrophils attracted to the focus of inflammation are some of the sources of soluble IL-6 receptor (sIL-6R), which is necessary for initiating trans-signaling in relation to the structural cellular elements of the lungs (fibroblasts, epithelial cells, endothelial cells, and smooth muscle cells) [27, 28]. In turn, excessive proinflammatory activity of the cellular components in the pulmonary interstitial matrix can lead to an increase in the permeability of the alveolar – capillary barrier, which is confirmed by the increase in the protein concentration in the BALF in the group of animals with MS (Table 3).

CONCLUSION

Experimental diet-induced MS is accompanied by the development of a systemic inflammatory response, laboratory signs of which are neutrophilic leukocytosis in the blood and an increase in the serum concentration of protein, TNFα, and IL-10. Organ-specific changes that characterize the negative impact of MS factors on the state of the bronchopulmonary system in the experimental animals are qualitative and quantitative changes in the composition of BALF, such as an increase in the protein concentration, an increase in the content of cellular elements (alveolar macrophages, neutrophil granulocytes, lymphocytes), and a rise in the concentration of proinflammatory cytokines IL -6 and MCP-1. Since these changes are inflammatory in nature, it seems relevant to evaluate structural, morphological, and functional changes in the bronchoalveolar system in laboratory animals that occur against the background of MS and assess their intensity in conjunction with systemic and local inflammation factors.

REFERENCES

1. Lee J., Lee K.S., Kim H., Jeong H., Choi M.J., Yoo H.W.et al. The relationship between metabolic syndrome and the incidence of colorectal cancer. *Environmental Health and Preventive Medicine.* 2020; 25(1):6. DOI: 10.1186/s12199-020-00845-w.
2. Segula D. Complications of obesity in adults: a short review of the literature. *Malawi Med. J*. 2014; 26(1):20–24.
3. Laakso M., Kuusisto J., Stančáková, A., Kuulasmaa T., Pajukanta P., Lusis A.J. et al. The Metabolic Syndrome in Men study: a resource for studies of metabolic and cardiovascular diseases. *Journal of Lipid Research*. 2017;58(3):481–493. DOI: 10.1194/jlr.O072629.
4. Budnevsky A.V., Malysh E.Y., Ovsyannikov E.S., Drobysheva E.S. Asthma and metabolic syndrome: clinical and pathogenetic relationships. *Terapevticheskii Arkhiv*. 2015;87(10):110–114 (in Russ.). DOI: 10.17116/terarkh20158710110-114.
5. Budnevsky A.V., Ovsyannikov E.S., Labzhania N.B. Chronic obstructive pulmonary disease concurrent with metabolic syndrome: pathophysiological and clinical features. *Terapevticheskii Arkhiv*. 2017;89(1):123–127 (in Russ.). DOI: 10.17116/terarkh2017891123-127.
6. Voronkova O.V., Saprina T.V., Bukreeva E.B., Zima A.P. Etiopathogenetic parallels and unresolved issues in the pathogenesis of COPD and concomitant metabolic syndrome (review). *Obesity and Metabolism*. 2020;17(3):292–298 (in Russ.). DOI: 10.14341/omet12378.
7. Zinov'ev S.V., Seliverstov S.S., Tselujko S.S., Gorbunov M.M., Semenov D.A. Morphological characteristics of open bronchoalveolar lavage of the rat lung. *Amur Medical Journal.* 2015;4(12):103–108 (in Russ.).
8. Alimkina O.V., Petrenko A.E., Savchenko E.S., Ogneva N.S., Taboyakova L.A., Maksimenko S.V., et al. Analysis of the cellular composition of bronchoalveolar lavage fluid in the modeling and treatment of acute respiratory distress syndrome in mouse biomodels. *Journal Biomed.* 2021;17(3):17–22 (in Russ.). DOI: 10.33647/2074-5982-17-3-17-22.
9. Matichin A.A., Katelnikova A.E., Kryshen K.L. Specific techniques for collecting bronchoalveolar lavage fluid from laboratory animals. *Laboratory Animals for Science.* 2019;4:6 (in Russ.). DOI: 10.29296/2618723X-2019-04-06.
10. Woods S.C., Seeley R.J., Rushing P.A., D'Alessio D., Tso P. A controlled high-fat diet induces an obese syndrome in rats. *J. Nutr.* 2003; 133(4):1081–1087. DOI: 10.1093/jn/133.4.1081.
11. Jawien J., Nastalek P., Korbut R. Mouse models of experimental atherosclerosis. *J. Physiol. Pharmacol.* 2004;55(3):503.
12. Tran L.T., Yuen V.G., McNeill J.H. The fructose-fed rat: a review on the mechanisms of fructose-induced insulin resistance and hypertension. *Mol. Cell. Biochem.* 2009;332(1-2):145–159. DOI: 10.1007/s11010-009-0184-4.
13. Riger N.A., Shipelin V.A., Apryatin S.A., Gmoshinski I.V. Immunological markers of alimentary-induced hyperlipidemia in Wistar rats. *Problems of Nutrition.* 2019;88(3):44–52 (in Russ.). DOI: 10.24411/0042-8833-2019-10028.
14. Romantsova T.I., Sych Y.P. Immunometabolism and metainflammation in obesity. *Obesity and Metabolism.* 2019;16(4):3–17 (in Russ.). DOI: 10.14341/omet12218.
15. Bespalova I.D., Ryazantseva N.V., Kalyuzhin V.V., et al. Systemic inflammation in the pathogenesis of metabolic syndrome and associated diseases. *Siberian Medical Journal (Irkutsk)*. 2013;117(2):5–9 (in Russ.).
16. Shvarts V. Adipose tissue inflammation. Part 1. Morphological and functional manifestations. *Problems of Endocrinology*. 2009;55(4):44–49 (in Russ.). DOI: 10.14341/probl200955444-49.

17. Kryukov N.N., Ginzburg M.M., Kiseleva E.V. Modern view of the role of sterile inflammation in the adipose tissue in the genesis of obesity and metabolic syndrome. *Arterial Hypertension*. 2013;19(4):305–310 (in Russ.). DOI: https://doi.org/10.18705/1607-419X-2013-19-4-.
18. McCracken E., Monaghan M., Sreenivasan S. Pathophysiology of the metabolic syndrome. *Clin. Dermatol*. 2018;36(1):14–20. DOI: 10.1016/j.clindermatol.2017.09.004.
19. Lee B.-C., Lee J. Cellular and molecular players in adipose tissue inflammation in the development of obesity-induced insulin resistance. *Biochimica et Biophysica Acta (BBA) – Molecular Basis of Disease*. 2014;1842(3):446–462. DOI: 10.1016/j.bbadis.2013.05.017.
20. Kologrivova I.V., Vinnitskaya I.V., Koshelskaya O.A., Suslova T.E. Visceral obesity and cardiometabolic risk: features of hormonal and immune regulation. *Obesity and Metabolism.* 2017;14(3):3–10 (in Russ.). DOI: 10.14341/OMET201733-10.
21. Kodavanti U.P. Respiratory toxicity biomarkers. Biomarkers in Toxicology. *Academic Press.* 2014:217–239. DOI: 10.1016/B978-0-12-404630-6.00012-9.
22. Lyamina S.V., Shimshelashvili S.L., Kalish S.V., Malysheva E.V., Larionov N.P., Malyshev I.Yu. Changes in phenotype and phenotypic flexibility of alveolar macrophages in inflammatory lung diseases. *Pulmonologiya*. 2012;6 83–89 (in Russ.). DOI: 10.18093/0869-0189-2012-0-6-83-89.
23. Kzhyshkowska Ju.G., Gratchev A.N. Monocyte and macrophage markers for diagnosis of immunopathologies. *Patogenez*. 2012;10(1):14–19 (in Russ.).
24. Murray P.J., Allen J.E., Biswas S.K., Fisher E.A., Gilroy D.W., Goerdt S. et al. Macrophage activation and polarization: nomenclature and experimental guidelines. *Immunity.* 2014;41(1):14–20. DOI: 10.1016/j.immuni.2014.06.008.
25. Kolotov K.A., Rasputin P.G. Monocytic chemotactic protein-1 in physiology and medicine (review of literature). P*ermskij Medicinskij Zhurnal.* 2018;35(3):99–105 (in Russ.). DOI: 10.17816/pmj35399-105
26. Rincon M., Irvin C.G. Role of IL-6 in asthma and other inflammatory pulmonary diseases. *Int. J. Biol. Sci.* 2012;8(9):1281–1290. DOI: 10.7150/ijbs.4874.
27. Durham A.L., Caramori G., Chung K.F., Adcock I.M. Targeted anti-inflammatory therapeutics in asthma andchronic obstructive lung disease. *Transl. Res.* 2016;167(1):192–203. DOI: 10.1016/j.trsl.2015.08.004.
28. Wolf J., Rose-John S., Garbers C. Interleukin-6 and its receptors: a highly regulated and dynamic system. *Cytokine*. 2014;70(1):11–20. DOI: 10.1016/j.cyto.2014.05.024.

Authors contribution

Voronkova O.V., Birulina J.G., Ivanov V.V.– conception and design, drafting of the manuscript. Buyko E.E., Grigorieva A.V., Chernyshov N.A., Motlokhova E.A. – carrying out of the experiment. Osikhov I.A., Esimova I.E. – analysis and interpretation of the data.

Authors information

Voronkova Olga V. – Dr. Sci. (Med.), Associate Professor, Head of the Biology and Genetics Division, SSMU, Tomsk, voronkova-ov@yandex.ru, http://orcid.org/0000-0001-9478-3429

Birulina Julia G. – Cand. Sci. (Biology), Associate Professor, Biophysics and Functional Diagnostics Division, SSMU, Tomsk, birulina20@yandex.ru, http://orcid.org/0000-0003-1237-9786

Ivanov Vladimir V. – Cand. Sci. (Biology), Head of the Center for Preclinical Research, Central Research Laboratory, SSMU, Tomsk, ivanovvv1953@gmail.com, http://orcid.org/0000-0001-9348-4945

Buyko Evgeny E. – Laboratory Assistant, Center for Preclinical Research, Central Research Laboratory, SSMU, Tomsk, buykoevgen@yandex.ru, http://orcid.org/0000-0002-6714-1938

Esimova Irina E. – Dr. Sci. (Med.), Associate Professor, Biology and Genetics Division, SSMU, Tomsk, orevi@mail.ru, http://orcid.org/0000-0002-7508-2878

Grigorieva Anna V. – Teaching Assistant, Biology and Genetics Division, SSMU, Tomsk, anna-grigoreva-87@mail.ru, http://orcid.org/0000-0002-1962-9584

Osikhov Ivan A. – Cand. Sci. (Med.), Associate Professor, Biology and Genetics Division, SSMU, Tomsk, osikhov.25-88@yandex.ru, http://orcid.org/0000-0002-4873-7680

Chernyshov Nikita A. – Student, SSMU, Tomsk, niki-rembo@mail.ru, http://orcid.org/0000-0002-4008-5606

Motlokhova Elizaveta A. – Student, SSMU, Tomsk, emotlohova@gmail.com, http://orcid.org/0000-0001-7409-3770

(✉) **Voronkova Olga V.,** voronkova-ov@yandex.ru

Received 04.04.2022;
approved after peer review 21.04.2022;
accepted 09.06.2022

УДК 616.348/.351-006.6-089.844
https://doi.org/10.20538/1682-0363-2022-4-37-43

Development and characterization of patient-derived xenograft models of colorectal cancer for testing new pharmacological substances

Goncharova A.S., Kolesnikov E.N., Egorov G.Yu., Maksimov A.Yu., Shevchenko A.N., Nepomnyashchaya E.M., Gvaldin D.Yu., Kurbanova L.Z., Khodakova D.V., Kit S.O., Kaymakchi O.Yu., Snezhko A.V.

National Medical Research Center for Oncology
63, 14th Liniya Str., Rostov-on-Don, 344037, Russian Federation

ABSTRACT

The aim of the study was to create a patient-derived xenograft (PDX) model of human colorectal cancer and to determine its histologic and molecular characteristics, such as the status of *KRAS, NRAS,* and *BRAF* genes and the presence of microsatellite instability.

Materials and methods. First generation xenograft models *in vivo* were created using tumors from patients with colorectal cancer (n = 4) and immunodeficient Balb/c Nude mice (n = 20); second, third, and fourth generation models were created in the same mouse line (n = 3 for each generation). A caliper was used to measure subcutaneous xenografts; their size was calculated by the ellipsoid formula. Cryopreservation involved immersing the samples in a freezing medium (80% RPMI 1640, 10% fetal bovine serum, 10% dimethyl sulfoxide (DMSO)) and storing them at –80 °C. The histologic analysis was performed according to the standard technique (preparation of paraffin blocks and staining of microsections with hematoxylin and eosin). Mutations in the *KRAS, NRAS*, and *BRAF* genes were determined by direct Sanger sequencing; microsatellite instability was determined by the fragment analysis at five loci: *Bat-25, Bat-26, NR21, NR24,* and *NR27*.

Results. Stable, transplantable xenografts of colorectal cancer were obtained from two out of four patients. The average waiting time from the implantation to the growth of the first generation xenograft was 28 days. The latency phase after cryopreservation was comparable to that at the creation of the first generation PDX model. The model reproduced the histotype, grade and mutational status of the *KRAS*, *NRAS*, and *BRAF* genes, as well as microsatellite instability of the donor tumor.

Conclusion. The developed model of human colorectal cancer was characterized in terms of growth dynamics, cryopreservation tolerance, and histologic and molecular genetic parameters.

Keywords: xenograft, colorectal cancer, *in vivo* models, PDX model, Balb/c Nude

Conflict of interest. The authors declare the absence of obvious or potential conflicts of interest related to the publication of this article.

Source of financing. The authors state that they received no funding for the study.

Conformity with the principles of ethics. All patients signed an informed consent to participate in the study. The study was approved by the local Ethics Committee at the National Medical Research Center for Oncology.

For citation: Goncharova A.S., Kolesnikov E.N., Egorov G.Yu., Maksimov A.Yu., Shevchenko A.N., Nepomnyashchaya E.M., Gvaldin D.Yu., Kurbanova L.Z., Khodakova D.V., Kit S.O., Kaymakchi O.Yu., Snezhko A.V. Development and characterization of patient-derived xenograft models of colorectal cancer for testing new pharmacological substances. *Bulletin of Siberian Medicine.* 2022;21(4):37–43. https://doi.org/10.20538/1682-0363-2022-4-37-43.

✉ *Goncharova Anna S.,* fateyeva_a_s@list.ru

Разработка и характеристика ксенотрансплантатов, полученных от пациентов с колоректальным раком, для тестирования новых фармакологических субстанций

Гончарова А.С., Колесников Е.Н., Егоров Г.Ю., Максимов А.Ю., Шевченко А.Н., Непомнящая Е.М., Гвалдин Д.Ю., Курбанова Л.З., Ходакова Д.В., Кит С.О., Каймакчи О.Ю., Снежко А.В.

Национальный медицинский исследовательский центр (НМИЦ) онкологии
Россия, 344037, г. Ростов-на-Дону, ул. 14-я Линия, 63

РЕЗЮМЕ

Цель. Создание модели ксенотрансплантата, полученного от пациента с колоректальным раком (КРР), и определение ее гистологических и молекулярных характеристик, таких как статус генов *KRAS, NRAS BRAF* и наличие микросателлитной нестабильности.

Материалы и методы. Для создания первого поколения модели *in vivo* использовали опухоли от пациентов с КРР (n = 4) и иммунодефицитных мышей линии Balb/c Nude (n = 20), для создания второго, третьего и четвертого поколения – мышей этой же линии (n = 3 для каждого поколения). Измерения подкожных ксенотрансплантатов выполняли штангенциркулем, их размеры вычисляли по формуле Шрека для эллипсоида. Криоконсервацию выполняли путем погружения образцов в микс для криоконсервации (80% RPMI 1640, 10% фетальной бычьей сыворотки, 10% диметилсульфоксида) и хранения их на –80 °С. Гистологическое исследование выполняли согласно стандартной методике (приготовление парафиновых блоков и окрашивание микросрезов гематоксилином и эозином). Мутации в генах *KRAS*, *NRAS* и *BRAF* определяли методом прямого секвенирования по Сэнгеру, микросателлитную нестабильность – методом фрагментарного анализа по пяти локусам: *Bat-25*, *Bat-26*, *NR21*, *NR24*, *NR27*.

Результаты. Стабильные перевиваемые ксенотрансплантаты КРР получены от двух пациентов из четырех. Среднее время ожидания между имплантацией и ростом трансплантата первого поколения составило 28 сут. Латентная фаза после криоконсервации была сопоставима с латентной фазой при создании первого поколения пациентоподобной модели. Показано, что в модели воспроизведены гистотип, степень дифференцировки и мутационный статус генов *KRAS*, *NRAS*, *BRAF* и микросаттелитная нестабильность донорской опухоли.

Заключение. Созданная модель КРР человека охарактеризована с учетом динамики роста, способности переносить криоконсервацию, гистологических и молекулярно-генетических параметров.

Ключевые слова: ксенотрансплантат, колоректальный рак, модели *in vivo*, PDX модель, Balb/c Nude

Конфликт интересов. Авторы декларируют отсутствие явных и потенциальных конфликтов интересов, связанных с публикацией настоящей статьи.

Источник финансирования. Авторы заявляют об отсутствии финансирования.

Соответствие принципам этики. Все пациенты подписали информированное согласие на участие в исследовании. Исследование одобрено локальным этическим комитетом НИМЦ онкологии.

Для цитирования: Гончарова А.С., Колесников Е.Н., Егоров Г.Ю., Максимов А.Ю., Шевченко А.Н., Непомнящая Е.М., Гвалдин Д.Ю., Курбанова Л.З., Ходакова Д.В., Кит С.О., Каймакчи О.Ю., Снежко А.В. Разработка и характеристика ксенотрансплантатов, полученных от пациентов с колоректальным раком, для тестирования новых фармакологических субстанций. *Бюллетень сибирской медицины.* 2022;21(4):37–43. https://doi.org/10.20538/1682-0363-2022-4-37-43.

INTRODUCTION

Colorectal cancer (CRC) is one the most common cancers worldwide. It is characterized by high lethality at advanced stages [1]. Mortality from CRC can be reduced by its early detection and an optimal treatment regimen in management of patients with advanced disease.

The treatment strategy for CRC depends on the stage and site of the tumor, as well as on its molecular

characteristics [2]. To date, treatment of patients with CRC involves surgical resection combined with standard adjuvant chemotherapy, and neoadjuvant radiochemotherapy is recommended for patients with locally advanced rectal cancer [2, 3]. A combination of chemotherapy with new targeted drugs, such as epidermal growth factor receptor (EGFR) inhibitors, and immunotherapy improves the median survival of patients [4]. Patients with wild-type *KRAS* genes in tumors have been found to respond favorably to targeted therapies, including anti-EGFR or anti-VEGFR drugs, while patients with high microsatellite instability in tumors (MSI-high tumors) benefit more from immunotherapy [5].

Despite advances in CRC treatment, the search for new anticancer drugs continues around the world. Early stages of development of potentially useful pharmacological substances involve the use of cancer cell line panels as a tool to study the biological mechanisms of action and test the activity of new compounds *in vitro*. However, cell lines fail to reproduce heterogeneity of human tumors both *in vitro* and *in vivo*. On the contrary, patient-derived xenograft (PDX) models better reflect the existing molecular heterogeneity of human cancers and, therefore, are considered more suitable for drug efficacy studies [6].

The use of PDX models as a platform for assessing therapeutic responses in preclinical studies requires standardization of these models, which is especially important for assessments at the molecular level [7].

Therefore, the aim of this study was to create a PDX model of human CRC and to determine its molecular characteristics, such as the status of *KRAS*, *NRAS, BRAF*, and *MSI* genes.

MATERIALS AND METHODS

The study included immunodeficient Balb/c Nude mice (29 female mice aged 5–6 weeks) obtained from the SPF-vivarium of the Institute of Cytology and Genetics, SB of RAS (Novosibirsk). The animals were kept in the SPF vivarium at the National Medical Research Center for Oncology. The animals were housed in the IVC system (Tecniplast, Italy) in a room with controlled climate parameters (temperature 21–26 °C, air humidity 50–60%). The animals had free access to food and water which were exposed to autoclave sterilization. All manipulations involving animals were performed in compliance with the Guidelines for the Use of Laboratory Animals.

Subcutaneous PDX models of human CRC were created using tumor samples obtained during surgery from patients receiving treatment at the Department of Abdominal Cancer No.1, National Medical Research Center for Oncology, from February to April 2020. All patients signed an informed consent to the use of biological material.

Subcutaneous PDX models were obtained by implanting a fragment of the donor tumor with a size of 3 × 3 × 3 mm under the skin of the right thigh in recipient animals (n = 5 for a sample obtained from one patient). Mice of the same line were used for the second, third, and fourth generation models (n = 3 for each generation). Implantation was performed under injectable anesthesia with Xyla (20 mg / kg) and Zoletil-100 (50 mg / kg). The animals were euthanized by cervical dislocation.

Subcutaneous xenografts were measured by a caliper (Griff, Russia), and their size was calculated by the ellipsoid formula: $V = a \times b \times c \times \pi / 6$, where V is the tumor volume (mm3), and a, b, and c are measurements of the ellipsoid in three planes (mm).

Isolated tumor nodules were divided into 3 × 3 × 3 mm fragments, placed in a freezing medium (80% RPMI 1640, 10% fetal bovine serum, 10% dimethyl sulfoxide (DMSO)), and then stored in the freezer at –80 °C. Frozen samples were thawed in a 37 °C water bath. Then the samples were placed in a container with the RPMI 1640 medium. After the thawing, the tumor fragments were implanted.

The fragments of donor tumors and xenografts were fixed in 10% formalin for 24 h and then embedded in paraffin. Then the histologic analysis was performed according to the standard technique: paraffin blocks were prepared, and the microsections were stained with hematoxylin and eosin.

Genomic DNA was isolated from PDX using the QIAamp DNA Mini Kit (Qiagen, Germany) and the QIAcube Connect automated nucleic acid purification system (Qiagen, Germany). Mutations in exons 2, 3, and 4 in the *KRAS* and *NRAS* genes and *BRAF* V600 mutations were identified by direct Sanger sequencing (AB3500 Genetic Analyzer, Life Technologies, USA). Microsatellite instability was determined by the fragment analysis (AB3500 Genetic Analyzer, Life Technologies, USA) at five loci: *Bat-25, Bat-26, NR21, NR24,* and *NR27*.

RESULTS

Tumor samples for the PDX model of human CRC were obtained from four patients during surgery for

colon tumors (sigmoid / transverse colon resection). Freshly resected tumor fragments from each patient were transported from the operating unit to the SPF vivarium in a sterile container with the RPMI 1640 medium and implanted into immunodeficient Balb/c Nude mice (n = 5 for a sample taken from one patient) within an hour.

Table 1 presents the characteristics of patients and the corresponding assessment of xenotransplantation results.

Table 1

Clinical characteristics of patients and assessment of the results of tumor xenotransplantation into immunodeficient Balb/c Nude mice

Procedure number	Sampling method	Tumor site	TNM stage	Histology	Implantation results	Latency phase duration. days
PDX-1	Surgical resection	Transverse colon	$T_{4в}N_{1c}M_0$	Moderately differentiated adenocarcinoma	2/5	25 (20–30)
PDX-2	Surgical resection	Sigmoid colon	$T_3N_{1b}M_0$	Moderately differentiated adenocarcinoma	3/5	31 (24–45)
PDX-3	Surgical resection	Sigmoid colon	$T_3N_0M_0$	Moderately differentiated adenocarcinoma	0/5	–
PDX-4	Surgical resection	Sigmoid colon	$T_3N_{1b}M_0$	Moderately differentiated adenocarcinoma	0/5	–

Stable, transplantable PDX models of CRC were obtained from two out of four patients. The average waiting time from the implantation to the growth of the first generation PDX (P1) was 28 days (the range of 20–45 days). Engraftment and growth rate of freshly implanted tumor fragments varied (Fig. 1).

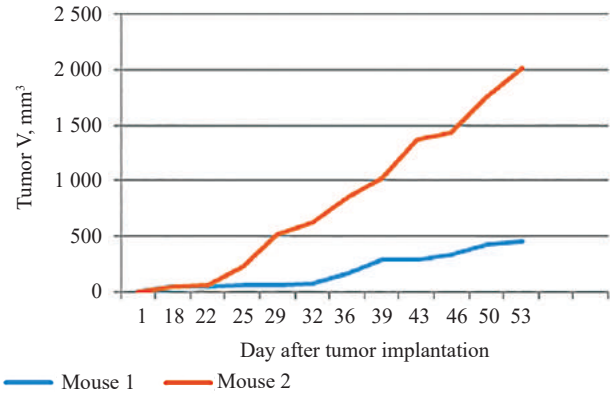

Fig. 1. Growth dynamics of the first generation PDX-1 model (P1)

If xenotransplantation did not result in the growth of subcutaneous tumor nodules within 60 days, the procedure was regarded as unsatisfactory, and the corresponding observations (PDX-3 and PDX-4) were stopped. Two successfully implanted PDX models (PDX-1 and PDX-2) were serially passaged to generate second (P2, n = 3) and third generation (P3, n = 3) models.

To assess the effect of cryopreservation on engraftment and growth rate, subcutaneous tumor nodules of the third generation PDX-1 were isolated, fragmented, cryopreserved according to the standard procedure, and stored at –80 °C. After recovery of PDX-1 from cryopreservation, two of the three samples showed linear growth forming the fourth generation (P4) (Fig. 2).

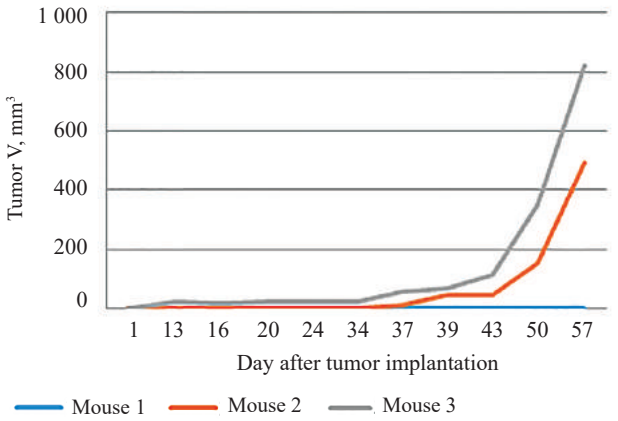

Fig. 2. Growth dynamics of PDX-1 thawed after cryopreservation, fourth generation (P4)

The latency phase of the fourth generation PDX-1 (P4) after cryopreservation was slightly longer than that of the first generation (P1).

The histologic characteristics of the primary tumor were preserved during serial passage, and they were reproduced in the fourth generation PDX-1 after cryopreservation. The preparations were described as moderately differentiated adenocarcinoma (G2). The tumor showed necrotic foci with pronounced infiltrative growth and areas with high mitotic activity. Slight lymphocytic infiltration was determined in the preparations obtained from the donor tumor material (Fig. 3).

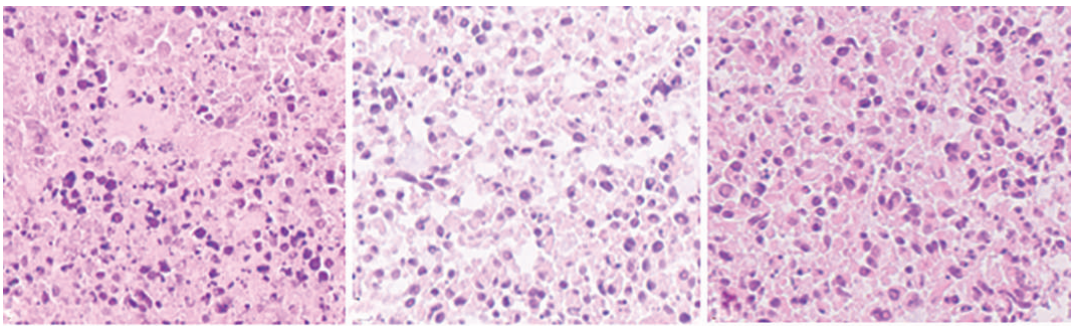

a *b* *c*

Fig. 3. Histologic samples of the patient tumor and corresponding PDX models: *a* – patient tumor; *b* – first generation PDX model; *c* – fourth generation PDX model (after cryopreservation). Staining with hematoxylin and eosin, ×400

Molecular and genetic tests showed no mutations in exons 2, 3, and 4 in the *KRAS* and *NRAS* genes and no *BRAF* V600 mutations. Microsatellite stability was also determined both in the sample of the donor tumor material and in the corresponding third (P3) and fourth generation (P4) PDX models.

DISCUSSION

In this study, we performed four subcutaneous implantations of tumor fragments from patients with CRC into immunodeficient Balb/c Nude mice, resulting in two stable, transplantable PDX-derived cell lines, which complied with earlier published engraftment-characterizing parameters [7, 8]. Successful engraftment of tumor fragments in a PDX model is not universal for all types of tumors; however, according to the literature, PDX models of human CRC have relatively high engraftment rates ranging from 50 to 70% [7–9].

A. Katsiampoura et al. (2017) demonstrated that surgically obtained samples had higher engraftment rates compared with biopsy samples, about 70 and 35%, respectively [8]. In this regard, we chose a surgical tumor sampling method to create PDX models. In addition, a small size of biopsy samples complicates the choice of the implantation site and creation of a series of xenografts with simultaneous sample duplication for biobanking [10, 11]. The growth dynamics of PDX models after cryopreservation (P4) showed that the duration of a latency phase was generally comparable to that during the creation of the first generation PDX model (P1).

We demonstrated the ability of PDX to reproduce the morphological features of the disease, namely the histotype and grade of the tumor. In addition, the study of sequentially created generations P1, P2, P3, and P4 allowed to conclude that PDX passaging did not significantly affect the ability to reproduce the histological subtype, at least at early stages of PDX creation, which is consistent with the literature data [7]. Some researchers demonstrated in larger-scale studies that differentiation of donor tumor cells did not affect the establishment of the PDX cell line [8].

PDX models can reproduce both morphological characteristics of tumors and molecular and genetic heterogeneity which is a fundamental feature of the human disease [12]. We noted in this study that wild-type *KRAS*, *NRAS,* and *BRAF* genes were preserved in serial passaging, and microsatellite stability was established in samples of the third generation PDX model (P3), which complied with the molecular and genetic characteristics of the donor tumor. This makes the resulting model suitable for testing both new pharmacological substances with a cytotoxic effect and monoclonal antibody drugs.

Other studies have found that clinically significant genetic mutations (*KRAS*, *BRAF*, and *PIK3CA*) do not affect the development of a PDX model, but the authors believe that three genes are not enough to fully reproduce the diversity of CRC biology. On the contrary, M. Cybulska et al. (2018) in a large-scale study on the stratification of PDX models of human CRC investigated transcriptomic and mutation profiles of primary tumors and xenografts derived from them using a panel of 409 cancer-associated genes. The differences were found in both genetic and transcriptomic profiles of donor tumors and PDX models, which might result from subclonal evolution at an early stage of PDX model development or technical errors. In this regard, the authors concluded that standardization of the PDX model requires taking into account more stable parameters, such as the presence of targets and a response to standard anticancer therapy [7].

CONCLUSION

To overcome certain shortcomings associated with drug testing on traditional tumor models, we attempted to develop and standardize PDX models of human CRC to reproduce a wide range of biological and clinical properties of human tumors. One of the PDX models obtained during the study was characterized in terms of growth dynamics, cryopreservation tolerance, histologic parameters, and molecular and genetic criteria for choosing a treatment strategy.

REFERENCES

1. Gevorkyan Yu.A., Kolesnikov V.E., Soldatkina N.V., Kharagezov D.A., Dashkov A.V., Kaymakchi D.O., et al. Minimally invasive surgery in treatment of patients with metastatic colorectal cancer. *Yuzhno-Rossiyskiy Onkologicheskiy Zhurnal*. 2020;1(2):22–27 (in Russ.). DOI: *10.37748/2687-0533-2020-1-2-3.*
2. Baran B., Ozupek N.M., Tetik N.Y., Acar E., Bekcioglu O., Baskin Y. Difference between left-sided and right-sided colorectal cancer: a focused review of literature. *Gastroenterology Research*. 2018;1(4):264–273. DOI: 10.14740/gr1062w.
3. Kit O.I., Gevorkyan Yu.A., Soldatkina N.V., Kolesnikov V.E., Kharagezov D.A. Laparoscopic combined surgical interventions for metastatic colorectal cancer. *Koloproktologiya.* 2015;4:19–23 (in Russ.).
4. Punt C.J.A., Koopman M., Vermeulen L. From tumour heterogeneity to advances in precision treatment of colorectal cancer. *Nature reviews Clinical Oncology*. 2017;14(4):235–246. DOI: 10.1038/nrclinonc.2016.171.
5. Wang F., Bai L., Liu T.S., Yu Y.Y., He M.M., Liu K.Y. et al. Right-and left-sided colorectal cancers respond differently to cetuximab. *Cancer Communications*. 2015;34(9):384–393. DOI: 10.1186/s40880-015-0022-x.
6. Ireson C.R., Alavijeh M.S., Palmer A.M., Fowler E.R., Jones H. The role of mouse tumour models in the discovery and development of anticancer drugs. *British Journal of Cancer*. 2019;121(2):101–108. DOI: 10.1038/s41416-019-0495-5.
7. Cybulska M., Olesinski T., Goryca K., Paczkowska K., Statkiewicz M., Kopczynski M. et al. Challenges in stratifying the molecular variability of patient-derived colon tumor xenografts. *BioMed Research International*. 2018;2018:2954208. DOI: 10.1155/2018/2954208.
8. Katsiampoura A., Raghav K., Jiang Z.Q., Menter D.G., Varkaris A., Morelli M.P. et al. Modeling of patient-derived xenografts in colorectal cancer. *Molecular Cancer Therapeutics*. 2017;16(7):1435–1442. DOI: 10.1158/1535-7163.MCT-16-0721.
9. Conte N., Mason J.C., Halmagui C., Neuhauser S., Mosaku A., Yordanova G. et al. PDX finder: a portal for patient-derived tumor xenograft model discovery. *Nucleic Acids Research.* 2019;47(D1):D1073–D1079. DOI: 10.1093/nar/gky984.
10. Jung J., Seol H.S., Chang S. The generation and application of patient-derived xenograft model for cancer research. *Cancer Research and Treatment: Official Journal of Korean Cancer Association.* 2018;50(1):1–10. DOI: 10.4143/crt.2017.307.
11. Ivanics T., John R., Bergquist J.R., Liu G., Kim M.P., Kang Y. et al. Patient-derived xenograft cryopreservation and reanimation outcomes are dependent on cryoprotectant type. *Laboratory Investigation.* 2018;98(7):947–956. DOI: 10.1038/s41374-018-0042-7.
12. Yoshida G.J. Applications of patient-derived tumor xenograft models and tumor organoids. *Journal of Hematology & Oncology*. 2020;13(1):4. DOI: 10.1186/s13045-019-0829-z.

Acknowledgments

The authors would like to thank Olesya A. Ossovskaya, translator at the National Medical Research Center for Oncology, for the translation of the manuscript in English.

Authors contribution

Goncharova A.S. – conception and design. Kolesnikov E.N. – carrying out of surgeries. Egorov G.Yu. – collection of patient clinical data. Maksimov A.Yu. – collection and analysis of data, carrying out of surgeries. Shevchenko A.N. – collection and analysis of data. Nepomnyashchaya E.M. – carrying out of the histologic study. Gvaldin D.Yu. – compilation of a list of references. Kurbanova L.Z. – drafting and technical editing of the manuscript. Khodakova D.V. – drafting of the manuscript. Kit S.O., Snezhko A.V. – editing of the manuscript. Kaymakchi O.Yu. – analysis and interpretation of the data.

Authors information

Goncharova Anna S. – Cand. Sci. (Biology), Head of the Experimental Laboratory Center, National Medical Research Center for Oncology, Rostov-on-Don, fateyeva_a_s@list.ru, http://orcid.org/0000-0003-0676-0871

Kolesnikov Evgeniy N. – Cand. Sci. (Med.), Head of the Department of Abdominal Cancer No.1, National Medical Research Center for Oncology, Rostov-on-Don, onko-sekretar@mail.ru, http://orcid.org/0000-0001-9749-709X

Egorov Georgiy Yu. – Post-Graduate Student, National Medical Research Center for Oncology, Rostov-on-Don, egorovgu@gmail.com, http://orcid.org/0000-0002-1413-6406

Maksimov Aleksey Yu. – Dr. Sci. (Med.)., Professor, Deputy Director General for Prospective Scientific Research, National Medical Research Center for Oncology, Rostov-on-Don, onko-sekretar@mail.ru, http://orcid.org/0000-0002-1397-837X

Shevchenko Aleksey N. – Dr. Sci. (Med.)., Professor, Head of the Department of Oncourology, Urologist, National Medical Research Center for Oncology, Rostov-on-Don, alexshew@mail.ru, http://orcid.org/0000-0002-9468-134X

Nepomnyashchaya Evgenia M. – Dr. Sci. (Med.)., Professor, Pathologist, Department of Anatomical Pathology, National Medical Research Center for Oncology, Rostov-on-Don, rnioi-patology@yandex.ru, http://orcid.org/0000-0003-0521-8837

Gvaldin Dmitriy Yu. – Cand. Sci. (Biology), Researcher, National Medical Research Center for Oncology, Rostov-on-Don, 89dmitry@mail.ru, http://orcid.org/0000-0001-8633-2660

Kurbanova Luiza Z. – Junior Researcher, National Medical Research Center for Oncology, Rostov-on-Don, luizacurbanowa@mail.ru, http://orcid.org/0000-0003-3436-1325

Khodakova Darya V. – Junior Researcher, National Medical Research Center for Oncology, Rostov-on-Don, coctail.moxuto@yandex.ru, http://orcid.org/0000-0003-3753-4463

Kit Sergey O. – Junior Researcher, National Medical Research Center for Oncology, Rostov-on-Don, onko-sekretar@mail.ru, http://orcid.org/0000-0002-1566-8906

Kaymakchi Oleg Yu. – Dr. Sci. (Med.)., Surgeon, Department of Abdominal Cancer No.2, National Medical Research Center for Oncology, Rostov-on-Don, onko-sekretar@mail.ru, http://orcid.org/0000-0002-7556-9897

Snezhko Aleksandr V. – Dr. Sci. (Med.), Surgeon, Department of Abdominal Cancer No.1 with a Group of X-ray Endovascular Methods of Diagnosis and Treatment, National Medical Research Center for Oncology, Rostov-on-Don, snezko.sania@yandex.ru, http://orcid.org/0000–0003–3998–8004

(✉) **Goncharova Anna S.,** fateyeva_a_s@list.ru

Received 03.02.2022;
approved after peer review 27.02.2022;
accepted 09.06.2022

УДК 616-006.6-085.28.065:616.1-02]-055.2
https://doi.org/10.20538/1682-0363-2022-4-44-53

Pharmacogenetics in treatment of anthracycline-induced cardiotoxicity in women without prior cardiovascular diseases

Grakova E.V.[1], Kopeva K.V.[1], Shilov S.N.[2], Berezikova E.N.[2], Popova A.A.[2], Neupokoeva M.N.[2], Ratushnyak E.T.[2], Kalyuzhin V.V.[3], Teplyakov A.T.[1]

[1] Cardiology Research Institute, Tomsk National Research Medical Center (NRMC), Russian Academy of Sciences
111a, Kievskaya Str., Tomsk, 634012, Russian Federation

[2] Novosibirsk State Medical University (NSMU)
1, Pirogova Str., Novosibirsk, 630091, Russian Federation

[3] Siberian State Medical University (SSMU)
2, Moscow Trakt, Tomsk, 634050, Russian Federation

ABSTRACT

Aim. To evaluate the role of polymorphisms in adrenoceptor beta 1 (*ADRB1*) (Arg389Gly, rs1801253) and angiotensin-converting enzyme (ACE) (I/D, rs4343) genes in assessing the effectiveness of β-blocker (carvedilol) and ACE inhibitor (enalapril) therapy in women with anthracycline-induced cardiotoxicity (AIC) without prior cardiovascular diseases (CVD) during 12-month follow-up.

Materials and methods. A total of 82 women (average age 45.0 (42.0; 50.0) years) with AIC and without prior CVD were included in the study. Echocardiography was performed and serum levels of NT-proBNP were determined at baseline and at 12 months after the enrollment. Gene polymorphisms in *ADRB1* and *ACE* genes were evaluated by polymerase chain reaction at baseline.

Results. Carriers of the G/G genotype in the *ADRB1* gene and G/G genotype in the *ACE* (I/D, rs4343) gene showed a significant increase in left ventricular ejection fraction (LVEF), a decrease in the size of the left ventricle (LV) and left atrium (LA), and a fall in the NT-proBNP level. Carriers of other genotypes had further progression of AIC which was manifested through a decrease in LVEF and an increase in the size of LV and LA.

Conclusion. Evaluation of gene polymorphisms in *ADRB1* (Arg389Gly, rs1801253) and *ACE* (I/D, rs4343) genes may be recommended before treatment initiation for AIC in women without prior CVD to determine who will benefit from carvedilol and enalapril therapy, as well as to identify a priority group of patients for personalized intensification and optimization of treatment for decreasing development of adverse cardiovascular events.

Keywords: anthracycline-induced cardiotoxicity, heart failure, gene polymorphisms, β-blocker, angiotensin-converting enzyme inhibitor

Conflict of interest. The authors declare the absence of obvious or potential conflicts of interest related to the publication of this article.

Source of financing. Basic research “Study of the mechanisms of structural and functional myocardial remodeling in different phenotypes in heart failure of ischemic and non-ischemic etiology” No. 122020300045-5.

Conformity with the principles of ethics. All patients signed an informed consent to participate in the study. The study was approved by the local Ethics Committee at Cardiology Research Institute of Tomsk NRMC.

For citation: Grakova E.V., Kopeva K.V., Shilov S.N., Berezikova E.N., Popova A.A., Neupokoeva M.N., Ratushnyak E.T., Kalyuzhin V.V., Teplyakov A.T. Pharmacogenetics in treatment of anthracycline-induced cardiotoxicity in women without prior cardiovascular diseases. *Bulletin of Siberian Medicine.* 2022;21(4):44–53. https://doi.org/10.20538/1682-0363-2022-4-44-53.

✉ *Kopeva Kristina V.,* Kristin-kop@inbox.ru

Фармакогенетика в лечении антрациклин-индуцированной кардиотоксичности у женщин без сопутствующих сердечно-сосудистых заболеваний

Гракова Е.В.[1], Копьева К.В.[1], Шилов С.Н.[2], Березикова Е.Н.[2], Попова А.А.[2], Неупокоева М.Н.[2], Ратушняк Е.Т.[2], Калюжин В.В.[3], Тепляков А.Т.[1]

[1] Научно-исследовательский институт (НИИ) кардиологии, Томский национальный исследовательский медицинский центр (НИМЦ) Российской академии наук
Россия, 634012, г. Томск, ул. Киевская, 111а

[2] Новосибирский государственный медицинский университет (НГМУ)
Россия, 630091, г. Новосибирск, Красный проспект, 52

[3] Сибирский государственный медицинский университет (СибГМУ)
Россия, 634050, г. Томск, Московский тракт, 2

РЕЗЮМЕ

Цель. Определить роль полиморфизмов генов β1-адренорецептора (*ADRB1*) (Arg389Gly, rs1801253) и ангиотензинпревращающего фермента (АПФ) (I/D, rs4343) в оценке эффективности терапии β-блокатором (карведилолом) и ингибитором АПФ (эналаприлом) у женщин с антрациклин-индуцированной кардиотоксичностью (АИК) и без сопутствующих сердечно-сосудистых заболеваний (ССЗ) в течение 12-месячного периода наблюдения.

Материалы и методы. В исследование включены 82 женщины в возрасте 45,0 (42,0; 50,0) лет с АИК и без ССЗ в анамнезе. Эхокардиографию и определение уровня NT-proBNP в сыворотке крови выполняли исходно и через 12 мес после включения в исследование. Оценку полиморфизмов генов *ADRB1* и *ACE* проводили с помощью полимеразной цепной реакции исходно.

Результаты. У носителей генотипа G/G гена *ADRB1* и генотипа G/G гена *ACE* (I/D, rs4343) диагностировано значительное увеличение фракции выброса левого желудочка (ФВ ЛЖ), уменьшение размеров ЛЖ и левого предсердия (ЛП), а также снижение уровней NT-proBNP. У носителей других генотипов наблюдалось дальнейшее прогрессирование АИК, что проявлялось снижением ФВ ЛЖ и увеличением размеров ЛЖ и ЛП.

Заключение. Оценка полиморфизмов генов *ADRB1* (Arg389Gly, rs1801253) и *ACE* (I/D, rs4343) может быть рекомендована до начала лечения АИК у женщин без ССЗ в анамнезе, чтобы определить, какие больные будут иметь преимущества от терапии карведилолом и эналаприлом, а также выделить приоритетную группу больных для персонифицированной интенсификации и оптимизации лечения с целью уменьшения развития неблагоприятных сердечно-сосудистых событий.

Ключевые слова: антрациклин-индуцированная кардиотоксичность, сердечная недостаточность, полиморфизмы генов, β-адреноблокатор, ингибитор ангиотензинпревращающего фермента

Конфликт интересов. Авторы декларируют отсутствие явных и потенциальных конфликтов интересов, связанных с публикацией настоящей статьи.

Источник финансирования. Фундаментальное научное исследование «Изучение механизмов структурного и функционального ремоделирования миокарда при разных фенотипах хронической сердечной недостаточности ишемической и неишемической этиологии» № 122020300045-5.

Соответствие принципам этики. Все пациенты подписали информированное согласие на участие в исследовании. Исследование одобрено локальным этическим комитетом НИИ кардиологии Томского НИМЦ.

Для цитирования: Гракова Е.В., Копьева К.В., Шилов С.Н., Березикова Е.Н., Попова А.А., Неупокоева М.Н., Ратушняк Е.Т., Калюжин В.В., Тепляков А.Т. Фармакогенетика в лечении антрациклин-индуцированной кардиотоксичности у женщин без сопутствующих сердечно-сосудистых заболеваний. *Бюллетень сибирской медицины.* 2022;21(4):44–53. https://doi.org/10.20538/1682-0363-2022-4-44-53.

INTRODUCTION

Anthracyclines are an important component of many chemotherapy regimens, but their use is associated with an increased risk of developing cardiotoxicity and heart failure (HF) [1]. As a result of the growing number of cancer survivors, the incidence of anthracycline-induced cardiotoxicity (AIC) is also increasing. However, neither optimal primary preventive strategies nor AIC-specific therapies have been developed for these patients [2]. Subclinical myocardial cell injury induced by anthracyclines is followed by asymptomatic left-sided heart failure and symptomatic HF, which can lead to irreversible cardiomyopathy. Although early AIC that develops in the first 12 months is often reversible, the late one involves a number of injuries that result in irreversible changes [3].

Treatment for patients with AIC currently includes standard therapies for congestive heart failure (HF) with ACE inhibitors, beta-blockers, and loop diuretics [4]. Enalapril and carvedilol are some of the main drugs for AIC treatment that appear effective in reducing the rates of left ventricular systolic dysfunction and preventing left ventricular ejection fraction (LVEF) decline in patients with AIC [2, 5, 6]. However, not all patients respond to therapy with these drugs. There are responders that have an increase in LVEF after the onset of congestive HF and non-responders that have no increase or even a decrease in LVEF despite receiving optimal drug therapy [7]. Genetic factors may be crucial in a patient's response to treatment and may help identify a subset of HP patients with AIC who might benefit from personalized intensification and optimization of treatment in order to reduce the development of adverse cardiovascular events [8].

Therefore, the aim of the study was to evaluate the role of polymorphisms in beta1-adrenoceptor (*ADRB1*) (Arg389Gly, rs1801253) and angiotensin-converting enzyme (ACE) (I/D, rs4343) genes in assessing the effectiveness of β-blocker (carvedilol) and ACE inhibitor (enalapril) therapy in women with anthracycline-induced cardiotoxicity (AIC) and without concomitant cardiovascular diseases (CVD) during a 12-month follow-up period.

MATERIALS AND METHODS

The study was conducted in accordance with the Declaration of Helsinki and was approved by the local Ethics Committee at Cardiology Research Institute, Tomsk National Research Medical Center. All patients signed an informed consent to participate in the study.

The study was prospective, observational, and single-center. A total of 82 women with AIC which developed 12 months after chemotherapy were enrolled in the study from February 2019 to February 2020.

Inclusion criteria were the following: 1) women with breast cancer who did not have a history of cardiovascular diseases and who developed AIC; 2) cancer treatment they received was either a combination of doxorubicin and cyclophosphamide (AC regimen), or a combination of doxorubicin, cyclophosphamide, and docetaxel (TAC regimen); 3) NT-proBNP levels ≥ 125 pg / ml; 4) breast cancer remission.

Criteria for the development of AIC included reduction of LVEF by ≥ 10 points from the baseline value or LVEF value of less than 55% with symptoms of HF and NT-proBNP levels ≥ 125 pg / ml 12 months after chemotherapy.

Exclusion criteria were the following: 1) type 1 and 2 diabetes mellitus; 2) coronary heart disease; 3) hypertension; 4) valve defects and prior cardiomyopathies of any etiology; 5) HF with an alternative cause of manifestation (severe lung diseases, primary pulmonary hypertension, anemia, body mass index > 50 kg / m^2); 6) previous treatment with any cardiovascular drugs, including ACE inhibitors and β-blockers; 7) concomitant severe renal or hepatic failure, or multiple organ dysfunction syndrome; 8) indications of poor drug tolerance; 9) chronic alcoholism or mental disorders; 10) ovarian pathology or hormonal imbalance.

Blood samples were obtained by venipuncture and adequate serum samples after centrifugation were stored at −24 °C with one freeze – thaw cycle. The serum levels of NT-proBNP were determined using an enzyme-linked immunosorbent assay (Biomedica Immunoassays, Austria).

Buccal epithelium was taken to determine gene polymorphisms. DNA was isolated from buccal epithelial cells using phenol - chloroform extraction. Genotyping of the *ADRB1* gene (polymorphism Arg389Gly, rs1801253) and I/D of the *ACE* gene (I/D, rs4343) was carried out by the real-time polymerase chain reaction.

The Hardy – Weinberg equilibrium was used to monitor genotyping results, testing was conducted using an online program on the website of the Institute of Human Genetics (http://ihg2.helmholtz-muenchen.de/cgi-bin/hw/hwa1.pl).

All patients received β-blocker (carvedilol) and ACE inhibitor (enalapril) therapies as AIC treatment. Drugs were titrated to the maximum tolerated dose. Given the fact that study participants were women without a history of cardiovascular diseases, the average up-titrated dose of carvedilol was 50 (25; 50) mg / day and that of enalapril was 10 (10; 20) mg / day.

An unfavorable course of AIC was defined as new or aggravating symptoms / signs of HF, reduction of LVEF by more than 5% 12 months after treatment initiation, or an increase in New York Heart Association (NYHA) class by 1 or more functional classes. Patients who did not meet these criteria had a favorable course of AIC.

Statistical processing of the results was carried out using Statistica 10.0 R software package version 2. Data were presented as the median and the interquartile range *Me* (Q_{25}; Q_{75}). To test statistical hypotheses, the Mann – Whitney test was used to analyze quantitative variables when comparing two groups. In the analysis of qualitative characteristics, the contingency tables were analyzed using the Pearson's χ2 test. If there were cells with an expected frequency of less than 5, then the two-sided Fisher's exact test or the Yates's correction was applied (for 2 × 2 tables). Odds ratios (OR) for gene polymorphisms were determined using logistic regression models. All *p* values were two-tailed. The differences were considered statistically significant at *p* value of 0.05 or less. Power calculation for the gene polymorphism test was 72.6%.

RESULTS

Initially, we examined a total of 303 women aged 45.0 (42.0; 50.0) years with breast cancer and without cardiovascular diseases and cardiovascular risk factors (LVEF of 67.0 (62; 70) %), who received chemotherapy. The cumulative dose of doxorubicin was 300–360 mg / m^2. 12 months after chemotherapy, 82 patients developed symptoms of HF (NYHA FC I0III) and had reduction of LVEF by 25.2%: from 65.5 (61; 70) to 49 (47; 52) %. These patients were included in the study, and for the treatment of AIC, they were prescribed carvedilol and enalapril at the maximum tolerated doses.

All patients were examined after 12 months of treatment and were divided into two groups: group 1 (n = 31) included patients with an unfavorable course of AIC, group 2 (n = 51) consisted of patients with a favorable course of the disease. Baseline demographic and clinical characteristics did not differ between the groups (Table 1). Baseline echocardiography parameters were also the same in both groups. However, 12 months after treatment initiation, in group 1, LVEF significantly ($p < 0.001$) decreased by 10.0% from 50 (47; 53) to 45 (44; 49) %; end-systolic diameter (ESD) increased by 3.0% ($p = 0.037$), end-diastolic diameter (EDD) rose by 4.0% ($p = 0.001$), left atrial (LA) size increased by 3.2% ($p = 0.001$), and 6-minute walk test (6MWT) distance decreased ($p = 0.046$) by 5.4%. In group 2, LVEF significantly ($p = 0.005$) increased by 6% from 49 (46; 51) to 52 (47; 55) %; the levels of NT-proBNP decreased by 22.5% ($p < 0.001$), and 6MWT distance increased ($p = 0.011$) by 11.6% (Table 2).

The presence of the C/G genotype in *ADRB1* rs1801253 (odds ratio (OR) = 2.01; $p = 0.004$) and the A/A genotype in *ACE* rs4343 (OR = 4.21; $p = 0.003$) was associated with further reduction of LVEF and progression of HF symptoms despite the therapy. The G/G genotype in the *ADRB1* rs1801253 gene (OR = 0.55; $p < 0.001$) and the G/G genotype in the *ACE* rs4343 gene (OR = 0.65; $p = 0.001$) were significantly associated with the improvement in HF symptoms and an increase in LVEF by 6%. Thus, patients with these genotypes may benefit from β-blocker (carvedilol) and ACE inhibitor (enalapril) therapy for AIC (Table 3).

No differences in echocardiography parameters and NT-proBNP levels were found at baseline and after 12 months of follow-up depending on NYHA functional class. The dynamics of the echocardiography parameters, NT-proBNP levels, and 6MWT distance during the follow-up were analyzed depending on polymorphisms in *ADRB1* (Arg389Gly, rs1801253) and *ACE* (I/D, rs4343) genes (Table 4). Women with the G/G genotype in the *ADRB1* gene (Arg389Gly, rs1801253) had the absolute benefit from carvedilol and enalapril therapies. In these patients, LVEF significantly ($p < 0.001$) increased by 10.7% from 50 (48; 51) to 56 (53; 57) %, ESD and EDD decreased by 5.8 ($p < 0.001$) and 6.0% ($p < 0.001$), respectively; LA size decreased by 9.7% ($p < 0.001$), 6MWT distance increased ($p = 0.008$) by 4.7%, and NT-proBNP decreased by 34.8% ($p < 0.001$). In carriers of the C/C and C/G genotypes, HF progressed further, which was manifested through a decrease in LVEF and an increase in LV and LA dimensions.

Women with the G/G genotype in the *ACE* (I/D, rs4343) gene benefited from carvedilol and enalapril therapies as well. In these patients, LVEF significantly ($p = 0.002$) increased by 7% from 50.5 (47; 51) to 54 (50; 57) %, ESD and EDD decreased by 5.3 ($p = 0.007$) and 3.0% ($p = 0.038$), respectively; LA size decreased

by 3.3% (p = 0.012), and NT-proBNP decreased by 20.4% (p = 0.007). In carriers of the A/A genotype, HF progressed further, which was manifested through a decrease in LVEF and an increase in LV dimensions, however, NT-proBNP levels tended to decrease by 20% (p = 0.052). Echocardiography parameters in patients with the A/G genotype in the *ACE* (I/D, rs4343) gene did not change, but NT-proBNP levels significantly decreased by 19.6% ($p < 0.001$).

Table 1

Clinical and demographic characteristics of patients at the time of inclusion in the study

Parameters	Group 1, n = 31	Group 2, n = 51	p
Age, years, *Me* (Q_{25}; Q_{75})	50 (47; 52)	48 (45; 50)	0.066
Body mass index, kg / m^2, *Me* (Q_{25}; Q_{75})	23.7 (21.3; 26.2)	24.3 (21; 26.3)	0.601
Heart rate, bpm, *Me* (Q_{25}; Q_{75})	75 (68; 83)	75 (69; 81)	0.825
Systolic blood pressure, mm Hg, *Me* (Q_{25}; Q_{75})	115 (110; 120)	115 (110; 120)	0.744
Diastolic blood pressure, mm Hg, *Me* (Q_{25}; Q_{75})	70 (70; 80)	75 (70; 80)	0.012
NYHA Class Class I, n (%) Class II, n (%) Class III, n (%)	 16 (51.6) 13 (41.9) 2 (6.5)	 26 (50.9) 20 (39.1) 5 (9.8)	 0.987 0.675 0.423
Smoking, n (%)	5 (16.1)	8 (15.7)	0.143
COPD, n (%)	4 (12.9)	7 (13.7)	0.981
Childbearing potential, n (%)	10 (32.2)	18 (35.3)	0.877
Menopause, n (%)	21 (67.8)	33 (64.7)	0.191
GFR, ml / min / m^2, *Me* (Q_{25}; Q_{75})	89 (78; 96)	88 (76; 98)	0.876
Six-minute walk test distance, m, *Me* (Q_{25}; Q_{75})	426 (349; 482)	426 (359; 472)	0.601
Total cholesterol, mg / dl, *Me* (Q_{25}; Q_{75})	93.6 (83.7; 102.6)	94.5 (84.6; 102.6)	0.882
LDL, mg / dl, *Me* (Q_{25}; Q_{75})	43.2 (39.6; 50.4)	43.2 (39.6; 50.5)	0.475
HDL, mg / dl, *Me* (Q_{25}; Q_{75})	41.44 (36.0; 42.2)	39.6 (36.0; 43.2)	0.323
Glucose, mmol / l, *Me* (Q_{25}; Q_{75})	5.3 (4.2; 6.1)	5.4 (4.1; 6.0)	0.541
Hemoglobin, g / l, *Me* (Q_{25}; Q_{75})	109.5 (100; 117)	109.5 (99; 117,5)	0.798
NT-proBNP, pmol / ml, *Me* (Q_{25}; Q_{75})	353.9 (265.4; 412.5)	317 (253; 372.9)	0.163

Note: GFR – glomerular filtration rate (CKD-EPI); HDL – high density lipoproteins; LDL – low density lipoproteins.

Table 2

Dynamics of echocardiography parameters, NT-proBNP levels, and 6-minute walk test distance during the follow-up period *Me* (Q_{25}; Q_{75})

Parameters	Before chemotherapy		p	12 months after chemotherapy (before carvedilol and enalapril treatment initiation)		p	12 months after carvedilol and enalapril treatment initiation		p
	Group 1, n = 31	Group 2, n = 51		Group 1, n = 31	Group 2, n = 51		Group 1, n = 31	Group 2, n = 51	
LVEF, %	67 (63; 70)	65 (60; 69)	0.119	50 (47; 53)	49 (46; 51)	0.117	45 (44; 49)#	52 (47; 55)#	<0.001
LA, mm	28 (26; 31)	28 (25.5; 31)		31 (29; 33)	31 (28; 32)	0.064	32 (30; 34)#	29 (27; 30)#	<0.001
EDD, mm	41 (39; 44)	42 (40; 44)	0.396	48 (45; 51)	50 (46; 51)	0.252	50 (48; 52)#	48 (47; 50)	0.005
ESD, mm	30 (27; 32)	29 (27; 30)	0.336	37 (34; 39)	36 (32; 38)	0.191	38 (37; 39)#	35 (32; 37)	<0.001
NT-proBNP, pg/ml	52.7 (45.9; 60.8)	51.1 (45; 61.9)	0.775	353.9 (265.4; 412.5)	317 (253; 372.9)	0.163	314.5 (259.3; 357.8)	245.6 (211.9; 276.8)#	<0.001
6-MWT distance, m	576 (552; 592)	575 (560; 589)	0.924	426 (349; 482)	426 (359; 472)	0.149	403 (341; 436)#	482 (375; 476)#	0.008

Note: here and in Table 4: 6-MWT – 6-minute walk test; LVEF – left ventricular ejection fraction; LA – left atrium; EDD – end-diastolic diameter; ESD – end-systolic diameter; NT-proBNP – N-terminal pro-B-type natriuretic peptide; # – statistically significant differences in comparison with the baseline levels.

Table 3

The frequency of genotypes, n, %, and odds ratio

Gene	Genotype	Group 1, *n* = 31	Group 2, *n* = 51	OR	95% confidence interval (CI)	χ2	*p*
ADRB1 (Arg389Gly, rs1801253)	C/C	10 (32.3)	11 (21.6)	0.98	0.87–1.12	1.16	0.282
	C/G	21 (67.7)	18 (35.3)	2.01	1.91–2.27	8.13	**0.004**
	G/G	0 (0.0)	22 (43.1)	0.55	0.18–1.11	18.27	<0.001
ACE (I/D, rs4343)	A/A	16 (51.5)	10 (19.6)	4.21	2.89–11.54	9.12	**0.003**
	A/G	14 (45.3)	24 (47.1)	0.98	0.9–1.13	0.04	0.867
	G/G	1 (3.2)	17 (33.3)	0.65	0.38–1.43	10.20	**0.001**

Table 4

Dynamics of echocardiography parameters, NT-proBNP levels, and 6-minute walk test distance during the follow-up period depending on gene polymorphisms in *ADRB1* (Arg389Gly, rs1801253) and ACE (I/D, rs4343) genes, *Me* (Q_{25}; Q_{75})

Parameters	12 months after chemotherapy (before carvedilol and enalapril treatment initiation)			*p*	12 months after carvedilol and enalapril treatment initiation			*p*
	ADRB1 (Arg389Gly, rs1801253)				*ADRB1* (Arg389Gly, rs1801253)			
	C/C, n = 21	C/G, n = 39	*G/G, n* = 22		C/C, *n* = 21	C/G, *n* = 39	G/G, *n* = 22	
LVEF, %	49 (47; 51)	49 (46; 53)	50 (48; 51)	0.859	48 (45; 49)#	46 (44; 49)#	56 (53; 57)#	<0.001
LA, mm	30 (29; 33)	31 (28; 33)	31 (29; 32)	0.431	31 (30; 33)#	31 (29; 33)	28 (27; 30)#	<0.001
EDD, mm	49 (45; 50)	48 (46; 52)	50 (48; 51)	0.377	49 (48; 51)#	48 (46; 52)#	47 (46; 48)#	<0.001
ESD, mm	35 (33; 38)	37 (33; 39)	34 (32; 37)	0.335	37 (35; 38)#	37 (36; 39)#	32 (31; 34)#	<0.001
NT-proBNP, pg/ml	324.8 (285.7; 394.7)	318.9 (259.7; 381.8)	327.5 (260.1; 387.5)	0.976	311.7 (248.9; 350.9)	276.8 (242.8; 337.8)#	213.55 (195.3; 256.7)#	<0.001
6-MWT distance, m	426 (359; 445)	433 (348; 488)	423 (364; 467)	0.667	403 (350; 418)#	430 (345; 476)	444 (402; 476)#	0.038
ACE (I/D, rs4343)				*p*	*ACE* (I/D, rs4343)			*p*
A/A, n = 26		A/G, n = 38	G/G, n = 18		A/A, n = 26	A/G, n = 38	G/G, n = 18	
LVEF, %	52 (47; 53)	48.5 (46; 51)	50.5 (47; 51)	0.052	48 (45; 50)#	47 (45; 51)	54 (50; 57)#	0.002
LA, mm	29 (27; 32)	31 (29; 33)	30 (29; 32)	0.125	32 (29; 33)#	32 (29; 33)	29 (27; 30)#	0.031
EDD, mm	49.5 (45; 50)	48 (46; 50)	50 (49; 52)	0.192	50 (48; 52)#	48 (47; 50)	48.5 (47; 50)#	0.116
ESD, mm	35.5 (33; 37)	36 (33; 39)	38 (34; 40)	0.237	37 (35; 38)#	36 (33; 38)	36 (32; 37)#	0.341
NT-proBNP, pg/ml	359.5 (265.4; 421.5)	321.1 (259.7; 387.5)	314.1 (279.6; 372.9)	0.678	287.6 (245.6; 350.9)	258 (214.7; 314.5)#	249.9 (195.3; 267.8)#	0.035
6-MWT distance, m	397 (335; 450)	433.5 (358; 482)	426 (378; 473)	0.252	397 (335; 432)	413.5 (376; 474)	449 (421; 487)	0.015

DISCUSSION

AIC largely develops due to doxorubicin-induced free radical formation through mitochondrial redox cycling of doxorubicin in cardiomyocytes, which ultimately leads to LV dysfunction and in the most severe cases – to irreversible congestive HF [4]. The clinical implications of this cardiotoxicity become more important with the increasing use of cardiotoxic drugs [9] and the growing number of cancer survivors, which leads to an increase in the incidence of AIC [3]. However, the optimal strategy for preventing and managing AIC requires further research. Various groups of drugs for AIC treatment and prevention are currently being investigated. ACE inhibitors and β-blockers slow down the progression of LV dysfunction in HF, but their effectiveness in AIC treatment is still controversial.

Oxidative stress as the main mechanism for the development and progression of AIC may also contribute to contractile LV dysfunction, cardiac remodeling, lethal arrhythmias, and sudden cardiac death. Several medications are known to have antioxidant effects, including some ACE inhibitors and β-blockers. Carvedilol is a non-selective β-blocker with antioxidant properties [10]. The results obtained in several studies indicate that carvedilol has a protective effect for primary prevention of AIC [2] and may inhibit its development even at low doses [11]. However, the CECCY (Carvedilol Effect in Preventing Chemotherapy Induced Cardiotoxicity) trial randomized 200 patients with breast cancer, who were to receive anthracyclines (doxorubicin 240 mg / m^2), to receive either carvedilol therapy or placebo for primary prevention. At 6 months, no difference

was found (carvedilol cohort = 14.5% vs. placebo = 13.5%; $p = 1.0$) in the frequency of AIC between the groups [12].

M. Guglin et al. studied 468 women with HER2-positive breast cancer receiving trastuzumab. The women were randomized to receive treatment with lisinopril, carvedilol, or placebo. No significant difference was found in the primary endpoint of AIC development (32% in the placebo group, 29% in the carvedilol group, and 30% in the lisinopril group) [13].

ACE inhibitors, such as enalapril, are another group of drugs with an antioxidant effect considered for AIC treatment and prevention. It was found that in patients with increased risk of AIC, defined by elevated troponin I values, early treatment with enalapril could prevent the development and progression of late cardiotoxicity [14]. In another study that investigated enalapril and candesartan against placebo, enalapril appeared to decrease the LV end-systolic wall stress, although it did not improve the maximum cardiac index according to exercise echocardiography [15].

D. Cardinale et al. showed that patients who were randomized to receive enalapril for primary prevention had lower incidence of cardiac events compared with the control group ($p < 0.001$) [16]. The randomized OVERCOME (Prevention of Left Ventricular Dysfunction with Enalapril and Carvedilol in Patients Submitted to Intensive Chemotherapy for the Treatment of Malignant Hemopathies) trial showed that combination therapy prevented LVEF reduction compared with the control group at 6 months ($p = 0.035$), but there was no difference in serious adverse events between the groups [17].

Based on all of the above, enalapril and carvedilol are among the main drugs for AIC treatment that appear effective in reducing the incidence rates of left ventricular systolic dysfunction and preventing reduction of LVEF in patients with AIC [2, 5]. However, not all patients respond to therapy with these drugs. There are responders that have an increase in LVEF after therapy initiation and non-responders in whom LVEF does not increase, but sometimes even decreases, despite optimal drug therapy [6]. Authors point out several reasons why some patients may not respond to therapy. Firstly, it may depend on the irreversibility of damage in AIC. Early type I toxicity is often reversible, late type II toxicity involves an injury cascade that leads to almost irreversible changes [3]. Since most studies include patients with early AIC, the benefits of carvedilol and enalapril for patients with type II AIC have not been established yet [12–14, 17]. Secondly, genetic factors may be crucial in a patient's response to treatment and may help identify a subset of HP patients with AIC who might benefit from personalized intensification and optimization of treatment in order to reduce the development of adverse cardiovascular events [7, 18].

This study assessed the impact of genetic factors (polymorphisms in the *ADRB1* gene (Arg389Gly, rs1801253) and *ACE* gene (I/D, rs4343)) on the effectiveness of β-blocker (carvedilol) and ACE inhibitor (enalapril) therapy in women with AIC and without prior cardiovascular diseases during a 12-month follow-up period. Beta-1 adrenergic receptors (AR) play a pivotal role in the regulation of the cardiovascular system. Changes in expression or properties of the beta-1 adrenoceptors may have phenotypic consequences affecting their cardiovascular or metabolic function or may contribute to the pathophysiology of disorders like hypertension, congestive HF, asthma or obesity [19]. Thus, assessing the beta-1 adrenoceptor genotype, may help predict responsiveness to β-blocker treatment in patients with ischemic HF: patients homozygous for the Arg389 beta-1-AR polymorphism should be good responders while patients homozygous for the Gly389 beta-1-AR polymorphism should be poor responders or non-responders [20, 21].

L.M. Baudhuin et al. showed that carriers of the G/G genotype should receive an increased dose of the drug to achieve a therapeutic effect in HF treatment [22]. Another study found no relationship between the genotypes of the Arg389Gly polymorphism in the *ADRB1* gene and the effectiveness of carvedilol therapy in 183 HF patients with ischemic or non-ischemic cardiomyopathy, and LVEF ≤ 35% [23]. The C/C genotype is associated with a significantly greater increase in LVEF during carvedilol therapy in patients with HF of non-ischemic etiology compared with the C/G or G/G genotypes in the *ADRB1* gene [24]. These differences in the pharmacogenetic efficacy of carvedilol in assessing the Arg389Gly polymorphism in the *ADRB1* gene in different studies indicate the need for further research. A combined assessment with the *CYP2D6* polymorphism, which affects the pharmacokinetic effects of the drug [25] and the dosage regimen of the drug, is also promising, even though R. Shihmanter et al. revealed that variations in the CYP2D6 genotype were not associated with a change in the carvedilol dose in HF patients [26].

In this study, we evaluated the impact of the Arg389Gly polymorphism in the *ADRB1* gene on the pharmacodynamic effects of carvedilol. Thus, women with the G/G genotype in the *ADRB1* gene (Arg389Gly, rs1801253) had the absolute benefit from carvedilol and enalapril therapies. In these patients, LVEF significantly ($p < 0.001$) increased by 10.7%; ESD and EDD decreased by 5.8 ($p < 0.001$) and 6.0% ($p < 0.001$), respectively; LA size decreased by 9.7% ($p < 0.001$), 6MWT distance increased by 4.7% ($p = 0.008$), and NT-proBNP levels decreased by 34.8% ($p < 0.001$). In patients with the C/C and C/G genotypes, HF progressed further, which was manifested through a decrease in LVEF and an increase in LV and LA dimensions. However, we found that patients with a further decrease in LVEF and progression of HF were rarely carriers of the G/G genotype, which does not contradict the literature data, according to which the G/G genotype is rare and may even be absent in the general population [27]. Therefore, there is a need for further observations regarding this genotype in patients with AIC.

In the general population, the *ACE* gene was found to be associated with cardiovascular diseases and multiple cardiovascular risk factors, although some studies did not reveal such associations [28]. Polymorphisms in the *ACE* gene are associated with a response to ACE inhibitor therapy, but researchers have not reached consensus as to which allele has a more pronounced effect. In this study, we established for the first time that women with the G/G genotype in the *ACE* gene (I/D, rs4343) benefited from carvedilol and enalapril therapies. In these patients, LVEF significantly ($p = 0.002$) increased by 7%, ESD and EDD decreased by 5.3 ($p = 0.007$) and 3.0% ($p = 0.038$), respectively; LA size decreased by 3.3% ($p = 0.012$), and NT-proBNP levels decreased by 20.4% ($p = 0.007$). Carriers of the A/A genotype had further progression of HF which manifested through a decrease in LVEF and an increase in LV dimensions, but NT-proBNP levels tended to decrease by 20% ($p = 0.052$). Echocardiography parameters in carriers of the A/G genotype in the *ACE* gene (I/D, rs4343) did not change, but NT-proBNP levels significantly decreased by 19.6% ($p < 0.001$), which was probably due to concomitant β-blocker therapy.

It should be noted that our data do not suggest that β -blocker and ACE inhibitor therapy should be withheld only when genetic analysis is not favorable. However, evaluating these genes may help identify a subset of HP patients with AIC and LV dysfunction who might benefit from personalized intensification and optimization of treatment in order to reduce the development of adverse cardiovascular events.

CONCLUSION

Our data suggest that evaluation of *ADRB1* (Arg389Gly, rs1801253) and *ACE* gene (I/D, rs4343) polymorphisms may be recommended prior to the initiation of AIC treatment in women without known history of CVDs to determine patients with AIC and left ventricular dysfunction who will benefit from intensification and optimization of treatment to reduce the development of adverse cardiovascular events. Carriers of the G/G genotypes in the *ADRB1* and *ACE* genes (I/D, rs4343) benefited from carvedilol and enalapril therapy.

RESEARCH LIMITATIONS

The main limitations of the study included the small sample of patients, short-term follow-up, and the absence of hard endpoints. Further studies are required to clarify the role of the *ADRB1* (Arg389Gly, rs1801253) and *ACE* genes (I/D, rs4343) in assessing the effectiveness of beta-adrenoceptor (carvedilol) and ACE inhibitor (enalapril) therapy in women with AIC.

REFERENCES

1. Teplyakov A.T., Shilov S.N., Popova A.A., Grakova E.V., Berezikova E.N., Neupokoeva M.N. et al. The cardiovascular system in patients with anthracycline cardiomiopathy. *Bulletin of Siberian Medicine.* 2017;16(3):127–136 (in Russ.). DOI: 10.20538/1682-0363-2017-3-127-136.
2. Kheiri B., Abdalla A., Osman M., Haykal T., Chahine A., Ahmed S. et al. Meta-Analysis of Carvedilol for the Prevention of Anthracycline-Induced Cardiotoxicity. *Am. J. Cardiol.* 2018;122(11):1959–1964. DOI: 10.1016/j.amjcard.2018.08.039.
3. McCune C., McGowan M., Johnston R., McCarthy A., Watson C., Dixon L. The prevalence of late anthracycline induced cardiotoxicity in survivors of childhood malignancy in Northern Ireland. *Heart.* 2019;105:A52. DOI: 10.1136/heartjnl-2019-ICS.64.
4. Volkova M., Russell R. Anthracycline cardiotoxicity: prevalence, pathogenesis and treatment. *Curr. Cardiol. Rev.* 2011;7(4):214–220. DOI: 10.2174/157340311799960645.
5. Janbabai G., Nabati M., Faghihinia M., Azizi S., Borhani S., Yazdani J. Effect of enalapril on preventing anthracycline-induced cardiomyopathy. *Cardiovasc. Toxicol.* 2017;17(2):130–139. DOI: 10.1007/s12012-016-9365-z.
6. Cardinale D., Colombo A., Lamantia G., Colombo N., Civelli M., De Giacomi G. et al. Anthracycline-induced cardiomyopathy: clinical relevance and response to pharmacologic therapy. *J. Am. Coll. Cardiol.* 2010;19;55(3):213–220. DOI: 10.1016/j.jacc.2009.03.095.

7. Aminkeng F., Ross C.J., Rassekh S.R., Hwang S., Rieder M.J., Bhavsar A.P. et al. CPNDS Clinical Practice Recommendations Group. Recommendations for genetic testing to reduce the incidence of anthracycline-induced cardiotoxicity. *Br. J. Clin. Pharmacol.* 2016;82(3):683–695. DOI: 10.1111/bcp.13008.
8. Elitok A., Oz F., Cizgici A.Y., Kilic L., Ciftci R., Sen F. et al. Effect of carvedilol on silent anthracycline-induced cardiotoxicity assessed by strain imaging: A prospective randomized controlled study with six-month follow-up. *Cardiol. J.* 2014;21(5):509–515. DOI: 10.5603/CJ.a2013.0150.
9. Bansal N., Adams M.J., Ganatra S., Colan S.D., Aggarwal S., Steiner R. et al. Strategies to prevent anthracycline-induced cardiotoxicity in cancer survivors. *Cardiooncology.* 2019;2;5:18. DOI: 10.1186/s40959-019-0054-5.
10. Book W.M. Carvedilol: a nonselective β blocking agent with antioxidant properties. *Congestive Heart Failure.* 2002;8:173–190. DOI: 10.1111/j.1527-5299.2002.00718.x.
11. Nabati M., Janbabai G., Baghyari S., Esmaili K., Yazdani J. Cardioprotective effects of carvedilol in inhibiting doxorubicin-induced cardiotoxicity. *J. Cardiovasc. Pharmacol.* 2017;69(5):279–285. DOI: 10.1097/FJC.0000000000000470.
12. Avila M.S., Ayub-Ferreira S.M., de Barros Wanderley M.R. et al. Carvedilol for Prevention of Chemotherapy-Related Cardiotoxicity: The CECCY Trial. *J. Am. Coll. Cardiol.* 2018;22;71(20):2281–2290. DOI: 10.1016/j.jacc.2018.02.049.
13. Guglin M., Krischer J., Tamura R., Fink A., Bello-Matricaria L., McCaskill-Stevens W. et al. Randomized Trial of Lisinopril Versus Carvedilol to Prevent Trastuzumab Cardiotoxicity in Patients With Breast Cancer. *J. Am. Coll. Cardiol.* 2019;11;73(22):2859–2868. DOI: 10.1016/j.jacc.2019.03.495.
14. Cardinale D., Colombo A., Sandri M.., Lamantia G., Colombo N., Civelli M. et al. Prevention of high-dose chemotherapy-induced cardiotoxicity in high-risk patients by angiotensin-converting enzyme inhibition. *Circulation.* 2006;5;114(23):2474–2481. DOI: 10.1161/CIRCULATIONAHA.106.635144.
15. Silber J.H., Cnaan A., Clark B.J., Paridon S.M., Chin A.J., Rychik J. et al. Enalapril to prevent cardiac function decline in long-term survivors of pediatric cancer exposed to anthracyclines. *J. Clin. Oncol.* 2004;1;22(5):820–828. DOI: 10.1200/JCO.2004.06.022.
16. Bosch X., Rovira M., Sitges M., Domènech A., Ortiz-Pérez J.T., de Caralt T.M. et al. Enalapril and carvedilol for preventing chemotherapy-induced left ventricular systolic dysfunction in patients with malignant hemopathies: the OVERCOME trial (preventiOn of left Ventricular dysfunction with Enalapril and caRvedilol in patients submitted to intensive ChemOtherapy for the treatment of Malignant hEmopathies). *J. Am. Coll. Cardiol.* 2013;11;61(23):2355–2362. DOI: 10.1016/j.jacc.2013.02.072.
17. Nazarenko M.S., Markov A.V., Sleptsov A.A. et al. Comparative analysis of gene expression in vascular cells of patients with advanced atherosclerosis. *Biomed. Khim.* 2018;64(5):416–442. DOI: 10.18097/PBMC20186405416.
18. Brodde O.E. Beta1- and beta2-adrenoceptor polymorphisms and cardiovascular diseases. *Fundam. Clin. Pharmacol.* 2008;22(2):107–125. DOI: 10.1111/j.1472-8206.2007.00557.x.
19. Baudhuin L.M., Miller W.L., Train L., Bryant S., Hartman K.A., Phelps M. et al. Relation of ADRB1, CYP2D6, and UGT1A1 polymorphisms with dose of, and response to, carvedilol or metoprolol therapy in patients with chronic heart failure. *Am. J. Cardiol.* 2010;1;106(3):402–408. DOI: 10.1016/j.amjcard.2010.03.041.
20. Metra M., Covolo L., Pezzali N., Zacà V., Bugatti S., Lombardi C. et al. Role of beta-adrenergic receptor gene polymorphisms in the long-term effects of beta-blockade with carvedilol in patients with chronic heart failure. *Cardiovasc. Drugs Ther.* 2010;24(1):49–60. DOI: 10.1007/s10557-010-6220-5.
21. Chen L., Meyers D., Javorsky G., Burstow D. et al. Arg-389Gly-beta1-adrenergic receptors determine improvement in left ventricular systolic function in nonischemic cardiomyopathy patients with heart failure after chronic treatment with carvedilol. *Pharmacogenet. Genomics*. 2007;17(11):941–949. DOI: 10.1097/FPC.0b013e3282ef7354.
22. Luzum J.A., Sweet K.M., Binkley P.F., Schmidlen T.J., Jarvis J.P., Christman M.F. et al. CYP2D6 genetic variation and beta-blocker maintenance dose in patients with heart failure. *Pharm. Res.* 2017;34(8):1615–1625. DOI: 10.1007/s11095-017-2104-8.
23. Shihmanter R., Nulman I., Goland S., Caspi A., Bar-Haim A., Harary I. et al. Variation in the CYP2D6 genotype is not associated with carvedilol dose changes in patients with heart failure. *J. Clin. Pharm. Ther.* 2014;39(4):432–438. DOI: 10.1111/jcpt.12154.
24. Katsarou M.S., Karathanasopoulou A., Andrianopoulou A., Desiniotis V., Tzinis E., Dimitrakis E. et al. Beta 1, Beta 2 and Beta 3 adrenergic receptor gene polymorphisms in a southeastern European population. *Front. Genet.* 2018;28;9:560. DOI: 10.3389/fgene.2018.00560.
25. Uemura K., Nakura J., Kohara K. Miki T. Association of ACE I/D polymorphism with cardiovascular risk factors. Hum Genet. 2000; 107(3):239-42. doi: 10.1007/s004390000358.
26. Niu T., Chen X., Xu X. Angiotensin converting enzyme gene insertion/deletion polymorphism and cardiovascular disease: therapeutic implications. *Drugs.* 2002;62(7):977–993. DOI: 10.2165/00003495-200262070-00001.

Authors information

Grakova Elena V. – Dr. Sci. (Med.), Leading Researcher, Department of Myocardial Pathology, Cardiology Research Institute, Tomsk NRMC, Tomsk, gev@cardio-tomsk.ru, http://orcid.org/0000-0003-4019-3735

Kopeva Kristina V. – Cand. Sci. (Med.), Researcher, Department of Myocardial Pathology, Cardiology Research Institute, Tomsk NRMC, Tomsk, Kristin-kop@inbox.ru, http://orcid.org/0000-0002-2285-6438

Shilov Sergey N. – Dr. Sci. (Med.), Associate Professor, Department of Pathological Physiology and Clinical Pathological Physiology, NSMU, Novosibirsk, newsib54@gmail.com, http://orcid.org/0000-0002-7777-6419

Berezikova Ekaterina N. – Dr. Sci. (Med.), Associate Professor, Department of Outpatient Therapy and General Medical Practice, NSMU, Novosibirsk, berezikova@ngs.ru, http://orcid.org/0000-0002-9630-0213

Popova Anna A. – Dr. Sci. (Med.), Head of the Department of Outpatient Therapy and General Medical Practice, NSMU, Novosibirsk, ann24@ngs.ru, http://orcid.org/0000-0003-2645-162X

Neupokoeva Maria N. – Teaching Assistant, Department of Outpatient Therapy and General Medical Practice, NSMU, Novosibirsk, maria.neupokoeva@mail.ru, http://orcid.org/0000-0003-3102-8156

Ratushnyak Elena T. – Teaching Assistant, Department of Outpatient Therapy and General Medical Practice, NSMU, Novosibirsk, lalala777elena@yandex.ru, http://orcid.org/0000-0002-4223-3457

Kalyuzhin Vadim V. – Dr. Sci. (Med.), Professor, Head of the Advanced Therapy Division with Rehabilitation Training, Physiotherapy and Sports Medicine, Siberian State Medical University, Tomsk.

Teplyakov Alexander T. – Dr. Sci. (Med.), Professor, Principal Researcher, Cardiology Research Institute, Tomsk NRMC, Tomsk, Vgelen1970@gmail.com, http://orcid.org/0000-0003-0721-0038

(✉) **Kopeva Kristina V.,** Kristin-kop@inbox.ru

Received 11.03.2022;
approved after peer review 05.07.2022;
accepted 08.09.2022

УДК 616.24-002.5-06:612.226:577.29
https://doi.org/10.20538/1682-0363-2022-4-54-62

Molecular mechanisms of inflammation in the pathogenesis of respiratory disorders in patients with pulmonary tuberculosis

Dyakova M.Ye.[1], Serebryanaya N.B.[2, 3, 4], Kiryukhina L.D.[1], Esmedlyaeva D.S.[1], Yablonskiy P.K.[1, 2]

[1] St. Petersburg State Research Institute of Phthisiopulmonology
2–4, Ligovsky Av., St. Petersburg, 191036, Russian Federation

[2] St. Petersburg University
7–9, Universitetskaya Emb., St. Petersburg, 199034, Russian Federation

[3] I.I.Mechnikov North-Western State Medical University
41, Kirochnaya Str., St. Petersburg, 191015, Russian Federation

[4] Institute of Experimental Medicine
12, Akademika Pavlova Str., St. Petersburg, 197376, Russian Federation

ABSTRACT

Aim. To assess external respiration (ER) and its relationship with the activity of enzymes involved in purine metabolism in patients with acute and chronic forms of pulmonary tuberculosis (TB).

Materials and methods. In patients with acute and chronic TB, we assessed the activity of adenosine deaminase (ADA)-1, 2 in the blood serum (eADA), mononuclear cells, and neutrophils, the concentration of ecto-5'-nucleotidase (eNT5E) in the blood serum, the level of CD26 (dipeptidyl peptidase-4, DPPIV) in the blood serum and mononuclear cells, production of reactive oxygen intermediates (ROI) and reactive nitrogen intermediates (RNI) in mononuclear cells and neutrophils, as well as parameters of ER.

Results. Patients with TB were found to have an increase in the concentration of eNT5E and eADA-2 activity in the blood serum, stimulated production of ROI in neutrophils, a decrease in the concentration of DPPIV (CD26) in mononuclear cells, and a fall in the production of RNI in mononuclear cells and neutrophils. In patients with chronic TB, a decrease in the activity of ADA-1 in mononuclear cells and a fall in the concentration of DPPIV (CD26) in the blood serum were noted. In patients with acute TB, a decrease in the activity of eADA-1 in the blood serum and ADA-1 in neutrophils, reduced production of ROI in mononuclear cells, and an increase in spontaneous production of ROI in neutrophils were revealed. Correlations were found between the parameters of ER and the concentration of eNT5E in the blood serum, spontaneous production of ROI in mononuclear cells and production of RNI in neutrophils in chronic TB, as well as between eADA-2 in the blood serum, ADA-1 in neutrophils, DPPIV (CD26) activity in mononuclear cells, and ROI and RNI production in mononuclear cells and neutrophils.

Conclusion. The data obtained make it possible to associate regulation of external respiration with parameters of purine metabolism, in particular with the concentration and activity of enzymes responsible for generation and metabolism of adenosine, that determine its level outside cells and inside mononuclear cells and neutrophils, with expression of cofactor molecules, as well as with the duration of activation of cells in innate immunity, neutrophils, and monocytes/ macrophages, determined largely by the potential of adenosine regulation.

Keywords: purine metabolism, inflammation, pulmonary tuberculosis, respiratory function

Conflict of interest. The authors declare the absence of obvious or potential conflicts of interest related to the publication of this article.

Source of financing. The authors state that they received no funding for the study.

✉ *Dyakova Marina Ye.,* marinadyakova@yandex.ru

Conformity with the principles of ethics. All patients signed an informed consent to participate in the study. The study was approved by the local Ethics Committee at St. Petersburg State Research Institute of Phthisiopulmonology (Protocol No. 57 of 11.09.2012).

For citation: Dyakova M.Ye., Serebryanaya N.B., Kiryukhina L.D., Esmedlyaeva D.S., Yablonskiy P.K. Molecular mechanisms of inflammation in the pathogenesis of respiratory disorders in patients with pulmonary tuberculosis. *Bulletin of Siberian Medicine.* 2022;21(4):54–62. https://doi.org/10.20538/1682-0363-2022-4-54-62.

Молекулярные механизмы воспаления в патогенезе нарушений внешнего дыхания у больных туберкулезом легких

Дьякова М.Е.[1], Серебряная Н.Б.[2, 3, 4], Кирюхина Л.Д.[1], Эсмедляева Д.С.[1], Яблонский П.К.[1, 2]

[1] Санкт-Петербургский научно-исследовательский институт фтизиопульмонологии (СПбНИИФ)
Россия, 191036, г. Санкт-Петербург, Лиговский проспект, 2-4

[2] Санкт-Петербургский государственный университет (СПбГУ)
Россия, 199034, г. Санкт-Петербург, Университетская наб., 7-9

[3] Северо-Западный государственный медицинский университет им. И.И. Мечникова (СЗГМУ им. И.М. Мечникова)
Россия, 191015, г. Санкт-Петербург, ул. Кирочная, 41

[4] Институт экспериментальной медицины (ИЭМ)
Россия, 197376, г. Санкт-Петербург, ул. Академика Павлова, 12

РЕЗЮМЕ

Цель. Оценить функцию внешнего дыхания и ее связь с активностью воспаления и активностью ферментов пуринового метаболизма у больных острой и хронической формой туберкулеза легких (ТЛ).

Материалы и методы. У больных острой (ОФТЛ) и хронической формой ТЛ (ХФТЛ) оценивали активность аденозиндезаминазы (ADA-1, 2) в сыворотке крови (eADA), мононуклеарах и нейтрофилах, концентрацию экто-5'-нуклеотидазы (eNT5E) в сыворотке крови, CD26 (дипептидилпептидазы-4, DPPIV) в сыворотке крови и мононуклеарах, продукцию активных форм кислорода (АФК) и азота (АФА) в мононуклеарах и нейтрофилах, функцию внешнего дыхания (ФВД).

Результаты. У больных ТЛ выявлено: увеличение концентрации eNT5E и активности eADA-2 в сыворотке крови, стимулированной продукции АФК нейтрофилами; снижение концентрации DPPIV (CD26) в мононуклеарах, продукции АФА мононуклеарами и нейтрофилами; при ХФТЛ снижение активности ADA-1 в мононуклеарах и концентрации DPPIV (CD26) в сыворотке крови; при ОФТЛ снижение активности eADA-1 в сыворотке крови, ADA-1 в нейтрофилах, продукции АФК мононуклеарами и увеличение спонтанной продукции АФК нейтрофилами. Выявлены корреляции между параметрами ФВД и концентрацией eNT5E в сыворотке крови, спонтанной продукцией АФК мононуклеарами, АФА нейтрофилами при ХФТЛ; активностью eADA-2 в сыворотке крови, ADA-1 в нейтрофилах, DPPIV (CD26) в мононуклеарах, продукцией АФК и АФА мононуклеарами и нейтрофилами.

Заключение. Полученные данные позволяют связать регуляцию внешнего дыхания с показателями пуринергического обмена, в частности с концентрацией и активностью ферментов, ответственных за образование и метаболизм аденозина, определяющих его уровень вне клеток и внутри мононуклеаров и нейтрофилов, с экспрессией кофакторных молекул, а также с длительностью активации клеток врожденного иммунитета, нейтрофилов и моноцитов/макрофагов, определяемой в значительной степени возможностями аденозиновой регуляции.

Ключевые слова: пуриновый метаболизм, воспаление, туберкулез легких, функция внешнего дыхания

Конфликт интересов. Авторы декларируют отсутствие явных и потенциальных конфликтов интересов, связанных с публикацией настоящей статьи.

Источник финансирования. Авторы заявляют об отсутствии финансирования при проведении исследования.

Соответствие принципам этики. Все пациенты подписали информированное согласие на участие в исследовании. Исследование одобрено независимым этическим комитетом Санкт-Петербургского научно-исследовательского института фтизиопульмонологии (протокол № 57 от 11.09.2012).

Для цитирования: Дьякова М.Е., Серебряная Н.Б., Кирюхина Л.Д., Эсмедляева Д.С., Яблонский П.К. Молекулярные механизмы воспаления в патогенезе нарушений внешнего дыхания у больных туберкулезом легких. *Бюллетень сибирской медицины.* 2022;21(4):54–62. https://doi.org/10.20538/1682-0363-2022-4-54-62.

INTRODUCTION

One third of the world's population is infected with *Mycobacterium tuberculosis (Mtb)*, and 10 million new cases of tuberculosis are registered annually [1–3]. In pulmonary tuberculosis (TB), granulomatous inflammation emerges, supported by a complex cascade of inflammatory signaling molecules – cytokines and autacoids, such as the purine nucleoside adenosine. Adenosine (ADO) regulates the activity, volume, duration, and resolution of the inflammatory response by changing the metabolism of involved cells through the activation of specific receptors (ADORA A_1, A_{2A}, A_{2B}, A_3), which are widely present on body cells [4].

ADO has been shown to have anti-inflammatory and tissue protective effects in acute inflammation, in particular, lung injury [5–7]. However, in chronic lung injury, ADO enhances proinflammatory and profibrotic processes [8].

During inflammation, ischemia, and cell death, the concentration of extracellular ADO increases. Stressed cells release adenosine triphosphate (ATP), which is gradually dephosphorylated to ADO by coordinated activity of ecto-nucleotidase, mainly ectonucleoside triphosphate diphosphohydrolase 1 (CD39, E-NTPDase1) and ecto-5'-nucleotidase (CD73, eNT5E). Extra- and intracellular ADO is deaminated by adenosine deaminase (ADA) or is transformed into adenosine monophosphate by the enzyme adenosine kinase [9].

ADA isoenzymes (ADA-1 and ADA-2) are key enzymes in purine rescue pathways and are essential in the regulation of purine metabolism [10]. ADA-1 is localized not only in the cytosol and nucleus of cells, but is also present as an "ecto" form on the cell membrane, where it forms complexes with dipeptidyl peptidase IV (CD26) and / or adenosine receptors A_1 and A_{2B} [11].

ADA-2 is localized mainly in the extracellular space, predominating in the blood serum. The main source of ADA-2 is macrophages / monocytes, in which both isoforms, ADA-1 and ADA-2, coexist [12]. With physiological concentrations of ADO, the catalytic activity of ADA-2 is close to zero; however, this isoform is effective for deamination at elevated levels of adenosine in a slightly acidic environment, for example, during hypoxia [13].

Since the purinergic regulation by ATP and ADO affects the functional state of cells in the respiratory and immune systems, the study of the molecular mechanisms of inflammation in the lung tissue can help understanding the pathogenesis of lung damage in patients with pulmonary TB and indicate new targets for targeted therapy, which is necessary to improve the effectiveness of treatment for pulmonary TB patients.

The aim of this study was to assess external respiration (ER) and its relationship with the activity of inflammation and expression and activity of enzymes involved in purine metabolism in patients with acute and chronic forms of pulmonary TB.

MATERIALS AND METHODS

The study included 60 patients with a verified diagnosis of pulmonary TB who were treated in the clinic of the St. Petersburg State Research Institute of Phthisiopulmonology. The group of patients with acute pulmonary TB (APTB) consisted of 15 patients with newly diagnosed infiltrative pulmonary tuberculosis, 6 men and 9 women aged 25.0–31.0 years (average age 29.0 years). A group of patients with chronic pulmonary TB (CPTB) encompassed 45 patients with fibrous – cavernous pulmonary TB, 30 men and 15 women aged 28.0–42.0 years (average age 32.0 years). All patients with pulmonary TB underwent a comprehensive study of the function of external respiration (ER). The exclusion criterion was chronic obstructive pulmonary disease. The control group (CG) included 20 practically healthy donors with comparable characteristics by sex and age.

The groups of patients with pulmonary TB significantly differed in the smoking status (smokers / non-smokers – 33.3 / 66.7% and 71.4 / 28.6%; $p = 0.01$) and disease duration (disease duration up to a year – 100.0 and 17.1%; $p = 0.00001$). Patients

with CPTB smoked 2 times more often and were ill for much longer.

Purine metabolism was assessed by the activity of adenosine deaminase-1 and 2 (ADA-1 and ADA-2) in the blood serum (eADA-1 and eADA-2) and mononuclear and neutrophil lysates (by triple freezing and thawing), determined by the ADA assay described by G. Giusti (1974) on a spectrophotometer PV 1251C (Belarus) as well as by concentrations of ecto-5'-nucleotidase (eNT5E) and CD26 (dipeptidyl peptidase-4, DPPIV) proteins (soluble form, sCD26 (DPPIV)) in the serum and mononuclear lysate by the enzyme-linked immunosorbent assay (ELISA) (Ecto NT5E, USCN, China and Human sCD26 Platinum ElISA, eBioscience, Austria).

Production of reactive oxygen species by phagocytes was assessed by respiratory burst parameters in the nitroblue tetrazolium test (NBT test): spontaneous NBT test (NBTs.) and zymosan-induced NBT test (NBTi).

Mononuclear cells (MNs) were isolated from peripheral blood using Ficoll – verografin density gradient centrifugation (1.077 g / l). From the remaining sediment (after erythrocyte lysis and additional centrifugation), neutrophils (NPHs) were isolated. Nitric oxide generation was determined by the level of nitrites (NO_2^-) and nitrates (NO_3^-) in MNs and NPHs by ELISA (R&D Systems, Canada).

A comprehensive study of the ER function included spirometry, body plethysmography, and a study of the diffusing capacity of the lungs using the MasterScreen Body Diffusion unit (VIASYS Healthcare, Germany) according to international recommendations for standardization of pulmonary function tests and the national guidelines for functional diagnostics [14–18]. We analyzed total lung capacity (TLC), vital capacity (VC), residual volume (RV), the RV / TLC ratio, inspiratory capacity (IC), expiratory reserve volume (ERV), and airway patency parameters, such as forced expiratory volume in 1 second (FEV_1) and the FEV_1 / forced vital capacity (FVC) ratio (the Tiffeneau – Pinelli index). Pulmonary gas exchange was assessed by diffusing capacity of the lungs (DLCO) and the carbon monoxide transfer coefficient – the DLCO to alveolar volume (DLCO / VA) ratio. To eliminate the influence of anthropometric characteristics, the values of parameters with due values (D) were expressed as percentage of D for the corresponding sex, height, body weight, and age. The due values proposed by the European Coal and Steel Community (1993) [19] were used as reference values.

The analysis of ER parameters in patients with APTB and CPTB revealed that the values of most functional characteristics were within the reference range, except for significantly reduced DLCO% (71.4 and 78.6% in patients with APTB and CPTB, respectively). Patients with pulmonary TB differed significantly only in the value of the Tiffeneau – Pinelli index, which was higher in the APTB group compared with the CPTB group (83.6 (75.9–85.7) and 76.5 (70.2–81.1), respectively, $p = 0.025$).

Statistical processing of the results was carried out using the Statistica software for Windows, version 13.0. Quantitative variables were presented as the median and the interquartile range *Me (LQ–UQ)*. Tests for homogeneity were performed for two samples using the Mann – Whitney *U* test. The Spearman's rank correlation coefficient was used in the correlation analysis of quantitative variables. The differences were considered statistically significant at $p < 0.05$.

RESULTS

Studying the parameters of purine metabolism in the examined patients with pulmonary TB revealed a significant increase in the concentration of eNT5E in the blood serum, which affects the production of ADO, and a decrease in the concentration of DPPIV (CD26) in mononuclear cell lysates, compared with the control group. It indicates a decrease in the expression of this protein on the membrane of these cells, which results in a decrease in its ability to form complexes with eADA-1 and impairs the immunoregulatory ability of monocytes in relation to T lymphocytes (Table 1). In patients with CPTB, the concentration of sCD26 (DPPIV) in the blood serum was also significantly reduced compared with the control group.

Table 1

Serum concentrations of enzymes involved in purine metabolism in patients with APTB and CPTB, *Me* (*LQ–UQ*)

Parameters	Groups		
	CG	APTB	CPTB
eNT5E, ng / ml	0.06 (0.01–0.6)	0.7 ($p = 0.006$) (0.46–1.3)*	0.9 ($p = 0.01$) (0.45–1.4)*
sDPPIV-(CD26), ng / ml	692.5 (625.0–875.0)	560.0 (550.0–585.0)	473.5 ($p = 0.04$) (265.0–628.2)*
DPPIV-(CD26) MN, ng /10^6 cells	19.2 (12.8–25.0)	1.46 ($p = 0.0004$) (1.03–3.0)*	3.95 ($p = 0.0008$) (1.2–6.6)*

Note: CG – control group, APTB – acute pulmonary TB, CPTB – chronic pulmonary TB, eNT5E – ecto-5'-nucleotidase, DPPIV (CD26) – dipeptidyl peptidase-4, sDPPIV(CD26) – its soluble form.
* the level of statistical significance of differences compared with the control group.

The activity of eADA-1 and eADA-2 in the blood serum (Fig. 1, *a*) in the groups of patients with pulmonary TB mainly changed in the same direction compared with the CG. A significant decrease in the eADA-1 activity was revealed in patients with APTB. For eADA-2, which main function is degradation of extracellular ADO, an increase in activity was recorded in both groups of patients with pulmonary TB. ADA-1 activity in the mononuclear cell lysate was lower in CPTB patients than in the CG. ADA-1 activity in the neutrophil lysate was lower in APTB patients compared with the CG. However, there were no differences in ADA-1 activity in mononuclear and neutrophil lysates in patients with APTB and CPTB ($p = 0.91$ and $p = 0.28$, respectively, Fig. 1, *b*).

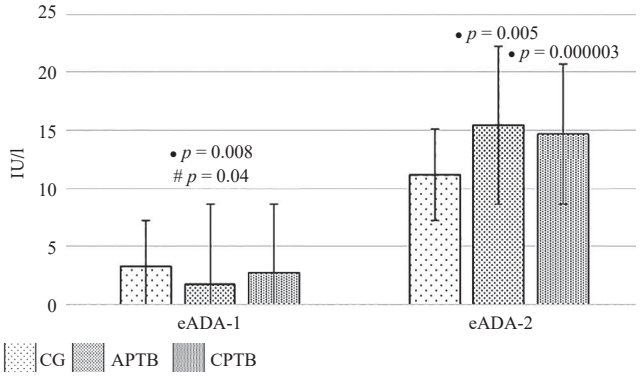

a

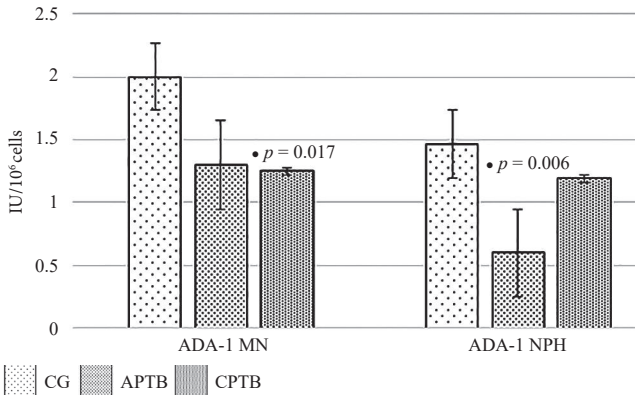

b

Fig. 1. Parameters of extracellular (*a*) and intracellular (*b*) activity of adenosine deaminase in groups of patients with APTB and CPTB and in the CG. Here and in Figures 2 and 3: CG – control group, APTB – acute pulmonary TB, CPTB – chronic pulmonary TB. eADA-1 and eADA-2 – activity of adenosine deaminase-1 and -2 in the blood serum, ADA-1 MN and NPH – activity of adenosine deaminase in mononuclear cells and neutrophils.

* level of statistical significance of differences compared with the control group, # level of statistical significance of differences between the groups; the level of significance is given in brackets.

Therefore, in both APTB and CPTB groups, the distribution of the activity of enzymes involved in purine metabolism and associated molecules indicates an increase in the concentration of extracellular ADO and a decrease in the immunoregulatory properties of cells of the immune system. At the same time, in patients with APTB, a significant decrease in eADA-1 activity provides conditions for a more pronounced increase in the ADO level and suppression of the function of monocytes and T lymphocytes.

Innate immune cells, such as monocytes, macrophages, and neutrophils, are known to play a key role in regulating the spread of *Mycobacterium tuberculosis (Mtb)* and the activity of tissue inflammation. The functional state of these cells can be assessed by their production of reactive oxygen species (ROS) and reactive nitrogen species (RNS).

The data presented in Figure 2 indicate that in both examined groups of patients with pulmonary TB, the production of ROS by neutrophils stimulated by bacteria was increased. It indicates a high degree of their activation. In the group of patients with APTB, spontaneous and stimulated production of ROS by mononuclear cells was significantly reduced compared with the CG. In patients with CPTB, stimulated production of ROS was reduced. It indicates significant impairment of the functional capabilities of these cells. At the same time, both spontaneous and stimulated ROS production by neutrophils in this group of patients was significantly higher than in the CG.

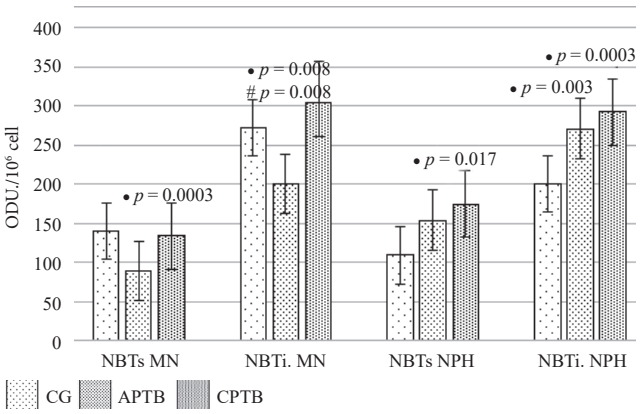

Fig. 2. Parameters of respiratory burst in groups of patients with APTB and CPTB and in the CG. Here and in Table 2: NBTs. MN, NPH and NBTi. MN, NPH – nitroblue tetrazolium test: spontaneous NBT test (NBTs.) and zymosan-induced NBT test (NBTi.) in mononuclear cells and neutrophils.

* level of statistical significance of differences compared with the control group, # level of statistical significance of differences between the groups; the level of significance is given in brackets.

An essential component for elimination of *Mtb* is RNS, which have a microbicidal effect against intracellular pathogens. The number of nitrite (NO_2^-) and nitrate (NO_3^-) radicals produced by mononuclear cells and neutrophils of TB patients was significantly reduced compared with the CG. At the same time, production of nitrite (NO_2^-) and nitrate (NO_3^-) radicals by neutrophils of the APTB patients was even more reduced than in the CPTB patients (Fig. 3). Neutrophils are actively involved in inflammation in pulmonary TB. Unlike activated macrophages, they do not produce a significant number of NO metabolites [20].

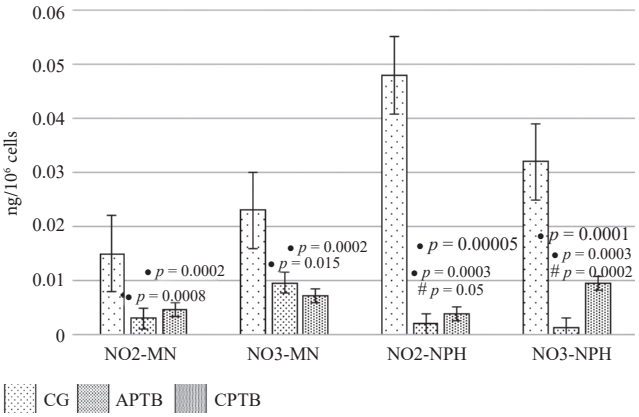

Fig. 3. Generation of RNS in groups of patients with APTB and CPTB and in the CG. Here and in Table 2: NO_2^- MN, NPH and NO_3^- MN and NPH are the levels of nitrites and nitrates in mononuclear cells and neutrophils.

* significant differences compared with the control group, # significant differences between the analyzed groups; the level of significance is given in brackets.

In general, the reduced production of NO metabolites by MNs and NPHs in patients with pulmonary TB impairs the immune response to *Mycobacterium tuberculosis*, and a more pronounced decrease in the production of NO metabolites by neutrophils, observed in patients with APTB, can be regarded as a more serious impairment of microbicidal functions, compared with patients with CPTB.

A revealed positive correlation ($r = 0.7$; $p = 0.037$) between the level of stimulated ROS production by neutrophils and the activity of intracellular ADA-1 in neutrophils indicates involvement of enzymes of purine metabolism in the regulation of phagocyte activity in patients with CPTB. Interestingly, for patients with APTB, a correlation of stimulated ROS production by neutrophils with the activity of intracellular ADA-1 in neutrophils was negative ($r = –0.4$; $p = 0.03$). Therefore, in patients with APTB, when neutrophils are activated, the level of intracellular ADO increases, which contributes to strong suppression of their functions.

The analysis of the relationship of abnormal ER parameters with the ability of phagocytes to produce ROS and RNS showed that in patients with CPTB, the parameters of static lung volumes (VC and ERV) and the DLCO /VA ratio, characterizing the gas exchange function of the lungs, were associated with spontaneous production of ROS by mononuclear cells and generation of nitrite and nitrate radicals by neutrophils ($r = –0.4$; $p = 0.04$, $r = –0.6$; $p = 0.04$, $r = –0.7$; $p = 0.01$, respectively). In patients with APTB, more correlations between phagocyte activity and ER parameters were revealed, which indicates greater tension in ER regulation [21].

The parameters of static lung volumes (TLC, VC, ERV, RV, RV / TLC ratio, IC), dynamic lung volumes, which characterize the airway patency (FEV_1, the Tiffeneau – Pinelli index), and DLCO, which characterizes the gas exchange function of the lungs, had significant correlations with spontaneous ROS production by mononuclear cells, spontaneous and induced ROS production by neutrophils, and generation of nitrate radicals by mononuclear cells and nitrite radicals by neutrophils (Table 2). Therefore, the revealed correlations confirm that the activation and dysfunction of neutrophils and mononuclear cells are associated with changes in the ER parameters in patients with pulmonary TB.

Table 2

Correlations between the respiratory burst parameters, nitric oxide metabolites, and external respiration parameters (correlation coefficient and its significance) in patients with acute pulmonary tuberculosis

Pairs of parameters		APTB
NBTs. MN	RV / TLC	0.7 (0.02)
	FEV_1	–0.6 (0.05)
NBTs. NPH	IC	–0.6 (0.01)
	TLC	–0.6 (0.04)
	DLCO	–0.7 (0.02)
NBTi. NPH	RV / TLC	0.6 (0.03)
	RV	0.6 (0.04)
NO_3^- MN	ERV	0.7 (0.02)
	IC	–0.7 (0.04)
	DLCO	–0.7 (0.02)
NO_2^- NPH	FEV_1 / FVC	0.7 (0.04)
	VC	–0.7 (0.03)

Note: TLC – total lung capacity, RV – residual volume, RV / TLC – their ratio, FEV_1 – forced expiratory volume in 1 second, IC – inspiratory capacity, DLCO – diffusing capacity of the lungs, ERV – expiratory reserve volume, VC – vital capacity, FEV_1 / FVC – the Tiffeneau – Pinelli index.

ADO plays an important role in modulating the activity of phagocytes and releasing microbicidal oxygen and nitrogen radicals. Our study showed that in CPTB, there is a significant correlation between the Tiffeneau – Pinelli index, which characterizes airway patency, and the serum concentration of eNT5E, an enzyme that synthesizes ADO ($r = 0.5$; $p = 0.02$).

In patients with APTB, positive correlations were revealed between the ER parameters (ERV, RV) and the activity of enzymes (eADA-2 in the blood serum, ADA-1 in neutrophils), which destroy ADO to cytoprotective inosine ($r = 0.7$; $p = 0.004$, $p = 0.04$, respectively). A decrease in the concentration of DPPIV (CD26) in mononuclear cells was negatively correlated with FEV_1 ($r = –0.7$; $p = 0.04$).

DISCUSSION

Fibrous – cavernous tuberculosis (FCTB) is defined as a chronic form of TB and an unfavorable outcome of untreated or ineffectively treated infiltrative TB. It should be noted that even after microbiological cure for pulmonary TB, 50% of patients still have post-tuberculous lung disease (PTLD) [22]. PTLD is caused by damage to the parenchyma, respiratory tract, blood vessels, and mediastinum, which determines pathomorphological changes in the organs. The cause of PTLD and its severity are associated with the influx of neutrophils and their excessive activity [23, 24].

Our data confirmed that in both examined groups of TB patients, neutrophils, indeed, produced an excess amount of ROS capable of damaging their own cells and intercellular structures (when the antioxidant system is depleted, which is typical of chronic inflammation). At the same time, the ability to produce NO metabolites important for microbicidal activity against mycobacteria was reduced both for neutrophils (more pronounced in patients with APTB) and for mononuclear cells in patients with pulmonary TB.

The results of our study showed that, judging by the activity of eNT5E, the level of ADO was equally increased in patients with pulmonary TB, regardless of the clinical form of the disease. In TB infection, at high levels of extracellular ADO, activated macrophages released eADA-2, which is a marker of the inflammatory response and the severity of the TB infection [25].

The regulatory effect of ADO on ER parameters (indirectly through the regulation of phagocyte activity) was confirmed by the revealed positive correlation between the activity of eADA-2 in the blood serum and ERV (a parameter characterizing the static lung volumes in patients with APTB). Another significant correlation was revealed between ADA-1 activity in neutrophils of patients with APTB (2.2 times lower than in the CG) and RV.

In patients with APTB, a decrease in intracellular ADA-1 activity can lead to a rise in the intracellular concentration of ADO, which determines an increase in the expression of P1 receptors, in particular, the low-affinity A_{2B} receptor, which stimulation inhibits inflammation and promotes tissue repair [4, 26]. When immune cells are activated at high levels of ADO, the expression of A_{2A}, A_{2B}, and A_3 receptors on macrophages increases, and their production of nitric oxide is inhibited [27]. Apparently, the differences in the duration of innate immune cell activation and their expression of P1 receptors determine the revealed multidirectional correlations between the intracellular activity of ADA-1 and the level of induced respiratory burst in neutrophils in APTB and CPTB.

Extracellular ADO not only regulates the inflammatory response, but also modulates the interaction between cells of innate and adaptive immunity. T. Hashikawa et al. (2006) showed that necrotic cells could become a source of eADA-1 during inflammation, which can subsequently form a complex with DPPIV (CD26). Our study revealed a decrease in the expression of DPPIV (CD26) by mononuclear cells (most pronounced in APTB) [28]. Apparently, a disruption of the monocyte – T lymphocyte interaction during decreased expression of DPPIV (CD26) by mononuclear cells and reduced activity of eADA-1 in the blood serum in patients with APTB caused impaired regulation of inflammation and a negative correlation between the level of DPPIV expression by mononuclear cells and FEV. The level of the soluble form of DPPIV in chronic diseases has been shown to inversely correlate with the severity of the disease, the severity of inflammation, and the prevalence of pulmonary fibrosis [29, 30].

In our study, a significantly reduced serum level of the soluble form of DPPIV (CD26) was registered in patients with CPTB. It caused a decrease in compensatory capabilities in the chronic course of the infectious and inflammatory process and explained the decrease in ER parameters that was found in patients with CPTB. At the same time, in patients with APTB, whose serum level of the soluble form of DPPIV was maintained within the reference values, the ER function was not impaired (measured parameters were within the reference values).

CONCLUSION

The data obtained make it possible to link the regulation of ER with the parameters of purine metabolism, in particular, with (1) the concentration and activity of enzymes that are responsible for the production and metabolism of ADO and that determine its level outside cells and inside mononuclear cells and neutrophils; (2) the expression of cofactor molecules; and (3) the duration of activation of innate immune cells, neutrophils, and monocytes / macrophages, affected to a large extent by ADO regulation potential. The revealed regularities make it possible to outline new approaches to modern diagnosis, prevention, and, possibly, treatment of developing respiratory failure in patients with pulmonary TB.

REFERENCES

1. Global tuberculosis report 2020. Geneva: World Health Organization. URL: https://www.who.int/tb/publications/global_report/en/ (accessed on 20.10.2020).
2. Voronchikhin T.A., Avetisyan A.O., Vasil'ev I.V., Kudryashov G.G., Yablonskiy P.K. The outcomes of complex treatment of limited fibrocavernous pulmonary tuberculosis. *Medical Alliance*. 2018;3:56–64 (in Russ.).
3. Bagishcheva N.V., Mordyk A.V., Gol'tyapin V.V. Predicting the outcomes of tuberculosis treatment in patients with chronic obstructive pulmonary disease. *Medical Alliance*. 2019;1:13–19 (in Russ.).
4. Antonioli L., Csóka B., Fornai M., Colucci R., Kókai E., Drandizzi C. et al. Adenosine and inflammation: what's new on the horizon? *Drug Discov. Today.* 2014;19(8):1051–1068. DOI: 10.1016/j.drudis.2014.02.010.
5. Ohta A., Sitkovsky M. Role of G-protein-coupled adenosine receptors in down-regulation of inflammation and protection from tissue damage. *Nature.* 2001;414(6866):916–920. DOI: 10.1038/414916a.
6. Rivo J., Zeira E., Galun E., Matot I. Activation of A3 adenosine receptors attenuates lung injury after *in vivo* reperfusion. *Anesthesiology*. 2004;101(5):1153–1159. DOI: 10.1097/00000542-200411000-00015.
7. Day Y.J., Marshall M.A., Huang L., McDuffie M.J., Okusa M.D., Linden J. Protection from ischemic liver injury by activation of A2A adenosine receptors during reperfusion: inhibition of chemokine induction. *Am. J. Physiol*. 2004;286(2):285–293. DOI: 10.1152/ajpgi.00348.203.
8. Chunn J.L., Molina J.G., Mi T., Xia Y., Kellems R.E., Blackburn M.R. Adenosine-dependent pulmonary fibrosis in adenosine deaminase-deficient mice. *The Journal of Immunology*. 2005;175(3):1937–1946. DOI: 10.4049/jimmunol.175.3.1937.
9. Antonioli L., Fornai M., Colucci R., Ghisu N., Tuccori M., Del Tacca M. et al. Pharmacological modulation of adenosine system: novel options for treatment of inflammatory bowel diseases. *Inflamm. Bowel. Dis.* 2008;14(4):566–574. DOI: 10.1002/ibd.20316.
10. Cristalli G., Costanzi S., Lambertucci C., Lupidi G., Vittori S., Volpini R. et al. Adenosine deaminase: functional implications and different classes of inhibitors. *Medicinal Research Reviews*. 2001;21(2):105–128. DOI: 10.1002/1098-1128(200103)21:2<105::aid-med1002>3.0.co;2-u
11. Gakis C. Adenosine deaminase (ADA) isoenzymes ADA1 and ADA2: diagnostic and biological role. *Eur. Respir. J.* 1996;9(4):632–633. DOI: 10.1183/09031936.96.09040632.
12. Zavialov A.V., Gracia E., Glaichenhaus N., Franco R., Zavialov A.V., Lauvau G. Human adenosine deaminase 2 induces differentiation of monocytes into macrophages and stimulates proliferation of t helper cells and macrophages. *J. Leukoc. Biol.* 2010;88(2):279–290. DOI: 10.1189/jlb.1109764.
13. Watanabe N., Gao S., Kajigaya S., Diamond C., Alemu L., Ombrello A. et al. Analysis of deficiency of adenosine deaminase 2 pathogenesis based on single cell RNA sequencing of monocytes. *J. Leukoc. Biol.* 2021;110(3):409–424. DOI: 10.1002/JLB.3HI0220-119.
14. Giusti G. Adenosine deaminase. Methods of enzymatic analysis. H. Bergmeyer (ed.). New York: Academic Press, 1974;2:1092–1099.
15. Miller M.R., Hankinson J., Brusasco V., Burgos F., Casaburi R., Coates A. et al. Standardisation of spirometry. *Eur. Respir. J.* 2005;26(2):319–338. DOI: 10.1183/09031936.05.00034805.
16. Wanger J., Clausen J.L., Coates A., Pedersen O.F., Brusasco V., Burgos F. et al. Standardisation of the measurement of lung volumes. *Eur. Respir. J.* 2005;26(3):511–522. DOI: 10.1183/09031936.05.00035005.
17. Graham B.L., Brusasco V., Burgos F., Cooper B.C., Jensen R., Kendrick A. et al. 2017 ERS/ATS standards for single-breath carbon monoxide uptake in the lung. *Eur. Respir. J.* 2017;49(1):1600016. DOI: 10.1183/13993003.00016-2016.
18. Functional diagnostics of the state of external respiration. Functional diagnostics: national guidelines. Edited by N.F. Beresten', V.A. Sandrikov, S.I. Fedorova. M.: GEOTAR-Media, 2019:566–645 (in Russ.).
19. Quanjer P.H., Tammeling G.J., Cotes J.E., Pedersen O.F., Peslin R., Yennauft J.-C. Lung volumes and forced ventilatory flows. Report Working Party Standardization of Lung Function Tests, European Community for Steel and Coal. Official Statement of the European Respiratory Society. *Eur. Respir. J.* 1993;6:5–40. URL: https://erj.ersjournals.com/content/erj/6/Suppl_16/5.full.pdf.
20. Mishra B.B., Lovewell R.R., Olive A.J., Zhang G., Wang W., Eugenin E. et al. Nitric oxide prevents a pathogen-permissive granulocytic inflammation during tuberculosis. *Nat. Microbiol.* 2017;2:17072. DOI: 10.1038/nmicrobiol.2017.72.
21. Lebedev K.A., Ponyakina I.D. Immunogram in clinical practice. *M., Science*, 1990:224 (in Russ.).
22. Chushkin M.I., Ots O.N. Impaired pulmonary function after treatment for tuberculosis: the end of the disease? *J. Bras. Pneumol.* 2017;43(1):38–43. DOI: 10.1590/s1806-37562016000000053.
23. Gopal R., Monin L., Torres D., Slight S., Mehra S., McKenna K.C. et al. S100A8/A9 proteins mediate neutrophilic inflammation and lung pathology during tuberculosis. *Am. J. Respir. Crit. Care Med*. 2013; 188(9):1137–1146. DOI: 10.1164/rccm.201304-0803OC.
24. Panteleev A.V, Nikitina I.Y., Burmistrova I.A., Kosmiadi G.A., Radaeva T.V., Amansahedov R.B. et al. Severe tuberculosis in

humans correlates best with neutrophil abundance and lymphocyte deficiency and does not correlate with antigen-specific CD4 T-cell response. *Front. Immunol*. 2017;8:963. DOI: 10.3389/fimmu.2017.00963.
25. Zavialov A.V., Gracia E., Glaichenhaus N., Franco R., Zavialov A.V., Lauvau G. Human adenosine deaminase 2 induces differentiation of monocytes into macrophages and stimulates proliferation of T helper cells and macrophages. *J. Leukoc. Biol.* 2010;88(2):279–290. DOI: 10.1189/jlb.1109764.
26. Sun Y., Huang P. Adenosine A2B Receptor: from cell biology to human diseases. *Front. Chem.* 2016;4:37. DOI: 10.3389/fchem.2016.00037.
27. Antonioli L., Fornai M., Blandizzi C., Pacher P., Haskó G. Adenosine signaling and the immune system: When a lot could be too much. *Immunology Letters*. 2019;205:9–15. DOI: 10.1016/j.imlet.2018.04.006.
28. Hashikawa T., Takedachi M., Terakura M., Yamada S., Thompson L.F., Shimabukuro Y., Murakami I. Activation of adenosine receptor on gingival fibroblasts. *J. Dent. Res.* 2006;85(8):739–744. DOI: 10.1177/154405910608500810.
29. Tamaki Z., Kubo M., Yazawa N., Mimura Y., Ashida R., Tomita M. et al. Serum levels of soluble CD26 in patients with scleroderma. *J. Dermatol. Sci.* 2008;52(1):67–69. DOI: 10.1016/j.jdermsci.2008.05.004.
30. Somborac-Bačura A., Buljević S., Rumora L., Čulić O., Detel D., Pancirov D. et al. Decreased soluble dipeptidyl peptidase IV activity as a potential serum biomarker for COPD. *Clin. Biochem*. 2012;45(15):1245–1250. DOI: 10.1016/j.clinbiochem.2012.04.023.

Authors contribution

Dyakova M.Ye. – conception and design, carrying out of the biochemical studies, analysis and interpretation of the data, drafting of the article, critical revision of the manuscript for important intellectual content. Serebryanaya N.B. – drafting and editing of the manuscript, critical revision of the manuscript for important intellectual content. Kiryukhina L.D. – carrying out and assessment of the comprehensive study of the external respiration. Esmedlyaeva D.S. – carrying out of the biochemical studies. Yablonskiy P.K. – final approval of the manuscript for publication.

Authors information

Dyakova Marina Ye. – Cand. Sci. (Biology), Senior Researcher, Research Institute of Phthisiopulmonology, St. Petersburg, marinadyakova@yandex.ru, http://orcid.org/0000-0002-7810-880X

Serebryanaya Natalia B. – Dr. Sci. (Med.), Professor, Head of the Laboratory for General Immunology, Institute of Experimental Medicine; Professor, Division of Cytology and Histology, Biology Department, St. Petersburg University; Professor, Department of Clinical Mycology, Allergology, and Immunology, I. I. Mechnikov North-Western State Medical University, St. Petersburg, nbvma@mail.ru, http://orcid.org/0000-0002-2418-9368

Kiryukhina Larisa D. – Cand. Sci. (Med.), Leading Researcher, Head of the Department of Functional Diagnostics, Research Institute of Phthisiopulmonology, St. Petersburg, kiryuhina_larisa@mail.ru, http://orcid.org/0000-0001-6550-817X

Esmedlyaeva Dilyara S. – Cand. Sci. (Biology), Senior Researcher, Research Institute of Phthisiopulmonology, St. Petersburg, diljara-e@yandex.ru, http://orcid.org/0000-0002-9841-0061

Yablonskiy Peter K. – Dr. Sci. (Med.), Professor, Director of the Research Institute of Phthisiopulmonology; Dean of the Medical Department, St. Petersburg University, St. Petersburg, piotr_yablonskii@mail.ru, http://orcid.org/0000-0003-4385-9643

(✉) **Dyakova Marina Ye.,** marinadyakova@yandex.ru

Received 14.12.2021;
approved after peer review 14.04.2022;
accepted 09.06.2022

УДК 577.1.08:611.36.018:615.37:616-089.943
https://doi.org/10.20538/1682-0363-2022-4-63-71

Local biocompatibility and biochemical profile of hepatic cytolysis in subcutaneous implantation of polylactide matrices

Ivanova E.A., Dzyuman A.N., Dvornichenko M.V.

Siberian State Medical University
2, Moscow Trakt, Tomsk, 634050, Russian Federation

ABSTRACT

The aim of the study was to investigate local biocompatibility and systemic effects of nonwoven polylactide (PLA) matrices on blood and liver parameters after their subcutaneous implantation in Wistar rats.

Materials and methods. Bioabsorbable fibrous PLA matrices were produced by electrospinning and had dimensions (10 × 10 mm², thickness of no more than 0.5 mm; fiber diameter in the matrix ~1 μm) appropriate for subcutaneous implantation in white laboratory rats. Polymer implants were sterilized in ethylene oxide vapor. Thirty days after the implantation of PLA matrices, local biocompatibility according to GOST ISO 10993-6-2011, cellular parameters (total leukocyte count, hemogram, erythrocyte count, hemoglobin concentration), and biochemical blood parameters (lactate concentration, alanine aminotransferase (ALT) and aspartate aminotransferase (AST) levels) were studied, and a standard histologic evaluation of the liver was performed.

Results. PLA matrix samples were mild local irritants on a scale of 1–1.9 points according to GOST ISO 10993-6-2011 criteria 30 days after the subcutaneous implantation. The median density of distribution of multinucleated giant cells (MNGCs) in the connective tissue around and in PLA matrices was 1,500 (1,350; 1,550) per 1 mm^2 of a slice. Pronounced leukocytic reaction due to lymphocytosis was noted (an increase by 1.7 times compared with a sham-operated (SO) control group, $p < 0.02$). The absence of a significant neutrophil count in the blood revealed sterile inflammation proceeding in the subcutaneous tissue around the PLA materials. Normalization of hepatic cytolysis markers (ALT and AST activity) in the blood without pronounced changes in the structure of the liver and the number of binuclear hepatocytes was noted. These markers were increased in SO controls (ALT up to 123% and AST up to 142%, $p < 0.001$ compared with values in the intact group).

Conclusion. Nonwoven PLA matrices are biocompatible with subcutaneous tissue, undergo bioresorption by MNGCs, and have a distant protective effect on the functional state of the liver in laboratory animals. Hypotheses on the detected systemic effect during subcutaneous implantation of PLA matrices were discussed; however, specific mechanisms require further study.

Keywords: nonwoven PLA matrix, rats, blood serum, alanine transaminase, aspartate transaminase, blood cells, binuclear hepatocytes

Conflict of interest. The authors declare the absence of obvious or potential conflict of interest related to the publication of this article.

Source of financing. The study was supported by Siberian State Medical University development program "Priority 2030".

Conformity to the principles of ethics. The study was approved by the local Ethics Committee at Siberian State Medical University (Protocol No. 7693/1 of 30.09.2019).

For citation: Ivanova E.A., Dzyuman A.N., Dvornichenko M.V. Local biocompatibility and biochemical profile of hepatic cytolysis in subcutaneous implantation of polylactide matrices. *Bulletin of Siberian Medicine.* 2022;21(4):63–71. https://doi.org/10.20538/1682-0363-2022-4-63-71

✉ *Dvornichenko Marina V.,* dochic@yandex.ru

Местная биосовместимость и биохимические маркеры цитолиза гепатоцитов при подкожной имплантации полилактидных матриц

Иванова Е.А., Дзюман А.Н., Дворниченко М.В.

Сибирский государственный медицинский университет (СибГМУ)
Россия, 634050, г. Томск, Московский тракт, 2

РЕЗЮМЕ

Цель. Исследование местной биосовместимости и системных эффектов нетканых полилактидных (PLA) матриксов на показатели крови и печени после подкожной имплантации крысам стока Wistar.

Материалы и методы. Биодеградируемые волокнистые PLA матриксы изготовлены методом электроспиннинга, имели размеры (10 × 10 мм^2, толщина не более 0,5 мм; диаметр волокон в матриксе ~1 мкм), пригодные для подкожного введения белым лабораторным крысам. Полимерные изделия стерилизовали в парах этиленоксида. Через 30 сут после имплантации PLA матриксов изучены местная биосовместимость согласно ГОСТ ISO 10993-6-2011, клеточные (общее количество лейкоцитов, гемограмма, число эритроцитов, концентрация гемоглобина) и биохимические показатели крови (концентрация лактата, активность аланинаминотрансферазы (АЛТ) и аспартатаминотрансферазы (АСТ)), определена стандартная гистологическая оценка состояния печени. Проведены компьютерная морфометрия цифровых изображений гистологических срезов и статистическая обработка результатов.

Результаты. Образцы PLA матрикса являлись легкими местными раздражителями в шкале 1–1,9 балла согласно критериям ГОСТ ISO 10993-6-2011 через 30 сут после подкожной имплантации. Медианная плотность распределения гигантских многоядерных клеток инородных тел (ГМКИТ) в соединительной ткани вокруг и в структуре PLA матриксов составила 1 500 (1 350; 1 550) на 1 мм^2 среза. Имела место выраженная лейкоцитарная реакция крови, обусловленная лимфоцитозом (в 1,7 раза по сравнению с ложнооперированным (ЛО) контролем, $p < 0,02$). Отсутствие значительного нейтрофилеза крови свидетельствовало об асептическом характере воспаления, протекающего в подкожной клетчатке вокруг PLA материалов. В крови отмечена нормализация маркеров цитолиза гепатоцитов (активности АЛТ и АСТ), повышенных у ЛО животных (АЛТ – до 123% и АСТ – до 142%, $p < 0,001$ в сравнении с интактными значениями), без выраженных изменений структуры печени и числа двуядерных гепатоцитов.

Заключение. Нетканые PLA матриксы биосовместимы с подкожной клетчаткой, подвергаются биорезорбции ГМКИТ, обладают дистантным протекторным действием на функциональное состояние печени у лабораторных животных. Обсуждены гипотезы обнаруженного системного эффекта при подкожной имплантации PLA матриц. Однако конкретные механизмы требуют дальнейшего изучения.

Ключевые слова: нетканый матрикс из полимолочной кислоты, крысы, сыворотка крови, аланинаминотрансфераза, аспартатаминотрансфераза, клетки крови, двуядерные гепатоциты

Конфликт интересов. Авторы декларируют отсутствие явных и потенциальных конфликтов интересов, связанных с публикацией настоящей статьи.

Источник финансирования. Исследование выполнено в рамках Программы стратегического академического лидерства «Приоритет – 2030».

Соответствие принципам этики. Исследование одобрено локальным этическим комитетом СибГМУ (протокол № 7693/1 от 30.09.2019).

Для цитирования: Иванова Е.А., Дзюман А.Н., Дворниченко М.В. Местная биосовместимость и биохимические маркеры цитолиза гепатоцитов при подкожной имплантации полилактидных матриц. *Бюллетень сибирской медицины.* 2022;21(4):63–71. https://doi.org/10.20538/1682-0363-2022-4-63-71.

INTRODUCTION

Polylactic acid (polylactide, PLA) is one of the synthetic biodegradable polymers consisting of analogs of natural monomers. It is actively used in various applications of tissue engineering [1] as implants [2], as well as in the form of matrices for drug and cell delivery [3].

PLA materials are approved for clinical use. The surface of nonwoven fibrous matrices makes it possible to use various methods of loading and release of significant concentrations of drugs and biological

molecules [4]. However, the accumulation of lactate, which depends on the rate of PLA degradation, can provoke local inflammation and/or systemic toxicity [5].

Electrospinning is a fast growing technology for obtaining nonwoven fibrous scaffolds made of nanosized interconnected fibers (5 nm – 1 μm in diameter) that form microsized (~100 μm) interconnected pores [6, 7]. Thereby their architecture allows to reproduce to a certain extent the structure of the natural extracellular matrix in various biological tissues. On the other hand, a large surface area at low density [6] promotes increased biodegradation of fibrous PLA materials [8] with the release of high doses of lactic acid, which can result in adverse events masking or eliminating the therapeutic effect of cells and drug and biological molecules immobilized on the implant.

Therefore, the aim of the study was to research local biocompatibility and systemic effects of nonwoven PLA matrices on blood and liver parameters after subcutaneous implantation in Wistar rats.

MATERIALS AND METHODS

The experimental study was conducted *in vivo* on 20 mature white male Wistar rats weighing 280–300 g. The animals were kept in standard vivarium conditions in the Laboratory of Biological Models at Siberian State Medical University (Tomsk) and received a standard diet. The study was carried out in compliance with the principles of the European Convention for the Protection of Vertebrate Animals used for Experimental and other Scientific Purposes (Strasbourg, 1986).

Nonwoven PLA matrices (10 × 10 mm^2, thickness of no more than 0.5 mm; average fiber diameter in the matrix ~1 μm) obtained in Tomsk Polytechnic University using electrospinning as described earlier [8] were used as test products. The raw material was poly(DL-lactide) PURASORB (Corbion, Netherlands). Nonwoven PLA matrices were sterilized in 100% ethylene oxide vapor at 37 ˚C for 9 hours in the 3M Steri-Vac Sterilizer/Aerator gas sterilizer (3M, USA) according to ISO 11135-2017 (Sterilization of healthcare products. Ethylene oxide. Requirements for the development, validation, and routine control of a sterilization process for medical devices).

PLA matrices were injected subcutaneously through a median abdominal incision and a formed lateral subcutaneous pocket in 10 rats under CO_2 anesthesia (1 matrix per animal) as described earlier [9]. After placing the samples in the axillary pocket, interrupted atraumatic sutures (thread 4.0) were applied. The skin around the sutures was treated with an aseptic agent. The control group consisted of 10 sham-operated rats. Sham surgery involved a median skin incision, via which forceps were inserted subcutaneously; a lateral pocket was formed, and then the wound was closed without implantation of a matrix. Blood biochemistry tests were also conducted in 10 intact animals.

Thirty days after the implantation, the animals were euthanized by carbon dioxide inhalation in compliance with the rules and norms of the European Community (86/609EEC), the Declaration of Helsinki, and orders of the USSR Ministry of Healthcare (No. 742 of 13.11.1984 and No. 48 of 23.01.1985).

Blood was collected from decapitated animals in Vacuette blood collection tubes (BD Diagnostics, USA) to obtain blood serum. We determined lactate concentrations and alanine aminotransferase (ALT) and aspartate aminotransferase (AST) levels using kits for the Random Access A25 Biochemistry Analyzer (BioSystems S.A., Spain) according to the manufacturer's instructions. Blood parameters (total leukocyte count (TLC), hemogram, erythrocyte count, hemoglobin) were examined using standard hematologic methods [10].

In accordance with ISO 10993-6-2011 (Medical devices. Biological evaluation of medical devices. Part 6. Tests for local effects after implantation), we conducted a macroscopic assessment of subcutaneous soft tissue surrounding the implantation site for the local tissue reaction (local biocompatibility *in vivo*): the presence or absence of signs of inflammation (alteration, exudation, proliferation), hyperemia of vessels in the recipient bed, and encapsulation of samples. The results of the semi-quantitative macroscopic assessment of the local reaction to PLA matrices were recorded on the following scale (in points): no irritating effect (0–0.9 points); mild irritant (1–1.9 points); moderate irritant (2–2.9 points); strong irritant (3–4 points).

For the microscopic analysis, the implants with surrounding tissues were carefully removed from the subcutaneous pocket; after opening the abdominal cavity, a part of the liver was taken for the histologic assessment after subcutaneous implantation of PLA matrices. The analyzed fragments were fixed in 10% neutral buffered formalin. The fragments were dehydrated in eight changes of isopropanol-based dehydrating solution (IsoPrep, BioVitrum, Russia) according to the manufacturer's instruction. The

studied objects were placed in the Histomix paraffin medium (BioVitrum, Russia), thin (5–7 μm) sections were prepared on a microtome perpendicular to the surface of the tissue plates and the studied samples.

Slices mounted on slides were stained with Gill's hematoxylin (BioVitrum, Russia) and eosin for histologic examinations under standard conditions. A total of 10 serial sections were obtained from each tissue sample. Then they were stained and examined. Microslides were studied in transmitted light of the ZEISS Axio Observer A1 microscope (Germany) at various magnifications (40–400). Digital images of the stained histologic sections were obtained using the AxioVision 4.8 software (ZEISS, Germany). We determined the intensity of cellular resorption of PLA matrices (based on the number of multinucleated foreign body giant cells, FBGCs) and the activity of regenerative processes in the liver (measured by the number of binuclear hepatocytes) in 10 randomly selected fields of vision in each histologic sample using computer morphometry of sections stained with hematoxylin and eosin, as described in the literature [11].

The standard Statistica software package v.13.3 was used for statistical description and testing of statistical hypotheses in order to evaluate the data obtained. We used the Shapiro – Wilk test to analyze normally distributed data. The data were presented as the median and the interquartile range *Me* (Q_1; Q_3). The nonparametric Mann – Whitney test was used to evaluate statistical differences in the samples. The differences were considered statistically significant at $p < 0.05$.

RESULTS AND DISCUSSION

In addition to their principal function, implants can activate local regenerative processes, cause a systemic reaction of the body mediated through the circulatory system. At the same time, biodegradable materials (for example, polylactides) can affect the body with the properties of their surface and biodegradation and bioresorption products [5]. The study of the local biocompatibility of PLA matrices established that there were no macroscopic signs of inflammation (alteration, exudation) in the tissues surrounding the implants 30 days after the subcutaneous implantation of the tested samples (Fig. 1). The severity of hyperemia in the recipient vascular bed and encapsulation of the samples (cell proliferation reaction) in the study groups corresponded mainly to the absence of irritation (0 points), mild irritation (1 point), and in a few cases (with encapsulation) – to moderate irritation (2 points) (Table 1). Thus, the studied PLA matrix samples were mild irritants on a scale of 1–1.9 points according to the criteria of ISO 10993-6-2011.

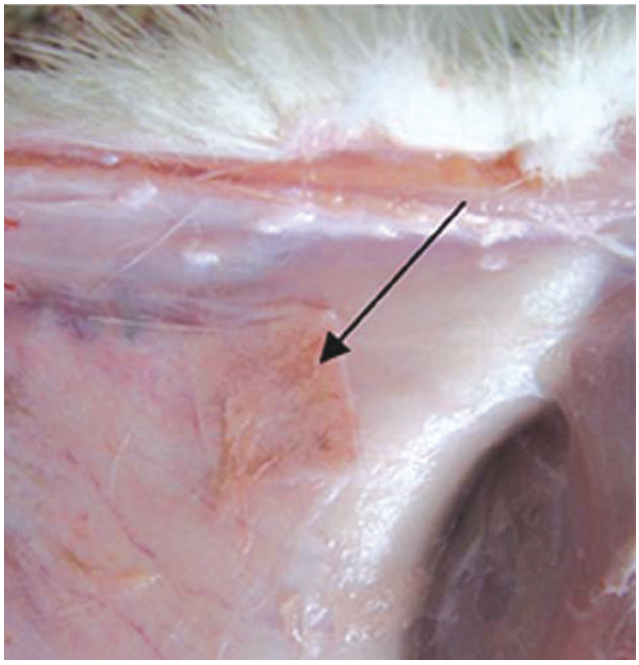

Fig. 1. The condition of the tissues surrounding the PLA matrix in the axillary subcutaneous pocket in rats 30 days after the implantation

Table 1

Macroscopic signs of changes in the tissues surrounding the PLA matrix 30 days after the subcutaneous implantation in Wistar rats, *Me* (Q_1; Q_3)

Study groups	Inflammation	Hyperemia around the sample (postoperative scar)	Matrix encapsulation
Sham surgery, $n = 10$	0 (0; 0)	0 (0; 1)	–
Implantation of PLA matrix, $n = 10$	0 (0; 0)	1 (1; 1.5)	1.5 (1; 1.5)

The presence of a well-formed connective tissue capsule around the implants was revealed during the examination of microscopic changes (Fig. 2). In the capsule, two layers could be well identified: a thin (thickness of no more than 50 μm) inner layer in contact with the PLA matrix formed by dense fibrous connective tissue. Encapsulation with a thin layer of connective tissue is characteristic of relatively bioinert artificial materials [5]. Thin collagen fiber bundles were parallel to the implant surface and grew into the implant structure, mainly from the edge of the tested samples. The second layer of the capsule was located outside the previous one. It directly contacted

the surrounding tissues and was formed by loose connective tissue with microvessels. Collagen fiber bundles diverged in different directions, regardless of the implant surface. Both fibroblasts and inflammatory cells (polymorphonuclear leukocytes, lymphocytes, and macrophages) were found between them.

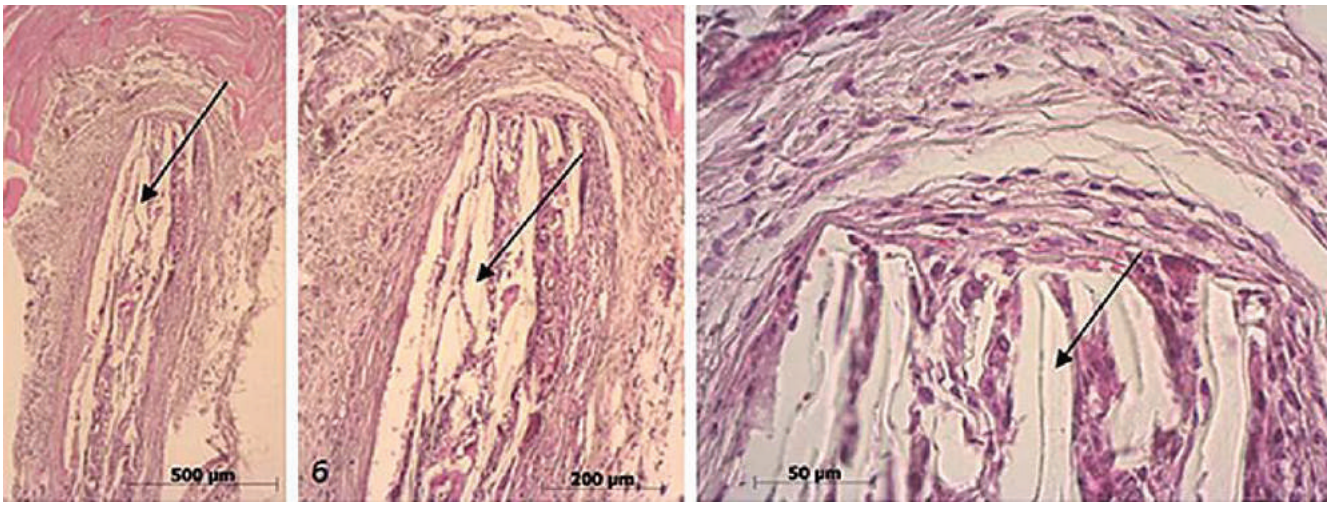

a *b* *c*

Fig. 2. The condition of the connective tissue capsule around and in the structure of the PLA scaffold at different magnifications (*a* – 50; *b* – 100; *c* – 400). Staining with hematoxylin and eosin. The arrows indicate the transparent substance of the polymer scaffold

The cellular composition of the connective tissue was represented, in particular, by FBGCs (Fig. 3). FBGCs were often found inside the implant cavity and were located separately (Fig. 3*a*) or in small clusters of up to three cells (Fig. 3*b*). According to computer morphometry data, the median distribution density of FBGCs in the connective tissue around and in the structure of PLA matrices was 1,500 (1,350; 1,550) per 1 mm^2 of the slice. The formation and accumulation of FBGCs at the site of implantation with a high surface-area-to-volume ratio is a typical reaction of the host organism that indicates active cellular resorption of the matrix substance [5].

Fibrocytes and fibroblasts were located between collagen fiber bundles (Fig. 3*c*). Mononuclear (lymphocytes, macrophages) and polymorphonuclear leukocytes (PMNs) diffused, but formed clusters near FBGCs (Fig. 3*a, b*).

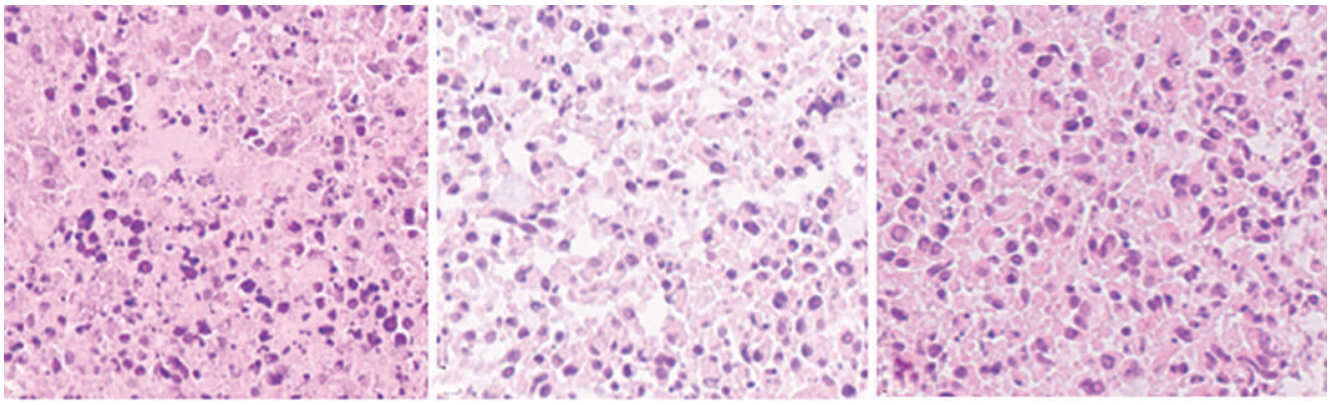

a *b* *c*

Fig. 3. Tissue response to PLA matrix 30 days after the subcutaneous implantation in Wistar rats: *a, b* – mononuclear and polymorphonuclear leukocytes, multinucleated FBGCs (marked with arrows); *c* – fibroblasts between the polymer fibers of the implant. Stained with hematoxylin and eosin

Thus, the local reaction to PLA matrices 30 days after the subcutaneous implantation in rats apparently reflected the transition from acute to chronic productive inflammation with the change of leukocytes infiltrating the damaged area from PMNs to mononuclear forms. After the catabolic phase, which promotes rehabilitation of the inflammatory focus, anabolic processes are activated [12], as secretion of proinflammatory cytokines stops and secretion of anti-inflammatory / regenerative factors begins [13–15].

On the one hand, the formation and accumulation of FBGCs at the site of implantation demonstrated pronounced cellular resorption of PLA matrices. At the same time, they are crucial for the development of a local granulomatous inflammatory reaction to the implant, mediated primarily through the tumor necrosis factor (TNF)α secreted by them [5]. TNFα is a systemic cytokine that induces the expression of epidermal growth factor receptors (EGFR) [16] and activates the production of growth hormone (GH) by cells of the adenohypophysis [17]. In turn, EGFR and GH have an anabolic effect and enhance regenerative processes in organs and tissues [18, 19].

On the other hand, the utilization of the PLA matrix is accompanied by the release of lactic acid, which can have a systemic effect on the body. The liver and the kidneys are target organs for lactate circulating in the bloodstream [20]. Therefore, biochemical blood parameters are assessed to determine the biological safety of polymer scaffold biodegradation products and the capacity of the liver.

The polylactic base of the tested materials could lead to an increase in lactate monomers in the blood of animals in case of massive biodegradation. However, statistically significant changes in the concentration of lactic acid in the blood were not observed 30 days after the implantation (Table 1). A fivefold increase in *in vitro* dissolution of the tested PLA matrices was noted by day 35 of immersion into the nutrient medium [8]. Cellular resorption of the implant can accelerate its destruction *in vivo*, however, the distribution density of FBGCs in the fibrous matrix was insignificant (Fig. 3). We cannot exclude the influence of implants and their biodegradation products on liver function, mediated through distant (stress-regulating) regulatory systems of the body.

It is known that subcutaneous implantation induces a stress reaction in animals [21], which is realized through local (cellular microenvironment) and distant life support systems of the body [19]. In our study, the activity of AST and ALT in the blood of intact Wistar rats (Table 2) was close to that in other vivaria [22]. The sham operation was accompanied by an increase in the activity of ALT (up to 123%) and AST (up to 142%, $p < 0.001$) in the blood serum compared with the values in intact animals 30 days after the surgery. These functional tests suggest damage to the liver parenchyma [23] caused by postoperative stress. At the same time, subcutaneous implantation of the PLA matrix led to normalization of hepatocyte cytolysis markers (almost to the baseline level), which indicated the distant hepatoprotective effect of the PLA material during surgery (Table 2).

Table 2

Biochemical blood parameters in Wistar rats 30 days after the subcutaneous implantation of PLA matrices, *Me* (Q_1; Q_3)

Group	Lactate, mM	ALT, UI / l	AST, UI / l
Intact animals, $n = 10$	–	67.14 (60.47; 69.59)	185.14 (174.16; 216.07)
Sham-operated animals, $n = 10$	4.93 (4.5; 5.71)	82.58 (75.61; 84.36)* $p < 0.001$	262.90 (246.60; 304.60)* $p < 0.001$
Implantation of PLA matrix, $n = 10$	4.28 (3.50; 5.40)	67.34 (65.61; 72.95)# $p < 0.003$	225.10 (209.10; 250.0)# $p < 0.02$

* with the baseline level (intact animals); # with sham-operated rats.

Having obtained data on the functional changes, we were to study the effect of PLA matrices on the liver structure, since subcutaneous implantation of scaffolds can stimulate hepatocyte regeneration [24]. The number of binuclear hepatocytes (dividing and non-dividing) is one of the principal indicators of liver regeneration. Slow subthreshold loss of hepatocytes is not compensated by the body when the loss becomes critical (10% of working hepatocytes for the liver), which leads to irreversible processes and death of the body due to liver failure [25].

During the examination of the histologic preparations of the liver in sham-operated (SO) rats, we observed moderate hyperemia of the central veins and sinusoidal capillaries, while the structure and shape of the classic hepatic lobules were preserved. Subcutaneous implantation of PLA matrices did not cause visible destructive changes in the liver by day 30 of the follow-up (Fig. 4). However, the increase in the number of binuclear hepatocytes (Fig. 4) did not reach statistical differences in comparison with the controls (Table 2).

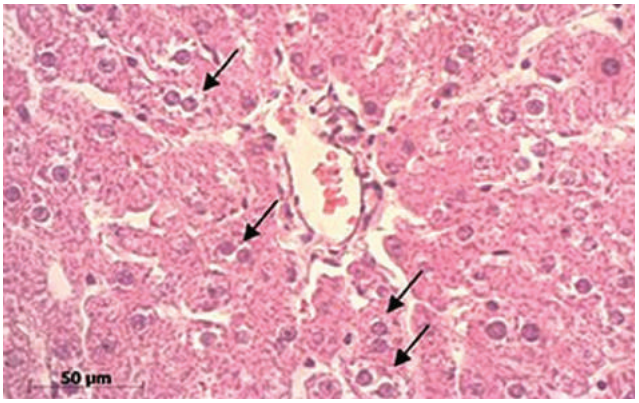

Fig. 4. Histologic image of the liver of Wistar rats 30 days after the subcutaneous implantation of PLA matrices: staining with hematoxylin and eosin; arrows indicate binuclear hepatocytes

Table 2

Distribution density of binuclear hepatocytes in Wistar rats 30 days after the subcutaneous implantation of PLA matrices, *Me* (Q_1; Q_3)

Group	Количество двуядерных клеток на 1 мм^2
SO animals, n = 10	4,600 (4,450; 4,800), n_1 = 100
Implantation of PLA matrix, n = 10	5,300 (4,700; 5,500), n_1 = 100

Note: n_1 is the number of calculated fields of vision.

According to our findings, subcutaneous implantation of PLA matrices has a functional hepatoprotective effect by day 30 after administration to laboratory rats. The mechanisms of the established phenomenon are not clear, but they are likely to be complex. Postoperative regeneration in subcutaneous adipose tissue may be important, as it leads to the release of EGFR and other growth factors activating liver regeneration into the blood [26]. In addition, lactate released during the degradation of PLA matrices can have a regulatory effect on migration and activity of T lymphocytes [27, 28], which are recruited as conductor cells of proliferative inflammation and subsequent regenerative processes in parenchymal organs [29].

Indeed, after subcutaneous implantation of PLA matrices, a pronounced leukemoid reaction was detected, due to an increase in the number of lymphocytes (by 1.7 times compared with the controls, $p < 0.02$) (Table 3). The absence of significant neutrophilia indicated sterile inflammation taking place in the subcutaneous tissue around the PLA material.

Table 3

Hemogram (10^9 / l), RBC count, and hemoglobin concentration (g / l) in the blood of Wistar rats 30 days after the subcutaneous implantation of PLA matrices, *Me* (Q_1; Q_3)

Group	Total WBC count	Lymphocytes	Monocytes	Neutrophils	Erythrocytes, 10^{12} / l	Hemoglobin, g / l
SO animals, n = 10	6.4 (4.6; 9.2)	3.6 (2.8; 6.1)	0.5 (0.2; 0.7)	2.5 (1.2; 2.8)	9.41 (7.93; 9.52)	146 (123; 147)
Implantation of PLA matrix, n = 10	8.7 (6.7; 13.3)	6.1* (5.2; 9.0) $p < 0.02$	0.4 (0.3; 0.6)	2.2 (1.3; 3.4)	9.43 (7.92; 9.94)	150 (148; 154)

* significant differences according to the Mann – Whitney test.

The systemic effect of PLA matrices on biochemical markers of hepatocyte cytolysis is largely similar to the effect of subcutaneous injection of hyaluronic acid implants in healthy women during cosmetic procedures [30]. Various chemical substances have a similar effect when injected subcutaneously, which suggests a non-specific mechanism of their long-term effect besides the specific impact of monomers (lactic or glucuronic acid). This mechanism may be linked to the controlled onset of low-grade local productive inflammation, which activates the compensatory – adaptive and adaptive reactions of the host organism.

CONCLUSION

Biodegradable scaffolds based on PLA and copolymers are of fundamental and clinical interest for soft and solid tissue bioengineering [31, 32], including the liver [33]. These scaffolds can be used as carriers of stem cells [34] and as a means of delivery and release of drugs and biological molecules [35].

According to the data obtained, bioabsorbable nonwoven PLA matrices are biocompatible with subcutaneous tissue and have a distant protective effect on the capacity of the liver in laboratory animals. Nonwoven PLA matrices can be used as cell carriers. The areas of application may include treating damage induced by cytostatic agents, radiation injuries, and chronic liver diseases. However, the specific mechanisms underlying the revealed effect that subcutaneous implantation of PLA matrices had on hepatocytes require further study.

REFERENCES

1. Jafari M., Paknejad Z., Rad M.R., Motamedian S.R., Eghbal M.J., Nadjmi N. et al. Polymeric scaffolds in tissue

engineering: a literature review. *J. Biomed. Mater. Res. B Appl. Biomater.* 2017;105(2):431–459. DOI: 10.1002/jbm.b.33547.
2. Jukkala-Partio K., Laitinen O., Vasenius J., Partio E.K., Toivonen T., Tervahartiala P. et al. Healing of subcapital femoral osteotomies fixed with self-reinforced poly-L-lactide screws: an experimental long-term study in sheep. *Arch. Orthop. Trauma Surg*. 2002;122(6):360–364. DOI: 10.1007/s00402-001-0379-y.
3. Zhou J., Han S., Dou Y., Lu J., Wang C., He H. et al. Nanostructured poly(L-lactide) matrix as novel platform for drug delivery. *Int. J. Pharm*. 2013;448(1):175–188. DOI: 10.1016/j.ijpharm.2013.03.038.
4. Wulf K., Arbeiter D., Matschegewski C., Teske M., Huling J., Schmitz K.P. et al. Smart releasing electrospun nanofibers-poly: L. lactide fibers as dual drug delivery system for biomedical application. *Biomed. Mater*. 2020;16(1):015022. DOI: 10.1088/1748-605X/abbec8.
5. Biomaterials science: an introduction to materials in medicine; 2nd ed.; ed. by B.D. Ratner, A.S. Hoffman, F.J. Schoen, J.E. Lemons. San Diego: Elsevier Academic Press; 2004:851.
6. Do A.V., Khorsand B., Geary S.M., Salem A.K. 3D printing of scaffolds for tissue regeneration applications. *Adv. Healthc. Mater.* 2015;4(12):1742–1762. DOI: 10.1002/adhm.201500168.
7. Daristotle J.L., Behrens A.M., Sandler A.D., Kofinas P.A Review of the Fundamental Principles and Applications of Solution Blow Spinning. *ACS Appl. Mater. Interfaces*. 2016;8(51):34951–34963. DOI: 10.1021/acsami.6b12994.
8. Tverdokhlebov S.I., Stankevich K.S., Bolbasov E.N., Khlusov I.A., Kulagina I.V., Zaytsev K.V. Nonwoven polylactide scaffolds obtained by solution blow spinning and the *in vitro* degradation dynamics. *Advanced Materials Research*. 2014;872:257–263.
9. Bolbasov E.N., Popkov A.V., Popkov D.A., Gorbach E.N., Khlusov I.A., Golovkin A.S.et al. Osteoinductive composite coatings for flexible intramedullary nails. *Mater Sci. Eng. C Mater. Biol. Appl.* 2017;75:207–220. DOI: 10.1016/j.msec.2017.02.073.
10. Menshikov V.V., Delektorskaya L.N., Zolotnitskaya R.P., et al. Laboratory methods of research in the clinic: handbook; ed. by V.V. Menshikov. Moscow: 1987:368 (in Russ.).
11. Avtandilov G.G. Diagnostic medical ploidometry. Moscow: Medicine; 2006:192 (in Russ.).
12. Clark D., Nakamura M., Miclau T., Marcucio R. Effects of aging on fracture healing. Curr. Osteoporos Rep. 2017;15(6):601–608. DOI: 10.1007/s11914-017-0413-9.
13. Loi F., Córdova L.A., Pajarinen J., Lin T.H., Yao Z., Goodman S.B. Inflammation, fracture and bone repair. Bone. 2016;86:119–130. DOI: 10.1016/j.bone.2016.02.020.
14. Yurova K.A., Khaziakhmatova O.G., Malashchenko V.V., Norkin I.K., Ivanov P.A., Khlusov I.A., et al. The role of γC cytokines (IL-2, IL-7, AND IL-15) in regulation of activation-induced cell death of memory T cells. A brief review. *Cell and Tissue Biology*. 2020;62(5):305–315 (in Russ.). DOI: 10.31857/S0041377120050090.
15. ElHawary H., Baradaran A., Abi-Rafeh J., Vorstenbosch J., Xu L., Efanov J.I. Bone healing and inflammation: Principles of fracture and repair. Semin. Plast. Surg. 2021;35(3):198–203. DOI: 10.1055/s-0041-1732334.
16. Fayers W. Biological methods of treatment with tumor necrosis factor: preclinical studies. In Biologic therapy of cancer: translated from Engli-sh; edited by Vincent T. DeVita, Samuel Hellman, Steven A. Rosenberg. Moscow: Medicine; 2002:309–343 (in Russ.).
17. Milenkovic L., Rettori V., Snyder G.D., Beutler B., McCann S.M. Cachectin alters anterior pituitary hormone release by a direct action in vitro. *Proc. Natl. Acad. Sci. U S A.* 1989;86(7):2418–2422. DOI: 10.1073/pnas.86.7.2418.
18. Hormone therapy: trans. from German; edited by H. Schambach, G. Knappe, W. Carol. Moscow: Medicine, 1988:416 (in Russ.).
19. Goldberg E.D., Dygai A.M., Udut V.V., Naumov S.A., Khlusov I.A. Regularities of the structural organization of life support systems in normal and in the development of the pathological process. Tomsk, 1996:283 (in Russ.).
20. Yang W.H., Park H., Grau M., Heine O. Decreased blood glucose and lactate: Is a useful indicator of recovery ability in athletes? *Int. J. Environ. Res. Public Health.* 2020;17(15):5470. DOI: 10.3390/ijerph17155470.
21. Selye H., Lemire Y., Bajusz E. Induction of bone, cartilage and hemopoietic tissue by subcutaneously implanted tissue diaphragms. Wilhelm Roux Arch. Entwickl. Mech. Org. 1960;151(5):572–585. DOI: 10.1007/BF00577813.
22. Voitenko N.G., Makarova M.N., Zueva A.A. Variability of blood biochemical parameters and establishment of reference intervals in nonclinical studies. Part 1: rats. *Laboratory animals for science.* 2020;(1):47–53 (in Russ.). DOI: 10.29296/2618723X-2020-01-06.
23. Lifshits V.M., Sidelnikova V.I. Biochemical analysis in the clinic: handbook. Moscow: MIA; 1998:303 (in Russ.).
24. Khlusov I.A., Khlusova M.Yu. Method of distant stimulation of hepatocyte regeneration: RF Patent for invention No. 2590859 of 15.06.2016 (published 10.07.2016, Issue No. 19) (in Russ.).
25. Severin M.V., Yushkov B.G., Yastrebov A.P. Tissue regeneration under extreme effects on the body. Yekaterinburg: USMI, 1993:187 (in Russ.).
26. Bader A. Method of tissue regeneration: RF Patent for invention No. 2392314 of 20.06.2010 (in Russ.).
27. Haas R., Smith J., Rocher-Ros V., Nadkarni S., Montero-Melendez T., D'Acquisto F. et al. Lactate regulates metabolic and pro-inflammatory circuits in control of T cell migration and effector functions. *PLoS Biol.* 2015;13(7):e1002202. DOI: 10.1371/journal.pbio.1002202.
28. Pucino V., Bombardieri M., Pitzalis C., Mauro C. Lactate at the crossroads of metabolism, inflammation, and autoimmunity. *Eur. J. Immunol.* 2017;47(1):14–21. DOI: 10.1002/eji.201646477.
29. Babaeva A.G. Regeneration and immunogenesis system. Moscow: Medicine; 1985:256 (in Russ.).
30. Khlusov I.A., Igumnov V.A., Chukhnova D.L., Mitasova O.L., Zaitsev K.V., Abdulkina N.G., et al. Local and system effects of hyaluronic acid implants in conditions of corrections of age-related changes in skin. *Bulletin of Siberian Medicine*. 2013;12(1):61–68 (in Russ.).
31. Grémare A., Guduric V., Bareille R., Heroguez V., Latour S., L'heureux N. et al. Characterization of printed PLA scaf-

folds for bone tissue engineering. *J. Biomed. Mater. Res. A.* 2018;106(4):887–894. DOI: 10.1002/jbm.a.36289.
32. Gangolphe L., Leon-Valdivieso C.Y., Nottelet B., Déjean S., Bethry A., Pinese C. et al. Electrospun microstructured PLA-based scaffolds featuring relevant anisotropic, mechanical and degradation characteristics for soft tissue engineering. *Mater Sci. Eng. C Mater. Biol. Appl.* 2021;129:112339. DOI: 10.1016/j.msec.2021.112339.
33. Wang M., Pei H., Zhang L., Guan L., Zhang R., Jia Y. et al. Hepatogenesis of adipose-derived stem cells on poly-lactide-co-glycolide scaffolds: in vitro and in vivo studies. *Tissue Eng. Part C Methods.* 2010;16(5):1041–1050. DOI: 10.1089/ten.TEC.2009.0244.
34. Diomede F., Gugliandolo A., Cardelli P., Merciaro I., Ettorre V., Traini T. et al. Three-dimensional printed PLA scaffold and human gingival stem cell-derived extracellular vesicles: A new tool for bone defect repair. *Stem. Cell Res. Ther.* 2018;9(1):104. DOI: 10.1186/s13287-018-0850-0.
35. Eğri S., Eczacıoğlu N. Sequential VEGF and BMP-2 releasing PLA-PEG-PLA scaffolds for bone tissue engineering: I. Design and in vitro tests. *Artif. Cells Nanomed. Biotechnol.* 2017;45(2):321–329. DOI: 10.3109/21691401.2016.1147454.

Authors contribution

Dvornichenko M.V. – conception and design, drafting of the manuscript. Ivanova E.A., Dzyuman A.N. – carrying out of the research, collection, translation, and processing of the material.

Authors information

Ivanova Ekaterina A. – Senior Lecturer, Human Anatomy Division with Topographic Anatomy and Operative Surgery Course; Assistant, Laboratory of Cellular and Microfluidic Technologies, Siberian State Medical University, Tomsk, http://orcid.org/0000-0002-4119-7562

Dzyuman Anna N. – Cand. Sci. (Med.), Associate Professor, Morphology and General Pathology Division, Siberian State Medical University, Tomsk, http://orcid.org/0000-0002-0795-0987 .

Dvornichenko Marina V. – Dr. Sci. (Med.), Professor, Human Anatomy Division with Topographic Anatomy and Operative Surgery Course; Researcher, Laboratory of Cellular and Microfluidic Technologies, Siberian State Medical University, Tomsk, dochic@yandex.ru, http://orcid.org/0000-0001-9783-0817

(✉) **Dvornichenko Marina V.,** dochic@yandex.ru

Received 12.02.2022;
approved after peer review 05.03.2022;
accepted 09.06.2022

УДК 618.39-02:616.127-018.63-002.88]-092.9:599323.4
https://doi.org/10.20538/1682-0363-2022-4-72-78

Effect of preterm birth in rats on proliferation and hyperplasia of cardiomyocytes

Ivanova V.V.[1], Milto I.V.[1, 2], Serebryakova O.N.[1], Sukhodolo I.V.[1]

[1] *Siberian State Medical University*
2, Moscow Tract, Tomsk, 634050, Russian Federation

[2] *Seversk Biophysical Research Center*
P.O. Box 130, Seversk-13, 636013, Russian Federation

ABSTRACT

Aim. To identify the effect of preterm birth on proliferation and hyperplasia of cardiomyocytes in the early postnatal period of ontogenesis in rats.

Materials and methods. Preterm birth (on day 21 and 21.5 of gestation) in Wistar rats was induced by subcutaneous administration of mifepristone. Immunohistochemistry was used to identify and calculate the number of Ki67-positive and Mklp2-positive cardiomyocytes in the left ventricle of preterm and full-term rats on days 1, 2, 3, 4, 5, and 6 of postnatal ontogenesis. Statistical analysis of morphometric parameters was performed using the Shapiro – Wilk test and Mann – Whitney test with the Bonferroni correction.

Results. We revealed an increase in the number of Ki67-positive cardiomyocytes in the left ventricle of the rats: on day 1 of postnatal ontogenesis (in the rats born on day 21 of gestation) and on days 3–5 of postnatal ontogenesis (in the rats born on day 21.5 of gestation). Preterm birth in rats did not result in a change in the number of Mklp2-positive cardiomyocytes in the left ventricular wall.

Conclusion. A change in the pattern of Ki67 expression by cardiomyocytes in the rats born 12 or 24 hours before full term was demonstrated in the early postnatal period of ontogenesis. An isolated increase in Ki67 expression without a change in Mklp2 expression by cardiomyocytes in the left ventricular wall of preterm rats indicates acceleration of cardiomyocyte hypertrophy. Shorter duration of prenatal development is associated with more pronounced morphological and functional rearrangements in the rat myocardium.

Keywords: preterm birth; cardiomyocyte; proliferation; hyperplasia; hypertrophy, experiment

Conflict of interest. The authors declare the absence of obvious or potential conflicts of interest related to the publication of this article.

Source of financing. The study was carried out within the strategic academic leadership program “Priority 2030”.

Conformity with the principles of ethics. The study was approved by the local Ethics Committee at Siberian State Medical University (Protocol No. 8475/1 of 30.11.2020).

For citation: Ivanova V.V., Milto I.V., Serebryakova O.N., Sukhodolo I.V. Effect of preterm birth in rats on proliferation and hyperplasia of cardiomyocytes. *Bulletin of Siberian Medicine.* 2022;21(4):72–78. https://doi.org/10.20538/1682-0363-2022-4-72-78.

✉ *Ivanova Vera V.,* ivvera92@rambler.ru

Влияние преждевременного рождения крыс на пролиферацию и гиперплазию кардиомиоцитов

Иванова В.В.[1], Мильто И.В.[1, 2], Серебрякова О.Н.[1], Суходоло И.В.[1]

[1] Сибирский государственный медицинский университет (СибГМУ)
Россия, 634050, г. Томск, Московский тракт, 2

[2] Северский биофизический научный центр (СБН Центр)
Россия, 636013, г. Северск-13, а/я № 130

РЕЗЮМЕ

Цель. Установить влияние преждевременного рождения на процессы пролиферации и гиперплазии кардиомиоцитов в раннем постнатальном периоде онтогенеза у крыс.

Материалы и методы. Преждевременные роды (на 21-е и 21,5-е сут беременности) крыс линии Вистар индуцировали подкожным введением мифепристона. Иммуногистохимически в левом желудочке преждевременно рожденных и доношенных крыс на 1, 2, 3, 4, 5 и 6-е сут постнатального периода онтогенеза выявляли и подсчитывали количество Ki67-позитивных и Mklp2-позитивных кардиомиоцитов. С помощью критерия Шапиро – Уилка и критерия Манна – Уитни с поправкой Бонферрони провели статистический анализ морфометрических показателей.

Результаты. Продемонстрировано увеличение количества Ki67-позитивных кардиомиоцитов в левом желудочке сердца крыс: на 1-е сут постнатального периода онтогенеза (у рожденных на 21-е сут беременности) и на 3–5-е сут постнатального периода онтогенеза (у рожденных на 21,5-е сут беременности). Преждевременное рождение не приводит к изменению количества Mklp2-позитивных кардиомиоцитов в стенке левого желудочка крыс.

Заключение. В раннем постнатальном периоде онтогенеза продемонстрировано изменение паттерна экспрессии Ki67 кардиомиоцитами крыс, рожденных на 12 или 24 ч ранее срока. Изолированное увеличение экспрессии Ki67 без изменения экспрессии Mklp2 кардиомиоцитами в стенке левого желудочка преждевременно рожденных крыс свидетельствует об акселерации гипертрофии кардиомиоцитов. Меньшая продолжительность внутриутробного периода развития ассоциирована с более выраженными морфофункциональными перестройками миокарда крыс.

Ключевые слова: преждевременное рождение, кардиомиоцит, пролиферация, гиперплазия, гипертрофия, эксперимент

Конфликт интересов. Авторы декларируют отсутствие явных и потенциальных конфликтов интересов, связанных с публикацией настоящей статьи.

Источники финансирования. Исследование выполнено в рамках Программы стратегического академического лидерства «Приоритет – 2030».

Соответствие принципам этики. Исследование одобрено локальным этическим комитетом СибГМУ (протокол № 8475/1 от 30.11.2020).

Для цитирования: Иванова В.В., Мильто И.В., Серебрякова О.Н., Суходоло И.В. Влияние преждевременного рождения крыс на пролиферацию и гиперплазию кардиомиоцитов. *Бюллетень сибирской медицины.* 2022;21(4):72–78. https://doi.org/10.20538/1682-0363-2022-4-72-78.

INTRODUCTION

Preterm birth (birth before 37 completed weeks of gestation) increases the risk of early development of cardiovascular diseases [1, 2], such as coronary heart disease [3], hypertension, and heart failure [4]. Preterm birth is associated with structural and functional immaturity of organs, which is the reason for their adaptive morphogenesis in the postnatal period. Thus, there are no differences in the heart structure between full-term and preterm children in the prenatal period; initial structural changes in the heart in preterm children emerge in the postnatal period [5]. It is known that the morphological and

functional features of the heart in preterm children are determined already at the third month of the postnatal period of ontogenesis: an increase in the relative mass of the right and left ventricles is observed, compared with that in full-term infants [5]. Over time, the structural features of the heart in preterm children are preserved [6] and serve as a prerequisite for earlier development of cardiovascular diseases in this group of individuals [7].

It remains unclear how preterm birth leads to the formation of structural and functional features of the heart, though researchers pay close attention to this problem [8]. At the same time, correction of structural features in the heart of preterm children in the early postnatal period of ontogenesis can prevent the development or reduce the risk of cardiovascular diseases in adulthood [9–11].

Determination and detailed characterization of morphological and functional changes in the heart of preterm children in the early postnatal period are priority tasks, which solution is hampered by the lack of histologic studies. Single studies devoted to the histologic characteristics of the myocardium in preterm children are difficult to interpret, since the hearts of stillborn babies are used as controls [12], while it is adaptation of the heart and blood vessels to the conditions of *ex utero* functioning that is of great interest. Therefore, it is relevant to identify and study the dynamics and consequences of postnatal morphological and functional features of the heart in preterm animals in the experiment. The aim of the study was to establish the effect of preterm birth on proliferation and hyperplasia of cardiomyocytes in the early postnatal period of ontogenesis in rats.

MATERIALS AND METHODS

Wistar rats of both sexes were used in the experiment. A full gestation period for Wistar rats is 22 days. Rats born two days before full term are not viable. Rats born one day before full term are characterized by a sufficient degree of structural and functional immaturity of organs and are used as models for studying the effects of preterm birth [13, 14]. Based on clinical data, according to which the severity of the morphological and functional changes in the heart and blood vessels correlates with the degree of prematurity [15, 16], as well as on the information that even a moderate degree of prematurity leads to impaired functioning of the cardiovascular system in adulthood [17], we formed two groups of rats in the study: rats born 12 and 24 hours before full term, respectively (Table 1).

Table 1

Characteristics of the experimental groups

Experimental group	Duration of prenatal development in experimental animals, days	Time of mifepristone injection, days of pregnancy
Control group, $n = 30$	22.0	–
Group 1, $n = 30$	21.5	20.5
Group 2, $n = 30$	21.0	20.0

The offspring were obtained from the intact male (aged 2 months, 180 ± 20 g) and female (aged 3 months, 180 ± 20 g) Wistar rats, the latter were kept in individual cages. In females, the phase of the estrous cycle was determined daily. In the proestrus, a male was placed with a female for a night. The following morning, the male was removed from the cage, and vaginal smear of the female rat was analyzed to verify coitus. The day of detection of spermatozoa in the vaginal smear was considered to be the first day of pregnancy. Pregnant females were kept in individual cages and fed with LbK 120 R-22 feed for pregnant laboratory rodents (Delta Feeds, Russia). Preterm labor was induced on days 21 and 21.5 of pregnancy by subcutaneous administration of mifepristone (1 ml, 10 mg / kg of body weight, Sigma-Aldrich, USA) to the rats [18].

The rats were euthanized on days 1, 2, 3, 4, 5, and 6 of postnatal ontogenesis by CO_2 inhalation. The rat heart was fixed in the buffered (pH 7.4) formalin solution (BioVitrum, Russia) for 24 h, then it was washed in running water, dehydrated in the Isoprep solution (BioVitrum, Russia), and embedded in the HISTOMIX paraffin mixture (BioVitrum, Russia). The sections obtained on the automatic microtome (HM355S, Thermo Fisher Scientific, China) were used for immunohistochemistry. Ki67 (a proliferation marker) and Mklp2 (a cytokinesis marker) were detected on the sections by the indirect peroxidase method. Ki67 is non-specific for determining true mitosis and is expressed during endomitosis as well [19]. On the contrary, Mklp2 (mitotic kinesin-like protein 2) is a marker of cytokinesis, the final stage of true mitosis. Therefore, Mklp2 makes it possible to identify cells undergoing the final stages of mitosis [20].

To unmask antigens, the deparaffinized sections were exposed to high temperatures in the citrate buffer (0.01 M, pH 6.0). Ab16667 (Anti-Ki67 antibody [SP6],

1:300) and bs-7750r (Anti-Mklp2 antibody, 1:500) were used as primary antibodies. Primary antibodies were visualized using the Mouse and Rabbit Specific HRP/DAB IHC Detection Kit – Micro-polymer (Abcam, UK). After the immunohistochemical staining, the sections were counterstained with Gill's hematoxylin.

Immunohistochemical slides were studied using the Axioscope 40 light microscope (Zeiss, Germany) and the Canon PowerShot G5 digital camera (Canon, China). To determine the localization of immunopositive cardiomyocytes, the thickness of the left ventricular myocardium was arbitrarily divided into three parts: subepicardial, middle, and subendocardial. The number of Ki67-positive and Mklp2-positive cardiomyocytes per 1 mm^2 of the left ventricular wall section area was counted.

Statistical analysis was carried out using SPSS 16.0 (IBM, USA). The Shapiro –Wilk test and the Mann – Whitney test with the Bonferroni correction were used. The results of the morphometric study were presented as the median and the interquartile range Me $(Q_1; Q_3)$. The differences were statistically significant at $p < 0.01$.

RESULTS

In the left ventricular myocardium of rats, Ki67 and Mklp-2 were detected in the cytoplasm of different cells: endotheliocytes, fibroblasts, and cardiomyocytes (Figure). In the observed periods, Ki67-positive cardiomyocytes were diffuse in the left ventricular myocardium in all experimental groups, while Mklp2-positive cardiomyocytes had predominantly subendocardial localization.

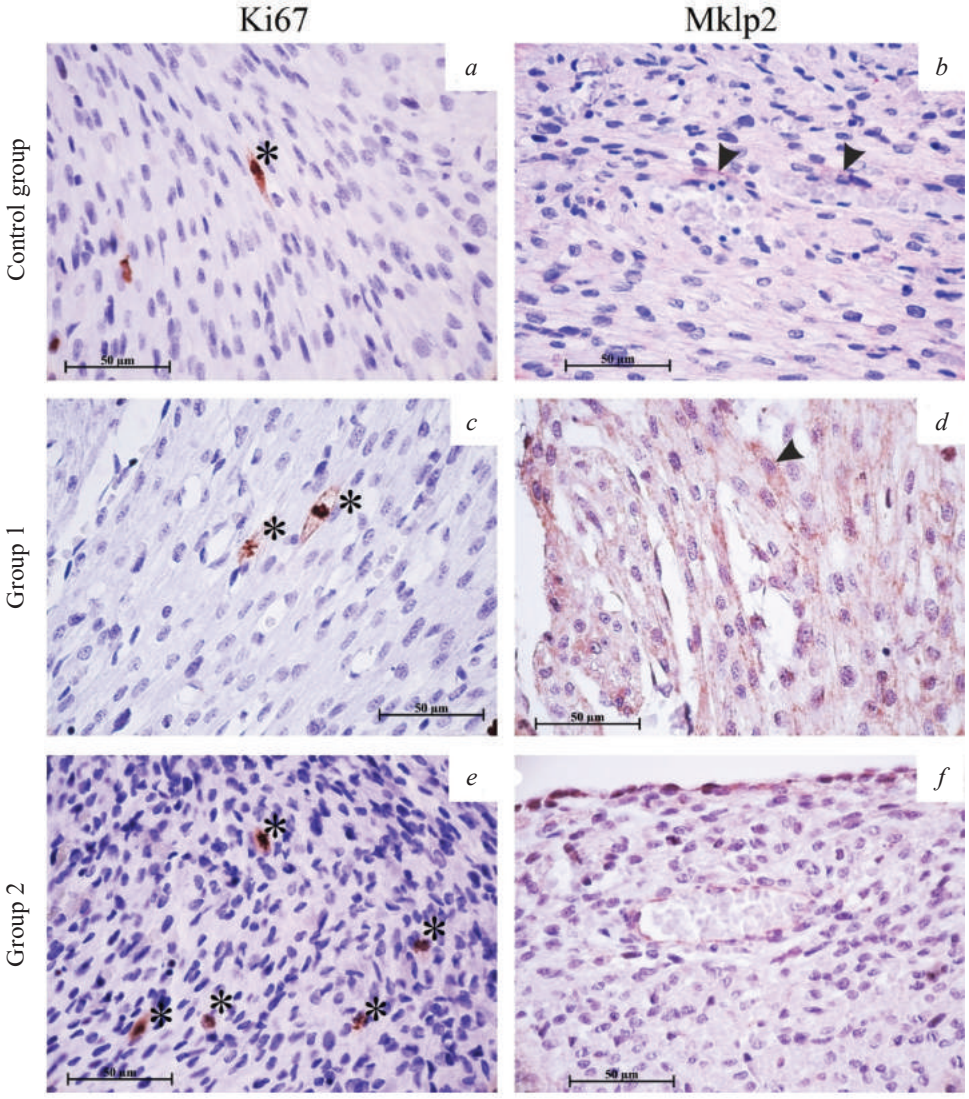

Figure. The left ventricular myocardium in rats: of the control group (full-term animals) (*a*, *b*), of group 1 – rats born on day 21.5 of gestation (*c, d*), of group 2 – rats born on day 21 of gestation (*e, f*), on day 1 of postnatal ontogenesis. Asterisks indicate Ki67-positive cardiomyocytes (*a, c, e*), and arrowheads indicate Mklp2-positive cardiomyocytes (*b, d, f*). Counterstaining with Gill's hematoxylin.

In the left ventricular myocardium of rats in all studied groups, the number of Ki67-positive cardiomyocytes exceeded the number of Mklp2-positive cardiomyocytes (Table 2). Changes in the number of Ki67-positive cardiomyocytes and Mklp2-positive cardiomyocytes per 1 mm^2 of the left ventricular section are shown in Table 2.

In all experimental groups, the number of Ki67-positive cardiomyocytes in the left ventricular wall of rats peaked on days 2–3 of postnatal ontogenesis, after which it progressively decreased. In the rats of group 1, a delayed increase in the number of Ki67-positive cardiomyocytes in the left ventricular wall was observed, compared with the control group. An increase in the number of Ki67-positive cardiomyocytes in the left ventricular wall of the rats from group 1 was found on days 3–5 of postnatal ontogenesis. On the contrary, in the rats of group 2, the number of Ki67-positive cardiomyocytes in the left ventricular wall exceeded that in the rats of group 1 and the control group on day 1 of postnatal ontogenesis.

The number of Mklp2-positive cardiomyocytes in the left ventricular wall of rats in all studied groups progressively decreased during the experiment. Preterm birth did not result in a change in the number of Mklp2-positive cardiomyocytes in the left ventricular wall of the rats.

Table 2

Changes in the number of immunopositive cardiomyocytes in the left ventricle of rats, number of cardiomyocytes in 1 mm^2, *Me* (Q_1; Q_3)

Group	Postnatal ontogenesis, day					
	1	2	3	4	5	6
Number of Ki67-positive cardiomyocytes						
Control group	43.8 (37.5; 50.0)	87.5 (68.8; 98.4)	68.8 (62.5; 85.9)	43.8 (25.0; 50.0)	46.9 (37.5; 50.0)	34.4 (20.3; 48.4)
	–	$p_2 = 0.000$	–	$p_2 = 0.001$	–	–
Group 1	28.1 (14.1; 42.2)	78.1 (68.8; 115.6)	96.9 (71.9; 123.4)	78.1 (57.8; 93.8)	62.5 (51.6; 75.0)	50.0 (37.5; 67.2)
	p =0.007	$p_2 = 0.000$	$p = 0.008$	$p = 0.000$	$p = 0.001$	
Group 2	71.9 (56.3; 81.3)	84.4 (75.0; 100.0)	65.6 (51.6; 95.3)	43.8 (37.5; 68.8)	46.9 (31.3; 62.3)	43.8 (31.3; 56.3)
	$p = 0.000$ $p_1 = 0.000$	$p_2 = 0.000$	–	$p_1 = 0.000$ $p_2 = 0.002$	–	–
Number of Mklp2-positive cardiomyocytes						
Control group	25.0 (0; 50.0)	12.5 (0; 50.0)	12.5 (0; 31.3)	0 (0; 25.0)	0 (0; 0)	0 (0; 0)
	$p_3 = 0.002$	$p_{33} = 0.000$	$p_3 = 0.000$	$p_3 = 0.000$	$p_3 = 0.000$	$p_3 = 0.000$
Group 1	25.0 (0; 50.0)	0 (0; 31.3)	0 (0; 31.3)	0 (0; 25.0)	0 (0; 0)	0 (0; 0)
	p_3 =.009	$p_3 = 0.000$	$p_3 = 0.000$	$p_3 = 0.000$	$p_3 = 0.000$	$p_3 = 0.000$
Group 2	12.5 (0; 31.3)	0 (0; 31.3)	0 (0; 25.0)	0 (0; 0)	0 (0; 0)	0 (0; 0)
	$p_3 = 0.000$	$p_3 = 0.000$	$p_3 = 0.000$	$p_3 = 0.000$	$p_3 = 0.000$	$p_3 = 0.000$

Note: the level of statistical significance of differences in comparison with the control group (p), in comparison with group 1 (p_1), in comparison with the corresponding parameter for the previous period (p_2). The level of statistical significance of differences in the number of Ki67-positive and Mklp2-positive cardiomyocytes per 1 mm^2 of the left ventricular wall section in rats of similar groups at corresponding times (p_3).

DISCUSSION

The study used a generally accepted model of preterm labor induction in rats [21–23]. Before delivery, a decrease in the concentration of progesterone is observed in the rat blood plasma. It is known that morphological and functional changes in the uterus and placenta of rats caused by injection of mifepristone, a competitive progesterone antagonist, are identical to those developing before delivery in full-term pregnancy [21–23]. Mifepristone does not inhibit lactation [24], has no toxic effect, and does not cause stillbirth and infant death [18, 25, 26].

During the last day of prenatal ontogenesis, the mass of the rat heart increases from 15.8 to 25.9 mg [27]; the volume of the left ventricle increases from 4.14 to 6.72 mm^3 [28]. An increase in the size of the rat heart in prenatal and early postnatal ontogenesis is due to proliferation of cardiomyocytes. It was demonstrated that on days 1–2 of postnatal ontogenesis, an increase in the pool of cardiomyocytes (hyperplasia of cardiomyocytes) continues, which is consistent with the data of F.Li et al. [29]. It was shown that hyperplastic myocardial growth in postnatal ontogenesis mainly affects the subendocardial part of the myocardium. On days 3–4 of postnatal ontogenesis, rat cardiomyocytes lose the ability to complete cytokinesis: true mitosis is completely replaced by endomitosis (hypertrophy of cardiomyocytes). To assess whether preterm

birth will alter the time of myocardial transition from hyperplasia to hypertrophy, we studied the dynamics in the number of Ki67- and Mklp2-positive cardiomyocytes in preterm rats from day 1 to day 6 of postnatal ontogenesis.

Preterm birth is not accompanied by a compensatory increase in the number of Mklp2-positive cardiomyocytes or a change in the temporal pattern of Mklp2 expression in the rat left ventricular myocardium. An isolated increase in Ki67 expression without a change in Mklp2 expression by cardiomyocytes in the left ventricular wall of preterm rats indicates acceleration of cardiomyocyte hypertrophy, which may be the cause of a decrease in the myocardial flow reserve. An increase in Ki67 expression by cardiomyocytes of the left ventricular wall in preterm rats reflects the so-called catch-up growth and is an adaptive response of a structurally immature heart to an increase in the hemodynamic load due to the birth and growth of the animal.

It should be noted that an increase in the number of Ki67-positive left ventricular cardiomyocytes in rats born on day 21 of gestation, compared with the animals of the control group and the animals born on day 21.5 of gestation, is observed already on the first day of postnatal ontogenesis. Greater structural immaturity of the heart may be the cause of more pronounced morphological and functional changes in the organ following the birth. Taking into account short duration of the fetal stage of prenatal ontogenesis in rats (for Wistar rats, it lasts from day 18 to day 22 of embryogenesis) and high intensity of organogenesis during this period, it is likely that the 0.5-day difference in the duration of pregnancy can be the cause of a different effect of preterm birth on the morphological and functional condition of the rat myocardium. Further studies are required to understand in detail the causes of the observed differences in the effect of preterm birth on the proliferation of cardiomyocytes in rats born 12 and 24 hours before full term.

CONCLUSION

In early postnatal ontogenesis, a change in the pattern of Ki67 expression by cardiomyocytes in the rats born 12 or 24 hours before full term was revealed. An isolated increase in Ki67 expression without a change in Mklp2 expression by cardiomyocytes in the left ventricular wall of preterm rats indicates acceleration of cardiomyocyte hypertrophy. Shorter duration of the intrauterine development is associated with more pronounced morphological and functional changes in the rat myocardium.

REFERENCES

1. Lewandowski A.J., Levy P.T., Bates M.L., McNamara P.J., Nuyt A.M., Goss K.N. Impact of the vulnerable preterm heart and circulation on adult cardiovascular disease risk. *Hypertension*. 2020;76 (4):1028–1037. DOI: 10.1161/HYPERTENSIONAHA.120.15574.
2. Huckstep O.J., Burchert H., Williamson W., Telles F., Tan C., Bertagnolli M. et al. Impaired myocardial reserve underlies reduced exercise capacity and heart rate recovery in preterm-born young adults. *Eur. Heart J. Cardiovasc. Imaging*. 2021;22(5):572–580. DOI: 10.1093/ehjci/jeaa060.
3. Crump C., Howell E.A., Stroustrup A., McLaughlin M.A., Sundquist J., Sundquist K. Association of preterm birth with risk of ischemic heart disease in adulthood. *JAMA Pediatr*. 2019;173 (8):736–743. DOI: 10.1001/jamapediatrics.2019.1327.
4. Carr H., Cnattingius S., Granath F., Ludvigsson J.F., Edstedt Bonamy A.K. Preterm birth and risk of heart failure up to early adulthood. *J. Am. Coll. Cardiol*. 2017;69(21):2634–2642. 10.1016/j.jacc.2017.03.572.
5. Aye C., Lewandowski A.J., Lamata P., Upton R., Davis E., Ohuma E.O. et al. Disproportionate cardiac hypertrophy during early postnatal development in infants born preterm. *Pediatr. Res*. 2017;82(1):36–46. DOI: 10.1038/pr.2017.96.
6. Mohlkert L.A., Hallberg J., Broberg O., Rydberg A., Halvorsen C.P., Liuba P. et al. The preterm heart in childhood: Left ventricular structure, geometry, and function assessed by echocardiography in 6-year-old survivors of periviable births. *J. Am. Heart Assoc*. 2018;7(2):e007742. DOI: 10.1161/JAHA.117.007742.
7. Burchert H., Lewandowski A.J. Preterm birth is a novel, independent risk factor for altered cardiac remodeling and early heart failure: Is it time for a new cardiomyopathy? *Curr. Treat. Options Cardio. Med*. 2019;21(2):8. DOI: 10.1007/s11936-019-0712-9.
8. Goss K.N., Haraldsdottir K., Beshish A.G., Barton G.P., Watson A.M., Palta M. et al. Association between preterm birth and arrested cardiac growth in adolescents and young adults. *JAMA Cardiol*. 2020;5(8):910–919. DOI: 10.1001/jamacardio.2020.1511.
9. Alsaied T., Omar K., James J.F., Hinton R.B., Crombleholme T.M., Habli M. Fetal origins of adult cardiac disease: a novel approach to prevent fetal growth restriction induced cardiac dysfunction using insulin like growth factor. *Pediatr. Res*. 2017;81(6):919–925. DOI: 10.1038/pr.2017.18.
10. Vrselja A., Pillow J.J., Black M.J. Effect of preterm birth on cardiac and cardiomyocyte growth and the consequences of antenatal and postnatal glucocorticoid treatment. *J. Clin. Med*. 2021;10(17):3896. DOI: 10.3390/jcm10173896.
11. Lewandowski A.J., Lamata P., Francis J.M., Piechnik S.K., Ferreira V.M., Boardman H et al. Breast milk consumption in preterm neonates and cardiac shape in adulthood. *Pediatrics*. 2016;138 (1): e20160050. DOI: 10.1542/peds.2016-0050.
12. Bensley J.G., Moore L., De Matteo R., Harding R., Black M.J.

Impact of preterm birth on the developing myocardium of the neonate. *Pediatr. Res*. 2018;83(4):880–888. DOI: 10.1038/pr.2017.324.
13. Tanswell A.K., Wong L., Possmayer F., Freeman B.A. The preterm rat: a model for studies of acute and chronic neonatal lung disease. *Pediatr. Res*. 1989;25(5):525–529. DOI: 10.1203/00006450-198905000-00020.
14. Grases-Pintó B., Torres-Castro P., Abril-Gil M., Castell M., Rodríguez-Lagunas M.J., Pérez-Cano F.J. et al. A preterm rat model for Immunonutritional studies. *Nutrients*. 2009;11(5):999. DOI: 10.3390/nu11050999.
15. Bensley J.G., De Matteo R., Harding R., Black M.J. The effects of preterm birth and its antecedents on the cardiovascular system. *Acta Obstet. Gynecol. Scand*. 2016;95(6) 652–663. DOI: 10.1111/aogs.12880.
16. Telles F., McNamara N., Nanayakkara S., Doyle M.P., Williams M., Yaeger L. et al. Changes in the preterm heart from birth to young adulthood: A meta-analysis. *Pediatrics*. 2020;146(2):e20200146. DOI: 10.1542/peds.2020-0146.
17. Allison B.J., Nguyen V., Yiallourou S.R., Nitsos I., Black M.J., Polglase G.R. The effect of sex and prematurity on the cardiovascular baroreflex response in sheep. *Exp. Physiol*. 2018;103(1):9–18. DOI: 10.1113/EP086494.
18. Dudley D.J., Branch D.W., Edwin S.S., Mitchell M.D. Induction of preterm birth in mice by RU486. *Biol. Reprod*. 1996;55(5):992–995. DOI: 10.1095/biolreprod55.5.992.
19. Alvarez R. Jr., Wang B.J., Quijada P.J., Avitabile D., Ho T., Shaitrit M et al. Cardiomyocyte cell cycle dynamics and proliferation revealed through cardiac-specific transgenesis of fluorescent ubiquitinated cell cycle indicator (FUCCI). *J. Mol. Cell. Cardiol*. 2019;127:154–164. DOI: 10.1016/j.yjmcc.2018.12.007.
20. Jiang Y.H., Zhu Y., Chen S., Wang H.L., Zhou Y., Tang F.Q. et al. Re-enforcing hypoxia-induced polyploid cardiomyocytes enter cytokinesis through activation of β-catenin. *Sci. Rep*. 2019;9:17865. DOI: 10.1038/s41598-019-54334-4.
21. Rechberger T., Abramson S.R., Woessner J.F. Jr. Onapristone and prostaglandin E2 induction of delivery in the rat in late pregnancy: a model for the analysis of cervical softening. *Am. J. Obstet. Gynecol*. 1996;175(3):719–723. DOI: 10.1053/ob.1996.v175.a74254.
22. Fang X., Wong S., Mitchell B.F. Effects of RU486 on estrogen, progesterone, oxytocin, and their Receptors in the rat uterus during late gestation. *Endocrinology*. 1997;138(7):2763–2768. DOI: 10.1210/endo.138.7.5247.
23. Li Y., Je H.D., Malek S., Morgan K.G. Role of ERK1/2 in uterine contractility and preterm labor in rats. *Am. J. Physiol. Regul. Integr. Compar. Physiol*. 2004;287(2):R328–R335. DOI: 10.1152/ajpregu.00042.2004.
24. Kuz'minykh T.U., Petrosyan M.A. The comparison of the effect of different synthetic antigestagens on the start of contractile activity in pregnant rats and postnatal development of their offspring. *Zhurnal Akusherstva i Zhenskikh Bolezney*. 2009;2:34–39 (in Russ.).
25. Cadepond F., Ulmann A., Baulieu E.E. RU486 (mifepristone): mechanisms of action and clinical uses. *Annu. Rev. Med*. 1997;48:129–156. DOI: 10.1146/annurev.med.48.1.129. PMID: 9046951.
26. Nielsen B.W., Bonney E.A., Pearce B.D., Donahue L.R., Sarkar I.N., Preterm Birth International Collaborative (PREBIC). A cross-species analysis of animal models for the investigation of preterm birth mechanisms. *Reprod. Sci*. 2016;23(4):482–491. DOI: 10.1177/1933719115604729.
27. Clark C.M. Jr. Characterization of glucose metabolism in the isolated rat heart during fetal and early neonatal development. *Diabetes*. 1973;22(1):41–49. DOI: 10.2337/diab.22.1.41.
28. Ito T., Harada K., Takada G. In situ morphometric analysis of left and right ventricles in fetal rats: changes in ventricular volume, mass, wall thickness, and valvular size. *Tohoku J. Exp. Med*. 2001;193(1):37–44. DOI: 10.1620/tjem.193.37.
29. Li F., Wang X., Bunger P.C., Gerdes A.M. Formation of binucleated cardiac myocytes in rat heart: I. Role of actin-myosin contractile ring. *J. Mol. Cell. Cardiol*. 1997;29(6):1541–1551. DOI: 10.1006/jmcc.1997.0381.

Authors information

Ivanova Vera V. – Cand. Sci. (Biology), Associate Professor, Morphology and General Pathology Division, Siberian State Medical University, Tomsk, ivvera92@rambler.ru, http://orcid.org/0000-0002-2530-1112

Milto Ivan V. – Dr. Sci. (Biology), Associate Professor, Professor, Morphology and General Pathology Division, Siberian State Medical University, Tomsk; Deputy Director for Research, Seversk Biophysical Research Center, Seversk-13, milto_bio@mail.ru, http://orcid.org/0000-0002-9764-4392

Serebryakova Olga N. – Teaching Assistant, Morphology and General Pathology Division, Siberian State Medical University, Tomsk, oserebryakovan@gmail.com, http://orcid.org/0000-0002-2924-0724

Sukhodolo Irina V. – Dr. Sci. (Med.), Professor, Head of the Morphology and General Pathology Division, Siberian State Medical University, Tomsk, staranie@mail.ru, http://orcid.org/0000-0001-9848-2068

(✉) **Ivanova Vera V.,** ivvera92@rambler.ru

Received 09.11.2021;
approved after peer review 18.01.2022;
accepted 09.06.2022

УДК 575.174.015.3:577.34
https://doi.org/10.20538/1682-0363-2022-4-79-87

Search for polymorphic variants of candidate genes contributing to individual radiosensitivity

Isubakova D.S.[1], Litviakov N.V.[1, 2], Tsymbal O.S.[1], Usova T.V.[1], Tsyplenkova M.Yu.[1], Milto I.V.[1, 3], Takhauov R.M.[1, 3]

[1] *Seversk Biophysical Research Center*
P.O. Box-130, Seversk-13, 636013, Russian Federation

[2] *Cancer Research Institute of Tomsk National Research Medical Center (NRMC), Russian Academy of Sciences*
5, Cooperativny Lane, Tomsk, 634009, Russian Federation

[3] *Siberian State Medical University*
2, Moscow Trakt, Tomsk, 634050, Russian Federation

ABSTRACT

Background. Cytogenetic damage (CD) in lymphocytes induced by low doses (up to 0.1 Sv) of ionizing radiation (IR) is the main cytogenetic sign of individual radiosensitivity of the human body. In addition to DNA repair and cell death, which affect the formation of CD and its elimination, IR effects on the cell can be manifested through changes in proliferation of cells with unrepaired DNA damage. The system of cyclins and cyclin-dependent kinases (CDK), which provide coordination of mitotic events during passage of a cell through the cell cycle, plays a crucial role in regulation of cell proliferation.

Aim To evaluate the relationship of single-nucleotide polymorphisms (SNPs) of cell cycle genes with an increased frequency of CD in workers of a nuclear power plant affected by chronic occupational radiation exposure in the dose range of 100–500 mSv.

Materials and methods. The object of the study was blood of 55 conditionally healthy workers of Siberian Chemical Plant (SCP) who were affected by chronic occupational radiation exposure (gamma radiation) in the dose range of 100–500 mSv. A standard cytogenetic analysis of blood lymphocytes was performed for all examined individuals. Genomic DNA was isolated from the blood of the workers using the QIAamp DNA Blood Mini Kit (QIAGEN, Germany). DNA was genotyped using 257 SNPs of cyclin genes and neighboring intergenic regions using DNA microarrays from the high-density CytoScan HD Array (Affymetrix, USA).

Results. Taking into account the Bonferroni correction, only statistically significant associations of SNPs with the frequency of dicentric chromosomes were found; all other types of chromosomal aberrations did not show statistical significance. The rs803054 *CCNI2* was associated with an increased frequency of dicentric chromosomes arising under the influence of chronic occupational radiation exposure.

Conclusion. The discovered SNP (rs803054), whose recessive genotype is associated with an increased frequency of dicentric chromosomes in workers of SCP exposed to radiation at doses of 100–500 mSv over a long time, can be considered as a potential marker of individual radiosensitivity. To confirm the identified associations, further validation studies are needed on an expanded sample of people affected by chronic occupational radiation exposure.

Keywords: ionizing radiation, individual radiosensitivity, chromosomal aberrations, gene polymorphism, microarray analysis

Conflict of interest. The authors declare the absence of obvious or potential conflicts of interest related to the publication of this article.

Source of financing. The study was carried out within the framework of state assignment No. 388-00162-22-00 dated 01.03.2022.

✉ *Isubakova Daria S.,* isubakova.daria@yandex.ru

Conformity with the principles of ethics. All donors signed an informed consent to participate in the study. The study was approved by the local Ethics Committee at Cancer Research Institute of Tomsk NRMC.

For citation: Isubakova D.S., Litviakov N.V., Tsymbal O.S., Usova T.V., Tsyplenkova M.Yu., Milto I.V., Takhauov R.M. Search for polymorphic variants of candidate genes contributing to individual radiosensitivity. *Bulletin of Siberian Medicine.* 2022;21(4):79–87. https://doi.org/10.20538/1682-0363-2022-4-79-87.

Поиск полиморфных вариантов кандидатных генов индивидуальной радиочувствительности

Исубакова Д.С.[1], Литвяков Н.В.[1, 2], Цымбал О.С.[1], Усова Т.В.[1], Цыпленкова М.Ю.[1], Мильто И.В.[1, 3], Тахауов Р.М.[1, 3]

[1] Северский биофизический научный центр (СБН Центр)
Россия, 636013, Томская обл., г. Северск-13, а/я 130

[2] Научно-исследовательский институт (НИИ) онкологии, Томский национальный исследовательский медицинский центр (НИМЦ) Российской академии наук
Россия, 634009, г. Томск, пер. Кооперативный, 5

[3] Сибирский государственный медицинский университет (СибГМУ)
Россия, 634050, г. Томск, Московский тракт, 2

РЕЗЮМЕ

Актуальность. Цитогенетические нарушения (ЦН) лимфоцитов, индуцированные «малыми» дозами (до 100 мЗв) ионизирующего излучения (ИИ), являются основными цитогенетическими признаками индивидуальной радиочувствительности организма человека. Помимо репарации ДНК и гибели клеток, которые влияют на формирование ЦН и их элиминацию, вклад в последствия воздействия ИИ на клетку может реализоваться за счет изменений пролиферации клеток с нерепарированными дефектами ДНК. Определяющую роль в регуляции пролиферации клеток играет система циклинов и циклин-зависимых киназ, которые обеспечивают координацию митотических событий при прохождении клеточного цикла.

Цель. Оценить связь однонуклеотидных полиморфизмов (ОНП) генов клеточного цикла с повышенной частотой ЦН, возникших у персонала объекта использования атомной энергии, под действием долговременного техногенного профессионального облучения ИИ в диапазоне доз 100–500 мЗв.

Материалы и методы. Объектом исследования служила кровь 55 условно здоровых работников Сибирского химического комбината (СХК), подвергавшихся в процессе профессиональной деятельности долговременному техногенному радиационному воздействию (γ-излучение) в дозах 100–500 мЗв. Для всех обследованных лиц проводили стандартный цитогенетический анализ лимфоцитов крови. Геномную ДНК из крови работников выделяли с помощью набора QIAamp DNA Blood mini Kit (Qiagen, Германия). Генотипировали ДНК по 257 ОНП генов циклинов и межгенных областей вблизи генов циклинов с помощью ДНК-чипов высокой плотности CytoScan HD Array (Affymetrix, США).

Результаты. Установлено, что с учетом поправки Бонферрони имеются только статистически значимые связи ОНП с высокой частотой дицентрических хромосом, все остальные типы изученных ЦН не показали достоверных отличий. С повышенной частотой дицентрических хромосом, возникающих под действием долговременного техногенного профессионального облучения ИИ, ассоциирован rs803054 *CCNI2*.

Заключение. Обнаруженный ОНП (rs803054), рецессивный генотип которого ассоциирован с повышенной частотой дицентрических хромосом у работников СХК, подвергавшихся в процессе профессиональной деятельности долговременному техногенному радиационному воздействию (γ-излучение) в дозах 100–500 мЗв, можно рассматривать в качестве потенциального маркера индивидуальной радиочувствительности. Для подтверждения выявленных ассоциаций необходимы дальнейшие валидационные исследования на расширенной выборке людей, подвергавшихся долговременному техногенному профессиональному облучению ИИ.

Ключевые слова: ионизирующее излучение, индивидуальная радиочувствительность, хромосомные аберрации, полиморфизм генов, микроматричный анализ

Конфликт интересов. Авторы декларируют отсутствие явных и потенциальных конфликтов интересов, связанных с публикацией настоящей статьи.

Источник финансирования. Исследование выполнено в рамках государственного задания № 388-00162-22-00 от 01.03.2022.

Соответствие принципам этики. Все доноры подписали добровольное информированное согласие на участие в исследовании. Исследование одобрено НИИ онкологии Томского НИМЦ.

Для цитирования: Исубакова Д.С., Литвяков Н.В., Цымбал О.С., Усова Т.В., Цыпленкова М.Ю., Мильто И.В., Тахауов Р.М. Поиск полиморфных вариантов кандидатных генов индивидуальной радиочувствительности. *Бюллетень сибирской медицины.* 2022;21(4):79–87. https://doi.org/10.20538/1682-0363-2022-4-79-87.

INTRODUCTION

Cytogenetic signs of individual radiosensitivity (IRS) of the human body include frequency of induced cytogenetic damage (CD) and formation of radiogenic disease, among which tumor diseases are the most prevalent [1–3]. Lymphocytes are cells in the human body that are the most sensitive to the effect of ionizing radiation (IR). Blood lymphocytes with induced CD are eliminated from the body through various types of cell death, such as apoptosis, necrosis, necroptosis, autophagic cell death, mitotic catastrophe, and accelerated aging of irradiated cells [4–6]. However, when these mechanisms of death are impaired or their activity decreases due to normal genomic variation, CD-affected lymphocytes can accumulate, which is manifested through an increase in the frequency of CD even at low doses of IR.

Another mechanism in the frequency of CD is proliferation of lymphocytes, since it is well known that chromosomal aberrations are eliminated during proliferation [1, 2]. A system of cyclins plays a crucial role in the regulation of proliferation. They function as regulators of cyclin-dependent kinases (CDKs) and contribute to temporal coordination of each mitotic event. Therefore, the formation and elimination of CD are directly affected by the variability in the mechanisms of DNA repair and cell death and indirectly affected by the variability in the mechanisms of proliferation of cells with unrepaired CD.

A genome-wide study of the association of 162 single-nucleotide polymorphisms (SNPs) in cyclin genes (*CCNA1, CCNA2, CCNB1, CCNB2, CCNB3, CCND1, CCND2, CCND3, CCNE1, CCNE2, CCNF, CCNG1, CCNH, CCNI, CCNI2, CCNJ, CCNJL, CCNK, CCNY*) and 95 neighboring intergenic SNPs with high frequency of CD was carried out in workers of Siberian Chemical Plant (SCP, 55 people) who experienced occupational radiation exposure in the dose range of 100–500 mSv. In a preliminary study on the dose – effect relationship, a plateau was observed, i.e. the frequency of CD did not change with the increasing dose [7, 8], and it is this dose range that should be used for studying the association of SNPs with increased frequency of CD to assess IRS.

The aim of the study was to evaluate the relationship of SNPs in cyclin genes and their promoters with the increased frequency of CD in workers of a nuclear power plant who experienced chronic occupational radiation exposure in the dose range of 100–500 mSv.

MATERIALS AND METHODS

The study used whole venous blood obtained from 38 conditionally healthy SCP workers who were not exposed to IR in their professional activities (the control group) and 55 conditionally healthy SCP workers who experienced chronic occupational radiation exposure (gamma radiation) in the dose range of 100–500 mSv (the experimental group). The characteristics of the studied groups are presented in Table 1.

Table 1

Characteristics of the studied groups of SCP workers

Parameter		Control group, $n = 38$	Experimental group, $n = 55$
Men / Women		38/0	55/0
Age, years	*Me*	52.00	59.00
	L–R	37.00–58.00	54.00–69.00
Work experience, years	*Me*	20.00	34.00
	L–R	12.00–34.00	29.00–42.00
External radiation dose, mSv	*Me*	–	203.35
	L–R	–	164.00–276.15

Information about donors of the biological material was collected and clarified using the database in the medical and dosimetric register of SCP staff and the Archives of Seversk Biophysical Research Center, containing medical information about all SCP workers [9]. In accordance with the Federal Law No. 323-FZ of 21.11.2011 "On the Basics of Public Health Protection in the Russian Federation", each donor signed an informed consent to participate in the study.

Blood was taken from donors from the ulnar vein. It was collected in the volume of 9 ml in Vacuette K3 EDTA tubes (Greiner Bio-one, Austria) using a Vacuette Visio Plus needle 38 × 0.8 mm, 21G × 11/2 (Greiner Bio-one, Austria) for subsequent DNA isolation and microarray. To prepare cytogenetic suspensions, blood was collected in the volume of 9 ml in Vacuette LH Lithium Heparin tubes (Greiner Bio-one, Austria) using a Vacuette Visio Plus needle 38 × 0.8 mm, 21G × 11/2 (Greiner Bio-one, Austria).

The individuals included in the study underwent a cytogenetic analysis of mononuclear leukocytes. For lymphocyte culture, whole venous blood was used. It was mixed with a nutrient medium (15% fetal bovine serum and 85% RPMI 1640 medium supplemented with glutamine, phytohemagglutinin, and penicillin) and incubated (at 37 °C) in culture tubes (Corning, USA) in the dry air shaker – incubator (Biosan, Latvia). The cytogenetic analysis was performed using the Leica DM2500 microscope (Leica, Germany). At least 300 metaphase plates were analyzed for each individual. The results were presented as the frequency of CD per 100 metaphase plates. The following types of CD were determined: aberrant cells, polyploid cells, multi-aberrant cells (more than 5 chromosomal aberrations), chromosomal and chromatid fragments, ring and dicentric chromosomes, chromatid exchanges (crossing over), and translocations.

DNA was isolated from mononuclear leukocytes using the QIAamp DNA Blood Mini Kit (Qiagen, Germany). The purity (A260 / A280 = 1.80–2.00, A260 / A230 = 1.90–2.15) and concentration (50–150 ng / ml) of DNA were determined on the NanoDrop 2000 spectrophotometer (Thermo Scientific, USA). DNA integrity was determined using capillary electrophoresis – DNA fragments were larger than 48 kb.

The studied SNPs were genotyped using DNA microarrays from the high-density CytoScan™ HD Array (Affymetrix, USA). Sample preparation, hybridization, and scanning were carried out in accordance with the manufacturer's protocol. The microarray results were processed using Chromosome Analysis Suite 4.3 software (Affymetrix, USA). To clarify and identify SNPs and genes to which they belong, the Affymetrix genotype database, NCBI, OMIM, GWAS Catalog, and SNPedia databases were used.

The following SNPs of cyclin genes (*CCN*) and neighboring intergenic regions were studied ($n = 257$):

– *CCNA1 (cyclin A1)*: rs7997378, rs3814803, rs17188012;

– *CCNA2* (*cyclin A2*): rs3217753, rs3217772, rs3217771;

– *CCNB1* (*cyclin B1*): rs1128761;

– *CCNB2* (*cyclin B2*): rs28383518, rs28383514, rs75767699, rs169410487, rs16941042, rs16941046, rs28383551;

– *CCNB3* (*cyclin B3*): rs12848359, rs12009873, rs7063886, rs6614336, rs12007902, rs17003332;

– *CCND1* (*cyclin D1*): rs3212869, rs649392;

– *CCND2* (*cyclin D2*): rs3217805, rs4765775, rs3217916, rs3217812, rs3217848, rs3217830, rs11063072, rs3217882, rs3217898, rs3217933;

– *CCND3* (*cyclin D3*): rs9369318;

– *CCNE1 (cyclin E1)*: rs3218071, rs3218035, rs3218036, rs41520849, rs3218038, rs3218068, rs3218042, rs3218064, rs3218066, rs3218044;

– *CCNE2* (*cyclin E2*): rs2467670, rs16893774, rs2278891;

– *CCNF* (*cyclin F*): rs8052046;

– *CCNG1* (*cyclin G1*): rs299322, rs2069345, rs2069347;

– *CCNH* (*cyclin H*): rs6879293, rs3752862, rs74582239, rs16902635, rs16902632, rs75949864, rs6891010, rs10067098, rs115516306, rs114916935, rs3827607, rs16902623, rs16902625, rs11745338, rs16902631, rs77996308, rs1062035;

– *CCNI* (*cyclin I*): rs803054, rs803057, rs10006033, rs62302339;

– *CCNJ* (*cyclin J*): rs4921132, rs57334361, rs17057562, rs6875660, rs4921270, rs74734346, rs17057596, rs78444213, rs17111275, rs2303059, rs915506, rs6874570, rs6556488, rs11949221, rs17057577, rs6899125, rs754112, rs2421777, rs2421778, rs17057631, rs10052876, rs2421779, rs2421780, rs10038395, rs28595384, rs72814336, rs12657051, rs17057641, rs9313842, rs11596126;

– *CCNK* (*cyclin K*): rs10144895, rs3918051, rs3918094, rs2069492, rs2069493, rs3918139, rs3918048;

– *CCNY* (*cyclin Y*): rs12261552, rs113182825, rs115589270, rs11816866, rs111374708, rs2295417, rs115469285, rs2504352, rs2504350, rs2474533, rs4934749, rs35745247, rs17593103, rs75954134,

rs16936030, rs3003980, rs16936032, rs3013364 rs114206731, rs12241755, rs16936035, rs74979754, rs10508817, rs10827506, rs11010151, rs4934753, rs112496700, rs11591533, rs4934754, rs1345561, rs12248732, rs10508818, rs116338411, rs75609581, rs11010178, rs74866156, rs2086153, rs12242002, rs10827509, rs112818779, rs11595699, rs11010213, rs16936102, rs3003981, rs7067539, rs61449529, rs10827512, rs4934551, rs11010225, rs7910421, rs17500653, rs116009947, rs12249814, rs112091952;

– neighboring intergenic regions: rs6817626, rs2138940, rs9566153, rs13153588, rs6509615, rs9547604, rs4865924, rs73537845, rs79959089, rs79226566, rs17053967, rs12508668, rs4241604, rs413127, rs11097684, rs115693938, rs9315437, rs2323125, rs12902628, rs5961171, rs59776629, rs6887755, rs6826342, rs4557282, rs375299, rs4502705, rs6818356, rs7682171, rs13133761, rs4518274, rs6849124, rs6849534, rs6871154, rs323746, rs112520532, rs9603050, rs114501411, rs323758, rs323757, rs1441709, rs2919902, rs984026, rs34383364, rs17285919, rs9547632, rs73770251, rs35556022, rs1517886, rs35000040, rs6892636, rs11749408, rs11749439, rs3909481, rs7250135, rs4805497, rs10422957, rs17002403, rs35204615, rs16963260, rs4998568, rs11882235, rs56400371, rs28582702, rs11881322, rs255259, rs1811302, rs255263, rs77475690, rs11084309, rs410468, rs17053969, rs10514840, rs17053994, rs76165140, rs74045329, rs17054069, rs12866109, rs1517893, rs9315426, rs7489996, rs7692898, rs9594152, rs9603064, rs1474085, rs6822060, rs17054113, rs9603072, rs4943389, rs7317651, rs17191516, rs17054217, rs9547595, rs660005, rs16963219, rs594452.

The genotyping data for each studied SNP were analyzed according to four genetic models: dominant, recessive, additive, and over-dominant. According to the dominant model, the frequency of CD was compared in homozygous recessive and heterozygous individuals and in homozygous dominant individuals. According to the recessive model, the frequency of CD was compared in homozygous dominant and heterozygous individuals and in homozygous recessive individuals. The additive model was used to compare the frequency of CD in homozygous dominant, homozygous recessive, and heterozygous individuals. The over-dominant model was used to compare the frequency of CD in homozygous dominant and homozygous recessive individuals, on the one hand, and heterozygous carriers, on the other hand.

Statistical processing of the results was carried out using Statistica 8.0 software (StatSoft, USA). The results were presented as the median and the interquartile range *Me (L–R)*.

The genotype distribution was tested for deviations from the Hardy – Weinberg equilibrium using the Court lab HW calculator program in Excel. The Mann – Whitney test with the Bonferroni correction ($p < 0.05$) was used to determine the significance of differences in the frequency of CD.

RESULTS

At the first stage, a cytogenetic study of the frequency of CD in the SCP workers of both groups was carried out to confirm the increased frequency of CD in the workers of the experimental group. The results are presented in Table 2.

Table 2

Comparison of the frequency of CD in SCP workers of the control and experimental groups, per 100 cells *Me* (*L–R*)

Parameter	Control group, *n* = 38	Experimental group, *n* = 55	*p*
Number of aberrant cells	1.0000 (0.3333–2.3333)	2.5641 (1.4285–3.3333)	**0.0002**
Chromatid fragments	0.3316 (0.0000–0.6666)	0.6269 (0.0000–1.3071)	0.1294
Chromosomal fragments	0.3268 (0.0000–0.6557)	0.3225 (0.0000–0.9118)	0.5140
Ring chromosomes	0.0000 (0.0000–0.0000)	0.2724 (0.0000–0.3333)	**0.0050**
Dicentric chromosomes	0.3322 (0.0000–0.9493)	0.7712 (0.0000–1.2578)	**0.0280**
Multi-aberrant cells	0.0000 (0.0000–0.0000)	0.0000 (0.0000–0.0000)	0.8819
Chromatid exchanges	0.0000 (0.0000–0.0000)	0.0000 (0.0000–0.0000)	0.2687
Translocations	0.0000 (0.0000–0.0000)	0.0000 (0.0000–0.0000)	0.8819
Polyploid cells	0.0000 (0.0000–0.0000)	0.0000 (0.0000–0.0000)	0.8820

Note: here and in Table 3, statistically significant differences are highlighted in bold.

As can be seen from Table 2, the frequency of most types of CD, which are not markers of radiation exposure, do not differ in both groups of SCP workers. It may be due to the fact that all the employees of SCP included in the study live and work in approximately identical conditions, i.e. the samples were thoroughly stratified, and the control and experimental groups do not differ significantly, except for markers of radiation exposure – ring and dicentric chromosomes.

It is well known that lifestyle (smoking, alcohol consumption, and other bad habits), environmental factors (to a lesser extent), and industrial exposure to harmful chemical and toxic substances can drastically increase the frequency of CD in humans. The absence of differences in the frequency of chromatid and chromosomal fragments, multi-aberrant cells, chromatid exchanges, translocations, and polyploid cells indicates the absence of the above differences in the workers of the studied groups. However, the frequency of radiation exposure markers (ring and dicentric chromosomes) and the frequency of aberrant cells (due to ring and dicentric chromosomes) are significantly higher in the workers who have been experiencing chronic occupational radiation exposure.

At the second stage, we assessed the association of the frequency of radiation-induced CD with the polymorphic variants of the studied genes in the experimental group. When analyzing the data, we excluded SNPs of any genotype with $n < 5$, since in conditions of a small sample, this increased the probability of type I errors. Further, we excluded SNPs that deviated from the Hardy – Weinberg equilibrium. Therefore, out of 257 SNPs, 58 SNPs were included in the final statistical analysis. Their association with high frequency of the identified CD was revealed.

Figure shows the significance levels for 58 selected SNPs (see above) by dicentric chromosomes.

The negative logarithm of the confidence level is depicted on the ordinate axis. The line above shows the confidence level with the Bonferroni correction.

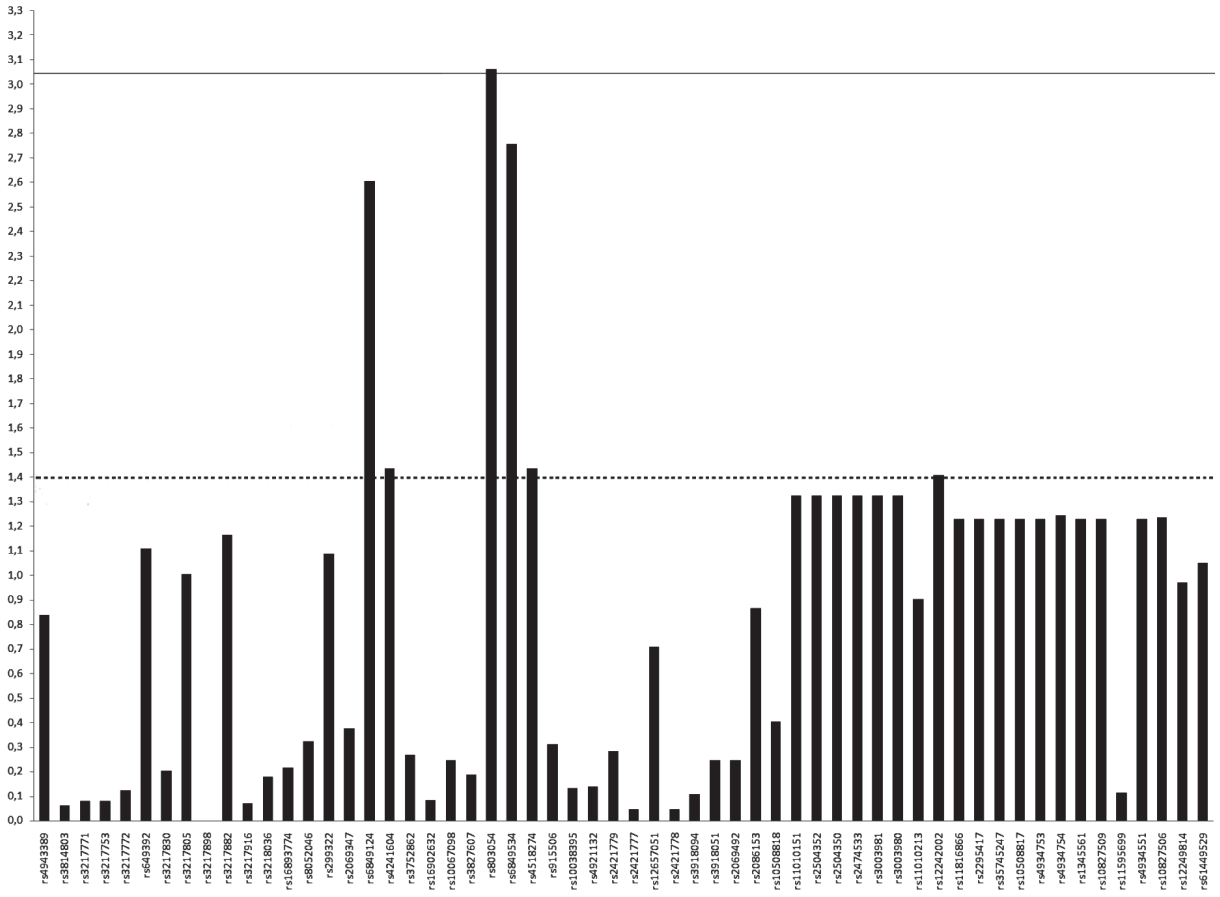

Figure. Significance levels for the recessive model based on the frequency of dicentric chromosomes. The ordinate axis is the p value on the logarithmic scale – (log10); the dotted line marks the significance level of $p < 0.05$ calculated according to the Mann – Whitney test; the red line denotes the Bonferroni correction.

It equals to –log(0.05/57) = 3.0644. Therefore, Figure shows that, taking into account the Bonferroni correction, only 1 SNP is associated with high frequency of dicentric chromosomes in the SCP workers of the experimental group.

Of the 58 identified SNPs, the genotyping data analysis carried out for all four genetic models (dominant, recessive, additive, and over-dominant) showed an association with high frequency of dicentric chromosomes (markers of radiation exposure) for the recessive model for 1 SNP: *CCNI2* (*rs803054*) (Table 3).

Table 3

The frequency of dicentric chromosomes depending on the genotypes of the studied genes in the experimental group of SCP workers, per 100 cells, *M (L–R)*

Parameter	Frequency of dicentric chromosomes by the genotype			*p*	Bonfer-roni correction
Dominant model					
CCNI2 rs803054	*A/G + G/G*, *n* = 39	*A/A*, *n* = 16		0.0865	0.000874
	0.9740 (0.0000–1.6666)	0.3928 (0.0000–1.0317)			
Recessive model					
CCNI2 rs803054	*A/A + A/G*, *n* = 42	*G/G*, *n* = 13		**0.0008**	0.000874
	0.5303 (0.0000–1.0899)	1.4285 (1.0256–1.8750)			
Over-dominant model					
CCNI2 rs803054	*A/A + G/G*, *n* = 28	*A/G*, *n* = 27		0.1116	0.000874
	0.9890 (0.3928–1.5476)	0.6060 (0.0000–1.0899)			
Additive model					
CCNI2 rs803054	*A/A*, *n* = 16	*A/G*, *n* = 26	*G/G*, *n* = 13	0.8645	0.000874
	0.3928 (0.0000–1.0317)	0.6298 (0.0000–1.0899)	1.4285 (1.0256–1.8750)		

DISCUSSION

The polymorphic variant rs803054 is intronic, located at chr5:132750285 (GRCh38.p13), and belongs to the *CCNI2* gene. In 2008, S. Choudhry et al. suggested that 5q23.3 (the authors indicated that rs803054 is located at position chr5:132162193) is a potential region containing asthma genes in Puerto Ricans [10]. There is no other information about the contribution of this SNP to the regulation of the functional activity of *CCNI2*, including information in the SNPedia database.

In contrast to the results described by S. Choudhry et al., our work showed the association of rs803054 with radiation-induced CD. Thus, it was revealed that for rs803054 *CCNI2,* the frequency of dicentric chromosomes was 2 times higher in carriers of the recessive genotype than in carriers of the dominant genotype at relatively identical doses of IR. One of the reasons for the higher frequency of ring and dicentric chromosomes in workers of the experimental group was chronic occupational exposure to IR [11].

CCNI2 is located at the long arm of chromosome 5 (5q31.1), it is considered a homolog of *CCNI*. *CCNI2* interacts with CDK5 and activates it. C. Liu et al. and J. Taneera et al. showed that the depletion of CCNI2 by siRNA inhibits passage of a cell through the cell cycle and cell proliferation [12, 13]. D.M.Lai et al. demonstrated a reduced level of CCNI2 expression, which, in turn, inhibited proliferation of colorectal cancer cells, stopped the cell cycle in the G2 phase, and stimulated apoptosis [14]. There are findings that a decrease in *CCNI2* expression slows down progression of gastric cancer by inhibiting proliferation of tumor cells, increasing susceptibility to apoptosis, and suppressing cell migration [15].

It is also known that CD is eliminated during proliferation, therefore, according to our results, carriers of the recessive rs803054 *CCNI2* allele may have a decrease in *CCNI2* expression, following which the proliferative potential of lymphocytes and the intensity of CD elimination (which includes dicentric chromosomes) decrease. The results obtained are in good agreement with the data obtained by [12, 13]. With chronic occupational exposure to IR, this leads to an increase in the frequency of dicentric chromosomes.

CONCLUSION

For the first time, the rs803054 SNP was identified, which can be considered a potential marker of IRS. It was shown that the SCP workers who are homozygous for the recessive rs803054 allele had increased frequency of dicentric chromosomes in blood lymphocytes during chronic occupational exposure to IR in the dose range of 100–500 mSv. The identified

candidate marker of IRS can be used to develop a test system for detection of genetically determined IRS using a real-time PCR system.

REFERENCES

1. Elisova T.V. Stable and unstable chromosome aberrations in humans and other mammals in relation to the problems of biological dosimetry. *Radiation Biology. Radioecology*. 2008;48(1):14–27 (in Russ.).
2. Balaeva L.S., Sipyagina A.E. Urgent problem of our time: the risk of developing radiation-induced stochastic diseases in the generations of children from irradiated parents. *Rossiyskiy Vestnik Perinatologii i Pediatrii*. 2019;64(1):7–14 (in Russ.). DOI: 10.21508/1027-4065-2019-64-1-7-14.
3. Kim B.M., Hong Y., Lee S., Liu P., Lim J.H., Lee Y.H. et al. Therapeutic implications for overcoming radiation resistance in cancer therapy. *Int. J. Mol. Sci*. 2015;16(11):26880–26913. DOI: 10.3390/ijms161125991.
4. Maier P., Hartmann L., Wenz F., Herskind C. Cellular pathways in response to ionizing radiation and their targetability for tumor radiosensitization. *Int. J. Mol. Sci*. 2016;17(1):102. DOI: 10.3390/ijms17010102.
5. Baskar R., Lee K.A., Yeo R., Yeoh K.W. Cancer and radiation therapy: current advances and future directions. *Int. J. Med. Sci*. 2012;9(3):193–199. DOI: 10.7150/ijms.3635.
6. Freidin M.B., Vasilyeva E.O., Skobelskaya E.V., Goncharova I.A., Karpov A.B., Takhauov R.M. The prevalence and spectrum of chromosomal aberrations in workers of the Siberian Group of Chemical Enterprises. *Bulletin of Siberian Medicine*. 2005;(2):75–81.
7. Litviakov N.V., Freidin M.B., Khalyuzova M.V., Sazonov A.E., Vasileva E.O., Albah E.N. et al. The frequency and spectrum of cytogenetic anomalies in employees of Siberian Chemical Plant. *Radiation Biology. Radioecology*. 2014;54(3):283–296 (in Russ.). DOI: 10.7868/S0869803114030084.
8. Isubakova D.S., Khalyuzova M.V., Litviakov N.V., Bronikovskaya E.V., Usova T.V., Takhauov R.M. et al. Cytogenetic anomalies in blood lymphocytes in employees of Siberian Chemical Plant exposed to occupational irradiation. *Radiation Biology. Radioecology*. 2021;61(4):353–366 (in Russ.). DOI: 10.31857/S0869803121040056.
9. Takhauov R.M., Karpov A.B., Albach E.N., Khalyuzova M.V., Freidin M.B., Litviakov N.V. et al. The bank of biological samples representing individuals exposed to long-term ionizing radiation at various doses. *Biopreserv Biobank*. 2015;13(2):72–78. DOI: 10.1089/bio.2014.0035.
10. Choudhry S., Taub M., Mei R., Rodriguez-Santana J., Rodriguez-Cintron W., Shriver M.D. et al. Genome-wide screen for asthma in Puerto Ricans: evidence for association with 5q23 region. *Hum Genet*. 2008;123(5):455–468. DOI: 10.1007/s00439-008-0495-7.
11. Snegireva G.P. Effects of ionizing radiation: cytogenetic changes in human blood lymphocytes. Moscow: Lomonosov Moscow State University, 2009:402 (in Russ.).
12. Liu C., Zhai X., Zhao B., Wang Y., Xu Z. Cyclin I-like (CCNI2) is a cyclin-dependent kinase 5 (CDK5) activator and is involved in cell cycle regulation. *Sci. Rep*. 2017;7:40979. DOI: 10.1038/srep40979.
12. Taneera J., Fadista J., Ahlqvist E., Zhang M., Wierup N., Renström E. et al. Expression profiling of cell cycle genes in human pancreatic islets with and without type 2 diabetes. *Mol. Cell Endocrinol*. 2013;375(1-2):35–42. DOI: 10.1016/j.mce.2013.05.003.
13. Lai D.M., Bi J.J., Chen Y.H., Wu Y.D., Huang Q.W., Li H.J. et al. CCNI2 plays a promoting role in the progression of colorectal cancer. *Cancer Med*. 2021;10(6):1913–1924. DOI: 10.1002/cam4.3504
14. Chen W., Zhou Y., Wu G., Sun P. CCNI2 promotes the progression of human gastric cancer through HDGF. *Cancer Cell Int*. 2021;21:661–673. DOI: 10.1186/s12935-021-02352-6.

Authors contribution

Isubakova D.S. – analysis and interpretation of the data, drafting of the article. Litviakov N.V. – conception and design. Tsymbal O.S., Usova T.V., Tsyplenkova M. Yu. – collection and processing of the material, carrying out of studies. Milto I.V. – critical revision of the manuscript for important intellectual content, editing of the article. Takhauov R.M. – critical revision of the manuscript for important intellectual content, editing of the article, final approval of the manuscript for publication.

Authors information

Isubakova Daria S. – Researcher, Department of Molecular and Cellular Radiobiology, Seversk Biophysical Research Center, Seversk, isubakova.daria@yandex.ru, http://orcid.org/0000-0002-5032-9096

Litviakov Nikolai V. – Dr. Sci. (Biology), Professor of the Russian Academy of Sciences, Leading Researcher, Seversk Biophysical Research Center, Seversk; Head of the Laboratory for Oncovirology, Cancer Research Institute, Tomsk NRMC, Tomsk, nvlitv72@yandex.ru, http://orcid.org/0000-0002-0714-8927

Tsymbal Olga S. – Researcher, Department of Molecular and Cellular Radiobiology, Seversk Biophysical Research Center, Seversk, olga-tsymbal@mail.ru, http://orcid.org/0000-0002-2311-0451

Usova Tatyana V. – Junior Researcher, Department of Molecular and Cellular Radiobiology, Seversk Biophysical Research Center, Seversk, vishnevskaya_seversk@mail.ru

Tsyplenkova Maria Yu. – Junior Researcher, Department of Molecular and Cellular Radiobiology, Seversk Biophysical Research Center, Seversk, mariatsyplenkova@yandex.ru.

Milto Ivan V. – Dr. Sci. (Biology), Deputy Director for Research, Seversk Biophysical Research Center, Seversk; Professor, Morphology and General Pathology Division, Siberian State Medical University, Tomsk, milto_bio@mail.ru, http://orcid.org/0000-0002-9764-4392

Takhauov Ravil M. – Honored Doctor of the Russian Federation, Dr. Sci. (Med.), Professor, Director of Seversk Biophysical Research Center, Seversk; Professor, Health Organization and Public Health Division, Siberian State Medical University, Tomsk, niirm2007@yandex.ru, http://orcid.org/0000-0002-1994-957X

(✉) **Isubakova Daria S.,** isubakova.daria@yandex.ru

Received 10.12.2021;
approved after peer review 24.10.2022;
accepted 26.10.2022

УДК 616.12-008.46:612.172
https://doi.org/10.20538/1682-0363-2022-4-88-97

Heart failure with preserved ejection fraction: the role of microvascular dysfunction

Kopeva K.V., Mochula A.V., Maltseva A.N., Grakova E.V., Shipulin V.V., Gusakova A.M., Zavadovsky K.V.

Cardiology Research Institute, Tomsk National Research Medical Center (NRMC), Russian Academy of Sciences
111a, Kievskaya Str., Tomsk, 634012, Russian Federation

ABSTRACT

Aim. To evaluate the relationship between coronary microvascular dysfunction (CMD), biomarkers of cardiac fibrosis and cardiac remodeling (soluble ST2 (sST2), fibroblast growth factor-23 (FGF-23), matrix metalloproteinase-9 (MMP-9), tissue inhibitor of metalloproteinase-1 (TIMP-1), and NT-proBNP), parameters of diastolic dysfunction (DD), and the presence of heart failure with preserved ejection fraction (HFpEF) in symptomatic patients.

Materials and methods. Study participants were 59 patients with non-obstructive coronary artery disease (CAD) and preserved left ventricular ejection fraction (LVEF) of 62 (56; 67) %. Non-obstructive CAD was verified by coronary computed tomography angiography. Stress- and rest-myocardial blood flow (MBF) and coronary flow reserve (CFR) parameters were evaluated by CZT SPECT. Serum levels of cardiac biomarkers were measured by the enzyme immunoassay. Two-dimensional transthoracic echocardiography was used to assess DD parameters.

Results. Decreased CFR was defined as CFR ≤ 2. Therefore, CMD was defined as the presence of decreased CFR in the absence of flow-limiting CAD. Distribution of patients was performed by CFR values: group 1 included patients with preserved CFR (>2, n = 35), and group 2 encompassed patients with decreased CFR (≤2, n = 24). In 87.5% of cases, patients with CMD were diagnosed with HFpEF, whereas in patients with preserved CFR, heart failure was diagnosed only in 51.4% of cases ($p < 0.0001$). CFR values were correlated with the left atrial volume ($r = –0.527$; $p = 0.001$), E / A ratio ($r = –0.321$, $p = 0.012$), and E / e' ($r = –0.307$; $p = 0.021$). Following the ROC analysis, the levels of sST2 ≥ 31.304 ng / ml (AUC = 0.730; p = 0.004) and NT-proBNP ≥ 0.034 pg / ml (AUC = 0.815; $p = 0.034$) were identified as cut-off values for the presence of CMD in patients with non-obstructive CAD.

Conclusion. The obtained data suggest that CMD may play an essential role in HFpEF. The values of CFR were correlated with DD parameters, and decreased CFR was associated with overexpression of biomarkers of cardiac fibrosis and cardiac remodeling. Serum levels of sST2 and NT-proBNP were identified as cut-off values for the presence of CMD in patients with non-obstructive CAD.

Keywords: heart failure, preserved left ventricular ejection fraction, diastolic dysfunction, coronary flow reserve, myocardial blood flow, microvascular dysfunction

Conflict of interest. The authors declare the absence of obvious or potential conflicts of interest related to the publication of this article.

Source of financing. The study was supported by the grant awarded by the President of the Russian Federation MK-4257.2022.3.

Conformity with the principles of ethics. All patients signed an informed consent to participate in the study. The study was approved by the local Ethics Committee at Cardiology Research Institute of Tomsk NRMC (Protocol No. 204 of 18.11.2020).

For citation: Kopeva K.V., Mochula A.V., Maltseva A.N., Grakova E.V., Shipulin V.V., Gusakova A.M., Zavadovsky K.V. Heart failure with preserved ejection fraction: the role of microvascular dysfunction. *Bulletin of Siberian Medicine.* 2022;21(4):88–97. https://doi.org/10.20538/1682-0363-2022-4-88-97.

✉ *Kopeva Kristina V.,* Kristin-kop@inbox.ru

Сердечная недостаточность с сохраненной фракцией выброса: роль микроваскулярной дисфункции

Копьева К.В., Мочула А.В., Мальцева А.Н., Гракова Е.В., Шипулин В.В., Гусакова А.М., Завадовский К.В.

Научно-исследовательский институт (НИИ) кардиологии, Томский национальный исследовательский медицинский центр (НИМЦ) Российской академии наук
Россия, 634012, Томск, ул. Киевская, 111а

РЕЗЮМЕ

Цель. Оценить взаимосвязь между коронарной микроваскулярной дисфункцией (КМД), биомаркерами фиброза и миокардиального ремоделирования (растворимый ST2 (sST2) и фактор роста фибробластов 23 (FGF-23), матриксная металлопротеиназа-9 (ММП-9), тканевой ингибитор металлопротеиназ-1 (ТИМП-1), NT-proBNP), параметрами диастолической дисфункции (ДД) и наличием сердечной недостаточности с сохраненной фракцией (СНсФВ) у симптоматичных пациентов.

Материалы и методы. В исследование включены 59 пациентов с необструктивным поражением коронарных артерий (КА) и сохраненной фракцией выброса левого желудочка (ФВ ЛЖ) 62 (56; 67)%. Необструктивное поражение КА было подтверждено компьютерной коронарной ангиографией. С помощью динамической CZT-SRECT оценивали параметры миокардиального кровотока в состоянии покоя (rest-MBF) и стресса (stress-MFR) и резерва коронарного кровотока (CFR). Сывороточные уровни сердечных биомаркеров измеряли с помощью иммуноферментного анализа. Всем пациентам проводилась двухмерная трансторакальная эхокардиография для оценки параметров ДД.

Результаты. Сниженный CFR определяли как CFR ≤2. Таким образом, КМД диагностировали на основании сниженного CFR при отсутствии окклюзирующего поражения КА. Распределение пациентов проводилось по значениям CFR: группа 1 включала больных с сохраненным CFR (>2, n = 35), группа 2 – со сниженным CFR (≤2, n = 24). В 87,5% случаев у больных с КМД была диагностирована СНсФВ, тогда как у больных без КМД – только в 51,4% (p < 0,0001). Значения CFR коррелировали с объемом левого предсердия (r = –0,527; p = 0,001), отношением E/A (r = –0,321; p = 0,012) и E/e' (r = –0,307; p = 0,021). На основании ROC-анализа уровни sST2 ≥ 31,304 нг/мл (AUC = 0,730; p = 0,004) и NT-proBNP ≥ 0,034 пг/мл (AUC = 0,815; p = 0,034) были определены как пороговые значения для диагностики КМД у пациентов с необструктивным поражением КА.

Заключение. КМД может играть важную роль в патогенезе развития СНсФВ. Значения CFR коррелировали с параметрами ДД, а снижение CFR было связано с гиперэкспрессией сердечных биомаркеров фиброза и ремоделирования. Уровни sST2 и NT-proBNP могут использоваться в качестве маркеров неинвазивной диагностики КМД.

Ключевые слова: сердечная недостаточность, сохраненная фракция выброса левого желудочка, диастолическая дисфункция, коронарный резерв, миокардиальный кровоток, микрососудистая дисфункция

Конфликт интересов. Авторы декларируют отсутствие явных и потенциальных конфликтов интересов, связанных с публикацией настоящей статьи.

Источник финансирования. Исследование поддержано грантом президента Российской Федерации (МК-4257.2022.3).

Соответствие принципам этики. Информированное письменное согласие было получено от всех пациентов до их включения в данное исследование. Исследование одобрено локальным комитетом по этике НИИ кардиологии Томского НИМЦ (протокол № 204 от 18.11.2020).

Для цитирования: Копьева К.В., Мочула А.В., Мальцева А.Н., Гракова Е.В., Шипулин В.В., Гусакова А.М., Завадовский К.В. Сердечная недостаточность с сохраненной фракцией выброса: роль микроваскулярной дисфункции. *Бюллетень сибирской медицины.* 2022;21(4):88–97. https://doi.org/10.20538/1682-0363-2022-4-88-97.

INTRODUCTION

Despite growing prevalence worldwide, heart failure with preserved ejection fraction (HFpEF) remains a poorly understood clinical syndrome [1, 2]. At the same time, a lack of clear understanding of its pathophysiology results in a lack of effective targeted therapy [3, 4]. Recent studies have implicated that coronary microvascular dysfunction (CMD) may be one of the possible causes of development and progression of HFpEF [5, 6].

Coronary flow reserve (CFR), quantified as the ratio of hyperemic myocardial blood flow to resting myocardial blood flow, reflects functional ischemia in large and small vessels. In the absence of obstructive coronary artery disease (CAD), it is a marker of CMD [7]. A new class of gamma cameras equipped with semiconductor cadmium – zinc – telluride (CZT) detectors has recently made it possible to measure CFR by noninvasive dynamic SPECT imaging [8, 9]. This method has been sufficiently tested and validated and may be a more accessible technique for visualization of changes in the coronary microcirculation [10] in addition to a comprehensive clinical assessment and traditional tests for assessing stress-induced ischemia [11].

The potential mechanisms of CMD appear to be heterogeneous, including impaired endothelial function, systemic inflammation, mitochondrial dysfunction, oxidative stress, etc. [12–16]. Moreover, all these processes cause adhesion and infiltration of monocytes and stimulation of integrated macrophages that promote myofibroblast differentiation and collagen secretion leading to fibrosis and cardiac remodeling [10, 11, 13–15]. Thus, CMD may play an important role in elevated left ventricular (LV) filling pressure, the development of diastolic dysfunction (DD), and the pathophysiology of HFpEF in general [7, 16].

The aim of the study was to evaluate the relationship between CMD, biomarkers of fibrosis and cardiac remodeling (soluble ST2 (sST2), fibroblast growth factor-23 (FGF-23), matrix metalloproteinase-9 (MMP-9), tissue inhibitor of metalloproteinase-1 (TIMP-1), NT-proBNP), diastolic dysfunction (DD) parameters, and the presence of HFpEF in symptomatic patients.

MATERIALS AND METHODS

The study was performed in accordance with the Declaration of Helsinki and was approved by the local Ethics Committee at Cardiology Research Institute, Tomsk NRMC (protocol No.204 of 18.11.2020). An informed written consent was obtained from all patients prior to their enrollment in the study.

Study population. From December 2020 to January 2022, a total of 59 patients (39 men, average age of 65.0 [58.0; 69.0] years) were enrolled in the study. All patients did not receive optimal medical treatment before the enrollment. Inclusion criteria: 1) non-obstructive (< 50%) coronary artery disease (CAD); 2) documented left ventricular ejection fraction (LVEF) ≥ 50% measured by echocardiography; 3) LVDD / elevated left ventricular filling pressure (LVFP) based on echocardiography; 4) sinus rhythm; 5) a signed informed consent to participate in the study.

Exclusion criteria were the following: 1) myocardial infarction in the medical history; 2) planned coronary revascularization and / or previous revascularization of the coronary artery (CA); 3) systolic blood pressure > 160 mm Hg); 4) symptomatic hypotension with the mean systolic blood pressure < 90 mm Hg; 5) second- or third-degree atrioventricular block, sick sinus syndrome; 6) persistent or chronic atrial fibrillation and / or flutter; 7) valvular insufficiency or stenosis of ≥ 2 degree; 8) hypertrophic and dilated cardiomyopathy; 9) previous pulmonary embolism with pulmonary hypertension of ≥ 45 mm Hg; 10) severe bronchial asthma and / or chronic obstructive pulmonary disease; 11) pathology of the thyroid gland; 12) glomerular filtration rate (CKD-EPI) of < 30 ml / min / m^2; 13) class 3 hepatic insufficiency according to Child-Pugh classification; 14) acute and chronic inflammatory heart diseases; 15) hemoglobin level of < 100 g / dl; 16) stroke or transient ischemic attack within 90 days prior to enrollment; 17) obesity (body mass index (BMI) > 35 kg / m^2); 18) life-threatening uncontrolled arrhythmias.

Echocardiography. Philips Affiniti 70 ultrasound scanner was used to perform two-dimensional transthoracic echocardiography. All studies were performed by one highly qualified specialist. Evaluation of LVDD was based on the following indices: E wave, E/A ratio, septal e′, average E/e′ ratio, indexed left atrial volume, and peak tricuspid regurgitation velocity [17].

Coronary computed tomography angiography and dynamic SPECT. Dynamic CZT SPECT and coronary computed tomography angiography (CCTA) were performed using a hybrid system (GE Discovery NM/CT 570C; GE Healthcare, USA) equipped with a dedicated cardiac CZT gamma camera and a 64-slice CT scanner.

Dynamic SPECT. Patient preparation, study protocol, as well as acquisition and analysis of static and dynamic scintigraphic data were described in the previous articles [9, 10]. It is important to note that patients were instructed to stop taking beta-blockers, nitrates, calcium channel blockers, caffeine, and methylxanthine-containing substances for at least 24 hours before the procedure. All studies were performed in the morning, on an empty stomach, against the background of a sinus heart rhythm [18]. A two-day rest – stress protocol was performed using the radiopharmaceutical 99mTc-methoxy-isobutyl-isonitrile (99mTc-MIBI), which was administered intravenously at a bolus dose of 260–444 MBq. Before the first dynamic study, a low-dose CT scan (tube voltage 100 kV, tube current 20 mA, rotation time 0.8 s, helical pitch 0.969 : 1, slice thickness 5 mm) had been performed to assess the heart position.

The pharmacological stress test was performed according to a standard 4-minute protocol [18]. Adenosine triphosphate (ATP) was used as a pharmacological stress agent, which was administered intravenously using an infusion pump at a dose of 160 μg / kg / min for 4 min. During the stress test, after 2 minutes of intravenous infusion of ATP, a dose of 99mTc-Sestamibi (3 MBq·kg-1) was injected. Dynamic data acquisition was started 610 seconds before the radiotracer injection. The infusion of ATP continued for additional 2 minutes.

To correct attenuation, low-dose CT of the chest was performed. All studies were performed on the Discovery NM/CT 570c hybrid computed tomography scanner (GE Healthcare, Milwaukee, WI, USA) equipped with a gamma camera with highly sensitive CZT detectors. The total effective radiation exposure of the study (rest / pharmacological stress test) was ~6.25 mSv.

The resulting scintigraphic images were processed on the specialized Xeleris II workstation (GE Healthcare, Haifa, Israel). Myocardial perfusion, myocardial blood flow (MBF), and coronary flow reserve (CFR)were assessed using specialized software Corridor 4DM SPECT and 4DM Reserve v.2015 (INVIA, Ann Arbor, MI, USA). The quantitative characteristics were processed using the Net Retention model with attenuation correction [19].

According to myocardial perfusion SPECT data, standard semi-quantitative indices of impaired myocardial perfusion were determined: Summed Stress Score (SSS) – the sum of scores during stress, Summed Rest Score (SRS) – the sum of scores at rest, Summed Difference Score (SDS) – the difference between exercise and rest, as well as quantitative parameters: stress-MBF – myocardial blood flow during stress, rest-MBF – myocardial blood flow at rest, and CFR.

Coronary computed tomography angiography. Preparation for CCTA was carried out according to the standard protocol and included beta-blockers and prednisolone, avoiding caffeinated drinks or food, and excluding the use of glucophage (metformin), viagra, etc., and pain medications (advil or motrin). Besides, patients were instructed about contraindications of the procedure related to allergies, pregnancy, and kidney disease. Heart rate and blood pressure were evaluated before each scan. All patients received 0.5 mg of sublingual nitroglycerin tablets.

For contrast-enhanced scans, 70–90 ml of a non-ionic contrast agent (iopamidol 370 mg, Bracco Diagnostics, Italy) was injected intravenously through an 18G antecubital catheter at a flow rate of 5–5.5 ml / s followed by 60 ml of 0.9% NaCl.

In patients with the heart rate ≥ 55 bpm, a retrospective electrocardiogram (ECG)-gated helical scan was acquired, and in those with the heart rate < 55, a prospective ECG-gated protocol was used. The recording parameters were the following: tube voltage of 120 kV, tube current of 300–600 mA using ECG modulation with maximum tube current of 40–80% between phases, and minimum tube current in the remaining phases.

Axial images, curved multiplanar and cross-section reformations, and thin-slab maximum intensity projections were used for dataset analysis. All studies were analysed on the hybrid CT scanner (Advantage Workstation 4.6, GE Healthcare, USA).

In the case of retrospective CCTA scans, images were reconstructed at 75% of the cardiac cycle with a slice thickness of 0.625 mm. In cases of heart rate artefacts, other reconstruction windows were used (from 10% to 90% of the R-R cycle). According to modified American Heart Association criteria, CAs were subdivided into 16 segments [20, 21].

Blood sampling and biochemical analysis. Blood samples were obtained by venipuncture. Adequate samples were centrifuged, serum was separated and stored at –24 °C with a single freeze – thaw cycle. Serum levels of sST2, NT-proBNP, FGF-23, MMP-9, and TIMP-1 were analyzed from the same blood sample by the enzyme immunoassay (NT-proBNP, FGF-23, and TIMP-1, Biomedica, Austria; Presage® ST2 Assay, Critical Diagnostics, San Diego, CA, USA; MMP-9; eBioscience, USA).

Statistical analysis. Statistical processing of the results was performed using Statistica 10.0 software package R, version 2. The data were presented as the median and the interquartile range *Me* (Q_{25}; Q_{75}). To test statistical hypotheses for quantitative variables, the Mann – Whitney test was used when comparing two independent groups. When analyzing qualitative variables, contingency tables were analyzed using the Pearson's $\chi 2$ test. If there were cells with an expected frequency less than 5, then a two-tailed Fisher's exact test or Yates' correction (for 2 × 2 tables) was applied. To search for relationships between the variables, the correlation analysis was used with the calculation of the Spearman's rank correlation coefficients. The cut off scores for the diagnosis of CMD were determined by the ROC-analysis. The critical significance level of the *p*-value was taken equal to 0.05.

RESULTS

Impaired CFR was defined as CFR ≤ 2. Thus, CMD was defined as the presence of impaired CFR in the absence of flow-limiting CAD. Patients were distributed according to CFR values: group 1 included patients with preserved CFR (> 2, *n* = 35), group 2 included patients with impaired CFR (CFR ≤ 2, *n* = 24). HFpEF was diagnosed according to 2021 ESC guidelines for the diagnosis and treatment of acute and chronic HF [22]. The baseline demographic and clinical characteristics of patients did not differ (Table 1). However, in patients with CMD, HFpEF was revealed in 87.5%, while in patients without CMD, it was diagnosed only in 51.4% ($p < 0.0001$). Echocardiography parameters did not differ significantly between the groups (Table 2).

In patients with CMD, CFR values were lower by 47.8% ($p < 0.0001$) than in patients without CMD (1.41 [1.23; 1.55] vs. 2.6 [2.49; 3.38], respectively). In group 1, rest-MBF was 0.74 (0.56; 0.93) ml / min / g, while in group 2, it was 0.48 (0.37; 0.67) ml / min / g ($p = 0.045$). In group 1, stress-MBF was 1.06 (0.91; 1.24) ml / min / g, and in group 2 it was 1.59 (1.19; 1.74) ml / min / g($p = 0.012$). The remaining indices did not differ significantly (Table 3).

Table 1

Clinical and demographic characteristics of patients, *Me* (Q_{25}; Q_{75})

Parameter	Patients with CMD, *n* = 24	Patients without CMD, *n* = 35	*p* value
Age, years	60 (52; 66)	62 (59; 67.5)	0.451
Sex / male, *n* (%)	14 (58.3)	23 (65.7)	0.767
BMI, kg / m^2	29.55 (27.1; 30.7)	31.2 (28.0; 33.41)	0.180
Hypertension, *n* (%)	20 (83.3)	32 (91.4)	0.812
Diabetes mellitus, *n* (%)	6 (25.0)	10 (28.6)	0.761
COPD, *n* (%)	3 (12.5)	5 (14.3)	0.824
Current smoker, *n* (%)	6 (25.0)	9 (25.8)	0.998
Heart failure, *n* (%)	21 (87.5)	18 (51.5)	< 0.0001
eGFR, ml / min / 1.73 m^2	73.5 (59; 81)	69 (65; 79)	0.775
Total cholesterol, mmol / l	4.15 (3.2; 5.98)	4.4 (3.6; 5.4)	0.874
LDL-cholesterol, mmol / l	1.79 (1.3; 3.34)	2.6 (1.8; 3.42)	0.606
HDL-cholesterol, mmol / l	1.36 (1.29; 1.78)	1.23 (1.06; 1.3)	0.239
Triglycerides, mmol / l	1.5 (1.14; 2.23)	1.6 (1.25; 2.2)	0.815
Hemoglobin, g / dl	152 (144; 159)	143 (137; 153.5)	0.121
Potassium, mmol / l	4.3 (4.0; 5.2)	4.2 (3.9; 5.1)	0.981
HbA1c, %	5.8 (5.5; 7.6)	5.6 (5.3; 7.5)	0.091
CRP, g / l	4.1 (3.6; 4.7)	5.2 (2.7; 10.1)	0.998
Fibrinogen, g / l	3.3 (2.9; 3.4)	3.2 (2.7; 3.4)	0.934
sST2, ng / ml	31.03 (27.03; 35.5)	25.0 (21.45; 31.15)	< 0.001
NT-proBNP, pg / ml	318.0 (169.7; 2,106.2)	196.8 (68.1; 510.4)	0.045
MMP-9, ng / ml	1538 (945.4; 1982)	1183 (720.9; 1725)	0.023
TIMP-1, ng / ml	230.2 (107.38; 285.8)	160.78 (58.66; 213.2)	0.012
FGF-23, ng / ml	0.683 (0.383; 0.999)	0.649 (0.5; 0.965)	0.565

Note: HbA1c – glycated hemoglobin; FGF-23 – fibroblast growth factor-23; LDL-cholesterol – low-density lipoprotein cholesterol; HDL-cholesterol – high-density lipoprotein cholesterol; CRP – C-reactive protein; eGFR – estimated glomerular filtration rate (CKD-EPI); TIMP-1 – tissue inhibitor of metalloproteinase-1; COPD – chronic obstructive pulmonary disease.

Table 2

Echocardiography parameters, *Me* (Q_{25}; Q_{75})			
Parameter	Patients with CMD, *n* = 24	Patients without CMD, *n* = 35	*p*-value
Left ventricular ejection fraction, %	65 (63; 66)	65 (64; 67)	0.531
End-systolic diameter, mm	32 (30; 33)	32 (31; 33)	0.886
End-diastolic diameter, mm	50.5 (48;51)	50.5 (49; 51)	0.752
LVMI, g / m^2	91 (88; 95)	84 (79; 90)	0.159
Interventricular septum, mm	10.2 (10; 11)	10.5 (10.5; 11)	0.371
Left ventricular posterior wall, mm	10 (10; 11)	10 (9.5; 10)	0.154
E / A ratio	0.98 (0.73; 1.38)	1.02 (0.86; 1.29)	0.829
Septal e′	5.89 (4.8; 6.45)	5.66 (5.35; 6.25)	0.949
PTRV, m / s	2.89 (2.8; 3.11)	2.91 (2.87; 2.99)	0.852
E / e’	14.75 (13.5; 15.1)	14 (13.3; 14)	0.181
LAVI	33 (29; 37)	32 (29; 33)	0.284
DD type 1, *n* (%)	19 (79.2)	26 (74.3)	0.761
DD type 2, *n* (%)	5 (20.8)	25.7	0.817

Note: DD – diastolic dysfunction; LAVI – left atrial volume index; LVMI – left ventricular mass index; PTRV – peak tricuspid regurgitation velocity.

Table 3

Dynamic SPECT parameters and standard semi-quantitative indices of impaired myocardial perfusion, *Me* (Q_{25}; Q_{75})			
Parameter	Patients with CMD, *n* = 24	Patients without CMD, *n* = 35	*p*-value
Dynamic SPECT indices			
Stress-MBF, ml / min / g	1.06 (0.91; 1.24)	1.59 (1.19; 1.74)	0.012
Rest-MBF, ml / min / g	0.74 (0.56; 0.93)	0.48 (0.37;0.67)	0.045
CFR	1.41 (1.23; 1.55)	2.6 (2.49; 3.38)	<0.0001
Standard semi-quantitative indices of impaired myocardial perfusion			
SSS	2.0 (1.0; 4.0)	2.0 (0; 4.0)	0.566
SRS	0 (0; 1)	0 (0; 1)	0.926
SDS	0.5 (0; 3.0)	2 (0; 3.0)	0.364
Standard semi-quantitative indices of myocardial dysfunction			
Stress ESV, ml	37.0 (30.0; 46.0)	33.5 (25.5; 40.0)	0.158
Stress EDV, ml	115.5 (97.0; 123.0)	106.5 (99.0; 122.5)	0.404
Stress EF, %	68.0 (61.0; 74.0)	70.0 (66.0; 73.5)	0.244
Rest ESV, ml	32.0 (28.0; 41.0)	32.5 (24.5; 36.0)	0.364
Rest EDV, ml	108.5 (100; 117)	102.5 (89.5;121.5)	0.250
Rest EF, %	70.5 (62.0; 72.0)	69.5 (65.5; 72.5)	0.698

Note: CFR – coronary flow reserve; stress-MBF – myocardial blood flow during stress; rest-MBF – myocardial blood flow at rest; SSS – summed stress score; SRS – summed rest scores; SDS – summed difference score as the difference between SSS and SRS; ESV – end-systolic volume; EDV – end-diastolic volume; EF – ejection fraction.

CFR values were correlated with the left atrial volume (r = –0.527; p = 0.001), E / A ratio (r = –0.321, p = 0.012), and E / e’ (r = –0.307; p = 0.021), as well as with the levels of NT-proBNP (r = –0.290; p = 0.04) and sST2 (r = –0.330; p = 0.012).

The levels of NT-proBNP were higher in group 1 by 36.4% (p = 0.045) than in group 2 (318.0 [169.7; 2,106.2] and 196.8 [68.1; 510.4] pg / ml, respectively). The sST2 levels were higher in patients with impaired CFR by 19.4% (p > 0.001) than in patients with preserved CFR (31.03 [27.03; 35.5] and 25.0 [21.45; 31.15] ng / ml, respectively). The serum levels of MMP-9 in group 1 were 1,538 (945.4; 1,982) pg / ml, and in group 2 they were 1,183 (720.9; 1,725) ng /ml (p = 0.023). The levels of TIMP-1 were higher by 30.1% (p = 0.012) in group 1 than in group 2 (230.2 [107.38; 285.8] and 160.78 [58.66; 213.2] ng / ml, respectively). The serum concentration of FGF-23 did not differ between the groups.

Following the ROC-analysis, the levels of sST2 ≥ 31.304 ng / ml (sensitivity 55.0%, specificity 90.3%; area under the curve (AUC) = 0.730; p = 0.004) (Fig. 1) and NT-proBNP ≥ 977.2 pg / ml (sensitivity 64.9%, specificity 84.6%; AUC = 0.815; p = 0.034) were identified as cut-off values for diagnosing CMD

in patients with non-obstructive CAD (Fig. 2). When comparing the ROC-curves of sST2 and NT-proBNP, no significant differences in the cut-off values for the presence of CMD were revealed (Fig. 3).

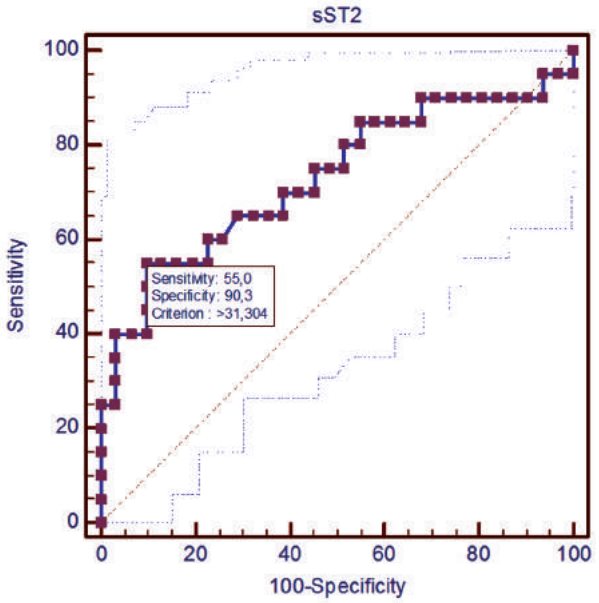

Fig. 1. Sensitivity and specificity of sST2 levels in the diagnosis of CMD (ROC-analysis)

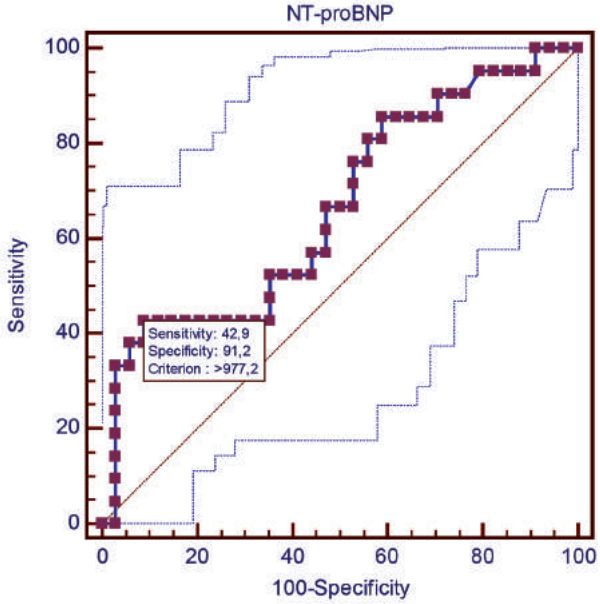

Fig. 2. Sensitivity and specificity of NT-proBNP levels in the diagnosis of CMD (ROC-analysis)

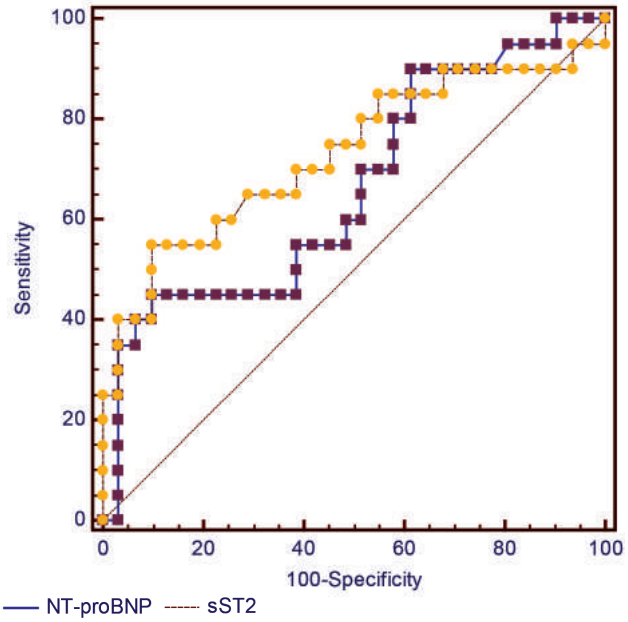

Fig. 3. Comparison of sensitivity and specificity of NT-proBNP and sST2 levels in the diagnosis of CMD (ROC-analysis)

DISCUSSION

This study demonstrated that patients with non-obstructive CAD and CMD had higher incidence of HFpEF than patients without CMD. The values of CFR were correlated with DD parameters and the concentrations of NT-proBNP and sST2. The levels of sST2 ≥ 31.304 ng / ml and NT-proBNP ≥ 977.2 pg / ml were identified as cut-off values for diagnosing CMD in patients with non-obstructive CAD.

HFpEF is one of the greatest problems in modern cardiology. Out of the estimated 5 million patients diagnosed with HF in the USA, approximately 50% have HFpEF [22]. In Europe, this proportion ranges from 22 to 73% [1]. Moreover, there is a growing understanding that HFpEF represents a heterogeneous syndrome with various phenotypes and comorbidities [23]. The results of a number of international studies using invasive or non-invasive diagnostic methods support the assumption that CMD occurs significantly more often than previously, including patients with HFpEF. V.L.Murthy et al. reported that 53% of patients with non-obstructive CAD and pain syndrome had evidence of inducible myocardial ischemia [11]. According to the latest meta-analysis data of 56 studies including 14,427 patients, the proportion of patients with CMD was 41% in the general population [12]. Moreover, when the prevalence of CMD was analyzed in patients with HFpEF, the incidence increased to 75–85% [13, 14]. Therefore, an innovative theory has been proposed recently according to which CMD represents “common soil” for the occurrence of both microvascular angina and HFpEF [4, 14, 24]. It is worth noting that patients with non-obstructive CAD,

despite preserved LVEF, are no less often subject to hospitalization due to HF decompensation [11].

CMD is a type of non-obstructive CAD in which small blood vessels feeding the cardiac muscle cannot cope with the load [14]. However, the potential mechanisms of CMD development have not yet been studied and include cellular metabolism disorders, systemic inflammation, reactive oxygen species (ROS) generation, increased coronary vasoconstrictor reactivity at the microvascular level, impaired endothelium-dependent and endothelium-independent vasodilator capacities, hormonal and electrolyte imbalance, etc., which results in development of fibrosis and increased myocardial stiffness and coronary microvascular resistance [12, 14–16, 25]. It is most likely that primary structural abnormalities in CMD are associated with damage to endothelial mitochondria and include their hyperplasia, reduction in size of organelles or their fragmentation, and structural damage, such as reduction of electron-dense matrix and disruption of inner and outer membranes [16, 23, 24]. The concomitant diseases, such as diabetes, hypertension, obesity, etc., not only activate superoxide overexpression via the mitochondrial electron-transport chain and NADPH oxidase, which partially contribute to impaired endothelial cell function, but also control parallel pathways causing the development of endothelial dysfunction [22]. It is worth noting, that endothelial dysfunction is one of the key mechanisms for the development and progression of CMD in HFpEF [18].

The endothelium plays a pivotal role in preventing platelet aggregation and leukocyte adhesion, regulating cell proliferation, and modulating vascular tone by synthesizing and releasing endothelium-derived relaxing factors, such as prostaglandins, nitric oxide (NO), and endothelium-dependent hyperpolarization (EDH) factors in different forms depending on the vessel size. NO predominantly mediates vasodilatation of relatively large coronary vessels, while EDH factors influence microvasculature resistance. As a consequence, alterations in both the myocytic and non-myocytic compartments can lead to the development of myocardial fibrosis and extracellular matrix remodeling and increase diastolic stiffness, which contributes to the progression of HFpEF [25, 26].

In the context of increased oxygen demand, impaired CFR, even in the absence of obstructive CAD, reflects myocardial ischemia at the microcirculatory level due to an imbalance in the ratio of oxygen demand and its delivery to the myocardium, which may predispose the myocardium to injury and impaired global ventricular mechanics and cardiac dysfunction [7]. Our data demonstrated that CMD was independently associated with DD parameters and the presence of HFpEF. This suggests that factors tipping the balance towards ischemic damage to cardiomyocytes in patients with existing CMD may impair LV function and increase the risk of HFpEF development, even in the absence of overt structural abnormalities or obstructive CAD. Thus, in the study including 385 patients with non-obstructive CAD, CMD was also significantly associated with echocardiography parameters of DD [27]. In patients with systolic dysfunction (LVEF < 35%) and non-obstructive CAD, CFR parameters were correlated with E / e' values [28]. In particular, microvascular endothelial dysfunction, decreased nitric oxide bioavailability, and increased profibrotic cytokine signaling may contribute to reduced coronary microvascular density or rarefaction and increased myocardial fibrosis, observed in HFpEF [7, 13, 14]. Correlation of CFR with biochemical markers of left ventricular volume overload, such as NT-proBNP (r = –0.290; p = 0.04), and cardiac fibrosis, such as sST2 (r = –0.331; p = 0.012), demonstrates a close relationship between these processes in the pathogenesis of HFpEF in patients without occlusive CAD.

In our study, only the levels of sST2 and NT-proBNP, but not MMP-9 and TIMP-1, were identified as cut-off values for diagnosing CMD in patients with non-obstructive CAD. Perhaps, in this population with non-obstructive CAD, the levels of sST2 reflect periarteriolar fibrosis that may occur in CMD [29]. In particular, CMD associated with chronic systemic inflammation may promote periarteriolar fibrosis and microvascular rarefaction, yielding decreased CFR, overexpression of sST2, and the development of HF symptoms and / or microvascular angina with "normal" CA [30]. In the study on mice models, decreased ST2 signaling with the progression of microvascular changes in the pressure overload state was associated with amplifying and sustaining arteriolar remodeling and periarteriolar fibrosis [29]. Furthermore, Aslan et al. (2019) established that serum sST2 levels were significantly higher in patients with microvascular angina compared with controls [31]. Hereinafter, chronic systemic inflammation causes adhesion and infiltration of monocytes and stimulation of integrated macrophages, which promotes myofibroblast differentiation and, eventually, collagen secretion leading to fibrosis and cardiac remodeling [10, 11, 32].

Thus, coronary microvascular ischemia may play an important role in the elevation of LV filling pressure, the development of DD, and the pathophysiology of HFpEF [8]. To support this fact, it was found that patients with CMD had higher levels of MMP-9 and TIMP-1 than those without it. But most likely, this process is secondary to CMD and is a consequence of HFpEF progression; therefore, these biomarkers did not show significance in the diagnosis of CMD, in contrast to sST2 and NT-proBNP.

CONCLUSION

It was established that CMD may play an important role in the pathogenesis of HFpEF. The values of CFR were correlated with DD parameters, and impaired CFR was associated with overexpression of cardiac biomarkers of fibrosis and remodeling. Serum levels of sST2 and NT-proBNP may be used as markers for non-invasive diagnosis of CMD.

REFERENCES

1. Ponikowski P., Voors A.A., Anker S.D., Bueno H., Cleland J.G., Coats A.J. et al. 2016 ESC Guidelines for the diagnosis and treatment of acute and chronic heart failure: the task force for the diagnosis and treatment of acute and chronic heart failure of the European Society of Cardiology (ESC) developed with the special contribution of the Heart Failure Association (HFA) of the ESC. *Eur. Heart J.* 2016;18(8):891–975. DOI: 10.1002/ejhf.592.
2. Groenewegen A., Rutten F.H., Mosterd A., Hoes A.W. Epidemiology of heart failure. 2020;22(8):1342–1356. DOI: 10.1002/ejhf.1858.
3. McDonagh T.A., Metra M., Adamo M., Gardner R.S. et al. 2021 ESC Guidelines for the diagnosis and treatment of acute and chronic heart failure: Developed by the Task Force for the diagnosis and treatment of acute and chronic heart failure of the European Society of Cardiology (ESC) With the special contribution of the Heart Failure Association (HFA) of the ESC. *Eur. Heart J.* 2021;42(36): 3599–3726. DOI: 10.1093/eurheartj/ehab368.
4. Tona F., Montisci R., Iop L., Civieri G. Role of coronary microvascular dysfunction in heart failure with preserved ejection fraction. *Rev. Cardiovasc. Med*. 2021;22(1):97–104. DOI: 10.31083/j.rcm.2021.01.277.
5. Vancheri F., Longo G., Vancheri S., Henein M. Coronary microvascular dysfunction. *J. Clin. Med.* 2020;9(9):2880. DOI: 10.3390/jcm9092880.
6. Crea F., Bairey Merz C.N., Beltrame J.F., Kaski J.C. et al. The parallel tales of microvascular angina and heart failure with preserved ejection fraction: a paradigm shift. *Eur. Heart J.* 2017;38(7):473–477. DOI: 10.1093/eurheartj/ehw461.
7. Taqueti V.R., Solomon S.D., Shah A.M., Desai A.S. et al. Coronary microvascular dysfunction and future risk of heart failure with preserved ejection fraction. *Eur. Heart J.* 2018;39(10):840–849. DOI: 10.1093/eurheartj/ehx721.
8. Rahman H., Scannell C.M., Demir O.M., Ryan M. et al. High-resolution cardiac magnetic resonance imaging techniques for the identification of coronary microvascular dysfunction. *JACC Cardiovasc. Imaging*. 2021 14(5):978–986. DOI: 10.1016/j.jcmg.2020.10.015.
9. Zavadovsky K.V., Mochula A.V., Boshchenko A.A. et al. Absolute myocardial blood flows derived by dynamic CZT scan vs invasive fractional flow reserve: Correlation and accuracy. *J. Nucl. Cardiol*. 2021;28(1):249–259. DOI: 10.1007/s12350-019-01678-z.;
10. Zavadovsky K.V., Mochula A.V., Maltseva A.N., Boshchenko A.A. et al. The diagnostic value of SPECT CZT quantitative myocardial blood flow in high-risk patients. *J. Nucl. Cardiol.* 2022; 29(3):1051–1063. DOI: 10.1007/s12350-020-02395-8.
11. Murthy V.L., Naya M., Foster C.R., Hainer J. et al. Improved cardiac risk assessment with noninvasive measures of coronary flow reserve. *Circulation.* 2011;124(20):2215–2224. DOI: 10.1161/CIRCULATIONAHA.111.050427.
12. Agostini D., Roule V., Nganoa C. et al. First validation of myocardial flow reserve assessed by dynamic 99mTc-sestamibi CZT-SPECT camera: head to head comparison with 15O-water PET and fractional flow reserve in patients with suspected coronary artery disease. The WATERDAY study. *Eur. J. Nucl. Med. Mol. Imaging*. 2018;45(7):1079–1090. DOI: 10.1007/s00259-018-3958-7.
13. Paulus W.J., Tschöpe C. A novel paradigm for heart failure with preserved ejection fraction: comorbidities drive myocardial dysfunction and remodeling through coronary microvascular endothelial inflammation. *J. Am. Coll. Cardiol*. 2013;62(4):263–271. DOI: 10.1016/j.jacc.2013.02.092.
14. Godo S., Suda A., Takahashi J., Yasuda S., Shimokawa H. Coronary microvascular dysfunction. *Arteriosclerosis, Thrombosis, and Vascular Biology*. 2021;41(5):1625–1637. DOI: 10.1161/ATVBAHA.121.316025.
15. Mileva N., Nagumo S., Mizukami T., Sonck J. et al. Prevalence of Coronary Microvascular Disease and Coronary Vasospasm in Patients With Nonobstructive Coronary Artery Disease: Systematic Review and Meta-Analysis. *J. Amer. Heart Ass*. 2022;11(7):e023207. DOI: 10.1161/JAHA.121.023207.
16. Zhou H., Toan S. Pathological roles of mitochondrial oxidative stress and mitochondrial dynamics in cardiac microvascular ischemia/reperfusion injury. *Biomolecules*. 2020;10(1):85. DOI: 10.3390/biom10010085.
17. Nagueh S.F., Smiseth O.A., Appleton C.P. Recommendations for the evaluation of left ventricular diastolic function by echocardiography: an update from the American Society of Echocardiography and the European Association of Cardiovascular Imaging. *Eur. Heart J. Cardiovasc. Imaging*. 2016;17(12):1321–1360. DOI: 10.1093/ehjci/jew082.
18. Henzlova M.J., Duvall W.L., Einstein A.J., Travin M.I., Verberne H.J. ASNC imaging guidelines for SPECT nuclear cardiology procedures: Stress, protocols, and tracers. *J. Nucl. Cardiol.* 2016;23 (3):606–639. DOI: 10.1007/s12350-015-0387-x.
19. Leppo J.A., Meerdink D.J. Comparison of the myocardial uptake of a technetium-labeled isonitrile analogue and thallium. *Circ. Res*. 1989;65(3):632–639. DOI: 10.1161/01.res.65.3.632.

20. Cerqueira M.D., Weissman N.J., Dilsizian V., Jacobs A.K. et al. Standardized myocardial segmentation and nomenclature for tomographic imaging of the heart: A statement for healthcare professionals from the cardiac imaging. *Circulation.* 2002;105(4):539–542. DOI: 10.1161/hc0402.102975.
21. Austen W.G., Edwards J.E., Frye R.L., Gensini G.G. et al. A reporting system on patients evaluated for coronary artery disease. Report of the Ad Hoc Committee for Grading of Coronary Artery Disease, Council on Cardiovascular Surgery, American Heart Association. *Circulation.* 1975;51(4):5–40. DOI: 10.1161/01.cir.51.4.5.
22. Clark K.A.A., Velazquez E.J. Heart failure with preserved ejection fraction: time for a Reset. *JAMA.* 2020;324(15):1506–1508. DOI: 10.1001/jama.2020.15566.
23. Triposkiadis F., Butler J., Abboud F.M., Armstrong P.W., Adamopoulos S., Atherton J.J. et al. The continuous heart failure spectrum: moving beyond an ejection fraction classification. *Eur. Heart J.* 2019;40(26):2155–2163. DOI: 10.1093/eurheartj/ehz158.
24. Graziani F., Varone F., Crea F., Richeldi L. Treating heart failure with preserved ejection fraction: learning from pulmonary fibrosis. *Eur. J. Heart Fail*. 2018;20(10):1385–1391. DOI: 10.1002/ejhf.1286.
25. Zile M.R., Baicu C.F., Ikonomidis J.S., Stroud R.E., Nietert P.J. et al. Myocardial stiffness in patients with heart failure and a preserved ejection fraction: contributions of collagen and titin. *Circulation*. 2015;131(14):1247–1259. DOI: 10.1161/CIRCULATIONAHA.114.013215.
26. Rahman H., Ryan M., Lumley M., Modi B. et al. Coronary microvascular dysfunction is associated with myocardial ischemia and abnormal coronary perfusion during exercise. *Circulation.* 2019;140:1805–1816. DOI: 10.1161/CIRCULATIONAHA.119.041595.
27. Kim I.C., Hwang J., Lee C.H., Cho Y.K. et al. Correlation of coronary microvascular function and diastolic dysfunction. *Eur. Heart J.* 2020;41(2):ehaa946.0903. DOI: 10.1093/ehjci/ehaa946.0903.
28. Snoer M., Monk-Hansen T., Olsen R.H., Pedersen L.R., Nielsen O.W. et al. Coronary flow reserve as a link between diastolic and systolic function and exercise capacity in heart failure. *Eur. Heart J. Cardiovasc. Imaging.* 2013;14(7):677–683. DOI: 10.1093/ehjci/jes269.
29. Garbern J.C., Williams J., Kristl A.C., Malick A., Rachmin I. et al. Dysregulation of IL-33/ST2 signaling and myocardial periarteriolar fibrosis. *J. Mol. Cell Cardiol*. 2019;128:179–186. DOI: 10.1016/j.yjmcc.2019.01.018.
30. Lewis G.A., Schelbert E.B., Williams S.G., Cunnington C., Ahmed F., McDonagh T.A. et al. Biological phenotypes of heart failure with preserved ejection fraction. *J. Am. Coll. Cardiol.* 2017;70(17):2186–2200. DOI: 10.1016/j.jacc.2017.09.006.
31. Aslan G., Polat V., Bozcali E., Opan S., Çetin N., Ural D. Evaluation of serum sST2 and sCD40L values in patients with microvascular angina. *Microvasc. Res*. 2019;122:85–93. DOI: 10.1016/j.mvr.2018.11.009.
32. Grakova E.V., Kopeva K.V., Teplyakov A.T., Ogurkova O.N., Soldatenko M.V., Garganeeva A.A. Clinical use of the new biomarker ST2 in patients with chronic heart failure of ischemic genesis: an exercise test. *Cardiovascular Therapy and Prevention.* 2019;18(4):12–18 (in Russ.). DOI: 10.15829/1728-8800-2019-4-12-18.

Authors information

Kopeva Kristina V. – Cand. Sci. (Med.), Researcher, Department of Myocardial Pathology, Cardiology Research Institute, Tomsk NRMC, Tomsk, http://orcid.org/0000-0002-2285-6438

Maltseva Alina N. – Post-Graduate Student, Laboratory for Radionuclide Research Methods, Cardiology Research Institute, Tomsk NRMC, Tomsk, http://orcid.org/0000-0002-1311-0378

Mochula Andrey V. – Cand. Sci. (Med.), Senior Researcher, Laboratory for Radionuclide Research Methods, Cardiology Research Institute, Tomsk NRMC, Tomsk, http://orcid.org/0000-0003-0883-466X

Grakova Elena V. – Dr. Sci. (Med.), Leading Researcher, Department of Myocardial Pathology, Cardiology Research Institute, Tomsk NRMC, Tomsk, http://orcid.org/0000-0003-4019-3735

Shipulin Vladimir V. – Cand. Sci. (Med.), Junior Researcher, Laboratory for Radionuclide Research Methods, Cardiology Research Institute, Tomsk NRMC, Tomsk, http://orcid.org/0000-0001-9887-8214

Gusakova Anna M. – Cand. Sci. (Biology), Researcher, Department of Clinical Laboratory Diagnostics, Cardiology Research Institute, Tomsk NRMC, Tomsk, http://orcid.org/0000-0003-0883-466X

Zavadovsky Konstantin V. – Dr. Sci. (Med.), Head of the Laboratory for Radionuclide Research Methods, Cardiology Research Institute, Tomsk NRMC, Tomsk, http://orcid.org/0000-0002-1513-8614.

(✉) **Kopeva Kristina V.,** Kristin-kop@inbox.ru

Received 17.03.2022;
approved after peer review 30.06.2022;
accepted 08.09.2022

УДК 613.2.038-02:617.735] -092.4:599.233.4
https://doi.org/10.20538/1682-0363-2022-4-98-104

Effects of a high-fat, high-carbohydrate diet on the retina of young and old rats

Logvinov S.V.[1], Mustafina L.R.[1], Kurbatov B.K.[2], Naryzhnaya N.V.[2], Varakuta E.Yu.[1], Potapov A.V.[1]

[1] *Siberian State Medical University*
2, Moscow Trakt, Tomsk, 634050, Russian Federation

[2] *Cardiology Research Institute, Tomsk National Research Medical Center (NRMC) of the Russian Academy of Sciences*
111a, Kievskaya Str., Tomsk, 634012, Russian Federation

ABSTRACT

Aim. To study the effect of a high-fat, high-carbohydrate diet on retinal morphology of young and old rats in the experiment.

Materials and methods. The study was carried out on male Wistar rats aged 60 and 450 days at the beginning of the experiment. The animals were divided into 4 groups: group 1 (n = 14) included intact rats aged 150 days at the end of the experiment; group 2 (n = 14) encompassed rats (60 days old) fed with a high-fat, high-carbohydrate diet (HFHCD) for 90 days; group 3 (n = 14) included intact rats (450 days old) receiving a standard diet for 90 days; group 4 (n = 14) included rats (450 days old) fed with HFHCD for 90 days. Immunoassay and histology were used in the work.

Results. HFHCD resulted in an increase in glucose concentration in animals of both age groups. In old animals, it caused a pronounced increase in the content of insulin, TGFβ, and fibronectin in the blood serum, neovascularization of outer retinal layers, as well as karyopyknosis and death of neurosensory cells, leading to destruction of photoreceptors and drastic thinning of the outer nuclear and outer plexiform layers. In young rats fed with HFHCD, no pronounced histologic disorders of the retina were noted.

Conclusion. HFHCD enhances age-related retinal changes in old (450-day-old) rats.

Keywords: retinopathy, age-related changes in the retina, high-fat, high-carbohydrate diet

Conflict of interest. The authors declare the absence of obvious or potential conflict of interest related to the publication of this article.

Source of financing. The authors state that they received no funding for the study.

Conformity with the principles of ethics. The study was approved by the local Ethics Committee at Cardiology Research Institute of Tomsk NRMC (Protocol No. 201 of 30.07.2020).

For citation: Logvinov S.V., Mustafina L.R., Kurbatov B.K., Naryzhnaya N.V., Varakuta E.Yu., Potapov A.V. Effects of a high-fat, high-carbohydrate diet on the retina of young and old rats. *Bulletin of Siberian Medicine.* 2022;21(4):98–104. https://doi.org/10.20538/1682-0363-2022-4-98-104.

✉ *Mustafina Liliia R.,* lrmustafina@yandex.ru

Влияние высокоуглеводной высокожировой диеты на сетчатку молодых и старых крыс

Логвинов С.В.[1], Мустафина Л.Р.[1], Курбатов Б.К.[2], Нарыжная Н.В.[2], Варакута Е.Ю.[1], Потапов А.В.[1]

[1] Сибирский государственный медицинский университет (СибГМУ)
Россия, 634050, г. Томск, Московский тракт, 2

[2] Научно-исследовательский институт (НИИ) кардиологии, Томский национальный исследовательский медицинский центр (НИМЦ) Российской академии наук
Россия, 634012, г. Томск, ул. Киевская, 111а

РЕЗЮМЕ

Цель: изучить в эксперименте влияние высокоуглеводной высокожировой диеты на сетчатку в молодом и старческом возрасте.

Материалы и методы. Исследование проводили на самцах крыс линии Вистар в возрасте 60 и 450 сут в начале эксперимента. Животных распределяли на четыре группы: 1-я (n = 14) – интактные крысы в возрасте 150 сут на момент окончания исследования; 2-я (n = 14) – 150-суточные крысы на момент окончания 90 сут высокоуглеводной высокожировой диеты (ВУВЖД); 3-я (n = 14) – интактные крысы 540-суточного возраста на момент окончания исследования; 4-я (n = 14) – 540-суточные крысы после окончания 90 сут ВУВЖД. В работе использовали иммуноферментный и гистологический методы исследования.

Результаты. ВУВЖД приводила к повышению концентрации глюкозы у животных обеих возрастных групп, а у старых животных вызывала выраженное увеличение содержания инсулина, TGFβ и фибронектина в сыворотке крови, неоваскуляризацию наружных слоев сетчатки, кариопикноз и массовую гибель нейросенсорных клеток, влекущую за собой разрушение слоя палочек и колбочек, резкое истончение наружного ядерного и наружного сетчатого слоев. У молодых крыс, содержавшихся на ВУВЖД, не было отмечено выраженных гистологических нарушений сетчатки.

Заключение. ВУВЖД усиливает возрастные изменения сетчатки у старых (450-суточных) крыс.

Ключевые слова: ретинопатия, возрастные изменения сетчатки, высокоуглеводная высокожировая диета

Конфликт интересов. Авторы декларируют отсутствие явных и потенциальных конфликтов интересов, связанных с публикацией настоящей статьи.

Источник финансирования. Авторы заявляют об отсутствии финансирования при проведении исследования.

Соответствие принципам этики. Исследование одобрено этическим комитетом НИИ кардиологии Томского НИМЦ (протокол № 201 от 30.07.2020).

Для цитирования: Логвинов С.В., Мустафина Л.Р., Курбатов Б.К., Нарыжная Н.В., Варакута Е.Ю., Потапов А.В. Влияние высокоуглеводной высокожировой диеты на сетчатку молодых и старых крыс. *Бюллетень сибирской медицины.* 2022;21(4):98–104. https://doi.org/10.20538/1682-0363-2022-4-98-104.

INTRODUCTION

Age-related changes in the retina, in particular age-related macular degeneration, cause vision loss in millions of people around the world. At the same time, excessive consumption of high-calorie food, especially in developed countries, leads to diabetic retinopathy, which is the main cause of blindness in the working age population [1, 2]. The mechanisms of development of senile macular degeneration and diabetic retinopathy have some common features [3]. Numerous studies are devoted to retinal aging [4–6], retinal pathology in metabolic syndrome, and type 2 diabetes [7–9], including models with high-fat and high-carbohydrate diets [3, 10, 11]. However, the impact of high-calorie diets on the development of age-related retinal diseases and the structural basis of retinopathy caused by a high-fat, high-carbohydrate

diet (HFHCD) in various age groups is poorly studied. Knowledge about the association of aging with HFHCD is essential for development of prevention and treatment strategies for age-related macular degeneration and diabetic retinopathy. The aim of the study was to investigate the effect of HFHCD on retinal morphology of young and old rats in the experiment.

MATERIALS AND METHODS

The study was carried out on male Wistar rats aged 60 and 450 days. All procedures were carried out in accordance with the European Parliament Directive 2010/63/ EU and the FASEB statement on the principles for the use of animals in research and education. The following experimental groups were formed: group 1 (n = 14) included intact 150-day-old rats fed with a standard diet for 90 days (from 60 days of age); group 2 (n = 14) included 150-day-old rats fed with HFHCD for 90 days (from 60 days of age); group 3 (n = 14) – intact 540-day-old rats fed with a standard diet for 90 days (from 450 days of age); group 4 (n = 14) – 540-day-old rats fed with HFHCD for 90 days (from 450 days of age).

HFHCD contained 16% proteins, 21% fats, and 46% carbohydrates, including 17% fructose and 0.125% cholesterol. The water was replaced with a 20% fructose solution. Rats of groups 1 and 3 (intact animals) received standard rodent feed (24% proteins, 6% fats, 44% carbohydrates) and pure water *ad libitum*. The animals were removed from the experiment by decapitation with preliminary anesthesia with chloralose (100 mg / kg intraperitoneally).

Before decapitation, blood samples were taken, which were centrifuged (for 15 min at 3,000 rpm). Serum samples were stored in a freezer at –70 °C. Glucose concentration in the blood serum was determined by the enzymatic colorimetric method using B-8054 kits (Vector-Best, Russia). The serum levels of insulin (ab100578, Abcam), fibronectin (ab108850, Abcam), and tissue growth factor beta (TGFβ) (ab119558, Abcam) were determined by the enzyme immunoassay. Sample measurements were performed using the Infinite 200 PRO microplate reader (Tecan GmbH, Austria). The homeostatic model assessment of insulin resistance (HOMA-IR) was calculated as the ratio of insulin * glucose / 22.5. For the histologic examination, the eyeballs were fixed in a 10% buffered formalin solution (BioVitrum LLC, Russia) and embedded in paraffin according to the standard method. Sections of the posterior wall of the eyes were stained with hematoxylin and eosin (BioVitrum LLC, Russia).

Micropreparations were viewed and photographed using the AxioStar Plus light microscope (Carl Zeiss, Germany) at 400x and 1,000x magnification. In 10 random fields of vision in sections for each retina, nuclei undergoing degeneration (%) were counted in the outer nuclear layer (ONL), inner nuclear layer (INL), and ganglion cell layer (GL). In the ONL and INL, rows of nuclei were counted.

Statistical data processing was performed using the Statistica 13.0 software (StatSoft Inc., USA). The data obtained were tested for normality of distribution using the Shapiro – Wilk test. Normally distributed data were presented as the mean and the standard error of the mean ($M \pm SEM$). Not normally distributed data were presented as the median and the interquartile range Me (Q_1; Q_3). Homogeneity of multivariate dispersions was tested using the Levene's test. When comparing several independent samples of quantitative data, a two-way ANOVA was used, followed by the Bonferroni correction for normally distributed variables. The nonparametric Kruskal – Wallis test was applied to compare samples with non-normal distribution. The threshold value of the significance level p was equal to 0.05.

RESULTS

Feeding the animals with HFHCD resulted in an increase in the concentration of glucose in the blood serum in the rats of both age groups (Table 1), as well as in a rise in the HOMA-IR values. However, only in old animals, HFHCD affected insulin levels, which led to a more pronounced increase in HOMA-IR values than in young rats (Table 1). Prescription of HFHCD contributed to an increase in the levels of TGFβ and fibronectin in the animals in group 4.

The histologic examination showed that the retinas in the rats of groups 1 and 2 had normal structural architecture of retinal layers (Figure, *a*). However, a small number of nuclei undergoing degeneration were detected in the ONL; they were characterized by diffuse hyperchromic staining and wrinkling (Figure, *b*).

In the retinas of rats in group 3, nuclei in the ONL were rarefied; in areas with the absence of nuclei, they were replaced by radial glial cell processes. Some of the outer and inner segments of the rods and cones were fragmented. In the subretinal space, fragments of the external processes of rods and cones were found, as well as small nuclei undergoing

degeneration, possibly displaced here from the ONL. Single larger nuclei in the subretinal space belonged to macrophages. Karyopyknosis was detected in the pigmented layer (PL) (Figure, *c*).

Degenerating cells were found not only in the ONL, but also in the INL and GL (Figure, *d*). The most pronounced changes were noted in the retinas of rats in group 4. Thus, the ONL was almost completely destroyed and contained a few nuclei arranged in one incomplete row. Most of these nuclei were also undergoing degeneration and in some areas were displaced close to the PL, since the layer of rods and cones was completely destroyed. The PL was unevenly altered and often had pyknotic nuclei. In some areas, it was very thin and destroyed. Among the pigmented cells, hemocapillaries were found containing blood cells in the lumen. Hemocapillaries were also detected in the ONL, which indicates neovasculogenesis. In areas with the destroyed pigmented and photoreceptor layers, the nuclei of photoreceptors were attached to the Bruch's membrane. In these areas, the choriocapillaries were few and narrowed. The INL and GL contained degenerating cells (Figure, *e, f*). The quantitative assessment did not reveal significant differences in 150-day-old animals of groups 1 and 2. However, the content of nuclei undergoing degeneration in the ONL in group 2 showed a distinct upward trend compared with group 1 (Table 1).

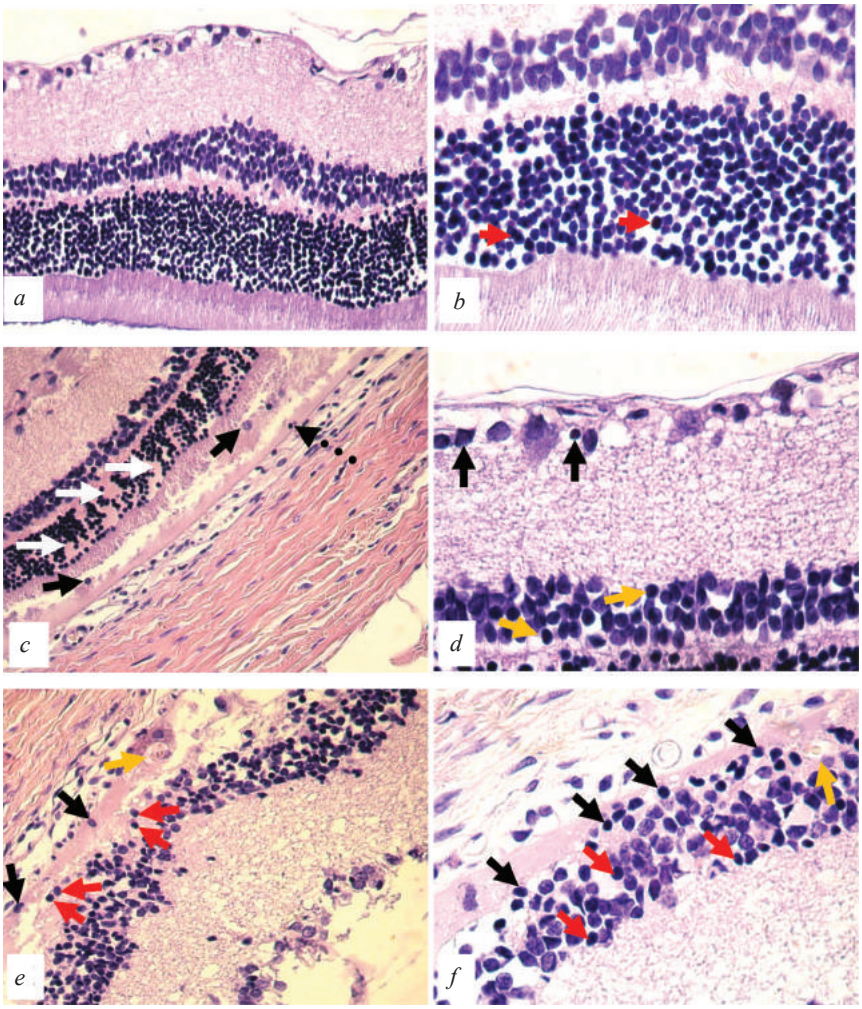

Figure. Histologic changes in the retina of rats associated with age and HFHCD: *a* – usual structural architecture of the retinal layers, group 2; *b* – single nuclei of rods and cones undergoing degeneration (indicated by arrows) in the ONL, group 2; *c* – rarefaction of nuclei in the ONL and their replacement by radial glial cell processes (white arrows), the presence of nuclei in the subretinal space (black arrows), a nucleus undergoing degeneration in the pigmented layer (dashed arrow), group 3; *d* – degenerating cells in the INL (yellow arrows) and the GL (black arrows), group 3; *e* – a blood vessel in the pigmented layer (yellow arrow), pyknosis of pigmented cell nuclei (black arrows), single nuclei undergoing degeneration in the ONL (black arrows) and GL (red arrows), group 4; *f* – nuclei of rods and cones (black arrows), arranged in one incomplete row, close to the pigmented layer, a blood capillary in the subretinal space (yellow arrow), degenerating cells in the INL (red arrows), group 4. Staining with hematoxylin and eosin, x400 (*a*, *c*, *e*); x1,000 (*b*, *d*, *f*)

Table 1

The levels of glucose and insulin in the blood serum of rats of different age fed with HFHCD, *M* ± *SEM*

Parameters	Group 1	Group 2	Group 3	Group 4
Glucose, mM / l	5.4 ± 0.2	7.3 ± 0.2[1]	6.0 ± 0.1	7.7 ± 0.2[1, 3]
Insulin, pM / l	12.2 ± 0.8	18.35 ± 2.57	19.99 ± 2.3	34.7 ± 8.6[1]
HOMA-IR	2.94 ± 0.28	5.97 ± 0.85[1]	5.36 ± 0.61[1]	12.05 ± 3.29[1, 2, 3]
Fibronectin, mg / dl	21.23 ± 1.55	27.58 ± 1.78	29.89 ± 2.38	43.00 ± 3.12[1, 2, 3]
Transforming growth factor β (TGFβ), ng /ml	14.0 ± 3.0	19.1 ± 2.6	35.3 ± 5.2[1]	31.9 ± 4.1[1]

Note: statistical significance of differences with: 1 group 1; 2 group 2; 3 group 3; 4 group 4; two-way ANOVA followed by the Bonferroni correction.

Table 2

Quantitative histologic changes in the retina of albino rats associated with age and HFHCD, *Me* (Q_1; Q_3)

Parameters	Group 1	Group 2	Group 3	Group 4
Nuclei undergoing degeneration in ONL, %	0.25 (0.20; 0.40)	0.80 (0.70; 0.90)	15.05[1] (13.65; 16.65)	88.30[1, 2] (72.80; 92.40)
Number of rows of nuclei in ONL	10.65 (9.70; 11.90)	10.20 (9.30; 10.40)	5.90[1] (4.85; 7.85)	1.40[1, 2] (1.10; 4.90)
Nuclei undergoing degeneration in INL, %	0.15 (0.10; 0.20)	0.10 (0.10; 0.20)	1.95 (1.65; 2.80)	8.10[1, 2] (7.00; 9.30)
Number of rows of nuclei in INL	4.65 (4.20; 4.90)	4.70 (4.60; 5.40)	4.20 (4.05; 4.90)	4.30 (3.70; 5.20)
Ganglion neurons undergoing degeneration	0.50 (0.25; 0.50)	0.75 (0.25; 1.00)	3.00[1] (1.50; 4.00)	9.50[1, 2] (9.00; 11.50)

Note: statistical significance of differences with: 1 group 1; 2 group 2; 3 group 3; 4 group 4; Kruskal – Wallis test.

In rats of group 3, the proportion of degenerating cells in the ONL, INL, and GL significantly increased compared with groups 1 and 2. The most pronounced increase in the proportion of such cells was observed among rods and cones. There was a significant decrease in the number of rows of nuclei in the ONL in group 3 compared with groups 1 and 2. The number of rows of nuclei in the INL did not differ in all 4 groups of animals. In group 4, the trend was similar to that in group 3, but the quantitative changes were significantly more pronounced. A drastic decrease in the number of rows of nuclei in the ONL and an increase in the proportion of nuclei undergoing degeneration among the remaining nuclei were worth noting, which indicates massive death of rods and cones. The proportion of degenerating cells in the INL and GL significantly increased in group 4 compared with group 3, but to a much lesser extent than the proportion of nuclei undergoing degeneration in the ONL.

DISCUSSION

In our opinion, the revealed neovasculogenesis played the most important role in tissue mechanisms of retinopathy in old rats fed with HFHCD. As shown, blood vessels containing blood cells in the lumen appeared in unusual places – among the pigmented cells, in the layer of outer and inner segments, and in the ONL. It is known that invasion of hemocapillaries into layers where they are not present in normal conditions leads to oxidative stress and, as a consequence, death of pigmented and photoreceptor cells, for example, under the combined effect of ionizing radiation and bright light [12]. Under light exposure, new vessels invaded the layer of the outer and inner segments, which was due to expression of VEGF and led to retinal degeneration [13].

C.Toma et al. emphasized the relationship of oxidative stress and neovascularization with changes in choroidal blood flow and degeneration of the pigmented layer and photoreceptor cells in age-related retinopathy [14]. Pathological retinal angiogenesis is associated with expression of VEGF in diabetic retinopathy [15]. The studies carried out by a group of authors [16] showed that HFHCD used in our work causes biochemical disturbances characteristic of the metabolic syndrome.

To date, the pathogenesis of diabetic retinopathy has been characterized in the context of signaling of glucose, insulin, VEGF, and other growth factors, among which TGFβ is of great importance [17]. At an early stage of diabetic retinopathy, TGFβ protects retinal vessels. At later stages, it contributes to the progression of vascular diseases, including proliferative ones [18]. TGFβ is known to control endothelial cell proliferation, cell adhesion, and deposition of the extracellular matrix and plays a key role in the development of diabetic retinopathy [19, 20]. In our study, an increase in the concentration of TGFβ was detected in old rats, which was accompanied

by proliferative changes in the retina in the form of neovasculogenesis in HFHCD. This occurred against the background of an increase in the blood levels of glucose and insulin and a rise in the HOMA-IR value. In old rats fed with HFHCD, the plasma level of fibronectin also increased. It is known that activation of fibronectin in endothelial cells and retinal pericytes is caused by TGFβ, which leads to thickening of capillary basement membranes and impairs permeability of the blood – retina barrier in diabetic retinopathy [21, 22]. Therefore, the changes in the studied growth factors involved in the pathogenesis of retinopathy corresponded to neovasculogenesis and other vascular diseases that play a key role in age-related and HFHCD-related structural retinal abnormalities. This makes determination of these biochemical parameters in the diagnosis and treatment of senile macular degeneration and diabetic retinopathy clinically significant.

CONCLUSION

Our study showed that HFHCD enhances age-related changes in the retina in old rats. Aging and HFHCD exhibit synergism in damaging photoreceptor cells, causing their karyopyknosis and massive death, which results in destruction of the layer of outer and inner segments, drastic thinning of the ONL to 1–2 rows of nuclei, and thinning of the outer retinal layer. Death of rods and cones in the retina is accompanied by focal destructive changes in pigmented cells and a decrease in the number of choriocapillaries in the foci of destruction. HFHCD causes an increase in the serum levels of TGFβ and fibronectin and neovascularization in the outer retinal layers, which, in our opinion, plays a key role in the mechanisms of their destruction. The inner retinal layers were affected to a lesser extent than the photoreceptor and pigmented layers in old rats fed with HFHCD. In young rats, HFHCD did not cause pronounced histologic abnormalities in the retina.

REFERENCES

1. Dai W., Dierschke S.K., Toro A.L., Dennis M.D. Consumption of a high fat diet promotes protein O-GlcNAcylation in mouse retina via NR4A1-dependent GFAT2 expression. *Biochim. Biophys. Acta Mol. Basis Dis.* 2018;1864(12):3568–3576. DOI: 10.1016/j.bbadis.2018.09.006.
2. Hammoum I., Mbarek S., Dellaa A., Dubus E., Baccouche B., Azaiz R. et alStudy of retinal alterations in a high fat diet-induced type ii diabetes rodent: Meriones shawi. *Acta Histochem.* 2017;119(1):1–9. DOI: 10.1016/j.acthis.2016.05.005.
3. Vidal E., Lalarme E., Maire M.-A., Febvret V., Grégoire S., Gambert S. et al. Early impairments in the retina of rats fed with high fructose/high fat diet are associated with glucose metabolism deregulation but not dyslipidaemia. *Sci. Rep.* 2019;9(1):5997. DOI: 10.1038/s41598-019-42528-9.
4. Lee K.S., Lin S., Copland D.A., Dick A.D., Liu J. Cellular senescence in the aging retina and developments of senotherapies for age-related macular degeneration. *J. Neuroinflammation*. 2021;18(1):32. DOI: 10.1186/s12974-021-02088-0.
5. Nag T.C., Wadhwa S. Ultrastructure of the human retina in aging and various pathological states. *Micron*. 2012;43(7):759–781. DOI: 10.1016/j.micron.2012.01.011.
6. Kovács-Valasek A., Etelka Pöstyéni E., Dénes V., Mester A., Sétáló G.Jr., Gábriel R. Age-related alterations of proteins in albino Wistar rat retina. *Cells Tissues Organs*. 2021;210(2): 135–150. DOI: 10.1159/000515447.
7. Karaca C., Karaca Z. Beyond hyperglycemia, evidence for retinal neurodegeneration in metabolic syndrome. *Invest. Ophthalmol. Vis. Sci.* 2018;59(3):1360–1367. DOI: 10.1167/iovs.17-23376.
8. Godisela K.K., Reddy S.S., Kumar C.U., Saravanan N., Reddy P.Y., Jablonski M.M. et al. Impact of obesity with impaired glucose tolerance on retinal degeneration in a rat model of metabolic syndrome. *Mol. Vis.* 2017;23:263–274.
9. Yau P.L., Kim M., Tirsi A., Convit A. Retinal vessel alterations and cerebral white matter microstructural damage in obese adolescents with metabolic syndrome. *JAMA Pediatr*. 2014;168(12):e142815. DOI: 10.1001/jamapediatrics.2014.2815.
10. Thierry M., Pasquis B., Buteau B., Fourgeux C., Dembele D., Leclere L. et al. Early adaptive response of the retina to a pro-diabetogenic diet: Impairment of cone response and gene expression changes in high-fructose fed rats. *Exp. Eye. Res.* 2015;135:37–46. DOI: 10.1016/j.exer.2015.04.012.
11. Paz M.C., Barcelona P.F., Subirada P.V., Ridano M.E., Chiabrando G.A., Castro C. et al. Metabolic syndrome triggered by fructosedDiet impairs neuronal function and vascular integrity in ApoE-KO mouse retinas: Implications of autophagy deficient activation. *Front. Cell Dev. Biol.* 2020;8:573987. DOI: 10.3389/fcell.2020.573987.
12. Logvinov S.V., Potapov A.V. Structural changes to the retina in combined exposure to light and X-ray. *Morfologiia.* 2000;117(1):19–23 (in Russ.).
13. Tisi A., Parete G., Flati V., Maccarone R. Up-regulation of pro-angiogenic pathways and induction of neovascularization by an acute retinal light damage. *Sci. Rep.* 2020;10(1):6376. DOI: 10.1038/s41598-020-63449-y.
14. Toma C., De Cillà S., Palumbo A., Garhwal D.P., Grossini E. Oxidative and Nitrosative Stress in Age-Related Macular Degeneration: A Review of Their Role in Different Stages of Disease. *Antioxidants (Basel)*. 2021;10(5):653. DOI: 10.3390/antiox10050653.
15. Rezzola S., Loda A., Corsini M., Semeraro F., Annese T., Presta M. et al. Angiogenesis-Inflammation Cross Talk in Diabetic Retinopathy: Novel Insights From the Chick Embryo Chorioallantoic Membrane/Human Vitreous Platform. *Front. Immunol.* 2020;11:581288. DOI: 10.3389/fimmu.2020.581288.
16. Birulina J.G., Ivanov V.V., Buyko E.E., Trubacheva O.A., Petrova I.V., Grechishnikova A.Yu., Nosarev A.V., Gusako-

va S.V. Effects of a high-fat, high-carbohydrate diet on blood cells of rats. *Bulletin of Siberian Medicine.* 2021;20(3):6–12 (in Russ.). DOI: 10.20538/1682-0363-2021-3-6-12.
17. Wheeler S.E., Lee N.Y. Emerging roles of transforming growth factor β signaling in diabetic retinopathy. *J. Cell. Physiol.* 2017;232(3):486–489. DOI: 10.1002/jcp.25506.
18. Huang H. Pericyte-endothelial interactions in the retinal microvasculature. *Int. J. Mol. Sci.* 2020;21(19):7413. DOI: 10.3390/ijms21197413.
19. Goumans M.-J., Valdimarsdottir G., Itoh S., Rosendahl A., Sideras P., Ten Dijke P. Balancing the activation state of the endothelium via two distinct TGF-beta type I receptors. *EMBO J.* 2002;21(7):1743–1753. DOI: 10.1093/emboj/21.7.1743.
20. Gacka M., Adamiec J. The role of transforming growth factor-beta in the pathogenesis of diabetic retinopathy. *Przegl. Lek.* 2006;63(5):296–298. (In Polish).
21. Van Geest R.J., Klaassen I., Vogels I.M., Van Noorden C.J., Schlingemann R.O. Differential TGF-{beta} signaling in retinal vascular cells: a role in diabetic retinopathy? *Invest. Ophthalmol. Vis. Sci.* 2010;51(4):1857–1865. DOI: 10.1167/iovs.09-4181.
22. Chaqour B., Karrasch C. Eyeing the extracellular matrix in vascular development and microvascular diseases and bridging the divide between vascular mechanics and function. *Int. J. Mol. Sci.* 2020;21(10):3487. DOI: 10.3390/ijms21103487.

Acknowledgments

The authors are grateful to Mukhomedzyanov A.V., Gorbunov A.S., and Voronkov N.S. for help in conducting the experiment, as well as to Ivanov V.V. and Birulina Yu.G. for methodological assistance in developing a diet.

Authors contribution

Logvinov S.V. – conception, drafting of the Morphology section of the article, substantiation of the manuscript, critical revision of the manuscript for important intellectual content, final approval of the manuscript for publication. Mustafina L.R. – carrying out of the morphologic studies, work on the illustrations, interpretation of the morphologic findings. Kurbatov B.K. – design of the study, carrying out of the studies, statistical analysis and interpretation of the results. Naryzhnaya N.V. – conception and design, carrying out of the studies, statistical processing of the results, drafting of the article, substantiation of the manuscript. Varakuta E.Yu. – carrying out of the morphologic studies, interpretation of the data. Potapov A.V. – conception, drafting of the article, substantiation of the manuscript, critical revision of the manuscript for important intellectual content.

Authors information

Logvinov Sergey V. – Dr. Sci. (Med.), Professor, Head of the Histology, Embryology and Cytology Division, Siberian State Medical University, Tomsk, s_logvinov@mail.ru, https://orcid.org/0000-0002-9876-6957

Mustafina Liliia R. – Dr. Sci. (Med.), Associate Professor, Professor, Histology, Embryology and Cytology Division, Siberian State Medical University, Tomsk, lrmustafina@yandex.ru, https://orcid.org/0000-0003-3526-7875

Kurbatov Boris K. – Junior Researcher, Laboratory for Experimental Cardiology, Cardiology Research Institute, Tomsk NRMC, Tomsk, bobersanker@gmail.com, https://orcid.org/0000-0001-9603-822X

Naryzhnaya Natalia V. – Dr. Sci. (Med.), Leading Researcher, Laboratory for Experimental Cardiology, Cardiology Research Institute, Tomsk NRMC, Tomsk, natalynar@yandex.ru, https://orcid.org/0000-0003-2264-1928

Varakuta Elena Yu. – Dr. Sci. (Med.), Associate Professor, Head of the Division of Human Anatomy with a Course in Topographic Anatomy and Operative Surgery, Siberian State Medical University, Tomsk, varelen@rambler.ru, https://orcid.org/0000-0003-3173-5336

Potapov Aleksey V. – Dr. Sci. (Med.), Professor, Histology, Embryology and Cytology Division, Siberian State Medical University, Tomsk, potalex@mail.ru, https://orcid.org/0000-0002-0468-3959

(✉) **Mustafina Liliia R.,** lrmustafina@yandex.ru

Received 19.01.2022;
approved after peer review 25.02.2022;
accepted 09.06.2022

УДК 616.858-056.7-092
https://doi.org/10.20538/1682-0363-2022-4-105-113

Environmental and genetic risk factors for Parkinson's disease

Nikitina M.A.[1], Alifirova V.M.[1], Bragina E.Yu.[2], Babushkina N.P.[2], Gomboeva D.E.[2], Nazarenko M.S.[1, 2]

[1] Siberian State Medical University
2, Moscow Trakt, Tomsk, 634050, Russian Federation

[2] Research Institute of Medical Genetics, Tomsk National Research Medical Center (NRMC), Russian Academy of Sciences
10, Ushaika Embankment, Tomsk, 634050, Russian Federation

ABSTRACT

Aim. To analyze risk factors in the group of patients with Parkinson's disease (PD) and compare them with the literature data.

Materials and methods. The study included 439 patients with PD and 354 controls, comparable by gender and age. For each individual, a registration card was filled in containing demographic, epidemiological, clinical, and neuropsychological data. The severity of the disease was studied according to the MDS-UPDRS scale; the stage of PD was determined according to the Hoehn and Yahr scale. Cognitive functions were assessed by the MoCA test and MMSE. The length of the (CAG)n repeat region in the *HTT* gene was determined using fragment analysis on the ABI 3730 DNA analyzer. The obtained results were analyzed using GeneMapper Software v4.1 (Applied Biosystems, USA).

Results. When comparing patients with PD and the control group, the odds ratio (OR) for PD in individuals with traumatic brain injury was 3.13 (95% confidence interval (CI): 2,27–4.34; $p = 4.94 \times 10^{-13}$), which showed the significance of this risk factor for PD. Consumption of coffee in the anamnesis distinguished the group of PD patients from the control group (OR = 0.41 (95% CI: 0.30–0.56); $p < 0.0001$), confirming its neuroprotective effect. Analysis of the variability in the length of the (CAG)n repeat regions in the *HTT* gene showed that patients whose genotype contained an allele with 17 repeats in combination with any allele other than an allele containing 18 repeats had a protective effect (OR = 0.50 (95% CI: 0.27–0.92); $p = 0.025$). All genotypes containing an allele with 18 repeats were predisposed to PD (OR = 2.57 (95% CI: 1.66–4.28); $p = 0.007$). The predisposing effect of the allele to PD, unrelated to the expansion of CAG repeats in the *HTT* gene, was revealed for the first time.

Conclusion. Traumatic brain injury and the allele with 18 CAG repeats in the *HTT* gene are risk factors for PD. Coffee consumption can be attributed to protective factors in relation to PD.

Keywords: Parkinson's disease, risk factors, coffee, traumatic brain injury, *HTT* gene

Conflict of interest. The authors declare the absence of obvious or potential conflict of interest related to the publication of this article.

Source of financing. The study was partially supported by the research grants for young scientists ("The role of repair genes in the pathogenesis of Parkinson's disease, Huntington's disease, and healthy ageing" 2021–2023). The study was partially supported by the state assignment of the Ministry of Science and Higher Education No.122020300041-7.

Conformity with the principles of ethics. The patients gave an informed consent to examination, neuropsychological testing, and sampling of venous blood. The study was approved by the local Ethics Committee at Siberian State Medical University (Protocol No. 7813 of 27.05.2019).

✉ *Nikitina Maria A.,* nikitina_ma@mail.ru

For citation: Nikitina M.A., Alifirova V.M., Bragina E.Yu., Babushkina N.P., Gomboeva D.E., Nazarenko M.S. Environmental and genetic risk factors for Parkinson's disease. *Bulletin of Siberian Medicine.* 2022;21(4):105–113. https://doi.org/10.20538/1682-0363-2022-4-105-113.

Средовые и генетические факторы риска болезни Паркинсона

Никитина М.А.[1], Алифирова В.М.[1], Брагина Е.Ю.[2], Бабушкина Н.П.[2], Гомбоева Д.Е.[2], Назаренко М.С.[1, 2]

[1] Сибирский государственный медицинский университет (СибГМУ)
Россия, 634050, г. Томск, Московский тракт, 2

[2] Научно-исследовательский институт (НИИ) медицинской генетики, Томский национальный исследовательский медицинский центр (НИМЦ) Российской академии наук
Россия, 634050, г. Томск, ул. Набережная реки Ушайки, 10

РЕЗЮМЕ

Цель. Проанализировать факторы риска в группе пациентов с болезнью Паркинсона (БП) и сопоставить их с литературными данными.

Материалы и методы. В исследование были включены 439 пациентов с БП и 354 индивида группы контроля, сопоставимых по полу и возрасту. На каждого индивидуума заполнена регистрационная карта, содержащая информацию о демографических, эпидемиологических, клинических и нейропсихологических данных. Тяжесть заболевания исследовалась по шкале MDS-UPDRS; стадия БП – согласно шкале Hoehn – Yahr. Когнитивные функции оценивались по MoCA-тесту и MMSE. Длину (CAG)n-повтора в гене *HTT* определяли с помощью фрагментного анализа на платформе ABI Genetic Analyzer 3730. Анализ полученных результатов проводился с помощью GeneMapper Software v4.1 (Applied Biosystems, США).

Результаты. При сравнении пациентов с БП и контрольной выборки отношение шансов развития БП у индивидов с травмой головы составило 3,13 (95% CI: 2,27–4,34; $p = 4{,}94 \times 10^{-13}$), показав значимость этого фактора риска БП. Употребление в анамнезе кофе отличает группу пациентов с БП от группы контроля (OR = 0,41 (95% CI: 0,30–0,56); $p < 0{,}0001$), подтверждая его нейропротективное действие. Анализ вариабельности длины (CAG)*n*-повторов в гене *HTT* показал, что пациенты, в генотипе которых присутствует аллель, содержащий 17 повторов в сочетании с любым другим аллелем, кроме аллеля, содержащего 18 повторов, обладает протективным эффектом (OR = 0,50 (95% CI: 0,27–0,92); $p = 0{,}025$). Все генотипы, содержащие аллель с 18 повторами, предрасполагают к БП (OR = 2,57 (95% CI: 1,66–4,28); $p = 0{,}007$). Предрасполагающий эффект аллеля, не связанный с экспансией CAG-повторов гена *HTT*, к БП выявлен впервые.

Заключение. Черепно-мозговая травма и аллель $(CAG)_{18}$-повторов гена *HTT* являются факторами риска для развития БП. Употребление кофе можно отнести к протективным факторам в отношении БП.

Ключевые слова: болезнь Паркинсона, факторы риска, кофе, черепно-мозговая травма, *HTT*

Конфликт интересов. Авторы декларируют отсутствие явных и потенциальных конфликтов интересов, связанных с публикацией настоящей статьи.

Источник финансирования. Исследование выполнено при частичной грантовой поддержке научно-исследовательских проектов, выполняемых молодыми учеными («Роль генов репарации в патогенезе болезни Паркинсона, болезни Гентингтона и нормального (здорового) старения», 2021–2023 гг.). Работа выполнена при частичном финансировании Министерства науки и высшего образования (госзадание № 122020300041-7).

Соответствие принципам этики. Обследование, нейропсихологическое тестирование и забор венозной крови всех лиц проводились только после подписания информированного согласия. Исследование одобрено локальным этическим комитетом СибГМУ (протокол № 7813 от 27.05.2019).

Для цитирования: Никитина М.А., Алифирова В.М., Брагина Е.Ю., Бабушкина Н.П., Гомбоева Д.Е., Назаренко М.С. Средовые и генетические факторы риска болезни Паркинсона. *Бюллетень сибирской медицины.* 2022;21(4):105–113. https://doi.org/10.20538/1682-0363-2022-4-105-113.

INTRODUCTION

Parkinson's disease (PD) is a chronic, progressive neurodegenerative disease, described by James Parkinson in 1817 in the essay about "shaking palsy" [1]. Degeneration of dopaminergic neurons in the substantia nigra and formation of Lewy bodies are pathological markers of PD [2]. Lewy bodies are cytoplasmic inclusions that contain insoluble aggregates of α-synuclein. However, pathological process is not restricted to the substantia nigra, it affects other brain regions and involves non-dopaminergic neurons.

PD is characterized by multifactorial etiology, which includes environmental and genetic components. Lifestyle and environmental factors [3] and multiple genetic variants have modifying effects both on predisposition to PD [4] and on the rate of PD progression [5–7]. Such factors as age, male gender [8], contact with pesticides [9], head injuries, depression, osteoporosis, therapy with beta-adrenergic antagonists or melanoma in the medical history [10] are associated with an increased risk for PD. At the same time, physical activity [11], coffee consumption [12], and long-term intake of nonsteroidal anti-inflammatory drugs, calcium channel blockers, and statins are associated with a decreased risk for PD [3]. Some studies revealed a decrease in the frequency of PD among people with alcohol abuse [11] and among smokers [13]. The latter two associations are controversial and can be caused by peculiarities of study group formation.

Monogenic forms of PD are encountered approximately in 5–10 % of PD cases. At least 18 different genes, mutations in which lead to PD, have been currently described [14]. The main pathogenic variants are found in genes encoding α-synuclein (SNCA), leucin-rich repeat kinase 2 (LRRK2), glucocerebrosidase (GBA), and parkin E3 ubiquitin protein ligase (PRKN) [15]. Nonetheless, PD mostly has sporadic nature, and the majority of PD patients do not have mutations in these genes [2, 16].

Moreover, the most frequent genetic mutations contributing to PD have incomplete penetrance, which indicates the presence of modifying factors. Twin studies have shown that inheritance of PD is 30%, which indicates that an increased risk for PD is associated with environmental and lifestyle factors [17]. The *HTT* gene is one of the possible modifier genes; expansion in its (CAG)n repeat regions (more than 36 repeats) results in Huntington's disease (HD). The length of repeat regions is assumed to be a physiological modifier for the adenosine diphosphate (ADP) / adenosine triphosphate (ATP) ratio, which implies a common pathological component in both diseases (PD and HD). Moreover, single cases with atypical PD were described in the literature: PD patients with pronounced clinical manifestations have some neurophysiological features typical of HD. Such patients have intermediate alleles in the *HTT gene* – $(CAG)_{27}$ and $(CAG)_{29}$ – which do not exceed the pathological (CAG)n repeat length in HD [18, 19]. Therefore, we considered the length of (CAG)n repeats in the *HTT* gene as one of the risk factors for PD.

The aim of the study was to evaluate the role of environmental and genetic factors in PD development.

MATERIALS AND METHODS

A group of PD patients was recruited at the Neurology and Neurosurgery Division of Siberian State Medical University. The diagnosis was established according to the Movement Disorder Society Clinical Diagnostic Criteria for Parkinson's Disease [20]. We examined 439 PD patients (179 males and 260 females) and 354 healthy individuals as a control group (143 males and 211 females). All these individuals were included in the study. The control group consisted of healthy individuals without neurodegenerative pathology. The study groups were comparable by age (66.3 ± 7.3 and 66.2 ± 9.1 years, $p > 0.05$) and sex (1:1.45 and 1:1.47, respectively).

All study participants underwent clinical neurological and neuropsychological testing. An individual registration card was filled in for each participant containing demographic, epidemiological, and clinical data. Information about risk factors for PD (head injury, exposure to toxic chemicals, smoking, coffee consumption) was obtained from interviews with the participants and their relatives (individuals with pronounced cognitive impairments were not included in the study). The above factors were taken into account only if they preceded PD symptoms.

The severity of the disease was assessed using the MDS-UPDRS scale; the stage of PD was determined according to the Hoehn and Yahr scale (1967) [21]. Cognitive functions were examined according to the Montreal Cognitive Assessment (MoCA) test [22] and MMSE [23].

The study complied with the principles of the Good Clinical Practice (GCP) and the Declaration of Helsinki. The study was approved by the local Ethics Committee at Siberian State Medical University.

Molecular and genetic testing was performed at the Center for Collective Use of Research Equipment and Experimental Biological Material "Medical Genomics" of the Research Institute of Medical Genetics, Tomsk NRMC. The length of (CAG)n repeats in the *HTT* gene was examined by the fragment analysis on the ABI Genetic Analyzer 3730 according to the earlier described method [24]. The obtained results were analyzed using GeneMapper Software v4.1. (Applied Biosystems).

Statistical data processing was performed using Statistica 10 software. Calculation of odds ratio (OR) and 95% confidence interval (95% CI) was performed using the online tool at https://www.medcalc.org/calc/odds_ratio.php.

RESULTS

Association of traumatic brain injury with Parkinson's disease. According to the literature data, traumatic brain injury (TBI) was studied as one of the risk factors for a range of neurodegenerative diseases [25]. Some studies have shown that head injury can cause neuroinflammation, affecting neurons either directly [26, 27] or indirectly – via blood – brain barrier impairment [28, 29].

Among the examined 439 PD patients, 208 (47.4%) individuals reported the presence of TBI in the medical history (42 females and 166 males, the average age was 66.2 ± 9.2 years). In the control group, only 79 (22.3%) individuals (18 females and 61 males, the average age was 65.5 ± 8.8 years) reported TBI in the past medical history (Fig.1).

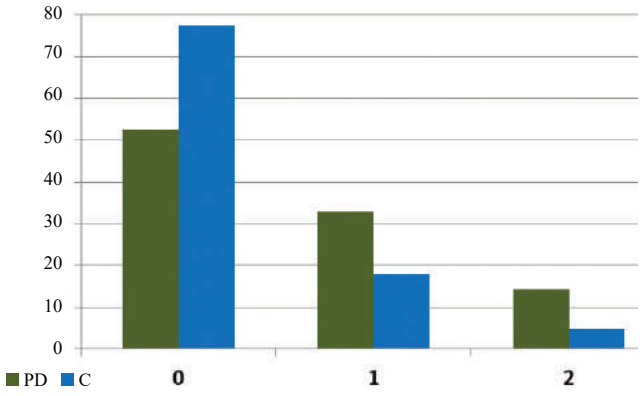

Fig. 1. Frequency of TBI in the past medical history of individuals with PD and the control group (C), %; 0 – no TBI; 1 – the presence of TBI without a loss of consciousness; 2 – the presence of TBI with a loss of consciousness

Comparing the frequency of TBI in PD patients and the control group, OR for PD in individuals with TBI was 3.13 (95 % CI: 2.27–4.34; p = 4.94 × 10^{-13}). Therefore, TBI is a significant risk factor for PD. 63 (14.3%) of PD patients and 17 (4.8%) individuals from the control group reported TBI with a loss of consciousness. The odds for development of PD increase in individuals with more severe TBI (TBI with a loss of consciousness). The OR for the development of PD in individuals with TBI with a loss of consciousness, compared with individuals without TBI, was 4.41 (95% CI: 2.44–8.07; $p = 7.39 \times 10^{-8}$). The average age of disease debut did not differ significantly between PD patients with and without TBI (66.2 ± 9.2 years vs. 67.8 ± 11.8 years, p = 0.82).

Exposure to toxic chemicals. Numerous studies that included populations from all over the world have shown that exposure to pesticides and farming or living in rural areas are considered risk factors for the development of PD [16]. Occupational hazards and accidental exposure to such pesticides as paraquat, rotenone, 2,4-dichlorophenoxyacetic acid, and some dithiocarbamates and organochlorines (for residents living near the areas treated with these pesticides) are associated with an increased risk of PD development [30]. Genetically determined impairments in individuals exposed to toxic chemicals may affect their health increasing the risk of PD manifestation [31]. And on the contrary, compliance with hygiene rules and healthy diet can protect from adverse effects of environmental factors and reduce the effect of pesticide exposure [32, 33].

Among the studied individuals, 116 patients (26.4%) reported exposure to toxic chemicals for more than 5 years: gasoline and petroleum products 8.7% (38), paints and organic solvents 8.0% (35), pesticides and fertilizers 4.3% (19), metals and ionizing radiation 3.6% (16); 8 individuals (1.8%) among the PD patients were welders with work experience of 10 ± 6 years. Nevertheless, comparing the group of PD patients and the control group in terms of exposure to toxic chemicals did not reveal significant differences (OR = 0.79 95 % CI: 0.58–1.08; p = 0.1409).

Lifestyle factors. Some lifestyle factors are associated with a decreased risk of PD development. The strongest association was found between a decreased risk of PD and cigarette smoking individuals and (according to other studies) other tobacco users. It is assumed that nicotine plays the central role in this association. However, a recently finished clinical trial did not reveal a modifying effect of a nicotine patch on manifestations and progression of the disease in PD patients [34, 35].

In the current study, about 42% (n = 184) of patients have never smoked, 53% (n = 233) of patients used to smoke, and 5% (n = 22) of patients are current smokers. In the control group, the values were 50.3% (n = 178), 43.5% (n = 154), and 6.2% (n = 22), respectively. No significant differences were revealed between smoking and non-smoking individuals (p = 0.6594).

In 2007, Dr. Xiang Gao published the first large, prospective study, which lasted 16 years, on the effect of diet and eating habits on the risk of PD development [36]. It was shown that coffee and caffeine consumption were linked with a decreased risk of PD development. This effect was more pronounced in men, was dose-dependent, and might depend on genetic factors. Similarly, some studies showed a decreased risk of PD in individuals drinking strong tea [37, 38].

Among the examined PD patients, only 20.5 % (n = 90) of individuals drink coffee, and about 38.7% (n = 137) of people drink coffee in the control group (OR = 0.41 (95%CI: 0.30–0.56); $p < 0.0001$). At the same time, about 16% of PD patients regularly drink coffee for more than 10 years. These results are consistent with the data obtained by the Xiang Gao et al. [36].

Alcohol consumption in the studied groups was evaluated at the time of the study and in the anamnesis in terms of the frequency of consumption of beer, wine, fortified wine, sweet liqueur or strong alcohol in grams per day (g / day) based on the standard volume of the container for a particular drink. Division into groups was the following: < 0.1 g / day (people who do not drink alcohol, I), 0.1–4.9 g / day (II), 5.0–14.9 g / day (III), 15.0–29.9 g / day (IV), 30.0–59.9 g / day (V), and ≥ 60 g / day (VI). For patients with PD, the following values were identified: 15% (I), 18% (II), 34% (III), 20% (IV), 10% (V), and ≥3% (VI). For the control group, the values were the following: 13% (I), 19% (II), 35% (III), 20% (IV), 10% (V), and ≥3% (VI) ($p > 0.05$). At the same time, the average amount of consumed alcohol did not differ between the groups: 3.01 ± 1.29 and 3.02 ± 1.26 (p = 0.9501).

Length of (CAG)n-repeats in the HTT gene. Despite incontrovertible evidence of the pathophysiological role of mitochondria in PD and their key role in cell signaling pathways, identification of mitochondrial dysfunction as a cause or effect of neurodegeneration is still a challenging task for researchers [39].

Earlier, we showed the associations of *NBN*, *ATM*, and *MLH1* genes with PD. Protein deficiency in these genes can also lead to mitochondrial dysfunction. Frequent alleles and genotypes of non-synonymous substitution of rs1801516 in *ATM* and rs1799977 in *MLH1* predispose to PD development; at the same time, heterozygotes exert a protective effect. A rare allele and genotype of promoter substitution in *NBN* (rs1805800) is also a risk allele for PD [40].

In the current study, we analyzed the length of (CAG)n repeats in the *HTT* gene in PD patients and healthy individuals. In both groups, we found a comparable number of alleles (16 and 17 in PD patients and in the control group, respectively) and a comparable length range (12–32 (CAG)n repeats in PD patients and 12–30 (CAG)n repeats in the control group) (Fig.2). Intermediate alleles $(CAG)_{26\text{-}35}$ were identified in both groups with alleles of normal length: $(CAG)_{16\text{-}19}$ in PD patients and $(CAG)_{15\text{-}24}$ in the control group. The frequency of intermediate alleles was 2.38% and 5.58% in the PD patients and in the control group, respectively.

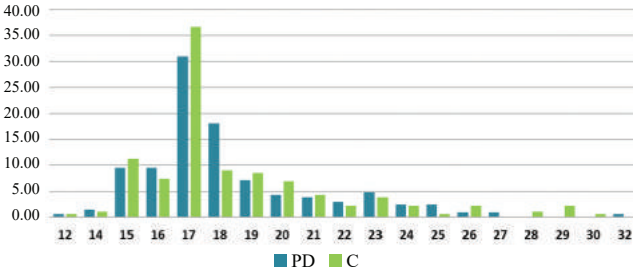

Fig. 2. Frequency of (CAG)n repeat regions in the HTT gene in patients with PD and in the control group, %

The distribution of alleles in both studied groups was similar, about 80% of alleles had 15–20 repeats (Fig.3); the $(CAG)_{17}$ allele was the most frequent in both groups (30.95% and 36.70% in PD patients and healthy individuals, respectively). However, the $(CAG)_{18}$ allele in PD patients was significantly more frequent than in the control group (OR = 2.22 (95%CI: 1.66–4.28), $\chi 2 = 6.09$, $p = 0.014$). Therefore, a risk allele was identified (18 repeats); the allele with 17 repeats was 5.75% more frequent in the control group; however, these differences were not significant (p = 0.269).

Since there was a great number of genotypes in each sample (38 in each group), we have grouped genotypes for the further analysis. The "18 / all" group included all genotypes which had one allele with 18 (CAG)n repeats and the other allele with any number of repeats except for 17. The genotype combining alleles with 17 and 18 repeats was studied

separately. The "17 / all" group included all genotypes which had one allele with 17 repeats and the other allele with any number of repeats, expect for 18. All remaining genotypes were included in the group "all / all". The "17 / all" genotype had a protective effect (OR = 0.50 (95%CI: 0.27–0.92), $\chi 2 = 5.05$, $p = 0.025$). At the same time, genotypes with 18 alleles were more prevalent in PD patients: "18 / all" was 2.98 times more frequent, and "17 / 18" was 1.47 times more frequent than in the control group. Therefore, we considered these genotypes together. The frequency of the genotype containing 18 alleles in combination with any other allele (including the allele with 17 repeats) in the group of PD patients was 36.19%, in the group of healthy individuals – 18.09%; the OR for these genotypes was 2.57 (95%CI: 1.66–4.28; $\chi 2 = 7.25$; $p = 0.007$).

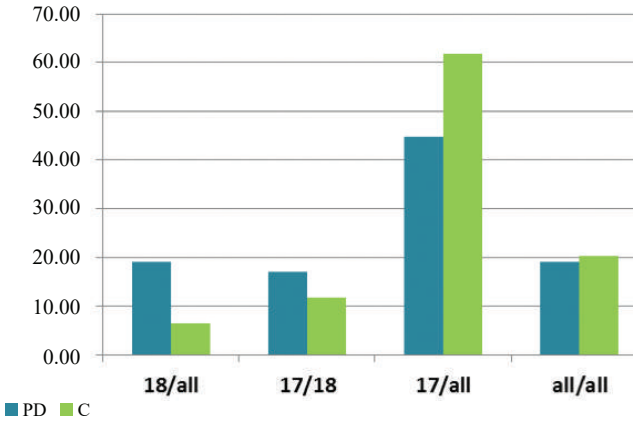

Fig. 3. Genotype frequencies for (CAG)n repeats in the HTT gene in patients with PD and in the control group

The obtained results indicate that the allele containing 17 (CAG)n repeats has a protective effect in combination with any allele, except for the one containing 18 repeats. In turn, all genotypes with 18 (CAG)n repeats predispose to PD. The predisposing effect to PD of the normal length allele in the *HTT* gene was identified in this study for the first time. It is hard to state how this association can manifest itself in the pathological phenotype, as there are no data on the involvement of normal alleles in the pathology. It is possible that the revealed associations can be explained by the involvement of the polyglutamine tract in the *HTT* gene in the regulation of energy production by mitochondria. I.S. Seong et al. showed in 2005 that the ADP / ATP ratio suggests the participation of not only pathological alleles, but also normal ones in this process [41]. Therefore, changes in the energy production function of mitochondria may contribute to the phenotypic manifestations of PD.

CONCLUSION

Our study in PD patients confirms modifying effects of lifestyle factors on PD progression, and changes in lifestyle can improve health-related quality of life of patients.

Coffee consumption in the anamnesis significantly distinguishes PD patients from healthy individuals. The obtained data suggest a possible neuroprotective effect of caffeine, which contributes to maintenance of cognitive and physical functioning, improving the quality of life of PD patients and their relatives. Caffeine is known as a psychostimulant and antioxidant, which boosts attention. According to the conducted studies, caffeine is able to protect low-density lipoproteins from oxidation and decrease oxidative DNA damage. Additionally, caffeine is an adenosine A2A-receptor antagonist and exerts a neuroprotective effect, decreasing dopamine deficiency [42]. The use of caffeine in animal models of PD led to a decrease in oxidative stress and restoration of dopamine level in the midbrain and the striatum, which, in turn, prevented reduction of motor activity and muscle strength and normalized the norepinephrine level [43].

TBI was widely studied as a risk factor of many neurodegenerative diseases [44]. Some studies have shown that TBI is accompanied by neuroinflammation, affecting neurons either directly [45-47] or indirectly – via blood – brain barrier impairment [48]. Moreover, individuals with TBI had elevated levels of α-synuclein in the cerebrospinal fluid [49]. The literature data suggest a possible association between TBI and PD, which was shown in our study.

The advantages of this study include personal interviews with patients, registered clinical and environmental data, a comprehensive neurological examination, and a sample size. However, we should consider some limitations when interpreting the results of the study. Due to the retrospective design of our study, we should take into account the recall bias: TBI in the past medical history was identified following interviews with patients, and PD patients may be more prone to recalling elements, which can justify their condition. Despite this, a previously conducted study showed high consistency between the assessment of medical history by the patient and TBI registered in the medical record [50].

Therefore, PD is a complex disease, the development of which is affected by both environmental and

molecular genetic factors that require further in-depth study. Reducing the burden of PD can be achieved through a two-pronged strategy: implementing interventions to correct modifiable risk factors, such as behavioral or environmental factors, and developing drugs aimed at correcting the functioning of protein products in genes associated with PD.

REFERENCES

1. Obeso J.A., Stamelou M., Goetz C.G., Poewe W., Lang A.E., Weintraub D. et al. Past, present, and future of Parkinson's disease: A special essay on the 200th Anniversary of the Shaking Palsy. *Mov. Disord.* 2017;32(9):1264–1310. DOI: 10.1002/mds.27115.
2. Poewe W., Seppi K., Tanner C.M., Halliday G.M., Brundin P., Volkmann J. et al. Parkinson disease. *Nat. Rev. Dis. Primers.* 2017;3:17013. DOI: 10.1038/nrdp.2017.13.
3. Ascherio A., Schwarzschild M.A. The epidemiology of Parkinson's disease: risk factors and prevention. *Lancet Neurol.* 201615(12):1257–1272. DOI: 10.1016/S1474-4422(16)30230-7.
4. Dong X., Liao Z., Gritsch D., Hadzhiev Y., Bai Y., Locascio J.J. et al. Enhancers active in dopamine neurons are a primary link between genetic variation and neuropsychiatric disease. *Nat. Neurosci.* 2018;21(10):1482–1492. DOI: 10.1038/s41593-018-0223-0.
5. Liu G., Boot B., Locascio J.J., Jansen I.E., Winder-Rhodes S., Eberly S. et al. Specifically neuropathic Gaucher's mutations accelerate cognitive decline in Parkinson's. *Ann. Neurol.* 2016;80(5):674–685. DOI: 10.1002/ana.24781.
6. Domínguez-Baleón C., Ong J.S., Scherzer C.R., Rentería M.E., Dong X. Understanding the effect of smoking and drinking behavior on Parkinson's disease risk: a Mendelian randomization study. *Sci. Rep.* 2021;11(1):13980. DOI: 10.1038/s41598-021-93105-y.
7. Liu G., Locascio J.J., Corvol J.C., Boot B., Liao Z., Page K. et al. Prediction of cognition in Parkinson's disease with a clinical-genetic score: a longitudinal analysis of nine cohorts. *Lancet Neurol.* 2017Aug.;16(8):620–629. DOI: 10.1016/S1474-4422(17)30122-9.
8. Balestrino R., Schapira A.H.V. Parkinson disease. *Eur. J. Neurol.* 2020;27(1):27–42. DOI: 10.1111/ene.14108.
9. Wang A., Costello S., Cockburn M., Zhang X., Bronstein J., Ritz B. Parkinson's disease risk from ambient exposure to pesticides. *Eur. J. Epidemiol.* 2011;26(7):547–555. DOI: 10.1007/s10654-011-9574-5.
10. Rybkina V.L., Azizova T.V. The risk factors for Parkinson's Disease. *The Neurological Journal*. 2017;22(6):287–294 (in Russ.). DOI: 10.18821/1560- 9545-2017-22-6-287-294.
11. Bettiol S.S., Rose T.C., Hughes C.J., Smith L.A. Alcohol Consumption and Parkinson's Disease Risk: A Review of Recent Findings. *J. Parkinsons Dis.* 2015;5(3):425–442. DOI: 10.3233/JPD-150533.
12. Costa J., Lunet N., Santos C., Santos J., Vaz-Carneiro A. Caffeine exposure and the risk of Parkinson's disease: a systematic review and meta-analysis of observational studies. *J. Alzheimers Dis.* 2010;20(1):S221–238. DOI: 10.3233/JAD-2010-091525.
13. Gallo V., Vineis P., Cancellieri M., Chiodini P., Barker R.A., Brayne C. et al. Exploring causality of the association between smoking and Parkinson's disease. *Int. J. Epidemiol.* 2019;48(3):912–925. DOI: 10.1093/ije/dyy230.
14. Cherian A., Divya K.P. Genetics of Parkinson's disease. *Acta. Neurol. Belg.* 2020;120(6):1297–1305. DOI: 10.1007/s13760-020-01473-5.
15. Cook L., Schulze J., Naito A., Alcalay R.N. The role of genetic testing for arkinson's disease. *Curr. Neurol. Neurosci. Rep.* 2021;21(4):17. DOI: 10.1007/s11910-021-01100-7.
16. Simon D.K., Tanner C.M., Brundin P. Parkinson disease epidemiology, pathology, genetics, and pathophysiology. *Clin. Geriatr. Med.* 2020;36(1):1–12. DOI: 10.1016/j.cger.2019.08.002.
17. Goldman S.M., Marek K., Ottman R., Meng C., Comyns K., Chan P. et al. Concordance for Parkinson's disease in twins: A 20-year update. *Ann. Neurol.* 2019;85(4):600–605. DOI: 10.1002/ana.25441.
18. Jot S. Parkinsonism with a Hint of Huntington's from 29 CAG repeats in HTT. *Brain Sci.* 2019;9(10):245. DOI: 10.3390/brainsci9100245.
19. Nikitina M.A., Bragina E.Yu., Nazarenko M.S., Zhukova N.G., Gomboeva D.E., Nurzhanova K.F., Tsentr N.V., Alifirova V.M. Atypical course of Parkinson's disease with clinical manifestations of Huntington's disease in a patient with an allele of 27 CAG repeats in the HTT gene. *Bulletin of Siberian Medicine*. 2020;19(4):235–240 (in Russ.). DOI: 10.20538/1682-0363-2020-4-235-240.
20. Postuma R.B., Berg D., Stern M., Poewe W., Olanow C.W., Oertel W. et al. MDS clinical diagnostic criteria for Parkinson's disease. *Mov. Disord.* 2015;30(12):1591–1601. DOI: 10.1002/mds.26424.
21. Hoehn M.M., Yahr M.D. Parkinsonism: onset, progression and mortality. *Neurology.* 196717(5):427–442. DOI: 10.1212/wnl.17.5.427.
22. Freud T., Vostrikov A., Dwolatzky T., Punchik B., Press Y. Validation of the Russian version of the MoCA test as a cognitive screening instrument in cognitively asymptomatic older individuals and those with mild cognitive impairment. *Front. Med. (Lausanne).* 2020;7:447. DOI: 10.3389/fmed.2020.00447.
23. Folstein M.F., Folstein S.E., McHugh P.R. "Mini-mental state". A practical method for grading the cognitive state of patients for the clinician. *J. Psychiatr. Res.* 1975;12(3):189–198. DOI: 10.1016/0022-3956(75)90026-6.
24. Bastepe M., Xin W. Huntington disease: molecular diagnostics approach. *Curr. Protoc. Hum. Genet.* 2015;87:9.26.1–9.26.23. DOI: 10.1002/0471142905.hg0926s87.
25. Crane P.K., Gibbons L.E., Dams-O'Connor K., Trittschuh E., Leverenz J.B., Keene C.D. et al. Association of traumatic brain injury with late-life neurodegenerative conditions and neuropathologic findings. *JAMA Neurol.* 2016;73(9):1062–1069. DOI: 10.1001/jamaneurol.2016.1948.
26. Ramlackhansingh A.F., Brooks D.J., Greenwood R.J., Bose S.K., Turkheimer F.E., Kinnunen K.M. et al. Inflammation after trauma: microglial activation and traumatic brain injury. *Ann. Neurol.* 2011;70(3):374–383. DOI: 10.1002/ana.22455.
27. Loane D.J., Kumar A., Stoica B.A., Cabatbat R., Faden A.I. Progressive neurodegeneration after experimental brain trau-

ma: association with chronic microglial activation. *J. Neuropathol. Exp. Neurol.* 2014;73(1):14–29. DOI: 10.1097/NEN.0000000000000021.
28. Nicoletti A., Vasta R., Mostile G., Nicoletti G., Arabia G., Iliceto G. et al. Head trauma and Parkinson's disease: results from an Italian case-control study. *Neurol. Sci.* 2017;38(10):1835–1839. DOI: 10.1007/s10072-017-3076-5.
29. Stoll G., Jander S., Schroeter M. Detrimental and beneficial effects of injury-induced inflammation and cytokine expression in the nervous system. *Adv. Exp. Med. Biol.* 2002;513:87–113. DOI: 10.1007/978-1-4615-0123-7_3.
30. Chia S.J., Tan E.K., Chao Y.X. Historical perspective: models of Parkinson's disease. *Int. J. Mol. Sci.* 2020;21(7):2464. DOI: 10.3390/ijms21072464.
31. Carmona A., Zogzas C.E., Roudeau S., Porcaro F., Garrevoet J., Spiers K.M. et al. SLC30A10 mutation involved in Parkinsonism results in manganese accumulation within nanovesicles of the Golgi apparatus. *ACS Chem. Neurosci.* 2019;10(1):599–609. DOI: 10.1021/acschemneuro.8b00451.
32. Aloizou A.M., Siokas V., Sapouni E.M., Sita N., Liampas I., Brotis A.G. et al. Parkinson's disease and pesticides: Are microRNAs the missing link? *Sci. Total. Environ.* 2020;744:140591. DOI: 10.1016/j.scitotenv.2020.140591.
33. Dardiotis E., Xiromerisiou G., Hadjichristodoulou C., Tsatsakis A.M., Wilks M.F., Hadjigeorgiou G.M. The interplay between environmental and genetic factors in Parkinson's disease susceptibility: the evidence for pesticides. *Toxicology.* 2013;307:17–23. DOI: 10.1016/j.tox.2012.12.016.
34. Breckenridge C.B., Berry C., Chang E.T., Sielken R.L. Jr., Mandel J.S. Association between Parkinson's disease and Cigarette Smoking, Rural Living, Well-Water Consumption, Farming and Pesticide Use: Systematic Review and Meta-Analysis. *PLoS One.* 2016;11(4):e0151841. DOI: 10.1371/journal.pone.0151841.
35. Martino R., Candundo H., Lieshout P.V., Shin S., Crispo J.A.G., Barakat-Haddad C. Onset and progression factors in Parkinson's disease: A systematic review. *Neurotoxicology.* 2017;61:132–141. DOI: 10.1016/j.neuro.2016.04.003.
36. Gao X., Chen H., Fung T.T., Logroscino G., Schwarzschild M.A., Hu F.B. et al. Prospective study of dietary pattern and risk of Parkinson disease. *Am. J. Clin. Nutr.* 2007;86(5):1486–1494. DOI: 10.1093/ajcn/86.5.1486.
37. Delamarre A., Meissner W.G. Epidemiology, environmental risk factors and genetics of Parkinson's disease. *Presse Med.* 2017;46(2-1):175–181. DOI: 10.1016/j.lpm.2017.01.001.
38. Paul K.C., Chuang Y.H., Shih I.F., Keener A., Bordelon Y., Bronstein J.M. et al. The association between lifestyle factors and Parkinson's disease progression and mortality. *Mov. Disord.* 2019;34(1):58–66. DOI: 10.1002/mds.27577.
39. Prasuhn J., Davis R.L., Kumar K.R. Targeting mitochondrial impairment in Parkinson's disease: challenges and opportunities. *Front. Cell Dev. Biol.* 2021;8:615461. DOI: 10.3389/fcell.2020.615461.
40. Nikitina M., Babushkina N., Bragina E., Alifirova V., Gomboeva D., Koroleva E. et al. The role of repair genes in the pathogenesis of Parkinson's disease. *J. Neurol. Sci.* 2021;429:119480.
41. Seong I.S., Ivanova E., Lee J.M., Choo Y.S., Fossale E., Anderson M. et al. HD CAG repeat implicates a dominant property of huntingtin in mitochondrial energy metabolism. *Hum. Mol. Genet.* 2005;14(19):2871–2880. DOI: 10.1093/hmg/ddi319.
42. Chen J.F., Xu K., Petzer J.P., Staal R., Xu Y.H., Beilstein M. et al. Neuroprotection by caffeine and A(2A) adenosine receptor inactivation in a model of Parkinson's disease. *J. Neurosci.* 2001;21(10):RC143. DOI: 10.1523/JNEUROSCI.21-10-j0001.2001.
43. Khadrawy Y.A., Salem A.M., El-Shamy K.A., Ahmed E.K., Fadl N.N., Hosny E.N. Neuroprotective and therapeutic effect of caffeine on the rat model of Parkinson's disease induced by rotenone. *J. Diet Suppl.* 2017;14(5):553–572. DOI: 10.1080/19390211.2016.1275916.
44. Crane P.K., Gibbons L.E., Dams-O'Connor K., Trittschuh E., Leverenz J.B., Keene C.D. et al. Association of traumatic brain injury with late-life neurodegenerative conditions and neuropathologic findings. *JAMA Neurol.* 2016;73(9):1062–1069. DOI: 10.1001/jamaneurol.2016.1948.
45. Ramlackhansingh A.F., Brooks D.J., Greenwood R.J., Bose S.K., Turkheimer F.E., Kinnunen K.M. et al. Inflammation after trauma: microglial activation and traumatic brain injury. *Ann. Neurol.* 2011Sept.;70(3):374-83. DOI: 10.1002/ana.22455.
46. Loane D.J., Kumar A., Stoica B.A., Cabatbat R., Faden A.I. Progressive neurodegeneration after experimental brain trauma: association with chronic microglial activation. *J. Neuropathol. Exp. Neurol.* 2014;73(1):14–29. DOI: 10.1097/NEN.0000000000000021.
47. Schmidt O.I., Heyde C.E., Ertel W., Stahel P.F. Closed head injury-an inflammatory disease? *Brain Res. Brain Res. Rev.* 2005;48(2):388–399. DOI: 10.1016/j.brainresrev.2004.12.028.
48. Stoll G., Jander S., Schroeter M. Detrimental and beneficial effects of injury-induced inflammation and cytokine expression in the nervous system. *Adv. Exp. Med. Biol.* 2002;513:87–113. DOI: 10.1007/978-1-4615-0123-7_3.
49. Mondello S., Buki A., Italiano D., Jeromin A. α-Synuclein in CSF of patients with severe traumatic brain injury. *Neurology.* 2013;80(18):1662–1668. DOI: 10.1212/WNL.0b013e3182904d43.
50. Goldman S.M., Tanner C.M., Oakes D., Bhudhikanok G.S., Gupta A., Langston J.W. Head injury and Parkinson's disease risk in twins. *Ann. Neurol.* 2006;60(1):65–72. DOI: 10.1002/ana.20882.

Authors contribution

Nikitina M.A. – conception and design, analysis and interpretation of the data. Alifirova V.M. – conception and design, final approval of the manuscript for publication. Bragina E.Yu. – analysis and interpretation of the data, substantiation of the manuscript, critical revision of the manuscript for important intellectual content. Babushkina N.P. – analysis and interpretation of the data. Gomboeva D.E. –

substantiation of the manuscript, critical revision of the manuscript for important intellectual content. Nazarenko M.S. – conception and design, critical revision of the manuscript for important intellectual content.

Authors information

Nikitina Maria A. – Cand. Sci. (Med.), Associate Professor, Neurology and Neurosurgery Division, Siberian State Medical University, Tomsk, nikitina_ma@mail.ru; http://orcid.org/0000-0002-2614-207X

Alifirova Valentina M. – Dr. Sci. (Med.), Professor, Head of the Neurology and Neurosurgery Division, Siberian State Medical University, Tomsk, v_alifirova@mail.ru, http://orcid.org/0000-0002-4140-3223

Bragina Elena Yu. – Cand. Sci. (Biology), Senior Researcher, Laboratory for Population Genetics, Research Institute of Medical Genetics, Tomsk NRMC, Tomsk, elena.bragina@medgenetics.ru, http://orcid.org/0000-0002-1103-3073

Babushkina Nadezhda P. – Cand. Sci. (Biology), Researcher, Laboratory for Population Genetics, Research Institute of Medical Genetics, Tomsk NRMC, Tomsk, nad.babushkina@medgenetics.ru, https://orcid.org/0000-0001-6133-8986

Gomboeva Densema E. – Resident Physician, Research Institute of Medical Genetics, Tomsk NRMC, Tomsk, Gombo-D@mail.ru, https://orcid.org/0000-0002-7882-2093

Nazarenko Maria S. – Dr. Sci. (Med.), Professor, Principal Researcher, Laboratory for Population Genetics, Research Institute of Medical Genetics, Tomsk NRMC, Tomsk; Professor, Medical Genetics Division, Siberian State Medical University, Tomsk, maria.nazarenko@medgenetics.ru, https://orcid.org/0000-0002-0673-4094

(✉) **Nikitina Maria A.,** nikitina_ma@mail.ru

Received 15.09.2022;
approved after peer review 30.09.2022;
accepted 03.10.2022

УДК 615.273.2:547.992
https://doi.org/10.20538/1682-0363-2022-4-114-120

Effects of plasma acid on rat uterine tissue *in vitro*

Salmin V.V.[1], Perevertov T.A.[1], Muradyan G.A.[1], Gudkova E.S.[2], Epova A.S.[1], Kutyakov V.A.[1, 3], Lychkovskaya E.V.[1], Chekisheva T.N.[1], Semichev E.V.[1], Malinovskaya N.A.[1], Medvedeva N.N.[1], Makarenko T.A.[1], Salmina A.B.[1, 4]

[1] *V.F. Voino-Yasenetsky Krasnoyarsk State Medical University*
1, Partizana Zheleznyaka Str., Krasnoyarsk, 660022, Russian Federation

[2] *St. Petersburg State Pediatric Medical University*
2, Litovskaya Str., St. Petersburg, 194100, Russian Federation

[3] *Krasnoyarsk Regional Bureau of Forensic Medical Examination*
25, Mira Av., Krasnoyarsk, 660049, Russian Federation

[4] *Scientific Center of Neurology*
80, Volokolamskoe Highway, Moscow, 125367, Russian Federation

ABSTRACT

The aim of the study was to evaluate the effect of plasma acid on the uterine tissue of laboratory animals *in vitro*.

Materials and methods. Treatment of dimethyl sulfoxide – water solution and water for injections with a spark discharge in air resulted in a decrease in pH, which contributed to generation of plasma acid in the solutions. We incubated uterine tissues *in vitro* in plasma acid at room temperature for 30 minutes. The treated tissues were examined histologically and immunohistochemically.

Results. We showed that plasma acid had pronounced biological activity. Immunohistochemistry was used to show that, depending on the type of a solution, plasma acid altered generation of nitrosative damage products (3-NT) and oxidative DNA damage (8-OHdG) and modulated the number of cells with high proliferative potential (including $CD133^+$ cells) and production of vascular endothelial growth factor (VEGF). These effects contributed to the general cytotoxicity of plasma acid solutions.

Conclusion. During 30-minute exposure *in vitro*, plasma acid prepared from the dimethyl sulfoxide (DMSO) – water mixture exhibits various biological effects in uterine tissue samples obtained from experimental animals. Plasma-treated water exerts cytotoxic effects associated with oxidative DNA damage and promotes induction of pro-angiogenic activity in the uterine tissue. Plasma-treated DMSO does not have a cytotoxic effect. It inhibits cell proliferation, reducing the population of $CD133^+$ cells and VEGF production in the tissue.

Keywords: uterine tissue, plasma acid, cytotoxicity

Conflict of interest. The authors declare the absence of obvious or potential conflict of interest related to the publication of this article.

Source of financing. The study was supported by the grant of Krasnoyarsk regional foundation of scientific and scientific – technical support (agreement No. 1/20 of 15.05.2020).

Conformity with the principles of ethics. The study was approved by the Bioethics Commission on the Use of Laboratory Animals at the local Ethics Committee and by the local Ethics Committee at V.F. Voino-Yasenetsky Krasnoyarsk State Medical University.

For citation: Salmin V.V., Perevertov T.A., Muradyan G.A., Gudkova E.S., Epova A.S., Kutyakov V.A., Lychkovskaya E.V., Chekisheva T.N., Semichev E.V., Malinovskaya N.A., Medvedeva N.N., Makarenko T.A.,

✉ *Salmin Vladimir V.*, vsalmin@gmail.com

Salmina A.B. Effects of plasma acid on rat uterine tissue *in vitro*. *Bulletin of Siberian Medicine.* 2022;21(4):114–120. https://doi.org/10.20538/1682-0363-2022-4-114-120.

Эффекты плазменной кислоты на ткани матки крыс *in vitro*

Салмин В.В.[1], Перевертов Т.А.[1], Мурадян Г.А.[1], Гудкова Е.С.[2], Эпова А.С.[1], Кутяков В.А.[1, 3], Лычковская Е.В.[1], Чекишева Т.Н.[1], Семичев Е.В.[1], Малиновская Н.А.[1], Медведева Н.Н.[1], Макаренко Т.А.[1], Салмина А.Б.[1, 4]

[1] Красноярский государственный медицинский университет (КрасГМУ) им. проф. В.Ф. Войно-Ясенецкого Россия, 660022, г. Красноярск, ул. Партизана Железняка, 1

[2] Санкт-Петербургский государственный педиатрический медицинский университет Россия, 194100, г. Санкт-Петербург, ул. Литовская, 2

[3] Красноярское краевое бюро судебно-медицинской экспертизы Россия, 660049, г. Красноярск, пр. Мира, 35

[4] Научный центр неврологии Россия, 125367, г. Москва, Волоколамское шоссе, 80

РЕЗЮМЕ

Целью исследования является оценка влияния плазменной кислоты на ткани матки лабораторных животных *in vitro*.

Материалы и методы. Обработка раствора диметилсульфоксида в воде и воды для инъекций искровым разрядом в атмосфере приводила к снижению pH, что соответствовало формированию в растворах плазменной кислоты. Мы инкубировали ткани матки *in vitro* в плазменной кислоте при комнатной температуре в течение 30 мин. Обработанные ткани исследовались гистологически и иммуногистохимически.

Результаты. Нами показано, что плазменная кислота обладает выраженной биологической активностью. Иммуногистохимическим методом мы зарегистрировали, что, в зависимости от типа раствора, плазменная кислота изменяет в клетках формирование продуктов нитрозативного повреждения белков (3-NT) и окислительного повреждения ДНК (8-OHdG), модулирует количество клеток с высоким пролиферативным потенциалом (в том числе CD133+ клеток), продукцию сосудисто-эндотелиального фактора роста (VEGF), что соответствует суммарному цитотоксическому эффекту вида раствора плазменной кислоты.

Заключение. Плазменная кислота, приготовленная на основе воды и диметилсульфоксида, проявляет различные биологические эффекты в образцах ткани матки экспериментальных животных при 30-минутной экспозиции *in vitro*. Вода, обработанная плазмой, реализует цитотоксический потенциал, связанный с окислительным повреждением ДНК, а также способствует индукции проангиогенной активности в ткани. Диметилсульфоксид, обработанный плазмой, не вызывает цитотоксического действия, подавляет пролиферацию клеток, снижая популяцию CD133+ клеток, а также продукцию VEGF в ткани.

Ключевые слова: ткани матки, плазменная кислота, цитотоксичность

Конфликт интересов. Авторы декларируют отсутствие явных и потенциальных конфликтов интересов.

Источник финансирования. Работа выполнена при поддержке гранта ККФПНиНТД (договор № 1/20 от 15.05.2020).

Соответствие принципам этики. Исследование одобрено представителями биоэтической комиссии по работе с лабораторными животными при локальном этическом комитете и локальным этическим комитетом КрасГМУ.

Для цитирования: Салмин В.В., Перевертов Т.А., Мурадян Г.А., Гудкова Е.С., Эпова А.С., Кутяков В.А., Лычковская Е.В., Чекишева Т.Н., Семичев Е.В., Малиновская Н.А., Медведева Н.Н., Макаренко Т.А., Салмина А.Б. Эффекты плазменной кислоты на ткани матки крыс *in vitro*. *Бюллетень сибирской медицины.* 2022;21(4):114–120. https://doi.org/10.20538/1682-0363-2022-4-114-120.

INTRODUCTION

In recent years, there has been an increasing interest in the use of gas discharge plasma when performing surgical interventions in gynecology. Argon plasma for coagulation and ablation is the leading technological solution in this area [1, 2]. The impact of cold atmospheric plasma at the final stage of reconstructive and plastic uterus operations (applied directly to the suture area) enhances repair of the myometrium and, consequently, formation of a consistent scar [3]. Interaction of a plasma jet with air entrained by a laminar flow results in an increased concentration of active particles, many of which, having good solubility, increase the concentration of reactive oxygen species (ROS) and reactive nitrogen species (RNS) in the tissue [4].

For standard coagulation and ablation, it is impossible to exclude the accumulation of ROS and RNS in tissues and the formation of the so-called plasma acid, as well as a significant decrease in pH (in case of prolonged exposure to plasma) [5, 6]. A significant increase in the RNS concentration in plasma devices for medical applications is achieved by replacing argon with air, which is used in the Plazon system [7] or kINPen MED® [8]. The results of assessing the possibility of using the Plazon unit during surgeries on the uterus and its appendages were discussed in the literature [3, 9–13]. However, the molecular and cellular mechanisms in uterine tissues induced by plasma have not been studied. The effect of plasma acid on the modification of proteins and lipids was described [6], but no data on its effects on cells of the reproductive system, including the uterus, are available in the literature. This prevents from a reasonable, scientifically grounded understanding of the safety and effectiveness of the use of plasma acid in clinical practice.

The aim of the study was to evaluate the effect of plasma acid on the uterus of laboratory animals *in vitro*.

MATERIALS AND METHODS

The study was carried out on female Wistar rats aged 3 months (n = 16), weighing 180–200 g. The selection of female rats was carried out at the end of proestrus and the beginning of estrus (by examining the vaginal opening and evaluating vaginal smears). Then surgery was performed, and after 1 day, the uterus was removed from the euthanized animals. Uterus samples after exposure to plasma acid were fixed in a 4% buffered paraformaldehyde solution and embedded into paraffin blocks for further sectioning.

Plasma acid was prepared by irradiating 5 ml of water for injections or 50% dimethyl sulfoxide (DMSO) – water solution with a nanosecond-pulsed spark discharge in a 50 ml leak-proof container. A spark discharge with a discharge gap length of 20 mm was created by a nanosecond high-voltage pulse generator with a pulse energy of 0.2 J and a voltage of 40 kV. When pH = 2 was reached, the treatment was stopped. The prepared solution was used to incubate freshly isolated uterine tissues of laboratory rats for 30 minutes.

The expression of DAPI, VEGF, CD133, 8-hydroxy-2-deoxyguanosine, 3-nitrotyrosine, and Ki67 in tissues was assessed according to standard protocols for direct and indirect immunohistochemistry (immunofluorescent variant). Microphotography of 10 different fields was performed at x175 magnification using the ZOE™ Fluorescent Cell Imager (Bio-Rad, USA). Digital images were processed using the ImageJ software. Each field was divided into nine frames, empty fields outside the tissue sample were rejected after manual sorting. Then the plugin [14] in the ImageJ software was used for automatic recognition and counting of labels.

We evaluated the median expression and the interquartile range of the number of labels in one frame Me (Q_1; Q_3). The method of non-parametric statistics was used for statistical processing of the obtained data: comparison of several independent samples (the Kruskal – Wallis test) with the subsequent use of a module for pairwise comparison of medians among the samples using the Statsoft Statistica 12.0 package.

RESULTS

Data on the expression of the markers used are shown in the diagrams (Figure). They demonstrate median values with the interquartile range in the control group and two experimental groups exposed to plasma acid (plasma-activated DMSO, plasma-activated water). We used the method of non-parametric statistics (the Kruskal – Wallis test).

The analysis of the number of 4',6-diamidino-2-phenylindole (DAPI)-stained ($DAPI^+$) cells was used to assess the effect of plasma acid on cell survival in a tissue sample in the tested solutions. At the same time, a smaller number of $DAPI^+$ cells in the tissue sample should be regarded as the result of death, exfoliation, and destruction of damaged cells upon exposure to plasma acid in the tested solutions. We

found that when using plasma-activated water, the number of DAPI+ cells was significantly smaller n_{DAPI+}=311 (233;368) compared with the control group n_{DAPI+}=350 (284; 435) (z = 7.638; p < 0.001), thereby suggesting the cytotoxic effect of the solution. In the tissue samples incubated in a plasma-activated DMSO solution, the median number of cells n_{DAPI+}= 351 (267; 414) did not significantly differ from the control group (z = 1.443; p = 0.44), so the cytotoxic effect of this solution should be considered unproven.

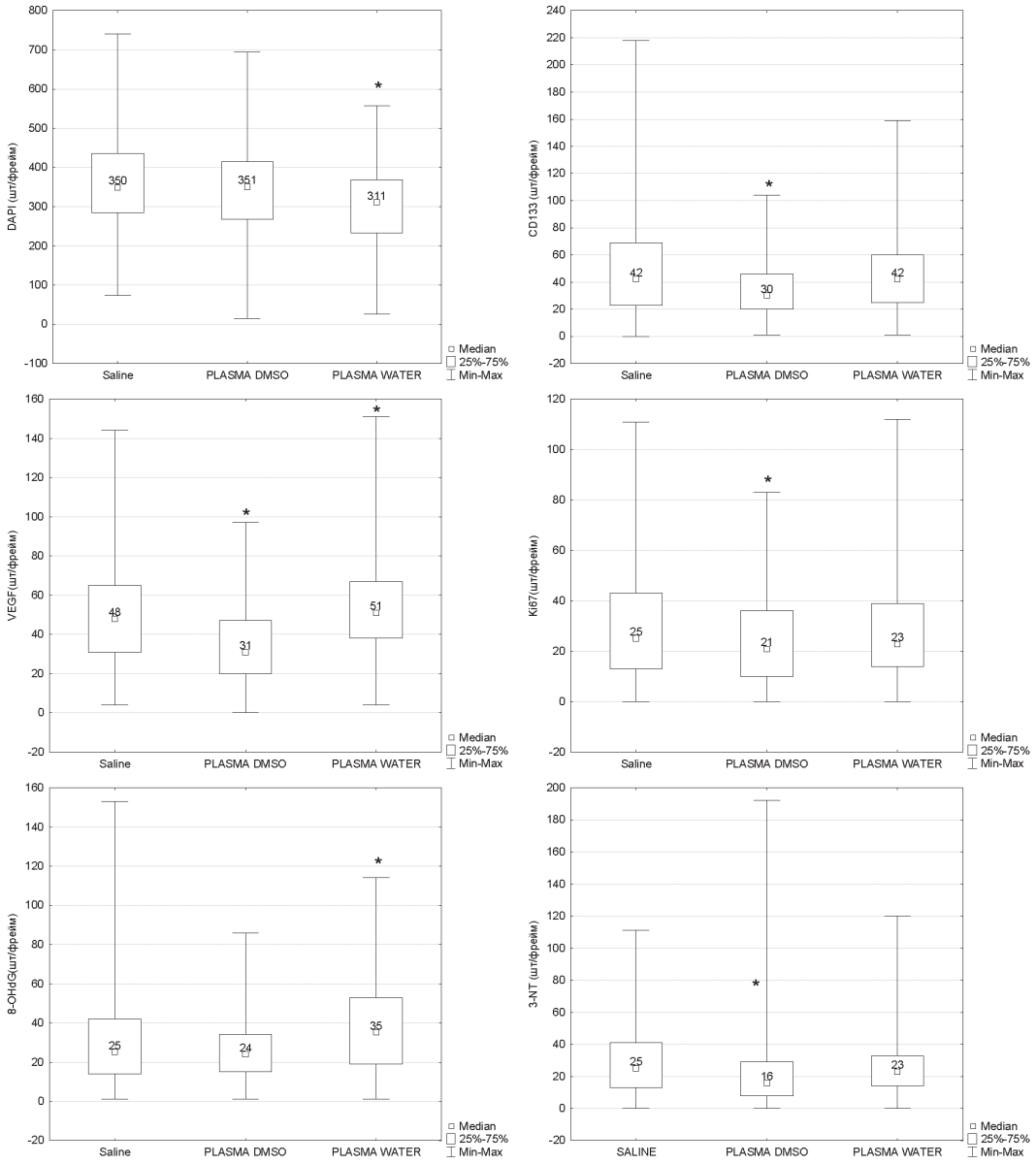

Figure. Results of the analysis of DAPI+ cell number, expression of VEGF, Ki67, CD133, 3-NT, and 8-OHdG during incubation of rat uterine tissue samples in solutions treated with spark discharge plasma, *Me* (Q_1; Q_3): * experimental groups with p < 0.05 compared with the control group; plasma-activated DMSO – 50% aqueous solution, plasma-activated water – water for injections compared with the control (saline)

Expression of 8-hydroxy-2-deoxyguanosine (8-OHdG) as a marker of oxidative DNA damage under the effect of plasma-activated water was significantly higher $n_{8\text{-OHdG}}$ = 35 (19; 53) (z = 5.98; p < 0.001) compared with the control group $n_{8\text{-OHdG}}$ = 25 (14; 42). In the group of samples incubated in plasma-activated DMSO solution, the expression level of $n_{8\text{-OHdG}}$=24 (15; 34) did not significantly differ from the control group (z = 2.16; p = 0.09). In the tissue samples incubated in the plasma-activated DMSO solution, tissue expression of 3-nitrotyrosine (3-NT) as a marker of nitrosative protein damage was significantly lower

$n_{3\text{-NT}}$ = 16 (8; 29) (z = 8.35; p < 0.001) compared with the control group $n_{3\text{-NT}}$ = 25 (13; 41), while plasma-activated water did not have such an effect $n_{3\text{-NT}}$ = 23 (14; 33) (z = 1.64; p = 0.29). It is worth noting that these effects of DMSO were accompanied by a lower proliferative potential of cells, as it could be concluded from the expression of Ki67 protein, n_{Ki67}= 21(10; 36) (z = 3.47; p = 0.0015) compared with the control group n_{Ki67}= 25 (13; 43). The cytotoxic effect of plasma-activated water was not associated with significant changes in cell proliferation n_{Ki67} = 23 (14; 39) (z = 1.18; p = 0.71).

To what extent do the revealed effects correspond to the response of cells with pro-angiogenic potential in the tissue? When fragments of the uterine wall were treated with the plasma-activated DMSO, there was a significantly smaller median number of cells expressing CD133, n_{CD133} = 30 (20; 46) (z = 5.78; p < 0.001) compared with the control group, n_{CD133} = 42 (23; 68). In the group of samples treated with plasma-activated water, n_{CD133} = 42 (25; 60), no significant differences were found (z = 1.30; p = 0.57). CD133 is a marker of stem and progenitor cells in the tissue, whereas VEGF expression characterizes the pro-angiogenic potential of the tissue and may also reflect the degree of hypoxic cell damage. We found that the median value of VEGF expression in the endometrium and uterine stroma was lower under the effect of plasma-activated DMSO, n_{VEGF} = 31 (20; 47) (z = 8.13, p < 0.001), or higher under the effect of plasma-activated water, n_{VEGF} = 51 (38; 67) (z = 3.36, p = 0.003) compared with the control group, n_{VEGF} = 48 (31; 65).

DISCUSSION

We found that plasma-activated DMSO did not have a pronounced cytotoxic effect and did not induce oxidative DNA damage or nitrosative damage to cellular proteins, but reduced the proliferation of cells (including $CD133^+$ cells) and suppressed VEGF expression, thereby affecting proliferative and pro-angiogenic activities. On the contrary, plasma-activated water demonstrated a pronounced cytotoxic effect due to the induction of oxidative DNA damage and VEGF expression. In general, this indicates that the cytotoxic effect of plasma-activated water was more determined by the action of ROS, but not by RNS. Interestingly, plasma-activated DMSO prevented the development of physiologically mediated nitrosative damage to cellular proteins. These differences in the effects of solutions were probably due to their physical and chemical properties that determined the ability to cross a cell membrane and / or trap ROS / RNS in the solution.

CD133 (prominin) is a stem cell marker present in various tissues, but it can also be detected in adult differentiated cells. It is believed that its expression is high in the endometrium [15; 16]. It is known that a decrease in CD133 expression is a consequence of an increase in the activity of the mTOR protein which, in turn, is activated by oxidative stress [17]. However, the observed decrease in the number of CD133+ cells under the effect of plasma-activated DMSO cannot be explained by oxidative stress (with no signs of oxidative DNA damage or general cytotoxicity). Presumably, it is associated with a decrease in VEGF expression. It is known that $CD133^+$ cells are very sensitive to the effects of this growth factor in various tissues, and CD133 can control the release of VEGF [18]. Hypoxia [19] and oxidative stress [20] are known to be powerful triggers of VEGF expression. Increased expression of VEGF was recorded in endometriosis [21]. In addition to stimulating angiogenesis, VEGF activates the mitochondrial biogenesis through the mTOR-dependent pathways as a response to insufficient mitochondrial activity due to oxygen deficiency, damage to mitochondria, or an increased demand for cells to produce ATP [22]. Thus, the increase in VEGF expression in cells under the effect of plasma-activated water might be associated with the development of mitochondrial dysfunction, oxidative stress, and hypoxia in the tissue. Indeed, plasma-activated water caused a cytotoxic effect accompanied by the formation of 8-OHdG, so an increase in VEGF expression is expected.

The two tested solutions had different effects on cell proliferation. Plasma-activated water had no significant effect, while plasma-activated DMSO inhibited Ki67 expression in tissue samples. On the one hand, this effect could be associated with the fact that actively proliferating cells predominantly die under the effect of plasma-activated DMSO. However, taking into consideration that DMSO generally showed no cytotoxic effect, we may assume that a decrease in the number of $Ki67^+$ cells in the tissue was associated with a decrease in the number of $CD133^+$ cells and suppression of VEGF expression.

CONCLUSION

Plasma-activated water and plasma-activated DMSO exhibited various biological effects in the uterine tissue samples of experimental animals at

30-minute exposure *in vitro*. Plasma-activated water demonstrated cytotoxicity associated with oxidative DNA damage and promoted pro-angiogenic activity in the tissue. Plasma-activated DMSO did not exert cytotoxic effects, but inhibited cell proliferation, reducing the number of $CD133^+$ cells and production of VEGF in the tissue. Generally, plasma acid solutions can be considered as promising agents for local use in gynecologic pathology.

REFERENCES

1. Bafort C., Beebeejaun Y., Tomassetti C., Bosteels J., Duffy J. Laparoscopic surgery for endometriosis. *Cochrane Database of Systematic Reviews*. 2020;(10):CD011031. DOI: 10.1002/14651858.CD011031.pub2.
2. Grund K.E., Storek D., Farin G. Endoscopic argon plasma coagulation (APC) first clinical experiences in flexible endoscopy. *Endoscopic Surgery and Allied Technologies*. 1994;2(1):42–46.
3. Davydov A.I., Chakvetadze L., Klindukhov I.A., Bakhtiyarov K.R., Voronoi S.V. Assessment of the morphological structure of the myometrium and uterine fibroids after contact exposure to air-plasma flow: Materials of the I All-Russian Conference "Women's health problems and ways to solve them". Moscow: 2007:17–18 (in Russ.).
4. Olovyannikova R., Makarenko T., Lychkovskaya E., Gudkova E., Muradyan G., Medvedeva N., et al. Chemical mechanisms of non-thermal plasma action on cells. *Fundamental and Clinical Medicine*. 2020;5(4):104–116 (in Russ.). DOI: 10.23946/2500-0764-2020-5-4-104-115.
5. Ivanova I., Trofimova S., Aristova N., Arkhipova E., Burkhina O., Sysoeva V., et al. The analysis of active products of spark discharge plasma radiation determining biological effects in tissues. *Modern Technologies in Medicine*. 2012;(2):20–30 (in Russ.).
6. Ivanova I., Trofimova S., Piskarev I., Ichetkina A., Burkhina O., Sysoeva V. The effect of spark discharge plasma radiation on the modification of proteins and lipids. *Fundamental Research*. 2013;3(1):572–575 (in Russ.).
7. Achkasov E., Esipov A., Pekshev A., Musailov V. Use of an exogenous nitric oxide generator for treatment of peritonitis. *Biomedical Engineering*. 2018;52(1):64–67. DOI: 10.1007/s10527-018-9783-2.
8. Schönebeck R. kINPen MED®. Comprehensive Clinical Plasma Medicine: Springer; 2018:485–494.
9. Davydov A., Strizhakov A., Pekshev A., Kuchukhidze S., Klindukhov I. Possibilities and prospects of plasma endosurgery with generation of nitrogen monoxide during operations on the womb and uterine appendages. *Gynecology, Obstetrics and Perinatology*. 2002;1(2):57–60 (in Russ.).
10. Davydov A., Strizhakov A., Chakvetadze L., Shekhter A., Pekshev A., Klindukhov I. Clinical and morphological analysis of the effect of new generation plasmatrons on uterine and ovarian tissues during laparoscopic operations. *Gynecology, Obstetrics and Perinatology*. 2007;6(5):5–10 (in Russ.).
11. Davydov A.I., Belotserkovtseva L.D. Diagnosis and treatment of benign diseases of the uterine cervix. *Gynecology, Obstetrics and Perinatology*. 2012;11(6):74–81 (in Russ.).
12. Davydov A.I., Kuchukhidze S., Shekhter A., Khanin A., Pekshev A., Pankratov V. Clinical evaluation of intraoperative use of an air-plasma stream enriched with nitrogen monoxide during operations on the uterus and uterine appendages. *Gynecology, Obstetrics and Perinatology*. 2004;3(4):12–17 (in Russ.).
13. Davydov A.I., Shakhlamova M.N., Chaban O.V., Pirogova M.N. High surgical energies in operative gynecology. *Gynecology, Obstetrics and Perinatology*. 2013;12(5):75–85 (in Russ.).
14. Salmin V.V., Salmina A.B., Morgun A.V. Plugin for the IMAGEJ program for counting fluorescent labels on microphotographs: RU 2020612777. 2020 (in Russ.).
15. Friel A.M., Zhang L., Curley M.D., Therrien V.A., Sergent P.A., Belden S.E. et al. Epigenetic regulation of CD133 and tumorigenicity of CD133 positive and negative endometrial cancer cells. *Reproductive Biology and Endocrinology*. 2010;8(1):147. DOI: 10.1186/1477-7827-8-147.
16. Sun Y., Yoshida T., Okabe M., Zhou K., Wang F., Soko C. et al. Isolation of stem-like cancer cells in primary endometrial cancer using cell surface markers CD133 and CXCR4. *Translational Oncology*. 2017;10(6):976–987. DOI: 10.1016/j.tranon.2017.07.007.
17. Li Z. CD133: a stem cell biomarker and beyond. *Experimental Hematology & Oncology*. 2013;2(1):17. DOI: 10.1186/2162-3619-2-17.
18. Qiu Y., Chen C., Zhang J., Chen M., Gong H., Gong L. et al. VEGF attenuates lung injury by inducing homing of CD133+ progenitors via VEGFR1. *Biochemical and Biophysical Research Communications*. 2019;511(3):650–657. DOI: 10.1016/j.bbrc.2019.02.071.
19. Sharkey A.M., Day K., McPherson A., Malik S., Licence D., Smith S.K. et al. Vascular endothelial growth factor expression in human endometrium is regulated by hypoxia. *J. Clin. Endocrinol. Metab*. 2000;85(1):402–409. DOI: 10.1210/jcem.85.1.6229.
20. Kim Y.-W., Byzova T.V. Oxidative stress in angiogenesis and vascular disease. *Blood*. 2014;123(5):625–631. DOI: 10.1182/blood-2013-09-512749.
21. Ren Q.Z., Qian Z.H., Jia S.H., Xu Z.Z. Vascular endothelial growth factor expression up-regulated by endometrial ischemia in secretory phase plays an important role in endometriosis. *Fertil. Steril*. 2011;95(8):2687–2689. DOI: 10.1016/j.fertnstert.2011.05.001.
22. Guo D., Wang Q., Li C., Wang Y., Chen X. VEGF stimulated the angiogenesis by promoting the mitochondrial functions. *Oncotarget*. 2017;8(44):77020–77027. DOI: 10.18632/oncotarget.20331.

Acknowledgement

The work was carried out using the material base of Shared Core Facilities of Molecular and Cell Technologies at V.F. Voino-Yasenetsky Krasnoyarsk State Medical University.

Authors contribution

Salmin V.V., Makarenko T.A., Salmina A.B. – conception and design, analysis and interpretation of data, substantiation of the manuscript and critical revision of the manuscript for important intellectual content, final approval of the manuscript for publication. Perevertov T.A., Muradyan G.A., Gudkova E.S., Epova A.S., Kutyakov V.A., Lychkovskaya E.V., Chekisheva T.N., Semichev E.V., Malinovskaya N.A., Medvedeva N.N. – carrying out of the experiments.

Authors information

Salmin Vladimir V. – Dr. Sci. (Physics and Mathematics), Associate Professor, Head of the Department of Medical and Biological Physics, V.F. Voino-Yasenetsky Krasnoyarsk State Medical University, Krasnoyarsk, vsalmin@gmail.com, https://orcid.org/0000-0003-4441-9025

Perevertov Timofey A. – Student, V.F. Voino-Yasenetsky Krasnoyarsk State Medical University, Krasnoyarsk, dmchernov26@mail.ru, https://orcid.org/0000-0001-6280-9233

Muradyan Goar A. – Laboratory Assistant, Laboratory of Medical Cybernetics and Management in Healthcare, V.F. Voino-Yasenetsky Krasnoyarsk State Medical University, Krasnoyarsk, muradyan.goar1@gmail.com, https://orcid.org/0000-0002-5656-4636

Gudkova Elizaveta S. – Resident Physician, St. Petersburg State Pediatric Medical University, St. Petersburg, miss.gudcova@mail.ru, https://orcid.org/0000-0002-7540-4144

Epova Anna S. – Post-Graduate Student, Department of Operative Gynecology of the Institute of Professional Education, V.F. Voino-Yasenetsky Krasnoyarsk State Medical University, Krasnoyarsk, annaepova23@mail.ru, https://orcid.org/0000-0001-9969-9808

Kutyakov Viktor A. – Cand.Sci. (Biology), Expert, Krasnoyarsk Regional Bureau of Forensic Medical Examination; Associate Professor, Department of Biological Chemistry with Courses in Medical, Pharmaceutical and Toxicological Chemistry, V.F. Voino-Yasenetsky Krasnoyarsk State Medical University, Krasnoyarsk, victor-koutjakov@yandex.ru, https://orcid.org/0000-0001-7814-4176

Lychkovskaya Elena V. – Senior Lecturer, Department of Biological Chemistry with Courses in Medical, Pharmaceutical and Toxicological Chemistry, V.F. Voino-Yasenetsky Krasnoyarsk State Medical University, lychk-elena@mail.ru, http://orcid.org/0000-0002-4017-1125

Chekisheva Tatiana N. – Teaching Assistant, Department of Human Anatomy, V.F. Voino-Yasenetsky Krasnoyarsk State Medical University, Krasnoyarsk, maksi726@mail.ru, https://orcid.org/0000-0001-6905-980X

Semichev Evgeny V. – Dr. Sci. (Med.), Leading Researcher, Research Institute of Molecular Medicine and Pathobiochemistry. V.F. Voino-Yasenetsky Krasnoyarsk State Medical University, Krasnoyarsk, evsemichev@yandex.ru, https://orcid.org/0000-0003-2386-5798

Malinovskaya Natalia A. – Dr. Sci. (Med.), Head of the Department of Biological Chemistry with Courses in Medical, Pharmaceutical and Toxicological Chemistry, V.F. Voino-Yasenetsky Krasnoyarsk State Medical University, Krasnoyarsk, malinovskaya-na@mail.ru, https://orcid.org/0000-0002-0033-3804

Medvedeva Nadezhda N. – Dr. Sci. (Med.), Professor, Head of the Department of Human Anatomy, V.F. Voino-Yasenetsky Krasnoyarsk State Medical University, Krasnoyarsk, medvenad@mail.ru, https://orcid.org/0000-0002-7757-6628

Makarenko Tatiana A. – Dr. Sci. (Med.), Associate Professor, Head of the Department of Operative Gynecology of the Institute of Professional Education, Prof. V.F. Voino-Yasenetsky Krasnoyarsk State Medical University, Krasnoyarsk, makarenko7777@yandex.ru, https://orcid.org/0000-0002-2899-8103

Salmina Alla B. – Dr. Sci. (Med.), Professor, Principal Researcher, Head of the Laboratory of Experimental Neurocytology, Department of Brain Research, Scientific Center of Neurology, Moscow; Principal Researcher, Research Institute of Molecular Medicine and Pathobiochemistry, Research Institute of Molecular Medicine and Pathobiochemistry. V.F. Voino-Yasenetsky Krasnoyarsk State Medical University, Krasnoyarsk, allasalmina@mail.ru, https://orcid.org/0000-0003-4012-6348

(✉) **Salmin Vladimir V.,** vsalmin@gmail.com

Received 01.11.2021;
approved after peer review 07.03.2022;
accepted 09.06.2022

УДК 616.153.96:616.132.2-004.6]-071
https://doi.org/10.20538/1682-0363-2022-4-121-129

Study of associations of blood proteins with development of unstable atherosclerotic plaques in coronary arteries by quantitative proteomics

Stakhneva E.M.[1], Kashtanova E.V.[1], Polonskaya Ya.V.[1], Striukova E.V.[1], Shramko V.S.[1], Sadovski E.V.[1], Kurguzov A.V.[2], Murashov I.S.[2], Chernyavskii A.M.[2], Ragino Yu.I.[1]

[1] Research Institute of Internal and Preventive Medicine – Branch of the Institute of Cytology and Genetics, Siberian Branch of the Russian Academy of Sciences
175/1, B. Bogatkova Str., Novosibirsk, 630089, Russian Federation

[2] Meshalkin National Medical Research Center
15, Rechkunovskaya Str., Novosibirsk, 630055, Russian Federation

ABSTRACT

Aim. To study the associations of blood proteins with the presence of unstable atherosclerotic plaques in the arteries in patients with coronary artery disease using the quantitative proteomic analysis.

Materials and methods. The study included patients with coronary artery disease (n = 40); the average age of patients was 58 ± 7 years. Material for the study was blood serum. Protein concentrations in serum samples were determined using the PeptiQuant Plus Proteomics Kit (Cambridge Isotope Laboratories, USA). Protein fractions were identified using the liquid chromatograph and tandem mass spectrometer Q-TRAP 6500.

Results. Mass spectrometry revealed an increased concentration of proteins, such as fibrinogen, fibulin-1, and complement factor H, in the serum samples of patients with unstable atherosclerotic plaques. It took place with a simultaneous decrease in the levels of α 2-antiplasmin, heparin cofactor II, coagulation factor XII, plasminogen, prothrombin, vitronectin, complement proteins (C1, C3, C7, C9), and complement factor B. The differences were considered significant at $p < 0.05$. It was revealed that the presence of unstable atherosclerotic plaques was associated with the level of fibulin-1 (Exp(B) = 1.008; $p = 0.05$), plasminogen (Exp(B) = 0.995; $p = 0.027$), and coagulation factor X (Exp(B) = 0.973; $p = 0.037$).

Conclusion. An increased concentration of fibulin-1 can be considered as a potential biomarker of unstable atherosclerotic plaque development in coronary artery disease. The possibility of using the studied proteins as biomarkers of unstable atherosclerotic plaques requires further studies on their potential role in the development of this disease.

Keywords: proteomic analysis, mass spectrometry, coronary artery disease

Conflict of interest. The authors declare the absence of obvious or potential conflict of interest related to the publication of this article.

Source of financing. The study was carried out within the budgetary topic of the state assignment No.122031700094-5 and within the grant of the Russian Science Foundation No. 21-15-00022.

Conformity with the principles of ethics. All patients signed an informed consent to participate in the study. The study was approved by the Ethics Committee at the Research Institute of Internal and Preventive Medicine – Branch of the Institute of Cytology and Genetics (Protocol No. 7 of 26.09.2017).

For citation: Stakhneva E.M., Kashtanova E.V., Polonskaya Ya.V., Striukova E.V., Shramko V.S., Sadovski E.V., Kurguzov A.V., Murashov I.S., Chernyavskii A.M., Ragino Yu.I. Study of associations of blood proteins with development of unstable atherosclerotic plaques in coronary arteries by quantitative proteomics. *Bulletin of Siberian Medicine.* 2022;21(4):121–129. https://doi.org/10.20538/1682-0363-2022-4-121-129.

✉ *Stakhneva Ekaterina M.,* stahneva@yandex.ru

Изучение ассоциаций белков в крови с наличием нестабильных атеросклеротических бляшек в коронарных артериях методом количественной протеомики

Стахнёва Е.М.[1], Каштанова Е.В.[1], Полонская Я.В.[1], Стрюкова Е.В.[1], Шрамко В.С.[1], Садовский Е.В.[1], Кургузов А.В.[2], Мурашов И.С.[2], Чернявский А.М.[2], Рагино Ю.И.[1]

[1] Научно-исследовательский институт терапии и профилактической медицины – филиал Федерального исследовательского центра «Институт цитологии и генетики Сибирского отделения Российской академии наук» (НИИТПМ – филиал ИЦиГ СО РАН)
630089, г. Новосибирск, ул. Б. Богаткова, 175/1

[2] Национальный медицинский исследовательский центр (НМИЦ) им. акад. Е.Н. Мешалкина
Россия, 630055, г. Новосибирск, ул. Речкуновская,15

РЕЗЮМЕ

Цель. Изучение ассоциаций белков крови с наличием нестабильных атеросклеротических бляшек в артериях у пациентов с коронарным атеросклерозом с использованием количественного протеомного анализа.

Материалы и методы. В исследование участвовали пациенты с ишемической болезнью сердца и коронарным атеросклерозом (n = 40), средний возраст пациентов 58 ± 7 лет. Материал исследования – сыворотка крови. Концентрации белков в образцах сыворотки определяли с помощью набора PeptiQuant Plus Proteomics Kit (Cambridge Isotope Laboratories, США). Идентификацию белковых фракций осуществляли методом мониторинга множественных реакций на масс-спектрометре Q-TRAP 6500, комбинированном с жидкостным хроматографом.

Результаты. Масс-спектрометрическая идентификация выявила в образцах сыворотки крови у пациентов с нестабильными атеросклеротическими бляшками повышенную концентрацию белков: фибриноген, фибулин-1 и фактор комплемента H. При одновременном сниженном уровне белков: витронектин, α-2-антиплазмин, кофактор гепарина 2, коагуляционный фактор XII, плазминоген и протромбин, белки комплемента (C1, C3, C7, C9) и фактор комплемента B. Различия считали значимыми при $p < 0,05$. Выявлено, что нестабильность атеросклеротических бляшек ассоциирована с концентрацией фибулина-1 (Exp(B) = 1,008; $p = 0,05$), плазминогена (Exp(B) = 0,995; $p = 0,027$) и коагуляционного фактора X (Exp(B) = 0,973; $p = 0,037$).

Заключение. Повышенная концентрация фибулина-1 в крови может рассматриваться как потенциальный биомаркер нестабильности атеросклеротических бляшек при коронарном атеросклерозе. Возможность использования исследованных белков как биомаркеров нестабильности атеросклеротических бляшек при коронарном атеросклерозе требует дальнейших исследований их потенциальной роли в развитии данного заболевания.

Ключевые слова: протеомный анализ, масс-спектрометрия, коронарный атеросклероз

Конфликт интересов. Авторы декларируют отсутствие явных и потенциальных конфликтов интересов, связанных с публикацией настоящей статьи.

Источник финансирования. Работа выполнена в рамках бюджетной темы по Государственному заданию № 122031700094-5 и в рамках гранта РНФ №. 21-15-00022.

Соответствие принципам этики. Все участники подписали информированное согласие на участие в исследовании. Исследование одобрено этическим комитетом НИИТПМ – филиал ИЦиГ СО РАН (протокол № 7 от 26.09.2017).

Для цитирования: Стахнёва Е.М., Каштанова Е.В., Полонская Я.В., Стрюкова Е.В., Шрамко В.С., Садовский Е.В., Кургузов А.В., Мурашов И.С., Чернявский А.М., Рагино Ю.И. Изучение ассоциаций белков в крови с наличием нестабильных атеросклеротических бляшек в коронарных артериях методом количественной протеомики. *Бюллетень сибирской медицины.* 2022;21(4):121–129. https://doi.org/10.20538/1682-0363-2022-4-121-129.

INTRODUCTION

Research in the field of etiology and pathogenesis of coronary atherosclerosis, which predetermine complications of this pathology, is currently relevant due to high prevalence and mortality from this disease. Atherosclerosis as the dominant cause of cardiovascular diseases (CVD) includes a number of pathological processes, namely: endothelial dysfunction, excessive lipid deposition in the intima, exacerbations of innate and adaptive immune responses, proliferation of smooth muscle cells, and remodeling of the extracellular matrix, eventually leading to the formation of atherosclerotic plaques (AP).

AP instability aggravates the pathological atherosclerotic process, leading to the development of complications of CVD. The composition of the plaque and internal hemorrhage in the atherosclerotic plaque are independent risk factors for stroke and CAD [1]. Genetically determined inhibition of fibrinogen α-, β- and γ-chains, factor II, and factor XI was associated with a reduced risk of venous thromboembolism ($p < 0.001$). Inhibition of fibrinogen β- and γ-chains was associated with a reduced risk of stroke in large arteries ($p = 0.001$) [2]. Various biomechanical and hemodynamic factors contribute to AP instability. The intact vascular endothelium is thromboresistant, and the damaged endothelium releases increased amounts of procoagulants. Hemostasis is carried out by blood cells and a plasma enzyme system represented by closely interacting protein components. In order to study the involvement of various proteins in the pathogenesis of coronary atherosclerosis, it is necessary to investigate the specific contribution of proteins with pro- or anticoagulation activity to the development of plaque instability in the coronary arteries.

Accumulation of data on the pathogenesis of coronary atherosclerosis and its complications and the development of modern research methods contribute to the search for proteins which may be used as prognostic and diagnostic biomarkers of CVD. A quantitative proteomic analysis which is used for identification and quantification of biological molecules using tandem mass tag mass spectrometry is a useful method in the accurate quantitative simultaneous determination of proteins in various biological samples. Despite the fact that the number of candidate proteins under study is constantly increasing, their role in the pathogenesis of coronary atherosclerosis is not completely clear. Understanding the changes in blood proteins in atherosclerosis will help identify new biomarkers that will give an insight into the conditions underlying the development of complications of this disease.

The aim of this study was to investigate the association of certain blood proteins with unstable AP in the arteries in men with coronary atherosclerosis using quantitative proteomic analysis.

MATERIALS AND METHODS

The study included patients with CAD and coronary atherosclerosis who were referred to coronary artery bypass surgery and who had intraoperative indications for coronary endarterectomy which was carried out during the surgery. Exclusion criteria were as follows: myocardial infarction (less than 6 months ago), acute and chronic infectious and inflammatory diseases or their exacerbations, renal failure, active liver diseases, cancer, hyperparathyroidism. The protocol of the study was approved by the Ethics Committee at the Research Institute of Internal and Preventive Medicine, branch of the Institute of Cytology and Genetics, SB RAS (Protocol No. 7 of 26.09.2017). All patients signed an informed consent to participate in the study.

Blood serum samples were the study material. In all patients, blood was taken from the ulnar vein in the morning on an empty stomach. Blood serum samples of 40 men were selected for the quantitative proteomic analysis. All patient samples were divided into two groups of 20 patients each. Group 1 consisted of patients (average age 58 ± 4 years) with stable AP only, which was determined by the histologic analysis. Group 2 consisted of 20 patients (average age 57 ± 10 years) with unstable AP only, which was also determined by the histologic analysis. We used the PeptiQuant Plus Proteomics Kit (Cambridge Isotope Laboratories, USA) to determine protein concentration in the serum samples according to the method suggested by the manufacturer with some modifications.

The technique of performing trypsinolysis was the following: 20 ml of a solution containing 9 M urea, 20 mM dithiothreitol, and 300 mM Tris-HCl (pH 8.0) was added to 10 ml of a serum sample. We added 10 µl of a bovine serum albumin (BSA) solution to a separate test tube, which was later used as a matrix solution for calibration points. The samples were incubated for 30 min at 37 °C. We added 20 µl of 100 mM iodoacetamide solution to all test tubes. Then the test tubes were incubated for 30 minutes in the dark at room temperature. Later we added 272 µl of

100 mM Tris-HCl (pH 8.0) and 35 µl of a trypsin solution. The test tubes were then incubated for 18 hours at 37 °C. Proteolysis was stopped by adding 343 µl of 2% formic acid.

A mixture of light (unlabeled) peptides was diluted in 60 µl of a solution of 30% acetonitrile and 0.1% formic acid. We prepared a series of dilutions for calibration according to the scheme. A mixture of peptides labeled with heavy stable isotopes was diluted in 450 µl of 30% acetonitrile and 0.1% formic acid and used as an internal standard.

We added 40 µl of serum samples to the test tubes after trypsinolysis and 40 µl of BSA solution after trypsinolysis. Then 10 µl of a labeled peptide solution was added to all tubes. We added 10 µl of diluting standards to the tubes with BSA to create a calibration curve. We added 10 µl of 30% acetonitrile and 0.1% formic acid to the test tubes with serum samples. Then 540 µl of 0.1% formic acid was added to all tubes.

The samples were purified with the Oasis HLB solidphase extraction cartridges (Waters, USA), 10 mg. The cartridges activated 600 µl of methanol and balanced 600 µl of 0.1% formic acid. We took 510 µl of the sample and rinsed it with 600 µl of water 3 times. Peptides were eluted with 300 µl of 50% acetonitrile and 0.1% formic acid. The obtained samples were frozen at –80 °C and dried using the FreeZone 2.5 Dryer designed for lyophilizing light sample loads (Labconco, USA). Dry sediments were diluted in 34 µl of 0.1% formic acid and then used for the analysis.

Peptides were detected by multiple reaction monitoring (MRM) on the Q-TRAP 6500 mass spectrometer (AB Sciex, USA) coupled with the high-performance liquid chromatograph Infinity 1290 (Agilent, USA). Chromatographic separation was carried out on the column Titan C18, 1.9 µm (Supelc, USA) in several stages. The flow rate was 0.4 ml / min, the separation temperature was 45 °C.

Positively charged ions obtained by electrospray ionization in the IonDrive Turbo V Ion Source were detected. We used the Multiquant 3.0.2 software (AB Sciex, USA) to create calibration curves and determine protein concentrations based on the peak area of the MRM transitions specific to each studied peptide.

Statistical data processing was carried out using the SPSS 20.0 software for Windows. The statistical analysis consisted in applying the Kolmogorov – Smirnov test and the Mann – Whitney *U* test to normally distributed data. The age of patients was presented as the mean and the standard root-mean-square deviation ($M \pm \sigma$). The results in the table were presented as the median and the interquartile range (Me [Q_{25};Q_{75}]). A multivariate logistic regression analysis was carried out to determine associations. The differences were considered statistically significant at $p < 0.05$.

RESULTS

Proteomic profiling of the blood serum samples was performed using the PeptiQuant Plus Proteomics Kit. A total of 125 proteins were identified. The identification of proteins was carried out by MRM using a triple quadrupole ultra-high resolution time-of-flight mass spectrometer with electrospray ionization coupled with a high-performance liquid chromatograph.

The differential protein expression analysis was carried out by two technical replicates for each sample. Following the comparative analysis, we isolated proteins, the concentration of which had a statistically significant difference in the study groups ($p < 0.05$).

Table

Quantitative mass spectrometry-based protein identification in the blood, Me [Q_{25};Q_{75}]

Protein	Protein concentration, fmol / µl		*p*
	Group 1	Group 2	
Fibrinogen, α-chain	143.5 [139.4;147.7]	254.4 [243.6;284.9]	0.006
Fibrinogen, γ-chain	45.9 [40.9;52.1]	120.9 [45.4;165.8]	0.005
Fibulin-1	663.9 [576.1;748.6]	735.2 [600.4;796.0]	0.038
Fibronectin	429.6 [234.0;522.5]	256.2 [197.9;402.3]	0.161
Thrombospondin-1	75.0 [63.0;95.2]	75.1 [53.8;89.8]	0.419
Vitronectin	2,839.5 [2,166.2;3,362.2]	2,151.0 [1,654.0;2,878.0]	0.005
α2-antiplasmin	522.2 [427.2;649.4]	472.2 [323.4;599.2]	0.034
α2-macroglobulin	4,885.0 [4,342.5;5,345.5]	4,714.5 [3,324.5;5,868.2]	0.376
Antithrombin III	3,880.0 [2,460.75;4,845.75]	3,272.5 [3,017.5;4,291.0]	0.844
Heparin cofactor II	4,274.5 [4,057.7;4,577.5]	3,803.0 [3,055.0;4,233.0]	0.0001
Coagulation factor IX	87.8 [67.7;107.9]	74.1 [48.2;124.0]	0.166
Coagulation factor X	136.0 [107.5;142.4]	105.3 [92.3;123.3]	0.065

Table (continued)

Protein	Protein concentration, fmol / µl		*p*
	Group 1	Group 2	
Coagulation factor XII	419.4 [294.9;525.0]	291.1 [265.8;380.6]	0.0001
Kininogen-1	178.3 [162.5;205.7]	175.5 [154.9;192.1]	0.346
Complement component C1q, subunit B	67.1 [53.3;95.9]	68.5 [57.2;80.2]	0.538
Complement component C1q, subunit C	106.2 [93.8;143.3]	112.1 [92.4;146.5]	0.939
Complement component C1r	251.2 [169.7;273.6]	194.0 [164.2;242.5]	0.106
Complement component C1s	47.4 [42.8;54.0]	43.8 [34.0;74.8]	0.729
Complement Component C3	586.8 [469.1;717.1]	471.8 [408.7;572.0]	0.008
Complement component C7	75.9 [56.4;82.0]	60.4 [54.2;74.9]	0.006
Complement component C9	191.3 [113.9;212.5]	137.7 [75.4;185.5]	0.026
Complement factor B	4,985.0 [3,585.0;6,251.2]	3,980.5 [3,698.0;4,358.7]	0.017
Complement factor H	526.4 [463.3;587.8]	581.4 [531.9;626.6]	0.018
Plasma protease C1 inhibitor	2,037.0 [1,565.0;2,294.0]	1,651.5 [1,092.0;2,234.7]	0.041
Plasma serine protease inhibitor	51.4 [48.2;62.1]	49.4 [46.5;74.6]	0.769
Plasminogen activator inhibitor-1	27.6 [21.1;36.4]	24.1 [19.2;32.1]	0.102
Plasminogen	933.1 [833.2;1,050.5]	803.5 [695.6;879.2]	0.001
Prothrombin	902.2 [711.1;1,044.2]	788.4 [718.7;821.1]	0.047

Fibrinogen, which is one of the main proteins in the coagulation system, differed significantly in the study groups. In the group of patients with unstable plaques, the concentration of each of the two fibrinogen isoforms (α- and γ-chain) was 1.8 and 2.5 times higher, respectively (Table). At the same time, the level of fibulin which binds to fibrinogen and incorporates into clots, was also higher in the group of patients with unstable plaques. In addition, the multivariate logistic analysis showed that the instability of atherosclerotic plaques was associated with the concentration of fibulin-1 (Exp(B) = 1.008; 95% confidence interval (CI) 1.000–1.015; $p = 0.05$).

In our study, the level of plasminogen, which is the main component of the fibrinolytic system, was higher in the group of patients with stable plaques ($p < 0.05$). Also, the multivariate logistic analysis showed that the instability of atherosclerotic plaques was reversely correlated with the levels of plasminogen (Exp(B) = 0.995; 95% CI 0.990–0.999; $p = 0.027$), heparin cofactor II (Exp(B) = 0.999; 95% CI 0.998–1.000; $p = 0.010$), and coagulation factor X (Exp(B) = 0.973; 95% CI 0.949–0.998; $p = 0.037$). Fibrinolytic activity of the blood also depends on fibrinolysis inhibitors. The concentration of plasminogen activator inhibitor-1 (PAI-1) was 13% higher in the group of patients with stable plaques, but did not reach the level of statistical significance ($p = 0.102$).

In addition, the concentration of proteins, primary anticoagulants (α2-antiplasmin, α2-macroglobulin, heparin cofactor II), was significantly higher in patients with stable plaques (Table). At the same time, the level of the anticoagulant antithrombin III was higher in the blood of patients with unstable plaques. Antithrombin III is a universal inhibitor of thrombin and almost all clotting factors, which is confirmed by our study; the levels of coagulation factors IX, X, and XII were lower in group 2.

At the same time, the level of coagulation factor XII was significantly higher in the group of patients with stable plaques. Highly activated factor XII in combination with kininogen activates fibrinolysis. In our study, the level of kininogen was higher in the group of patients with stable plaques, but it did not reach the level of statistical significance.

Blood clotting mechanisms are linked with the activation of the immune system. In our study, there was no significant difference between the C1 (C1q; C1r; C1s) complement components in the study groups (Table). However, the total level of the complement component C1 was higher in the group of patients with stable AP and amounted to 471.37 fmol / µl vs. 446.48 fmol / µl, compared with the group of patients with unstable AP ($p < 0.0001$). The content of complement components C3, C7, C9, and complement factor B was higher in the group of patients with stable AP ($p < 0.05$). The level of the complement factor H involved in C3b inactivation was 10% higher in the group of patients with unstable AP (Table).

Fibronectin, thrombospondin, and vitronectin are also involved in the coagulation cascade, promoting platelet adhesion. In our study, no significant difference was revealed in the content of fibronectin and thrombospondin between the study groups. The

concentration of vitronectin was significantly higher in patients with stable plaques ($p = 0.005$).

DISCUSSION

Atherosclerosis is associated with inflammation and vascular endothelial dysfunction. The intact vascular endothelium is thromboresistant, and the damaged endothelium releases increased amounts of procoagulants.

In our study, the levels of fibrinogen and fibulin-1, which is related to it, differed significantly in the study groups. The concentrations of each of the two fibrinogen isoforms (α- and γ-chain) and fibulin-1 were higher in the group of patients with unstable plaques. The multivariate logistic analysis showed that AP instability was associated with the concentration of fibulin-1. Previously, we found that the maximum amount of fibrinogen was in the tissue of stable fibrous AP, and the protein level was slightly lower in unstable AP [3]. Thus, the study suggests that high concentrations of fibrinogen and fibulin-1 may be a promising biomarker of AP instability in the blood of patients with coronary atherosclerosis.

Fibronectin, thrombospondin, and vitronectin are involved in the coagulation cascade. Platelet activation caused a local release of fibrinogen, fibronectin, vWF, thrombospondin, vitronectin, and clotting factors, promoting platelet adhesion and increased coagulation [4]. In our study, no significant difference was revealed in the content of fibronectin and thrombospondin between the study groups.

Vitronectin is the main glycoprotein of cell adhesion contained in plasma and extracellular matrix. Increased expression of vitronectin may contribute to the development of chronic vascular diseases, such as atherosclerosis, playing an important role in vascular homeostasis and pathological vascular remodeling. Plasminogen activator inhibitor-1 (PAI-1) stimulated vitronectin expression by binding low-density protein receptor-related protein-1 (LRP1). The concentration of vitronectin in the blood plasma was significantly reduced in mice with PAI-1 deficiency compared with the control [5]. When binding to PAI-1, vitronectin participates in the activation of fibrinolysis. In atherosclerosis of the carotid arteries, it was shown that the level of PAI-1 in blood plasma was reduced in the experimental group compared with the controls. At the same time, the level of PAI-1 was positively correlated with the level of vitronectin in the group of patients with atherosclerosis, which may be due to increased fibrinolytic activity and disease progression, promoted by increased vascular remodeling [6]. The level of vitronectin was significantly higher in the blood of patients with CAD than in the control group. Vitronectin is assumed to be a marker of CAD [7]. In our study, the concentration of fibronectin in the blood was significantly higher in patients with stable plaques.

Earlier, a prospective cohort study revealed that high levels of factors IX and XI and α2-antiplasmin were associated with an increased risk of CAD, and did not depend on other coronary risk factors [8]. Correlations between the level of factor XII in the blood and the presence of vulnerable atherosclerotic plaques in the coronary arteries were shown [9].

In our study, the concentrations of proteins α2-antiplasmin, α2-macroglobulin, heparin cofactor II, and coagulation factor XII were significantly higher in patients with stable plaques than in group 2. Antithrombin III (AT-III) is a universal inhibitor of thrombin and almost all clotting factors, but in our study, the concentration of antithrombin III in the blood was higher in patients with unstable plaques, although the level of statistical significance was not reached.

The levels of coagulation factors IX, X, and XII were lower in group 2. At the same time, the logistic regression analysis showed that the instability of AP was negatively correlated with the concentrations of coagulation factor X, heparin cofactor II, and plasminogen.

Previously, it was shown that the level of AT-III was reduced in the high-risk subgroup of acute coronary syndrome (ACS) compared with the control group ($p < 0.05$). The logistic regression model demonstrated that AT-III was a protective factor (odds ratio (OR) = 0.958; $p = 0.012$) for ACS. The level of AT-III demonstrated prognostic value in patients with ACS and was associated with the severity of CAD [10]. At the same time, a reduced level of antithrombin III is not an independent risk factor for myocardial infarction [11].

Highly activated factor XII in combination with kininogen activates fibrinolysis. Kininogen is a precursor of bradykinin and kallidin, proteins that cause vasodilation and smooth muscle contraction. Besides the fact that kinins are known for their ability to induce nitric oxide and prostacyclin, which mediate cardioprotection, bradykinin promotes inflammation, fibroplasia, and fibrosis after myocardial infarction in rats [12]. Thus, kininogen is involved in inflammation, blood pressure control, coagulation, and emergence

of pain. With kininogen deficiency, the level of bradykinin decreases, which does not affect the function of the left ventricle, but affects the risk of CAD [13]. In our study, the level of kininogen did not differ in the study groups. However, high levels of plasminogen and fibrinolysis inhibitor PAI-1 were found in the group of patients with stable plaques.

There is a relationship between the activation of the immune system, inflammation, and blood clotting mechanisms. The complement system is not only a component of the innate immune response, but also a key mediator of inflammation [14]. Complement system proteins have been repeatedly associated with vascular remodeling and atherosclerosis [15, 16].

Research data indicate that the anomaly of complement components and the resulting excessive complement activation are associated with atherogenesis. C3b / iC3b and MAC deposition in the clogged arteries indicates increased complement activation [17]. The complement system can modulate platelet activation and subsequent formation of blood clots. It was reported that several components of the complement system, including C3 and the membrane attack complex, are associated with platelets and become functionally active when platelets are activated [18]

The complement system can be activated through three pathways: classical, lectin, and alternative. All three pathways converge at the C3 level to form the C5 convertase, which ultimately leads to the polymerization of C9 and the formation of membrane attack complexes. The classical pathway is triggered by the recognition of C1q antibodies or apoptotic cells associated with antigens or microbial surfaces. Exposure of C1q to its target results in activation of serine proteases C1r and C1s, followed by C1s-mediated cleavage of C4 into anaphylatoxin C4a and opsonin C4b. [14, 18]. Platelets can also release C1q upon activation, thereby activating other platelets [19]. There are several points of interaction in the complement cascade and the blood coagulation system. For example, factor XIIa can activate C1q and, consequently, the classical complement pathway [20].

In our study, no significant difference was found between the C1 (C1q; C1r; C1s) complement components in the study groups. However, the total content of the complement component C1 was higher in the group of patients with stable AP. The levels of complement components C3, C7, C9 and complement factor B were higher in the group of patients with stable AP ($p < 0.05$) (Table). The level of complement factor H involved in C3b inactivation was higher in the group of patients with unstable AP (Table).

Earlier ELISA studies showed high levels of C5b-9 in intimal thickening and fibrous plaques compared with normal tissue. At the same time, the levels of C5b-9 in intimal thickening were higher than in fibrous plaques, which allowed the authors to assume that complement activation occurs directly in the artery wall and plays an important role in atherogenesis [16].

Inflammation and activation of the C5b-9 complement system predispose to rupture of an intracranial aneurysm [21]. In an animal experiment, it was shown that the complement factor C5a and its receptor C5aR are expressed in vulnerable atherosclerotic plaques. A significant increase in C5aR in the plaque was found in mice treated with C5a, while local treatment with C5a led to a significant increase in plaque destruction with concomitant bleeding. In addition, the authors demonstrated that smooth muscle cells and endothelial cells after C5a treatment *in vitro* showed a marked increase in apoptosis, which may contribute to the instability of the lesion *in vivo* [22]. It was also found that the membrane attack complex can play a crucial role in the formation of plaques and rupture of aneurysms [23]. In our study, the concentration of complement components C7 and C9 involved in the formation of the membrane attack complex did not increase in the blood of patients with unstable plaques. Apparently, this process is local in the tissue of the atherosclerotic plaque.

CONCLUSION

The possibility of using the studied proteins as biomarkers of AP instability in coronary atherosclerosis requires further research devoted to their potential role in the development of this disease. The data of this study, obtained using a modern method of quantitative proteomics, revealed elevated concentrations of complement factor H, fibrinogen, and fibulin-1 in the blood serum samples of patients with unstable AP. When the levels of proteins which are involved in the coagulation cascade and fibrinolysis and proteins related to them functionally (α2-antiplasmin, α2-macroglobulin, heparin cofactor II, coagulation factor XII, prothrombin, plasminogen, PAI-1, vitronectin) reduced simultaneously, the concentrations of complement proteins (C1, C3, C7, C9) and complement factor B associated with coagulation and fibrinolysis were also found to be reduced in the group of patients with unstable AP.

Our data showed that the inhibition of coagulation and fibrinolysis in the blood of patients with unstable AP significantly increased the concentrations of fibulin-1 and fibrinogen. This was confirmed by the multivariate logistic regression analysis, which showed the relationship of instability with the concentration of fibulin-1 (Exp(B) = 1.008; $p = 0.05$).

Thus, an increased concentration of fibulin-1 in the blood may be considered as a promising potential biomarker of AP instability in coronary atherosclerosis.

REFERENCES

1. Bos D., Arshi B., van den Bouwhuijsen Q.J.A., Ikram M.K., Selwaness M., Vernooij M.W. et al. Atherosclerotic carotid plaque composition and Incident stroke and coronary events. *J. Am. Coll. Cardiol*. 2021;77(11):1426–1435. DOI: 10.1016/j.jacc.2021.01.038
2. Yuan S., Burgess S., Laffan M., Mason A.M., Dichgans M., Gill D. et al. Genetically roxied Inhibition of Coagulation Factors and Risk of Cardiovascular Disease: A Mendelian Randomization Study. *J. Am. Heart Assoc*. 2021;10(8):e019644. DOI: 10.1161/JAHA.120.019644.
3. Stakhneva E.M., Meshcheryakova I.A., Demidov E.A., Starostin K.V., Sadovski E.V., Peltek S.E. et al. A Proteomic Study of Atherosclerotic Plaques in Men with Coronary Atherosclerosis. *Diagnostics*. 2019;9(4):E177. DOI: 10.3390/diagnostics9040177.
4. Badimon L., Vilahur G. Thrombosis formation on atherosclerotic lesions and plaque rupture. *J. Intern. Med*. 2014;276(6):618–632. DOI: 10.1111/joim.12296.
5. Luo M., Ji Y., Luo Y., Li R., Fay W.P., Wu J. Plasminogen activator inhibitor-1 regulates the vascular expression of vitronectin. *J. Thromb. Haemost*. 2017;15(12):2451–2460. DOI: 10.1111/jth.13869.
6. Ekmekçi H., Güngör Öztürk Z., Ekmekçi O.B., Işler Bütün I., Beşirli K., Gode S. et al. Significance of vitronectin and PAI-1 activity levels in carotid artery disease: comparison of symptomatic and asymptomatic patients. *Minerva Med*. 2013;104(2):215–223.
7. Ekmekci H., Sonmez H., Ekmekci O.B., Ozturk Z., Domanic N., Kokoglu E. Plasma vitronectin levels in patients with coronary atherosclerosis are increased and correlate with extent of disease. *J. Thromb. Thrombolysis*. 2002;14(3):221–225. DOI: 10.1023/a:1025000810466.
8. Yamagishi K., Aleksic N., Hannan P.J., Folsom A.R.; ARIC Study Inverstigators. Coagulation factors II, V, IX, X, XI, and XII, plasminogen, and alpha-2 antiplasmin and risk of coronary heart disease. *J. Atheroscler. Thromb*. 2010;17(4):402–409. DOI: 10.5551/jat.3673.
9. Ragino Y.I., Striukova E.V., Murashov I.S., Polonskaya Y.V., Volkov A.M., Kurguzov A.V. et al. Association of some hemostasis and endothelial dysfunction factors with probability of presence of vulnerable atherosclerotic plaques in patients with coronary atherosclerosis. *BMC Res. Notes*. 2019;12(1):336. DOI: 10.1186/s13104-019-4360-7.
10. Lu J., Niu D., Zheng D., Zhang Q., Li W. Predictive value of combining the level of lipoprotein-associated phospholipase A2 and antithrombin III for acute coronary syndrome risk. *Biomed. Rep.* 2018;9(6):517–522. DOI: 10.3892/br.2018.1162.
11. Elmissbah T.E., Iderous M.E., Al-Qahtani F.M., Elaskary A., Dahlawi H. Assessment of antithrombin III and protein C in Saudi myocardial infarction patients. *Clin. Lab*. 2021;67(10). DOI: 10.7754/Clin.Lab.2021.201206.
12. Sridharan V., Tripathi P., Sharma S.K., Moros E.G., Corry P.M., Lieblong B.J. et al. Cardiac inflammation after local irradiation is influenced by the kallikrein-kinin system. *Cancer Res*. 2012;72(19):4984–4992. DOI: 10.1158/0008-5472.CAN-12-1831
13. Koch M., Bonaventura K., Spillmann F., Dendorfer A., Schultheiss H.P., Tschöpe C. Attenuation of left ventricular dysfunction by an ACE inhibitor after myocardial infarction in a kininogen-deficient rat model. *Biol. Chem*. 2008;389(6):719–723. DOI: 10.1515/BC.2008.083.
14. Lubbers R., van Essen M.F., van Kooten C., Trouw L.A. Production of complement components by cells of the immune system. *Clin. Exp. Immunol*. 2017;188(2):183–194. DOI: 10.1111/cei.12952.
15. Martin-Ventura J.L., Martinez-Lopez D., Roldan-Montero R., Gomez-Guerrero C., Blanco-Colio L.M. Role of complement system in pathological remodeling of the vascular wall. *Mol. Immunol.* 2019;114:207–215. DOI: 10.1016/j.molimm.2019.06.016.
16. Vlaicu S.I., Tatomir A., Rus V., Mekala A.P., Mircea P.A., Niculescu F. et al. The role of complement activation in atherogenesis: the first 40 years. *Immunol. Res*. 2016;64(1):1–13. DOI: 10.1007/s12026-015-8669-6.
17. Ge X., Xu C., Liu Y., Zhu K., Zeng H., Su J. et al. Complement activation in the arteries of patients with severe atherosclerosis. *Int. J. Clin. Exp. Pathol*. 2018;11(1):1–9.
18. Rawish E., Sauter M., Sauter R., Nording H., Langer H.F. Complement, inflammation and thrombosis. *Br. J. Pharmacol.* 2021;178(14):2892–2904. DOI: 10.1111/bph.15476.
19. Speth C., Rambach G., Würzner R., Lass-Flörl C., Kozarcanin H., Hamad O.A. et al. Complement and platelets: Mutual interference in the immune network. *Mol. Immunol.* 2015;67(1):108–118. DOI: 10.1016/j.molimm.2015.03.244.
20. Amara U., Rittirsch D., Flierl M., Bruckner U., Klos A., Gebhard F. et al. Interaction between the coagulation and complement system. *Adv. Exp. Med. Biol*. 2008;632:71–79. DOI: 10.1007/978-0-387-78952-1_6.
21. Tulamo R., Frösen J., Paetau A., Seitsonen S., Hernesniemi J., Niemelä M. et al.. Lack of complement inhibitors in the outer intracranial artery aneurysm wall associates with complement terminal pathway activation. *Am. J. Pathol*. 2010;177(6):3224–3232. DOI: 10.2353/ajpath.2010.091172.
22. Wezel A., de Vries M.R., Lagraauw H.M., Foks A.C., Kuiper J., Quax P.H. et al. Complement factor C5a induces atherosclerotic plaque disruptions. *J. Cell Mol. Med*. 2014;18(10):2020–2030. DOI: 10.1111/jcmm.12357.
23. Wu G., Hu W., Shahsafaei A., Song W., Dobarro M., Sukhova G.K. et al. Complement regulator CD59 protects against atherosclerosis by restricting the formation of complement membrane attack complex. *Circ. Res*. 2009;104(4):550558. DOI: 10.1161/CIRCRESAHA.108.191361.

Authors contribution

Stakhneva E.M. – conception and design; analysis and interpretation of data. Kashtanova E.V. – critical revision of the manuscript for important intellectual content. Polonskaya Ya.V., Striukova E.V., Shramko V.S., Sadovski E.V., Kurguzov A.V., Murashov I.S. – analysis and interpretation of data. Chernyavskii A.M., Ragino Yu.I. – final approval of the manuscript for publication.

Authors information

Stakhneva Ekaterina M. – Cand. Sci. (Biology), Senior Researcher, Laboratory for Clinical Biochemical and Hormonal Studies on Internal Diseases, Research Institute of Internal and Preventive Medicine, branch of the Institute of Cytology and Genetics, SB RAS, Novosibirsk, stahneva@yandex.ru, http://orcid.org/0000-0003-0484-6540 .

Kashtanova Elena V. – Dr. Sci. (Biology), Leading Researcher, Head of the Laboratory for Clinical Biochemical and Hormonal Studies on Internal Diseases, Research Institute of Internal and Preventive Medicine, branch of the Institute of Cytology and Genetics, SB RAS, Novosibirsk, elekastanova@yandex.ru, http://orcid.org/0000-0003-2268-4186

Polonskaya Yana V. – Dr. Sci. (Biology), Senior Researcher, Laboratory for Clinical Biochemical and Hormonal Studies on Internal Diseases, Research Institute of Internal and Preventive Medicine, branch of the Institute of Cytology and Genetics, SB RAS, Novosibirsk, yana-polonskaya@yandex.ru, http://orcid.org/0000-0002-3538-0280;

Striukova Elena V. – Cand. Sci. (Med.), Researcher, Laboratory for Clinical Biochemical and Hormonal Studies on Internal Diseases, Research Institute of Internal and Preventive Medicine, branch of the Institute of Cytology and Genetics, SB RAS, Novosibirsk, stryukova.j@mail.ru, http://orcid.org/0000-0001-5316-4664

Shramko Victoria S. – Cand. Sci. (Med.), Researcher, Laboratory for Clinical Biochemical and Hormonal Studies on Internal Diseases, Research Institute of Internal and Preventive Medicine, branch of the Institute of Cytology and Genetics, SB RAS, Novosibirsk, nosova@211.ru, http://orcid.org/0000-0002-0436-2549

Sadovski Evgeny V.– Junior Researcher, Laboratory for Clinical Biochemical and Hormonal Studies on Internal Diseases, Research Institute of Internal and Preventive Medicine, branch of the Institute of Cytology and Genetics, SB RAS, Novosibirsk, stinger000@mail.ru, http://orcid.org/0000-0001-7350-534X

Kurguzov Alexey V. – Cardiologist, Cardiosurgical Department of Aorta and Coronary Arteries, Meshalkin National Medical Research Center, Novosibirsk, aleksey_kurguzov@mail.ru, http://orcid.org/0000-0003-1345-2199

Murashov Ivan S. – Cand. Sci. (Med.), Researcher, Laboratory for Pathomorphology, Meshalkin National Medical Research Center, Novosibirsk, ivmurashov@gmail.com, http://orcid.org/0000-0002-3712-1258

Chernyavskii Alexander M. – Dr. Sci. (Med.), Professor, Director of Meshalkin National Medical Research Center, Novosibirsk, amchern@mail.ru, http://orcid.org/0000-0001-9818-8678

Ragino Yulia I. – Dr. Sci. (Med.), Professor, Corresponding Member of RAS, Head of the Research Institute of Internal and Preventive Medicine, branch of the Institute of Cytology and Genetics, SB RAS, Novosibirsk, ragino@mail.ru, http://orcid.org/0000-0002-4936-8362

(✉) **Stakhneva Ekaterina M.,** stahneva@yandex.ru

Received 06.05.2022;
approved after peer review 27.06.2022;
accepted 08.09.2022

УДК 616.127-005.8-021.3-037:616.132..2-089.86
https://doi.org/10.20538/1682-0363-2022-4-130-139

Prognostic value of short-term trajectories of left ventricular ejection fraction in patients with first myocardial infarction and percutaneous coronary intervention

Timofeeva T.M.[1, 2], Kobalava Zh.D.[1], Safarova A.F.[1, 2], Cabello M. F.E.[1], Tigay Zh.G.[1]

[1] *Peoples' Friendship University of Russia (RUDN University)*
8, Mikluho-Maklaya Str., Moscow, 117198, Russian Federation

[2] *Vinogradov City Clinical Hospital*
61, Vavilova Str., Moscow, 117292, Russian Federation

ABSTRACT

Aim. To assess periprocedural dynamics of left ventricular ejection fraction (LVEF) in patients with first acute myocardial infarction (AMI) and percutaneous coronary intervention (PCI) without heart failure (HF) in the medical history, as well as its prognostic value in the development of cardiovascular complications in the postinfarction period.

Materials and methods. A prospective, single-center observational study included 131 patients with first AMI without HF in the past medical history and successful PCI. LVEF was assessed before PCI at admission and before discharge. In patients with reduced baseline LVEF of less than 50%, the criteria for its periprocedural improvement were chosen: 1) LVEF ≥ 50%; 2) ΔLVEF of more than 5%, but EF < 50%. The endpoints were hospitalization for the development of HF and death from cardiovascular disease in combination with the development of HF. The average follow-up period was 2.5 years.

Results. At admission, LVEF was < 50% in 74 (56.5%) patients. At discharge, according to the criteria for LVEF improvement, the proportion of patients in this group was 40.5 and 14.9%, respectively. In 44.6% of cases, no increase in LVEF was noted.

The predictors of the absence of periprocedural dynamics in LFEF included impaired regional contractility index > 1.94, left ventricular end-systolic volume > 57 ml, left ventricular end-diastolic diameter > 5.1 cm, pulmonary artery systolic pressure >27 mm Hg, NT-proBNP > 530 pg / ml, and E / A ratio > 1.06. During the follow-up period, 28 (21.4%) patients were hospitalized for the development of HF, 33 (25.2%) patients had a combined endpoint.

The absence of periprocedural improvement in left ventricular contractility was independently associated with higher odds of hospitalization for HF (relative risk (RR) 3.5; 95% confidence interval (CI) 1.63–7.55; $p = 0.001$) and the combined endpoint (RR 2.6; 95% CI 1.28–5.48; $p = 0.009$) in the postinfarction period.

Conclusion. In patients with first AMI and left ventricular systolic dysfunction, periprocedural evaluation of LVEF is reasonable to stratify the risk of adverse cardiovascular outcomes.

Keywords: acute myocardial infarction, periprocedural dynamics, ejection fraction, heart failure

Conflict of interest. The authors declare the absence of obvious or potential conflict of interest related to the publication of this article.

Source of financing. The authors state that they received no funding for the study.

Conformity with the principles of ethics. All individuals signed an informed consent to participate in the study. The study was approved by the Ethics Committee at RUDN University.

For citation: Timofeeva T.M., Kobalava Zh.D., Safarova A.F., Cabello M. F.E., Tigay Zh.G. Prognostic value of short-term trajectories of left ventricular ejection fraction in patients with first myocardial infarction and percutaneous

✉ *Timofeeva Tatiana M.,* timtan@bk.ru

coronary intervention. *Bulletin of Siberian Medicine.* 2022;21(4):130–139. https://doi.org/10.20538/1682-0363-2022-4-130-139.

Прогностическое значение перипроцедурной динамики фракции выброса левого желудочка у пациентов с первым инфарктом миокарда и чрескожным коронарным вмешательством

Тимофеева Т.М.[1, 2], Кобалава Ж.Д.[1], Сафарова А.Ф.[1, 2], Кабельо М.Ф.Э.[1], Тигай Ж.Г.[1]

[1] *Российский университет дружбы народов (РУДН)*
Россия, 117198, г. Москва, ул. Миклухо-Маклая, 8

[2] *Городская клиническая больница (ГКБ) им. В.В. Виноградова*
117292, Россия, г. Москва, ул. Вавилова, 61

РЕЗЮМЕ

Цель исследования. Оценка перипроцедурной динамики фракции выброса левого желудочка (ФВ ЛЖ) у пациентов с первым острым инфарктом миокарда (ОИМ) и чрескожным коронарным вмешательством (ЧКВ) без анамнеза сердечной недостаточности (СН) и ее прогностическое значение в развитии сердечно-сосудистых осложнений в постинфарктный период.

Материалы и методы. В проспективное одноцентровое наблюдательное исследование включен 131 пациент с первым ОИМ без анамнеза СН и успешным ЧКВ. ФВ ЛЖ оценивалась до ЧКВ при поступлении и перед выпиской. У пациентов с исходно сниженной ФВ ЛЖ менее 50% были выбраны критерии перипроцедурного ее улучшения: 1) ФВ ЛЖ ≥ 50%; 2) ΔФВ ЛЖ более 5%, но ФВ < 50%. Конечными точками являлись госпитализация по поводу развития СН и смерть от сердечно-сосудистых заболеваний в комбинации с развитием СН. Средний период наблюдения составил 2,5 года.

Результаты. При поступлении у 74 (56,5%) пациентов отмечена ФВ ЛЖ менее 50%. При выписке в этой группе по критериям улучшения ФВ ЛЖ доля пациентов составила 40,5 и 14,9% соответственно. В 44,6% случаев прирост ФВ ЛЖ отсутствовал.

Предикторами перипроцедурного отсутствия динамики ФВ ЛЖ явились индекс нарушения локальной сократимости >1,94, конечно-систолический объем ЛЖ >57 мл, конечно-диастолический размер ЛЖ >5,1 см, систолическое давление легочной артерии >27 мм рт. ст, уровень NT-proBNP > 530 пг/мл, соотношение скоростей трансмитрального кровотока в фазу раннего наполнения к кровотоку в систолу предсердий >1,06. За период наблюдения 28 (21,4%) пациентов были госпитализированы по поводу развития СН, у 33 (25,2%) зарегистрирована комбинированная конечная точка.

Отсутствие перипроцедурного улучшения сократительной способности ЛЖ независимо ассоциировано с более высокой вероятностью госпитализации по поводу СН (относительный риск (ОР) 3,5; 95%-й доверительный интервал (ДИ) 1,63–7,55; $p = 0,001$) и наступления комбинированной конечной точки (ОР 2,6; 95%-й ДИ 1,28–5,48; $p = 0,009$) в постинфарктном периоде.

Заключение. У пациентов с первым ИМ и систолической дисфункцией ЛЖ целесообразна перипроцедурная оценка ФВ ЛЖ для стратификации риска развития неблагоприятных сердечно-сосудистых исходов.

Ключевые слова: острый инфаркт миокарда, перипроцедурная динамика, фракция выброса, сердечная недостаточность

Конфликт интересов. Авторы декларируют отсутствие явных и потенциальных конфликтов интересов, связанных с публикацией настоящей статьи.

Источник финансирования. Авторы заявляют об отсутствии финансирования при проведении исследования.

Соответствие принципам этики. Все пациенты подписали информированное согласие на участие в исследовании. Исследование одобрено комитетом по этике Медицинского института РУДН.

Для цитирования: Тимофеева Т.М., Кобалава Ж.Д., Сафарова А.Ф., Кабельо М.Ф.Э., Тигай Ж.Г. Прогностическое значение перипроцедурной динамики фракции выброса левого желудочка у пациентов с пер-

вым инфарктом миокарда и чрескожным коронарным вмешательством. *Бюллетень сибирской медицины.* 2022;21(4):130–139. https://doi.org/10.20538/1682-0363-2022-4-130-139.

INTRODUCTION

Left ventricular (LV) systolic dysfunction is one of the key negative prognostic factors in patients with acute myocardial infarction (AMI) [1]; therefore, an assessment of left ventricular ejection fraction (LVEF) is recommended for all patients in this group [2, 3]. At the same time, LVEF is the only echocardiography parameter which is currently used as a predictor of the outcome in patients with ST-elevation myocardial infarction (STEMI) [4]. Depending on the value of LVEF after the first myocardial infarction (MI) at discharge, the authors recommend to identify groups with a high risk of mortality with follow-up periods of 1 year [5, 6] and 3 years [7]. However, several studies showed that a significant proportion of MI patients with reduced baseline LVEF may improve over time [8, 9], which results in a reduced risk of cardiovascular events in the postinfarction period. Conversely, patients who do not show an improvement in LVEF values after MI have an increased risk of adverse LV remodeling [10], life-threatening arrhythmias, cardiac arrest, cardiovascular disease, and all-cause mortality, regardless of revascularization, drug therapy, peak troponin level, and baseline LVEF [11, 12]. Studies on the dynamics of left ventricular contractility revealed the association of an improvement in LVEF with baseline levels of natriuretic peptide and MB-creatine kinase and the affected artery [13, 14]. Patients, whose LVEF improved from 2 weeks to several months after MI, had a better disease prognosis [11, 12, 15]. The rate of improvement in LVEF within a shorter period after percutaneous coronary intervention (PCI) and its relationship with distant outcomes are not well understood in patients with the first MI and without heart failure (HF) in the past medical history.

Despite recent advances in diagnosis and treatment, the incidence of complications after MI remains high [16–18]. Moreover, a lack of compliance and a possibility of long-term follow-up in such patients indicates relevance of assessing the role of short-term trajectories of LVEF after PCI at discharge and their impact on the development of HF and cardiovascular mortality. Since much attention is paid to the development of HF in the distant postinfarction period, the aim of this study was to assess the periprocedural dynamics of LVEF in patients with first MI and PCI without HF in the medical history, as well as its prognostic value in the development of cardiovascular complications in the postinfarction period.

MATERIALS AND METHODS

Our prospective, single-center observational study included 131 patients hospitalized in the Intensive Care Unit (ICU) of Vinogradov City Clinical Hospital. The average age was 61.85 ± 11.3 years; 68% of patients were men. STEMI was diagnosed in 74% of patients; the average LVEF at admission was 46 (44; 50)%. In 57 (43.6%) patients, LVEF was more than 50%, in 56 (42.7%) patients, it was 40–49%, in 18 (13. 7%) patients, it was less than 40%.

Inclusion criteria were the following: the first AMI diagnosed according to the Fourth Universal Definition of MI [19]; successful primary PCI in patients with STEMI, early (within 24 hours) PCI in patients with non-ST elevation myocardial infarction (NSTEMI), i.e. achieving TIMI grade III blood flow in the affected vessel; the sum of B-lines of less than 5 during lung ultrasound; no history of HF and dyspnea at admission, Killip 1.

Exclusion criteria were the following: intake of diuretics and vasopressors, the presence of primary pathology of the lungs (pneumonia), lung cancer, development of AMI complications (ventricular septal rupture, papillary muscle rupture with detachment), severe arrhythmia at the time of inclusion, including atrial fibrillation and(or) flutter.

The study was performed in compliance with the ethical principles of the Declaration of Helsinki developed by the World Medical Association "Ethical Principles for Medical Research Involving Human Subjects" and Rules of Clinical Practice in the Russian Federation.

All patients underwent a routine physical examination, electrocardiography, chest X-ray, echocardiography (EchoCG), lung ultrasound, coronary angiography, and coronary angioplasty with stenting. Laboratory studies were performed in accordance with Russian standards of medical care. Complete blood count and blood biochemistry were performed, including measurement of the troponin level twice (at admission and 6–12 hours after hospitalization) and additional measurement of N-terminal pro-brain natriuretic peptide (NT-proBNP).

EchoCG was performed at admission to the ICU before PCI and at discharge, followed by post-processing using the EchoPAC station (General Electric Healthcare, USA) with an automatic assessment of LVEF [20–22]. LV diastolic function was assessed by the following parameters: E, E / A, e'lat, E / e'lat, left atrial volume index, peak tricuspid regurgitation velocity [23].

Patients with the baseline LVEF of less than 50% were additionally stratified based on the periprocedural dynamics of LV contractility. In patients with baseline LVEF of less than 50%, criteria for short-term improvement of LVEF were selected: 1) ≥ 50%; 2) ΔLVEF of more than 5%, but EF < 50% [15].

To assess pulmonary edema, eight-point lung ultrasound at admission was performed along the anterior surface of the chest. The sum of B-lines of less than 5 corresponded to the absence of pulmonary edema [4, 22]. During the hospital stay and within a year after the discharge, all patients received standard dual antiplatelet therapy before and after the intervention.

Endpoints. The main endpoints were hospitalization for HF and death from cardiovascular disease. These data were collected in a unified medical information and analytical system, as well as via telephone interviews with patients during a follow-up period of 2.5 years.

Statistical analysis. A data analysis was performed using SPSS software (version 23.0) and MedCalc Version 19. Quantitative variables were presented as the arithmetic mean and the standard deviation M ± *SD* (for normal distribution) and as the median and the interquartile range *Me* (Q_1; Q_3) (for non-normal distribution). Qualitative variables were described by absolute and relative values *n* (%). The distributions were checked using the Kolmogorov – Smirnov test. The Spearman's rank correlation coefficient was used to measure rank correlation. To assess the differences in quantitative variables between two independent samples, the Mann – Whitney *U* test was used. The Pearson's chi-square test ($\chi 2$) was used to compare the frequencies of qualitative variables. Results were considered statistically significant at two-tailed $p < 0.05$. The impact of a lack of improvement in LVEF on the risk of developing endpoints was assessed by the univariate and multivariate Cox regression model. Using logistic regression, predictors of changes in LVEF were studied, the odds ratio (OR) and 95% confidence interval (CI) were determined. Threshold values for quantitative predictors were set based on the ratio of marginal probabilities with the selected cut-off score. The cut-off score was chosen for the optimal trade-off between sensitivity and specificity. The primary criterion for evaluating survival was cumulative survival – the interval between the date of discharge and the date of the endpoint. The survival probability was estimated by constructing Kaplan-Meier survival curves; comparison was made using the log-rank test.

RESULTS

Comparative characteristics of patients with LVEF of more and less than 50% at admission are summarized in Table 1. Patients were matched by sex and age. In the group of patients with LVEF of less than 50%, atrial fibrillation in the past medical history was significantly more frequent; laboratory tests revealed significantly higher levels of troponin and NT-proBNP at admission and 6–12 hours after hospitalization. In addition, they had a higher risk of mortality according to the GRACE score.

Table 1

Characteristics of patients with AMI, *n* = 131

Parameter	LVEF 50%, *n* = 57 (43.5%)	LVEF < 50%, *n* = 74 (56.5%)	*p*
Age, years, *M* ± *SD*	57 ± 10.97	62.5 ± 11.8	0.172
Men / women, *n* (%)	39(68)/18(32)	50(68)/24(32)	0.917
Body mass index, kg / m^2, *M* ± *SD*	28.03 ± 4.26	28.71 ± 4.56	0.375
Atrial fibrillation in the past medical history, *n* (%)	2 (3.5)	10 (14)	0.049
NT-proBNP, pg / ml, *Me* (Q_1; Q_3)	330.70 (199; 988)	785 (314; 1768)	0.011
Troponin 1, ng / ml, *Me* (Q_1; Q_3)	0.11 (0.03; 0.73)	0.39 (0.07; 2.93)	0.005
Troponin 2, ng / ml, *Me* (Q_1; Q_3)	3.64 (0.68; 19.73)	23.68 (3.45; 61.24)	<0.000
STEMI / NSTEMI, *n* (%)	38(67)/19(33)	59(80)/15(20)	0.090

Note: Troponin 1 – at admission in the ICU; Troponin 2 – 6–12 hours after the hospitalization.

In a repeated EchoCG study before discharge of patients with baseline LVEF of less than 50%, an improvement in LV systolic function was observed in 55.4% of cases, which was assessed as 1) improvement in LVEF ≥ 50% (in 30 patients); 2) Δ LVEF of more than 5%, but not reaching 50% (in 11 patients). There was a slight decrease in LVEF in 4.6% of cases, and these patients were assigned to the group without changes in LVEF, which consisted of 33 patients.

Comparative characteristics of patients with improved LVEF and patients with no changes in this parameter are presented in Table. 2.

Predictors of the absence of short-term recovery of LVEF are listed in Table 3.

The relative risk of developing HF and the combined endpoint, obtained by univariate and multivariate analysis, was statistically significant in the group of patients with no short-term recovery of LVEF (Table 4).

Table 2

Comparative characteristics of patients with recovered LVEF and patients without changes in LVEF, *n* = 74

Patients	Patients with improved LVEF, *n* = 41	Patients without changes in LVEF, *n* = 33	*p*
IRCI, *M* ± *SD*	1.87 ± 0.15	1.96 ± 0.15	0.025
LVESV, ml	41 (35; 56)	58 (42; 71)	0.0055
SV, ml	47 (41;59)	41 (37; 47)	0.040
LVRWT	0.47 ± 0.1	0.53 ± 0.1	0.041
Patterns of LV geometry, *n* (%)			
Normal	6 (14.6)	2 (6)	0.244
CR	9 (22)	7 (21.2)	0.937
CH	24 (58.5)	15 (45.5)	0.293
EH	2 (4.9)	9 (27.3)	0.006
E, cm / s	0.44 (0.40;0.60)	0.56 (0.42;0.66)	0.197
E / A	0.70 (0.60;0.82)	0.77 (0.57;1.36)	0.002
LAVI, ml / m^2	28.4 (24; 33)	30 (23.5; 40)	0.333
PTRV, m / s	1.9 (1.40; 2.20)	2.5 (2.2; 2.8)	< 0.000
Systolic pressure in the pulmonary artery, mm Hg	20 (14;27)	30 (25;37)	< 0.000

Note: A – rate of transmitral blood flow in the atrial systole; E – rate of transmitral blood flow in the early filling phase; PTRV – peak tricuspid regurgitation velocity; IVLC – impaired regional contractility index; LAVI – left atrial volume index ; CH – concentric hypertrophy; CR – concentric remodeling; ESV – end-systolic volume; LVRWT – left ventricular relative wall thickness; SV – stroke volume; EH – eccentric hypertrophy.

Table 3

Predictors of the absence of short-term recovery of LVEF

Parameter	OR	95% CI	*p*
IRCI > 1.94	7.86	2.57–24.06	0.0001
LVESV > 57 ml	6.94	2.82–17.05	< 0.0001
LVEDD > 5.1 cm	8.45	2.99–23.87	< 0.0001
Systolic pressure in the pulmonary artery >27 mm Hg	5.39	2.31–12.56	0.0001
NTproBNP > 530 pg / ml	3.22	1.42–7.29	0.0044
E / A > 1.06	6.32	1.81–22.0	0.004
PTRV > 2.1 m / s	10.87	3.57–33.04	0.000

Note: IRCI – impaired regional contractility index; LVESV – left ventricular end-systolic volume; LVEDD – left ventricular end-diastolic diameter; E / A – ratio of transmitral blood flow rates in the early filling phase to blood flow in atrial systole; PTRV – peak tricuspid regurgitation velocity.

Table 4

Risk ratio for development of heart failure and a combined endpoint in patients, depending on the periprocedural dynamics of LVEF

Parameter	Development of HF					Combined endpoint				
	Frequency of the events,%	Univariate analysis, 95% CI	*p*	Multivariate analysis, 95% CI	*p*	Frequency of the events,%	Univariate analysis, 95% CI	*p*	Multivariate analysis, 95% CI	*p*
LVEF ≥ 50%, *n* = 30	14	0.50 (0.27–1.89)	0.71	0.75 (0.28–2.05)	0.58	19	0.73 (0.30–1.77)	0.48	0.69 (0.27–1.74)	0.44
Increase in LVEF ≥ 5%, *n* = 11	17	0.75 (0.18–3.18)	0.70	0.53 (0.12–2.35)	0.40	22	0.62 (0.14–2.61)	0.51	0.41 (0.09–1.81)	0.24

Table 4 (continued)

Parameter	Development of HF					Combined endpoint				
	Frequency of the events,%	Univariate analysis, 95% CI	*p*	Multivariate analysis, 95% CI	*p*	Frequency of the events,%	Univariate analysis, 95% CI	*p*	Multivariate analysis, 95% CI	*p*
No dynamics of LVEF, *n* = 33	39	3.1 (1.46–6.47)	0.003	3.5 (1.63–7.55)	0.001	42	2.3 (1.17–4.86)	0.017	2.6 (1.28–5.48)	0.009

Note: the multivariate analysis included sex, age, atrial fibrillation, diabetes mellitus, multivessel damage.

Patients without changes in LVEF at discharge after AMI were significantly more likely to develop endpoints (hospitalization for HF and CVD) than patients with normal baseline and improved LVEF (Fig. 1).

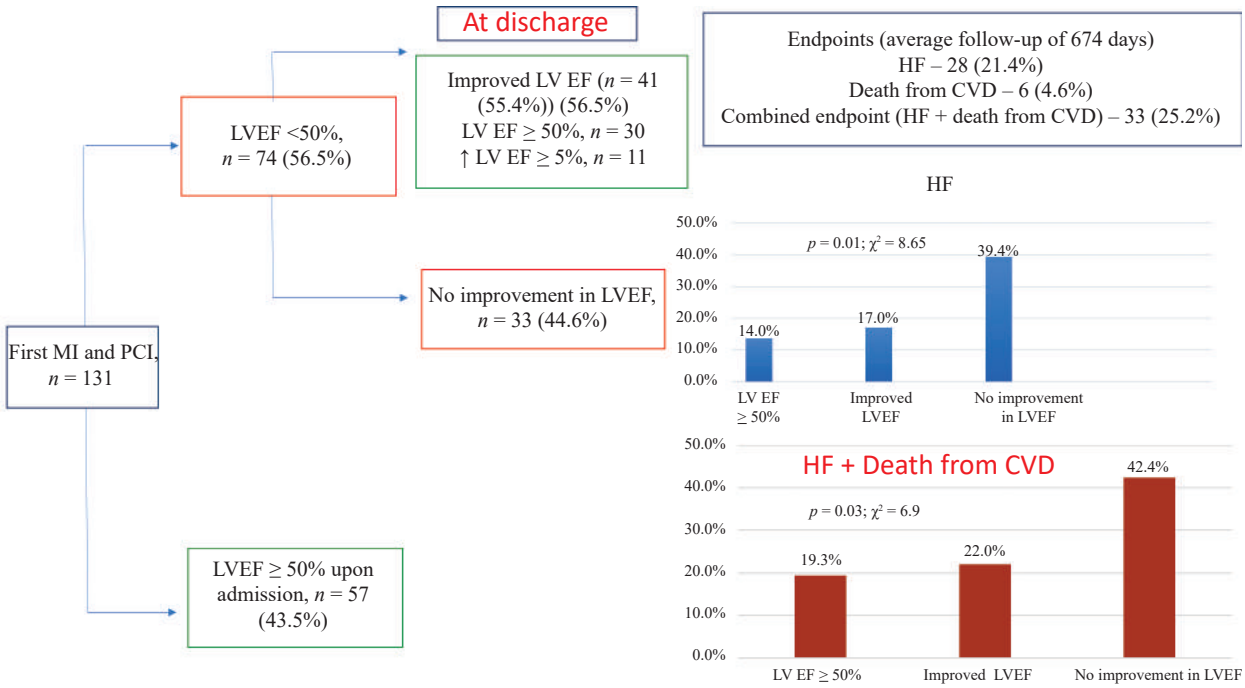

Fig. 1. Distribution of patients with AMI and PCI by LVEF at admission and discharge. Kaplan – Meier curves for cumulative survival probability depending on the improvement in LVEF at discharge are presented on fig. 2,3

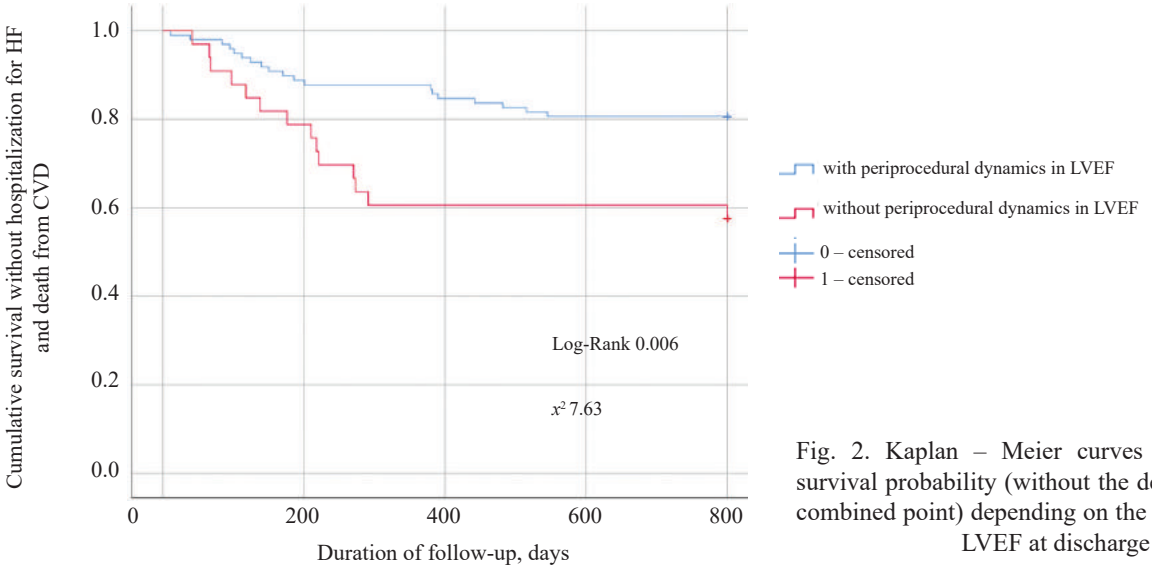

Fig. 2. Kaplan – Meier curves for cumulative survival probability (without the development of a combined point) depending on the improvement in LVEF at discharge

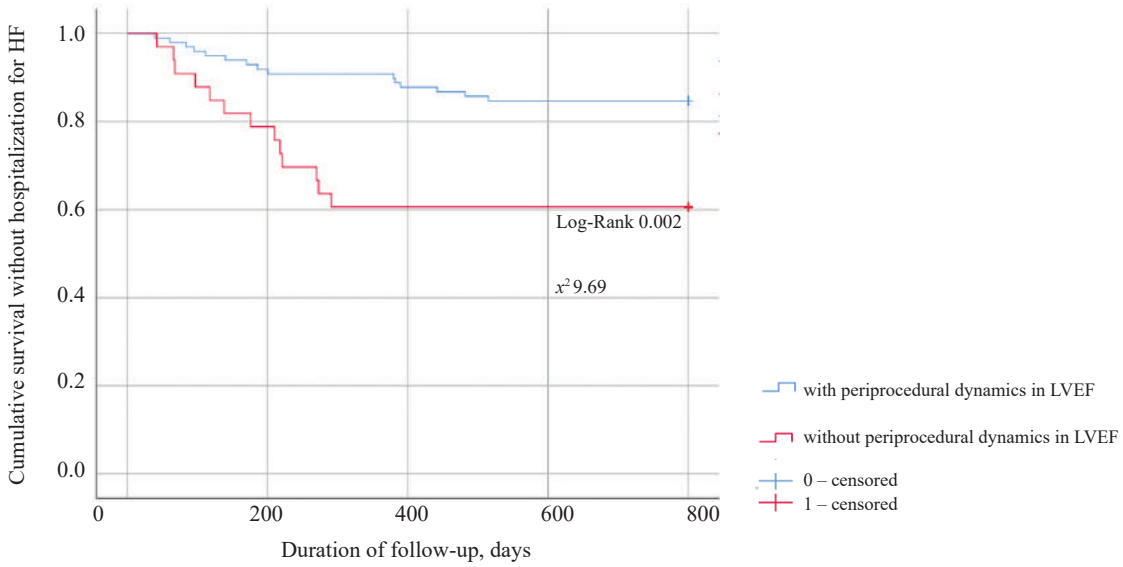

Fig. 3. Kaplan – Meier curves for cumulative survival probability (without hospitalization for HF) versus improvement in LVEF at discharge

DISCUSSION

Our study is the first attempt to assess the prognostic value of short-term improvement in LVEF in patients after the first MI and PCI. We demonstrated the association between the absence of improvement in LVEF at discharge according to the selected criteria and a significantly increased risk of developing HF and a combined endpoint. At the time of admission, more than half of the patients had LV systolic dysfunction and 44.6% of them did not recover at discharge.

Patients with and without positive dynamics in LVEF were comparable in terms of sex, age, risk factors for cardiovascular diseases, and the extent of coronary lesion. However, patients without LVEF dynamics had significantly higher LVESV, LVRWT, higher systolic pressure in the pulmonary artery, and eccentric LV hypertrophy, which emphasizes more significant structural and functional damage to the heart [23, 24].

Our data are consistent with the study by M.F Minicucci et al. [14], who revealed the recovery of LV function in the period from 2 weeks to 6 months in 25% of patients after MI. Y.Wu Wanda et al. [15, 25] demonstrated 8-fold reduction of all-cause mortality and a 10-fold decrease in the CVD risk in young AMI patients with improved LVEF. D.S.Chew et al. [11, 12] also found that elderly patients with MI and an improvement in LVEF of > 40% within 2 weeks had a 4-fold lower risk of future adverse events, all-cause mortality, and CVD compared with patients without changes in LVEF.

It was noted in the earlier studies that low LVEF at discharge in elderly patients after MI was correlated with an increased risk of mortality and rehospitalization [26]. In our study a decrease in baseline LVEF below 50% was not significantly associated with higher rates of hospitalization for HF and CVD per se ($p = 0.070$). However, we found an association of the absence of short-term dynamics in LV contractility with high frequency of hospitalizations for HF during the follow-up, as well as with the development of a combined endpoint. In addition, we identified predictors of the absence of LVEF dynamics in patients with the first MI, such as IRCI > 1.94, LVESV > 57 ml, LVEDD > 5.1 cm, systolic pressure in the pulmonary artery > 27 mm Hg, concentration of NT-proBNP > 530 pg / ml, and the E / A ratio > 1.06.

We did not find studies on periprocedural dynamics of LVEF in patients with the first MI and successful PCI and its effect on the prognosis of CVD. A detailed study of the contractility dynamics before and after PCI during hospitalization may be of great importance, since there is no decrease in the incidence of MI, and patients' compliance with follow-up, as well as its possibility, is not always optimal.

Assessment of LV EF is recommended in all patients presenting with AMI (grade 1 recommendation); however, recommendations are less clear in terms of the dynamic assessment of LVEF [2, 3]. It has been shown that many traditional EchoCG parameters, such as LV volumes, LVEF, and IRCI, can be used as prognostic markers [27]. Our work demonstrates

that in patients with the first AMI, assessment of LV linear dimensions, LV diastolic function, and dynamic assessment of LVEF before and after PCI can provide valuable information on long-term prognosis, outcomes, and potential ongoing need for drug therapy.

Limitations and prospects of the study. Our study was limited by a small sample size and a relatively short follow-up period. There were also inherent limitations to the evaluation of LVEF using echoCG. However, echoCG has shown its accuracy in the assessment of LVEF compared with other imaging modalities and is widely used in clinical trials. In our work, all echoCG studies were performed by one doctor using one device, followed by post-processing on the EchoPAC station (General Electric Healthcare, USA) with an automatic assessment of LVEF, which allowed to minimize errors [20, 21]. There is an obvious need for a multicenter clinical study that would research the significance of short-term dynamics of LVEF in patients with the first AMI in relation to long-term prognosis.

CONCLUSION

In patients with the first MI, the frequency of LV systolic dysfunction at admission was 58.8%. 44.6% of patients had no improvement in LV contractility after successful PCI. The absence of improvement in LVEF is associated with a significantly increased risk of hospitalization for HF and a combined point. Therefore, in patients with the first AMI and LV systolic dysfunction, a short-term assessment of LVEF is reasonable to stratify the risk of developing adverse cardiovascular outcomes.

REFERENCES

1. Ye Q., Zhang J., Ma L. Predictors of all-cause 1-year mortality in myocardial infarction patients. *Medicine (Baltimore)*. 2020;99(29):e21288. DOI: 10.1097/MD.0000000000021288.
2. Amsterdam E.A., Wenger N.K., Brindis R.G., Casey D.E. Jr., Ganiats T.G., Holmes D.R. Jr. et al. 2014 AHA/ACC Guideline for the Management of Patients with Non-ST-Elevation Acute Coronary Syndromes: a report of the American College of Cardiology/American Heart Association Task Force on Practice Guidelines. *J. Am. Coll. Cardiol*. 2014;64(24):e139–e228. DOI: 10.1016/j.jacc.2014.09.017. Erratum in: *J. Am. Coll. Cardiol*. 2014;64(24):2713–2714. Dosage error in article text. DOI: 10.1016/j.jacc.2014.09.017.
3. O'Gara P.T., Kushner F.G., Ascheim D.D., Casey D.E. Jr., Chung M.K., de Lemos J.A. et al. 2013 ACCF/AHA guideline for the management of ST-elevation myocardial infarction: a report of the American College of Cardiology Foundation/American Heart Association Task Force on Practice Guidelines. *Circulation.* 2013;127(4):e362–425. DOI: 10.1161/CIR.0b013e3182742cf6.
4. Ibanez B., James S., Agewall S., Antunes M.J., Bucciarelli-Ducci C., Bueno H. et al. 2017 ESC Guidelines for the management of acute myocardial infarction in patients presenting with ST-segment elevation: The Task Force for the management of acute myocardial infarction in patients presenting with ST-segment elevation of the European Society of Cardiology (ESC). *Eur. Heart J.* 2018;39(2):119–177. DOI: 10.1093/eurheartj/ehx393.
5. Ahnve S., Gilpin E., Dittrich H., Nicod P., Henning H., Carlisle J. et al. First myocardial infarction: age and ejection fraction identify a low-risk group. *Am. Heart J*. 1988;116(4):925–932. DOI: 10.1016/0002-8703(88)90142-1.
6. Fedorova N.V., German A.I., Kokov A.N., Brel N.K., Pecherina T.B., Kashtalap V.V., et al. Echocardiography correlations between myocardial fibrosis and preserved ejection fraction of the left ventricle. *Fundamental and Clinical Medicine*. 2019;4(2):17–27 (in Russ.). DOI: 10.23946/2500-0764-2019-4-2-17-27.
7. Garganeeva A.A., Borel K.N., Okrugin S.A., Kuzheleva E.A. The effect of left ventricular ejection fraction on distant prognosis of patients after vascular catastrophe. Analysis of 5-year monitoring within the population program "Registry of acute myocardial infarction". *Serdechnaya Nedostatochnost.* 2014;15(4):218–223 (in Russ.).
8. Oh P.C., Choi I.S., Ahn T., Moon J., Park Y., Seo J.G. et al. Predictors of recovery of left ventricular systolic dysfunction after acute myocardial infarction: from the korean acute myocardial infarction registry and korean myocardial infarction registry. *Korean Circ. J.* 2013;43(8):527–533. DOI: 10.4070/kcj.2013.43.8.527.
9. Sjöblom J., Muhrbeck J., Witt N., Alam M., Frykman-Kull V. Evolution of left ventricular ejection fraction after acute myocardial infarction: implications for implantable cardioverter-defibrillator eligibility. *Circulation.* 2014;130(9):743–748. DOI: 10.1161/CIRCULATIONAHA.114.009924.
10. Zharikova E.S., Villevalde S.V., Kobalava Zh.d. Predictors of unfavorable left ventricular remodeling in patients after myocardial infarction. *Bulletin of Russian People's Friendship University. Series: Medicine.* 2017;21(2):219–226 (in Russ.). DOI: 10.22363/2313-0245-2017-21-2-219-226.
11. Chew D.S., Heikki H., Schmidt G., Kavanagh K.M., Dommasch M., Bloch Thomsen P.E. et al. Change in left ventricular ejection fraction following first myocardial infarction and outcome. *JACC Clin. Electrophysiol*. 2018;4(5):672–682. DOI: 10.1016/j.jacep.2017.12.015.
12. Chew D.S., Wilton S.B., Kavanagh K., Southern D.A., Tan-Mesiatowsky L.E., Exner D.V. et al. Left ventricular ejection fraction reassessment post-myocardial infarction: Current clinical practice and determinants of adverse remodeling. *Am. Heart J.* 2018;198:91–96. DOI: 10.1016/j.ahj.2017.11.014.
13. Ohashi J., Sakakura K., Yamamoto K., Taniguchi Y., Tsukui T., Seguchi M. et al. Determinants of improvement of mid-term ejection fraction in patients with acute myocardial infarc-

tion. *Int. Heart J*. 2019;60(6):1245–1252. DOI: 10.1536/ihj.19-126.
14. Minicucci M.F., Farah E., Fusco D.R., Cogni A.L., Azevedo P.S., Okoshi K. et al. Infarct size as predictor of systolic functional recovery after myocardial infarction. *Arq. Bras. Cardiol*. 2014;102(6):549–556. DOI: 10.5935/abc.20140051.
15. Wu W.Y., Biery D.W., Singh A., Divakaran S., Berman A.N., Ayuba G. et al. Recovery of left ventricular systolic function and clinical outcomes in young adults with myocardial infarction. *J. Am. Coll. Cardiol*. 2020;75(22):2804–2815. DOI: 10.1016/j.jacc.2020.03.074.
16. Gupta A., Wang Y., Spertus J.A., Geda M., Lorenze N., Nkonde-Price C. et al. Trends in acute myocardial infarction in young patients and differences by sex and race, 2001 to 2010. *J. Am. Coll. Cardiol*. 2014;64(4):337–345. DOI: 10.1016/j.jacc.2014.04.054.
17. Wilmot K.A., O'Flaherty M., Capewell S., Ford E.S., Vaccarino V. Coronary heart disease mortality declines in the United States from 1979 through 2011: Evidence for stagnation in young adults, especially women. *Circulation*. 2015;132(11):997–1002. DOI: 10.1161/CIRCULATIONAHA.115.015293.
18. Yandrapalli S., Nabors C., Goyal A., Aronow W.S., Frishman W.H. Modifiable risk factors in young adults with first myocardial infarction. *J. Am. Coll. Cardiol*. 2019;73(5):573–584. DOI: 10.1016/j.jacc.2018.10.084.
19. Thygesen K., Alpert J.S., Jaffe A.S., Chaitman B.R., Bax J.J., Morrow D.A. et al. Fourth Universal Definition of Myocardial Infarction (2018). *Circulation*. 2018;138(20):e618-e651. DOI: 10.1161/CIR.0000000000000617.
20. Belghitia H., Brette S., Lafitte S., Reant P., Picard F., Serri K. et al. Automated function imaging: a new operator-independent strain method for assessing left ventricular function. *Arch. Cardiovasc. Dis*. 2008;101(3):163–169. DOI: 10.1016/s1875-2136(08)71798-4.
21. Amundsen B.H., Helle-Valle T., Edvardsen T., Torp H., Crosby J. et al. Noninvasive myocardial strain measurement by speckle tracking echocardiography: validation against sonomicrometry and tagged magnetic resonance imaging. *J. Am. Coll. Cardiol*. 2006;47(4):789–793. DOI: 10.1016/j.jacc.2005.10.040.
22. Mamedov S., Kobalava Zh., Safarova A., Timofeeva T., Cabello F., Meray I. et al. Prognostic value of subclinical pulmonary congestion in patients with primary acute myocardial infarction and percutaneous coronary intervention. *Eur. J. Heart Fail.* 2021;23(S2):34–35.
23. Nagueh S.F., Smiseth O.A., Appleton C.P., Byrd B.F. 3rd., Dokainish H., Edvardsen T. et al. Recommendations for the evaluation of left ventricular diastolic function by echocardiography: an update from the American Society of Echocardiography and the European Association of Cardiovascular Imaging. *J. Am. Soc. Echocardiogr*. 2016;29(4):277–314. DOI: 10.1016/j.echo.2016.01.011.
24. Cohn J.N., Ferrari R., Sharpe N. Cardiac remodeling--concepts and clinical implications: a consensus paper from an international forum on cardiac remodeling. Behalf of an International Forum on Cardiac Remodeling. *J. Am. Coll. Cardiol*. 2000;35(3):569–582. DOI: 10.1016/s0735-1097(99)00630-0. Colvin M.M., Sutton N.R. Left ventricular recovery in young patients with myocardial infarction: How much is enough? *J. Am. Coll. Cardiol*. 2020;75(22):2816–2818. DOI: 10.1016/j.jacc.2020.04.020.
25. Sutton N.R., Li S., Thomas L., Wang T.Y., de Lemos J.A., Enriquez J.R. et al. The association of left ventricular ejection fraction with clinical outcomes after myocardial infarction: Findings from the Acute Coronary Treatment and Intervention Outcomes Network (ACTION) Registry-Get With the Guidelines (GWTG) Medicare-linked database. *Am. Heart J.* 2016;178:65–73. DOI: 10.1016/j.ahj.2016.05.003.
26. Krikunov P.V., Vasyuk Yu.A., Krikunova O.V. Prognostic value of echocardiography after acute myocardial infarction. Part 1. Russian Journal of Cardiology. 2017;22(12):120–128 (in Russ.). DOI: 10.15829/1560-4071-2017-12-120-128.
27. Gillam L.D., Leipsic J., Weissman N.J. Use of Imaging Endpoints in Clinical Trials. *JACC Cardiovasc. Imaging.* 2017;10(3):296–303. DOI: 10.1016/j.jcmg.2016.12.003.

Authors contribution

Timofeeva T.M. – conception and design; acquisition, analysis, and interpretation of the data. Kobalava Zh.D. – critical revision of the manuscript for important intellectual content; final approval of the manuscript for publication. Safarova A.F. – conception and design; analysis and interpretation of the data; critical revision of the manuscript for important intellectual content; final approval of the manuscript for publication. Cabello M.F.E. – analysis and interpretation of the data. Tigay Zh.G. – critical revision of the manuscript for important intellectual content.

Authors information

Timofeeva Tatiana M. – Teaching Assistant, Department of Internal Medicine with a Course In Cardiology and Functional Diagnostics named after V.S. Moiseev, RUDN University; Physician, Department of Functional Diagnostics, Vinogradov City Clinical Hospital, Moscow, timtan@bk.ru, https://orcid.org/0000-0001-6586-7404

Kobalava Zhanna D. – Dr. Sci. (Med.), Professor, RAS Corresponding Member, Head of the Department of Internal Medicine with a Course in Cardiology and Functional Diagnostics named after V.S. Moiseev, RUDN University, Moscow, zkobalava@mail.ru, https://orcid.org/0000-0002-5873-1768

Safarova Ayten F. – Dr. Sci. (Med.), Professor, Department of Internal Medicine with a Course in Cardiology and Functional Diagnostics named after V.S. Moiseev, RUDN University; Physician, Department of Functional Diagnostics, Vinogradov City Clinical Hospital, Moscow, aytensaf@mail.ru, https://orcid.org/0000-0003-2412-5986

Cabello Montoya Flora Elisa – Cand. Sci. (Med.), Teaching Assistant, Department of Internal Medicine with a Course in Cardiology and Functional Diagnostics named after V.S. Moiseev, RUDN University, Moscow, flora.cabello@mail.ru, https://orcid.org/0000-0002-2334-6675

Tigay Zhanna G. – Dr. Sci. (Med.), Professor, Director of the Accreditation and Simulation Center, RUDN University, Moscow, tigay_zhg@rudn.university, https://orcid.org/0000-0001-6586-7404

(✉) **Timofeeva Tatiana M.,** timtan@bk.ru

Received 29.06.2022;
approved after peer review 15.07.2022;
accepted 08.09.2022

УДК 616.24-002.5:578.233.22
https://doi.org/10.20538/1682-0363-2022-4-140-149

Expression of scavenger receptors CD163, CD204, and CD206 on macrophages in patients with pulmonary tuberculosis

Churina E.G.[1, 2], Popova A.V.[1], Urazova O.I.[1], Patysheva M.R.[2, 3], Kolobovnikova Ju.V.[1], Chumakova S.P.[1]

[1] *Siberian State Medical University*
2 Moscow Trakt, Tomsk, 634050, Russian Federation

[2] *National Research Tomsk State University*
36, Lenina Av., Tomsk, 634050, Russian Federation

[3] *Cancer Research Institute, Tomsk National Research Medical Center (NRMC), Russian Academy Sciences*
5, Kooperativny Str., Tomsk, 634009, Russian Federation

ABSTRACT

The aim of the study was to evaluate the expression of scavenger receptors (CD163, CD204, CD206) on macrophages in patients with pulmonary tuberculosis, depending on the clinical form of the disease and sensitivity of the pathogen to anti-tuberculosis drugs.

Materials and methods. 64 patients with pulmonary tuberculosis (TB) were examined: 26 patients with disseminated pulmonary tuberculosis (DTB) and 38 patients with infiltrative pulmonary tuberculosis (ITB). Of these, 42 patients secreted *Mycobacterium tuberculosis* (MBT) sensitive to basic antituberculosis drugs (ATBD), and 22 patients secreted MBT resistant to first-line anti-TB drugs. Material for the study was venous blood.

To isolate monocytes from the whole blood in order to transform them into macrophages, Ficoll density gradient centrifugation with a density of 1.077 g / cm^3 was used followed by immunomagnetic separation of CD14+ cells. Monocytes were cultured in the X-VIVO 10 medium with gentamicin and phenol red with the addition of macrophage colony-stimulating factor (M-CSF) (5 ng / ml) at a concentration of 1×10^6 cells / ml with stimulators: interleukin (IL)-4 (10 ng / ml) and interferon (IFN) γ (100 ng / ml). Immunophenotyping of macrophages was performed using monoclonal antibodies to CD163, CD204, and CD206 on the Beckman Coulter CytoFLEX LX Flow Cytometer. The analysis of the obtained data was carried out using the CytExpert 2.0 software. The results were analyzed using statistical methods.

Results. Switching the phenotype of macrophages from the M1-like proinflammatory phenotype to M2-like anti-inflammatory one contributes to the chronic course of pulmonary TB, dissemination, and persistence of infection. In the present study, we analyzed the features of the expression of CD163, CD204, and CD206 scavenger receptors on macrophages in patients with pulmonary TB. An increase in the number of macrophages carrying markers of the M2 subpopulation (CD163, CD204, and CD206) on their surface was noted, regardless of the clinical form of pulmonary TB and drug resistance of M. tuberculosis.

Conclusion. Studying the mechanisms underlying M1 or M2 activation of macrophages is necessary for a deeper understanding of the immunopathogenesis of TB and the role of innate immunity cells in protecting the body from mycobacteria. The analysis of the expression of scavenger receptors CD163, CD204, and CD206 on macrophages allowed to conclude that, in pulmonary TB, especially in patients with drug resistant *M. tuberculosis* and infiltrative TB, regulatory mechanisms that suppress the activation of innate immunity are implemented together with polarization of macrophage differentiation towards the M2 phenotype. It may be the cause of immune deficiency induced by the pathogen.

Keywords: macrophages, pulmonary tuberculosis, innate immunity, immune response, scavenger receptors, IL-4, IFNγ, CD163, CD204, CD206

Conflict of interest. The authors declare the absence of obvious or potential conflicts of interest related to the publication of this article.

✉ *Churina Elena G.,* Lena1236@yandex.ru

Source of financing. The reported study was funded by the Council for Grants of the President of the Russian Federation for leading scientific schools (SS-2690.2018.7) and the RFBR grant, project number 19-315-90018.

Conformity with the principles of ethics. All patients signed an informed consent to participate in the study. The study was approved by the local Ethics Committee at Siberian State Medical University (Protocol No. 5648 of 27.11.2017).

For citation: Churina E.G., Popova A.V., Urazova O.I., Patysheva M.R., Kolobovnikova Ju.V., Chumakova S.P. Expression of scavenger receptors CD163, CD204, and CD206 on macrophages in patients with pulmonary tuberculosis. *Bulletin of Siberian Medicine.* 2022;21(4):140–149. https://doi.org/10.20538/1682-0363-2022-4-140-149.

Экспрессия скавенджер-рецепторов CD163, CD204 и CD206 на макрофагах у больных туберкулезом легких

Чурина Е.Г.[1, 2], Попова А.В.[1], Уразова О.И.[1], Патышева М.Р.[2, 3], Колобовникова Ю.В.[1], Чумакова С.П.[1]

[1] Сибирский государственный медицинский университет (СибГМУ)
Россия, 634050, г. Томск, Московский тракт, 2

[2] Национальный исследовательский Томский государственный университет (НИ ТГУ)
Россия, 634050, г. Томск, пр. Ленина, 36

[3] Научно-исследовательский институт (НИИ) онкологии, Томский национальный исследовательский медицинский центр (НИМЦ) Российской академии наук
Россия, 634009, г. Томск, пер. Кооперативный, 5

РЕЗЮМЕ

Цель работы – оценка экспрессии скавенджер-рецепторов (CD163, CD204, CD206) на макрофагах у больных туберкулезом легких в зависимости от клинической формы заболевания и чувствительности возбудителя к противотуберкулезным средствам.

Материалы и методы. Обследованы 64 пациента с туберкулезом легких (ТБ): 40 мужчин и 24 женщины, из которых 26 человек с диссеминированным туберкулезом легких (ДТБ) и 38 – с инфильтративным туберкулезом легких (ИТБ). Из них было 42 пациента, выделяющих *Mycobacterium tuberculosis* (МВТ), чувствительные к основным противотуберкулезным средствам (ПТС), и 22 пациента, выделяющих МВТ, устойчивые к лекарственным средствам основного ряда противотуберкулезной терапии. Материалом исследования являлась венозная кровь.

Для выделения моноцитов из цельной крови с целью их трансформации в макрофаги использовали метод центрифугирования в градиенте фиколла плотностью 1,077 г/см^3 с последующей иммуномагнитной сепарацией CD14+ клеток. Моноциты культивировали в полной питательной среде X-VIVO 10 with gentamicin and phenol red с добавлением колониестимулирующего фактора макрофагов (M-CSF) (5 нг/мл) в концентрации 1 × 10^6 клеток/мл со стимуляторами: интерлейкином (IL) 4 (10 нг/мл) и интерфероном (IFN) γ (100 нг/мл). Иммунофенотипирование макрофагов проводили с использованием моноклональных антител к CD163, CD204, CD206 на проточном цитометре Beckman Coulter CytoFLEX LX. Анализ полученных данных осуществляли при помощи программного приложения CytExpert 2.0. Полученные результаты анализировали статистическими методами.

Результаты. Переключение фенотипа макрофагов с провоспалительного М1 на противовоспалительный М2, установленное нами в ходе настоящего исследования, способствует хроническому течению туберкулеза легких, диссеминации и персистенции инфекции. Мы проанализировали особенности экспрессии скавенджер-рецепторов CD163, CD204 и CD206 на макрофагах у больных туберкулезом легких. Анализ экспрессии скавенджер-рецепторов на макрофагах показал значимое увеличение численности CD163, CD204 и CD206-позитивных клеток у больных ТБ независимо от клинической формы заболевания и лекарственной чувствительности *M. tuberculosis* к ПТС по сравнению с группой здоровых доноров.

Заключение. Исследование механизмов, лежащих в основе М1- или М2-активации макрофагов, необходимо для более глубокого понимания иммунопатогенеза туберкулезной инфекции и роли клеток врожденного иммунитета в защите организма от микобактерий. Анализ экспрессии скавенджер-рецепторов CD163, CD204 и CD206 на макрофагах позволил нам прийти к заключению, что при туберкулезе легких, особенно у больных с лекарственной устойчивостью *M. tuberculosis* и при инфильтративной форме заболевания, реализуются механизмы регуляции, подавляющие активацию врожденного иммунитета, с поляризацией

дифференцировки макрофагов в направлении М2-фенотипа, что, вероятно, является причиной формирования иммунодефицита, индуцированного возбудителем.

Ключевые слова: макрофаги, туберкулез легких, врожденный иммунитет, иммунный ответ, скавенджер-рецепторы, IL-4, IFNγ, CD163, CD204, CD206

Конфликт интересов. Авторы декларируют отсутствие явных и потенциальных конфликтов интересов, связанных с публикацией настоящей статьи.

Источник финансирования. Исследование выполнено при финансовой поддержке Совета по грантам Президента Российской Федерации для ведущих научных школ (НШ-2690.2018.7) и РФФИ в рамках научного проекта № 19-315-90018.

Соответствие принципам этики. От каждого обследованного было получено добровольное информированное согласие на проведение исследования. Исследование одобрено локальным этическим комитетом СибГМУ (протокол № 5648 от 27.11.2017).

Для цитирования: Чурина Е.Г., Попова А.В., Уразова О.И., Патышева М.Р., Колобовникова Ю.В., Чумакова С.П. Экспрессия скавенджер-рецепторов CD163, CD204 и CD206 на макрофагах у больных туберкулезом легких . *Бюллетень сибирской медицины.* 2022;21(4):140–149. https://doi.org/10.20538/1682-0363-2022-4-140-140.

INTRODUCTION

Macrophages play a crucial role in the defense of the body from *Mycobacterium tuberculosis.* They are involved in both innate and adaptive immune responses and also regulate remodeling and repair processes in damaged tissues [1, 2]. Macrophages are characterized by versatility and plasticity; they are capable of switching a functional phenotype in tissues [3–6]. This heterogeneity is determined by the ability of macrophages to implement different activation programs in response to different stimuli, such as cytokine signals, damage-associated molecular patterns, or pathogenicity patterns in the body.

According to the recent WHO Global Tuberculosis Report, there was a decline in deaths from tuberculosis (TB) in 2018: 1.5 million people died in comparison with 1.6 million in 2017. However, the incidence of TB remains high: about 10 million people worldwide were diagnosed with TB in 2018 [7]. *M. tuberculosis* develops resistance to anti-tuberculosis drugs (ATBD), which is an important problem. A variant of extensively drug-resistant tuberculosis (XDR-TB), when *M. tuberculosis* does not respond to any of the existing antibiotics, has been registered in 117 countries [8].

Dysregulation of the immune response during the development of pulmonary tuberculosis (TB) occurs even at its earliest stages, primarily at the stage of macrophage activation and antigen presentation to T-helper cells. Macrophages play an important role in successful immune defense when *M. tuberculosis* components penetrate into mucous membranes of the respiratory tract. M1 macrophages trigger acute lung inflammation and rapidly activate the mechanisms of innate immunity, inflammatory and cytotoxic T-cell responses. It causes the development of acute destructive, clinical and pathogenetic forms of pulmonary TB, such as infiltrative and disseminated TB [9]. Later an immune control of the *M. tuberculosis* infection depends on the direction of the macrophage differentiation and the effectiveness of the inflammatory response implemented by CD4+ type 1 T-helper cells (Th1) [10–12]. Switching the phenotype of macrophages to the M2-like anti-inflammatory one leads to chronic and persistent TB infection. Mechanisms of innate immunity in pulmonary TB require more detailed consideration, first of all, through analyzing the receptor profile of macrophages. The scavenger receptors of monocytes and (or) macrophages, which include CD206 mannose receptor, scavenger receptor A – SR-A (CD204), and CD163 membrane marker, are of the greatest interest [12, 13–16]. Many questions remain open related to the plasticity, polarization, and activation of macrophages in various clinical forms of pulmonary TB and depending on the resistance or sensitivity of *M. tuberculosis* to ATBD.

Therefore, the aim of the study was to evaluate the expression of scavenger receptors (CD163, CD204, CD206) on macrophages in patients with pulmonary TB depending on its clinical form and sensitivity of the pathogen to ATBD.

MATERIALS AND METHODS

We examined 64 patients (40 men and 24 women) aged 23–50 years (average age 43.10 ± 10.00 years) with newly diagnosed pulmonary TB. The disease was diagnosed at Tomsk Phthisiopulmonology Medical Center. The diagnosis was established based on the past medical history, clinical presentation of the disease, as well as the results of the X-ray examination of the lungs and bacteriological and microscopic examination of the sputum. All patients were examined before the initiation of anti-TB chemotherapy. The clinical form of the disease was diagnosed using an X-ray examination of the lungs. In most patients, both lungs were affected by the pathological process. In ITB, the examination detected one or more heterogeneous infiltration shadows (3–6 cm in diameter) in the lungs. In DTB, multiple small- and medium-sized foci with heterogeneous structures were detected. Bacterial excretion (MTB+) was registered in all patients. *Mycobacterium tuberculosis* (MTB) was identified by Ziehl – Neelsen stained sputum smear microscopy as well as by fluorescence microscopy of auramine-stained sputum smears. To determine the species of *M. tuberculosis* and MBT sensitivity to ATBD, the absolute concentration method and sputum culture in Lowenstein – Jensen and Finn-2 solid nutrient media were used.

TB patients were divided into two groups depending on the clinical form of the disease: 26 patients with disseminated pulmonary tuberculosis (DTB) and 38 patients with infiltrative pulmonary tuberculosis (ITB). In all examined TB patients, the causative agent had drug sensitivity to basic ATBD. This criterion was used to identify 42 patients secreting *M. tuberculosis* (MBT), sensitive to the basic ATBD, and 22 patients secreting MBT resistant to the first-line drugs (isoniazid, rifampicin, streptomycin, ethambutol). Exclusion criteria for TB patients to participate in the study were: 1) cancer, diabetes mellitus, allergies and autoimmune diseases, viral hepatitis, and HIV; 2) treatment with ATBD and immunosuppressants. The comparison group consisted of 30 healthy donors (20 men and 10 women) aged 23–50 years (average age 41.31 ± 7.47 years) without past medical history of pulmonary TB. All patients signed an informed consent to participate in the study.

Immunomagnetic separation of blood monocytes. The material for the study was venous blood taken from healthy donors and patients with pulmonary TB. Blood sampling was carried out once, during the most intense phase of the disease, before the initiation of the anti-TB chemotherapy. To isolate monocytes from the whole blood for their further transformation into macrophages, the method of magnetic separation of CD14+ monocytes (MACS MultiStand, Germany) was used according to the manufacturer's instructions for the Monocyte isolation kit, Miltenyi Biotec GmbH (Germany). 30 ml of whole venous blood was collected into vacuum blood collection systems with an anticoagulant (K3-EDTA). The blood was diluted with phosphate – buffer saline (PBS) at a ratio of 1:1 and layered on 15 ml of the Ficoll cushion with a density of 1.077 g / cm^3. The samples were centrifuged for 30 min at 0.016 g. The resulting mononuclear fraction was collected and washed from PBS twice. After that, 5 ml of PBS was added and mixed; then the number of mononuclear cells was counted using the automated cell counter Scepter 2.0 (Merck Millipore, Germany). The cell suspension was centrifuged, the supernatant was removed, and the appropriate volumes of MACS Separation Buffer (containing bovine serum albumin (BSA), EDTA, and 0.09% sodium azide) and CD14+ magnetic particles (Micro Beads, Germany) were added based on the number of cells, and the suspension was incubated for 40 min. The resulting suspension underwent positive magnetic separation according to the manufacturer's protocol (Miltenyi Biotec, Germany).

Cultivation of macrophages in vitro. Monocytes were cultivated in the X-VIVO 10 complete growth medium with gentamicin and phenol red (Lonza, Switzerland) at a concentration of 1×10^6 cells / ml with the addition of macrophage colony stimulating factor M-CSF (5 ng / ml; R&D Systems, USA). Recombinant cytokines IL-4 (10 ng / ml; PeproTech, USA) (for M2 macrophage activation) and IFNγ (100 ng / ml; PeproTech, USA) (for M1 macrophage activation) were used for additional cell induction. The samples were cultured for 6 days in the CO_2-incubator set to 7.5% CO_2 at 37 °C without additional stimulation and with the addition of cytokines for M1 and M2 macrophage activation.

Immunophenotyping of macrophages. Macrophage phenotyping was performed on day 6 of cultivation. To collect cells, a plate with a cell culture was placed on ice and held for 10 minutes, and then the cells were harvested using a cell scraper (Cell-scraper, USA). For immunophenotyping of macrophages, monoclonal antibodies to CD163, CD204, and CD206 (eBioscience, USA) were added.

Cell suspensions were measured on the Beckman Coulter CytoFLEX flow cytometer (Beckman Coulter, USA). The obtained data were analyzed using the CytExpert 2.0 software application (Beckman Coulter, USA).

SPSS Statistics 17.0 and Microsoft Excel were used for statistical analysis of the obtained results. The data were presented as the median and the interquartile range *Me* (Q_1–Q_3). To perform a comparative analysis, the non-parametric Mann – Whitney test with the Benjamini – Hochberg correction was applied. The results of statistical analysis were considered significant at $p < 0.05$.

RESULTS

Expression of CD163, CD204, and CD206 scavenger receptors on macrophages transformed *in vitro* from CD14+ blood monocytes in TB patients depending on the clinical form of the disease

The analysis of the expression of scavenger receptors on macrophages showed a significant increase in the number of CD163- and CD206-positive cells in TB patients compared with the group of healthy donors, regardless of the clinical form of the disease and sensitivity of *M. tuberculosis* to ATBD (Table 1, 2; Fig. 1, 2).

Table 1

The expression of scavenger receptors on macrophages in patients with pulmonary tuberculosis depending on the clinical form of the disease, %, *Me* (Q_1–Q_3)

Markers of macrophages	Groups of examined persons	Conditions for *in vitro* cultivation of macrophages		
		No stimulation	IL-4 stimulation	IFNγ stimulation
CD163	Healthy donors	12.43 (6.51–22.33)	4.11 (2.17–8.34) $p_3 = 0.011$	13.24 (7.41–16.71) $p_3 = 0.511$ $p_4 = 0.014$
	ITB patients	44.23 (24.14–64.35) $p_1 = 0.012$	48.55 (27.31–59.54) $p_1 = 0.015$	26.70 (14.74–38.02) $p_1 = 0.010$ $p_3 = 0.011$ $p_4 = 0.027$
	DTB patients	40.81 (25.42–61.27) $p_1 = 0.010$	26.30 (17.11–41.72) $p_1 = 0.025$ $p_2 = 0.027$ $p_3 = 0.011$	27.83 (16.01–34.73) $p_1 = 0.010$ $p_3 = 0.014$
CD204	Healthy donors	11.31 (6.75–20.14)	8.05 (4.11–17.76)	10.26 (7.11–19.33)
	ITB patients	24.52 (14.27–34.36) $p_1 = 0.041$	40.83 (24.35–59.21) $p_1 = 0.017$ $p_3 = 0.037$	32.19 (16.14–50.36) $p_1 = 0.010$ $p_3 = 0.013$
	DTB patients	9.56 (6.02–20.33) $p_2 = 0.014$	8.91 (5.63–21.30) $p_2 = 0.025$	19.62 (11.38–35.17) $p_1 = 0.017$ $p_2 = 0.011$ $p_3 = 0.045$ $p_4 = 0.037$
CD206	Healthy donors	17.16 (9.17–28.43)	13.4 (6.35–22.45)	4.41 (2.15–9.37) $p_3 = 0.017$ $p_4 = 0.035$
	ITB patients	57.59 (28.12–68.18) $p_1 = 0.014$	58.27 (27.01–66.22) $p_1 = 0.037$	46.31 (26.45–61.27) $p_1 = 0.020$
	DTB patients	33.01 (18.34–52.43) $p_1 = 0.021$ $p_2 = 0.021$	29.37 (19.17–44.36) $p_1 = 0.012$ $p_2 = 0.021$	23.44 (13.16–37.46) $p_1 = 0.037$ $p_2 = 0.014$ $p_3 = 0.012$

Note: the level of statistical significance of differences compared with healthy donors – p_1; in ITB patients – p_2; in *in vitro* cell cultivation with no stimulation – p_3; in *in vitro* cell cultivation with IL-4 (M2 stimulation) – p_4.

After adding IL-4 to the cell culture (M2 macrophage activation), the expression of CD163 in ITB patients did not significantly change in comparison with its value in the absence of cytokine stimulation. In the group of healthy donors, the number of CD163-positive macrophages in M2 macrophage activation was 3.2 times lower relative to the number of cells in M1 macrophage activation (when cells were induced

by IFNγ). In DTB patients, the CD163 expression on macrophages was almost 1.5 times lower than that in the absence of stimulation both in M1 and M2 macrophage activation (Table 1, Fig. 1).

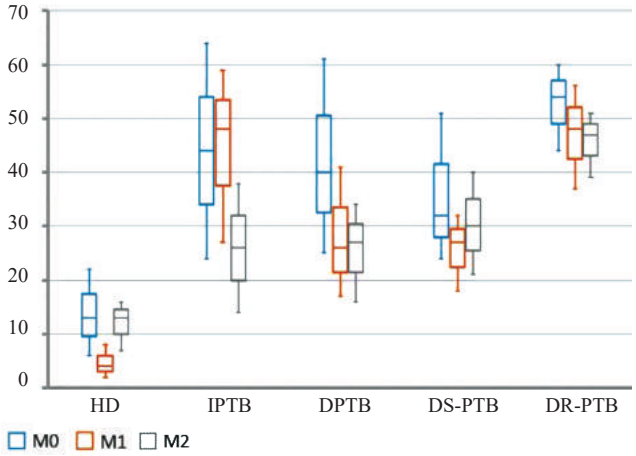

Fig. 1. The expression of the CD163 scavenger receptor on macrophages in patients with pulmonary tuberculosis, *Me* (Q_1–Q_3): HD – healthy donors, ITB – infiltrative pulmonary tuberculosis, DTB – disseminated pulmonary tuberculosis, DR TB – drug-resistant pulmonary tuberculosis, DS TB – drug-sensitive pulmonary tuberculosis, M0 – cell culture of macrophages without stimulation by cytokines, M1 – cell culture of macrophages stimulated by IFNγ, M2 – cell culture of macrophages stimulated by IL-4 (here and in Fig. 2, 3)

In cytokine stimulation, the number of CD206-positive macrophages in ITB patients did not change significantly in comparison with its basal level. In healthy donors and DTB patients, the expression of the CD206 molecule on macrophages significantly decreased in response to the IFNγ stimulation of cells, compared with the intact culture (Table 1, Fig. 2).

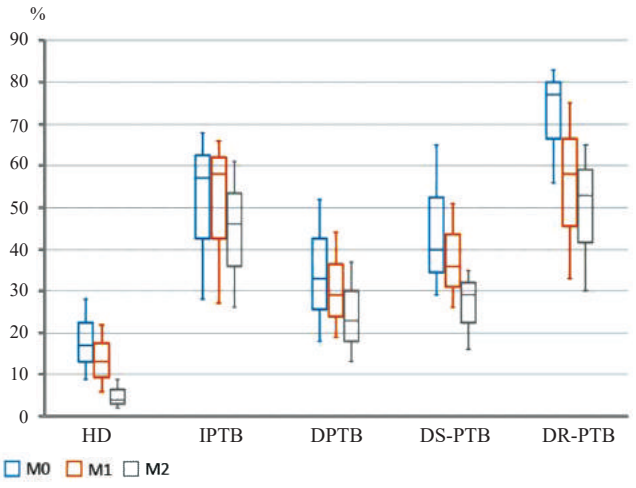

Fig. 2. The expression of the CD206 scavenger receptor on macrophages in patients with pulmonary tuberculosis, *Me* (Q_1–Q_3)

In patients with ITB, the induced expression of the CD204 scavenger receptor on macrophages more significantly increased after IL-4 stimulation of the cell culture than after IFNγ stimulation, compared with that in the intact cell culture. In the case of IL-4 stimulation, it increased by 5.1 times compared with its value in healthy donors and by 4.6 times compared with DTB patients. In DTB patients, the number of CD204-positive macrophages increased to a greater extent (by more than 2 times) in response to IFNγ stimulation of cells compared with that in the control group and after IL-4 stimulation (Table 1, Fig. 3).

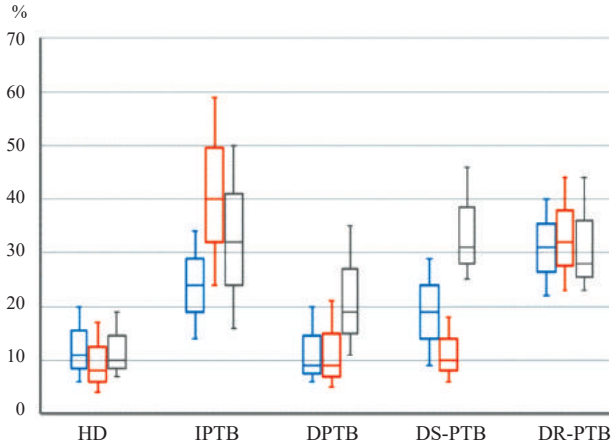

Fig. 3. The expression of the CD204 scavenger receptor on macrophages in patients with pulmonary tuberculosis, *Me* (Q_1–Q_3)

Expression of CD163, CD204, and CD206 scavenger receptors on macrophages transformed *in vitro* from CD14+ blood monocytes in TB patients depending on drug sensitivity of the pathogen to ATBD

The expression of M2 macrophage activation markers in TB patients, depending on the sensitivity of the pathogen to ATBD, was analyzed. It was found that the highest expression (basal and with stimulation by both cytokines) of the CD163 molecule on macrophages was observed in patients with DR TB. In DS TB patients, the cytokine-stimulated CD163 expression did not significantly change compared with the basal level, but it was higher (as in DR TB patients) than in healthy donors (Table 2, Fig. 1).

In cell cultivation without stimulation and with stimulation by cytokines, patients with DR TB also had the maximum number of CD206-positive macrophages. It was higher than in the control group and in patients with DS TB. However, in DR TB in both M1 and M2 stimulation by cytokines, the number of CD206+ macrophages was smaller than in the unstimulated cell culture (Table 2, Fig. 3).

Similarly, the highest expression of CD204 on macrophages was registered in DR TB. When cells were cultured without stimulation, the expression was higher than in the control group and in patients with DS TB. At the same time, it remained at the same level when cells were induced by cytokines. However, after adding IFNγ to the macrophage culture (M1 macrophage activation), patients with DS TB showed an increase in the expression of the CD204 receptor – by 1.6 times compared with its basal level and by 3.1 times compared with M2 macrophage activation and the control group (Table 2, Fig. 2).

Table 2

The expression of the scavenger receptors on macrophages in patients with pulmonary tuberculosis depending on the sensitivity of *M. tuberculosis* to ATBD, %, *Me* (Q_1–Q_3)

Markers of macrophages	Groups of examined persons	Conditions for *in vitro* cultivation of macrophages		
		No stimulation	IL-4 stimulation	IFNγ stimulation
CD163	Healthy donors	12.43 (6.51–22.33)	4.11 (2.17–8.34) $p_3 = 0.012$	13.24 (7.41–16.71) $p_4 = 0.015$
	DS TB patients	32.52 (24.45–51.23) $p_1 = 0.031$	27.25 (18.12–32.65) $p_1 = 0.012$	30.56 (21.65–40.28) $p_1 = 0.024$
	DR TB patients	54.23 (44.23–60.56) $p_1 = 0.021$ $p_2 = 0.012$	48.77 (37.56–56.44) $p_1 = 0.024$ $p_2 = 0.043$	47.32 (39.11–51.22) $p_1 = 0.035$ $p_2 = 0.044$
CD204	Healthy donors	11.31 (6.75–20.14)	8.05 (4.11–17.76)	10.26 (7.11–19.33)
	DS TB patients	19.23 (9.54–29.11) $p_1 = 0.032$	10.26 (6.23–18.25)	31.33 (25.4–46.12) $p_1 = 0.031$ $p_3 = 0.012$ $p_4 = 0.032$
	DR TB patients	31.23 (22.56–40.12) $p_1 = 0.034$ $p_2 = 0.011$	32.44 (23.56–44.36) $p_1 = 0.025$ $p_2 = 0.023$	28.56 (23.54–44.2) $p_1 = 0.037$
CD206	Healthy donors	17.16 (9.17–28.43)	13.40 (6.35–22.45)	4.41 (2.15–9.37) $p_3 = 0.017$ $p_4 = 0.035$
	DS TB patients	40.13 (29.14–65.45) $p_1 = 0.012$	36.45 (26.17–51.45) $p_1 = 0.027$	29.03 (16.54–35.47) $p_1 = 0.015$ $p_3 = 0.014$
	DR TB patients	77.36 (56.45–83.12) $p_1 = 0.031$ $p_2 = 0.022$	58.36 (33.47–75.16) $p_1 = 0.010$ $p_2 = 0.025$ $p_3 = 0.013$	53.27 (30.45–65.44) $p_1 = 0.014$ $p_2 = 0.042$ $p_3 = 0.014$

Note: the level of statistical significance of differences compared with values in healthy donors – p_1; in DS TB patients – p_2; in *in vitro* cell cultivation with no stimulation – p_3; in *in vitro* cell cultivation with IL-4 (M2 stimulation) – p_4.

DISCUSSION

High efficiency of innate immunity activation in TB plays a crucial role in the development of the disease and its outcomes. Abnormalities in the immune response induction are often associated with the development of tolerance to the antigen already at the stage of its presentation. In this case, instead of macrophage activation and differentiation into M1 cells, a tolerogenic and anti-inflammatory M2 phenotype is formed. Mobilization of monocytes and their entry into the systemic circulation from the bone marrow are always caused by an increased antigenic load and a need for resident macrophages for the immune system during lung inflammation. More and more studies on the macrophage population heterogeneity indicate that

a timely switch of the macrophage phenotype from the M1-like proinflammatory phenotype to the M2-like anti-inflammatory one and vice versa affects the clinical outcome of TB [17–20].

The analysis of the expression of scavenger receptors on macrophages showed, in general, an increase in the number of cells carrying markers of the M2 phenotype (CD163, CD204, and CD206) on their surface, regardless of the clinical form of the disease and sensitivity of *M. tuberculosis* (Table 1, 2, Fig. 1–3).

We registered the largest number of CD163-positive macrophages in ITB patients, especially in M2 macrophage activation. In case of M1 macrophage activation, on the contrary, the number of CD163+ macrophages decreased compared with that in the absence of cytokine stimulation of cells. In DR TB, the number of CD163-positive macrophages was higher than in DS TB in both the intact culture of cells and in the cells stimulated with IL-4 and IFNγ (Table 1, 2, Fig. 1). It is known that the hemoglobin scavenger CD163 receptor is expressed by monocytes and mainly by M2 macrophages [21]. The surface CD163 receptor on macrophages functions as an innate immunity receptor for recognizing patterns of bacterial pathogenicity. Its overexpression may be a mechanism to reduce an acute severe inflammatory response [22]. It is logical that macrophages expressing CD163 should have a regulatory and regenerative potential in order to timely suppress the immune response that damages tissues.

When evaluating the CD204 expression on macrophages in TB patients, we determined its highest intensity in ITB compared with DTB. In DTB, the CD204 expression increased only in M1 macrophage activation. Drug sensitivity or drug resistance of MBT did not affect the expression of the CD204 molecule – it increased in both cases (Table 1, 2, Fig. 2).

CD204 is a scavenger receptor A (SR-A). It is mainly expressed on macrophages, dendritic cells, and epithelial cells of the respiratory tract. It is a multifunctional receptor with a big ligand-binding potential [23, 24]. The CD204 molecule recognizes modified lipid proteins, apoptotic cells, and pathogen-associated molecules [25]. Studies of CD204 knockout mice have shown that the CD204 expression plays an important role in polarizing the differentiation of macrophages towards the M2 phenotype by inhibiting TLR signaling [26].

The CD206 molecule is a C-type lectin or mannose receptor type 1 (MR1), which is usually expressed on tissue macrophages, dendritic cells, and endothelial cells. It binds structures with a high mannose content on the surface of potentially pathogenic bacteria, viruses, and fungi [27]. The CD206 molecule plays an essential role in immune homeostasis. Cells in the microenvironment of malignant tumors have high expression of this receptor. An increase in CD206-positive tumor-associated macrophages is associated with a poor disease prognosis and indicates the development of chronic inflammation in metastatic niches [28]. In the examined patients, the CD206 expression on macrophages was the most significant in ITB and DR TB. However, in the latter, the number of CD206-positive cells decreased when the culture was induced with both M1 and M2 stimulators (Table 1, 2, Fig. 3).

There is evidence in the literature that the population of macrophages involved in the fight against *M. tuberculosis* is heterogeneous [29, 4]. Studies have examined various mechanisms by which the antigen transforms M1 macrophages into M2 macrophages with immunoregulatory activity, creating a favorable environment for its existence. The study conducted on a model of the staphylococcal lung infection in mice concluded that *Staphylococcus aureus* induced the Akt1 signaling pathway (Akt1 – protein kinase B), shifting the phenotype of macrophages from the anti-microbial M1 phenotype towards the functionally dormant M0 phenotype [30]. Another work showed that *M. tuberculosis* secretes LAM (lipoarabinomannan) and ESAT-6 virulence factors, which inhibit M1 macrophage activation by blocking maturation of phagolysosomes and activation of nuclear factor κB (NF-κB) [17].

Therefore, high expression of scavenger receptors on macrophages in pulmonary TB may be associated with predisposition of patients to the implementation of regenerative and anti-inflammatory functions of macrophages and their polarization towards the M2 phenotype.

CONCLUSION

Studying the mechanisms underlying the M1 or M2 macrophage activation is necessary for a deeper understanding of TB immunopathogenesis and the role of innate immune cells in protecting the body from MBT. The analysis of the expression of CD163, CD204, and CD206 scavenger receptors on macrophages allowed to make the following conclusion. In pulmonary TB, especially in DR TB and ITB, there are regulatory mechanisms that suppress the activation of innate immunity with polarization

of macrophages towards the M2 phenotype. It might cause immune deficiency induced by the pathogen.

REFERENCES

1. Davies L.C., Taylor P.R. Tissue-resident macrophages: then and now. *Immunology*. 2015;144(4):541–548. DOI: 10.1111/imm.12451.
2. Mills C.D. M1 and M2 macrophages: oracles of health and disease. *Crit. Rev. Immunol.* 2012;32(6):463–488. DOI: 10.1615/critrevimmunol. v32.i6.10.
3. Khan A., Singh V.K., Hunter R.L., Jagannath C. Macrophage heterogeneity and plasticity in tuberculosis. *J. Leukoc. Biol*. 2019;106(2):275–282. DOI: 10.1002/JLB.MR0318-095RR.
4. Guilliams M., Svedberg F.R. Does tissue imprinting restrict macrophage plasticity? *Review Nat. Immunol.* 2021;22(2):118–127. DOI: 10.1038/s41590-020-00849-2.
5. Cheah F.C., Presicce P., Tan T.L., Carey B.C., Kallapur S.G. Studying the effects of granulocyte-macrophage colony-stimulating factor on fetal lung macrophages during the perinatal period using the mouse model. *Front. Pediatr.* 2021;9:614209. DOI: 10.3389/fped.2021.614209.
6. Global tuberculosis report. Health Organization Report. Geneva, 2019. URL: https://www.who.int/teams/global-tuberculosis-programme/tb-reports/global-report-2019.
7. Global tuberculosis report World Health Organization Report. Geneva, 2018. URL: https://apps.who.int/iris/handle/10665/274453.
8. Leopold Wager C.M., Arnett E., Schlesinger L.S. Macrophage nuclear receptors: Emerging key players in infectious diseases. *PLoS Pathog.* 2019;15(3):e1007585. DOI: 10.1371/journal.ppat.1007585.
9. Santos J.H.A., Bührer-Sékula S., Melo G.C., Cordeiro-Santos M., Pimentel J.P.D., Gomes-Silva A. et al. Ascaris lumbricoides coinfection reduces tissue damage by decreasing IL-6 levels without altering clinical evolution of pulmonary tuberculosis or Th1/Th2/Th17 cytokine profile. *Rev. Soc. Bras. Med. Trop.* 2019;52:e20190315. DOI: 10.1590/0037-8682-0315-2019.
10. Zhai W., Wu F., Zhang Y., Fu Y., Liu Z. The Immune escape mechanisms of *Mycobacterium tuberculosis*. *Int. J. Mol. Sci.* 2019;20(2):340. DOI: 10.3390/ijms20020340.
11. Shim D., Kim H., Shin S.J. *Mycobacterium tuberculosis* infection-driven foamy macrophages and their implications in tuberculosis control as targets for host-directed therapy. *Front. Immunol.* 2020;11:910. DOI: 10.3389/fimmu.2020.00910.
12. Maler M.D., Nielsen P.J., Stichling N., Cohen I., Ruzsics Z., Wood C. et al. Role of the scavenger receptor MARCO in mediating adenovirus infection and subsequent innate responses of macrophages. *mBio.* 2017;8(4):e00670–17. DOI: 10.1128/mBio.00670-17.
13. Gayer F.A., Reichardt S.D., Bohnenberger H., Engelke M., Reichardt H.M. Characterization of testicular macrophage subpopulations in mice. *Immunol. Lett*. 2022;243:44–52. DOI: 10.1016/j.imlet.2022.02.003.
14. Prabhu Das M.R., Baldwin C.L., Bollyky P.L., Bowdish D.M.E., Drickamer K., Febbraio M. et al. A consensus definitive classification of scavenger receptors and their roles in health and disease. *J. Immunol.* 2017;198(10):3775–3789. DOI: 10.4049/jimmunol.1700373.
15. Wong C.K., Smith C.A., Sakamoto K., Kaminski N., Koff J.L., Goldstein D.R. Aging impairs alveolar macrophage phagocytosis and increases influenza-induced mortality in mice. *J. Immunol.* 2017;199(3):1060–1068. DOI: 10.4049/jimmunol.1700397.
16. Wolfsberger J., Sakil H.A.M., Zhou L., van Bree N., Baldisseri E., Ferreira S.S. et al. TAp73 represses NF-κB-mediated recruitment of tumor-associated macrophages in breast cancer. *Proc. Natl. Acad. Sci. U S A.* 2021;118(10):e2017089118. DOI: 10.1073/pnas.2017089118.17.
17. Pisu D., Huang L., Narang V., Theriault M., Lê-Bury G., Lee B. et al. Single cell analysis of M. tuberculosis phenotype and macrophage lineages in the infected lung. *J. Exp. Med*. 2021;218(9):e20210615. DOI: 10.1084/jem.20210615.
18. Rocha D.M.G.C., Magalhães C., Cá B., Ramos A., Carvalho T., Comas I. et al. Heterogeneous streptomycin resistance level among mycobacterium tuberculosis strains from the same transmission cluster. *Front. Microbiol*. 2021;12:659545. DOI:10.3389/fmicb.2021.659545.
19. Marino S., Cilfone N.A., Mattila J.T., Linderman J.J., Flynn J.L., Kirschner D.E. Macrophage polarization drives granuloma outcome during Mycobacterium tuberculosis infection. *Infect. Immun.* 2015;83(1):324–338. DOI: 10.1128/IAI.02494-14.
20. Weaver L.K., Hintz-Goldstein K.A., Pioli P.A., Wardwell K., Qureshi N., Vogel S.N. et al. Pivotal advance: activation of cell surface Toll-like receptors causes shedding of the hemoglobin scavenger receptor CD163. *J. Leukoc. Biol.* 2006;80(1):26–35. DOI: 10.1189/jlb.1205756.
21. Fabriek B.O., van Bruggen R., Deng D.M., Ligtenberg A.J.M., Nazmi K., Schornagel K. et al. The macrophage scavenger receptor CD163 functions as an innate immune sensor for bacteria. *Blood.* 2009;113(4):887–892. DOI: 10.1182/blood-2008-07-167064.
22. Dieudonné A., Torres D., Blanchard S., Taront S., Jeannin P., Delneste Y. et al. Scavenger receptors in human airway epithelial cells: role in response to double-stranded RNA. *PLoS One.* 2012;7(8):e41952. DOI: 10.1371/journal.pone.0041952.
23. Canton J., Neculai D., Grinstein S. Scavenger receptors in homeostasis and immunity. *Nat. Rev. Immunol.* 2013;13(9):621–634. DOI: 10.1038/nri3515.
24. Kubota K., Moriyama M., Furukawa S., Rafiul H.A.S.M., Maruse Y., Jinno T. et al. $CD163^{+}CD204^{+}$ tumor-associated macrophages contribute to T cell regulation via interleukin-10 and PD-L1 production in oral squamous cell carcinoma. *Sci. Rep.* 2017;7(1):1755. DOI: 10.1038/s41598-017-01661-z.
25. Komohara Y., Takemura K., Lei X.F., Sakashita N., Harada M., Suzuki H. et al. Delayed growth of EL4 lymphoma in SR-A-deficient mice is due to upregulation of nitric oxide and interferon-gamma production by tumor-associated macrophages. *Cancer Sci.* 2009;100(11):2160–2166. DOI: 10.1111/j.1349-7006.2009.01296-x.
26. Barreto-Bergter E., Figueiredo R.T. Fungal glycans and the innate immune recognition. *Front. Cell Infect. Microbiol.* 2014;4:145. DOI: 10.3389/fcimb.2014.00145.
27. Azad A.K., Rajaram M.V., Schlesinger L.S. Exploitation of the macrophage mannose receptor (CD206) in infectious disease diagnostics and therapeutics. *J. Cytol. Mol. Biol.* 2014;1(1):1000003. DOI: 10.13188/2325-4653.1000003.

28. Kaku Y., Imaoka H., Morimatsu Y., Komohara Y., Ohnishi K., Oda H. et al. Overexpression of CD163, CD204 and CD206 on alveolar macrophages in the lungs of patients with severe chronic obstructive pulmonary disease. *PLoS One.* 2014;9(1):e87400. DOI: 10.1371/journal.pone.0087400.
29. Weiss G., Schaible U.E. Macrophage defense mechanisms against intracellular bacteria. *Immunol. Rev.* 2015;264(1):182–203. DOI: 10.1111/imr.12266.
30. Xu F., Kang Y., Zhang H., Piao Z., Yin H., Diao R. et al. Akt1-mediated regulation of macrophage polarization in a murine model of Staphylococcus aureus pulmonary infection. *J Infect. Dis.* 2013;208(3):528–538. DOI: 10.1093/infdis/jit177.

Authors contribution

Churina E.G. – design of the study, review of the literature, statistical processing and interpretation of research results, drafting of the manuscript. Popova A.V. – preparation of samples, carrying out of immunomagnetic separation and flow cytometry, drafting of the manuscript. Urazova O.I. – material and technical assistance in carrying out the laboratory research, interpretation of results, drafting and translation of the manuscript. Patysheva M.R. – carrying out of immunomagnetic separation and flow cytometry, consulting assistance in designing the study. Kolobovnikova Yu.V. – interaction with patients, consultations on phthisiological and pulmonological aspects of the study. Chumakova S.P. – interaction with patients, collection of the biomaterial.

Authors information

Churina Elena G. – Dr. Sci. (Med.), Professor, Pathophysiology Division, Siberian State Medical University; Professor, Department of Natural Compounds, Pharmaceutical and Medicinal Chemistry, National Research Tomsk State University, Tomsk, Lena1236@yandex.ru, 0000-0002-8509-9921

Popova Anjelika V. – Post-Graduate Student, Pathophysiology Division, Siberian State Medical University, Tomsk, anjelika.sitnikova@yandex.ru.

Urazova Olga I. – Dr. Sci. (Med.), Professor, Corresponding Member of the RAS, Head of the Pathophysiology Division, Siberian State Medical University, Tomsk, urazova72@yandex.ru, 0000-0002-9457-8879

Patysheva Marina R. – Junior Researcher, Laboratory for Cancer Progression Biology, Cancer Research Institute, Tomsk NRMC; Junior Researcher, Laboratory for Translational Cell and Molecular Biomedicine, National Research Tomsk State University, Tomsk, marinapatysh@gmail.com, 0000-0001-5758-7330

Kolobovnikova Yulia V. – Dr. Sci. (Med.), Professor, Pathophysiology Division, Siberian State Medical University, Tomsk, kolobovnikova.julia@mail.ru, 0000-0001-7156-2471

Chumakova Svetlana P. – Dr. Sci. (Med.), Professor, Pathophysiology Division, Siberian State Medical University, Tomsk, chumakova_s@mail.ru, 0000-0003-3468-6154

(✉) **Churina Elena G.,** Lena1236@yandex.ru

Received 24.04.2022;
approved after peer review 06.05.2022;
accepted 09.06.2022

УДК 616.24:[616.98:578.834.1-036.21]-022.14-073.432.1
https://doi.org/10.20538/1682-0363-2022-4-150-159

Lung ultrasound in the diagnosis of COVID-19-associated pneumonia

Balabanova A.A., Kurazhov A.P., Zavadovskaya V.D.

Siberian State Medical University
2, Moscow Trakt, Tomsk, 634050, Russian Federation

ABSTRACT

Over the past decades, lung ultrasound in the diagnosis of lung diseases has become widespread. Ultrasound examination has a number of advantages (no radiation exposure, real-time imaging, clear visualization of the subpleural lung regions and costophrenic angles), which make it possible to use ultrasound to monitor the dynamics of pneumonia in children and pregnant women. Currently, in the context of the COVID-19 pandemic, lung ultrasound is widely used due to its high diagnostic efficiency, which is comparable with classical radiography and X-ray computed tomography (CT) by a number of parameters.

The article describes the method of lung ultrasound and the radiographic pattern of COVID-19-associated pneumonia. It also provides a review of the literature, according to which the severity of pneumonia was determined, depending on the radiographic pattern, and the need for a lung ultrasound was identified.

The article indicates that information on assessment of the radiographic pattern of the lungs at runtime in different variants of the course of coronavirus infection, as well as many methodological issues, including the frequency of second-look lung ultrasound, has not been sufficiently studied.

Keywords: ultrasound, pneumonia, COVID-19, interstitial syndrome, white lung, consolidation, B-lines, pleural line

Conflict of interest. The authors declare the absence of obvious or potential conflicts of interest related to the publication of this article.

Source of financing. The authors state that they received no funding for the study.

For citation: Balabanova A.A., Kurazhov A.P., Zavadovskaya V.D. Lung ultrasound in the diagnosis of COVID-19-associated pneumonia. *Bulletin of Siberian Medicine.* 2022;21(4):150–159. https://doi.org/10.20538/1682-0363-2022-4-150-159.

Ультразвуковая диагностика COVID-19-ассоциированных пневмоний

Балабанова А.А., Куражов А.П., Завадовская В.Д.

Сибирский государственный медицинский университет (СибГМУ)
Россия, 634050, г. Томск, Московский тракт, 2

РЕЗЮМЕ

В течение последних десятилетий ультразвуковая диагностика заболеваний легких получила широкое распространение. Ультразвуковое исследование (УЗИ) имеет ряд преимуществ: отсутствие лучевой нагрузки, получение изображения в режиме реального времени, отчетливая визуализация субплевральных отделов легких и реберно-диафрагмальных синусов, которые дают возможность использовать ультразвук

✉ *Kurazhov Aleksei P.,* kurazhovap@mail.ru

для динамики пневмонии у детей и беременных женщин. В условиях пандемии COVID-19 УЗИ легких получило широкое применение в связи с высокой диагностической эффективностью, сопоставимой по ряду показателей с классической рентгенографией и рентгеновской компьютерной томографией.

Излагается методика УЗИ легких, ультразвуковая картина COVID-19-ассоциированных пневмоний. Предоставлен обзор литературы, согласно которой выявлены степени тяжести пневмонии в зависимости от ультразвуковой картины и необходимость использования УЗИ легких.

Указано, что недостаточно изучены информация об оценке ультразвуковой картины легких в динамике при различных вариантах течения коронавирусной инфекции, а также многие вопросы методического характера, включая периодичность и частоту динамического УЗИ легких.

Ключевые слова: ультразвуковое исследование, пневмония, COVID-19, интерстициальный синдром, белое легкое, консолидация, В-линии, плевральная линия

Конфликт интересов. Авторы декларируют отсутствие явных и потенциальных конфликтов интересов, связанных с публикацией настоящей статьи.

Источник финансирования. Авторы заявляют об отсутствии финансирования при проведении исследования.

Для цитирования: Балабанова А.А., Куражов А.П., Завадовская В.Д. Ультразвуковая диагностика COVID-19-ассоциированных пневмоний. *Бюллетень сибирской медицины.* 2022;21(4):150–159. https://doi.org/10.20538/1682-0363-2022-4-150-159.

INTRODUCTION

Coronavirus disease 2019 (COVID-19) [1–3] is a potentially severe acute respiratory infection caused by SARS-CoV-2 (2019-nCoV) [4]. It is a dangerous disease [3], which can occur both as mild [5, 6] and severe [7] acute respiratory infection. The most common complication of the disease is viral pneumonia, which can result in acute respiratory distress syndrome and subsequent acute respiratory failure, most often requiring oxygen therapy and respiratory support [8].

Medical imaging methods are used to identify COVID-19-associated pneumonias and their complications, to carry out differential diagnosis with other lung diseases, to determine severity of the disease and its progression, and to assess therapy effectiveness [6]. The main medical imaging methods for detecting chest pathologies in patients with suspected or confirmed COVID-19-associated pneumonia include lung computed tomography (CT), plain chest radiography (CR), and lung and pleural ultrasound (US).

CT is the gold standard imaging modality for examining patients with suspected or confirmed COVID-19-associated pneumonia. For example, it has been determined that specificity of CT versus US and CR can reach 100% in certain patient groups [9]. At the same time, it should be taken into account that many infectious and non-infectious diseases, such as various HIV-associated lung lesions and interstitial lung disease, can reduce CT specificity in the diagnosis of COVID-19-associated lung lesions [10, 11]. Typical CT changes in the lungs in COVID-19-associated pneumonia are bilateral subpleural ground-glass opacities in the lung tissue or lung consolidation areas of an irregular, sometimes rounded shape with predominantly peripheral distribution in the lungs, which emerge in case of bacterial coinfection [12].

In the Russian Federation, according to the Temporary Guidelines of the Russian Society of Radiologists and Russian Association of Specialists in Ultrasound Diagnostics in Medicine, in the context of the COVID-19 pandemic, the so-called "empirical" visual scale for a rapid assessment of pathological CT changes in the lungs is recommended. It is based on the visual assessment of the approximate volume of the damaged lung tissue and the nature of lung changes [13]. This scale has 5 grades (Table 1).

Table 1

Visual scale for assessing the degree of lung damage detected on CT

Degree of lung damage	Characteristics
CT-0	Normal pattern and the absence of CT signs of viral pneumonia despite typical clinical manifestations and relevant epidemiological history

Table 1 (continued)

Degree of lung damage	Characteristics
CT-1	Mild degree – ground-glass opacities. Lung parenchyma involvement ≤ 25%
CT-2	Moderate degree – ground-glass opacities. Lung parenchyma involvement of 25–50%
CT-3	Severe degree – ground-glass opacities, lung consolidation areas. Lung parenchyma involvement of 50–75%
CT-4	Critical degree – diffuse ground-glass opacities and lung consolidation in combination with reticular changes. Hydrothorax. Lung parenchyma involvement ≥ 75%.

To date, this scale is the mainstay for determining the severity of morphological changes in the lungs in patients with COVID-19-associated pneumonia. Its high efficiency has been proven by its wide use in clinical practice. The only limiting factor for CT is the impossibility of its use in intensive care units and mechanically-ventilated patients.

Another frequently used diagnostic radiology technique in detecting COVID-19-associated pneumonia is plain chest radiography (CR) [14]. This method has lower diagnostic efficiency, but due to its greater availability and lower cost, it has become widespread during the COVID-19 pandemic [15]. Typical CR changes in COVID-19 are multiple diffuse, peripheral, irregularly shaped opacities, localized mainly in the lower lobes of both lungs [16].

Over the past decades, one of the topical issues in diagnostic US has been the assessment of its information value in lung diseases [17–20]. It has been determined that this modality has a high diagnostic value in the assessment of some lung diseases and, in certain clinical situations, outperforms CR in sensitivity and specificity [21]. For example, the results of the study by Russian researchers indicated greater accuracy of US compared with CR in the diagnosis of pneumonia in children, and the same authors provided evidence that in some cases US can compete with CT, for example, in the diagnosis of lung abscess [22]. In addition, lung US has been quite widely used in monitoring pathologies associated with lung tissue, including cardiogenic pulmonary edema, pneumothorax, pleural effusion, atelectasis, pneumonia, and peripheral lung nodules [23–27]. A number of other publications also indicate that, in recent decades, US has been in great demand in the diagnosis of various lung diseases, including, in addition to the above, emphysema and pleural diseases [17–19, 28–30].

It is believed that lung US in patients with suspected or confirmed COVID-19-associated pneumonia is an additional imaging method that does not replace or exclude CR and CT as traditional diagnostic modalities with high information value, proven by many years of clinical practice. In this regard, lung US is not included in the clinical guidelines and standards for the diagnosis and treatment of community-acquired pneumonia [5, 13]. This is partly because the effectiveness of US is largely dependent on the experience and qualifications of the doctor performing the study.

Many researchers provide evidence that US can compete in accuracy with CT in the diagnosis of COVID-19-associated pneumonia [31, 32], and in some aspects it outperforms CR [33]. So, according to a study by R. Gibbons et al. [33], the sensitivity of US in detecting intrapulmonary changes in COVID-19 was 97.6%, while that of CR was only 69.9%. However, lung US was less specific than CR (33.3 and 44.4%, respectively). This study included 143 patients aged 18 years and older with symptoms of COVID-19 (all registered patients had a body temperature of 38 °C or higher, a heart rate of 100 beats per minute or higher, a respiratory rate of 16 breaths per minute or more, SpO_2 less than 94% with cough, dyspnea, myalgia, malaise, ageusia, and anosmia).

It was also previously found that lung US makes it possible to control the course of pneumonia directly at the bedside, including mechanically-ventilated patients [34]. An additional advantage of lung US due to the absence of radiation exposure is the ability to examine pregnant women [35], who may have a more severe course of COVID-19-associated pneumonia [28, 36, 37]. Lung US reveals initial signs of lung damage caused by SARS-CoV-2, which is especially important when triaging patients in the emergency rooms of medical institutions. An increase in the intensity of interstitial changes in the lungs up to the emergence of a white lung in the US scan may be a predictor of a need for intubation and transfer of patients to mechanical ventilation [31]. In such cases, lung US strongly affects the treatment strategy, reducing decision-making time, which is crucial, since the condition of patients with COVID-19 can deteriorate rapidly [34].

LUNG ULTRASOUND TECHNIQUE

Routine lung US is performed using the B-mode with a microconvex transducer with a frequency of 5 MHz. At the same time, it is possible to use linear or

convex transducers in the frequency ranges of 5–15 and 3–5 MHz, respectively [17, 38]. The linear transducer is used to detail and better visualize pleural sliding and search for alveolar consolidation [18]. Depending on the severity of the patient's condition, the examination is performed in an upright, sitting or lying position. It is believed that if the patient is mechanically ventilated or in the prone position, then it is necessary to scan the accessible chest areas and note this feature of the US examination in its protocol [39].

To date, a standard technique for lung US has been developed and is actively used [40]. In 2008, D. Lichtenstein developed the so-called BLUE protocol, which is an algorithmic approach to examining the lungs in acute respiratory pathology [18]. Its advantages are simplicity and speed, since it allows to get the main diagnostic information with the maximum ease of performing the study in a short period of time. The basic principle of the BLUE protocol is a simple sonographic evaluation of the lungs. If pulmonary embolism (PE) is suspected, this protocol is extended by a simplified study of lower extremity veins and echocardiography performed to detect extrapulmonary thrombi as possible causes of PE. The study of only anterior lung regions makes it possible to confirm or exclude such conditions as pneumothorax and pulmonary edema within a few seconds. In the absence of US signs of pneumothorax and pulmonary edema, further, according to the diagnostic algorithm, a study of the lower extremity veins and lateral and posterior lung regions is performed in order to diagnose possible pulmonary infarction and pleural effusion [18]. Sonographic signs of PE are pulmonary consolidation, predominantly wedge-shaped or rounded, fluid located directly above the subpleural lung lesion, and local interstitial changes [41].

According to the BLUE protocol [18], when performing a routine lung US examination to diagnose intrapulmonary lesions, the chest is arbitrarily divided into 12 zones. On the right and left, the chest surface is divided into anterior, lateral, and posterior regions, each of which, in turn, is subdivided into upper and lower zones (Table 2). Then the US transducer is placed perpendicular to the ribs or parallel to the intercostal spaces, and all regions accessible for inspection are scanned [18].

To minimize the risk of COVID-19 for medical personnel, lung US is preferably performed directly in the patient's ward quickly and according to a pre-verified protocol, using a portable device. In the study of patients with mild or moderate disease severity, to reduce the time of the examination, lung US is performed in a vertical, hands-behind-the-head position of the patient.

Table 2

Zones and anatomical landmarks in lung US

Surface	Vertical borders	Zones	Horizontal borders
Anterior	From the parasternal to the anterior axillary line	Upper	From the supraclavicular region to the IV rib
		Lower	From the IV rib to the diaphragmatic sinus
Lateral	From the anterior axillary to the posterior axillary line	Upper	From axillary fossa to the IV rib
		Lower	From the IV rib to the diaphragmatic sinus
Posterior	From the posterior axillary to the paravertebral line	Upper	From the II rib to the inferior angle of the scapula
		Lower	From the inferior angle of the scapula to the diaphragmatic sinus

NORMAL LUNG US PATTERN

In normal conditions, lung tissue is visualized in the intercostal spaces and is represented on diagnostic images by multiple parallel hyperechoic lines (called A-lines) due to lung sliding and movements of the visceral pleura [18]. A-lines are located directly below the pleural line, which, in turn, has the form of a thin hyperechoic strip in normal conditions (Fig. 1). Also, in normal conditions, US examination reveals single B-lines (no more than 3 in 1 intercostal space), which are linear vertical hyperechoic comet tail artifacts, coming from the pleural line [17, 18] (Fig. 2). B-lines are formed due to reverberation between the visceral pleura and air in the alveoli on the lung surface and because of thickening of the subpleural interlobular septa [18].

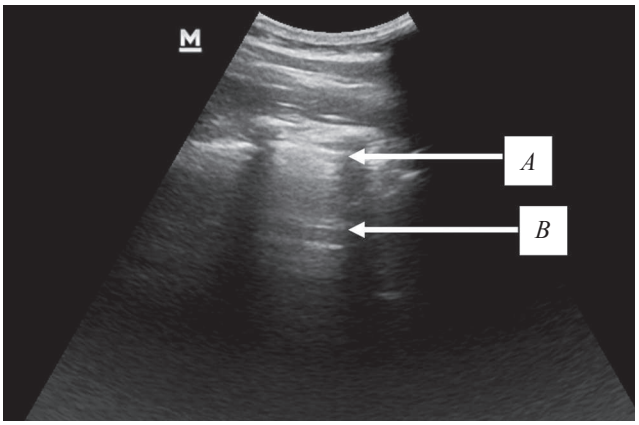

Fig. 1. US pattern of unchanged lung tissue: *A* – pleural line, *B* – multiple parallel white A-lines

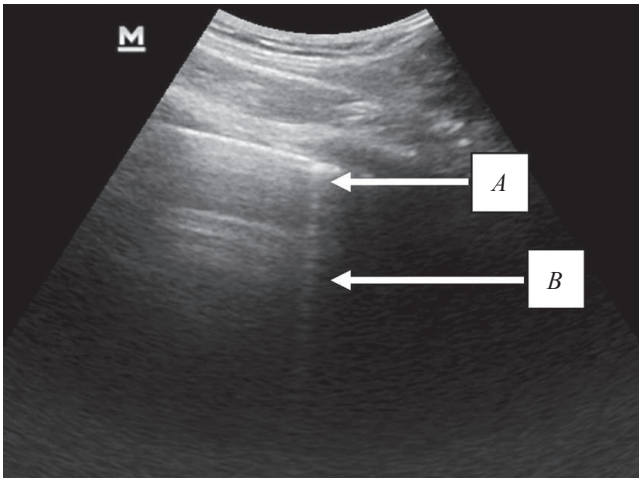

Fig. 2. US pattern of unchanged lung tissue with a single vertical B-line: *A* – pleural line, *B* – single B-line

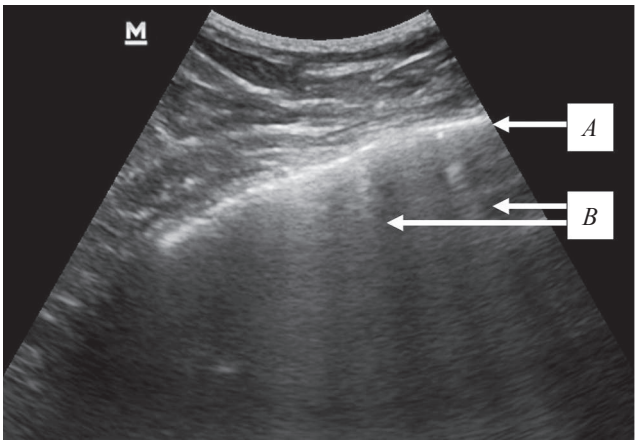

Fig. 3. US pattern of the interstitial syndrome in a patient with COVID-19-associated pneumonia: *A* – thickened pleural line with uneven contours, *B* – multiple vertical B-lines

US PATTERNS OF LUNG CHANGES IN PATIENTS WITH COVID-19-ASSOCIATED PNEUMONIA

For the first time, US patterns of lung lesions in COVID-19 were described by scientists from China [42]. According to their results, the main US signs of lung damage in COVID-19-associated pneumonia were: 1) thickening and uneven costal pleura; 2) different variants of B-patterns in the form of focal, confluent or multifocal B-lines; 3) subpleural and lobar lung consolidation, sometimes with air bronchograms (hyperechoic bright elements representing air trapped in the bronchioles); 4) small rare pleural effusion [42].

To date, it is believed that qualitative US signs of lung tissue damage in COVID-19-associated pneumonia are: 1) interstitial lung disease, 2) white lung, and 3) lung consolidation [43, 44] (Fig. 3–5).

The US pattern of interstitial lung disease is visualization of more than three vertical B-lines in one intercostal space. It is believed that the interstitial syndrome is a consequence of an infectious and inflammatory process that affects the interstitium [45]. In this case, B-lines are usually more pronounced in the lower zones with the same distribution on both sides, and the anterior and upper lateral lung zones are affected to a lesser extent. Besides, in interstitial lung disease, in addition to multiple B-lines, lung US reveals thickening of the pleural line (Fig. 3) [18]. This syndrome occurs due to local changes in the acoustic properties of the lung, caused by changes in the density and subpleural interlobular septa thickening [46–48].

The US pattern of the white lung is commonly understood as visualization of multifocal confluent B-lines, since it was found that an increase in their number reflects an increase in the amount of extravascular lung water, which is observed in interstitial pulmonary edema [49, 50]. Diffuse white lung is characterized by the alveolar – interstitial syndrome, which implies both alveolar and interstitial pulmonary edema [18] (Fig. 4).

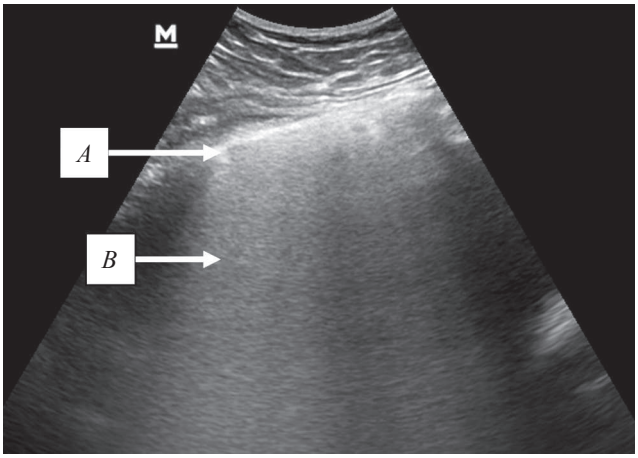

Fig. 4. US pattern of the white lung in a patient with COVID-19-associated pneumonia: *A* – thickened pleural line, *B* – multiple merging vertical B-lines

The alveolar – interstitial syndrome has no physical basis and is well detected by CT scan, as well as by lung US [51–53]. The alveolar – interstitial syndrome occurs in many pathological conditions, including cardiogenic pulmonary edema, bacterial, viral and fungal pneumonia, and chronic interstitial lung disease during an exacerbation [21, 51, 53].

In addition to the visualization of multifocal confluent B-lines, lung US detects an uneven, thickened, interrupted pleural line. This also includes visualization of single hypoechoic areas in the subpleural regions of the lungs corresponding to the alveoli completely filled with fluid [46–48].

Lung consolidation occurs when inflammation spreads to the subpleural lung areas and sonographically manifests itself as uneven thickening and discontinuity of the costal pleura. In addition, hypoechoic areas appear in the subpleural lung regions, which are formed due to the filling of the alveoli with fluid (Fig. 5). The emergence of these hypoechoic areas indicates a loss of lung tissue airiness. Acoustic properties of the lungs become the same as in soft tissues, significantly different from the lungs containing air [46–48].

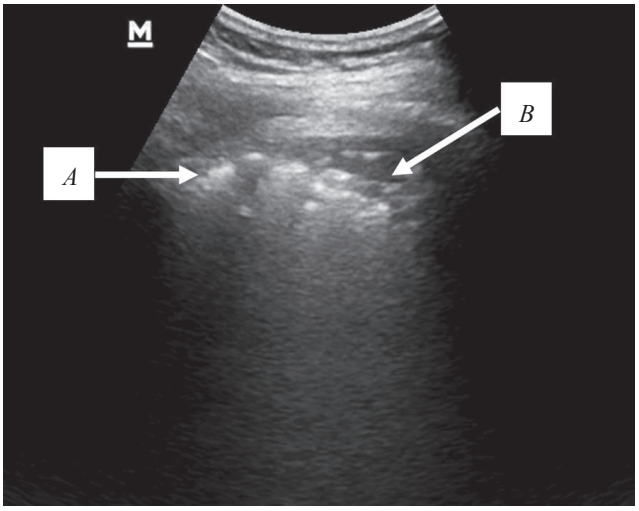

Fig. 5. US pattern of lung consolidation in a patient with COVID-19-associated pneumonia: *A* – thickened interrupted pleural line, *B* – hypoechoic areas in the subpleural lung regions

A study by Chinese scientists [54] showed that in patients with confirmed severe SARS-CoV-2 infection, bacterial and fungal coinfection develops in 25.5 and 10.9% of cases, respectively. In studies by Italian scientists [55], it was found that in 16,654 patients who died from COVID-19, bacterial and fungal coinfection occurred in 11% of cases.

When bacterial coinfection develops, typical US signs of pneumonia are lung consolidation, air bronchogram, pleural effusion, subpleural destruction foci, and compressive atelectasis in combination with pleural effusion [56–58] (Fig. 6).

Another direction of research in the use of US in the diagnosis of COVID-19-associated pneumonia is developing US semiotics of lung damage, depending on the stage of the disease. So, Q.Y.Peng et al. [42] revealed certain correlations of the US pattern with stages of pneumonia caused by SARS-CoV-2 (Table 3).

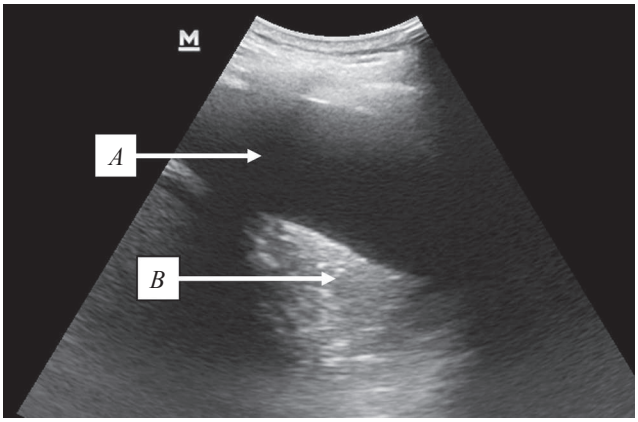

Fig. 6. US pattern of compressive atelectasis in the lower lung regions combined with pleural effusion in a patient with COVID-19-associated pneumonia complicated by bacterial coinfection: *A* – pleural effusion, *B* – area of compressive atelectasis

Table 3

US pattern of lung tissue damage in COVID-19-associated pneumonia depending on the disease severity according to Q.Y. Peng et al. [42]

Stages of pneumonia	US pattern
Initial stage or mild form	Unevenly distributed focal B-lines and an unevenly thickened pleural line are visualized
Stage of progression or moderate form	The number of B-lines in the affected lung zones increases, primarily in the basal lung regions, and then it spreads to other lung zones. The number of B-lines increases and they merge.
Severe form	Lung consolidation areas are visualized. Lung «hepatization» is noted, and pleural effusion emerges
Resolution stage	Reduction of the number of B-lines, emergence of A-lines in the affected lung area

Apart from identifying qualitative US signs of lung damage in COVID-19, attempts were made to perform a semi-quantitative assessment of pathological lung changes in this disease. For example, G. Soldati et al. proposed a scoring scale for assessing the severity of pneumonia caused by SARS-CoV-2, according to lung US data [58]. In accordance with this scale, a semi-quantitative assessment of the degree of lung damage is performed on the scale from 0 to 3 for each of the 12 examined areas (Table 4) [58].

Table 4

US pattern of lung tissue damage in COVID-19-associated pneumonia depending on the degree of lung damage according to G. Soldati et al. [58]

Degree of lung damage	US pattern
0	Normal, the pleural line is smooth and continuous, A-lines are visualized
1	The pleural line has serrated margins; three or more vertical B-lines are visualized under the altered pleural line in one zone
2	The pleural line is interrupted; under the altered pleural line, lung consolidation areas of different sizes are visualized; below them, multiple confluent B-lines (white lung) are detected
3	In the scanned area, increased white lung is detected with or without larger consolidation areas

In this paper [58], the average scores calculated according to the method proposed by the authors was 29.2 ± 7.3 and 20.4 ± 8.5 in patients with and without deterioration of the clinical condition, respectively. Therefore, when conducting the univariate and multivariate analyses, it was found that the total score calculated from the US data was directly associated with the likely deterioration of the patient's condition. Moreover, an overall mean US score above 24 was associated with an almost 6-fold increase in the odds for the deterioration of the patient's condition.

Another foreign study [39] showed that lung US in patients with COVID-19 can be used as a predictor of the disease course and outcome. In this work [39], lung US was performed only in six zones (anterior, anterolateral, and posterolateral on both sides), since the examined patients were in the intensive care unit, and to interpret the US data, a scoring scale for the assessment of the lung damage severity was also proposed (Table 5).

Table 5

US pattern of lung damage in COVID-19-associated pneumonia depending on the degree of severity according to Y. Lichter et al. [39]

Degree of lung damage	US pattern
0	Normal, A-lines are visualized due to normal lung aeration
1	Three or more vertical B-lines are visualized in one zone due to a moderate loss of lung aeration; the pleural line is altered
2	Multiple confluent B-lines are visualized due to a severe loss of lung aeration; the pleural line is altered
3	Lung consolidation areas are visualized; the pleural line is altered

In this study [39], the median scores for patients with mild, moderate, and severe lung damage were 12, 19, and 23, respectively. As a result, the authors of this study obtained a survival curve for patients with COVID-19-associated pneumonia, based on which patients with a score of more than 18 had a 2.6-fold higher mortality risk compared with mortality in patients with a lower score [39].

In turn, another study [59] demonstrated that lung US in the diagnosis of COVID-19 associated pneumonia is comparable to chest CT in terms of sensitivity, which is 93–94%. However, given that lung US can only assess peripheral lung areas [60], this method turned out to have low specificity (less than 50%). In addition, lung US is limited when used in obese patients [61] and depends on the experience and skill of the operator [62].

At the same time, a poorly studied field of lung US in COVID-19-associated pneumonia is a dynamic assessment of the lung sonographic pattern in different forms of coronavirus infection, as well as many methodological issues, including the frequency of second-look lung US.

CONCLUSION

Therefore, in the context of the COVID-19 pandemic, lung US plays an essential role in the diagnosis of COVID-19-associated lung lesions caused by SARS-CoV-2 due to its relatively high diagnostic efficiency (which is comparable in a number of parameters to that of CR and CT) and a possibility of examining non-transported patients and patients with reduced mobility (including pregnant women) during their stay in specialized medical institutions in the absence of radiation exposure. Lung US can also be used as a predictor of the course and outcome of COVID-19-associated pneumonia. At the same time, US patterns of lung damage in this disease and practical methodological aspects of US application require more in-depth study and clarification.

REFERENCES

1. Khachfe H.H., Chahrour M., Sammouri J., Salhab H.A. An epidemiological study on COVID-19: a rapidly spreading disease. *Cureus.* 2020;12(3):e7313. DOI: 10.7759/cureus.7313.
2. Zhu N., Zhang D., Wang W., Li X., Yang B., Song J. et al. *N. Engl. J. Med*. 2020;38(8):727–733. DOI: 10.1056/NEJMoa2001017.
3. Coronaviridae Study Group of the International Committee on Taxonomy of Viruses. The species Severe acute respiratory syndrome-related coronavirus: classifying 2019-nCoV and

naming it SARS-CoV-2. *Nat. Microbiol*. 2020;5(4):536–544. DOI: 10.1038/s41564-020-0695-z.
4. Heymann D.L., Shindo N. COVID-19: what is next for public health? *The Lancet.* 2020;395(10224):542–545. DOI: 10.1016/S0140-6736(20)30374-3.
5. Prevention, diagnosis and treatment of novel coronavirus infection (COVID-19). Temporary guidelines. Ministry of Health of the Russian Federation (September 3, 2020). 2020:227 (in Russ.).
6. Li K., Fang Y., Li W., Pan C., Qin P., Zhong Y. et al. CT image visual quantitative evaluation and clinical classification of coronavirus disease (COVID-19). *Eur. Radiol*. 2020;30(8):4407–4416. DOI: 10.1007/s00330-020-06817-6.
7. Avdeev S.N., Tsareva N.A., Merzhoeva S.N., Trushenko N.V., Yaroshetskiy A.I. Practical recommendations for oxygen therapy and respiratory support for patients with COVID-19 at the pre-resuscitation stage. *Pulmonology*. 2020;30(2):151–163 (in Russ.). DOI: 10.18093/0869-0189-2020-30-2-151-163.
8. Salehi S., Abedi A., Balakrishnan S., Gholamrezanezhad A. Coronavirus Disease 2019 (COVID-19): A systematic review of imaging findings in 919 patients. *AJR Am. J. Roentgenol*. 2020;215(1):87–93. DOI: 10.2214/AJR.20.23034.
9. Rongrong Y., Xien G., Yongxi Z., Yong X., Shicheng G., Hengning K. Clinical characteristics of COVID-19 patients with HIV coinfection in Wuhan, China. *Expert Review of Respiratory Medicine*. 2021;15(3):403–409. DOI: 10.1080/17476348.2021.1836965.
10. Chen J., Cheng X., Wang R., Zeng X. Computed tomography imaging of an HIV-infected patient with coronavirus disease 2019. *J. Med. Virol*. 2020;92(10):1774–1776. DOI: 10.1002/JMV.25879.
11. Chung M., Bernheim A., Mei X., Zhang N., Huang M., Zeng X. et al. CT Imaging Features of 2019 Novel Coronavirus (2019-nCoV). *Radiology*. 2020;295(1):202–207. DOI: 10.1148/radiol.2020200230.
12. Torres P., Irion K., Marchiori E. COVID-19: chest X-rays to predict clinical outcomes. *J. Bras. Pneumol*. 2020;46(5):e20200464. DOI: 10.36416/1806-3756/E20200464.
13. Sinitsyn V.E., Tyurin I.E., Mitkov V.V. Consensus Guidelines of Russian Society of Radiology (RSR) and Russian Association of Specialists in Ultrasound Diagnostics in Medicine (RASUDM) "Role of Imaging (X-ray, CT and US) in Diagnosis of COVID-19 Pneumonia" (version 2). *Journal of Radiology and Nuclear Medicine*. 2020;101(2):72–89 (in Russ.). DOI: 10.20862/0042-4676-2020-101-2-72-89.
14. Osterwalder J. COVID-19 – more lung pocus and sparing use of stethoscope, chest X-ray and lung CT. *Praxis (Bern 1994)*. 2020;109(8):583–591. DOI: 10.1024/1661-8157/a003512.
15. Jacobi A., Chung M., Bernheim A., Eber C. Portable chest X-ray in coronavirus disease-19 (COVID-19): A pictorial review. *Clin. Imaging*. 2020;64:35–42. DOI: 10.1016/j.clinimag.2020.04.001.
16. Kunze G., Kovacikova E., Haller H., Kumle B. Lungenultraschall bei Patienten mit SARS-CoV-2-Infektion. *Notf. Rett. Med*. 2020;7:1–9. DOI: 10.1007/S10049-020-00767-8.
17. Reissig A., Copetti R., Kroegel C. Current role of emergency ultrasound of the chest. *Critical Care Medicine*. 2011;39(4):839–845. DOI: 10.1097/CCM.0b013e318206d6b8.
18. Lichtenstein D.A. BLUE-protocol and FALLS-protocol: two applications of lung ultrasound in the critically ill. *Chest*. 2015;147(6):1659–1670. DOI: 10.1378/chest.14-1313.
19. Shakhov B.E., Safonov D.V. Diagnostic capabilities of transthoracic ultrasound examination of the lungs. *Mezhdunarodnyj Zhurnal Eksperimental'nogo Obrazovaniya*. 2008;3–8 (in Russ.).
20. Kharnas S.S. New technologies in the diagnosis and treatment of patients with surgical diseases of the lungs and pleura. M.: *Medicina*, 2005:96 (in Russ.).
21. Mojoli F., Bouhemad B., Mongodi S., Lichtenstein D. Lung ultrasound for critically ill patients. *Am. J. Respir. Crit. Care Med.* 2019;199(6):701–714. DOI: 10.1164/rccm.201802-0236CI.
22. Safonov D.V., Dianova T.I., Rodionov V.A., Gerasimova L.A. X-ray – ultrasound comparison and dynamic echographic control for pneumonia in children. *Politematicheskij Setevoj Elektronnyj Nauchnyj Zhurnal Kubanskogo Gosudarstvennogo Agrarnogo Universiteta.* 2014;104(10):1591–1605 (in Russ.).
23. Husain L.F., Hagopian L., Wayman D., Baker W.E., Carmody K.A. Sonographic diagnosis of pneumothorax. *J. Emerg. Trauma Shock.* 2012;5(1):76–81. DOI: 10.4103/0974-2700.93116.
24. Wang G., Ji X., Xu Y., Xiang X. Lung ultrasound: a promising tool to monitor ventilator-associated pneumonia in critically ill patients. *Crit. Care*. 2016;20(1):320. DOI: 10.1186/s13054-016-1487-y.
25. Cortellaro F., Colombo S., Coen D., Duca P.G. Lung ultrasound is an accurate diagnostic tool for the diagnosis of pneumonia in the emergency department. *Emerg. Med. J*. 2012;29(1):19–23. DOI: 10.1136/emj.2010.101584.
26. Cardinale L., Ardissone F., Garetto I., Marci V., Volpicelli G., Solitro F. et al. Imaging of benign solitary fibrous tumor of the pleura: a pictorial essay. *Rare Tumors*. 2010;2(1): e1. DOI: 10.4081/rt.2010.e1.
27. Gargani L., Frassi F., Soldati G., Tesorio P., Gheorghiade M., Picano E. Ultrasound lung comets for the differential diagnosis of acute cardiogenic dyspnoea: a comparison with natriuretic peptides. *Eur. J. Heart Fail*. 2008;10(1):70–77. DOI: 10.1016/j.ejheart.2007.10.009.
28. Lichtenstein D.A., Mezière G.A. Relevance of lung ultrasound in the diagnosis of acute respiratory failure: the BLUE protocol. *Chest*. 2008;134(1):117–125. DOI: 10.1378/chest.07-2800.
29. Repik V.I. Ultrasound in the diagnosis of pleural effusion. *Ul'trazvukovaya Diagnostika.* 1996;3:62 (in Russ.).
30. Trezzi M., Torzillo D., Ceriani E., Costantino G., Caruso S., Damavandi P.T. et al. Lung ultrasonography for the assessment of rapid extravascular water variation: evidence from hemodialysis patients. *Intensive Care Med*. 2013;8(5):409–415. DOI: 10.1007/s11739-011-0625-4.
31. Perrone T., Soldati G., Padovini L., Fiengo A., Lettieri G., Sabatini U. et al. A new lung ultrasound protocol able to predict worsening in patients affected by severe acute respiratory syndrome Coronavirus 2 pneumonia. *J. Ultrasound Med.* 2021;40(8):1627–1635. DOI: 10.1002/jum.15548.
32. Wang M., Luo X., Wang L., Estill J., Lv M., Zhu Y. et al. A Comparison of Lung Ultrasound and Computed Tomog-

raphy in the Diagnosis of Patients with COVID-19: A Systematic Review and Meta-Analysis. *Diagnostics (Basel)*. 2021;11(8):1351. DOI: 10.3390/diagnostics11081351.
33. Gibbons R.C., Magee M., Goett H., Murrett J., Genninger J., Mendez K. et al. Lung Ultrasound vs. Chest X-Ray Study for the Radiographic Diagnosis of COVID-19 Pneumonia in a High-Prevalence Population. *J. Emerg. Med*. 2021;60(5):615–625. DOI: 10.1016/j.jemermed.2021.01.041.
34. Moro F., Buonsenso D., Moruzzi M.C., Inchingolo R., Smargiassi A., Demi L. et al. How to perform lung ultrasound in pregnant women with suspected COVID-19infection. *Ultrasound Obstet. Gynecol*. 2020;55(5):593–598. DOI: 10.1002/uog.22028.
35. Yee J., Kim W., Han J.M., Lee N., Lee K.E., Gwak H.S. Clinical manifestations and perinatal outcomes of pregnant women with COVID-19: a systematic review and meta-analysis. *Sci. Rep*. 2020;10(1):18126. DOI: 10.1038/s41598-020-75096-4.
36. Zaigham M., Andersson O. Maternal and perinatal outcomes with COVID-19: A systematic review of 108 pregnancies. *Acta Obstet. Gynecol. Scand.* 2020;99(7):823–829. DOI: 10.1111/aogs.13867.
37. Moghadam S.A., Dini P., Nassiri S., Motavaselian M., Hajibaba M., Sohrabi M. Clinical features of pregnant women in Iran who died due to COVID-19. *Int. J. Gynaecol. Obstet*. 2021;152(2):215–219. DOI: 10.1002/ijgo.13461.
38. Lichtenstein D., Mézière G., Biderman P., Gepner A., Barré O. The comet-tail artifact an ultrasound sign of alveolar-interstitial syndrome. *Am. J. Respir. Crit. Care Med.* 1997;156(5):1640–1646. DOI: 10.1164/AJRCCM.156.5.96-07096.
39. Lichter Y., Topilsky Y., Taieb P., Banai A., Hochstadt A., Merdler I. et al. Lung ultrasound predicts clinical course and outcomes in COVID-19 patients. *Intensive Care Med*. 2020;46(10):1873–1883. DOI: 10.1007/s00134-020-06212-1.
40. Gargani L., Volpicelli G. How I do it: Lung ultrasound. *Cardiovasc. Ultrasound*. 2014;12:25. DOI: 10.1186/1476-7120-12-25.
41. Buda N., Kosiak W., Wełnicki M., Skoczylas A., Olszewski R., Piotrkowski J. et al. Recommendations for lung ultrasound in internal medicine. *Diagnostics (Basel)*. 2020;10(8):597. DOI: 10.3390/diagnostics10080597.
42. Peng Q.Y., Wang X.T., Zhang L.N., Chinese Critical Care Ultrasound Study Group (CCUSG). Findings of lung ultrasonography of novel corona virus pneumonia during the 2019–2020 epidemic. *Intensive Care Med*. 2020;46(5):849–850. DOI: 10.1007/s00134-020-05996-6.
43. Volpicelli G., Elbarbary M., Blaivas M., Lichtenstein D.A., Mathis G., Kirkpatrick A.W. et al. International evidence-based recommendations for point-of-care lung ultrasound. *Intensive Care Medicine*. 2012;38(4):577–591. DOI: 10.1007/s00134-012-2513-4.
44. Poggiali E., Dacrema A., Bastoni D., Tinelli V., Demichele E., Ramos P.M. et al. Can lung US help critical care clinicians in the early diagnosis of novel Coronavirus (COVID-19) pneumonia? *Radiology*. 2020;295(3):e6. DOI: 10.1148/radiol.2020200847.
45. Soldati G., Demi M., Smargiassi A., Inchingolo R., Demi L. The role of ultrasound lung artifacts in the diagnosis of respiratory diseases. *Expert Rev. Respir. Med*. 2019;13(2):163–172. DOI: 10.1080/17476348.2019.1565997.
46. Demi M., Prediletto R., Soldati G., Demi L. Physical mechanisms providing clinical information from ultrasound lung images: hypotheses and early confirmations. *IEEE Trans. Ultrason. Ferroelectr. Freq. Control*. 2020;67(3):612–623. DOI: 10.1109/TUFFC.2019.2949597.
47. Soldati G., Demi M., Inchingolo R., Smargiassi A., Demi L. On the physical basis of pulmonary sonographic interstitial syndrome. *J. Ultrasound Med*. 2016;35(10):2075–2086. DOI: 10.7863/ultra.15.08023.
48. Bradley B., Branley H.M., Egan J.J., Greaves M.S., Hansell D.M., Harrison N.K. et al. British Thoracic Society Interstitial Lung Disease Guideline Group, British Thoracic Society Standards of Care Committee, Thoracic Society of Australia, New Zealand Thoracic Society, Irish Thoracic Society. Interstitial lung disease guideline: the British Thoracic Society in collaboration with the Thoracic Society of Australia and New Zealand and the Irish Thoracic Society. *Thorax*. 2008;63. Suppl.5:v1–58. DOI: 10.1136/thx.2008.101691.
49. Tsung J.W., Kessler D.O., Shah V.P. Prospective application of clinician-performed lung ultrasonography during the 2009 H1N1 influenza A pandemic: distinguishing viral from bacterial pneumonia. *Crit. Ultrasound J*. 2012;4(1):16. DOI: 10.1186/2036-7902-4-16.
50. Zhao Z., Jiang L., Xi X., Jiang Q., Zhu B., Wang M. et al. Prognostic value of extravascular lung water assessed with lung ultrasound score by chest sonography in patients with acute respiratory distress syndrome. *BMC Pulm. Med*. 2015;15:98. DOI: 10.1186/s12890-015-0091-2.
51. Khosla R. Lung Sonography. Sonography. K. Thoirs (ed.). University Campus STeP Ri Slavka Krautzeka, 2012:111–130. DOI: 10.5772/27400.
52. Lichtenstein D., Mezière G. A lung ultrasound sign allowing bedside distinction between pulmonary edema and COPD: the comet-tail artifact. *Intensive Care Med*. 1998;24(12):1331–1334. DOI: 10.1007/s001340050771.
53. Akilov Kh.A., Aminov U.S., Amirova Z.F. Ultrasonic semiotics of bacterial lung destruction in children. *The Bulletin of Emergency Medicine*. 2017;10(2):55–60 (in Russ.).
54. Zhang G., Hu C., Luo L., Fang F., Chen Y., Li J. et al. Clinical features and short-term outcomes of 221 patients with COVID-19 in Wuhan, China. *J. Clin. Virol*. 2020;127:104364. DOI: 10.1016/j.jcv.2020.104364.
55. Huttner B., Catho G., Pano-Pardo J.R., Pulcini C., Schouten J. COVID-19: don't neglect antimicrobial stewardship principles! *Clin. Microbiol. Infect*. 2020;26(7):808–810. DOI: 10.1016/j.cmi.2020.04.024.
56. Chuyashenko E.V., Zavadovskaya V.D., Ageeva T.S., Prosekina N.M., Perova T.B. Ultrasound examination of the lungs for pneumonia. *Bulletin of Siberian Medicine*. 2017;16(2):47–59 (in Russ.). DOI: 10.20538/1682-0363-2017-2-47-59.
57. Chuyashenko E.V., Zavadovskaya V.D., Ageeva T.S., Zorkal'tsev M.A., Fedorova E.I., Bukreeva E.B. et al. Possibilities of ultrasound examination in the diagnosis of inflammatory infiltration of the lungs. *Radiation Diagnostics and Therapy*. 2020;11(2):107–115 (in Russ.). DOI: 10.22328/2079-5343-2020-11-2-107-115.
58. Soldati G., Smargiassi A., Inchingolo R., Buonsenso D., Perrone T., Briganti D.F. et al. Proposal for international standardization of the use of lung ultrasound for COVID-19 patients; a

simple, quantitative, reproducible method. *J. Ultrasound Med*. 2020;39(7):1413–1419. DOI: 10.1002/jum.15285.
59. Colombi D., Petrini M., Maffi G., Villani G.D., Bodini F.C., Morelli N. et al. Comparison of admission chest computed tomography and lung ultrasound performance for diagnosis of COVID-19 pneumonia in populations with different disease prevalence. *Eur. J. Radiol*. 2020;133:109344. DOI: 10.1016/j.ejrad.2020.109344.
60. Sperandeo M., Tinti M.G., Rea G. Chest ultrasound versus chest X-rays for detecting pneumonia in children: Why compare them each other if together can improve the diagnosis? *Eur. J. Radiol*. 2017;93:291–292. DOI: 10.1016/j.ejrad.2017.05.038.
61. Serafino M.D., Notaro M., Rea G., Iacobellis F., Paoli V.D., Acampora C. et al. The lung ultrasound: facts or artifacts? In the era of COVID-19 outbreak. *Radiol. Med*. 2020;125(8):738–753. DOI: 10.1007/s11547-020-01236-5.
62. Mozzini C., Pasini A.M.F., Garbin U., Cominacini L. Lung ultrasound in internal medicine: training and clinical practice. *Crit. Ultrasound J*. 2016;8(1):10. DOI: 10.1186/s13089-016-0048-6.

Authors information

Balabanova Aleksandra A. – Doctor of Ultrasound Diagnostics, Siberian State Medical University Hospital, Tomsk, balasasha@icloud.com, http://orcid.org/0000-0003-0974-9213,

Kurazhov Alexei P. – Dr. Sci. (Med.), Professor, Head of the Radiation Diagnostics Division, Siberian State Medical University Hospital, Tomsk, kurazhovap@mail.ru, http://orcid.org/0000-0003-1316-5421

Zavadovskaya Vera D. – Dr. Sci. (Med.), Professor, Acting Head of the Radiation Diagnostics and Radiation Therapy Division, Siberian State Medical University, Tomsk, WDZav@mail.ru, http://orcid.org/0000-0001-6231-7650

(✉) **Kurazhov Aleksei P.,** kurazhovap@mail.ru

Received 20.10.2020;
approved after peer review 22.09.2021;
accepted 05.10.2021

УДК 616.24-002-039.3:575.174.015.3
https://doi.org/10.20538/1682-0363-2022-4-160-169

Genetic factors contributing to a severe course of pneumonia: a systematic review

Karnaushkina M.A.[1], Sviridov P.S.[1, 6], Korchagin V.I.[3], Salamaikina S.A.[3], Vasilyeva I.S.[4], Litvinova M.M.[2, 4], Vatsik-Gorodetskaya M.V.[5]

[1] *Peoples' Friendship University of Russia (RUDN University)*
6, Miklukho-Maklaya Str., Moscow, 117198, Russian Federation

[2] *The Loginov Moscow Clinical Scientific Center*
86, Entuziastov Highway, Moscow, 111123, Russian Federation

[3] *Central Research Institute of Epidemiology*
3A, Novogireevskaya Str., Moscow, 111123, Russian Federation

[4] *I.M. Sechenov First Moscow State Medical University of the Ministry of Health of the Russian Federation (Sechenov University)*
8–2, Trubetskaya Str., Moscow, 119991, Russian Federation

[5] *Vinogradov City Clinical Hospital*
61, Vavilova Str., Moscow, 117292, Russian Federation

[6] *Research Centre for Medical Genetics*
1, Moskvorechye Str., Moscow, 115522, Russian Federation

ABSTRACT

The article presents a systematic review of publications devoted to the study of genetic markers of severe pneumonia.

The **aim** of the study was to compile a list of genetic markers that contribute to a severe course of pneumonia on the basis of the published data.

In the current study, we searched for and analyzed articles published between January 2000 and April 2021. Following the search for and subsequent selection of articles, a list of 10 publications was compiled, which demonstrated a clear association of certain gene variants with severe and complicated pneumonia. Finally, we made a list of genetic markers of severe pneumonia consisting of 16 polymorphisms in 12 genes (*CD86, IL6, IL10, PAI1, TNFα, HMGB1, ATG16L1, AGTR1, GCLC, CAT, IFNγ, FCGR2A*).

These genetic markers of severe and complicated pneumonia are responsible for various innate immune responses. The odds ratio for complicated pneumonia with a risk allele in the polymorphisms in the mentioned genes ranges from 1.39 to 4.28. To understand molecular and genetic mechanisms of severe pneumonia, further investigation of the effect of these genetic factors on the outcomes of pneumonia in different groups of patients with a simultaneous assessment of the cumulative effect of genetic variants and genetic interactions is required.

Keywords: pneumonia, genes, polymorphism, innate immunity, severity criteria, cytokines, secreted proteins

Conflict of interest. The authors declare the absence of obvious or potential conflicts of interest related to the publication of this article.

Source of financing. The authors state that they received no funding for the study.

For citation: Karnaushkina M.A., Sviridov P.S., Korchagin V.I., Salamaikina S.A., Vasilyeva I.S., Litvinova M.M., Vatsik-Gorodetskaya M.V. Genetic factors contributing to a severe course of pneumonia: a systematic review. *Bulletin of Siberian Medicine.* 2022;21(4):160–169. https://doi.org/10.20538/1682-0363-2022-4-160-169.

✉ *Vasilyeva Irina S.,* emmans@rambler.ru

Генетические факторы риска тяжелого течения пневмонии: систематический обзор

Карнаушкина М.А.[1], Свиридов Ф.С.[1, 6], Корчагин В.И.[3], Саламайкина С.А.[3], Васильева И.С.[4], Литвинова М.М.[2, 4], Вацик-Городецкая М.В.[5]

[1] Российский университет дружбы народов (РУДН)
Россия, 117198, г. Москва, ул. Миклухо-Маклая, 6

[2] Московский клинический научно-практический центр (МКНЦ) им. А.С. Логинова
Россия, 111123, г. Москва, шоссе Энтузиастов, 86

[3] Центральный научно-исследовательский институт (НИИ) эпидемиологии
Россия, 111123, г. Москва, ул. Новогиреевская, 3а

[4] Первый Московский государственный медицинский университет им. И.М. Сеченова Министерства здравоохранения Российской Федерации (Сеченовский Университет)
Россия, 119991, г. Москва, ул. Трубецкая, 8, стр. 2

[5] Городская клиническая больница (ГКБ) им. В.В. Виноградова
Россия, 117292, г. Москва, ул. Вавилова, 61

[6] Медико-генетический научный центр имени академика Н.П. Бочкова
Россия, 115522, г. Москва, ул. Москворечье, 1

РЕЗЮМЕ

Представлен систематический обзор публикаций, посвященных поиску генетических маркеров тяжелого течения пневмонии.

Цель исследования: на основании опубликованных данных сформировать перечень генетических маркеров, способствующих тяжелому течению пневмонии.

В ходе исследования выполнен поиск и анализ статей, опубликованных в период с января 2000 г. по апрель 2021 г. В результате проведенного поиска и последующего отбора статей сформирован список из 10 публикаций, в которых продемонстрирована четкая ассоциативная связь определенных генных вариантов с тяжелым и осложненным течением пневмонии, и список генетических маркеров тяжелого течения пневмонии, состоящий из 16 полиморфизмов в 12 генах (*CD86, IL6, IL10, PAI1, TNFα, HMGB1, ATG16L1, AGTR1, GCLC, CAT, IFNγ, FCGR2A*).

Приведенные генетические маркеры тяжелого и осложненного течения пневмонии отвечают за разнообразные реакции врожденного иммунитета. Отношение шансов при наличии рискового аллеля по соответствующим полиморфным локусам этих генов колеблется от 1,39 до 4,28. Необходимо дальнейшее изучение влияния данных генетических факторов на исходы пневмонии в группах пациентов различных популяций с одновременной оценкой совокупного влияния генетических вариантов и взаимодействия генов между собой.

Ключевые слова: пневмония, гены, полиморфизм, врожденный иммунитет, критерии тяжести, цитокины, секретируемые белки

Конфликт интересов. Авторы декларируют отсутствие явных и потенциальных конфликтов интересов, связанных с публикацией настоящей статьи.

Источник финансирования. Авторы заявляют об отсутствии финансирования при проведении исследования.

Для цитирования: Карнаушкина М.А., Свиридов Ф.С., Корчагин В.И., Саламайкина С.А., Васильева И.С., Литвинова М.М., Вацик-Городецкая М.В. Генетические факторы риска тяжелого течения пневмонии: систематический обзор. *Бюллетень сибирской медицины.* 2022;21(4):160–169. https://doi.org/10.20538/1682-0363-2022-4-160-169.

INTRODUCTION

Pneumonia is a form of acute respiratory infection characterized by focal parenchymal lung lesions with intra-alveolar exudate [1]. In 2019, pneumonia and other lower respiratory infections were ranked fourth among the leading causes of death as the deadliest group of infectious diseases [2]. According to the World Health Organization, pneumonia is currently one of the three main causes of death in the world, and among respiratory diseases, pneumonia accounts for 41.5% of deaths [3]. The incidence of community-acquired pneumonia in Russia in 2019 was 410 per 100,000 population according to the data of official statistics of the Russian Federation [4].

Pneumonia is a typical multifactorial disease as it can be caused by a wide range of bacteria, viruses, and fungi. Its course and prognosis are determined by human genetic characteristics, environmental factors, and the features of the pathogen. Numerous multicenter clinical trials discovered a large number of risk factors for a severe course of pneumonia and development of its complications in order to optimize treatment regimens and prevent the incidence of pneumonia. However, additional risk factors remained undetected in a significant proportion of patients [5]. In this regard, identifying reliable predictors of severe and complicated pneumonia is an urgent issue in modern medicine.

Researchers have made repeated attempts to solve this issue by identifying candidate genes and their variants associated with susceptibility to pneumonia and the course and clinical outcomes of the disease. Currently, a large number of studies devoted to this problem have been published. Particularly, in a systematic review, A.T. Kloek et al. (2019) analyzed 1,219 studies published from 2000 to 2018 [5]. When conducting a meta-analysis, the authors found a statistically significant association between the alleles in the *MBL2* and *CD14* genes and the risk of developing pneumococcal pneumonia. As it was noted in the research, there were contradictory results in the literature on the role of gene polymorphisms in susceptibility to pneumonia and the course and outcome of the disease. This fact can be explained by methodological flaws and poor reproducibility of the studies [5].

In this article, we provided a systematic analysis of the effect of genetic factors on the severity of pneumonia, compiled a list of genetic markers contributing to its severe course, and discussed possible directions for further research in this field.

The aim of the study was to compile a list of genetic markers that contribute to a severe course of pneumonia based on the published data on genetic aspects that determine the features of the course of this disease.

MATERIALS AND METHODS

In this study, we searched for and analyzed articles from the database of medical and biological articles PubMed (https://pubmed.ncbi.nlm.nih.gov/) which were published from January 2000 to April 2021 and then analyzed the publications found. The search query contained the words “pneumonia” and derivatives, “gene” and derivatives, “polymorphism” and derivatives. To narrow down the search, articles containing the words “children” and “covid” with their variations were excluded. So, the search algorithm looked like this: (“pneumonia”[MeSH Terms] OR “pneumonia”[All Fields] OR “pneumoniae”[All Fields] OR “pneumonias”[All Fields] OR “pneumoniae s”[All Fields]) AND (“genes”[MeSH Terms] OR “genes”[All Fields] OR “gene”[All Fields]) AND (“polymorphic”[All Fields] OR “polymorphics”[All Fields] OR “polymorphism s”[All Fields] OR “polymorphism, genetic”[MeSH Terms] OR (“polymorphism”[All Fields] AND “genetic”[All Fields]) OR “genetic polymorphism”[All Fields] OR “polymorphism”[All Fields] OR “polymorphisms”[All Fields])) NOT (“child”[MeSH Terms] OR “child”[All Fields] OR “children”[All Fields] OR “child s”[All Fields] OR “children s”[All Fields] OR “childrens”[All Fields] OR “childs”[All Fields])) NOT (“sars cov 2”[MeSH Terms] OR “sars cov 2”[All Fields] OR “covid”[All Fields] OR “covid 19”[MeSH Terms] OR “covid 19”[All Fields])) AND (2000:2021[pdat]). When applying the presented search algorithm, we initially found 795 articles. After further investigation, 761 articles were excluded because they did not fully meet the aim of this study as they were devoted to genetic characteristics of microorganisms causing bronchopulmonary diseases or studied the odds for the disease, but not its course. Therefore, the list was reduced to 34 articles.

After a thorough analysis of these publications, several articles were additionally excluded from the study, as they examined groups of patients unsuitable for our study or did not contain data relevant to the aim of this study. Particularly, several excluded works studied patients under the age of 18, and other publications did not analyze the association

of genetic markers with the severity of pneumonia, but with predisposition to pneumonia. In addition, studies that demonstrated a statistically insignificant ($p > 0.05$) association of a gene polymorphism with a severe course of pneumonia were eliminated from the list.

Thus, at the last stage of the detailed evaluation, 24 publications were excluded from 34 articles. As a result, we formed a list of 10 publications, which demonstrated a clear association of certain gene variants with a severe and complicated course of pneumonia (Figure).

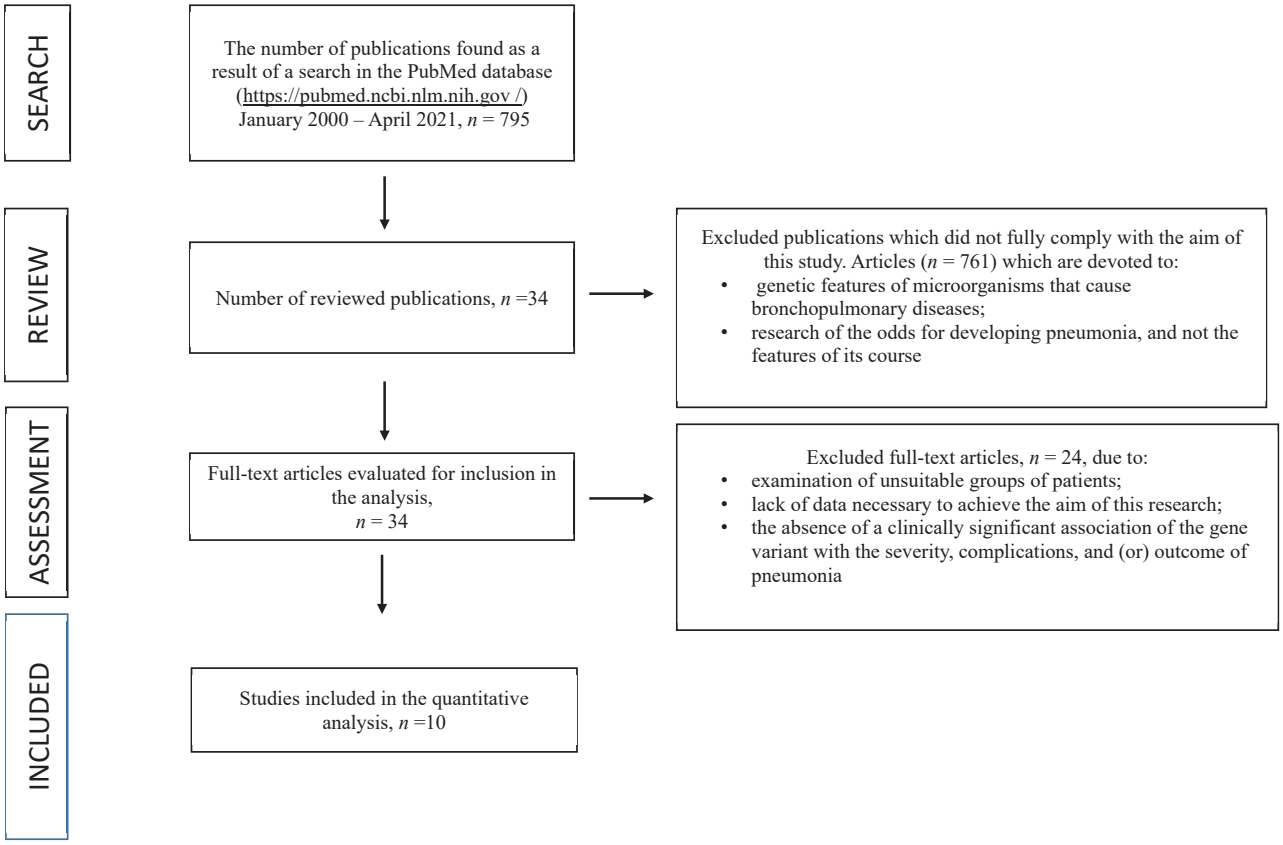

Figure. Schematic representation of the selection of publications devoted to the identification of genetic markers associated with severe pneumonia in accordance with PRISMA guidelines

The contribution of various polymorphisms to the development of the disease was determined using the odds ratio (OR), which is a traditional parameter for such studies. The results obtained were interpreted as follows: if the OR was equal to 1, then there was no correlation between a gene polymorphism and clinical and laboratory features of the course of pneumonia; if the OR was > 1, then there was an increased risk of severe pneumonia; if the OR was < 1, then there was a protective marker against the complicated course of pneumonia. Associations with $p < 0.05$ were considered statistically significant.

Furthermore, genetic databases and genomic browsers dbSNP (https://www.ncbi.nlm.nih.gov/snp/), Ensembl (https://www.ensembl.org/index), SNPedia (https://www.snpedia.com/), and OMIM (https://www.omim.org/) were analyzed to assess the results of the identified genetic associations, clarify the frequency characteristics of gene polymorphisms, and determine their biological role in the processes responsible for innate immune responses.

According to the Russian clinical guidelines for the diagnosis, management, and prevention of severe pneumonia in adults, it is advisable to use the IDSA / ATS criteria, containing two major and nine minor criteria, to determine the severity of the disease (Table 1) [6]. The presence of one major and three minor criteria in a patient indicates a severe course of pneumonia [7].

Table 1

IDSA / ATS criteria for the severity of pneumonia

Major criteria	Severe respiratory failure requiring MV
	Septic shock requiring vasopressors
Minor criteria	RR ≥ 30 per min
	PaO_2 / FiO_2 ≤ 250
	Multilobar infiltration
	Impaired consciousness
	Uremia (blood urea nitrogen ≥ 20 mg / dl)
	Leukopenia (leukocytes < 4×10^9 / l)
	Thrombocytopenia (platelets < 100×10^9 /l)
	Hypothermia (< 36 °C)
	Hypotension requiring aggressive fluid resuscitation

Note: IDSA – Infectious Diseases Society of America; ATS – American Thoracic Society; MV – mechanical ventilation; RR – respiratory rate; PaO_2 / FiO_2 – partial pressure of arterial oxygen / fraction of inspired oxygen; WBC – white blood cells.

RESULTS

As a result of a systematic literature review, we have formed a list of genetic markers of severe pneumonia, consisting of 16 polymorphisms in 12 genes (Table 2).

These genetic markers of a severe and complicated course of pneumonia are responsible for various innate immune responses. In general, the selected genes can be grouped according to the functional principle: extracellular cytosolic opsonizing proteins (proinflammatory cytokines) (*IFNG, IL6, IL10, TNFα*), secreted proteins (genes of the complement system and Fc receptors) (*FCGR2A*) and genes encoding synthesis of other proteins (*CAT, GCLC, AGTR1, PAI1 (SERPINE1)*).

Table 2

Genetic factors associated with the risk of severe and complicated pneumonia

Gene	Polymorphism	OR for allele and / or genotype (complication of pneumonia)	Features of the sample under study	Source (PubMed ID), population features
CB86	rs17281995 G/C	Allele C – 1.75 (95% CI; 1.04–2.95). Genotype GC – 1.85 (95% CI; 1.07–3.20) (sepsis)	Chinese population, 192 patients with pneumonia and sepsis and 201 healthy individuals	25129060 [8]
	rs2332096 T/G	Allele G – 1.65 (95% CI; 1.21–2.24). Genotype GG – 2.75 (95% CI; 1.46–5.16) (sepsis)	Chinese population, 186 patients with pneumonia and sepsis and 196 healthy individuals	25912130 [9]
IL6	rs1800795 G/C	Allele C – 2.83 (95% CI; 2.1–3.78). Genotype CC – 4.45 (95% CI; 2.69–5.37) (sepsis)	Chinese population, 188 patients with pneumonia and sepsis, 162 patients with pneumonia, and 200 healthy individuals	27388228 [10]
	rs1800795 G/C	Allele C – 2.42 (95% CI; 1.08–5.45) (septic shock)	Chinese population. The group of 277 patients was divided into two subgroups depending on the severity of sepsis and its outcome	26025100 [11]
IL10	rs1800896 A/G	Allele A – 2.08 (95% CI; 1.15–2.80) (sepsis)	Chinese population, 188 patients with pneumonia and sepsis, 162 patients with pneumonia, and 200 healthy individuals	27388228 [10]
PAI1 (SERPINE1)	rs1799768 4G/5G and 4G/4G	4G/5G and 4G/4G genotypes – 2.74 (95% CI; 1.34–5.60) (multiple organ dysfunction syndrome), 2.57 (95% CI; 1.18–5.62) (septic shock)	208 Caucasian patients with pneumonia and sepsis. Patients were stratified depending on the presence of multiple organ dysfunction syndrome, septic shock or death	20429897 [12]
TNFα	rs1800629 G/A	Allele A – 4.28 (95% CI; 2.24–8.18) (septic shock)	Chinese population.The group of 277 patients was divided into two subgroups depending on the severity of sepsis and its outcome	26025100 [11]
HMGB1	rs1412125 T/C	Genotype TC – 1.74 (95% CI; 1.025–2.958) (severe course). Genotype CC – 4.73 (95% CI; 2.24–10.08) (severe course)	Chinese population, 328 patients with community-acquired pneumonia (depending on the severity of the condition, patients were divided into severe (125) and non-severe community-acquired pneumonia (203) groups) and 317 healthy individuals	30562142 [13]
	rs2249825 C/G	Genotype CG – 1.75 (95% CI; 1.02–3.01) (severe course). Genotype GG – 3.87 (95% CI; 1.58–9.58) (severe course)		
ATG16L1	rs2241880 G/A	Allele A – 2.4 (95% CI; 1.06–5.60) (septic shock and failure of at least one organ in patients with ventilator-associated pneumonia)	Greek population, 155 patients with ventilator-associated pneumonia	24791954 [14]

Table 2 (continued)

Gene	Polymorphism	OR for allele and / or genotype (complication of pneumonia)	Features of the sample under study	Source (PubMed ID), population features
AGTR1	rs5186 A/C	Allele C – 1.86 (95% CI; 1.31–2.64) (complications of pneumonia)	Russian population, 350 patients with ventilator-associated pneumonia, 432 healthy individuals	24068433 [15]
GCLC	rs17883901 C/T	Allele T – 1.90 (95% CI; 1.15–3.15) (complications of pneumonia)		
CAT	rs17880664 T/A	Genotype AA – 1.85 (95% CI; 1.06–3.25) (complications of pneumonia)		
IFNγ	rs2069705 T/C	Allele T – 1.39 (95% CI; 1.03–1.89) (sepsis). Genotype TT – 1.22 (95% CI; 0.58–2.57) TC + TT – 1.84 (95% CI; 1.24–2.73) (sepsis)	Chinese population, 196 patients with sepsis and pneumonia, 213 healthy individuals	24475220 [16]
	rs2430561 A/T	Allele A – 1.49 (95% CI; 1.05–2.12) (sepsis). Genotype AA – 1.70 (95% CI; 0.61–2.12) TA + AA – 1.68 (95% CI; 1.11–2.54)		
FCGR2A	rs1801274 T/C	Allele C – 1.57 (95% CI; 1.00–2.45) Genotype CC – 2.55 (95% CI; 1.30–5.00) (sepsis)	Netherlands, 200 patients with ventilator-associated pneumonia and sepsis, 313 healthy individuals	19494086 [17]

Note: SNV – single nucleotide variant; OR – odds ratio; 95% CI – 95% confidence interval.

According to Table 1, the OR in the presence of a risk allele for the presented polymorphic loci ranges from 1.39 to 4.28.

Here we would like to provide more detailed information on the genetic associations found in the literature. The *CD86* gene is located on the long arm of chromosome 3 (3q13.33) and encodes a membrane protein of the immunoglobulin superfamily expressed by antigen-presenting cells. CD86 protein acts as a co-stimulatory signal for the activation and survival of T lymphocytes [18]. A study by H. Song et al. (2015) which included 192 patients with pneumonia-induced sepsis showed that the frequency of the rs17281995 G/C gene variant in these patients was significantly higher than in the control group. The OR for allele C and genotype GC was 1.75 and 1.85, respectively. In the study by C. Wang et al. (2015), where 186 patients with pneumonia-induced sepsis were examined, a correlation was found between the rs2332096 T/G gene variant and the severe course of the disease. The OR for allele G and genotype GG was 1.65 and 2.75, respectively [8, 9].

The *IL6* gene is located on the short arm of chromosome 7 (7p15.3) and encodes interleukin (IL)-6. IL-6 is a proinflammatory cytokine and one of the most important mediators of the acute-phase response. It stimulates synthesis of acute-phase proteins, proliferation and differentiation of B and T cells and leukopoiesis, and is involved in the development of oxidative stress. IL-6 is secreted by macrophages, fibroblasts, vascular endothelial cells, T cells, glial cells, and epithelial and skin keratinocytes after their activation by pathogen-associated molecules mediated by toll-like receptors [10]. The study by Z.-R. Mao et al. (2017), which included 188 patients with pneumonia-induced sepsis and 162 patients with pneumonia, showed that the rs1800795 G/C variant increases the risk of sepsis. The OR for allele C and genotype CC was 2.83 and 4.45, respectively. B. Feng et al. studied 277 patients with pneumonia-induced sepsis and found a correlation between the rs1800795 G/C gene variant and the development of septic shock. The OR for allele C was 2.42 [11].

The *IL-10* gene is located on the long arm of chromosome 1 (1q32.1) and encodes IL-10. IL-10 has multiple pleiotropic effects on immunoregulation and inflammation. It reduces the expression of Th1 cytokines, MHC class II antigens, and co-stimulatory molecules on macrophages, increases the survival of B cells, their proliferation and antibody production, blocks NF-κB activity, and regulates the JAK-STAT signaling pathway [20]. The study by Z.-R.Mao et al. (2017) which examined 188 patients with pneumonia-induced sepsis and 162 patients with pneumonia showed an increased risk of severe pneumonia in the rs1800896 A/G variant. The OR for allele A was 1.58 [10].

The *PAI1* gene (*SERPINE1*) is located on the long arm of chromosome 7 (7q22.1) and encodes plasminogen activator inhibitor 1 involved in

fibrinolysis. Polymorphisms in this gene are usually considered as risk factors for the development of cardiovascular diseases [21]. K. Madách et al. conducted a study involving 208 patients with pneumonia-induced sepsis and demonstrated the relationship between the genotypes 4G/5G and 5G/5G of the *PAI1* gene (*SERPINE1*) and the development of multiple organ dysfunction syndrome and septic shock. The OR for these two genotypes was 2.74 and 2.57, respectively [12].

The *TNFα* (*TNF*) gene is located on the long arm of chromosome 7 (*6p21.33*) and encodes tumor necrosis factor alpha. This extracellular protein is a multifunctional proinflammatory cytokine synthesized mainly by monocytes and macrophages. TNFα affects lipid metabolism, coagulation, insulin resistance, endothelial function, stimulates the production of IL-1, IL-6, IL-8, interferon gamma, activates leukocytes, and plays a pivotal role in the protection against intracellular parasites and viruses [22]. In the article by B. Feng et al., which studied 277 patients with pneumonia-induced sepsis, a correlation was found between the rs1800629 G/A gene variant and the development of septic shock. The OR for allele A was 4.28 [11].

The *HMGB1* gene is located on the long arm of chromosome 13 (13q12.3) and encodes the HMGB1 protein (amphoterin), which is secreted by activated macrophages and monocytes as a cytokine mediator. In addition, as a nuclear protein, HMGB1 can be released during cell and tissue necrosis. In the extracellular compartment, it can bind to the innate immune receptor TLR4, activating cytokine secretion by macrophages and a subsequent inflammatory response. The HMGB1 protein is highly toxic when released in large amounts, so it is considered as one of the possible therapeutic targets for sepsis [23]. In the study by W. Song et al. which involved 328 patients with pneumonia, a relationship was found between the rs1412125 T/C and rs2249825 C/G gene variants and the severity of pneumonia. When OR for genotype TC was equal to 1.740, OR for genotype TT was 4.728 (rs1412125 T/C). When OR for genotype CG was 1.754, OR for genotype GG was 3.869 (rs2249825 C/G) [13].

The *ATG16L1* gene is located on the long arm of chromosome 2 (2q37.1) and is responsible for synthesis of an intracellular protein involved in the autophagy process which interacts with other proteins of this complex [24]. The research by A. Savva et al. examined 200 patients with sepsis caused by ventilator-associated pneumonia and showed that the rs2241880 G/A gene variant affects the severity of ventilator-associated pneumonia. The OR for allele A was 2.4 [14].

The *AGTR1* gene is located on the long arm of chromosome 3 (*3q24)* and *encodes* production of angiotensin II type 1B receptor, which mediates the main cardiovascular effects of angiotensin II [25]. L. Salnikova et al. studied 350 patients (Slavs, including Russians) with pneumonia and found a relationship of the rs5186 A/C gene variant with complications of pneumonia, as well as with the development of acute respiratory failure (ARF). The risk of complicated pneumonia in the presence of allele C is quite high; OR is 1.862 [15].

The *GCLC* gene is located on the short arm of chromosome 6 (6p12.1) and encodes glutamate-cysteine ligase catalytic subunit, which is involved in synthesis of glutathione from L-cysteine and L-glutamate [26]. In the previously discussed study by L. Salnikova et al., where 350 patients (Slavs, including Russians) with pneumonia were examined, a relationship was found of the rs17883901 C/T variant with complications of pneumonia, as well as with the development of ARF. OR for complicated pneumonia for allele T was 3.36, and OR for ARF was 1.33 [15].

The *CAT* gene is located on the short arm of chromosome 11 (11p13) and encodes catalase, an enzyme involved in cellular respiration and in converting reactive oxygen species hydrogen peroxide into water and molecular oxygen [27]. L. Salnikova et al. (2013) studied a population of 350 patients (Slavs, including Russians) with pneumonia and described a relationship between the rs17880664 T/A variant and pneumonia complications. OR for genotype AA was 1.85 [15].

The *IFNG* gene is located on the long arm of chromosome 12 (12q15) and encodes a soluble cytokine. It is a member of the interferon type II class. It is secreted by cells of both adaptive and innate immunity. In its active form, this protein binds to the interferon gamma receptor and activates the cellular response to viral or bacterial infection [28]. The study by D. Wang et al. (2014), which involved 196 patients with pneumonia-induced sepsis, showed that the rs2069705 T/C and rs2430561 A/T gene variants are associated with the development of sepsis in patients with pneumonia. For a single-nucleotide substitution rs2069705 T/C, OR for TC, TT, and TC + TT genotypes was 1.99, 1.22, and 1.84, respectively. OR for T allele was 1.39. For a single-nucleotide

substitution rs2430561 A/T, OR for TA, AA, and TA+AA genotypes was 1.68, 1.70, and 1.68, respectively. OR for A allele was 1.49 [16].

The *FCGR2A* gene is located on the long arm of chromosome 1 (*1q23.3*), encodes the low-affinity immunoglobulin Fc receptor IIa (CD32A), and participates in the activation of the cellular response [29]. H. Endeman et al. (2009) examined 201 patients with pneumonia and pneumonia-induced sepsis and found a correlation between the rs1801274 T/C gene variant and the development of severe sepsis. OR for CC genotype was 2.55 [17].

DISCUSSION

According to the analyzed studies, the severity of pneumonia and its outcome are determined by the development of complications through a systemic inflammatory response [8–17]. Systemic inflammatory response syndrome, acute respiratory distress syndrome, multiple organ failure syndrome, as well as pleurisy, empyema, and the development of necrotizing pneumonia are the most significant complications in terms of the most unfavorable prognosis and outcome [30].

As it was shown in our systematic review, at least 12 genes and polymorphisms in them were proven to be associated with a severe course of pneumonia. These genes mostly include the ones responsible for various innate immune responses.

Despite the rigorous selection of genes, which polymorphisms are associated with a risk of severe pneumonia, it is worth noting that the selected genes included the ones responsible for synthesis of multifunctional, often nonspecific factors, such as proteins regulating vascular homeostasis (*PAI1* and *AGTR1*). This fact significantly reduces the significance of the interpretation of the role of these polymorphisms as predictors of clinical features of pneumonia and requires further in-depth study.

In addition, each of the presented gene variants does not act in isolation, but contributes to the risk of developing the disease in the context of the overall genetic constitution of the patient. Several years ago, a number of researchers put forward a hypothesis that a combination of two or more risk alleles in candidate genes is of greater importance for assessing the prognosis and the course of pneumonia. So, J.N. Siebert et al. (2018) demonstrated that a combination of nucleotide polymorphisms in *TLR1* or *TLR6* and *TIRAP* was associated with decreased release of IL-6 and predisposition to pneumonia [31].

In this regard, special attention should be paid to studying genetic interactions and the role of the combination of polymorphisms in receptor genes and opsonizing proteins involved in innate immune responses. Therefore, approaches to determining the presence of genetic associations should include a variety of genetic markers.

In this review we deliberately did not discuss human genetic characteristics that contribute to the development of an infectious process associated with certain types of microorganisms; this issue requires in-depth research. Currently, studies have described more than 100 microorganisms that can cause pneumonia under certain conditions. In most cases, these include *S. pneumoniae, M. pneumoniae, C. pneumoniae, H. influenzae*, respiratory viruses, enterobacteriaceae (*K. pneumoniae and E. coli*), and *S. aureus* [30].

The question of the influence of genetic factors on the course of pneumonia, depending on the causative agent, requires a detailed review and analysis of the available data from the literature.

CONCLUSION

We analyzed data published from 2000 to 2021 and identified a list of 16 polymorphisms in 12 human genes that can affect the severity of pneumonia. The OR for severe pneumonia in the presence of these risk alleles is 1.4–4.3. There is a need for further research of the influence of these genetic factors on the outcomes of pneumonia in groups of patients from different populations with a simultaneous assessment of the cumulative effect of genetic variants and genetic interactions. Therefore, molecular marker systems for the detection of relevant genetic variations should be developed.

In addition, in order to understand the genetic predisposition to severe pneumonia in Russia, it is essential to analyze allele frequencies of the related polymorphisms in Russian populations. The next step in studying the influence of gene polymorphisms on the development of respiratory diseases should be investigation of their molecular effects in combination with large-scale clinical trials involving patients with pneumonia.

REFERENCES

1. Chuchalin A.G., Sinopalnikov A.I., Kozlov R.S., Tyurin I.E., Rachina S.A. Community-acquired pneumonia in adults: practical recommendations for diagnosis, treatment and prevention. *Infectious diseases: news, opinions, training*. 2013;2(3):91–123 (in Russ.).

2. WHO statistics on mortality and disability worldwide: URL: https://www.who.int/ru/news/item/09-12-2020-who-reveals-leading-causes-of-death-and-disability-worldwide-2000-2019 (дата обращения: 11.02.2022).
3. Rachina S.A., Sinopalnikov A.I. Clinical recommendations for community-acquired pneumonia in adults: prognosis for year 2019. *Practical pulmonology.* 2018;3:8–13 (in Russ.).
4. Shapoval I.N., Nikitina S.Yu., Ageeva L.I., Aleksandrova G.A., Zaichenko N.M., Kirillova G.N., et al. Public health in Russia. 2019. Moscow: Rosstat, 2019:170 (in Russ.).
5. Kloek A.T., Brouwer M.C., Van de Beek D. Host genetic variability and pneumococcal disease: a systematic review and meta-analysis. *BMC Med. Genet.* 2019;12(1):130. DOI: 10.1186/s12920-019-0572-x.
6. Metlay J.P., Waterer G.W., Long A.C., Anzueto A., Brozek J., Crothers K. et al. Diagnosis and Treatment of Adults with Community-acquired Pneumonia. An Official Clinical Practice Guideline of the American Thoracic Society and Infectious Diseases Society of America. *Am. J. Respir. Crit. Care Med.* 2019;200(7):e45–e67. DOI: 10.1164/rccm.201908-1581ST.
7. Rachina S.A., Dekhnich N.N., Kozlov R.S., Bobylev A.A., Batishcheva G.A., Gordeeva S.A. et al. Severity assessment of community9acquired pneumonia in real clinical practice in a multi-profile hospital in Russia. *Pulmonologiya [Pulmonology]*. 2016;26(5):521–528. DOI: 10.18093/0869-0189-2016-26-5-521-528.
8. Song H., Tang L., Xu M., Li H., Xu S., Li G. et al. CD86 polymorphism affects pneumonia-induced sepsis by decreasing gene expression in monocytes. *Inflammation.* 2015;38(2):879–885. DOI: 10.1007/s10753-014-9997-8.
9. Wang C., Gui Q., Zhang K. Functional polymorphisms in CD86 gene are associated with susceptibility to pneumonia-induced sepsis. *APMIS.* 2015;123(5):433–438. DOI: 10.1111/apm.12364.
10. Mao Z.R., Zhang S.L., Feng B. Association of IL-10 (-819T/C, -592A/C and -1082A/G) and IL-6 -174G/C gene polymorphism and the risk of pneumonia-induced sepsis. *Biomarkers*. 2017;22(2):106 0150112. DOI: 10.1080/1354750X.2016.1210677.
11. Feng B., Mao Z.R., Pang K., Zhang S.L., Li L. Association of tumor necrosis factor α -308G/A and interleukin-6 -174G/C gene polymorphism with pneumonia-induced sepsis. *J. Crit. Care*. 2015;30(5):920–923. DOI: 10.1016/j.jcrc.2015.04.123.
12. Madách K., Aladzsity I., Szilágyi A., Fust F., Gál J., Pénzes I. et al. 4G/5G polymorphism of PAI-1 gene is associated with multiple organ dysfunction and septic shock in pneumonia induced severe sepsis: prospective, observational, genetic study. *Crit. Care.* 2010;14(2):R79. DOI: 10.1186/cc8992.
13. Song W., Tan H., Wang S., Zhang Y., Ding Y. Association of High Mobility Group Box Protein B1 Gene Polymorphisms with Pneumonia Susceptibility and Severity. *Genet. Test. Mol. Biomarkers.* 2019;23(1):3–11. DOI: 10.1089/gtmb.2018.0174.
14. Savva A., Plantinga T.S., Kotanidou A., Farcas M., Baziaka F., Raftogiannis M. et al. Association of autophagy-related 16-like 1 (ATG16L1) gene polymorphism with sepsis severity in patients with sepsis and ventilator-associated pneumonia. *Eur. J. Clin. Microbiol. Infect. Dis.* 2014;33(9):1609–1614. DOI: 10.1007/s10096-014-2118-7.
15. Salnikova L.E., Smelaya T.V., Golubev A.M., Rubanovich A.V., Moroz V.V. CYP1A1, GCLC, AGT, AGTR1 gene-gene interactions in community-acquired pneumonia pulmonary complications. *Mol. Biol. Rep.* 2013;40(11):6163–6176. DOI: 10.1007/s11033-013-2727-8.
16. Wang D., Zhong X., Huang D., Chen R., Bai G., Li Q. et al. Functional polymorphisms of interferon-gamma affect pneumonia-induced sepsis. *PLoS One*. 2014;9(1):e87049. DOI: 10.1371/journal.pone.0087049.
17. Endeman H., Cornips M.C.A., Grutters J.C., Van den Bosch J., Ruven H.J.T., Van Velzen-Blad H. et al. The Fcgamma receptor IIA-R/R131 genotype is associated with severe sepsis in community-acquired pneumonia. *Clin. Vaccine Immunol.* 2009;16(7):1087–1090. DOI: 10.1128/CVI.00037-09.
18. Van Coillie S., Wiernicki B., Xu J. Molecular and cellular functions of CTLA-4. *Adv. Exp. Med. Biol.* 2020;1248:7–32. DOI: 10.1007/978-981-15-3266-5_2.
19. Rose-John S. The Soluble interleukin 6 receptor: advanced therapeutic options in inflammation. *Clin. Pharmacol. Ther*. 2017;102(4):591–598. DOI: 10.1002/cpt.782.
20. Feng H., Feng J., Zhang Z., Xu Q., Hu M., Wu Y. et al. Role of IL-9 and IL-10 in the pathogenesis of chronic spontaneous urticaria through the JAK/STAT signaling pathway. *Cell Biochem. Funct.* 2020;38(4):480–489. DOI: 10.1002/cbf.3481.
21. Jacobs A., Schutte A.E., Ricci C., Pieters M. Plasminogen activator inhibitor-1 activity and the 4G/5G polymorphism are prospectively associated with blood pressure and hypertension status. *J. Hypertens.* 2019;37(12):2361–2370. DOI: 10.1097/HJH.0000000000002204.
22. Holbrook J., Lara-Reyna S., Jarosz-Griffiths H., McDermott M. Tumour necrosis factor signaling in health and disease. *F1000Res*. 2019;8:F1000. DOI: 10.12688/f1000research.17023.1.
23. Andersson U., Yang H., Harris H. Extracellular HMGB1 as a therapeutic target in inflammatory diseases. *Expert Opin. Ther. Targets.* 2018;22(3):263–277. DOI: 10.1080/14728222.2018.1439924.
24. Gammoh N. The multifaceted functions of ATG16L1 in autophagy and related processes. *J. Cell Sci.* 2020;133(20):jcs249227. DOI: 10.1242/jcs.249227.
25. Carlus S.J., Carlus F.H., Al-Harbi M.K., Al-Mazroea A.H., Al-Harbi K.M., Abdallah A.M. The Polymorphism at the microRNA-155 binding site in the AGTR1 gene is not significantly associated with rheumatic heart disease in Saudi Arabia Population. *Microrna.* 2020; 9(4):266–270. DOI: 10.2174/2211536609666200108093657.
26. Lu S.C. Glutathione synthesis. *Biochim. Biophys. Acta.* 2013;1830(5):3143–3153. DOI: 10.1016/j.bbagen.2012.09.008.
27. Bašić J., Vojinović J., Jevtović-Stoimenov T., Despotović M., Cvetković T., Lazarević D. et al. The association of CAT-262C/T polymorphism with catalase activity and treatment response in juvenile idiopathic arthritis. *Rheumatol. Int.* 2019;39(3):551–559. DOI: 10.1007/s00296-019-04246-3.
28. Wu S., Wang Y., Zhang M., Wang M., He J.Q. Genetic variants in IFNG and IFNGR1 and tuberculosis susceptibility. *Cytokine.* 2019;123:e154775. DOI: 10.1016/j.cyto.2019.154775.
29. Anania J.C., Chenoweth A.M., Wines B.D., Hogarth P.M. The

Human FcγRII (CD32) family of leukocyte FcR in health and disease. *Front. Immunol.* 2019;10:e464. DOI: 10.3389/fimmu.2019.00464.
30. Clinical guidelines for community-acquired pneumonia of the Russian Pulmonological Society (accessed: 11.02.2022) (in Russ.).
31. Siebert J.N., Hamann L., Verolet C.M., Gameiro C., Grillet S., Siegrist C.A. et al. Toll-interleukin 1 receptor domain-containing adaptor protein 180l single-nucleotide polymorphism is associated with susceptibility to recurrent pneumococcal lower respiratory tract infections in children. *Front. Immunol.* 2018;9:e1780. DOI: 10.3389/fimmu.2018.01780.

Authors contribution

Karnaushkina M.A. – conception and design, drafting of the manuscript, final approval of the manuscript, responsibility for the integrity of all parts of the manuscript. Litvinova M.M. – conception and design, editing, statistical processing of the results, and drafting of the manuscript. Korchagin V.I., Salamaikina S.A., Vasilyeva I.S., Sviridov F.S., Vatsik – Gorodetskaya M.V. – search and review of the literature, processing of the obtained results.

Authors information

Karnaushkina Maria A. – Dr. Sci. (Med.), Associate Professor, Professor of the Department of Internal Diseases with the Course in Cardiology and Functional Diagnostics named after academician V.S. Moiseeva, RUDN University, Moscow, kar3745@yandex.ru, http://orcid.org/0000-0002-8791-2920

Sviridov Filip S. – Junior Researcher, the Loginov Moscow Clinical Scientific Center, Moscow, philipp.sviridov96@gmail.com, https://orcid.org/0000-0003-3767-9339

Korchagin Vitaly I. – Cand. Sci. (Med.), Researcher, Scientific Group for the Development of New Methods for the Detection of Genetic Polymorphisms, Central Research Institute for Epidemiology, Moscow, vitaly_korchagin@rambler.ru, https://orcid.org/0000-0003-2264-6294

Salamaikina Svetlana A. – Junior Researcher, Central Research Institute of Epidemiology, Moscow, Russian Federation.

Vasilyeva Irina S. – Cand. Sci. (Med.), Assistant, Department of Advanced-Level Therapy No. 2, I.M. Sechenov First Moscow State Medical University, Moscow, emmans@rambler.ru, https://orcid.org/0000-0003-2654-1561

Litvinova Maria M. – Cand. Sci. (Med.), Associate Professor of the Department of Medical Genetics, I.M. Sechenov First Moscow State Medical University; Clinical Geneticist, the Loginov Moscow Clinical Scientific Center, Moscow, mariya.litvinova@gmail.com, http://orcid.org/0000-0002-1863-3768

Vatsik-Gorodetskaya Maria V. – Cand. Sci. (Med.), Deputy Chief Physician for Anesthesiology and Resuscitation, Vinogradov City Clinical Hospital, Moscow, m.vatsyk@gmail.com, http://orcid.org/0000-0002-6874-8213, SPIN 5531-0698

(✉) **Vasilyeva Irina S.,** emmans@rambler.ru

Received 24.03.2022;
approved after peer review 16.05.2022;
accepted 09.06.2022

УДК 577.218:577.216
https://doi.org/10.20538/1682-0363-2022-4-170-182

Methods for assessing the effect of microRNA on stemness genes

Pershina A.G.[1], Nevskaya K.V.[1], Morozov K.R.[1], Litviakov N.V.[1, 2]

[1] Siberian State Medical University
2, Moscow Trakt, Tomsk, 634050, Russian Federation

[2] Cancer Research Institute, Tomsk National Research Medical Center (NRMC), Russian Academy of Sciences
5, Kooperativnii Str., Tomsk, 634009, Russian Federation

ABSTRACT

According to the latest concepts, for micrometastasis to develop into macrometastasis, differentiated cancer cells must revert to a dedifferentiated state. Activation of stemness genes plays a key role in this transition. Suppression of stemness gene expression using microRNAs can become the basis for the development of effective anti-metastatic drugs. This article provides an overview of the existing methods for assessing the effect of microRNAs on stemness genes and cancer cell dedifferentiation.

Keywords: microRNA, cancer, stemness genes

Conflict of interest. The authors declare the absence of obvious or potential conflicts of interest related to the publication of this article.

Source of financing. The study was funded by the Ministry of Science and Higher Education of the Russian Federation (agreement No. 075-15-2021-1073 of 29.09.2021).

For citation: Pershina A.G., Nevskaya K.V., Morozov K.R., Litviakov N.V. Methods for assessing the effect of microRNA on stemness genes. *Bulletin of Siberian Medicine.* 2022;21(4):170–182. https://doi.org/10.20538/1682-0363-2022-4-170-182.

Методы оценки влияния микроРНК на гены стволовой пластичности

Першина А.Г.[1], Невская К.В.[1], Морозов К.Р.[1], Литвяков Н.В.[1, 2]

[1] Сибирский государственный медицинский университет (СибГМУ)
Россия, 634050, г. Томск, Московский тракт, 2

[2] Научно-исследовательский институт (НИИ) онкологии, Томский национальный исследовательский медицинский центр (НИМЦ) Российской академии наук
Россия, 634009, г. Томск, пер. Кооперативный, 5

РЕЗЮМЕ

Согласно современным представлениям, для перехода микрометастаза в макрометастаз дифференцированная раковая клетка должна перейти в дедифференцированное состояние. Ключевую роль в данном переходе играет активация генов стволовой пластичности. Подавление экспрессии генов стволовой пластичности с использованием микроРНК может стать основой для разработки эффективных антиметастатических пре-

✉ *Nevskaya Kseniya V.,* nevskayaksenia@gmail.com

паратов. Приведен обзор существующих методов оценки влияния микроРНК на гены стволовой пластичности и процесс дедифференцировки раковой клетки.

Ключевые слова: микроРНК, рак, гены стволовой пластичности

Конфликт интересов. Авторы декларируют отсутствие явных и потенциальных конфликтов интересов, связанных с публикацией настоящей статьи.

Источник финансирования. Работа выполнена при финансовой поддержке Министерства науки и высшего образования Российской Федерации (соглашение № 075-15-2021-1073 от 29.09.2021).

Для цитирования: Першина А.Г., Невская К.В., Морозов К.Р., Литвяков Н.В. Методы оценки влияния микроРНК на гены стволовой пластичности. *Бюллетень сибирской медицины.* 2022;21(4):170–182. https://doi.org/10.20538/1682-0363-2022-4-170-182.

INTRODUCTION

The study of fundamental mechanisms of carcinogenesis and the search for new drugs for therapy of malignant neoplasms are some of the leading tasks in oncology [1]. Metastatic cancer is a serious problem that complicates successful treatment of malignant neoplasms. Depending on the localization of the tumor and the stage of the disease, the proportion of patients who develop metastases ranges from 15 up to 90%. In the vast majority of tumor localizations, cancer patients die from metastases [2, 3]. At relatively early stages of tumor development, some cancer cells enter blood vessels and are further carried to various organs and tissues via the circulatory system, which leads to the formation of the so-called micrometastases. In micrometastases, cancer cells can remain dormant for a long time and under certain conditions trigger macrometastases. According to up-to-date concepts, for transition from micrometastasis to macrometastasis, differentiated cancer cells revert to a dedifferentiated state. Stemness genes play a key role in this transition.

It has been shown that stem cell plasticity is associated with the expression of a number of genes (*SOX2, MYC, OCT, NANOG*, etc.) [4–6]. Changes in the expression of these genes can be mediated by a wide range of factors, including non-coding RNAs (long non-coding RNA, short interfering RNA, microRNA) [7–9]. Currently, there are many studies on approaches to changing the expression of genes contributing to stem cell plasticity using microRNAs [10], since they can provide the basis for developing an effective anti-metastatic drug. This article provides an overview of existing methods for assessing the effect of microRNAs on stemness genes and dedifferentiation of cancer cells.

STEMNESS GENES

Transcription factors associated with stemness play a key role in the carcinogenesis. *SOX2, OCT4, NANOG*, and *MYC* genes are required for self-renewal and reprogramming of stem cells, as well as for maintenance of stem cell homeostasis. Overexpression of these transcription factor genes is associated with the development and progression of a wide range of cancers – breast cancer [11–14], melanoma [15–17], osteosarcoma [18–20], head and neck squamous cell carcinoma [21–23], colorectal cancer [24–26], cervical cancer [27, 28], pancreatic cancer [29–31], and stomach cancer [32–35]. At the same time, the highest level of *SOX2*, *OCT4, NANOG*, and *MYC* expression is typical of aggressive, metastatic, and chemoresistant tumors [17, 35–42].

Expression of stemness genes ensures maintenance of the phenotypic profile, self-renewal of cancer stem cells (CSCs), and proliferation of cancer progenitor cells and stimulates dedifferentiation of non-stem cancer cells [43, 44]. Stemness-related genes implement their functions by participating in almost all signaling pathways related to proliferation (WNT / B-catenin, Notch, Hedgehog (HH) and Sonic Hedgehog (SHH), NRF2, PI3K / AKT / mTOR, etc.) [45]. Activation of the self-renewal program is an integral part of CSC stemness, actively contributing to tumor progression and metastasis and causing high cell turnover and production of progenitor cells [46]. Moreover, the ability of CSCs to self-renew in the long term is one of the main reasons for the development of resistance to antitumor drugs [47, 48]. For example, the development of *SOX2*-mediated chemotherapy resistance was demonstrated for colorectal cancer, squamous cell carcinoma of the head and neck, pancreatic ductal adenocarcinoma, and breast cancer

[21, 38, 49, 50]. Ectopic co-expression of Oct4 and Nanog results in non-small cell lung cancer (NSCLC) cells acquiring the properties of CSCs, including self-renewal, drug resistance, epithelial – mesenchymal transition (EMT), and high tumor-initiating activity [51]. Directly in the focus of possible metastasis, ectopic expression of stemness-related genes can provide acquisition of metastatic potential by differentiated cancer cells due to their dedifferentiation to CSCs [5, 52]. Thus, stemness-related genes can be considered key factors in tumor metastasis, resistance of cancer cells to treatment, and maintenance of the CSC population.

EFFECT OF microRNAS ON STEMNESS GENES

MicroRNAs (miRNAs) are short double-stranded RNAs containing 20-23 nucleotides which have a unique seed sequence of 6–7 nucleotides at 5' end. This sequence binds to mRNA, implementing post-transcriptional regulation of gene expression (Fig. 1, *a*). Currently, more than 2,500 miRNAs are known to be present in the human genome. These miRNAs regulate normal processes of development and homeostasis in cells. Information about miRNAs can be obtained from databases, such as https://www.mirbase.org/, where the description of the published miRNA sequences can be found, or https://miRTarBase.cuhk.edu.cn/ for experimentally confirmed target genes for miRNAs, etc.

Extracellular miRNAs in microvesicles, when getting into target cells, are capable of acting as autocrine, paracrine, and / or endocrine regulators of cellular processes [53]. Taken together, they can affect up to 60% of the cell transcriptome with a significant impact on both protein expression and on the function of the cell as a whole [54–56]. More information about the biogenesis and mechanism of action of miRNA can be found in the articles [57, 58].

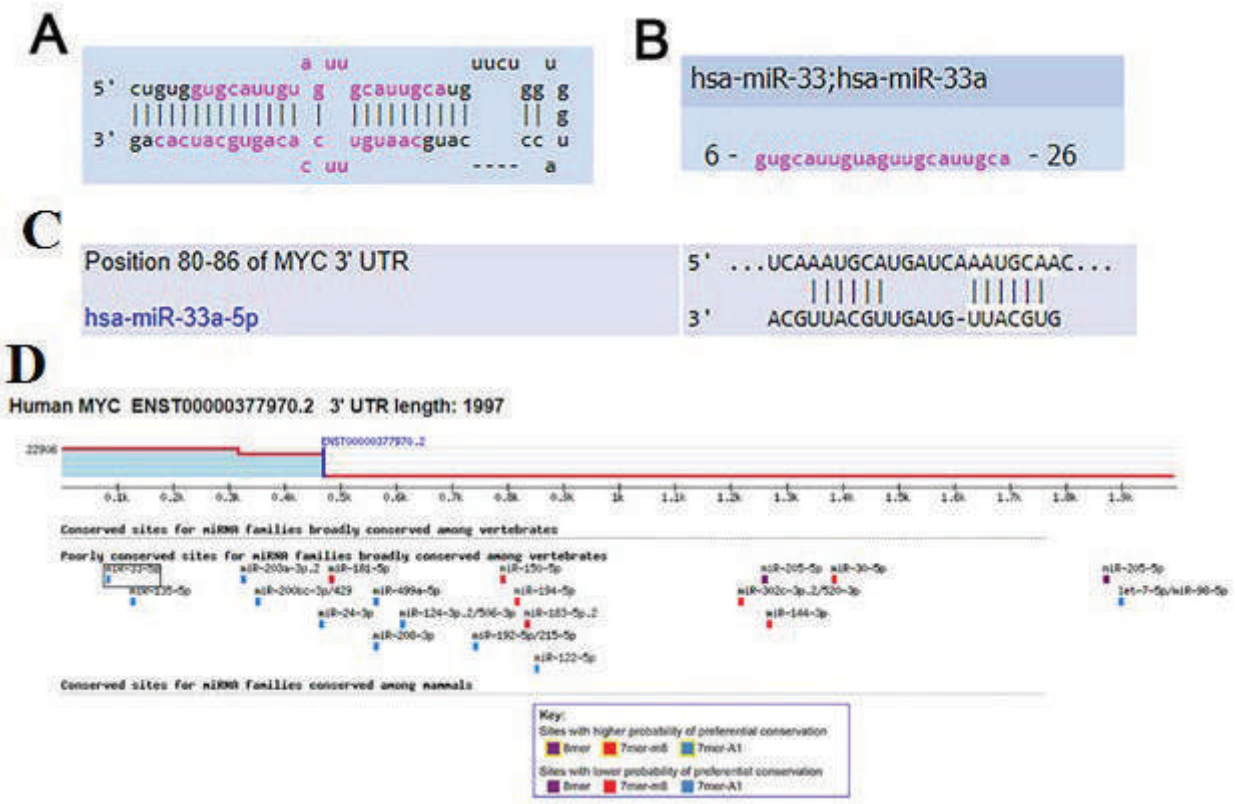

Fig. 1. Post-transcriptional regulation of gene expression: *a* – structure of immature miRNA; *b* – structure of mature miRNA, entering the active site of the Argonaute protein, hsa-miR-33 (miRBase database); *c* – hsa-miR-33 binding to a 3'-untranslated mRNA region encoding the c-Myc transcription factor; *d* – binding sites for various microRNAs in the 3'-untranslated region of the mRNA in the *MYC* gene predicted by TargetScan

Global microRNA dysregulation is observed in cancer cells [59]. There are published studies that confirm the involvement of miRNAs in the regulation of all processes leading to changes characteristic of cancer cells (Fig. 2) [60] – maintenance of proliferative signaling, avoidance of cellular growth suppression, resistance to cell death, unlimited cell division (cell immortality), induction of angiogenesis (growth of new vessels), activation of invasion (penetration into surrounding tissues) and metastasis, reprogramming of energy metabolism, avoidance of destruction by the immune system, epigenetic reprogramming, influence of polymorphic microbiomes, cellular aging, phenotypic plasticity, and closely related to it regulation of stemness genes.

It should be noted that identification of pro- or anti-oncogenic properties for each specific microRNA is a rather difficult task, since the patterns of their expression are tissue specific. Each type of miRNA can bind to multiple mRNA and, at the same time, one type of mRNA can be a target for a subset of miRNAs [61]. Moreover, one miRNA is able to regulate several targets that control different signaling pathways [62] (Fig. 1, *d*). The role of specific miRNA depends on the context – it can act as a tumor suppressor in one situation and as an oncogene in another. Miscellaneous tissues / cells express different sets of long non-coding RNAs (ncRNAs) and circular RNAs, as well as RNA-binding, RNA-modifying, and RNA-editing proteins [63]. Interaction with these proteins allows for microRNA binding sites on mRNA to become available or unavailable. Long ncRNAs and circular RNAs with a miRNA binding site can act as RNA sponges or traps that remove miRNA from the process. An additional factor is alternative polyadenylation, which affects the presence of a miRNA binding site [63].

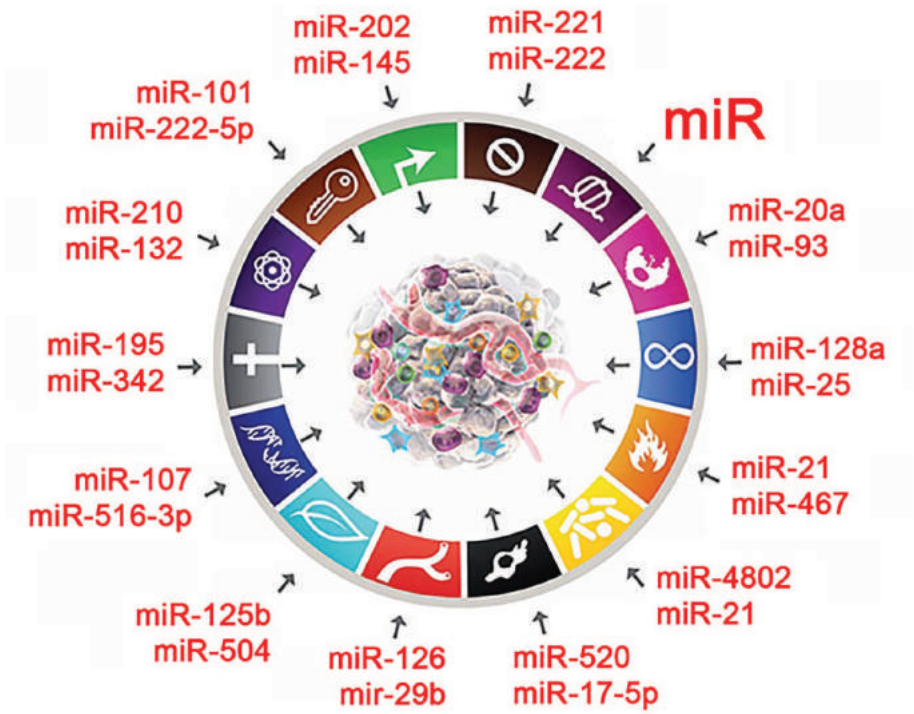

Fig. 2. Examples of microRNAs involved in the regulation of processes in the cell which are responsible for the difference between a normal cell and a cancer cell (adapted from [60])

METHODS FOR ASSESSING THE EFFECT OF MIRNAS ON TARGET GENES

The ability of miRNAs to maintain stem plasticity and regulate EMT, autophagy, resistance, and dedifferentiation of cancer cells is studied using a relatively small range of *in vitro* and *in vivo* methods (Table). At the first stage, to confirm the possible effect of a specific microRNA on a specific gene, researchers use a bioinformatic analysis of the presence of binding sites and a luciferase reporter assay allowing to validate microRNA target genes. The second phase includes an assessment of the effect of microRNA on the expression of the target gene (for example, by a real-time PCR) and, as a result, on protein production (for example, by the Western blotting). The third stage

includes an assessment of the effect of miRNAs on the functional cell activity – proliferation, mammosphere formation, migration, etc.

To predict the target genes of specific miRNAs, online analysis tools in databases, such as TargetScan (https://www.targetscan.org/) and miRDB (https://www.mirdb.org) [83, 84] are used. After conducting the bioinformatic analysis of the data to check for functional relevance of the predicted miRNA – mRNA pairs in the target gene, different modifications of the luciferase reporter assay are used, where luciferase acts as a reporter protein [85]. By gene cloning, the sequence of the 3'-untranslated region of the mRNA in the gene of interest is added at the 3' end of the luciferase gene. If the cell has successfully synthesized a reporter protein (luciferase), the addition of a substrate leads to a chemical reaction. The course of the reaction can be registered by the emergence of bioluminescence, and the intensity of bioluminescence is proportional to the number of successfully translated mRNAs [86]. Thus, the decrease in bioluminescence after miRNA treatment of cells indicates its interaction with mRNA.

To determine the level of gene expression under the effect of miRNAs, real-time PCR is widely used. It allows to evaluate gene expression based on data on the amount of mRNA in the sample [87]. The protein product of the target gene is determined mainly by the Western blotting. This method includes SDS-PAGE electrophoresis of the biosample, transfer of target proteins on a hydrophobic membrane, and their detection using specific antibodies [88]. To analyze the proliferative activity of cells under the effect of microRNA, different cell counting methods are used, ranging from basic techniques with trypan blue stain to more complex multi-stage protocols. One of the most common methods for assessing cell proliferative activity is an MTT assay based on enzymatic reduction of 3-(4,5-dimethyl thiazol-2-yl)-2,5-diphenyl-2H-tetrazolium bromide (yellow soluble tetrazolium dye) with mitochondrial dehydrogenases to purple – violet formazan crystals. The crystals are dissolved in DMSO, after which the optical density of the obtained samples is analyzed [89]. Analogs of the MTT assay are the MTS assay, which uses a different type of tetrazolium dye – (3- (4,5-dimethyl thiazol-2-yl)-5-(3-carboxymethoxyphenyl)-2-(4-sulfophenyl)-2H-tetrazolium)), and the CCK-8 test using the tetrazolium salt WST-8. These types of dyes are water soluble and do not require a solubilization step, which reduces the probability of error in the analysis [90].

Another approach to assessment of the proliferative activity of cells is the analysis using the nucleoside analog BrdU, which is able to incorporate into a replicating DNA and can be determined using specific antibodies [91]. The impedance-based RTCA iCELLIgence instrument is a new technology for assessing cell proliferation and cell death in real time. This technique requires no dyes, and cells can be observed for a long time. However, this method is applicable only to adherent cell cultures [92]. To analyze survival of cells and their ability to proliferate after miRNA treatment, the clonogenic assay is used, which measures the capacity of single cells to form colonies. Cells are seeded at very low density and incubated for 1–3 weeks, after which formed colonies are fixed and stained with crystal violet, and their number is counted [93].

Cell viability in a number of studies is assessed by the presence or absence of flow cytometry signs of necrosis, apoptosis, and secondary necrosis using appropriate fluorescently labeled antibodies, such as Annexin V, caspase-Glo 3/7, and DNA-binding dyes, such as propidium iodide or 7-aminoactinomycin D [94]. It is also possible to use flow cytometry to determine the effect of miRNAs on phases of the cell cycle in pre-fixed cells using DNA-binding dyes [95].

To assess the phenotypic profile of cells, the expression of CSC markers CD24, CD44, CD133, and ALDH is studied using fluorescently labeled antibodies [96]. The expression of stem cell plasticity markers CD44, CD24, CD133, LGR5 and EMT markers Snail, Slug, Zeb1, Cloudin1, B-catenin, E-cadherin, and vimentin is estimated by immunocytochemistry and Western blotting.

Several tests are used to study cell migration. In one of the migration assay variations, after cells reach the monolayer, a streak is made across the bottom of the plate with the use of a cell scraper or pipette tip, and then the dynamics of cell migration and recovery confluency are assessed [97]. A Transwell cell migration assay is also quite popular. The bottom of Transwell inserts has pores that allow cells to move from the insert to the well of the plate. Thus, the assessment of cell migratory ability is based on the number of cells that have passed through the pores of the insert and reached the well of the plate [97]. Transwell inserts are also used to evaluate the ability of cells to invade. Before testing, the bottom of the insert is coated with solubilized extracellular matrix protein mixture Matrigel. During polymerization of

the matrix, a structure similar in composition and properties to the basement membrane is formed. As a result, the number of cells which are able to pass through Matrigel and end up in the main well correlates with their ability to invade [97].

The ability of cancer cells to initiate tumor growth is determined by the spheroid formation assay (for breast cancer cells – mammospheres). For this purpose, a suspension of single cells is placed in wells with hydrophobic coating of the bottom in a serum-free medium supplemented with growth factors or MammoCult medium. After 5–14 days, the number of formed spheroids with a diameter of 35–100 μm is assessed, depending on the cell line used and the design of the experiment [98, 99]. The formation of spheroids in this case is an *in vitro* prototype of metastasis. It is also possible to evaluate the ability of cells in the spheroids to self-renew by disaggregating primary spheroids and placing them again on low surface energy plastic in a serum-free medium for the formation of secondary and, similarly, tertiary spheroids [100]. To prevent migration of spheroids and their aggregation, spheroid formation in soft agar, a modification of the method, is used [101].

Several studies on the role of miRNAs in carcinogenesis are based on *in vivo* experiments on immunodeficient mice (nude, NOD / SCID). For a tumorigenicity assessment, cells transfected with miRNA mimics or genetically modified cell lines that express the target miRNA are used. After subcutaneous injection of cells, the rate of tumor growth, the histological structure of the tumor, and expression of markers of interest via immunohistochemical staining are evaluated [69, 71, 73, 75].

MicroRNAs IN THE REGULATION OF STEMNESS GENES

Over the past 5–7 years, microRNAs have been widely studied as a component of tumor suppressor and oncogenic pathways. There are separate studies on stemness gene regulation using miRNAs in tumor tissues of various localizations. *SOX2* knockdown inhibits invasion and migration of breast cancer cells via antisense RNA [8]. MiR-302b, P21, and miR-145 miRNAs suppress expression of stemness genes *SOX2* and *MYC* in intestinal and diffuse gastric cancer [102]. Overexpression of miR-145 inhibits stem cell transcription factors SOX2, NANOG, and OCT4 in cervical CSCs and also reduces tumor invasion and colony formation *in vitro*. Knockdown of miR-145 leads to a significant decrease in cervical tumor growth in nude mice [9].

It has been shown that miR-148a inhibits stemness properties of glioblastoma cells and the metastatic potential of glioma through inhibition of *SOX2* and *OCT4.* In addition, decreased expression of pre-miR-29a, pre-miR-181, pre-miR-let7b, and pre-miR-124a is observed in CSCs expressing SOX2 and OCT4. MiR-148a has been recognized as one of the most significant microRNAs that negatively regulate in response to co-expression of Oct4 and Sox2. MiR-148a expression inhibits induced Oct4 / Sox2 CSC phenotypes in glioma, including *in vitro* sphere-formation and tumor formation *in vivo* [103]. It was shown that targets for miR-221-3p and miR-221-5p are 3'-untranslated regions of mRNA transcripts in the main transcription factors maintaining pluripotency (OCT4, Nanog, and Sox2) in mouse embryonic cells [104]. MiR-296, miR-470, and miR-134, as well as many others, regulate mouse embryonic stem cells by inhibiting Nanog, OCT4, and Sox2 [105]. MiR-371-5p is capable of suppressing EMT associated with stemness induction via the Wnt / beta-catenin signaling pathway. MiR-371-5p reduces spheroid formation by colorectal cancer cells. Demethylation of the *Sox17* gene induces miR-371-5 expression, which is suppressed by Sox2 expression. The Wnt inhibitory factor 1 (WIF1) is a member of the protein family that binds Wnt and inhibits transmission of the Wnt signaling pathway. WIF1 stimulates miR-200c expression, which reduces the expression of pluripotency and stemness markers *OCT4, c-MYC, c-KIT*, and *MYB*, as well as *BMI1, ZEB1* and *ZEB2,* which results in an increase in the expression of E-cadherin [106].

CONCLUSION

Currently, there are microRNAs known for their ability to regulate expression of stemness genes in embryonic stem cells, as well as in CSCs in different localizations. Extensive research in this area has been conducted since tumor origin from CSCs was proven. Significant achievements have been made in this area, which hopefully will result in the development of drugs that will regulate the activity of CSCs and thereby control tumor growth. In general, the current stage of research involves accumulation of knowledge about the mechanisms of regulation of the metastatic cascade and identification of targets for the development of RNA-based drugs for suppression of metastasis.

Table

Methods for the analysis of microRNA effects on stemness plasticity, EMT stimulation, and reprogramming of differentiated cancer cells.

Gene	miR	Tumor location	Cell line	Gene expression	Effects	Method	Ref.
c-MYC	miR-340	Breast cancer	MDA-MB231	↓ RT, WB	↓ proliferation ↓ migration ↓ invasion	MTT assay Transwell migration assay Transwell migration assay in Matrigel	64
	miR-320a	Hepatocellular carcinoma	HepG2, QGY-7703	↓ RT, WB	↓ proliferation ↓ invasion	MTT assay Transwell migration assay in Matrigel	65
	miR-320a	Breast cancer	MCF-7, T47D	↓ RT, WB	↓ proliferation ↓ resistance to tamoxifen ↓ number of mammospheres	MTT assay CCK-8-test Mammosphere formation assay in soft agar	66
	miR-145	Pancreatic cancer	PDAC	↓ RT, WB	↓ migration	Migration test	67
	miR-34a	Pancreatic cancer	MiaPaCa2	↓ WB	↓ colony formation	Colony formation assay	68
SOX2	miR-590-5p	Breast cancer	MCF-7, ZR75-1	↓ RT, WB	↓ ALDH expression ↓ number of mammospheres ↓ tumorigenicity *in vivo*	Flow cytometry Mammosphere formation assay Xenotransplantation in NOD / SCID mice	69
	miR-590-5p	Non-small cell lung cancer	A549, H1299	↓ RT, WB	↑ expression of E-cadherin ↓ expression of vimentin, Snail, Slug	WB WB	70
	miR-101	Breast cancer	MCF-7, MDA-MB231	↓ RT, WB	↓ colony formation ↓ migration ↓ invasion ↓ proliferation ↑ apoptosis ↓ tumorigenicity *in vivo*	Colony formation assay Migration test Transwell migration in Matrigel MTT assay Flow cytometry Xenotransplantation in nude mice	71
	miR-129-5p	Breast cancer	MCF-7, MDA-MB231	↓ RT	↓ migration ↓ invasion ↑ apoptosis ↓ colony formation ↓ resistance to adriamycin	Migration test Transwell migration in Matrigel Flow cytometry Colony formation assay CCK-8 test	72
NANOG	miR-760	Breast cancer	MCF-7, BT-549	↓ RT, WB	↓ proliferation ↓ migration ↓ tumorigenicity *in vivo*	MTT assay Transwell migration assay Xenotransplantation in nude mice	73
	miR-142-3p	Breast cancer	MCF-7, MDA-MB468	↓ RT	↓ colony formation ↓ number of mammospheres ↑ apoptosis ↑ cells in G2M phase ↓ SOX2, ALDH, c-MYC expression	Colony formation assay Mammosphere formation assay Flow cytometry Flow cytometry WB	74

	miR-134	Glioblastoma	U87	↓ RT, WB	↓ invasion ↓ migration ↓ tumorigenicity *in vivo*	Transwell-migration in Matrigel Transwell-migration Migration test Xenotransplantation in nude mice	75
	miR-128a	Prostate cancer	PC3, DU145, PPC-1, LAPC9, LNCaP, VCAP, NHP9	↓ RT, WB	↓ proliferation ↓ invasion ↓ number of cells in the S-phase ↓ number of mammospheres ↓ self-renewal ↓ tumorigenicity *in vivo*	BrdU assay Transwell migration in Matrigel Flow cytometry Spheroid formation assay Formation of secondary spheroids Xenotransplantation in NOD / SCID mice	76
	miR-203	Breast cancer	MDA-MB231	↓ RT	↓ population of $CD44^+CD24^-$ stem cells	Flow cytometry	77
	miR-150	Breast cancer	MDA-MB231	↑ RT	↑ population of $CD44^+CD24^-$ stem cells	Flow cytometry	77
	miR-126	Prostate cancer	PC3, DU145, LNCaP	↑ RT	↑ proliferation	MTS assay	78
	miR-149	Prostate cancer	PC3, DU145, LNCaP	↑ RT	↑ proliferation	MTS assay	78
Oct4	miR-598	Stomach cancer	MKN-45	↓ RT, WB	↓ proliferation ↓ colony formation ↓ migration ↓ invasion ↑apoptosis	MTT assay Colony formation assay Migration test Transwell migration in Matrigel Flow cytometry	79
	miR-299-3p	Breast cancer	MDA-MB231, HT1080	↓ RT, WB	↓ invasion ↓ proliferation ↑ apoptosis	LOC-analysis CellToxGreen Flow cytometry	80
	miR-145	Lung adenocarcinoma	A549	↓ RT, WB	↓ invasion ↓ proliferation ↓ number of cells in S-phase ↓ $CD133^+$ cells ↓ number of tumor spheres	Transwell migration in Matrigel CCK-8 test Flow cytometry Flow cytometry Mammosphere formation assay	81
	miR-3658	Colorectal cancer	SW480	↓ RT, WB	↓ CyclinD1, PCNA expression ↓ proliferation ↓ migration ↓ Snail, Zeb1 expression ↑ Cloudin1, B-catenin expression ↑ proportion of cells in the SubG1 phase	WB MTT assay Migration test WB WB Flow cytometry	82

Note: ↑ – increase, ↓ – decrease, RT – Real-time reverse transcription PCR, WB – Western blotting.

REFERENCES

1. Sung H., Ferlay J., Siegel R.L., Laversanne M., Soerjomataram I., Jemal A. et al. Global Cancer Statistics 2020: GLOBOCAN Estimates of Incidence and Mortality Worldwide for 36 Cancers in 185 Countries. *CA Cancer J. Clin*. 2021;71(3):209–249. DOI: 10.3322/caac.21660.
2. Sopik V., Narod S.A. The relationship between tumour size, nodal status and distant metastases: on the origins of breast cancer. *Breast Cancer Research and Treatment.* 2018;170(3):647–656. DOI: 10.1007/s10549-018-4796-9.
3. Yu K.D., Jiang Y.Z., Shao Z.M. Difference between observed and expected number of involved lymph nodes reflects the metastatic potential of breast cancer independent to intrinsic subtype. *Oncotarget*. 2015;6(18):16686–16697. DOI: 10.18632/oncotarget.3647.
4. Miranda A., Hamilton P.T., Zhang A.W., Pattnaik S., Becht E., Mezheyeuski A. et al. Cancer stemness, intratumoral heterogeneity, and immune response across cancers. *Proc. Natl. Acad. Sci USA*. 2019;116(18):9020–9029. DOI: 10.1073/pnas.1818210116.
5. Litviakov N., Ibragimova M., Tsyganov M., Kazantseva P., Deryusheva I., Pevzner A. et al. Amplifications of stemness genes and the capacity of breast tumors for metastasis. *Oncotarget*. 2020;11:1988–2001. DOI: 10.18632/oncotarget.27608.
6. Hatina J., Kripnerová M., Houdek Z., Pešta M., Tichánek F. Pluripotency stemness and cancer: more questions than answers. *Adv. Exp. Med. Biol*. 2022;1376:77–100. DOI: 10.1007/5584_2021_663.
7. Almairac F., Turchi L., Sakakini N., Debruyne D.N., Elkeurti S., Gjernes E. et al. ERK-mediated loss of miR-199a-3p and induction of EGR1 act as a "Toggle Switch" of GBM cell dedifferentiation into NANOG- and OCT4-positive cells. *Cancer Res*. 2020;80(16):3236–3250. DOI: 10.1158/0008-5472.CAN-19-0855.
8. Liu K., Xie F., Gao A., Zhang R., Zhang L., Xiao Z. et al. SOX2 regulates multiple malignant processes of breast cancer development through the SOX2/miR-181a-5p, miR-30e-5p/TUSC3 axis. *Mol. Cancer*. 2017;16(1):62. DOI: 10.1186/s12943-017-0632-9.
9. Zhou X., Yue Y., Wang R., Gong B., Duan Z. MicroRNA-145 inhibits tumorigenesis and invasion of cervical cancer stem cells. *Int. J. Oncol*. 2017;50(3):853–862. DOI: 10.3892/ijo.2017.3857.
10. Jiao X., Qian X., Wu L., Li B., Wang Y., Kong X. et al. MicroRNA: the impact on cancer stemness and therapeutic resistance. *Cells*. 2019;9(1):8. DOI: 10.3390/cells9010008.
11. Cho Y., Kang H.G., Kim S.J., Lee S., Jee S., Ahn S.G. et al. Post-translational modification of OCT4 in breast cancer tumorigenesis. *Cell Death Differ*. 2018;25(10):1781–1795. DOI: 10.1038/s41418-018-0079-6.
12. Leis O., Eguiara A., Lopez-Arribillaga E., Alberdi M.J., Hernandez-Garcia S., Elorriaga K. et al. Sox2 expression in breast tumours and activation in breast cancer stem cells. *Oncogene*. 2012;31(11):1354–1365. DOI: 10.1038/onc.2011.338.
13. Fallah Y., Brundage J., Allegakoen P., Shajahan-Haq A.N. MYC-driven pathways in breast cancer subtypes. *Biomolecules*. 2017;7(3):53. DOI: 10.3390/biom7030053.
14. Lu X., Mazur S.J., Lin T., Appella E., Xu Y. The pluripotency factor nanog promotes breast cancer tumorigenesis and metastasis. *Oncogene*. 2014;33(20):2655–2664. DOI: 10.1038/onc.2013.209.
15. Santini R., Pietrobono S., Pandolfi S., Montagnani V., D'Amico M., Penachioni J.Y. et al. SOX2 regulates self-renewal and tumorigenicity of human melanoma-initiating cells. *Oncogene*. 2014;33(38):4697–4708. DOI: 10.1038/onc.2014.71.
16. Silva C.T.X., Saddi V.A., Silva K.S.F.E., Sugita D.M., Guillo L.A. Expression of the cancer stem cell marker OCT4 is associated with worse prognosis and survival in cutaneous melanoma. *Melanoma Res*. 2021;31(5):439–448. DOI: 10.1097/CMR.0000000000000767.
17. Lin X., Sun R., Zhao X., Zhu D., Zhao X., Gu Q. et al. C-myc overexpression drives melanoma metastasis by promoting vasculogenic mimicry via c-myc/snail/Bax signaling. *J. Mol. Med. (Berl.)*. 2017;95(1):53–67. DOI: 10.1007/s00109-016-1452-x.
18. Basu-Roy U., Seo E., Ramanathapuram L., Rapp T.B., Perry J.A., Orkin S.H. et al. Sox2 maintains self renewal of tumor-initiating cells in osteosarcomas. *Oncogene*. 2012;31(18):2270–2282. DOI: 10.1038/onc.2011.405.
19. Feng W., Dean D.C., Hornicek F.J., Spentzos D., Hoffman R.M., Shi H. et al. Myc is a prognostic biomarker and potential therapeutic target in osteosarcoma. *Ther. Adv. Med. Oncol*. 2020;12:1758835920922055. DOI: 10.1177/1758835920922055.
20. Yan G.N., Tang X.F., Zhang X.C., He T., Huang Y.S., Zhang X. et al. TSSC3 represses self-renewal of osteosarcoma stem cells and Nanog expression by inhibiting the Src/Akt pathway. *Oncotarget*. 2017;8(49):85628–85641. DOI: 10.18632/oncotarget.20429.
21. Lee S.H., Oh S.Y., Do S.I., Lee H.J., Kang H.J., Rho Y.S. et al. SOX2 regulates self-renewal and tumorigenicity of stem-like cells of head and neck squamous cell carcinoma. *Br. J. Cancer*. 2014;111(11):2122–2130. DOI: 10.1038/bjc.2014.528.
22. Lin S.H., Wang H.K., Yeh K.T., Tai H.C., Wang H.Y., Huang L.R. et al. c-MYC expression in T (III/IV) stage oral squamous cell carcinoma (OSCC) patients. *Cancer Manag. Res*. 2019;11:5163–5169. DOI: 10.2147/CMAR.S20194.
23. Pedregal-Mallo D., Hermida-Prado F., Granda-Díaz R., Montoro-Jiménez I., Allonca E., Pozo-Agundo E. et al. Prognostic significance of the pluripotency factors NANOG, SOX2, and OCT4 in head and neck squamous cell carcinomas. *Cancers (Basel)*. 2020;12(7):1794. DOI: 10.3390/cancers12071794.
24. Lundberg I.V., Edin S., Eklöf V., Öberg Å., Palmqvist R., Wikberg M.L. SOX2 expression is associated with a cancer stem cell state and down-regulation of CDX2 in colorectal cancer. *BMC Cancer*. 2016;16:471. DOI: 10.1186/s12885-016-2509-5.
25. He W.L., Weng X.T., Wang J.L., Lin Y.K., Liu T.W., Zhou Q.Y. et al. Association Between c-Myc and Colorec-

tal Cancer Prognosis: A Meta-Analysis. *Front. Physiol*. 2018;9:1549. DOI: 10.3389/fphys.2018.01549.
26. Roudi R., Barodabi M., Madjd Z., Roviello G., Corona S.P., Panahei M. Expression patterns and clinical significance of the potential cancer stem cell markers OCT4 and NANOG in colorectal cancer patients. *Mol. Cell Oncol*. 2020;7(5):1788366. DOI: 10.1080/23723556.2020.1788366.
27. Liu X.F., Yang W.T., Xu R., Liu J.T., Zheng P.S. Cervical cancer cells with positive Sox2 expression exhibit the properties of cancer stem cells. *PLoS One*. 2014;9(1):e87092. DOI: 10.1371/journal.pone.0087092.
28. Kim B.W., Cho H., Choi C.H., Ylaya K., Chung J.Y., Kim J.H. et al. Clinical significance of OCT4 and SOX2 protein expression in cervical cancer. *BMC Cancer*. 2015;15:1015. DOI: 10.1186/s12885-015-2015-1.
29. Herreros-Villanueva M., Zhang J.S., Koenig A., Abel E.V., Smyrk T.C., Bamlet W.R. et al. SOX2 promotes dedifferentiation and imparts stem cell-like features to pancreatic cancer cells. *Oncogenesis*. 2013;2(8):e61. DOI: 10.1038/oncsis.2013.23.
30. Gzil A., Zarębska I., Bursiewicz W., Antosik P., Grzanka D., Szylberg Ł. Markers of pancreatic cancer stem cells and their clinical and therapeutic implications. *Mol. Biol. Rep*. 2019;46(6):6629–6645. DOI: 10.1007/s11033-019-05058-1.
31. Schneider G., Wirth M., Keller U., Saur D. Rationale for MYC imaging and targeting in pancreatic cancer. *EJNMMI Res*. 2021;11(1):104. DOI: 10.1186/s13550-021-00843-1.
32. Tian T., Zhang Y., Wang S., Zhou J., Xu S. Sox2 enhances the tumorigenicity and chemoresistance of cancer stem-like cells derived from gastric cancer. *J. Biomed. Res*. 2012;26(5):336–345. DOI: 10.7555/JBR.26.20120045.
33. Calcagno D.Q., Leal M.F., Assumpcao P.P., Smith M.A., Burbano R.R. MYC and gastric adenocarcinoma carcinogenesis. *World. J. Gastroenterol*. 2008;14(39):5962–5968. DOI: 10.3748/wjg.14.5962.
34. Chen B., Zhu Z., Li L., Ye W., Zeng J., Gao J. et al. Effect of overexpression of Oct4 and Sox2 genes on the biological and oncological characteristics of gastric cancer cells. *OncoTargets Ther*. 2019;12:4667–4682. DOI: 10.2147/OTT.S209734.
35. Lin T., Ding Y.Q., Li J.M. Overexpression of Nanog protein is associated with poor prognosis in gastric adenocarcinoma. *Med. Oncol*. 2012;29(2):878–885. DOI: 10.1007/s12032-011-9860-9.
36. Annovazzi L., Mellai M., Caldera V., Valente G., Schiffer D. SOX2 expression and amplification in gliomas and glioma cell lines. *Cancer Genomics Proteomics*. 2011;8(3):139–147.
37. Auffinger B., Spencer D., Pytel P., Ahmed A.U., Lesniak M.S. The role of glioma stem cells in chemotherapy resistance and glioblastoma multiforme recurrence. *Expert. Rev. Neurother*. 2015;15 (7):741– 752. DOI: 10.1586/14737175.2015.1051968.
38. Rothenberg S.M., Concannon K., Cullen S., Boulay G., Turke A.B., Faber A.C. et al. Inhibition of mutant EGFR in lung cancer cells triggers SOX2-FOXO6-dependent survival pathways. *Elife*. 2015;4:e06132. DOI: 10.7554/eLife.06132.
39. Piva M., Domenici G., Iriondo O., Rábano M., Simões B.M., Comailles V. et al. Sox2 promotes tamoxifen resistance in breast cancer cells. *EMBO Mol. Med*. 2014;6(1):66–79. DOI: 10.1002/emmm.
40. Keysar S.B., Le P.N., Miller B., Jackson B.C., Eagles J.R., Nieto C. et al. Regulation of head and neck squamous cancer stem cells by PI3K and SOX2. *J. Natl. Cancer Inst*. 2016;109(1):djw189. DOI: 10.1093/jnci/djw189.
41. Rasti A., Mehrazma M., Madjd Z., Abolhasani M., Saeednejad Zanjani L., Asgari M. Co-expression of cancer stem cell markers OCT4 and NANOG predicts poor prognosis in renal cell carcinomas. *Sci. Rep*. 2018;8(1):11739. DOI: 10.1038/s41598-018-30168-4.
42. Gao S., Pan Y., Song L., Dong L., Weng L.I., Wang P. et al. Nanog predicts poor prognosis in human pancreatic cancer and is downregulated by oingyihuaJi formula in pancreatic cancer stem cells. *Evid. Based Complement. Alternat. Med*. 2016;2016:7028289. DOI: 10.1155/2016/7028289.
43. Zhang Q., Han Z., Zhu Y., Chen J., Li W. The Role and Specific Mechanism of OCT4 in Cancer Stem Cells: A Review. *Int. J. Stem Cells*. 2020;13(3):312–325. DOI: 10.15283/ijsc20097.
44. Jing N., Gao W.Q., Fang Y.X. Regulation of formation, stemness and therapeutic resistance of cancer stem cells. *Front. Cell Dev. Biol*. 2021 9:641498. DOI: 10.3389/fcell.2021.641498.
45. Ibragimova M., Tsyganov M., Litviakov N. Tumour stem cells in breast cancer. *Int. J. Mol. Sci*. 2022;23(9):5058. DOI: 10.3390/ijms23095058.
46. Cabrera M.C., Hollingsworth R.E., Hurt E.M. Cancer stem cell plasticity and tumor hierarchy. *World J. Stem Cells*. 2015;7(1):27–36. DOI: 10.4252/wjsc.v7.i1.27.
47. Clarke M.F., Dick J.E., Dirks P.B., Eaves C.J., Jamieson C.H. Jones D.L. et al. Cancer stem cells – perspectives on current status and future directions: AACR Workshop on cancer stem cells. *Cancer Res*. 2006;66(19):9339–9344. DOI: 10.1158/0008-5472.CAN-06-3126.
48. Dean M., Fojo T., Bates S. Tumour stem cells and drug resistance. *Nat. Rev. Cancer*. 2005;5(4):275–284. DOI: 10.1038/nrc1590.
49. Han X., Fang X., Lou X., Hua D., Ding W., Foltz G. et al. Silencing SOX2 induced mesenchymal-epithelial transition and its expression predicts liver and lymph node metastasis of CRC patients. *PLoS One*. 2012;7(8):e41335. DOI: 10.1371/journal.pone.0041335.
50. Mukherjee P., Gupta A., Chattopadhyay D., Chatterji U. Modulation of SOX2 expression delineates an end-point for paclitaxel-effectiveness in breast cancer stem cells. *Sci. Rep.* 2017;7:9170. DOI: 10.1038/s41598-017-08971-2.
51. Liu L., Zhu H., Liao Y., Wu W., Liu L., Liu L. et al. Inhibition of Wnt/β-catenin pathway reverses multi-drug resistance and EMT in Oct4+/Nanog+ NSCLC cells. *Biomed. Pharmacother*. 2020;127:110225. DOI: 10.1016/j.biopha.2020.110225.
52. Fumagalli A., Oost K.C., Kester L., Morgner J., Bornes L., Bruens L. et al. Plasticity of Lgr5-negative cancer cells drives metastasis in colorectal cancer. *Cell Stem*

Cell. 2020;26(4):569–578.e7. DOI: 10.1016/j.stem.2020.02.008.
53. Iftikhar H., Carney G.E. Evidence and potential *in vivo* functions for biofluid miRNAs: from expression profiling to functional testing: potential roles of extracellular miRNAs as indicators of physiological change and as agents of intercellular information exchange. *Bioessays.* 2016;38:367–378. DOI: 10.1002/bies.201500130.
54. Bartel D.P. Metazoan microRNAs. *Cell*. 2018;173(1):20–51. DOI: 10.1016/j.cell.2018.03.006.
55. Gebert L.F.R., MacRae I.J. Regulation of microRNA function in animals. *Nat. Rev. Mol. Cell Biol*. 2019;20(1):21–37. DOI: 10.1038/s41580-018-0045-7.
56. Thomson D.W., Dinger M.E. Endogenous microRNA sponges: evidence and controversy. *Nat. Rev. Genet*. 2016;17(5):272– 283. DOI: 10.1038/nrg.2016.20.
57. Van Rooij E., Kauppinen S. Development of microRNA therapeutics is coming of age. *EMBO Mol. Med*. 2014;6(7):851–864. DOI: 10.15252/emmm.201100899.
58. Nakanishi K. Anatomy of RISC: how do small RNAs and chaperones activate Argonaute proteins? *Wiley Interdiscip. Rev. RNA*. 2016;7(5):637–660. DOI: 10.1002/wrna.1356.
59. Croce C.M. Causes and consequences of microRNA dysregulation in cancer. *Nat. Rev. Genet*. 2009;10(10):704–714. DOI: 10.1038/nrg2634.
60. Hanahan D. Hallmarks of cancer: new dimensions. *Cancer Discovery*. 2022;12(1):31–46. DOI: 10.1158/2159-8290.CD-21-1059.
61. Bartel D.P. MicroRNAs. *Cell*. 2004;116:281–297. DOI: 10.1016/S0092-8674(04)00045-5.
62. Krek A., Grün D., Poy M.N., Wolf R., Rosenberg L., Epstein E.J. et al. Combinatorial microRNA target predictions. *Nat. Genet*. 2005;37(5):495–500. DOI: 10.1038/ng1536.
63. Chen P., Liao K., Xiao C. MicroRNA says no to mass production. *Nat. Immunol.* 2018;19(10):1040–1042. DOI: 10.1038/s41590-018-0215-y.
64. Mohammadi-Yeganeh S., Paryan M., Arefian E., Vasei M., Ghanbarian H., Mahdian R. et al. MicroRNA-340 inhibits the migration, invasion, and metastasis of breast cancer cells by targeting Wnt pathway. *Tumour Biol*. 2016;37(7):8993–9000. DOI: 10.1007/s13277-015-4513-9.
65. Xie F., Yuan Y., Xie L., Ran P., Xiang X., Huang Q. et al. miRNA-320a inhibits tumor proliferation and invasion by targeting c-Myc in human hepatocellular carcinoma. *Onco. Targets Ther*. 2017;10:885–894. DOI: 10.2147/OTT.S122992.
66. Lü M., Ding K., Zhang G., Yin M., Yao G., Tian H. et al. MicroRNA-320a sensitizes tamoxifen-resistant breast cancer cells to tamoxifen by targeting ARPP-19 and ERRγ. *Sci. Rep*. 2015;5:8735. DOI: 10.1038/srep08735.
67. Azmi A.S., Li Y., Muqbil I., Aboukameel A., Senapedis W., Baloglu E. et al. Exportin 1 (XPO1) inhibition leads to restoration of tumor suppressor miR-145 and consequent suppression of pancreatic cancer cell proliferation and migration. *Oncotarget*. 2017;8(47):82144–82155. DOI: 10.18632/oncotarget.19285.
68. Gibori H., Eliyahu S., Krivitsky A., Ben-Shushan D., Epshtein Y., Tiram G. et al. Amphiphilic nanocarrier-induced modulation of PLK1 and miR-34a leads to improved therapeutic response in pancreatic cancer. *Nat. Commun*. 2018;9(1):16. DOI: 10.1038/s41467-017-02283-9.
69. Zhou L., Zhao L.C., Jiang N., Wang X.L., Zhou X.N., Luo X.L. et al. MicroRNA miR-590-5p inhibits breast cancer cell stemness and metastasis by targeting SOX2. *Eur. Rev. Med. Pharmacol. Sci*. 2017;21(1):87– 94.
70. Chang Z. Downregulation of SOX2 may be targeted by miR-590-5p and inhibits epithelial-to-mesenchymal transition in non-small-cell lung cancer. *Exp. Ther. Med*. 2019;18(2):1189– 1195. DOI: 10.3892/etm.2019.7642.
71. Wang J., Zeng H., Li H., Chen T., Wang L., Zhang K. et al. MicroRNA-101 Inhibits Growth, Proliferation and Migration and Induces Apoptosis of Breast Cancer Cells by Targeting Sex-Determining Region Y-Box 2. *Cell Physiol. Biochem.* 2017;43:717–732. DOI: 10.1159/000481445.
72. Zeng H., Wang L., Wang J., Chen T., Li H., Zhang K. et al. MicroRNA-129-5p suppresses Adriamycin resistance in breast cancer by targeting SOX2. *Arch. Biochem. Biophys*. 2018;651:52–60. DOI: 10.1016/j.abb.2018.05.018.
73. Han M.L., Wang F., Gu Y.T., Pei X.H., Ge X., Guo G.C. et al. MicroR-760 suppresses cancer stem cell subpopulation and breast cancer cell proliferation and metastasis: By down-regulating NANOG. *Biomed. Pharmacother*. 2016;80:304–310. DOI: 10.1016/j.biopha.2016.03.024.
74. Mansoori B., Duijf P.H.G., Mohammadi A., Safarzadeh E., Ditzel H.J., Gjerstorff M.F. et al. MiR-142-3p targets HMGA2 and suppresses breast cancer malignancy. *Life Sci*. 2021;276:119431. DOI: 10.1016/j.lfs.2021.119431.
75. Niu C.S., Yang Y., Cheng C.D. MiR-134 regulates the proliferation and invasion of glioblastoma cells by reducing Nanog expression. *Int. J. Oncol*. 2013;42(5):1533–1540. DOI: 10.3892/ijo.2013.1844.
76. Jin M., Zhang T., Liu C., Badeaux M.A., Liu B., Liu R. et al. miRNA-128 suppresses prostate cancer by inhibiting BMI-1 to inhibit tumor-initiating cells. *Cancer Res*. 2014;74(15):4183–4195. DOI: 10.1158/0008-5472.CAN-14-0404.
77. El-Osaily H.H., Ibrahim I.H., Essawi M.L., Salem S.M. Impact of miRNAs expression modulation on the methylation status of breast cancer stem cell-related genes. *Clin. Transl. Oncol*. 2021;23(7):1440–1451. DOI: 10.1007/s12094-020-02542-0.
78. Fujii T., Shimada K., Tatsumi Y., Fujimoto K., Konishi N. Syndecan-1 responsive microRNA-126 and 149 regulate cell proliferation in prostate cancer. *Biochem. Biophys. Res. Commun*. 2015;456(1):183–189. DOI: 10.1016/j.bbrc.2014.11.056.
79. Ma Y., Yan F., Wei W., Deng J., Li L., Liu L. et al. MicroRNA-598 inhibits the growth and maintenance of gastric cancer stem-like cells by down-regulating RRS1. *Cell Cycle.* 2019;18(20):2757–2769. DOI: 10.1080/15384101.2019.1657338.
80. Göhring A.R., Reuter S., Clement J.H., Cheng X., Theobald J., Wölfl S. et al. Human microRNA-299-3p decreases invasive behavior of cancer cells by downregulation of Oct4 expression and causes apoptosis. *PLoS One*. 2017;12(4):e0174912. DOI: 10.1371/journal.pone.0174912.

81. Yin R., Zhang S., Wu Y., Fan X., Jiang F., Zhang Z. et al. microRNA-145 suppresses lung adenocarcinoma-initiating cell proliferation by targeting OCT4. *Oncol. Rep*. 2011;25(6):1747–1754. DOI: 10.3892/or.2011.1252.
82. Hosseini F., Soltani B.M., Baharvand H., Hosseinkhani S. Hsa-miR-3658 down-regulates OCT4 gene expression followed by suppressing SW480 cell proliferation and migration. *Biochem. J*. 2020;477(12):2281–2293. DOI: 10.1042/BCJ20190619.
83. Chen Y., Wang X. miRDB: an online database for prediction of functional microRNA targets. *Nucleic Acids Res*. 2020;48(D1):D127– D131. DOI: 10.1093/nar/gkz757.
84. Moradi S., Kamal A., Aboulkheyr Es.H., Farhadi F., Ebrahimi M., Chitsaz H. et al. Pan-cancer analysis of microRNA expression profiles highlights microRNAs enriched in normal body cells as effective suppressors of multiple tumor types: A study based on TCGA database. *PLoS One*. 2022;17(4):e0267291. DOI: 10.1371/journal.pone.0267291.
85. Clément T., Salone V., Rederstorff M. Dual luciferase gene reporter assays to study miRNA function. *Methods Mol. Biol*. 2015;1296:187–198. DOI: 10.1007/978-1-4939-2547-6_17.
86. Tomasello L., Cluts L., Croce C.M. Experimental Validation of MicroRNA Targets: Luciferase Reporter Assay. *Methods Mol. Biol*. 2019;1970:315–330. DOI: 10.1007/978-1-4939-9207-2_17.
87. Arya M., Shergill I.S., Williamson M., Gommersall L., Arya N., Patel H.R. Basic principles of real-time quantitative PCR. *Expert Rev. Mol. Diagn*. 2005;5(2):209–219. DOI: 10.1586/14737159.5.2.209.
88. Mahmood T., Yang P.C. Western blot: technique, theory, and trouble shooting. *N. Am. J. Med. Sci*. 2012;4(9):429–434. DOI: 10.4103/1947-2714.100998.
89. Kumar P., Nagarajan A., Uchil P.D. Analysis of cell viability by the MTT assay. *Cold Spring Harb. Protoc*. 2018;2018(6). DOI: 10.1101/pdb.prot095505.
90. Kamiloglu S., Sari G., Ozdal T., Capanoglu E. Guidelines for cell viability assays. *Food Frontiers*. 2020;1(3):332–349. DOI: 10.1002/fft2.44.
91. Salic A., Mitchison T.J. A chemical method for fast and sensitive detection of DNA synthesis *in vivo*. *Proc. Natl. Acad. Sci. USA*. 2008;105(7):2415–2420. DOI: 10.1073/pnas.0712168105.
92. Türker Şener L., Albeniz G., Dinç B., Albeniz I. iCELLigence real-time cell analysis system for examining the cytotoxicity of drugs to cancer cell lines. *Exp. Ther. Med*. 2017;14(3):1866–1870. DOI: 10.3892/etm.2017.4781.
93. Franken N.A., Rodermond H.M., Stap J., Haveman J., van Bree C. Clonogenic assay of cells *in vitro*. *Nat. Protoc*. 2006;1(5):2315–2319. DOI: 10.1038/nprot.2006.339.
94. Telford W.G. Multiparametric analysis of apoptosis by flow cytometry. *Methods Mol. Biol*. 2018;1678:167–202. DOI: 10.1007/978-1-4939-7346-0_10.
95. Kim K.H., Sederstrom J.M. Assaying cell cycle status using flow cytometry. *Curr. Protoc. Mol. Biol*. 2015;111:28.6.1–28.6.11. DOI: 10.1002/0471142727.mb2806s111.
96. Walcher L., Kistenmacher A.K., Suo H., Kitte R., Dluczek S., Strauß A. et al. Cancer stem cells-origins and biomarkers: perspectives for targeted personalized therapies. *Front. Immunol*. 2020;11:1280. DOI: 10.3389/fimmu.2020.01280.
97. Pijuan J., Barceló C., Moreno D.F., Maiques O., Sisó P., Marti R.M. et al. *In vitro* cell migration, invasion, and adhesion assays: from cell imaging to data analysis. *Front. Cell Dev. Biol*. 2019;7:107. DOI: 10.3389/fcell.2019.00107.
98. Bailey P.C., Lee R.M., Vitolo M.I., Pratt S.J., Ory E., Chakrabarti K. et al. Single-cell tracking of breast cancer cells enables prediction of sphere formation from early cell divisions. *Iscience*. 2018;8P:29–39. DOI: 10.1016/j.isci.2018.08.015.
99. Lombardo Y., de Giorgio A., Coombes C.R., Stebbing J., Castellano L. Mammosphere formation assay from human breast cancer tissues and cell lines. *JoVE (Journal of Visualized Experiments)*. 2015;97:e52671. DOI: 10.3791/52671.
100. Yousefnia S., Ghaedi K., Seyed Forootan F., Nasr Esfahani M.H. Characterization of the stemness potency of mammospheres isolated from the breast cancer cell lines. *Tumor Biology*. 2019;41(8). DOI: 10.1177/1010428319869101.
101. Du F., Zhao X., Fan D. Soft agar colony formation assay as a hallmark of carcinogenesis. *Bio. Protoc*. 2017;7(12):e2351. DOI: 10.21769/BioProtoc.2351.
102. Khalili M., Vasei M., Khalili D., Alimoghaddam K., Sadeghizadeh M., Mowla S.J. Downregulation of the jenes involved in reprogramming (SOX2, c-MYC, miR-302, miR-145, and P21) in gastric adenocarcinoma. *J. Gastrointest. Cancer*. 2015;46(3):251–258. DOI: 10.1007/s12029-015-9695-2.
103. Lopez-Bertoni H., Lal B., Li A., Caplan M., Guerrero-Cázares H., Eberhart C.G. et al. DNMT-dependent suppression of microRNA regulates the induction of GBM tumor-propagating phenotype by Oct4 and Sox2. *Oncogene*. 2015;34(30):3994–4004. DOI: 10.1038/onc.2014.334.
104. Chen T.Y., Lee S.H., Dhar S.S., Lee M.G. Protein arginine methyltransferase 7-mediated microRNA-221 repression maintains Oct4, Nanog, and Sox2 levels in mouse embryonic stem cells. *J. Biol. Chem*. 2018;293(11):3925–3936. DOI: 10.1074/jbc.RA117.000425.
105. Beh-Pajooh A., Cantz T. The role of microRNAs in embryonic and induced pluripotency. *J. Stem. Cells Regen. Med*. 2018; 14 (1): 3–9. DOI: 10.46582/jsrm.1401002.
106. McCubrey J.A., Lertpiriyapong K., Steelman L.S., Abrams S.L.,Yang L.V., Murata R.M. et al. Effects of resveratrol, curcumin, berberine and other nutraceuticals on aging, cancer development, cancer stem cells and microRNAs. *Aging (Albany NY)*. 2017;9(6):1477–1536. DOI: 10.18632/aging.101250.

Authors information

Pershina Alexandra G. – Cand. Sci. (Biology), Head of the Center for Bioscience and Bioengineering, Central Research Laboratory, Siberian State Medical University, Tomsk, allysyz@mail.ru, https://orcid.org/0000-0001-7604-9722

Nevskaya Kseniya V. – Cand. Sci. (Med.), Researcher, Center for Bioscience and Bioengineering, Central Research Laboratory, Siberian State Medical University, Tomsk, nevskayaksenia@gmail.com, https://orcid.org/0000-0003-1659-8812

Morozov Konstantin R. – Student, Department of Pediatrics, Siberian State Medical University, Tomsk, morozov.tom@gmail.com, https://orcid.org/0000-0002-1847-2685

Litviakov Nikolay V. – Dr. Sci. (Biology), Professor of the Russian Academy of Sciences, Head of the Laboratory for Oncovirology, Cancer Research Institute, Tomsk NRMC, Tomsk; Researcher, Laboratory for Genetic Technologies, Central Research Laboratory, Siberian State Medical University, Tomsk, nvlitv72@yandex.ru, https://orcid.org/0000-0002-0714-8927

(✉) **Nevskaya Kseniya V.,** nevskayaksenia@gmail.com

Received 05.09.2022;
approved after peer review 19.09.2022;
accepted 26.09.2022.

УДК 616.314.18-002.4-002.2:616.72-002:616.517]-092
https://doi.org/10.20538/1682-0363-2022-4-183-192

Pathogenetic aspects of the development of psoriatic arthritis in people with generalized chronic periodontitis

Poryadin G.V.[1], Zakhvatov A.N.[2], Parshina A.Yu.[2]

[1] Pirogov Russian National Research Medical University
1, Ostrovityanova Str., Moscow, 117997, Russian Federation

[2] Medical institute, National Research Ogarev Mordovia State University
68, Bolshevistskaya Str., Saransk, 430005, Republic of Mordovia, Russian Federation

ABSTRACT

The pathogenetic mechanisms of progression of chronic periodontitis and psoriatic arthritis have common components in immune and inflammatory responses.

The pathogenesis of chronic periodontitis involves interaction of microbial and immunological components. As a chronic immune-mediated inflammatory disease and a consequence of an infectious trigger that originally affects gingival soft tissue, periodontitis is typically characterized by periodontal destruction and damage to adjacent connective tissues. Neutrophils contribute to the development of periodontitis and participate in its progression by recruiting T helper 17 cells and stimulating synthesis of the receptor activator of the nuclear factor kappa-β ligand (RANKL), contributing to bone resorption.

Macrophages as producers of proinflammatory cytokines (interleukin (IL)-1β, IL-6, IL-22, IL-23, tumor necrosis factor (TNF)), free radicals, and matrix metalloproteinases contribute to the chronic course of the disease. Tissue destruction results in generation of reactive oxygen species by neutrophils, which, against the background of a decrease in the antioxidant potential, leads to development of oxidative stress. These processes together lead to tooth mobility, formation of periodontal pockets, and bone resorption.

The key factors in the formation of psoriatic arthritis against the background of periodontitis are overproduction of proinflammatory cytokines in target tissues (skin, joints, gingival microflora) and development of an excessive systemic immune response to the microbiota inhabiting the epithelial and periodontal tissues. A statistically confirmed correlation of the progression of periodontal destruction with the presence of psoriatic arthritis proves the significance of the effects of inflammation as a background for the progression of a comorbidity. Increased IL-17 synthesis plays a crucial role in the development of immune responses of pathological bone remodeling and bone resorption in periodontitis and psoriatic arthritis.

Keywords: periodontitis, psoriatic arthritis, cytokines, free radical oxidation, inflammatory response, bone resorption

Conflict of interest. The authors declare the absence of obvious or potential conflicts of interest related to the publication of this article.

Source of financing. The authors state that they received no funding for the study.

For citation: Poryadin G.V., Zakhvatov A.N., Parshina A.Yu. Pathogenetic aspects of the development of psoriatic arthritis in people with generalized chronic periodontitis. *Bulletin of Siberian Medicine.* 2022;21(4):183–192. https://doi.org/10.20538/1682-0363-2022-4-183-192.

✉ *Zakhvatov Alexey N.,* zachvatan78@mail.ru

Патогенетические аспекты взаимосвязи хронического генерализованного пародонтита и псориатического артрита

Порядин Г.В.[1], Захватов А.Н.[2], Паршина А.Ю.[2]

[1] Российский национальный исследовательский медицинский университет (РНИМУ) им. Н.И. Пирогова Россия, 117997, г. Москва, ул. Островитянова, 1

[2] Медицинский институт, Национальный исследовательский Мордовский государственный университет (МГУ) им. Н.П. Огарёва
Россия, Республика Мордовия, 430005, г. Саранск, ул. Большевистская, 68

РЕЗЮМЕ

Патогенетическое единство механизмов прогрессирования хронического пародонтита и псориатического артрита подтверждается общими звеньями иммуновоспалительных реакций.

Патогенез хронического пародонтита заключается во взаимодействии микробного и иммунологического компонентов. Как хроническое иммуновоспалительное заболевание и следствие инфекционного триггера, который первоначально поражает мягкие ткани десен, пародонтит классически характеризуется разрушением периодонта и окружающих соединительных тканей. Нейтрофилы способствуют развитию пародонтита и участвуют в его прогрессировании, рекрутируя Т-хелперы 17 и стимулируя синтез активатора мембраносвязанного рецептора ядерного фактора каппа-β (RANKL), способствуя остеорезорбции.

Макрофаги как продуценты провоспалительных цитокинов (интерлейкин (IL)-1β, IL-6, IL-22, IL-23, фактор некроза опухоли), свободных радикалов, матриксных металлопротеиназ способствуют хронизации процесса. Деструкция тканей влечет за собой генерацию нейтрофилами активных форм кислорода, что на фоне снижения антиоксидантного потенциала ведет к развитию оксидативного стресса. Данные процессы в совокупности ведут к формированию патологической подвижности зубов, пародонтальных карманов, процессам остеорезорбции.

Ключевым фактором в формировании псориатического артрита на фоне пародонтита является гиперпродукция провоспалительных цитокинов в тканях-мишенях (кожа, суставы, микросреда десен) и развитие чрезмерного системного иммунного ответа на микробиоту, населяющую поверхность эпителия и ткани пародонта. Статистически подтвержденная корреляция развития деструкции пародонта с наличием псориатического артрита доказывает значимость эффектов воспалительного процесса как фона для развития коморбидной патологии. Повышенный синтез IL-17 выполняет ключевую роль в развитии иммунных реакций патологического костного ремоделирования и остеорезорбции при пародонтите и псориатическом артрите.

Ключевые слова: пародонтит, псориатический артрит, цитокины, свободнорадикальное окисление, воспалительный ответ, остеорезорбция

Конфликт интересов. Авторы декларируют отсутствие явных и потенциальных конфликтов интересов, связанных с публикацией настоящей статьи.

Источник финансирования. Авторы заявляют об отсутствии финансирования при проведении исследования.

Для цитирования: Порядин Г.В., Захватов А.Н., Паршина А.Ю. Патогенетические аспекты взаимосвязи хронического генерализованного пародонтита и псориатического артрита. *Бюллетень сибирской медицины.* 2022;21(4):183–192. https://doi.org/10.20538/1682-0363-2022-4-183-192.

INTRODUCTION

Currently, inflammatory periodontal diseases are some of the urgent and socially sensitive problems of health care [1]. About 95% of the adult population in the world suffer from this pathology, which, in the absence of proper and timely treatment, leads to defects in the dentition, thereby reducing the ability to work and decreasing the quality of life of the population [2–6]. The prevalence of periodontal disease in Russia is about 85%, 53% of the population have initial manifestations of inflammations, and 12% have moderate and severe inflammation [7–9].

In chronic periodontitis, systemic lesions occur that involve not only periodontal tissues, but also other organs and systems, which leads to disruption of various components of homeostasis, including the immune system [10]. The inflammatory process and increased synthesis of proinflammatory cytokines result in the development of a number of systemic autoimmune pathologies, of which rheumatic diseases and severe forms of psoriasis with joint damage have the greatest significance [11].

Despite the widespread interest in periodontitis and systemic disorders over the past decade, only a few studies have considered the association between psoriatic arthritis (PsA) and chronic periodontitis [12, 13].

The analysis of the conducted studies showed an increase in the frequency of periodontitis in patients with PsA. For example, in Denmark, a large cohort study of 6,428 patients who were diagnosed with PsA revealed that the frequency of periodontitis in this group of patients was significantly higher than in the control group [14]. C. Ancuta et al. (2017) showed a significant decrease in the intensity of the disease and an improvement in the periodontal condition in patients with PsA 6 months after the initiation of anti-cytokine therapy [15].

The association between chronic periodontitis and PsA is bidirectional. An increased risk of psoriasis was noted in patients with chronic periodontal diseases [13, 15–17]. This suggests the existence of common mechanisms that determine mutual aggravation of the course of these common diseases.

IMMUNOPATHOGENESIS OF CHRONIC GENERALIZED PERIODONTITIS

The pathogenesis of chronic generalized periodontitis is multifactorial and is considered to be a result of an ongoing cross-interaction of bacterial, immunological, inflammatory, and genetic factors [18]. As a chronic immune-mediated inflammatory disease and a consequence of an infectious trigger that originally affects gingival soft tissue, periodontitis is typically characterized by periodontal destruction and damage to adjacent connective tissues [19].

Microbiological aspects of the development of chronic periodontitis consist mainly in colonization of the periodontal pockets by gram-negative microorganisms, the most significant of which are *Aggregatibacter actinomycetemcomitans*, *Porphyromonas gingivalis*, *Tannerella forsythia,* and *Treponema denticola* [17].

The inflammatory response is triggered by the interaction of resident cells with bacterial biofilm attached to the tooth surface, which, via fixation, makes it impossible for the immune system to destroy gram-negative microorganisms, thereby increasing damage to periodontal tissues [20]. The epithelium of the periodontal ligamnent is the first periodontal structure to experience bacterial exposure [21]. Production of the main enzymes (proteinase, peptidyl-arginine deiminase (PPAD), hemolysins) and metabolites (methyl mercaptan and dimethyl sulfide) by gram-negative anaerobic microorganisms contributes to destruction of fibronectin and laminin and hydrolysis of collagen. It facilitates passage of bacteria through the periodontium into the gingival connective tissue, where they stimulate gingival epithelial cells and fibroblasts to trigger initial inflammatory responses [22].

Resident periodontal cells detect bacterial pathogen-associated molecular patterns (PAMP) [23], which connect to toll-like receptors (TLR4/2), triggering the recruitment of protein kinases. It ultimately causes activation of proinflammatory transcription factors, such as nuclear factor kappa B (NF-kB) and activator protein-1 (AP-1), stimulating the expression of genes responsible for synthesis of proinflammatory cytokines, thereby leading to an increase in inflammation [24]. In addition, gingival fibroblasts stimulate destruction and disorganization of the fibrous component of the extracellular matrix by increasing the production and activity of matrix metalloproteinases (MMP) [25].

Due to migration of immunocompetent cells into the subgingival space, infiltration of periodontal tissues by neutrophils occurs, which leads to an increase in synthesis of cytokines and chemokines with proinflammatory and anti-inflammatory properties [22]. Neutrophils induce recruitment of CD4+ T helper 17 (Th17) cells responsible for the production of IL-17 and stimulate synthesis of the receptor activator of the nuclear factor kappa-β ligand (RANKL), which leads to bone resorption by osteoclasts [25].

Macrophages are important sources of pro-inflammatory cytokines, such as interleukin (IL)-1, tumor necrosis factor (TNF), MMP, and prostaglandin E2 [26], which are elevated in the gingival tissue of patients with chronic periodontitis [25]. Studies have shown a direct correlation of macrophage infiltration with the severity of periodontitis, which significantly contributes to the degradation of the collagen matrix in the connective tissue of the periodontium [27].

Macrophages can undergo classical (M1) or alternative (M2) activation. M1 macrophages are induced by microbial agents or Th1 cytokines and exhibit high phagocytic capacity and increased expression of proinflammatory cytokines and costimulatory and antimicrobial molecules. In contrast, M2 macrophages are induced by Th2 cytokines and secrete high levels of IL-10 and transforming growth factor-β1 (TGF-β1). Consequently, they have immunoregulatory properties and promote cell proliferation and tissue regeneration [28]. In experimental models of periodontitis, the presence of both M1 and M2 macrophages was noted, but with the predominance of M1 macrophages, which indicates the activation of the immune response with increased production of proinflammatory cytokines [27].

When the inflammatory process becomes chronic, lymphocytes penetrate into periodontal tissues, releasing inflammatory and immune molecular mediators that change the balance of bone metabolism, determining the transition from gingivitis to periodontitis [25]. Activation of adaptive immunity has a great impact on bone loss associated with B and T lymphocytes, since these cells are the main cellular sources of RANKL during periodontal inflammation [28].

RANKL is a cytokine belonging to the TNF family that can bind to receptors on membranes and stimulate osteoclast differentiation, cell fusion and activation, which results in bone resorption [28]. Osteoblasts and bone marrow stromal cells predominantly express membrane-bound RANKL which induces osteoclastogenesis through cell contact with osteoclast precursors. Activated T and B cells produce both membrane-bound and soluble RANKL [22]. Soluble RANKL can induce osteoclastogenesis independently of the direct contact between infiltrating lymphocytes and osteoclast precursors on the bone surface. RANKL is an osteoclast activator and a molecular signal directly responsible for bone resorption. It interacts with the associated RANK receptor on the surface of osteoclasts and their precursors, which triggers its recruitment on the bone surface with subsequent activation of cells [29].

Osteoprotegerin (OPG) is a soluble protein that has the ability to block biological functions of RANKL by competitive inhibition [30]. In periodontitis, an increase in RANKL / OPG promotes the recruitment of osteoclast precursors, which contribute to bone resorption via the interaction with proinflammatory cytokines expressed by Th1 lymphocytes [29].

In addition, Th1 lymphocytes play an important role in the emergence and progression of periodontitis by increasing the level of interferon γ (IFNγ) [24]. IL-1ß and TNF secreted by Th1 lymphocytes cause vasodilation, stimulate activation of endothelial cells, increase the production of chemokines, participate in activation of neutrophils, and stimulate secretion of MMP [25]. Th2 lymphocytes are the main cellular source of IL-4, which promotes secretion of IgE by plasma cells and alternative activation of macrophages via the IFN-dependent pathway.

Lipid peroxidation processes play a significant role in the pathogenesis of chronic periodontitis [31]. Progressive periodontal destruction entails generation of reactive oxygen species (ROS) by neutrophils and subsequent peroxidation of lipid structures in cell membranes [32]. Insufficient antioxidant potential of cells, manifested by the inability to neutralize ROS, leads to development of oxidative stress, formation of metabolic disorders, and development of secondary destructive changes [32]. In such conditions, a violation of regeneration, formation of periodontal pockets, and progression of bone resorption are noted [30].

IMMUNOPATHOGENETIC ASPECTS OF PSA DEVELOPMENT

Psoriatic arthritis is a chronic progressive inflammatory process associated with psoriasis, characterized by predominant localization in the tissues of the musculoskeletal system and leading to the development of erosive arthritis, intra-articular osteolysis, and spondyloarthritis [33].

Etiological factors underlying the development of PsA are currently insufficiently studied. The disease develops following a complex interaction of genetic, immunological, and environmental factors [34]. About 40% of patients with PsA have this disease in the family history, and, therefore, the risk of developing this disease in such patients increases by 27–50 times [35, 36]. In recent years, studies have been conducted to identify genetic markers of PsA, during which the antigen of the histocompatibility complex HLA-B27 was detected in every third patient [33–36]. Genetic associations in PsA include HLA-B*08:01, HLA-B*27:05, HLA-B*38:01, HLA-B*39:01, HLA-B*57:01, and HLA-C*06:02 [36]. HLA-B27 is associated with axial lesion, whereas HLA-B38 and HLA-B39 are associated with polyarthritis [37]. Non-HLA genes associated with PsA include IL-23R [34].

Bacterial infection, smoking, obesity, stress, and trauma are environmental factors that increase the risk of developing PsA, especially in young people [38]. PsA is considered a T-cell-mediated disease in which cellular immunity is activated in the skin and synovia, followed by overproduction and imbalance of key pro- and anti-inflammatory cytokines, such as TNF, IL-1ß, IL-6, IL-12, IL-17, IL-23, and chemokines [39].

A genetic predisposition in combination with environmental factors (bacterial infection, mechanical injury) initiate a chronic inflammatory process affecting primarily the tissues of the joints [38]. Repeated mechanical injury contributes to formation of inflammatory infiltrates consisting of monocytes, dendritic cells, neutrophils, and T cells in the synovial membrane [40]. Dendritic cells release IL-12 and IL-23, which leads to differentiation of naive T cells into Th1 and Th17, respectively, and to a decrease in the production of regulatory T (Treg) cells [41]. Abnormal activation of the IL-23 / Th17 axis is the dominant pathology in PsA. IL-23 triggers the activation of tyrosine kinase 2 (TYK2) and Janus kinase 2 (JAK2) signaling pathways, which promote phosphorylation and activation of the signal protein STAT3 (signal transducer and activator of transcription 3). It increases the expression of the transcription factor RORγt, which stimulates the production of IL-17, IL-21, IL-22, granulocyte-macrophage colony stimulating factor (GM-CSF), and tumor necrosis factor (TNF), thereby contributing to tissue inflammation [42]. In addition to IL-23, the differentiation of naive T cells into Th17 cells is stimulated by IL-1ß, IL-6, and transforming growth factor β (TGFβ) [41].

In PsA, enthesis is considered to be the initial focus of inflammation, which spreads to other periarticular and articular structures, leading to the development of synovitis, dactylitis, spondylitis, and osteitis [43]. An important early mediator of enthesitis is prostaglandin E2 (PGE2), which causes vasodilation and facilitates recruitment of neutrophils from the bone marrow to tendon-to-bone attachment sites. Neutrophils increase inflammation by releasing proteases and ROS. PGE2 also promotes IL-17 production by T cells [44].

Inflammation in extra-articular structures, i.e. extensor tendon enthesitis and peritendon inflammation, progresses to intra-articular inflammation, taking the form of synovitis [43]. Synovitis in PsA is characterized by hyperplasia of the mucous layer with an increase in the number of fibroblast-like synoviocytes and macrophages, hypervascularization of tortuous arteries, and the presence of hyperemic villi and subsynovial infiltrate consisting of T cells, B cells, neutrophils, mast cells, and monocytes / macrophages. Elongated, dilated, thick, and tortuous vessels indicate increased angiogenesis [45, 46]. In the synovial membrane in PsA, high expression of IL-17A and IL-17 receptors is noted, where the cytokine IL-17A is directly involved in bone and cartilage destruction [44].

Remodeling is a unique feature of PsA [46]. In PsA, IL-17 enhances osteoclastogenesis, whereas IL-22 promotes osteoblastogenesis. Thus, the presence of a balance between IL-17, IL-22, and IL-23 is necessary to maintain bone homeostasis [47]. Prominent signs of PsA are subchondral perienthesial edema and diffuse bone marrow edema [45]. The subenthesis bone in PsA exhibits increased vascularity and hyperosteoclastic cystic and erosive changes [47]. Physiologically, bone homeostasis is maintained by a balance between osteoclasts capable of bone resorption and osteoblasts responsible for osteoblastogenesis. In systemic inflammation, stimulation of CD14+ monocytes by macrophage colony stimulating factor (M-CSF), TNF, and RANKL leads to the formation of osteoclast precursors in peripheral blood.

In addition, IL-23 and IL-17 independently induce osteoclast formation in myeloid cells [43]. In the subchondral bone, binding of the receptor activator of nuclear factor kappa B (RANK), present on the surface of monocytes / macrophages, to membrane-bound RANKL, present on the surface of Th17 cells, stimulates differentiation of monocytes / macrophages into osteoclasts [47]. Activated osteoclasts begin to secrete enzymes of bone matrix degradation: acid phosphatases, matrix metalloproteinase-9 (MMP-9), and cathepsin K (CatK), which promote bone resorption. In addition, the osteoclast-associated receptor (OSCAR) located on the surface of monocytes, after TNF induction, potentiates the action of RANKL, thereby enhancing osteoclastogenesis [46]. RANKL also increases the activation of T cells and their production of proinflammatory cytokines, including TNF, IL-1β, IL-6, IL-15, IL-17, and IL-23 [45].

In PsA, IL-22 induces osteoproliferation in the enthesis and periosteum by activating STAT3 on osteoblasts, causing the formation of new bone tissue, manifested by fusion of peripheral joints, enthesophytes, spurs, ankylosis, syndesmophytes in the axial skeleton, and changes in the sacroiliac joints [43, 47].

Proinflammatory cytokines secreted in PsA can stimulate chondrocytes to produce destructive

proteases, which leads to proteoglycan loss, damage to collagen bundles with concomitant release of cartilaginous oligomeric matrix protein (COMP). COMP, a glycoprotein belonging to the family of thrombospondins, is one of the components of the articular cartilage extracellular matrix. An increased level of COMP in the synovial fluid and serum contributes to remodeling and restoration of cartilage [48].

PATHOGENETIC RELATIONSHIP BETWEEN CHRONIC PERIODONTITIS AND PSORIATIC ARTHRITIS

A number of authors consider joint damage in PsA in the context of periodontitis to be a complex interaction of immunological and inflammatory phenomena involving bacterial infection [12, 35]. Psoriasis can occur in genetically predisposed people with an abnormal innate and / or adaptive immune response to components of oral microbiota in chronic periodontitis (such as *Porphyromonas gingivalis*), which can cause various psoriasis manifestations [49]. In addition, a certain composition of the microbiota in the body folds in patients with inverse psoriasis may also play a role in triggering local inflammation in the periodontium [50].

A closer look indicates an association between the immunopathogenesis of diseases: hypersecretion of proinflammatory cytokines produced by activated T lymphocytes and other mononuclear cells (monocytes, macrophages); increased proliferative activity of fibroblasts in the synovial membrane and periodontium, their ability to secrete platelet growth factors; increased collagenolytic activity of MMR and increased tissue proteolysis, disruptions in humoral immunity (autoantibodies to nuclear antigens, cytokeratins); pathological remodeling of bone tissue [49, 51].

The interaction between innate and adaptive immunity in chronic periodontitis, which maintains chronic inflammation, leads to dysregulation and overproduction of various proinflammatory cytokines, such as TNF, IL-17, IL-1β, IL-22, and IL-23 [49, 52]. Activation of IL-23R receptors induces phosphorylation of Jak2 and Tyk2 protein kinases, which mediate activation of STAT3 and RORγ transcription factors, thereby contributing to Th17 cell differentiation. The resulting Th17 cells produce IL-17, a powerful proinflammatory cytokine [52].

IL-17 and TNF induce synthesis of MMP in the synovial fluid and cartilage, which mediates loss of collagen structures and erosion-like changes in the cartilage surface. It also stimulates production of IL-1 and TNF by macrophages, induces secretion of IL-6 and IL-8 by synovial fibroblasts, and promotes recruitment of neutrophils and other immune cells into the synovial membrane [53]. IL-17 stimulates synthesis of RANKL in osteoblasts and its ligation with RANK in osteoclast precursors, contributing to the differentiation and activation of osteoclasts [30]. Mature osteoclasts, being bone resorbing cells, secrete lysosomal enzymes, thereby leading to destruction of the bone matrix. [53]. Therefore, Th17-mediated induction of osteoclastogenesis plays an important role in the pathogenesis of bone and cartilage destruction in PsA [49].

In addition, lymphocytic infiltration in PsA is localized not only on the skin or joints, but also in isolated blood cells, thereby confirming the presence of a systemic inflammatory response in such patients [55].

The production of TNF by macrophages promotes activation and recruitment of immune cells to the synovial membrane and synovial hyperplasia and induces secretion of MMR involved in cartilage degradation. Besides, together with other angiogenic factors, it promotes formation of new blood vessels [56]. TNF is responsible for regulation of genes responsible for synthesis of IL-1, interferon γ, granulocyte – macrophage colony stimulating factor (GM-CSF), IL-6, proinflammatory chemokine IL-8, and other inflammatory mediators [53]. It is assumed that angiogenesis and development of oxidative stress due to an increase in ROS production are apparently present in the early phase of diseases and can be considered as important processes linking periodontitis and PsA [50].

Therefore, PsA and periodontitis are chronic inflammatory diseases with similar pathophysiological mechanisms: overproduction of proinflammatory cytokines in target tissues (skin, joints, gingival microenvironment) and development of an excessive systemic immune response to the microbiota inhabiting the surface of the epithelium and periodontium [52]. Impaired interaction of innate and adaptive immunity present in chronic periodontitis leads to systemic overexpression of proinflammatory cytokines (TNF, IL-17, IL-1β, IL-22, and IL-23) and differentiation of Th0 into Th17, which play an important role in mutual aggravation of these pathologies. In addition, among the common pathophysiological mechanisms in the development of these pathologies, pathological bone

remodeling and bone resorption can be distinguished [49, 54].

CONCLUSION

Based on the studies listed above, it is possible to confirm the presence of a pathogenetic relationship between chronic periodontitis and PsA. Significance of the prevalence of the hyperergic systemic inflammatory response in both cases and the unity of the cytokine profile and bone resorption processes also confirm this statement.

A key factor in the formation and progression of PsA against the background of periodontitis is a disturbance in the interaction of innate and adaptive immunities, leading to overexpression of proinflammatory cytokines (TNF, IL-17, IL-1β, IL-22, and IL-23) and differentiation of Th0 into Th17. It further leads to increased synthesis of IL-17, which plays a significant role in the initiation of immune responses in PsA. IL-17 stimulates production of IL-1 and TNF by macrophages, secretion of neutrophil-attracting IL-6 and IL-8 by synovial fibroblasts, and induces synthesis of RANKL by them and osteoblasts, thus mediating secretion of osteoclastogenic factors (TNF and IL-1ß) and pathological bone remodeling and bone resorption (Figure) [31, 33, 45–47]. The statistically confirmed correlation between the development of periodontal destruction and the severity of PsA proves the commonality of immunological and inflammatory processes in the development and mutual aggravation of the studied comorbidity [6, 7, 9, 14].

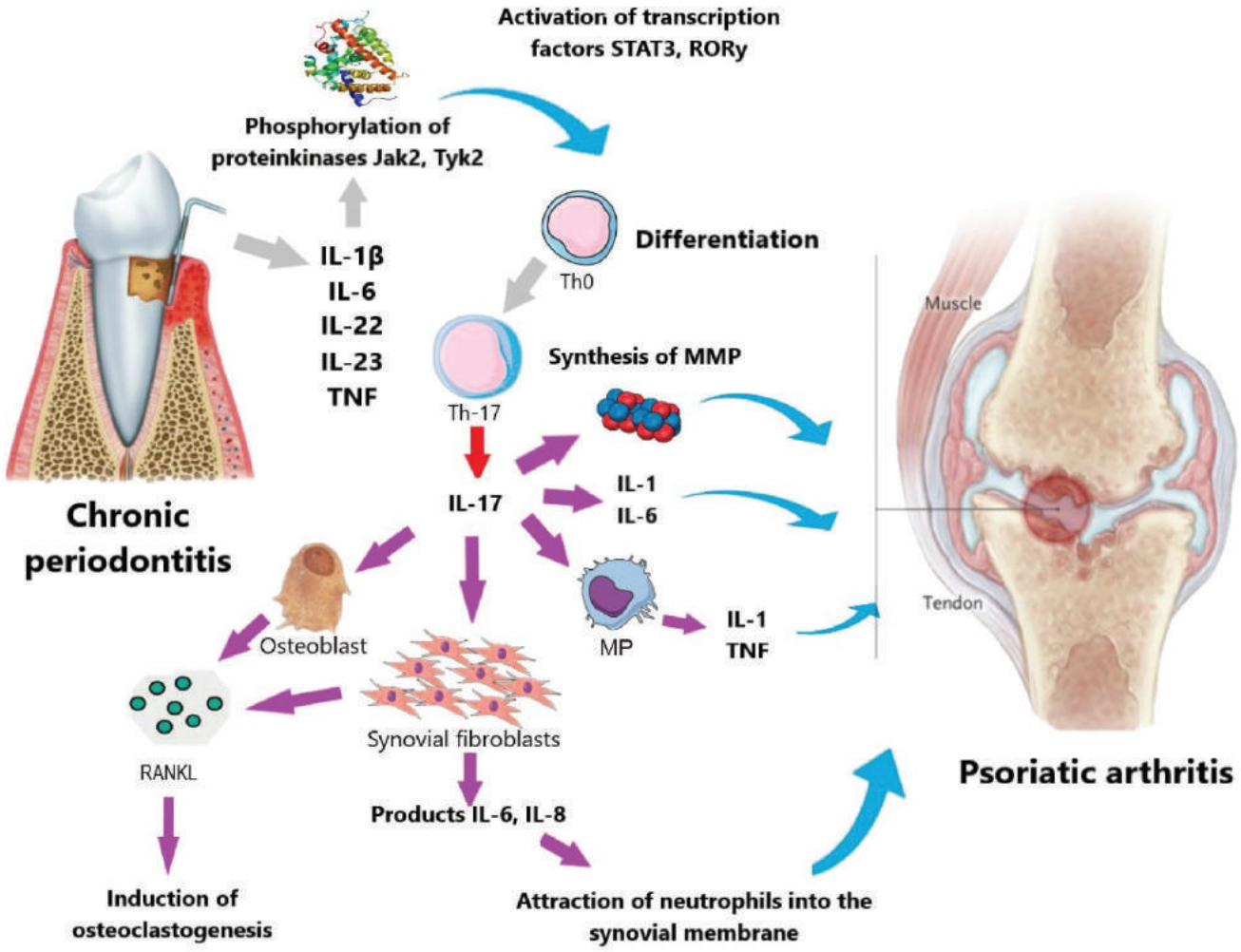

Figure. Pathogenetic relationship of chronic generalized periodontitis and psoriatic arthritis [31, 33, 45–47]. IL-1β – interleukin-1β; IL-1 – interleukin-1; IL-6 – interleukin-6; IL-8 – interleukin-8; IL-22 – interleukin-22; IL-23 – interleukin-23; TNF – tumor necrosis factor; Th0 – undifferentiated T helper cell; Th17 – T helper 17 cell; IL-17 – interleukin-17; MMP – matrix metalloproteinase; MP – macrophage; RANKL – receptor activator of nuclear factor kappa-β

Therefore, the established pathogenetic relationship makes it possible to develop new methods of early diagnosis, treatment, and prophylaxis for early detection and prevention of the progression of these pathologies. Close collaboration between dentists and rheumatologists for prescribing complex therapy for these diseases, as well as screening immunological examinations of people (especially working-age population) with chronic periodontitis will allow for early detection and prediction of the development of psoriatic arthritis.

REFERENCES

1. Tibúrcio-Machado C.S., Michelon C., Zanatta F.B., Gomes M.S., Marin J.A., Bier C.A. The global prevalence of apical periodontitis: a systematic review and meta-analysis. *Int. Endod. J*. 2021;54(5):712–735. DOI: 10.1111/iej.13467.
2. Jakovljevic A., Nikolic N., Jacimovic J., Pavlovic O., Miličić B., Beljić-Ivanović K.R. et al. Prevalence of Apical Periodontitis and Conventional Nonsurgical Root Canal Treatment in General Adult Population: An Updated Systematic Review and Meta-analysis of Cross-sectional Studies Published between 2012 and 2020. *J. Endod*. 2020;46(10):1371–1386. DOI: 10.1016/j.joen.2020.07.007.
3. Nijakowski K., Gruszczyński D., Surdacka A. Oral Health Status in Patients with Inflammatory Bowel Diseases: A Systematic Review. *International Journal of Environmental Research and Public Health.* 2021;18(21):11521. DOI: 10.3390/ijerph182111521.
4. González-Febles J., Sanz M. Periodontitis and rheumatoid arthritis: What have we learned about their connection and their treatment? *Periodontology 2000*. 2021;87(1):181–203. DOI: 10.1111/prd.12385.
5. Xiao F., Li C., Lin Y., Peng Z., Xu X., Wen Y. et al. Increased risk of periodontitis occurrence in patients with rheumatoid arthritis and its association with the levels of IL-1β and TNF-α in gingival crevicular fluid. *Annals of Palliative Medicine*. 2021;10(8):9078–9087. DOI: 10.21037/apm-21-1782.
6. Dannewitz B., Holtfreter B., Eickholz P. Periodontitis-therapy of a widespread disease. *Bundesgesundheitsblatt, Gesundheitsforschung, Gesundheitsschutz*. 2021;64(8):931–940. DOI: 10.1007/s00103-021-03373-2.
7. Blashkova S.L., Martyanova M.V. The role of preventive hygiene in the prevention of caries and periodontal disease in young age. *Russian Stomatology*. 2016;9(4):51–53 (in Russ.). DOI: 10.17116/rosstomat20169451-53.
8. Sabirova A.I., Akramov I.A., Ramazanova Z.D., Sergeeva V.V., Ibisheva L.K. Modern aspects of epidemiological issues of periodontal tissue diseases. *The Scientific Heritage.* 2021;73(2):31–38 (in Russ.). DOI: 10.24412/9215-0365-2021-73-2-31-38.
9. Avanesov A.M., Kulchenko A.A., Meladze Z.A., Arzuni V.A., Tsvetkova E.P., Marinicheva E.G., Chibisov S.M. Assessment of periodontal condition against the background of vitamin E use in a complex of therapeutic measures for generalized periodontitis. *Scientific review. Medical Sciences*. 2014;1:23–24 (in Russ.).
10. Barros F.C., Sampaio J.N., Figueredo C.M., Carneiro S., Fischer R.G. Higher prevalence of periodontitis and decayed, missing and filled teeth in patients with psoriasis. *European Journal of Dentistry.* 2020;14(3):366–370. DOI: 10.1055/S-0040-1713465.
11. Madianos P.N., Bobetsis Y.A., Offenbacher S. Adverse pregnancy outcomes (APOs) and periodontal disease: pathogenic mechanisms. *Journal of Clinical Periodontology*. 2013;40(14):170–180. DOI: 10.1111/jcpe.12082.
12. Monson C.A., Silva V., Porfírio G., Riera R., Tweed J.A., Petri V., Atallah Á.N. Oral Health Issues in Psoriasis: An Overview of the Literature. *International Journal of Clinical Dermatology & Research*. 2016;4(4):94–98. DOI: 10.19070/2332-2977-1600025.
13. Monson C.A., Porfírio G.J., Riera R., Tweed J.A., Petri V., Nagi A. et al. Periodontal Aspects for Psoriasis: A Systematic Review. *Journal of Clinical Research in Dermatology*. 2016;3(1):1–8. DOI: 10.15226/2378-1726/3/4/00141.
14. Egeberg A., Mallbris L., Gislason G., Hansen P.R., Mrowietz U. Risk of periodontitis in patients with psoriasis and psoriatic arthritis. *J. Eur. Acad. Dermatol. Venereol.* 2017;31(2):288–293. DOI: 10.1111/jdv.13814.
15. Ancuta C., Ancuta E., Chirieac R.M., Anton C.R., Surlari Z., Iordache C. TNF inhibitors and periodontal inflammation in psoriatic arthritis. *Rev. Chim.* 2017;68(8):1914–1918. DOI: 10.37358/RC.17.8.5790.
16. Esberg A., Johansson L., Johansson I., Dahlqvist S.R. Oral microbiota identifies patients in early onset rheumatoid arthritis. *Microorganisms*. 2021;9(8):1657. DOI: 10.3390/microorganisms9081657.
17. Lundmark A., Hu Y.O.O., Huss M., Johannsen G., Andersson A.F., Yucel-Lindberg T. Identification of salivary microbiota and its association with host inflammatory mediators in periodontitis. *Front. Cell Infect. Microbiol*. 2019;(9):216. DOI: 10.3389/fcimb.2019.00216.
18. Banjar W., Alshammari M.H. Genetic factors in pathogenesis of chronic periodontitis. *Journal of Taibah University Medical Sciences*. 2014;9(3):245–247. DOI: 10.1016/j.jtumed.2014.04.003.
19. Yousef A. AlJehani. Risk Factors of Periodontal Disease: Review of the Literature. *International Journal of Dentistry*. 2014;2014:182513. DOI: 10.1155/2014/182513.
20. Fadel H.T., Flytström I., Calander A., Bergbrant I.M., Heijl L., Birkhed D. Profiles of dental caries and periodontal disease in individuals with or without psoriasis. *Journal of Periodontology*. 2013;84(4):477–485. DOI: 10.1902/jop.2012.120119.
21. Noguchi S., Ukai T., Kuramoto A., Yoshinaga Y., Nakamura H., Takamori Y. et al. The histopathological comparison on the destruction of the periodontal tissue between normal junctional epithelium and long junctional epithelium. *Journal of Periodontal Research*. 2017;52(1):74–82. DOI: 10.1111/jre.12370.
22. Cavalla F., Osorio C., Paredes R., Valenzuela M.A., García-Sesnich J., Sorsa T. et al. Matrix metalloproteinases regulate extracellular levels of SDF-1/CXCL12, IL-6 and VEGF in hydrogen peroxide-stimulated human periodontal ligament fibroblasts. *Cytokine*. 2015;73(1):114–121. DOI: 10.1016/j.cyto.2015.02.001.

23. Han M.X., Ding C., Kyung H.M. Genetic polymorphisms in pattern recognition receptors and risk of periodontitis: Evidence based on 12,793 subjects. *Human Immunology*. 2015;76(7):496–504. DOI: 10.1016/j.humimm.2015.06.006.
24. Song B., Zhang Y., Chen L., Zhou T., Huang W., Zhou X. et al. The role of Toll-like receptors in periodontitis. *Oral Diseases*. 2017;23(2):168–180. DOI: 10.1111/odi.12468.
25. Hajishengallis G., Korostoff J.M. Revisiting the Page & Schroeder model: The good, the bad and the unknowns in the periodontal host response 40 years later. *Periodontology 2000*. 2017;75(1):116–151. DOI: 10.1111/prd.12181.
26. Cekici A., Kantarci A., Hasturk H., Van Dyke T.E. Inflammatory and immune pathways in the pathogenesis of periodontal disease. *Periodontology 2000*. 2014;64(1):57–80. DOI: 10.1111/prd.12002.
27. Gupta M., Chaturvedi R., Jain A. Role of monocyte chemoattractant protein-1 (MCP-1) as an immune-diagnostic biomarker in the pathogenesis of chronic periodontal disease. *Cytokine*. 2013;61(3):892–897. DOI: 10.1016/j.cyto.2012.12.012.
28. Braga T.T., Agudelo J.S., Camara N.O. Macrophages during the fibrotic process: M2 as friend and foe. *Front. Immunology*. 2015;6:602. DOI: 10.3389/fimmu.2015.00602.
29. Huang N., Dong H., Luo Y., Shao B. Th17 Cells in Periodontitis and Its Regulation by A20. *Front. Immunology*. 2021;12:125–137. DOI: 10.3389/fimmu.2021.742925.
30. Kikuta J., Wada Y., Kowada T., Wang Z., Sun-Wada G.H., Nishiyama I. et al. Dynamic visualization of RANKL and Th17-mediated osteoclast function. *The Journal of Clinical Investigation*. 2013;123(2):866–873. DOI: 10.1172/JCI65054.
31. Belibasakis G.N., Bostanci N. The RANKL-OPG system in clinical periodontology. *Journal of Clinical Periodontology.* 2012;39(3):239–248. DOI: 10.1111/j.1600-051X.2011.01810.x.
32. Almubarak A., Tanagala K.K.K., Papapanou P.N., Lalla E., Momen-Heravi F. Disruption of monocyte and macrophage homeostasis in periodontitis. *Front. Immunol.* 2020;11:330. DOI: 10.3389/fimmu.2020.00330.
33. Smirnova S.V., Smolnikova M.V. Immunopathogenesis of psoriasis and psoriatic arthritis. *Medical Immunology.* 2014;16(2):127–138 (in Russ.).
34. Fang C., Wu L., Zhao M.J., Deng T., Gu J.M., Guo X.P. et al. Periodontitis exacerbates benign prostatic hyperplasia through regulation of oxidative stress and inflammation. *Oxid. Med. Cell Longev*. 2021;2021:2094665. DOI: 10.1155/2021/2094665.
35. Korotaeva T.V., Korsakova Yu.L., Loginova E.Yu., Gubar E.E., Chamurlieva M.N. Psoriatic arthritis. Clinical guidelines for diagnosis and treatment. *Modern Rheumatology Journal.* 2018;12(2):22–35 (in Russ.). DOI: 10.14412/1996-7012-2018-2-22-35.
36. Mease P., Hall S., FitzGerald O., van der Heijde D., Merola J F., Avila-Zapata F. et al. Tofacitinib or adalimumab versus placebo for psoriatic arthritis. *N. Engl. J. Med.* 2017;377(16):1537–1550. DOI: 10.1056/NEJMoa1615975.
37. FitzGerald O., Haroon M., Giles J T., Winchester R. Concepts of pathogenesis in psoriatic arthritis: genotype determines clinical phenotype. *Arthritis Research and Therapy*. 2015;17(1):115. DOI: 10.1186/s13075-015-0640-3.
38. Kavanaugh A., Gladman D.D., Edwards C.J., Schett G., Guerette B., Delev N. et al. Long-term experience with apremilast in patients with psoriatic arthritis: 5-year results from a PALACE 1-3 pooled analysis. *Arthritis Res. Ther*. 2019;21(1):118. DOI: 10.1186/s13075-019-1901-3.
39. Coates L.C., Savage L.J., Chinoy H., Laws P.M., Lovell C.R., Korendowych E. et al. Assessment of two screening tools to identify psoriatic arthritis in patients with psoriasis. *Journal of the European Academy of Dermatology and Venereology: JEADV*. 2018;32(9):1530–1534. DOI: 10.1111/jdv.14971.
40. Emmungil H., İlgen U., Direskeneli R.H. Autoimmunity in psoriatic arthritis: pathophysiological and clinical aspects. *Turk. J. Med. Sci*. 2021;51(4):1601–1614. DOI: 10.3906/sag-2011-235.
41. Chimenti M.S., Triggianese P., De Martino E., Conigliaro P., Fonti G.L., Sunzini F. et al. An update on pathogenesis of psoriatic arthritis and potential therapeutic targets. *Expert Review of Clinical Immunology*. 2019;15(8):823–836. DOI: 10.1080/1744666X.2019.1627876.
42. Tateiwa D., Yoshikawa H., Kaito T. Cartilage and Bone Destruction in Arthritis: Pathogenesis and Treatment Strategy: A Literature Review. *Cells*. 2019;8(8):818. DOI: 10.3390/cells8080818.
43. Eder L., Aydin S.Z. Imaging in psoriatic arthritis-insights about pathogenesis of the disease. *Current Rheumatology Reports.* 2018;20(12):77. DOI: 10.1007/s11926-018-0793-6.
44. Coras R., Kavanaugh A., Boyd T., Huynh Q., Pedersen B., Armando A.M. et al. Pro- and anti-inflammatory eicosanoids in psoriatic arthritis. *Metabolomics: Official Journal of the Metabolomic Society*. 2019;15(4):65. DOI: 10.1007/s11306-019-1527-0.
45. Adebajo A., Boehncke W.H., Gladman D.D., Mease P.J. Psoriatic arthritis and psoriasis: pathology and clinical aspects. *Springer.* 2016;45:52. DOI: 10.1007/978-3-319-19530-8.
46. Celis R., Cuervo A., Ramírez J., Cañete J.D. Psoriatic synovitis: singularity and potential clinical implications. *Front. Medicine*. 2019;6:14. DOI: 10.3389/fmed.2019.00014.
47. Paine A., Ritchlin C. Bone remodeling in psoriasis and psoriatic arthritis: an update. *Current Opinion in Rheumatology*. 2016;28(1):66–75. DOI: 10.1097/BOR.0000000000000232.
48. Bartosińska J., Michalak-Stoma A., Juszkiewicz-Borowiec M., Kowal M., Chodorowska G. The Assessment of selected bone and cartilage biomarkers in psoriatic patients from Poland. *Mediators of Inflammation*. 2015;2015:194535. DOI: 10.1155/2015/194535.
49. Mishra S., Johnson L., Agrawal S., Rajput S. Assessment of Periodontal status in Patients with Psoriatic Arthritis: A retrospective, case-control study. *Journal of Clinical and Experimental Dentistry.* 2021;13(8):776–783. DOI: 10.4317/jced.58125.
50. Wójcik P., Biernacki M., Wroński A., Łuczaj W., Waeg G., Žarković N. et al. Altered lipid metabolism in blood mononuclear cells of psoriatic patients indicates differential changes in psoriasis vulgaris and psoriatic arthritis. *International Journal of Molecular Sciences*. 2019;20(17):4249. DOI: 10.3390/ijms20174249.
51. Üstün K., Sezer U., Kısacık B., Şenyurt S.Z., Özdemir E.Ç., Kimyon G. et al. Periodontal disease in patients with psoriatic

arthritis. *Inflammation.* 2013;36(3):665–669. DOI: 10.1007/s10753-012-9590-y.
52. Carvalho A.L., Hedrich C.M. The Molecular pathophysiology of psoriatic arthritis – the complex interplay between genetic predisposition, epigenetics factors, and the microbiome. *Front. Molecular Biosciences*. 2021;8:190–205. DOI: 10.3389/fmolb.2021.662047.
53. Zakhvatov A.N., Belyaev A.N., Tarasova T.V., Avanesov A.M., Zakharkin I.A., Chekmaeva A.A. Pathogenetic correction of cytokine imbalance in experimental post-traumatic arthritis. *Ulyanovsk Medical and Biological Journal*. 2018;3:101–108 (in Russ.) DOI: 10.23648/UMBJ.2018.31.17221.
54. Hawkes J.E., Chan T.C., Krueger J.G. Psoriasis pathogenesis and the development of novel targeted immune therapies. *The Journal of Allergy and Clinical Immunology*. 2017;140(3):645–653. DOI: 0.1016/j.jaci.2017.07.004.
55. Blauvelt A., Chiricozzi A. The Immunologic role of IL-17 in psoriasis and psoriatic arthritis pathogenesis. *Clinical Reviews in Allergy & Immunology*. 2018;55(3):379–390. DOI: 10.1007/s12016-018-8702-3.
56. Seeling M., Hillenhoff U., David J.P., Schett G., Tuckermann J., Lux A. et al. Inflammatory monocytes and Fcγ receptor IV on osteoclasts are critical for bone destruction during inflammatory arthritis in mice. *Proceedings of the National Academy of Sciences of the United States of America*. 2013;110(26):10729–10734. DOI: 10.1073/pnas.1301001110.

Authors information

Poryadin Gennady V. – Dr. Sci. (Med.), Professor, Corresponding Member of RAS, Department of Pathophysiology and Clinical Pathophysiology, Pirogov Russian National Research Medical University, Moscow, poryadin_gv@rsmu.ru, http://orcid.org/0000-0003-2010-3296

Zakhvatov Alexey N. – Dr. Sci. (Med.), Professor, Department of General Surgery named after Professor N. I. Atyasov, Medical Institute, National Research Ogarev Mordovia State University, Saransk, zachvatan78@mail.ru, http://orcid.org/0000-0003-1433-0337

Parshina Alina Yu. – Student, National Research Ogarev Mordovia State University, Saransk, alinaparshina2000@gmail.com, http://orcid.org/0000-0003-0415-1132

(✉) **Zakhvatov Alexey N.,** zachvatan78@mail.ru

Received 04.02.2022;
approved after peer review 16.05.2022;
accepted 09.06.2022

УДК 616.12-005.4:616.894-053.8:577.2.08
https://doi.org/10.20538/1682-0363-2022-4-193-204

Bioinformatic analysis of biological pathways in coronary heart disease and Alzheimer's disease

Chasovskikh N.Y., Chizhik E.E.

Siberian State Medical University
2, Moscow Trakt, Tomsk, 634050, Russian Federation

ABSTRACT

Aim. Using bioinformatic tools, to perform a pathway enrichment analysis in Alzheimer's disease and coronary heart disease (CHD).

Materials and methods. Genes contributing to susceptibility to CHD and Alzheimer's disease were obtained from the public database DisGeNET (Database of Gene – Disease Associations). A pathway enrichment analysis was performed in the ClueGO Cytoscape plug-in (version 3.6.0) using hypergeometric distribution and the KEGG and Reactome databases.

Results. The identified genes contributing to susceptibility to Alzheimer's disease and CHD are included in 69 common signaling pathways, grouped into the following subgroups: cell death signaling pathways (1); signaling pathways regulating immune responses (2); signaling pathways responsible for fatty acid metabolism (3); signaling pathways involved in the functioning of the nervous system (4), cardiovascular system (5), and endocrine system (6).

Conclusion. Following the performed analysis, we identified possible associations between processes involving genetic factors and their products in CHD and Alzheimer's disease. In particular, we assumed that susceptibility genes involved in the implementation of these pathways regulate apoptosis, production of inflammatory cytokines and chemokines, lipid metabolism, β-amyloid formation, and angiogenesis.

Keywords: coronary heart disease, Alzheimer's disease, ClueGO Cytoscape plug-in, susceptibility genes, pathway enrichment analysis

Conflict of interest. The authors declare the absence of obvious or potential conflict of interest related to the publication of this article.

Source of financing. The authors state that they received no funding for the study.

For citation: Chasovskikh N.Y., Chizhik E.E. Bioinformatic analysis of biological pathways in coronary heart disease and Alzheimer's disease. *Bulletin of Siberian Medicine.* 2022;21(4):193–204. https://doi.org/10.20538/1682-0363-2022-4-193-204.

Биоинформационный анализ биологических путей при ишемической болезни сердца и болезни Альцгеймера

Часовских Н.Ю., Чижик Е.Е.

Сибирский государственный медицинский университет (СибГМУ)
Россия, 634050, г. Томск, Московский тракт, 2

РЕЗЮМЕ

Цель исследования – провести анализ обогащения биологических путей при болезни Альцгеймера и ишемической болезни сердца (ИБС) с помощью биоинформационных инструментов.

✉ *Chizhik Evgenia E.,* evgenika06@gmail.com

Гены предрасположенности к ИБС и гены предрасположенности к болезни Альцгеймера извлечены из публичной базы данных DisGeNET (база данных ассоциаций генов и заболеваний). Анализ обогащения биологических путей проведен в плагине ClueGO Cytoscape version 3.6.0 при помощи гипергеометрического теста с использованием баз данных KEGG и REACTOME.

Выявленные гены предрасположенности к болезни Альцгеймера и ИБС включены в 69 общих сигнальных путей, объединенных в следующие подгруппы: сигнальные пути, участвующие в гибели клеток (1); сигнальные пути, вовлеченные в процессы иммунной системы (2); сигнальные пути, ответственные за метаболизм жирных кислот (3); сигнальные пути, принимающие участие в функционировании нервной системы (4), сердечно-сосудистой системы (5), эндокринной системы (6).

В результате проведенного анализа выявлены возможные общие процессы, в которые вовлечены генетические факторы и их продукты при ишемической болезни сердца и болезни Альцгеймера. В частности, предполагается, что гены предрасположенности, участвующие в реализации данных путей, регулируют процессы апоптоза, наработки воспалительных цитокинов и хемокинов, метаболизма липидов, формирования β-амилоида, ангиогенеза.

Ключевые слова: ишемическая болезнь сердца, болезнь Альцгеймера, ClueGO Cytoscape, гены предрасположенности, анализ обогащения путей

Конфликт интересов. Авторы декларируют отсутствие явных и потенциальных конфликтов интересов, связанных с публикацией настоящей статьи.

Источник финансирования. Авторы заявляют об отсутствии финансирования при проведении исследования.

Для цитирования: Часовских Н.Ю., Чижик Е.Е. Биоинформационный анализ биологических путей при ишемической болезни сердца и болезни Альцгеймера. *Бюллетень сибирской медицины.* 2022;21(4):193–204. https://doi.org/10.20538/1682-0363-2022-4-193-204.

INTRODUCTION

Currently, Alzheimer's disease (AD) is a serious health problem. According to the estimates by Alzheimer's Disease International in 2019, more than 50 million people suffer from this disease worldwide [1]. Numerous studies on the genetic basis of AD have identified genes contributing to the development of this disease [2, 3]. Besides, the results of genetic association studies of various diseases showed that AD manifestations can be combined with other pathologies, for example, with cardiovascular diseases, such as myocardial infarction [4] and atrial fibrillation [5]. According to M.K.Aronson et al., who studied the association between dementia and coronary heart disease (CHD) in elderly patients, CHD, especially long-term, is associated with a smaller cortical thickness and brain volume (according to magnetic resonance imaging data) [6]. In addition, a number of epidemiological studies showed that patients with CHD have higher incidence of AD [7, 8].

However, the association between AD and CHD remains debatable, since data of some studies suggest that CHD is associated with cognitive impairment [9], while other studies suggest that there is no relationship between these conditions [10]. For example, the Rotterdam Study (a prospective cohort study that started in 1990 in the Netherlands and is aimed at finding the causes of chronic diseases common among elderly people and increasing with the population aging) showed that unrecognized (asymptomatic) myocardial infarction was associated with a risk of developing AD, whereas recognized MI was not [5, 11].

In 2014, G. Liu et al. integrated data of three GWAS using a gene-based meta-analysis to identify new risk factors for AD. The pathway analysis was performed using the Kyoto Encyclopedia of Genes and Genomes and the gene ontology database [12]. The authors revealed for the first time the involvement of signaling pathways associated with cardiovascular diseases, cellular processes, and infectious diseases in the development of AD. However, there are no other studies describing joint processes of signal transduction in AD and CHD. Thus, a pathway enrichment analysis, which makes it possible to assess the involvement of susceptibility genes in possible mechanisms of simultaneous presentation of these pathologies, is of particular interest.

The aim of this work was to identify signaling and metabolic pathways involved in the processes of signal transduction in both AD and CHD.

Genes contributing to susceptibility to CHD and AD were extracted from the public database DisGeNET [13]. DisGeNET is a platform containing a complete catalog of genes and their variants related to human diseases. The catalog combines data from expert databases, such as CTD, UniProt, ClinVar, Orphanet, GWAS, GAD, with information obtained by the scientific literature analysis [13]. The pathway enrichment analysis presumably involved in the mechanisms of simultaneous presentation of CHD and AD was carried out in the ClueGO Cytoscape plug-in (version 3.6.0) [14] using the KEGG [15] and Reactome [16] databases.The studied susceptibility genes for CHD and AD in the ClueGO Cytoscape plug-in were presented in the form of clusters 1 and 2, respectively. For the analysis, the hypergeometric test with $p < 0.05$ and kappa K = 0.4 was used.

Susceptibility gene sets for AD and CHD were formed on the basis of the DisGeNET data analysis. For AD, the set consisted of 446 genes, and for CHD – 324 protein-coding genes. Following the pathway enrichment analysis, we revealed 90 pathways which include susceptibility genes for AD, 28 pathways which include susceptibility genes for CHD, and 69 pathways associated with both diseases (the latter are presented in the Table).

These pathways were grouped into the following blocks by their involvement in biological processes and functioning of body systems: cell death signaling pathways (1); signaling pathways regulating immune responses (2); signaling pathways responsible for fatty acid metabolism (3); signaling pathways involved in the functioning of the nervous system (4), cardiovascular system (5), and endocrine system (6). In addition, pathways that include genes required for implementing physiological processes and changes in typical pathological processes (such as inflammation and hypoxia) were considered separately.

Table

Common biological pathways associated with CHD and AD

Biological pathways	Genes that are common to diseases and are included in the signaling pathway
1. Cell death signaling pathways	
Apoptosis	*NFKB1*, *TNF*
Necroptosis	*IL1A*, *IL1B*, *TLR4*, *TNF*
TNF signaling pathway	*CCL2*, *IL1B*, *IL6*, *MMP3*, *MMP9*, *NFKB1*, *PTGS2*, *TNF*
p53 signaling pathway	*SERPINE1*
2. Signaling pathways regulating immune responses	
Hematopoietic cell lineage	*IL1A*, *IL1B*, *IL6*, *IL6R*, *TNF*
Innate immunity	*AGER*, *CFH*, *CRP*, *F2*, *IGF2R*, *IL1B*, *MMP9*, *MPO*, *NFKB1*, *NOS3*, *OLR1*, *PLA2G2A*, *PLCG2*, *TLR4*
Signaling by interleukins	*AGER*, *CCL2*, *CCR5*, *HMOX1*, *ICAM1*, *IL10*, *IL18*, *IL1A*, *IL1B*, *IL1RN*, *IL6*, *IL6R*, *IRS1*, *MMP3*, *MMP9*, *NFKB1*, *PTGS2*, *TGFB1*, *TNF*, *VEGFA*
Complement cascade	*CFH*, *CRP*, *F2*
Fc γ R-mediated phagocytosis	PLCG2
Phagosome	*MPO*, *OLR1*, *TLR4*
Cell surface interactions at the vascular wall	*F2*, *OLR1*, *TGFB1*
Leukocyte transendothelial migration	*MMP9*, *PLCG2*
Interleukin (IL)-4 and IL-13 signaling pathways	*CCL2*, *HMOX1*, *IL10*, *IL18*, *IL1A*, *IL1B*, *IL6*, *IL6R*, *MMP3*, *MMP9*, *PTGS2*, *TGFB1*, *TNF*, *VEGFA*
IL-17 signaling pathway	*CCL2*, *IL1B*, *IL6*, *MMP3*, *MMP9*, *NFKB1*, *PTGS2*, *TNF*
PI3K-Akt signaling pathway	*BDNF*, *IL6*, *IL6R*, *IRS1*, *NFKB1*, *NOS3*, *TLR4*, *VEGFA*
Fc ε RI-mediated signaling pathway	*PLCG2*
C-type lectin receptor signaling pathway	*IL10*, *IL1B*, *IL6*, *NFKB1*, *PLCG2*, *PTGS2*, *TNF*
Toll-like receptor signaling pathway	*IL1B*, *IL6*, *NFKB1*, *TLR4*, *TNF*
Clathrin-mediated endocytosis	*IGF2R*, *LDLR*
3. Signaling pathways responsible for fatty acid metabolism	
Plasma lipoprotein assembly	*ABCA1*, *APOA1*, *APOE*
Plasma lipoprotein remodeling	*ALB*, *APOA1*, *APOE*, *CETP*, *LPL*

Table (continued)

Biological pathways	Genes that are common to diseases and are included in the signaling pathway
Plasma lipoprotein assembly, remodeling, and clearance	*ABCA1*, *ALB*, *APOA1*, *APOE*, *CETP*, *LDLR*, *LPL*, *NPC1*
Cholesterol metabolism	*ABCA1*, *APOA1*, *APOE*, *CETP*, *LDLR*, *LPA*, *LPL*, *LRP1*, *NPC1*, *SORT1*
Ether lipid metabolism	*PLA2G1B*, *PLA2G2A*
Fat digestion and absorption	*ABCA1*, *APOA1*, *PLA2G1B*, *PLA2G2A*
Bile secretion	*ABCB1*, *HMGCR*, *LDLR*
Sphingolipid signaling pathway	*NFKB1*, *NOS3*, *TNF*
4. Signaling pathways involved in the functioning of the nervous system	
Signaling by NTRKs	*BDNF*, *IRS1*
Signaling by NTRK2 (TRKB)	*BDNF*
Neurotrophin signaling pathway	*BDNF*, *IRS1*, *NFKB1*, *PLCG2*, *SORT1*
Amyloid fibril formation	*APOA1*
Axon guidance	*MMP9*, *UNC5C*
Serotonergic synapse	*PTGS2*
Neurotransmitter clearance	*ALDH2*
Endocrine and other factor-regulated calcium reabsorption	*ESR1*, *VDR*
5. Signaling pathways involved in the functioning of the cardiovascular system	
VEGFA – VEGFR2 Pathway	*NOS3*, *VEGFA*
Signaling by VEGF	*NOS3*, *VEGFA*
Complement and coagulation cascades	*F2*, *PLG*, *SERPINE1*
Platelet activation, signaling, and aggregation	*ALB*, *APOA1*, *F2*, *PLCG2*, *PLG*, *SERPINE1*, *TGFB1*, *VEGFA*
Platelet activation	*F2*, *NOS3*, *PLCG2*
Signaling by PDGF	*PLG*
Fluid shear stress and atherosclerosis	*CCL2*, *HMOX1*, *IL1A*, *IL1B*, *MMP9*, *NFKB1*, *NOS3*, *TNF*, *VEGFA*
Platelet homeostasis	*NOS3*
Apelin signaling pathway	*NOS3*, *SERPINE1*
Aldosterone synthesis and secretion	*AGT*, *LDLR*
6. Signaling pathways involved in the functioning of the endocrine system	
Ovarian steroidogenesis	*LDLR*, *PTGS2*
Peptide hormone metabolism	*ACE*, *AGT*
Aldosterone-regulated sodium reabsorption	*IRS1*
7. Signaling pathways involved in processes in normal conditions and in pathology	
Signal transduction	*AGT*, *APOA1*, *APOE*, *BDNF*, *CCR5*, *ESR1*, *ESR2*, *F2*, *IL6*, *IL6R*, *IRS1*, *LDLR*, *LPL*, *LRP1*, *MMP3*, *MMP9*, *NFKB1*, *NOS3*, *NR3C1*, *PLCG2*, *PLG*, *PPARG*, *SERPINE1*, *TGFB1*, *TNF*, *VEGFA*
Cellular responses to stress	*IL1A*, *IL6*, *NFKB1*, *NR3C1*, *VEGFA*
Signaling by receptor tyrosine kinases	*BDNF*, *ESR1*, *IRS1*, *MMP9*, *NOS3*, *PLG*, *VEGFA*
FOXO-mediated transcription	*NR3C1*
FoxO signaling pathway	*IL10*, *IL6*, *IRS1*, *TGFB1*
MAPK signaling pathway	*BDNF*, *IL1A*, *IL1B*, *NFKB1*, *TGFB1*, *TNF*, *VEGFA*
Phospholipase D signaling pathway	*AGT*, *F2*, *PLCG2*
TGF-β signaling pathway	*TGFB1*, *TNF*
HIF-1 signaling pathway	*HMOX1*, *IL6*, *IL6R*, *NFKB1*, *NOS3*, *PLCG2*, *SERPINE1*, *TLR4*, *VEGFA*
Biological oxidation	*ALDH2*, *HPGDS*
Extracellular matrix organization	*MMP3*, *MMP9*, *PLG*, *SERPINE1*, *TGFB1*
Degradation of the extracellular matrix	*MMP3*, *MMP9*, *PLG*
Focal adhesion	*VEGFA*

Table (continued)

Biological pathways	Genes that are common to diseases and are included in the signaling pathway
Regulation of insulin-like growth factor (IGF) transport and uptake by insulin-like growth factor binding proteins (IGFBPs)	*ALB*, *APOA1*, *APOE*, *F2*, *IL6*, *PLG*
RAS signaling pathway	*BDNF*, *NFKB1*, *PLA2G1B*, *PLA2G2A*, *PLCG2*, *VEGFA*
G-α(i) signaling events	*AGT*, *APOA1*, *APOE*, *LDLR*, *LPL*, *LRP1*
Circadian clock	*NR3C1*, *SERPINE1*
ABC transporters	*ABCA1*, *ABCB1*
SUMOylation of intracellular receptors	*ESR1*, *NR3C1*, *PPARG*, *VDR*
G-α (q) signaling events	*AGT*, *F2*, *MMP3*
Glycolysis / gluconeogenesis	*ALDH2*

CELL DEATH SIGNALING PATHWAYS

These pathways include genes associated with AD and CHD. The TNF signaling pathway [KEGG:04668] initiates apoptotic or necroptotic pathway implementation. Namely, TNFR1 signaling pathway triggers the NF-κB signaling pathway, as well as apoptosis and necroptosis [17]. In addition, apoptosis can be triggered following the implementation of the p53 signaling pathway [18]. The necroptosis signaling pathway [KEGG:04217] is involved in the pathogenesis of many diseases, including neurological diseases, ischemic injury, and viral infections [19].

Changes in the regulation and activation of these pathways are of great importance for the development of both CHD and AD. However, the role of apoptosis in AD is ambiguous. Some researchers report that AD activates caspases, in particular caspase-6, which initiates apoptosis in the brain [20]. Other researchers argue that the theory of apoptotic cell death in AD and the clinical presentation of the disease are incompatible, since cells that are to undergo apoptosis die within a few days, maintaining a high level of caspase-3, which should lead to acute and massive neuronal loss. In this case, clinical symptoms of AD should be identified at an early stage of the disease, and not decades after its onset [21]. It is also known that apoptosis is a key component in the CHD pathogenesis [22].

SIGNALING PATHWAYS REGULATING IMMUNE RESPONSES

The signaling pathway of the hematopoietic cell lineage [KEGG:04640] reflects the transition of blood cells from hematopoietic stem cells to mature blood cells, including immune cells. It is known that an increase in the total number of leukocytes and in each of their subtypes separately makes it possible to predict the development of CHD. In addition, almost all cellular elements of blood, including leukocytes, erythrocytes, and platelets, are involved in the pathogenesis of atherosclerosis [23]. It is also known that platelets are involved in the development of the amyloid precursor protein, and their functional similarity with neurons makes it possible to use platelets as a model for AD studies [24].

Signaling by interleukins (ILs) [R-HSA:449147] is associated with their pleiotropic effect on cells (which affects tissue growth and repair, hematopoietic stem cell homeostasis, as well as multiple lines of body defense against pathogens) [25]. For example, IL-1β is the main mediator in the implementation of the acute phase response at the level of the entire body, as well as in the development of a local inflammatory response [26]. It is known that impaired coronary circulation with myocardial ischemia increases its concentration in the blood [27]. What is more, an increased level of this interleukin is observed in AD, which is associated with inflammation during the disease progression [28].

IL-4 and IL-13 signaling [R-HSA:6785807] in the central nervous system is associated with the neuroprotective effect of IL-4 and IL-13, which suppress the production of inflammatory mediators. It was confirmed by the results of the experiment with an animal AD model [29].

IL-17 signaling pathway [KEGG:04657] includes a family of cytokines consisting of IL-17A-F and plays an important role in acute and chronic inflammatory responses [30]. The IL-17 family cytokines transmit signals through their respective

receptors and activate downstream pathways, which include NF-κB, MAPK, and C/EBP, inducing the expression of antimicrobial peptides, cytokines, and chemokines [31].

Phagocytosis is an important process in the implementation of the protective function of the body against infectious pathogens. The Fc γ R-mediated phagocytosis pathway [KEGG:04666] implements this function via γ receptors on Fc cells, opsonized by antibodies that recognize foreign substances. Cross-linking of Fc-γ receptors initiates a series of signals mediated by tyrosine phosphorylation of several proteins, which, in turn, lead to the formation of phagosomes following cytoskeletal actin rearrangement and membrane remodeling [32]. The phagosome signaling pathway [KEGG:04145] is triggered when specific receptors on the surface of phagocytes recognize ligands on the surface of foreign particles. The acquisition of lysosomal proteases by phagosomes during maturation and the release of reactive oxygen species are important for the breakdown of foreign substances contained in them [33].

The Fc ε-RI signaling pathway [KEGG:04664] in mast cells identified by the bioinformatic analysis is initiated by antigen interaction with IgE bound to the extracellular domain of the Rc ε-RI α-chain. Mast cells activate the release of preformed granules containing biogenic amines and proteoglycans. Activation of phospholipase A2 causes the release of membrane lipids with subsequent development of lipid mediators, such as leukotrienes, namely LTC4, LTD4, LTE4, and prostaglandins, in particular PDG2. Cytokines are secreted; the most important cytokines are TNF-α, IL-4, and IL-5 [34, 35].

The C-type lectin receptor signaling pathway [KEGG:04625] is responsible for the functioning of CLRs as pattern recognition receptors (PRRs) for pathogen-derived ligands in dendritic cells, macrophages, neutrophils, etc. After ligand binding, CLRs stimulate intracellular signaling cascades, which induce the production of inflammatory cytokines and chemokines, and therefore trigger innate and adaptive immunity to pathogens [36].

The involvement of common susceptibility genes for the studied diseases in the above biological pathways can affect:

the production of cytokines and chemokines involved in inflammation in nervous and cardiovascular systems. Microglia have been shown to play the key role in the activation of inflammation. The amount of microglia increases in people with AD and in the experimental model of AD in transgenic mice [37]. *In vitro* studies showed that cytokines secreted by microglial cells, in particular IL-1β, IL-6, TNF-α, and INF-γ, and chemokines can increase the immune response [37]. It is also known that many cytokines, for example, IL-12, IL-23, IL-6, and IL-1β, are involved both in neurodegeneration and in neuroinflammation mediated by leukocyte invasion of the brain [38]. In CHD, an increase in the levels of IL-6 and C-reactive protein indicates an increase in the damage to coronary arteries [39, 40];

a change in the immune response when exposed to pathogens. In the experimental model of AD in mice, it was found that the administration of microbial mimics, apart from inducing a strong systemic inflammatory response, enhances neurodegeneration [41]. In CHD, various pathogenic microorganisms can reside in the atherosclerotic plaque and support the local inflammatory response [42]. However, regardless of the pathogens found in the plaque, systemic inflammation develops due to the release of cytokines. For example, periodontal pathogens, such as P. gingivalis and Actinomycetemcomitans, promote Th17 responses in both the spleen and atherosclerotic plaques, which, in turn, increases the release of a variety of powerful cytokines, such as IL-1β, IL-6, and IL-17 [42].

SIGNALING PATHWAYS RESPONSIBLE FOR FATTY ACID METABOLISM

The identified common susceptibility genes for the studied diseases are also involved in plasma lipoprotein assembly [R-HSA:8963898] and plasma lipoprotein remodeling [R-HSA:8963899]. Very-low-density lipoproteins (VLDL) are produced in the liver and transport triacylglycerol synthesized there to other tissues in the body. High-density lipoproteins (HDL) are generated mainly in the liver and transport several types of lipids between tissues and other lipoproteins [43]. Plasma lipoprotein remodeling is a sequence of events that begins with circulating chylomicrons acquiring apolipoprotein C and E molecules; interacting with endothelial lipases, they often lose most of their triacylglycerol. Under the effect of the described changes, they

become chylomicron remnants, which bind to LDL receptors, primarily on the surface of liver cells. As chylomicrons circulate, VLDLs are exposed to lipoprotein lipases located on the endothelium of blood vessels and secreting fatty acids and glycerol. Then they are absorbed by tissues, and VLDLs are converted first into intermediate-density lipoproteins (IDL) and then into low-density lipoproteins (LDL) [44]. HDL remodeling includes conversion of HDL-bound cholesterol to cholesterol esters (spherical HDL remodeling), transfer of HDL into target cells with regeneration of pre-βHDL, and conversion of pre-β HDL to discoidal HDL [45].

Impaired functioning of the identified biological pathway of cholesterol metabolism [KEGG:04979] can lead to an increased risk of various endocrine disorders and cardiovascular diseases [46]. Common susceptibility genes for CHD and AD *PLA2G1B, PLA2G2A* are involved in the implementation of ester metabolism [KEGG:00565].

The identified pathways of fat digestion and absorption [KEGG:04975] and bile secretion [KEGG:04976] are pathways that are involved in lowering cholesterol levels. The sphingolipid signaling pathway [KEGG:04071] reflects the role of sphingomyelin and its metabolic products as second messengers in various metabolic processes.

Thus, a change in lipid metabolism with the participation of these signaling and metabolic pathways can violate the state of the vascular wall, lead to infiltration of arterial walls with atherogenic lipoproteins, formation of sclerotic plaques and stenosis, and formation of blood clots, and be a key component in the pathogenesis of CHD [47].

In the brain in AD, impaired lipid metabolism, namely, an increase in cholesterol levels, promotes the integration of β-amyloid into the cell membrane, which ultimately increases the level of cytosolic calcium in astrocytes and leads to neuronal death [48]. A high level of plasma cholesterol under certain conditions can destroy the blood – brain barrier, which allows systemic macrophages to penetrate into the brain parenchyma and initiate neuroinflammation [49]. A high level of LDPs enhances BACE-1 activity, affects the amyloid precursor protein, and impairs synaptic activity [49]. Besides, apolipoprotein E, which acts as a cholesterol transporter, can bind to cell surface receptors and allow for the production of cholesterol oxidation products [50]. Disturbances in sphingolipid metabolism, in particular, its hydrolysis, can lead to the formation of ceramide, which causes apoptosis of brain cells in AD [51].

SIGNALING PATHWAYS INVOLVED IN THE FUNCTIONING OF THE NERVOUS SYSTEM

The susceptibility genes for CHD and AD are involved in signaling via NTRK2 (TRKB) [RHSA:9006115] and in the neurotrophin signaling pathway [KEGG:04722], where signaling via NTRK2 (TRKB) [RHSA:9006115] is a component of the identified NTRK pathway [R-HSA:166520]. NTRK signaling pathway transduces signal from neurotrophins (NGF, BDNF, NTF3, and NTF4) via NTRK tyrosine kinase receptors, which have a preferred neurotrophin ligand, and via the p75NTR death receptor, which interacts with all neurotrophins [52].

The identified biological pathway for amyloid fibril formation [R-HSA:977225] was originally described as a nucleation-dependent polymerization mechanism [53], but now it is thought to be more complex, with multiple events outside the pathway leading to the formation of multiple oligomeric structures, in addition to fibrils [54].

Thus, the signaling pathways considered in this block affect the formation of amyloid fibrils and signal transmission via neurotrophins, which can mediate changes in the nervous system in AD and in the cardiovascular system in CHD.

In AD, the amyloid fibril formation pathway is responsible for the formation of β-amyloid (Aβ), which underlies the amyloid cascade hypothesis in AD. It suggests that $A\beta_{42}$ fragments accumulate in the brain with age [55]. Neurotrophic factors modulate synaptic plasticity and are involved in memory formation; their reduced levels, for example, BDNF, can contribute to the degeneration and progressive atrophy of neurons in the brain affected by AD [56].

In patients with AD, the level of $A\beta_{42}$ is increased and the accumulation of this protein in the myocardium is also observed [57, 58]. Circulating $A\beta_{40}$ aggravates atherosclerosis and predicts disease progression and cardiovascular mortality in patients with diagnosed CHD [58].

SIGNALING PATHWAYS INVOLVED IN THE FUNCTIONING OF THE CARDIOVASCULAR SYSTEM

The biological pathway VEGFA – VEGFR2 [R-HSA:4420097] is an integral part of VEGF signaling [R-HSA:194138] and is related to angiogenesis. VEGFA signaling via VEGFR2 is the main pathway that activates angiogenesis through induction of proliferation, survival, sprouting, and migration of endothelial cells, as well as by increasing endothelial permeability [59]. Dysfunction of VEGF is associated with inflammatory diseases, including atherosclerosis [60, 61].

The identified biological pathway of complement and coagulation cascades [KEGG:04610] combines the complement system and blood coagulation. The main consequences of complement activation are opsonization of pathogens, recruitment of inflammatory and immunocompetent cells, and direct destruction of pathogens [62].

The biological pathways of platelet activation, signaling, and aggregation [R-HSA:76002] and platelet activation [KEGG:04611] are analogs and are implemented using common susceptibility genes for CHD and AD. Activation of integrin αIIbβ3 (glycoprotein IIb / IIIa), the most common platelet receptor, enhances adhesion and leads to platelet interaction and aggregation [63].

Susceptibility genes for the studied diseases are involved in PDGF signaling [R-HSA:186797]. Platelet-derived growth factor (PDGF) is a potent stimulator of growth and motility of connective tissue cells (fibroblasts, smooth muscle cells), capillary endothelial cells, and neurons. PDGF binds and activates α and β protein tyrosine kinase (PTK) receptors, which, in turn, dimerize and undergo autophosphorylation. Phosphorylation sites then recruit downstream effectors for signal transduction into the cell [64].

The biological pathway of platelet hemostasis [R-HSA:418346] is regulated by susceptibility genes for CHD and AD. Under normal conditions, vascular endothelium supports vasodilation, inhibits platelet adhesion and activation, inhibits coagulation, enhances fibrin breakdown, and is anti-inflammatory in nature. In acute vascular injury, vasoconstrictor mechanisms predominate, and the endothelium becomes prothrombotic, procoagulant, and proinflammatory. This is achieved by reducing endothelial dilating agents (adenosine, NO, and prostacyclin), as well as through the direct effect of ADP, serotonin, and thromboxane on vascular smooth muscle cells, which causes their contraction. Under normal conditions, laminar flow induces COX-2 expression and prostacyclin (PGI2) synthesis, which, in turn, stimulates endothelial nitric oxide synthase (eNOS) activity. PGI2 and NO counteract platelet activation and aggregation, as does CD39 ecto-ADPase, which reduces platelet activation and recruitment by metabolizing platelet-released ADP [65].

Thus, susceptibility genes common for AD and CHD are involved in signal transduction, which affects angiogenesis, blood coagulation, and production of inflammatory cytokines. Impairment of these processes plays an essential role in the development of CHD and AD.

Elevated levels of VEGF, a hypoxia-induced vascular endothelial growth factor, have been found in blood vessel walls, perivascular deposits, astrocytes, and the intrathecal space of patients with AD and are consistent with chronic cerebral hypoperfusion and hypoxia that have been observed in these individuals [66]. Also, in addition to VEGF, cerebral vessels in AD release molecules that can affect angiogenesis, including IL-1β, IL-6, IL-8, TNF, TGFβ, MCP1, thrombin, angiopoietin 2, integrins αVβ3 and αVβ5, and HIF1α [66].

SIGNALING PATHWAYS INVOLVED IN THE FUNCTIONING OF THE ENDOCRINE SYSTEM

Peptide hormone metabolism [R-HSA:2980736] includes modification of peptide hormones after secretion and their degradation by extracellular proteases. For example, insulin metabolism proceeds in 4 stages: formation of intramolecular disulfide bonds, formation of proinsulin – zinc – calcium complexes, proteolytic cleavage of proinsulin by PCSK1 (PC1/3) and PCSK2 to form insulin, and translocation of granules through the cytosol to the plasma membrane. During the metabolism of angiotensinogen to angiotensin, renin cleaves angiotensinogen to form angiotensin I. The two C-terminal amino acid residues of angiotensin I are then removed by an angiotensin-converting enzyme (ACE) located on the surface of endothelial cells to form angiotensin II – an active peptide that causes

vasoconstriction, sodium and chloride resorption, potassium excretion, water retention, and aldosterone secretion. [67].

The biological pathway of aldosterone-regulated sodium reabsorption [KEGG:04960] reflects the role of aldosterone in sodium and potassium metabolism by binding to epithelial mineralocorticoid receptors in renal collecting duct cells located in the distal nephron, promoting sodium reabsorption and potassium excretion [68].

The pathway enrichment analysis also identified pathways that are ubiquitous under normal conditions; changes in the regulation of these pathways are observed in a large number of different diseases. This group included the following pathways: signal transduction [R-HSA:162582], cellular responses to stress [R-HSA:2262752], signaling by receptor tyrosine kinases [R-HSA:9006934], MAPK signaling pathway [KEGG:04010], FoxO signaling pathway [KEGG:04068] and FOXO-mediated transcription [R-HSA:9614085], phospholipase D signaling pathway [KEGG:04072], TGF-β signaling pathway [KEGG:04350], HIF-1 signaling pathway [KEGG:04066], biological oxidations [R-HSA:211859], extracellular matrix organization [R-HSA:1474244], degradation of the extracellular matrix [R-HSA:1474228], focal adhesion [KEGG:04510], regulation of insulin-like growth factor (IGF) transport and uptake by insulin-like growth factor binding proteins (IGFBPs) [R-HSA:381426], RAS signaling pathway [KEGG:04014].

The role of the *ApoE4* gene in the development of the diseases under study should be described separately. A study investigating the association between postmortem neuropathology of AD and CHD revealed a significant association in carriers of the ApoE4 allele [69]. Apolipoprotein E (ApoE), which is involved in AD susceptibility, regulates lipid transport and metabolism [44]. Also, in 2018, an article was published by W. Chen et al., who considered the *ApoE4* gene as a target for the treatment of CHD and AD. It was shown that mutation in the apolipoprotein E gene leads to impaired cholesterol metabolism, which can result in the development of CHD and AD; mutation in the *ABCA1* gene leads to the same result [6].

The obtained results are consistent with those in a study that investigated gene variants promoting inflammation and cholesterol metabolism due to acute myocardial infarction and AD. As a result, it was found that acute myocardial infarction and AD have common genetic prerequisites associated with cholesterol metabolism and upregulation of inflammation [70].

Thus, the study of signaling and metabolic pathways demonstrated that the genes contributing to AD and CHD are involved in processes associated with cell death, maintenance of inflammation, and fatty acid metabolism, as well as with the functioning of the nervous, cardiovascular, and endocrine systems.

CONCLUSION

As a result of the study, 69 biological pathways common for AD and CHD were identified. Among them, pathways involved in cell death; associated with the innate immunity; responsible for fatty acid metabolism; as well as for signal transduction processes that affect the functioning of the nervous, cardiovascular, and endocrine systems, can play an important role in changing intra- and intercellular interactions in cellular homeostasis. The obtained results suggest the presence of a number of mechanisms of influence in genetic factors of AD and CHD that affect the development of these diseases.

Based on the involvement of signaling pathways in the processes described above, it can be assumed that susceptibility genes involved in the implementation of these pathways regulate the following processes:

– apoptosis of both neurons and cardiomyocytes;

– production of inflammatory cytokines and chemokines, and, as a result, maintenance of inflammation;

– lipid metabolism, which, when changed, can form sclerotic plaques on the blood vessel walls and lead to the development of CHD; under certain conditions, neuroinflammation in the brain can occur;

– formation of β-amyloid, both in the brain and in the myocardium;

– angiogenesis, in particular, the level of VEGF in the walls of blood vessels increases in AD.

The results of this study provide a deeper understanding of the molecular genetic mechanisms of the combined development of the studied diseases

and their proper treatment. The results of this study are prerequisites for further study of these pathologies.

REFERENCES

1. Alzheimer's Disease International. The costs of dementia: advocacy, media and stigma. *World Alzheimer Rep. 2019 Attitudes to Dement.* 2019;100–101.
2. Naj A.C., Schellenberg G.D. (ADGC) for the ADGC. Genomic variants, genes, and pathways of Alzheimer's disease: An overview. *Am. J. Med. Genet. Part B Neuropsychiatr. Genet.* 2017;174(1):5–26. DOI: 10.1002/ajmg.b.32499.
3. Barber R.C. The genetics of Alzheimer's disease. *Scientifica (Cairo)*. 2012;2012:246210. DOI: 10.6064/2012/246210.
4. Tini G., Scagliola R., Monacelli F., La Malfa G., Porto I., Brunelli C., Rosa G.M. Alzheimer's Disease and Cardiovascular Disease: A Particular Association. *Cardiol. Res. Pract.* 2020;2020:2617970. DOI: 10.1155/2020/2617970.
5. De Bruijn R.F., Ikram M.A. Cardiovascular risk factors and future risk of Alzheimer's disease. *BMC Med*. 2014;12:130. DOI: 10.1186/s12916-014-0130-5.
6. Aronson M.K., Ooi W.L., Morgenstern H., Hafner A., Masur D., Crystal H. et al. Women, myocardial infarction, and dementia in the very old. *Neurology.* 1990;40(7):1102 LP–1102. DOI: 10.1212/wnl.40.7.1102.
7. Levin O. S., Trusova N. A. Vascular risk factors for Alzheimer's disease. *Korsakov Journal of Neurology and Psychiatry (Special Issues).* 2013;113(7–2):3–12 (in Russ.).
8. Wolf P.A. Contributions of the Framingham Heart Study to Stroke and Dementia Epidemiologic Research at 60 Years. *Arch. Neurol*. 2012;69(5):567–571. DOI: 10.1001/archneurol.2011.977.
9. Newman A.B., Fitzpatrick A.L., Lopez O., Jackson S., Lyketsos C., Jagust W. et al. Dementia and Alzheimer's disease incidence in relationship to cardiovascular disease in the Cardiovascular Health Study Cohort. *J. Am. Geriatr. Soc.* 2005;53(7):1101–1107. DOI: 10.1111/j.1532-5415.2005.53360.x.
10. Knopman D.S., Petersen R.C., Cha R.H., Edland S.D., Rocca W.A. Coronary artery bypass grafting is not a risk factor for dementia or Alzheimer disease. *Neurology*. 2005;65(7):986LP–990. DOI: 10.1212/01.wnl.0000171954.92119.c7.
11. Ikram M.A., Brusselle G., Ghanbari M., Goedegebure A., Ikram M.K., Kavousi M. et al. Objectives, design and main findings until 2020 from the Rotterdam Study. *Eur. J. Epidemiol.* 2020;35(5):483–517. DOI: 10.1007/s10654-020-00640-5.
12. Liu G., Yao L., Liu J., Jiang Y., Ma G.; Genetic and Environmental Risk for Alzheimer's disease (GERAD1) Consortium et al. Cardiovascular disease contributes to Alzheimer's disease: evidence from large-scale genome-wide association studies. *Neurobiol. Aging.* 2014;35(4):786–792. DOI: 10.1016/j.neurobiolaging.2013.10.084.
13. Piñero J., Bravo À., Queralt-Rosinach N., Gutiérrez-Sacristán A., Deu-Pons J., Centeno E. et al. DisGeNET: a comprehensive platform integrating information on human disease-associated genes and variants. *Nucleic Acids Res.* 2017;45(D1):D833–839. DOI: 10.1093/nar/gkw943.
14. Bindea G., Mlecnik B., Hackl H., Charoentong P., Tosolini M., Kirilovsky A. et al. ClueGO: a Cytoscape plug-in to decipher functionally grouped gene ontology and pathway annotation networks. *Bioinformatics.* 2009;25(8):1091–1093. DOI: 10.1093/bioinformatics/btp101.
15. Kanehisa M., Goto S. KEGG: Kyoto Encyclopedia of Genes and Genomes. *Nucleic Acids Res.* 2000;28(1):27–30. DOI: 10.1093/nar/28.1.27.
16. Fabregat A., Jupe S., Matthews L., Sidiropoulos K., Gillespie M., Garapati P. et al. The Reactome Pathway Knowledgebase. *Nucleic Acids Res.* 2018;46(D1):D649–655. DOI: 10.1093/nar/gkx1132.
17. Chu W.-M. Tumor necrosis factor. *Cancer Lett.* 2013;328(2):222–225. DOI: 10.1016/j.canlet.2012.10.014.
18. Jacobs S.B.R., Basak S., Murray J. I., Pathak N., Attardi L.D. Siva is an apoptosis-selective p53 target gene important for neuronal cell death. *Cell Death Differ.* 2007;14(7):1374–1385. DOI: 10.1038/sj.cdd.4402128.
19. Vandenabeele P., Galluzzi L., Vanden Berghe T., Kroemer G. Molecular mechanisms of necroptosis: an ordered cellular explosion. *Nat. Rev. Mol. Cell Biol.* 2010;11(10):700–714. DOI: 10.1038/nrm2970.
20. Guo H., Albrecht S., Bourdeau M., Petzke T., Bergeron C., LeBlanc A.C. Active caspase-6 and caspase-6-cleaved tau in neuropil threads, neuritic plaques, and neurofibrillary tangles of Alzheimer's disease. *Am. J. Pathol.* 2004;165(2):523–531. DOI: 10.1016/S0002-9440(10)63317-2.
21. Zhu X., Raina A.K., Perry G., Smith M.A. Apoptosis in Alzheimer disease: a mathematical improbability. *Curr. Alzheimer Res.* 2006;3(4):393–396. DOI: 10.2174/156720506778249470.
22. Dong Y., Chen H., Gao J., Liu Y., Li J., Wang J. Molecular machinery and interplay of apoptosis and autophagy in coronary heart disease. *J. Mol. Cell Cardiol.* 2019;136:27–41. DOI: 10.1016/j.yjmcc.2019.09.001.
23. Madjid M., Awan I., Willerson J.T., Casscells S.W. Leukocyte count and coronary heart disease: implications for risk assessment. *J. Am. Coll. Cardiol.* 2004;44(10):1945–1956. DOI: 10.1016/j.jacc.2004.07.056.
24. Dukhinova M.S., Ponomarev E.D. Role of platelets in neuroinflammatory disorders. A review. *Bulletin of Moscow University. Series 16. Biology.* 2018;73(3):125–131 (in Russ.).
25. Vosshenrich C.A.J., Di Santo J.P. Interleukin signaling. *Curr. Biol.* 2002;12(22):R760-763. DOI: 10.1016/s0960-9822(02)01286-1.
26. Simbirtsev A.S. Interleukin-1: from experiment to the clinucal practice. *Medical Immunology.* 2001;3(3):431–438 (in Russ.).
27. Rebrov A.P., Voskoboy I.V. Role of inflammatory and infectious factors in the development of athorosclerosis. *Terapevticheskii Arkhiv.* 2004;79(1):78–82 (in Russ.).
28. Ng A., Tam W.W., Zhang M.W., Ho C.S., Husain S.F., McIntyre R S. et al. IL-1β, IL-6, TNF-α and CRP in Elderly Patients with Depression or Alzheimer's disease: Systematic Review and Meta-Analysis. *Sci. Rep.* 2018; 8(1):12050. DOI: 10.1038/s41598-018-30487-6.
29. Kawahara K., Suenobu M., Yoshida A., Koga K., Hyodo A., Ohtsuka H. et al. Intracerebral microinjection of interleukin-4/interleukin-13 reduces β-amyloid accumulation in the ipsilateral side and improves cognitive deficits in young amyloid

precursor protein 23 mice. *Neuroscience.* 2012;207:243–260. DOI: 10.1016/j.neuroscience.2012.01.049.
30. Song X., Qian Y. IL-17 family cytokines mediated signaling in the pathogenesis of inflammatory diseases. *Cell Signal.* 2013;25(12):2335–2347. DOI: 10.1016/j.cellsig.2013.07.021
31. Gaffen S.L. Structure and signalling in the IL-17 receptor family. *Nat. Rev. Immunol.* 2009;9(8):556–567. DOI: 10.1038/nri2586.
32. Joshi T., Butchar J.P., Tridandapani S. Fcγ receptor signaling in phagocytes. *Int. J. Hematol.* 2006;84(3):210–216. DOI: 10.1532/IJH97.06140.
33. Stuart L.M., Ezekowitz R.A.B. Phagocytosis: elegant complexity. *Immunity.* 2005;22(5):539–50. DOI: 10.1016/j.immuni.2005.05.002.
34. Nadler M.J., Matthews S.A., Turner H., Kinet J.P. Signal transduction by the high-affinity immunoglobulin E receptor Fc epsilon RI: coupling form to function. *Adv. Immunol.* 2000;76:325–355. DOI: 10.1016/s0065-2776(01)76022-1.
35. Siraganian R.P. Mast cell signal transduction from the high-affinity IgE receptor. *Curr. Opin. Immunol.* 2003;15(6):639–646. DOI: 10.1016/j.coi.2003.09.010.
36. Geijtenbeek T.B.H., Gringhuis S.I. C-type lectin receptors in the control of T helper cell differentiation. *Nat. Rev. Immunol.* 2016;16(7):433–448. DOI: 10.1038/nri.2016.55.
37. Combs C.K. Inflammation and microglia actions in Alzheimer's disease. *J. Neuroimmune Pharmacol.* 2009;4(4):380–388. DOI: 10.1007/s11481-009-9165-3.
38. Becher B., Spath S., Goverman J. Cytokine networks in neuroinflammation. *Nat. Rev. Immunol.* 2017;17(1):49–59. DOI: 10.1038/nri.2016.123.
39. Grammas P. Neurovascular dysfunction, inflammation and endothelial activation: implications for the pathogenesis of Alzheimer's disease. *J. Neuroinflammation.* 2011;8:26. DOI: 10.1186/1742-2094-8-26.
40. Fioranelli M., Bottaccioli A.G., Bottaccioli F., Bianchi M., Rovesti M., Roccia M.G. Stress and Inflammation in Coronary Artery Disease: A Review Psychoneuroendocrineimmunology-Based. *Front. Immunol.* 2018;9:2031. DOI: 10.3389/fimmu.2018.02031.
41. Field R., Campion S., Warren C., Murray C., Cunningham C. Systemic challenge with the TLR3 agonist poly I:C induces amplified IFNalpha/beta and IL-1beta responses in the diseased brain and exacerbates chronic neurodegeneration. *Brain Behav. Immun.* 2010;24(6):996–1007. DOI: 10.1016/j.bbi.2010.04.004.
42. Pothineni N.V.K., Subramany S., Kuriakose K., Shirazi L.F., Romeo F., Shah P.K. et al. Infections, atherosclerosis, and coronary heart disease. *Eur. Heart J.* 2017;38(43):3195–3201. DOI: 10.1093/eurheartj/ehx362.
43. Vance J.E., Vance D.E. The assembly of lipids into lipoproteins during secretion. *Experientia.* 1990;46(6):560–569. DOI: 10.1007/BF01939694.
44. Gibbons G.F., Wiggins D., Brown A.-M., Hebbachi A.-M. Synthesis and function of hepatic very-low-density lipoprotein. *Biochem. Soc. Trans.* 2004;32(1):59–64. DOI: 10.1042/bst0320059.
45. Rye K.A., Clay M.A., Barter P.J. Remodelling of high density lipoproteins by plasma factors. *Atherosclerosis.* 1999;145(2):227–238. DOI: 10.1016/s0021-9150(99)00150-1.
46. Cortes V.A., Busso D., Maiz A., Arteaga A., Nervi F., Rigotti A. Physiological and pathological implications of cholesterol. *Front Biosci.* 2014;19(3):416–428. DOI: 10.2741/4216.
47. Didigova R.T., Inarokova A.M., Imagozheva M.Ya., Mamedov M.N. Current opinions about the etiology and diagnosis of coronary artery disease. *Lechebnoe Delo.* 2011;4:11–17 (in Russ.).
48. Abramov A.Y., Ionov M., Pavlov E., Duchen M.R. Membrane cholesterol content plays a key role in the neurotoxicity of β-amyloid: implications for Alzheimer's disease. *Aging Cell.* 2011;10(4):595–603. DOI: 10.1111/j.1474-9726.2011.00685.x.
49. Chen X., Hui L., Geiger J.D. Role of LDL cholesterol and endolysosomes in amyloidogenesis and Alzheimer's disease. *J. Neurol. Neurophysiol*. 2014;5(5):236. DOI: 10.4172/2155-9562.1000236.
50. Liu C.C., Kanekiyo T., Xu H., Bu G. Apolipoprotein E and Alzheimer disease: risk, mechanisms and therapy. *Nature Reviews. Neurology*. 2013;9(2):106–118. DOI: 10.1038/nrneurol.2012.263.
51. Mullen T.D., Obeid L.M. Ceramide and apoptosis: exploring the enigmatic connections between sphingolipid metabolism and programmed cell death. *Anticancer Agents Med. Chem.* 2012;12(4):340–363. DOI: 10.2174/187152012800228661.
52. Skaper S.D. The neurotrophin family of neurotrophic factors: an overview. *Methods Mol. Biol.* 2012;846:1–12. DOI: 10.1007/978-1-61779-536-7_1.
53. Teplow D.B. Structural and kinetic features of amyloid beta-protein fibrillogenesis. *Amyloid.* 1998;5(2):121–142. DOI: 10.3109/13506129808995290.
54. Roychaudhuri R., Yang M., Hoshi M.M., Teplow D.B. Amyloid beta-protein assembly and Alzheimer disease. *J. Biol. Chem.* 2009;284(8):4749–4753. DOI: 10.1074/jbc.R800036200.
55. Ricciarelli R., Fedele E. The amyloid cascade hypothesis in Alzheimer's disease: it's time to change our mind. *Curr. Neuropharmacol.* 2017;15(6):926–935. DOI: 10.2174/1570159X15666170116143743.
56. Amidfar M., de Oliveira J., Kucharska E., Budni J., Kim Y.K. The role of CREB and BDNF in neurobiology and treatment of Alzheimer's disease. *Life Sci.* 2020;257:118020. DOI: 10.1016/j.lfs.2020.118020.
57. Troncone L., Luciani M., Coggins M., Wilker E.H., Ho C.Y., Codispoti K.E. et al. Aβ amyloid pathology affects the hearts of patients with Alzheimer's disease: mind the heart. *J. Am. Coll. Cardiol.* 2016;68(22):2395–2407. DOI: 10.1016/j.jacc.2016.08.073.
58. Janelidze S., Stomrud E., Palmqvist S., Zetterberg H., van Westen D., Jeromin A. et al. Plasma β-amyloid in Alzheimer's disease and vascular disease. *Sci. Rep.* 2016;6:26801. DOI: 10.1038/srep26801.
59. Lohela M., Bry M., Tammela T., Alitalo K. VEGFs and receptors involved in angiogenesis versus lymphangiogenesis. *Curr. Opin. Cell Biol.* 2009;21(2):154–165. DOI: 10.1016/j.ceb.2008.12.012.
60. Shibuya M., Claesson-Welsh L. Signal transduction by VEGF receptors in regulation of angiogenesis and lymphangiogenesis. *Exp. Cell Res.* 2006;312(5):549–560. DOI: 10.1016/j.yexcr.2005.11.012.
61. Matsumoto T., Mugishima H. Signal transduction via vascular

endothelial growth factor (VEGF) receptors and their roles in atherogenesis. *J. Atheroscler. Thromb.* 2006;13(3):130–5. DOI: 10.5551/jat.13.130.
62. Mathern D.R., Heeger P.S. Molecules great and small: The complement system. *Clin. J. Am. Soc. Nephrol.* 2015;10(9):1636–1650. DOI: 10.2215/CJN.06230614.
63. Phillips D.R., Charo I.F., Scarborough R.M. GPIIb-IIIa: The responsive integrin. *Cell.* 1991;65(3):359–362. DOI: 10.1016/0092-8674(91)90451-4.
64. Tallquist M., Kazlauskas A. PDGF signaling in cells and mice. *Cytokine Growth Factor Rev.* 2004;15(4):205–213. DOI: 10.1016/j.cytogfr.2004.03.003.
65. Kunapuli S.P., Dorsam R.T., Kim S., Quinton T.M. Platelet purinergic receptors. *Curr. Opin. Pharmacol.* 2003;3(2):175–180. DOI: 10.1016/s1471-4892(03)00007-9.
66. Steiner D.F. On the discovery of precursor processing. *Methods Mol. Biol.* 2011;768:3–11. DOI: 10.1007/978-1-61779-204-5_1.
67. Rozansky D.J. The role of Aldosterone in Renal Sodium Transport. *Semin. Nephrol.* 2006;26(2):173–181. DOI: 10.1016/j.semnephrol.2005.09.008.
68. Beeri M.S., Rapp M., Silverman J.M., Schmeidler J., Grossman H.T., Fallon J.T. et al. Coronary artery disease is associated with Alzheimer disease neuropathology in APOE4 carriers. *Neurology.* 2006;66(9):1399 LP–1404. DOI: 10.1212/01.wnl.0000210447.19748.0b.
69. Martins I.J., Hone E., Foster J.K., Sünram-Lea S.I., Gnjec A., Fuller S.J. et al. Apolipoprotein E, cholesterol metabolism, diabetes, and the convergence of risk factors for Alzheimer's disease and cardiovascular disease. *Mol. Psychiatry.* 2006;11(8):721–736. DOI: 10.1038/sj.mp.4001854.
70. Licastro F., Chiappelli M., Caldarera C.M., Porcellini E., Carbone I., Caruso C. et al. Sharing pathogenetic mechanisms between acute myocardial infarction and Alzheimer's disease as shown by partially overlapping of gene variant profiles. *J. Alzheimers Dis.* 2011;23(3):421–431. DOI: 10.3233/JAD-2010-090871.

Authors information

Chasovskikh Nataliya Yu. – Dr. Sci. (Med.), Professor, Acting Head of the Medical and Biological Cybernetics Division, Siberian State Medical University, Tomsk, nch03@mail.ru, https://orcid.org/0000-0001-6077-0347

Chizhik Evgenia E. – Teaching Assistant, Medical and Biological Cybernetics Division, Siberian State Medical University, Tomsk, evgenika06@gmail.com

(✉) **Chizhik Evgenia E.,** evgenika06@gmail.com

Received 25.01.2022;
approved after peer review 04.05.2022;
accepted 09.06.2022

УДК 616.24/.56-003.2-008.6/.8-056.7:575.224]-07: 618.2:618.4
https://doi.org/10.20538/1682-0363-2022-4-205-211

Clinical features of the course of cystic fibrosis during pregnancy and childbirth

Teteneva A.V.[1, 3], Chernyavskaya G.M.[1], Bespalova I.D.[1], Skorokhodova T.V.[1, 4], Koshchavtseva Yu.I.[1], Radionov D.I.[1], Kalyuzhina E.V.[1], Romanov D.S.[1], Radionova E.V.[1], Ustyuzhanina E.A.[2], Varfolomeeva I.A.[2], Stepanov I.A.[4], Karmanova A.V.[4], Golubyatnikova E.V.[4]

[1] *Siberian State Medical University*
2, Moscow Trakt, Tomsk, 634050, Russian Federation

[2] *Tomsk Regional Clinical Hospital*
96, I. Chernykh Str., Tomsk, 634063, Russian Federation

[3] *Medical and Sanitary Hospital No. 2*
3, Bela Kuna Str., Tomsk, 634040, Russian Federation

[4] *Regional Perinatal Center*
96/1, I. Chernykh Str., Tomsk, 634063, Russian Federation

ABSTRACT

Cystic fibrosis is one of the urgent medical and social problems of health care systems in most countries due to fairly high prevalence, development of multi-organ lesions, and poor outcomes.

Due to modern advances in the diagnosis and treatment of cystic fibrosis, not only has the average life expectancy of patients increased, but their quality of life has also improved, and it has become possible to maintain pregnancy and childbearing. Since cystic fibrosis can adversely affect the course of pregnancy, childbirth, and health of both mother and child, proper management of women with cystic fibrosis during pregnancy and childbirth is of particular relevance. The presented clinical case is an example of competent supervision at all stages of monitoring of a patient with cystic fibrosis during pregnancy and childbirth.

Keywords: cystic fibrosis, maintenance of pregnancy, childbearing, CF

Conflict of interest. The authors declare the absence of obvious or potential conflicts of interest related to the publication of this article.

Source of financing. The authors state that they received no funding for the study.

For citation: Teteneva A.V., Chernyavskaya G.M., Bespalova I.D., Skorokhodova T.V., Koshchavtseva Yu.I., Radionov D.I.1, Kalyuzhina E.V., Romanov D.S., Radionova E.V., Ustyuzhanina E.A., Varfolomeeva I.A., Stepanov I.A., Karmanova A.V., Golubyatnikova E.V. Clinical features of the course of cystic fibrosis during pregnancy and childbirth. *Bulletin of Siberian Medicine.* 2022;21(4):205–211. https://doi.org/10.20538/1682-0363-2022-4-205-211.

✉ *Bespalova Inna D.,* innadave@mail2000.ru

Клинические особенности течения муковисцидоза на фоне беременности и родов

Тетенева А.В.[1, 3], Чернявская Г.М.[1], Беспалова И.Д.[1], Скороходова Т.В.[1, 4], Кощавцева Ю.И.[1], Радионов Д.И.[1], Калюжина Е.В.[1], Романов Д.С.[1], Радионова Е.В.[1], Устюжанина Е.А.[2], Степанов И.А.[4], Карманова А.В.[4], Голубятникова Е.В.[4]

[1] *Сибирский государственный медицинский университет (СибГМУ)*
Россия, 634050, г. Томск, Московский тракт, 2

[2] *Томская областная клиническая больница (ТОКБ)*
Россия, 634063, г. Томск, ул. Ивана Черных, 96

[3] *Медико-санитарная часть (МСЧ) № 2*
Россия, 634040, г. Томск, ул. Бела Куна, 3

[4] *Областной перинатальный центр (ОПЦ) им. И.Д. Евтушенко*
Россия, 634063, г. Томск, ул. Ивана Черных, 96/1

РЕЗЮМЕ

Муковисцидоз (МВ) представляет собой одну из актуальных медико-социальных проблем систем здравоохранения большинства стран в связи с достаточно высоким уровнем распространенности, развитием полиорганных поражений и неблагоприятными исходами.

Благодаря современным достижениям диагностики и лечения муковисцидоза в настоящее время не только увеличилась средняя продолжительность жизни пациентов, но и улучшилось её качество, появилась возможность сохранения беременности и деторождения. В связи с тем, что МВ может неблагоприятно влиять на течение беременности, родов, состояние здоровья как матери, так и ребенка, вопросы правильного ведения больных во время беременности и родов у женщин, страдающих МВ, приобретают особую актуальность. Примером грамотной курации на всех этапах наблюдения за пациенткой в период беременности и родов на фоне МВ является представленный клинический случай.

Ключевые слова: муковисцидоз, сохранение беременности, деторождение, МВ.

Конфликт интересов. Авторы декларируют отсутствие явных и потенциальных конфликтов интересов, связанных с публикацией настоящей статьи.

Источник финансирования. Авторы заявляют об отсутствии финансирования при проведении исследования.

Для цитирования: Тетенева А.В., Чернявская Г.М., Беспалова И.Д., Скороходова Т.В., Кощавцева Ю.И., Радионов Д.И., Калюжина Е.В., Романов Д.С., Радионова Е.В., Устюжанина Е.А., Степанов И.А., Карманова А.В., Голубятникова Е.В. Клинические особенности течения муковисцидоза на фоне беременности и родов. *Бюллетень сибирской медицины.* 2022;21(4):205–211. https://doi.org/10.20538/1682-0363-2022-4-205-211.

INTRODUCTION

Cystic fibrosis (CF) is one of the urgent medical and social problems of health care systems in most countries due to fairly high prevalence, development of multi-organ lesions, and poor outcomes [1–3]. CF is a genetic disease caused by a mutation in the cystic fibrosis transmembrane conductance regulator (CFTR) gene and is characterized by damage to exocrine glands in a number of vital organs: respiratory tract, gastrointestinal tract, liver, pancreas, salivary and sweat glands, reproductive organs [2–6]. At the same time, pathology of the respiratory tract is the most common cause of complications and mortality; it is accompanied by persistent infection and inflammation in the respiratory tract, with formation of viscous bronchial secretions [2, 5, 6 –8]. The first clinical symptoms usually appear in early childhood [2, 9]. A chronic, pronounced pathological process contributes to formation of bronchiectasis and development of pulmonary hypertension and cor pulmonale. However,

lower respiratory tract infection is considered to be the key factor which underlies the severity of CF and its prognosis [2, 10].

Due to modern advances in the diagnosis and treatment of CF, not only has the average life expectancy of patients increased to an average of 36.8 years, but their quality of life has also improved, and it has become possible to maintain pregnancy and childbearing [9, 11]. However, it should be understood that in women with CF, pregnancy is associated with an increased risk for disease decompensation up to death, and decompensated liver pathology can contribute to an unfavorable course of pregnancy and childbirth [4, 12, 13].

Recent studies have confirmed that fertility in women with CF is not impaired, except for cases when more viscous secretion accumulates in the cervical canal [12, 14]. Often, patients with CF are characterized by multifetal pregnancies, gestational diabetes mellitus, preterm labor, and indications for operative delivery [13, 15]. Severe respiratory disorders underlie pneumonia, with the development of acute respiratory failure and a need for invasive mechanical ventilation [13]. Nevertheless, a sufficient number of observations have shown that most pregnancies in women with CF end in spontaneous childbirth through the birth canal; caesarean section is resorted to in cases of complications associated with a risk to the health of the mother or the baby [15, 16].

Therefore, considering that CF can adversely affect the course of pregnancy, childbirth, and the health of both the mother and the child, proper management of women with CF during pregnancy and childbirth is of particular relevance. The presented clinical case is an example of competent supervision at all stages of monitoring of a patient with CF during pregnancy and childbirth.

CLINICAL CASE

Patient P., 22 years old, was routinely admitted to the pulmonology department of the Regional Clinical Hospital on October 10, 2019 for a follow-up examination and inpatient treatment and for resolving the issue of maintaining pregnancy. The pregnancy was first and desired.

From the anamnestic data: at the age of 1.5 months, the patient experienced right-sided lower lobe pneumonia; since childhood, she had been experiencing rare dry cough, sometimes with a difficulty in clearing the chest of viscous sputum, which intensified after hypothermia. She was followed up by a pediatrician with the diagnosis of chronic bronchitis. For the first time, CF was diagnosed at the age of 4 years 10 months; the examination revealed an increase in the sweat chloride level up to 119 mEq / l. The patient has been followed up at the Research Institute of Medical Genetics with the diagnosis: Cystic fibrosis, mixed form (affects the lungs and the intestines), a moderately severe, continuously relapsing course. Compound heterozygous for Dele 2.3/E92,K. Chronic pancreatic insufficiency.

In 2011, a thoracoscopic lobectomy was performed for bronchiectasis in the right lower lobe in S8–10. The patient constantly receives basic therapy: Pulmozyme (dornase alfa) 1 ampule per day using a jet nebulizer, Bramitob 300 mg 2 times a day using a jet nebulizer in courses (28-day administration / 28 day-break, the last course was completed on October 9), Kreon 25,000 IU (6,000 IU /kg of body weight), 10 capsules per day with meals, Ursofalk 250 mg, 5 capsules per day. The patient undergoes inpatient treatment 1–2 times a year and receives antibiotic therapy (ABT). The last hospitalization in the pulmonology department was in December 2018, during which the patient received another course of ABT with Co-trimoxazole, Piperacillin / Tazobactam following the microbiological examination of the sputum (*St. aureus* 10^5, *Stenotrophomonas maltophilia* 10^5).

Two weeks before the current hospitalization, the patient noted an increase in coughing with light yellow sputum in the volume of up to 20 ml per day (the amount and color of the sputum did not change), decreased exercise tolerance, low-grade body temperature in the evenings, once up to 38 °C (took Paracetamol). On October 09, 2019, a pelvic ultrasound was performed, and an early intrauterine pregnancy was detected.

Past medical history: appendectomy in 2010, removal of the lower lobe of the right lung due to bronchiectasis in 2011, removal of nasopharyngeal polyps in 2014. The patient suffered from chicken pox as a child. Menstruation started at the age of 14, is regular, moderate, pain-free; the menstrual cycle is 30 days; bleeding lasts 5 days; the patient denies menstrual irregularities.

The patient has disability group 3.

Family history of CF is positive: the middle sister (the patient is the elder sister) also has CF, she is followed up at the Research Institute of Medical Genetics.

Upon admission: the patient's condition was satisfactory. The skin was pale, clean, moist, with no cyanosis of the lips. Height – 165 cm, weight – 51 kg, BMI – 18.7, blood pressure – 100 / 60 mm Hg, pulse – 80 beats per minute, body temperature – 37.1 °C, respiratory rate – 20 breaths per minute. Oxygen saturation (SpO_2) in the ambient air was 98%, after a six-minute walk test – 96%. The chest had a cylindrical shape and was elastic upon palpation. Percussion sound was resonant and the same over symmetrical areas. Auscultation of the lungs revealed rough vesicular breathing without wheezing. The borders of cardiac dullness were not changed. Heart sounds were loud

and rhythmic. The abdomen was soft and not tender on palpation in all departments. The liver and spleen were not enlarged. No dysuria was noted. The Murphy's punch sign was negative.

Complete blood count: hemoglobin – 122 g / l, leukocytes – 17.8 x10^9 / l: band neutrophils – 6%, segmented neutrophils – 78%, eosinophils – 1%, lymphocytes – 13%, monocytes – 2%. Platelets 180 x 10^9 / l, ESR – 27 mm / h. Biochemical blood parameters were without significant deviations from the normal values: glucose – 4.25 mmol / l, total protein – 68 g / l, albumins – 33.9 g / l, bilirubin – 13.3 / 3.5 μmol / l, alanine aminotransferase (ALT) – 11.2 IU, aspartate aminotransferase – 7.1 IU, alpha-amylase – 91.6 IU / l, creatinine – 66.3 μmol / l, C-reactive protein (CRP) – 57.8 mg / l, fibrinogen – 7.4 g / l.

10.15.19. Blood culture for sterility testing revealed no growth of bacterial flora.

The microbiological examination of the sputum of 10.12.19: *Acinetobacter baumanii* 10^5 (pan-drug resistant strain, insensitivity to carbapenems); the examination of 07.15.19: *Stenotrophomonas maltophilia* 10^6, *St.aureus* 10^5, *candida albicans* 10^6 (pan-drug resistant); the examination of 10.24.19: *Stenotrophomonas maltophilia* 10^2, *candida albicans* 10^3 (pan-drug resistant).

10.12.19. Spirometry. Forced expiratory volume in one second (FEV1) – 78%, forced vital capacity (FVC) – 84%, FEV1 / FVC – 82.8. Impression: vital capacity of the lungs is within the conditional norm. Stage 0–1 obstructive ventilation abnormalities.

10.11.19. ECG: sinus tachycardia, heart rate – 92 beats per min. Right axis deviation. A turn around the longitudinal axis with the right ventricle facing forward.

10.11.19. Echocardiography: cardiac cavities were not enlarged, no hypertrophy was noted. The contractility of the left and right ventricles was within normal values. Violations of local contractility were not revealed. Left ventricular diastolic dysfunction with the pseudonormal filling pattern. The valves were unchanged. Mild tricuspid valve regurgitation, right ventricular systolic pressure was not increased. The pericardium was unchanged, no fluid was detected.

10.12.19. Abdominal ultrasound: the liver was not enlarged, the contours were even, the edge was sharp, echogenicity was within normal values, the structure was homogeneous, the bile ducts were not dilated, the walls were dense, the vascular pattern was without irregularities; the portal vein – 8 mm. Gallbladder: dimensions: 80 x 30 mm, wall density 3 mm, biliary sludge was detected. The pancreas was not enlarged, the contours were even, the echogenicity was normal, the structure was homogeneous. The pancreatic duct – 1 mm. The spleen was not enlarged, the structure was homogeneous. The kidneys were not enlarged, the thickness of the renal parenchyma was normal, the contours were even, the mobility was preserved, the position was normal, the structure of the parenchyma was homogeneous, the boundaries of the renal sinuses were fuzzy, no signs of urodynamic disturbances were noted. Impression: signs of chronic cholecystitis. Moderate diffuse changes in the kidneys.

10.14.19. Thyroid and parathyroid ultrasound. Impression: no pathology detected.

The patient categorically refused to undergo a chest X-ray, despite the physician's explanation of its necessity and safety.

17.12.18. Spiral computed tomography of the chest. Impression: Condition after right-sided lower lobe lobectomy. Infiltrative areas, focal infiltrative changes in the lungs with interstitial thickening along the contour in the lobes of the lungs on both sides. Bronchial wall thickening. Small saccular bronchiectasis, a few calcified pulmonary nodules on both sides. Small areas of stringy fibrosis on both sides.

Taking into account chronic excretion of *Pseudomonas aeruginosa* from the sputum in the past medical history, the presence of other non-fermenting gram-negative bacteria (*Acinetobacter baumannii, Stenotrophomonas maltophilia*) in the bacteria culture tests, the presence of clinical and laboratory signs of exacerbation of bronchopulmonary infection, and an unfavorable prognosis in the absence of ABT, ABT was prescribed for health reasons. The prescription of ABT and further management of the patient were carried out taking into account pregnancy, with an informed consent obtained from the patient. The prescribed initial therapy (Meronem 1.0 g, 3 times a day via intravenous drip infusion) had no effect: the body temperature remained low-grade, leukocytosis was up to 21.3 x 10^9 / l with a left shift. Therefore, ABT was changed to a combination of Cefoperazone / Sulbactam 6 g (Cefoperazone 3 g + Sulbactam 3 g) per day via intravenous drip infusion and Fosfomycin 2.0 2 times a day via intravenous drip infusion. In the context of the therapy, the patient's condition improved: the body temperature did not exceed 37 °C, the volume of yellow sputum was about 15 ml per day. In the CBC, a positive trend was observed – a decrease in leukocytosis (as of 24.10.2019, leukocytes – 9.43 x 10^9 / l: band neutrophils – 6%, segmented neutrophils – 71%, eosinophils – 0.5%, lymphocytes – 16.8%, monocytes – 5.7%; the level of CRP decreased to 4.3 mg / l.

A consultation was held with the participation of pulmonologists, geneticists, and obstetricians – gynecologists in order to choose further treatment strategy and decide on the possibility of maintaining pregnancy.

Taking into account the patient's condition, the features of the clinical presentation of CF were the following: moderate course, no significant changes in the pulmonary ventilation parameters (they are close to normal values), no signs of respiratory failure (SpO2 in the ambient air – 98%), no pulmonary hypertension, and right ventricular hypertrophy, childbearing is possible. At the same time, the presence of vital indications for massive ABT at the present time (the first trimester of pregnancy) is associated with a risk of negative effects on the fetus. The patient and relatives were informed about this in order to make a decision. In addition, they were explained that after birth, given the condition of the patient, she may be hospitalized and may need help in caring for the baby. The patient decided to maintain the pregnancy.

Obstetric and gynecological status upon admission. 10.12.19. Examination by a gynecologist. The external genital organs are developed correctly, without pathological changes. The vaginal mucosa is not changed, the cervix is not visually changed. The cervix is positioned posteriorly from the pelvic axis, it is not shortened, its shape is cylindrical, the consistency is normal, the cervical os is closed, the uterus is enlarged up to 5–6 weeks of pregnancy; the uterus is normotonic, mobile, and not tender. At the time of examination, there are no data for acute obstetric pathology. The patient is 6–7 weeks pregnant.

10.14.19. Transvaginal ultrasound of the uterus and appendages. The uterus is positioned in the center and is retroverted; the contours of the uterus are even; the structure of the myometrium is homogeneous; in the uterine cavity, a fetal egg (d 24 mm) is visualized; pregnancy 6 weeks and 3 days. Cervix: the structure is not changed; no masses projected at the uterine appendages are detected. There is no free fluid in the posterior cul-de-sac. Impression: Pregnancy 6 weeks and 3 days.

10.21.19. Gynecological status. The external genitalia are developed correctly. Female pattern hair growth. The vagina is narrow, the folds are preserved. The cervix is posterior, up to 3.0 cm long, dense; the cervical os is closed. The uterus is enlarged because of pregnancy (up to 8 weeks), spherical in shape, soft, and not tender. Appendages on both sides are without pathology.

Dynamic transvaginal ultrasound of the uterus and appendages: 10.21.19. Following fetometry, the patient is 7 weeks 3 days pregnant.

The patient was discharged against medical advice on 31.10.19.

Diagnosis at discharge: 9 weeks pregnant. Cystic fibrosis, mixed form (affects the lungs and the intestines), a moderately severe, continuously relapsing course. Compound heterozygous for Dele 2.3/E92,K. Chronic infection of the respiratory tract with *St. aureus, Pseudomonas aeruginosa, Stenotrophomonas maltophilia, Acinetobacter baumannii*. Chronic bronchitis. Bronchiectasis of both lungs, condition after thoracoscopic lobectomy for bronchiectasis in the right lower lobe (03.04.2011). Fibrosis of the upper lobe of the right lung. Chronic pansinusitis. Exocrine pancreatic insufficiency. Chronic erosive antral gastritis, duodenitis HP(-), insufficiency of the gastric cardia. Gastroesophageal reflux disease (GERD). Bacterial overgrowth syndrome. Secondary intestinal dysbiosis. Asthenic syndrome.

Pregnancy follow-up was carried out in the Regional Perinatal Center from 13 weeks pregnant. The follow-up was carried out by an obstetrician – gynecologist together with a pulmonary internist. The patient's high adherence to follow-up and treatment was noted.

There were no exacerbations of the disease that required ABT prescription. No significant negative trend in spirometry parameters and oxygen saturation values was noted.

During pregnancy, shortness of breath on exertion, most pronounced in the last trimester of pregnancy, nausea, and repeated vomiting were common.

During pregnancy, in accordance with the recommendations, the patient received: vaginal Utrogestan 200 mg 1 time per day, vitamin D 2,000 IU, Calcemin Advance 1 capsule per day (500 mg calcium), Ursofalk 5 capsules per day in 2 doses, Kreon 10 capsules per day in 3 doses, Pulmozyme inhalations 1 time per day, Iodomarin 200 mcg / day, Tobramycin inhalation (28-day therapy – 28-day break), on-demand Salbutamol inhalation.

Weight gain during pregnancy was 9 kg.

The following ultrasound screenings were carried out:

1. 12 weeks pregnant (Research Institute of Medical Genetics) – no pathology was detected.

2. 19.6 weeks pregnant (Research Institute of Medical Genetics) – no pathology was detected.

3. 30 weeks pregnant (Regional Perinatal Center) – no pathology was detected.

At 35.2 weeks pregnant, the patient was admitted to antenatal hospital unit to resolve the issue of delivery. A plan for childbirth was drawn up: high degree of risk (15 points), estimated fetal weight was 2,600 g +\- 26 g.

Due to the appearance of shortness of breath on minimal exertion and the gestational age close to full term (35.2 weeks), a decision was made on elective operative delivery on 04.30.2020. The patient agreed with the strategy. Regional anesthesia with antibiotic prophylaxis were planned: Ampicillin + Sulbactam 1.5 g parenterally, further prescription of ABT according to indications.

On 04.30.2020, elective operative delivery was performed. A premature boy was born (weight 2,620 g, height 49 cm, the Apgar score of 8/8). During the operation, delayed umbilical cord clamping was performed. Amniotic fluid was light (400 ml). Blood loss was 600 ml.

The caesarean section went without technical difficulties.

The postoperative period proceeded without complications. The new mother was discharged on day 13 (delay in discharge due to the condition of the child). The newborn was in the Neonatal Intensive Care Unit for 7 days and in the Neonatal and Premature Infant Pathology Unit for 10 days. Primary diagnosis: late preterm baby (35.3 weeks). Postconceptional age 37.4 weeks. Secondary diagnosis: newborn respiratory distress syndrome of moderate severity. Incomplete ureteral duplication in the left kidney. Premature infant jaundice. Right-sided choroid plexus cyst.

The condition at birth was severe due to respiratory disorders. The Silverman Andersen Respiratory Severity Score of 4–5 points. Infusion therapy and respiratory support were carried out (6 days): nCPAP was performed in the delivery room, CPAP with positive dynamics and phototherapy were carried out in the intensive care unit for newborns (increased jaundice, unconjugated hyperbilirubinemia). A positive trend was noted in the context of the therapy. The condition at discharge was satisfactory. The neurological status corresponded to the gestational age.

Bottle-feeding with expressed breast milk. Attachment to the breast.

Nasal breathing was free, the pharynx was not irritated. The skin was subicteric, pink, and clean. The umbilical wound was epithelialized. Breath sounds were heard throughout all lung fields, no wheezing was heard. Heart sounds were clear and rhythmic. The abdomen was soft and not tender on palpation. The liver and spleen were not enlarged. Urination. No vaccinations were given.

Currently, the child is followed up in the pediatric hospital: he develops according to age, no abnormalities and developmental delays have been identified.

CONCLUSION

Modern advances in pulmonology, obstetrics, and neonatal and anesthetic services have enabled women with CF to have successful pregnancies without apparent significant impairment of their lung function. When considering the use of drugs during pregnancy, the known and unknown risks of the effects of drug treatment on the fetus must be weighed against the risk to the mother's health resulting from discontinuation of therapy. The choice of a method for delivering a baby is determined by the state of the mother's health, and in case external respiration deteriorates, a decision can be made to perform a caesarean section.

A number of conditions underly a successful pregnancy and successful delivery in this clinical case: firstly, the patient was diagnosed with CF in childhood, she has been followed up by pulmonologists and geneticists for her disease for a long time; secondly, the patient had no disorders of external respiration at early stages of pregnancy and no obstetric and gynecological diseases in the past medical history; and, thirdly, the coordinated work of specialists (pulmonologists, obstetrician – gynecologists, and neonatologists) in patient's management and delivery support.

REFERENCES

1. Bucher J., Oualha M., Dupic L., Lebourgeois M., Lesage F., Renolleau S. et al. 312 Outcomes and factors associated with poor outcome of children with cystic fibrosis admitted to the intensive care unit. *Journal of Cystic Fibrosis.* 2015;14(1):138. DOI: 10.1016/S1569-1993(15)30486-0.
2. Chen Q., Shen Y., Zheng J. A review of cystic fibrosis: basic and clinical aspects. *Animal Model Exp. Med.* 2021;4(3):220–232. DOI: 10.1002/ame2.12180.
3. Shteinberg M., Haq I.J., Polineni D., Davies J.C. Cystic fibrosis. *Lancet.* 2021;397(10290):2195–2211. DOI: 10.1016/S0140-6736(20)32542-3.
4. Clinical guidelines on cystic fibrosis. Union of Pediatricians of Russia, Association of Medical Geneticists, Russian Respiratory Society, Russian Transplant Society, Association of Pediatricians of the Moscow Region. 2021 (in Russ.).
5. Hao S., Roesch E.A., Perez A., Weiner R.L., Henderson L.C., Cummings L. et al. Inactivation of CFTR by CRISPR/Cas9 alters transcriptional regulation of inflammatory pathways and other networks. *Journal of Cystic Fibrosis.* 2020;19(1):34–39. DOI: 10.1016/j.jcf.2019.05.003.
6. Elborn J.S. Cystic Fibrosis. *Lancet.* 2016;388(10059):2519–2531. DOI: 10.1016/S0140-6736(16)00576-6.
7. Deschamp A.R., Hatch J.E., Slaven J.E., Gebregziabher N., Storch G., Hall G.L. et al. Early respiratory viral infections in infants with cystic fibrosis. *Journal of Cystic Fibrosis.* 2019;18(6):844–850. DOI: 10.1016/j.jcf.2019.02.004.
8. Krasovsky S.A., Chernyak A.V., Amelina E.L., Nikonova V.S., Voronkova A.Yu., Samoilenko V.A. et al. Survival trends in cystic fibrosis patients in Moscow and Moscow region in 1992–2001 and 2002–2011. *Russian Pulmonology Journal.* 2012;(3) 79–86 (in Russ.). DOI: 10.18093/0869-0189-2012-0-3-79-86.
9. Kashirskaya N.Yu., Kondrat'eva E.I., Krasovsky S.A., Starinova M.A., Voronkova A.Yu., Amelina E.L. et al. Register of patients with cystic fibrosis in the Russian Federation. 2019. M.: Medpraktika-M, 2021:68 (in Russ.).
10. Khan T.Z., Wagener J.S., Bost T., Martinez J., Accurso F.J., Riches D.W. Early pulmonary inflammation in infants with cystic fibrosis. *Am. J. Respir. Crit. Care Med.* 1995;151(4):1075–1082. DOI: 10.1164/ajrccm/151.4.1075.

11. Kashirskaya N.Yu., Krasovsky S.A., Chernyak A.V., Sherman V.D., Voronkova A.Yu., Shabalova L.A. et al. Trends in life expectancy of cystic fibrosis patients in Moscow and their association with the treatment received: retrospective study for 1993–2013. *Voprosy Sovremennoi Pediatrii.* 2015;14(4):503–508 (in Russ.). DOI: 10.15690/vsp.v14.i4.1390.
12. McArcdle J.R. Pregnancy in cystis fibrosis. *Clin. Chest. Med.* 2011;32(1):111–120. DOI: 10.1016/j.ccm.2010.10.005.
13. Patel E.M., Swamy G.K., Heine R.P., Kuller J.A., James A.H., Grotegut C.A. Medical and obstetric complications among pregnant women with cystis fibrosis. *Am. J. Obstet. Gynecol.* 2015;212(1):98.E1–E9. DOI: 10.1016/j.ajog.2014.07.018.
14. Shteinberg M., Taylor-Cousar J.L., Durieu I., Cohen-Cymberknoh M. Fertility and Pregnancy in Cystic Fibrosis. *Chest.* 2021;160(6):2051–2060. DOI: 10.1016/j.chest.2021.07.024.
15. Reynaud Q., Jablonski C.R., Poupon-Bourdy S., Denis A., Rabilloud M., Lemonnier L. et al. Pregnancy outcome in women with cystic fibrosis and poor pulmonary function. *Journal of Cystic Fibrosis.* 2020;19(1):80–83. DOI: 10.1016/j.jcf.2019.06.003.
16. Jaina R., Kazmerski T.M., Zuckerwisec L.C., West N.E., Montemayor K., Aitken M.L. et al. Pregnancy in cystic fibrosis: Review of the literature and expert recommendations. *Journal of Cystic Fibrosis.* 2021;21(3):1569–1993. DOI: 10.1016/j.jcf.2021.07.019.

Authors contribution

Teteneva A.V. – conception and design, analysis of the nosology. Chernyavskaya G.M., Skorokhodova T.V., Stepanov I.A., Karmanova A.V., Golubyatnikova E.V., Ustyuzhanina E.A., Varfolomeeva I.A., Radionov D.I., Kalyuzhina E.V., Romanov D.S., Radionova E.V. – analysis of the clinical case, selection of the material. Bespalova I.D. – editing of the article, communication with the editorial board. Koshchavtseva Yu.I. – work with the reference list, translation of the article.

Authors information

Teteneva Anna V. – Dr. Sci. (Med.), Deputy Chief Physician for Medicine, Medical and Sanitary Hospital No. 2; Professor, Division of Introduction into Internal Diseases with a Course in Therapy, Siberian State Medical University, Tomsk, anna.dubodelova@mail.ru, http://orcid.org/0000-0002-4323-2798

Chernyavskaya Galina M. – Dr. Sci. (Med.), Professor, Division of Advanced-Level Therapy with a Course in Physiotherapy, Rehabilitation and Sports Medicine, Siberian State Medical University, Tomsk, chernyavskayag@gmail.com, http://orcid.org/0000-0003-0105-2307

Bespalova Inna D. – Dr. Sci. (Med.), Head of the Division of Introduction into Internal Diseases with a Course in Therapy, Siberian State Medical University, Tomsk, innadave@mail2000.ru, http://orcid.org/0000-0002-4513-6329

Skorokhodova Tatyana V. – Cand. Sci. (Med.), Deputy Chief Physician for Clinical and Expert Work, Regional Perinatal Center; Associate Professor, Obstetrics and Gynecology Division, Siberian State Medical University, Tomsk, itv7@yandex.ru

Ustyuzhanina Elena A. – Cand. Sci. (Med.), Head of the Pulmonology Department, Tomsk Regional Clinical Hospital, Tomsk, u_elan@mail.ru

Varfolomeeva Irina A. – Pulmonologist, Tomsk Regional Clinical Hospital, Tomsk, varfolomeeva.irina@lust.ru

Koshchavtseva Yuliya I. – Teaching Assistant, Division of Introduction into Internal Diseases with a Course in Therapy, Siberian State Medical University, Tomsk, kossy09@mail.ru, http://orcid.org/0000-0001-5260-4832

Radionov Denis I. – Post-Graduate Student, Division of Introduction into Internal Diseases with a Course in Therapy, Siberian State Medical University, Tomsk, radionovdenis12@gmail.com.

Kalyuzhina Elena V. – Dr. Sci. (Med.), Professor, Division of Advanced-Level Therapy with a Course in Physiotherapy, Rehabilitation and Sports Medicine, Siberian State Medical University, Tomsk, kalyuzhina.e@mail.ru, http://orcid.org/0000-0002-7978-5327.

Romanov Dmitriy S. – Post-Graduate Student, Division of Introduction into Internal Diseases with a Course in Therapy, Siberian State Medical University, Tomsk, romanovds92@yandex.ru

Radionova Ekaterina V. – Resident, Division of General Medical Practice and Polyclinic Therapy, Siberian State Medical University, Tomsk, Opoldnik@yandex.ru

Stepanov Igor A. – Cand. Sci. (Med.), Chief Physician, Regional Perinatal Center, Tomsk, stepanovopc@mail.ru

Karmanova Alla V. – Cand. Sci. (Med.), Deputy Chief Physician for Obstetric and Gynecological Care, Regional Perinatal Center, Tomsk, karmanovaav@opc.tomsk.ru

Golubyatnikova Ekaterina V. – Obstetrician-Gynecologist, Regional Perinatal Center, Tomsk, ketrintomsk@mail.ru

(✉) **Bespalova Inna D.,** innadave@mail2000.ru

Received 17.05.2022;
approved after peer review 21.07.2022;
accepted 08.09.2022

On the 70th birthday of Evgeny L. Choynzonov, the member of the Russian Academy of Sciences

On December 14, 2022, Evgeny L. Choynzonov, Doctor of Medical Sciences, Professor, Academician of the Russian Academy of Sciences, Honored Scientist of Russia, Director of the Cancer Research Institute of Tomsk NRMC, turned 70 years old.

Evgeny L. Choynzonov is an outstanding Russian scientist and a talented organizer who has made a significant personal contribution to the development of medical science.

Evgeny L. Choynzonov was born in the village of Zhargalantuy in the Buryat ASSR. After graduating from the General Medicine Department of Tomsk Medical Institute in 1976, he entered clinical residency at the Otorhinolaryngology Division of the same institute.

At the opening of the Siberian branch of the All-Union Cancer Research Center of the Academy of Medical Sciences of the USSR in Tomsk, Evgeny L. Choynzonov was offered the position of a junior researcher at the Head and Neck Cancer Unit. In 1984, he successfully defended his PhD thesis on the topic "Treatment of patients with oral cancer and its effect on the parameters of the immune system" and was promoted to senior researcher. After defending his doctoral dissertation in 1995 on the topic "Cancer of the upper respiratory and digestive tract (epidemiological, immunological, and virological aspects, evaluation of the treatment effectiveness)", he became a leading researcher at the same department of the Cancer Research Institute. In 2002, he was awarded the academic title of Professor of Oncology. Since 2002, Evgeny L. Choynzonov has been the Director of the Cancer Research Institute of the SB RAMS.

Evgeny L. Choynzonov has outstanding organizational skills. He is able to determine the prospects for the development of modern medical science and is engaged in social activities. So, he managed to merge the academic institutes of the Tomsk Research Center into the current Tomsk National Research Medical Center (NRMC) of the Russian Academy of Sciences in order to achieve breakthrough scientific results that ensure the competitive global position of Russia in biomedicine and transfer them into healthcare. Tomsk NRMC, the director of which in 2016–2018 was academician Evgeny L. Choynzonov, is one of the largest and most authoritative medical research institutions in Russia, which cooperates with international research organizations in the fields as oncology, cardiology, pediatric cardiology, medical genetics, pharmacology, and psychiatry.

Academician Evgeny L. Choynzonov makes a great contribution to the training of senior biomedical staff. In 2006, he promoted the establishment of the Oncology Division at Siberian State Medical University (SibMed) on the basis of the Institute, the head of which he has been ever since. Evgeny Choynzonov is the Chairman of the Dissertation Committee 24.1.215.02 in the specialty "3.1.6. Oncology, Radial Therapy (medical sciences)" at the Cancer Research Institute of Tomsk NRMC and is a member of the Dissertation Committee 24.1.215.03 in the specialty "21.5.7. Genetics (Medical Sciences)" at the Research Institute of Medical Genetics of Tomsk NRMC.

Academician Evgeny L. Choynzonov is the founder of the scientific school "Malignant tumors of the head and neck. Development of personalized approaches to the

implementation of modern treatment and rehabilitation methods for patients with malignant neoplasms based on the study of clinical, morphological, and molecular genetic features of the tumor". The representatives of this scientific school include renowned scientists, professors who hold high positions in research, educational, and medical institutions, and young professionals who mastered modern high-tech methods of scientific research and treatment of patients. Under his scientific supervision, 16 doctoral and 21 candidate dissertations were completed and defended.

Evgeny L. Choynzonov is a recognized leader in Russia in the field of treatment and rehabilitation of patients with malignant neoplasms of the maxillofacial region, which is one of the most difficult groups of cancer patients. Back in the 1980s, he began to develop a new direction in the rehabilitation of patients with head and neck cancers to preserve their quality of life and social and labor adaptation. Today the Cancer Research Institute is one of the main organizations in Russia, providing assistance to patients from all over Siberia, the Far East, and the Far North.

Evgeny L. Choynzonov and his students developed methods of reconstructive surgeries using the latest achievements in the field of medical materials science and additive technologies. New high-tech methods of organ-preserving and reconstructive plastic surgical interventions using microsurgical equipment and biocompatible implants have been developed and introduced into clinical practice, which allows to ensure high quality of life for patients, their ability to work, and successful social adaptation. A unique technology was developed for creating artificial individual implants with a functionalized surface which could be integrated into bones and soft tissues of the body.

The proposed technologies reduce disability rate and improve the quality of life of patients and their social and labor adaptation, with more than 70% of patients being able to live their lives fully.

Evgeny L. Choynzonov made a huge contribution to the development of practical healthcare, providing scientific and methodological guidance to medical and prevention institutions of the Siberian Federal District on oncology issues and actively introducing advanced scientific developments into the practical healthcare in the region. He is a highly qualified specialist in oncosurgery and has been recognized as the leading professional in Russia in the treatment of socially sensitive tumors with complex localization. He is an actively operating oncologist of the highest category. He has conducted about 3,000 surgical interventions. Evgeny L. Choynzonov performs the most complex operations, and patients with the most severe course of cancer are treated under his personal supervision.

He introduced into clinical practice unique surgical interventions using simultaneous replacement of postoperative defects with endoprostheses made of porous titanium nickelide and microsurgical autotransplantation of tissues, which eliminates the need for repeated surgery. He has developed and implemented new approaches to the treatment of thyroid, parotid gland, nasal and paranasal sinus cancer based on organ-preserving operations in combination with intraoperative electronic and remote neutron therapy.

Having worked in this field for many years, Evgeny L. Choynzonov published 27 monographs, 1 manual for doctors, 1 methodological manual, and 7 clinical guidelines. He obtained 53 Russian patents for inventions, 25 certificates of state registration of software products, 5 license agreements granting the right to use patents, which proves the high priority of his research. He is the author of more than 1,000 printed works, about 350 Russian and foreign articles indexed in the Russian and foreign citation databases of the RSCI, Scopus, and Web of Science.

Being one of the leading oncologists in Russia, Evgeny L. Choynzonov actively participates in the publishing of many Russian and foreign scientific journals. He is the editor-in-chief of "Siberian Journal of Oncology", a member of the editorial board of the journals: "P.A. Herzen Journal of Oncology", "Problems in Oncology," "Oncosurgery", "Head and Neck Tumors", "Siberian Scientific Medical Journal", "The Siberian Journal of Clinical and Experimental Medicine"; member of the editorial board of the journals "Annals of Oncology. New Approaches in Oncology", "Bone and Soft Tissue Sarcomas, Tumors of the Skin", "Head and Neck Journal", "Eurasian Journal of Oncology", "Journal of Oncology", "Creative Surgery and Oncology", "The Territory of Intelligence", and "CA: A Cancer Journal for Clinicians. Russian Edition".

Academician Evgeny L. Choynzonov is a member of the Presidium of the Russian Academy of Sciences, a member of the Council of the Russian Academy of Sciences on Evolutionary Medicine and Medical Heritage, an expert of the Russian Academy of Sciences, a member of the Presidium of the Association of Oncologists of Russia, the Council on the priority scientific and technological development of the Russian Federation "Transition to personalized medicine, high-tech healthcare, and health-saving technologies, including through the rational use of drugs, primarily antibacterial drugs", Deputy Chairman of the task group

"Head and Neck Cancers" of the Scientific Council on Malignant Neoplasms of the Russian Federation, Chairman of the task group "Oncology" of the Scientific Council on Medical Problems of Siberia, the Far East and the Far North of the Russian Federation; member of the commission under the Governor of Tomsk region for monitoring the achievement of goals in socioeconomic development in the Tomsk region, determined by the President of the Russian Federation; chief freelance oncologist of the Siberian Federal District, Chairman of the Tomsk Regional Society of Oncologists, representative of the Russian Federation in the International Federation of Head and Neck Oncology Specialists (IFHNOS, USA) and the Eurasian Community of Specialists in Head and Neck Tumors; he is a member of the Coordinating Council (Board of Directors) and Academic Council of Tomsk NRMC; the Chairman of the Academic Council of the Cancer Research Institute of Oncology of Tomsk NRMC.

Under the leadership of academician Evgeny L. Choynzonov, the following works and research were successfully completed: 10 projects within federal targeted programs (2006–2007, 2010–2012, 2016), 6 grants of the Russian Foundation for Basic Research (2008–2015), the integration project of Siberian Branch of the Russian Academy of Medical Sciences (2006–2007), the grant of the Tomsk City Administration (2008), 3 major grants of the Russian Science Foundation (2016–2018, 2019–2021, 2022–2024), a project within the federal targeted program "Development of Pharmaceutical and Medical Industry of the Russian Federation up to 2020 and beyond" (2017–2019), 2 projects within the federal targeted program "Research and Development in Priority Areas of Development of the Scientific and Technological Complex of Russia in 2014–2020" (2017–2019, 2019–2020).

The long-term research, organizational, and pedagogical activity of Evgeny L. Choynzonov has been highly appreciated and recognized. He was awarded the title of "Honored Scientist of the Russian Federation". In 2021, Evgeny L. Choynzonov and a group of authors won the State Prize of the Russian Federation in the field of science and technology for 2020 for the creation of a fundamental interdisciplinary biomedical approach to the treatment, reconstruction, and rehabilitation of head and neck cancers. He won the Tomsk Region Prize in education, science, health, and culture (2012). Evgeny L. Choynzonov was awarded the medal of the Order "For Merit to the Fatherland" II class (2015), the badge "Excellent Health Worker" (2004), the jubilee medal "400 Years of Tomsk" (2004), the Certificate of Honor of the State Duma of the Tomsk Region (2004), the R. Virkhov Medal of Honor (2005), the Certificate of Honor of the Trade Union of Health Workers of the Russian Federation (2009), the medal "For Merit to Siberian State Medical University" (2011), the Certificate of Commendation of the Department of Healthcare of the Tomsk Region (2011), the Certificate of Honor of the Tomsk Region (2012), the Certificate of Honor of the Russian Academy of Medical Sciences (2012), the silver badge "Coat of Arms of the Tomsk Region" (2012), the Honorary Silver Order "Public Recognition" (2012), the badge of the Federation of Independent Trade Unions of Russia "For the Fellowship" (2012), the medal "For Achievements" (2014), the Certificate of Honor of the Tomsk City Administration (2014), the jubilee medal "120 Years of TPU" (2016), the honorary title "Honored Veteran of the Siberian Branch of the Russian Academy of Sciences" (2017), the badge of merit of the Federal Agency of Research Organizations of Russia "For Merits in the Development of Science" (2017), the badge of honor "Pride of Tomsk" (2017), the badge of merit "For Merit to the Tomsk Region" (2017), the Certificate of Honor of the Federation Council of the Federal Assembly of the Russian Federation (2017), the diploma of the Tomsk City Chamber of the Public (2017), the Certificate of Honor of the Federal Agency of Research Organizations of Russia (2018), the commemorative jubilee sign "Legislative Duma of the Tomsk Region: 25 Years" (2019), the jubilee badge "75 years of the Tomsk Region" (2019). Evgeny L. Choynzonov was listed in the Book of Honor of the Federation of Trade Union Organizations of the Tomsk Region (2013); awarded the title of chevalier of the golden badge of honor "Heritage of Siberia" (2016) and the title "Honorary Professor of Siberian State Medical University" (2017). He received the Certificate of Commendation from the President of the Russian Federation, the Certificates of Commendation from the Head of the People's headquarters of public support for the presidential candidate of the Russian Federation and the plenipotentiary representative of the President of the Russian Federation in the Siberian Federal District (2012), and the Certificate of Commendation of the Council of Rectors of Universities of the Tomsk Region (2019). Evgeny L. Choynzonov was awarded the medal "For Outstanding Achievements in Oncology" named after the founder of Russian oncology, Professor N.N. Petrov (2021), and the medal named after P.A. Herzen for outstanding achievements in the development of oncology (2022). He was awarded the title of Honorary Citizen of the Tomsk Region (2022).

K

L

M

N

O

P

R

S

T

U

V

Y

Z

20 ЛЕТ ЖУРНАЛУ «БЮЛЛЕТЕНЬ СИБИРСКОЙ МЕДИЦИНЫ»

bulletin.tomsk.ru

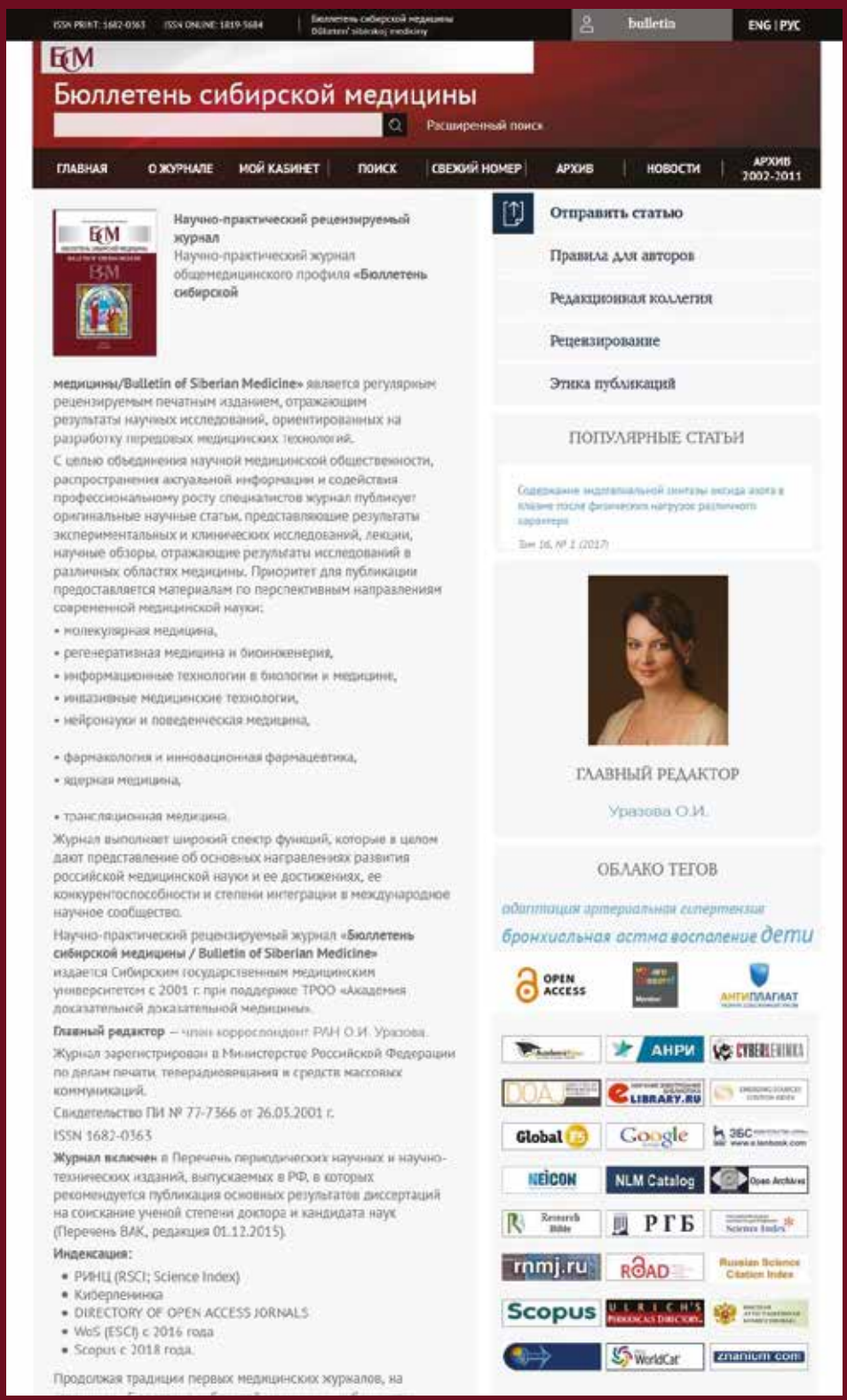

ISSN 1682-0363 (print)
ISSN 1819-3684 (online)
БЮЛЛЕТЕНЬ СИБИРСКОЙ МЕДИЦИНЫ
2022. Т. 21. № 4. 1–218